ASHES TO ASHES

IDENTIFYING ARCHAEOLOGICAL FUELS

GREGGORY A. GRIFFIN

Ph.D

UNIVERSITY OF BRADFORD

2018

Gregg Griffin

Abstract

Ashes to Ashes: Identifying archaeological fuels

Keywords: Orkney, magnetic, ashing, Neolithic, Pictish, resources, experimental, SEM-EDX

Abstract: Understanding fuel use is important in researching ancient communities. This project developed methods to identify archaeological fuel from midden, hearth, and ash samples using comparison to modern analogues. Modern analogue fuels were ashed at 200^0C, 400^0C, and 900^0C then analysed with a suite of methods, the results were then used to inform the development of an approach for the identification of archaeological fuels. These methods were tested using samples from Ness of Brodgar, Knowe of Swandro, and Smerquoy/Muckquoy in Orkney.

Magnetic susceptibility, scanning electron microscopy with energy dispersive X-ray spectroscopy, pH and Munsell colour assignment were chosen based upon previous archaeological, biofuel, and soil pollution research. The methodologies were refined with the analysis of ash from fuels including peat, seaweed, driftwood, willow, hazel, heather, grasses, cow dung, sheep dung, and bone. Modern analogue fuels at increasing temperatures showed an intensification in magnetism and alkalinity, and an alteration to mineral components during the chemical reaction of combustion that is indicative of fuel type and temperature.

Principal components analysis confirmed matches between archaeological samples and modern ash, indicating a strong relationship between peat fuels and the archaeological samples. A correlation is also demonstrated between some of the archaeological samples and sheep dung, driftwood, willow, and animal bone.

It is evident that each archaeological site has unique patterns of both fuel type and temperature. This shows that in the absence of abundant traditional wood fuel resources, the occupants of these sites used a combination of alternative fuels.

ASHES TO ASHES

IDENTIFYING ARCHAEOLOGICAL FUELS

GREGGORY A. GRIFFIN

Ph.D

UNIVERSITY OF BRADFORD

2018

Acknowledgements

This process has been a journey, and without help I never would have completed it. First and foremost, I would like to thank Cathy Batt and Julie Bond for their guidance and being such a great supervisory team. I would also like to Steve Dockrill for the encouraging chats and guidance in the field. Without Ruth Maher I never would have started this journey into academia and archaeology, so thanks are owed to her as well. My lab analysis never would have been completed without the help and support of Stuart Fox and Belinda Hill. There would have been no samples to analyse or a research project without archaeological samples provided by Nick Card for the Ness of Brodgar, Chris Gee and Colin Richards for the Smerquoy and Muckquoy excavations, Julie Bond and Steve Dockrill for the Knowe of Swandro. I would like to thank my wife Jacqui for being a constant source of encouragement and support, regardless of how bogged down I may have been or how hopeless I thought it all seemed she was always there. Without the support of my mother to take the leap and move to Bradford to pursue this crazy dream, and her unwavering support along the way, I never would have made it to this point. It is also necessary to thank Dani Farrar, Jenny West, and Helen Phillips for their support, encouragement while away in the field, rides to and from Orkney for 5 years, and allowing me to put bags full of dung in their car boots. I would also like to thank Highland Park, not only for making a delicious and nerve soothing spirit, but for providing with the heather peat to use for my modern analogue ashing experiments. In addition, it is also necessary to thank Neil Leask for providing peat samples from the Corrigall farm house museum. I would also like to thank Keith Wildman, my boss at the Record Café, for always being so understanding and accommodating when I needed to book weeks off for excavations. Along the way there were many other people who provided help or encouraging words, and they all deserve my thanks.

Contents

List of Figures

List of Tables

Chapter 1: Creating the spark (Introduction)

1.1 Overview

This research aimed to produce a methodology for identifying fuels from archaeological deposits using comparison to modern ash. This initial chapter introduces the concepts that are the framework for the Ashes to Ashes research project, and provide an outline of what is to come in this thesis.

This chapter presents the aims and objectives that were the basis for this project, followed by the research questions that were used to guide the investigation. Next, the key points of the research are introduced including the benefits of fire and dependence on fuel, the formation of ash through combustion, how ash is deposited in archaeological contexts, and the climate and archaeology of Orkney. The archaeological sites being examined in this project and the methods used are also introduced. This is followed by a discussion of the research contexts and archaeological significance of this project. This chapter concludes with an overview of what is discussed in the subsequent chapters.

1.2 Aims and objectives

The aim of this research was to develop a method capable of identifying fuel from archaeological deposits using comparison to modern analogue ash. Then to use the developed methods to investigate fuel use in the past within Orkney, to gain an insight into the fuel use among multi-period sites by examining functional area deposits and combustion features such as hearths, hearth rake outs, ash dumps, and middens. A large factor of this research involved producing ashes from modern analogues such as peat, seaweed, driftwood, grasses, dung, bone, heather, hazel, and willow at 200^0C, 400^0C, and 900^0C and recording the changes to the characteristics of fuels throughout combustion including magnetic susceptibility, pH, elemental abundance, and colour.

The aims of this research were addressed by the following objectives:

- To record the changes to the attributes of ashes from modern analogue fuel sources such as wood (hazel, heather and willow), plant brush and grasses, seaweed, peat (various cuts from several sources), and animal by-product (dung and bone) heated to 200^0C, 400^0C, and 900^0C to determine diagnostic signatures that could be used to identify archaeological fuel material from ashes within archaeological deposits.
- Using the attributes established by the modern analogue analyses, create an approach to identify archaeological fuel material based on the characteristics of modern ash.
- Review archaeological samples from multiple sites throughout Orkney to attempt to determine what fuel sources were in use for given settlement areas.

1.3 Research questions

The research questions were asked at the onset of this project, and were used to inform the investigation, and guide the development of the methods. With consideration to ash formation, the identification of fuels, and fuel use the research questions provide a comprehensive basis for this project. This research set out to answer the following questions using the results of recording the changes to modern analogue fuels and the investigation into fuel use within Orkney.

- What changes do fuels go through during the burning process?
- What markers present in modern analogue ash are indicative of fuel types within archaeological deposits?
- Can changes in fuel use be detected?
- What fuels are being used?
- What potential factors affect the selection of resources?

1.4 Introduction to the research

Understanding what fuel resources were being utilised by past populations is a vital component to comprehending a sites relationship with the environment and insight into its economy (Giles 2007). Since before the existence of modern humans, our evolutionary ancestors possessed the ability to control fire (Gowlett 2006). Fuel resources for fire are a constant component of society; wherever there is a settlement or occupation group, there is a need for the collection of fuel to sustain the demand for fire. For as long as groups have had the ability to control and use fire, there has been a necessity to gather fuel, and bring it to the fire (Heizer 1963; Pyne 2001: 124-126). The ability to control fire provides pure water, cooked food, warmth and light. Fire is also used to transform materials such as clay and iron into pottery and tools; however, the need for fire creates a dependence on fuel (Simpson *et al.* 2003). As the ability to use fire increases so do the consumption rates of fuel. A small settlement using fire for cooking, light, and heat uses less fuel than a settlement of similar size using fire for cooking, light, heat, pottery firing, and ore smelting. The procurement and processing of fuel in some capacity; felling trees, cutting peat, harvesting dung, etc. would have been part of everyday life in prehistory (Heizer 1963).

The fuel for fire as used in prehistory consisted of only three categories of carbon rich organic material capable of creating fire (Braadbaart et al 2012); vegetation such as wood and scrub plants, fossil fuel such as peat, and animal by-products including dung and bone. Wood is recognized as the most obvious fuel source, and according to Heizer (1963), all other fuels can be considered a surrogate. Location dictates what fuels are available, but the needs of the population determines which of the fuels are used for fire and which are

deemed too important to other industries to be burned away (Church *et al.* 2007; Rotherham 2005). For example, wood can also be used for building homes (roofing, fencing) making tool handles, weapons, transportation (boats, carts, wagons) making wood too value a resource to be used for fuel in environments with scarce woodlands like Orkney. This project investigated what fuel resources were utilised within Orkney to sustain the combustion requirements among various settlements throughout the Neolithic and Pictish periods in the absence of a woodland fuel resource capable of sustaining the needs of the population within the region. The Orkney Islands provide a well-suited region for the research of changes to fuel use over time. The extent of artefact survival within Orkney and the multitude of previously investigated sites and current excavations provide a wealth of material to aid in the understanding of the climate, economy, and technology level that was available within the region to further the interpretation of the data gathered pertaining to fuel use within this research.

Orkney is known for its vast archaeological record spanning from the Neolithic age through the Viking age, and closer to recent history (Wickham-Jones 2015: 1-2; Miller 1976: 59). Yet since the Mesolithic Age, woodland areas of Orkney were in decline. By the time the sites being discussed in this research were occupied, the Neolithic and Pictish periods, most of the Orkney woodlands were gone (Farrel *et al.* 2014; Berry 1985: 31-34). The remaining woodlands would not have sustained the fuel needs of the abundant populations flourishing in the region during the Neolithic through the Pictish period as is the chronological scope of this project.

The occupants of Orkney's Neolithic settlements and Pictish occupation sites seem to have thrived despite the formidable climate (Dockrill & Bond 2009), yet

wood fuel is not available in an abundance befitting the fuel needs for people to warm their homes, cook food, and produce pottery or metal work as is clearly evident from the copious artefacts found at countless archaeological excavations in the region (Wickham-Jones 2015). The prehistoric landscape/climate of Orkney has been well researched, since c. 4300 BP the Orkney landscape has been relatively treeless with the exception of pockets of birch/hazel scrub (Bond 1994: 32-39; Berry 1985: 31-34). This lack of traditional wood fuel resources indicates that inhabitants of prehistoric Orkney would have needed to find alternatives that were abundant and comparable to the heating properties of wood fuel (Fenton 1997: 206-209). This investigation aims to identify what fuels were being utilised in Orkney to supplement the requirements for fire.

Fires are lit within an enclosure to stop the fire from spreading such as a hearth or fire pit, or to insulate the fire to reach higher temperatures such as a kiln or oven, these structures were also used for economic and social activities according to Mentzer (2014). These enclosures are referred to by the blanket term of combustion feature, and are usually constructed from stone or clay (Courty 2017). Use of a combustion feature (hearth, oven, kiln, forge, or fire pit) to aid in the handling of fire was ubiquitous in survival and a large part of everyday life throughout prehistory (Costa Vaz *et al.* 2017; Pyne: 102-106; Miller *et al.* 2009). Combustion is an exothermic chemical reaction in which a fuel and oxidant are combined with heat and converted to energy (light and heat), throughout this reaction the combined fuel and oxidant produce exhaust (carbon dioxide and water), and the fuel is reduced to ash (Sullivan & Ball 2012). Ash contains mineral material and other components from the fuel that were not released as exhaust during the chemical reaction of combustion

(Vassilev *et al.* 2014). Over time the constant use of a combustion feature causes an accumulation of ash. This ash is deposited in middens and floor surfaces or remains within the combustion feature it was created in (Bellomo 1993). The ash from combustion features and subsequent midden deposition often survives into the archaeological record. The ashes from within archaeological deposits can offer insight into the fuel resource management and economy of a population, by identifying what fuels were in use, and to what temperatures said fuels were being heated. Studying fuel use within the marginal climate of Orkney provides insight into the alternative fuel resources utilised in the absence of a traditional wood based fuel resource.

This project investigated the use of different fuel resources by the prehistoric populations of Orkney through the application of archaeological, observational, and analytical methods. Ash has many properties that can be quantified, and modern research has expanded our knowledge on the formation of ash through combustion and the effect temperature variation can have on the resulting ash (Vassilev *et al.* 2017). The magnetic susceptibility, pH, elemental content, colour, and mass of ash can be used to identify fuel material with the use of comparison to modern analogues. This is discussed in further detail in chapter 3.

The three archaeological sites whose fuel use was examined for this research were not only chosen for their availability. Each site offers a different perspective of the use of the natural landscape in respect to fuels use and resource management. The Knowe of Swandro, a multi-period site (Neolithic – Viking Age) located on a bay. The Ness of Brodgar, a large Neolithic complex situated on a narrow peninsula between a fresh water and brackish loch, and Smerquoy/Muckquoy two Neolithic settlements that are landlocked and not

adjacent to a water source (figure 1.1). The variations in these settlement locations offer a potential insight into the way the topography and proximity to other resources may affect the acquisition and management of fuel, and the potential difference in fuel use between sites of different status and functionality. The background for each site is discussed individually in section 2.10.

Modern analogue fuel representative of what was available to archaeological inhabitants of Orkney (Bunting 1994) including peat, seaweed, driftwood, grasses, animal dung and bone, heather, willow, and hazel were collected from Orkney and reduced to ash in a muffle furnace at 200^0C, 400^0C, and 900^0C. The ashes from these fuels were then used to establish a method for the identification of archaeological fuel. The ash produced from the modern analogues was used to investigate the comparative properties of fuel resources available within Orkney, identify trends among fuel types at various temperatures, and recognize what characteristics would best aid in the subsequent identification of archaeological fuel. Results of the modern analogue analyses were then used to establish a database of fuel characteristics developed with consideration to elemental signatures and magnified images obtained through SEM/EDX analysis, magnetic properties established using a magnetic susceptibility bridge, pH, Munsell colour number assignment, and calculating the mass lost (as observed during the preparation of modern analogue ash). The methods developed throughout the analysis of modern analogue ash were then tested identifying the fuel from ashes within archaeological deposits. The source material for the archaeological analyses was ash residues, hearth surfaces, Hearth rake out, and middens collected from existing excavations in the Orkneys, Ness of Brodgar, Smerquoy/Muckquoy,

and Knowe of Swandro. The complete methodology for all the techniques used are laid out and fully explained throughout chapter 5.

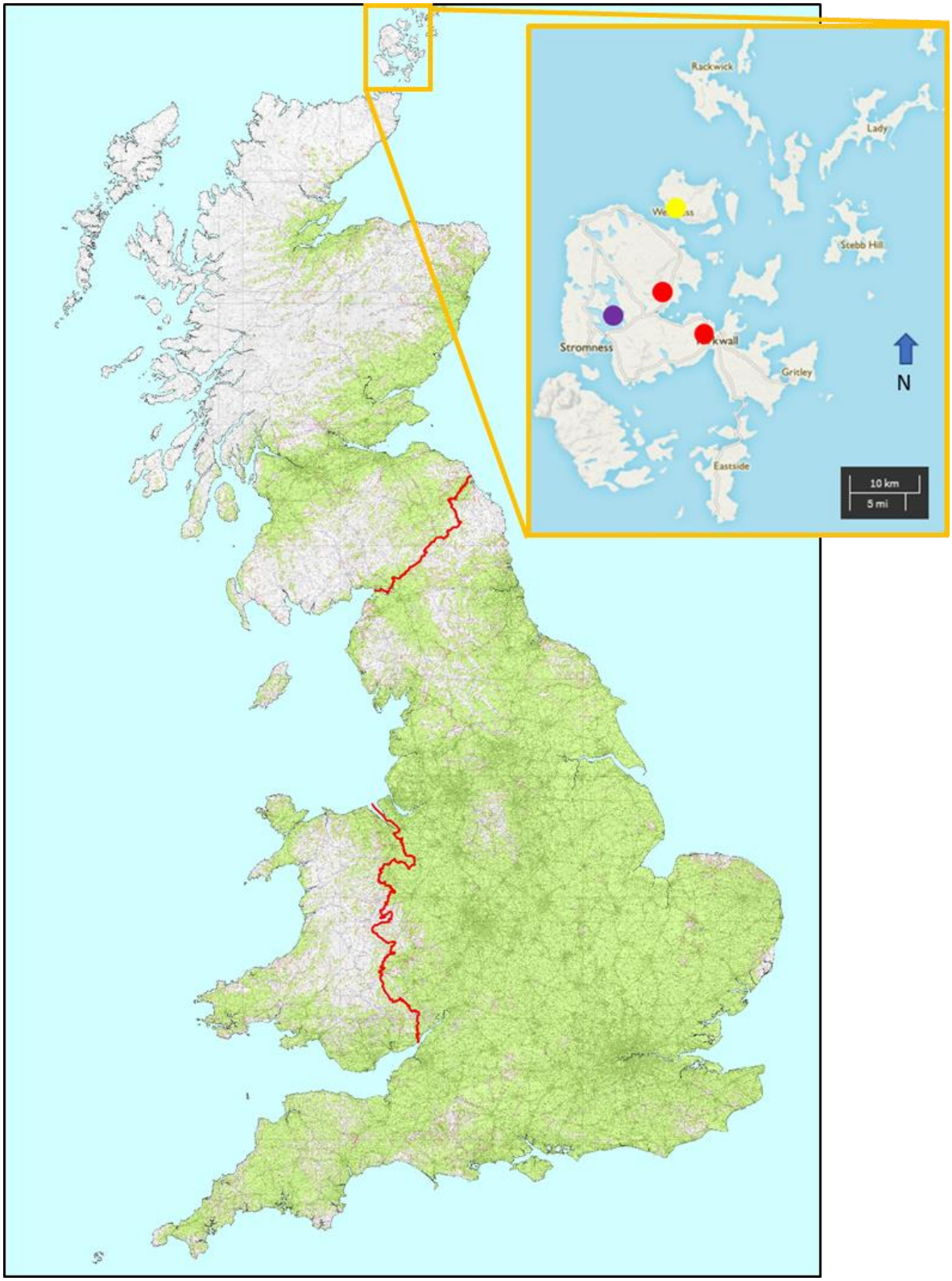

Figure 1.1 A map of Orkney in relation to the United Kingdom with the excavations used for this research indicated in dots; purple for the Ness of Brodgar, red for Smerquoy and Muckquoy, and yellow for the Knowe of Swandro. Source: https://osmaps.ordnancesurvey.co.ukmodified by Author

1.5 Research contexts

The investigation into fuel use within Orkney necessitated examination of literature from combustion science, environmental science, geology, archaeology, fuel design, and the consideration of techniques suited for modern material as well as archaeological samples (this is discussed in greater detail in chapter 3). Understanding of what happens to fuels throughout combustion at different temperatures increases the ability to interpret data from combustion features in archaeological contexts. Discerning fuel type and approximate combustion temperature using the methods developed in this project can provide a means to determine the function of a combustion feature based on the fuel being used and the approximate temperature to which it was heated. Data on fuel use would also afford a means to gain insight into the impact fuel resource management had on the local environment, level of technology possessed by the population, and establish an understanding of the economy. For example, some methods of production require certain functional temperatures such as pottery firing (400^0 – 900^0C), forging(900^0C), smelting (900^0C+), smoking meat (c. 200^0C), cooking/heat (200^0C - 400^0C) (Pyne 2001: 129-133; Pausus & Keeley 2009; Thér 2004; Heizer 1963; MacLeod 1925).

Research into the fuel resource utilization of fringe/marginal societies like Orkney offers insight into the innovations and adaptations of past populations to compensate for resource scarcity, with the lack of a means to import the required resources from an abundant source. Developing a more comprehensive understanding of how past peoples have dealt with the scarcity of natural resources and their subsequent impact on the environment associated with fuel resource management has beneficial implications in the search for sustainable fuel sources today. Modern concerns about biomass fuel

are hazards in the exhaust/smoke or smell, ash yield, the effects in the soil and water, and efficiency as a fuel. Ancient populations would have used trial and error to find the fuels that worked best in their environment based on the aforementioned criteria. The use of alternative, recycled and bio fuels has become a popular area of study, the analyses used to characterise fuel attributes can be useful in determining the efficacy or detriment of burning alternative fuels even today. This project has relevance in archaeological investigation as well as current fuel research.

1.6 Archaeological significance

The project aimed to achieve the development of a method for the analyses and classification of archaeological fuel sources, along with a database of the characteristic changes to modern analogue fuel sources through increasing temperatures. This research used 14 modern analogue fuel sources ashed at various temperatures (200^0C, 400^0C and 900^0C) to develop a method for the identification of fuel sources from archaeological ash deposits. The analyses of modern ash samples also offered in-depth analyses of the changes to selected fuels throughout various heating temperatures, and to observe the chemical changes in fuel throughout the combustion process from charring to complete ashing.

The methods used in this project could be applied to other locations and time periods. The initial environmental, geological, and vegetation research would need to be conducted with focus on the region of study, and a new set of modern analogues fuels would need to be selected, collected, and ashed based on the potential fuel sources available according to the literature and modern availability. Applying these techniques to previously excavated sites with existing sample material could offer new understanding on the socioeconomic structure of a population and fuel resource management protocols based on what fuels are in use and to what temperature they are being heated. This method will also help to expand the interpretation and knowledge from previous excavations using existing evidence such as artefacts and previous analyses of the archaeological deposits. Fire ecology data can be extremely useful to understanding palaeo-environmental data and past human dependency on fuel resources (Alperson-Afil 2012). The fuel resources used by ancient peoples can offer insight into the socio-economic activities associated with fire (Braadbaart

et al. 2012) such as cooking, lighting, heat, pottery, weapon and tool production, and metal casting and forging. In recent years, the analysis of combustion remains has become a more useful tool in understanding the relationship between culture and climate as changes in environment effect fuel resource management through obvious change in the ambient climate and the subsequent changes to the local environment based on the climate fluctuations and the changes brought forth anthropogenically to combat the environmental change and increase chances for immediate survival. This includes discussion on the selection of materials as fuel resources for different activities, social and environmental regulation of fuel resource utilization, and the contribution that fuel resource availability may have made to the success or failure of early settlement sites.

An explanation of what's to come: Outline of the thesis

Chapter 2 Background: This chapter provides a background to the key concepts of the research including the climate history of Orkney, the management of fuel resources, fire technology, and the formation of ash through combustion. This chapter also discusses the science behind the chosen analytical methods magnetic susceptibility, pH analysis, and SEM/EDX analysis. This chapter also explains principal components analysis which is used for interpretation of the analytical data. Finally, the background chapter provides the location and excavation history of the archaeological excavation sites chosen for this investigation.

Chapter 3 Literature review: This chapter presents reviews of the literature that was the basis for this research, and discusses the implications of past investigations on fuels for this project. Previous archaeological fuel investigations are discussed in depth with sections that focus on Orkney based fuel investigation, modern analogue experimentation, and modern fuel research. There is also discussion on the analytical methods chosen for this investigation, and their use in previous projects.

Chapter 4 Materials: All the materials chosen for this project are presented. The locations that samples were drawn from are discussed for both modern and archaeological sample material. Harris matrices for all the archaeological sites are also presented for each excavation site to demonstrate the stratigraphic relationships between the archaeological sample material.

Chapter 5 Methods: The methods that were employed for this investigation are laid out. This chapter shows the steps taken throughout preparation of modern analogue ash and the analyses of both modern and archaeological samples to ensure the repeatability and accuracy of the results. The methods are

presented with consideration to the previous investigations discussed within the literature review chapter.

Chapter 6 Results: The results are shown for the modern analogue and archaeological samples. The modern analogue material is presented by fuel type to demonstrate the changes that fuels undergo at increasing ashing temperatures, the archaeological material results are shown in stratigraphic sequence to illustrate the relationships between associated contexts. The analytical results are displayed using both plots and tables.

Chapter 7 Discussion: This chapter presents the interpretation of the results and their implications for the investigation. The relationship between the modern analogue and archaeological samples are discussed, and the fuels in use for each site as determined by this research are discussed. This chapter also presents the principal components analysis that was employed to display the relationships between all the sample material according to the multiple variables from the analytical techniques used

Chapter 8 Conclusions: The final chapter discusses the findings of the investigation, and their implications for archaeological fuel research. The research questions from the introduction chapter are answered using the findings from this research.

Chapter 2: Feeding the ember (Background)

2.1 Overview

This second chapter expands on what was presented in the introduction to increase the understanding of the concepts that are the framework of the Ashes to Ashes project; the climate and archaeology of Orkney, the benefits of fire technologies and dependence on fuel, and the formation of ash through combustion. A comprehensive understanding of these concepts is vital to the development of a method for the identification of archaeological fuel material through comparison to modern analogue ash. While the literature review focuses on examining previous work, this background chapter establishes a foundation of regional knowledge and understanding of fuel use, combustion, and the techniques being used that aid in the understanding of this project.

First the background to the environment of Orkney and the use of fuel resources in the region are reviewed. Previous excavation literature and regional history provide a background to the geology, climate, and fuel availability in Orkney within the chronological periods being investigated. This is followed by a more detailed discussion on fuel resource management. Next, fire technology and transformation of raw fuel material to ash is presented. Primitive survival techniques and ancient fire technology are discussed to establish the functions of fire and the means of manipulation of fire that are available to ancient populations. Biomass fuel examination and combustion research are evaluated to demonstrate the changes that a fuel undergoes during the chemical reaction of combustion and transformation from raw fuel to ash. Finally, the archaeological sites being investigated for this project, their respective backgrounds, and previous investigations of these sites are discussed.

2.2 Why Orkney?

Orkney is renowned for its extensive archaeological record spanning from the Mesolithic period to the 19th century (Wickham-Jones 2015: 1-2; Miller 1976: 59;). Orkney also boasts a historical record of references in texts including Diodorous c. 56 BCE, Tacitus c. 98 CE, and the *Orkneyinga Saga* c. 1192 – 1206 CE (Wickham-Jones 2015: 98; Laing 1974: 2; Pálsson & Edwards 1978: 13; Tacitus 2014: 10). Orkney is mentioned throughout history first referred to as the Orcades in the work of Diodorous and Tacitus and on Ptolemy's map; it is called Orkney throughout the *Orkneyinga Saga* (Tacitus *et al.* 2015; Pálsson & Edwards 1978; Miller 1976:11). Among the Orkney's archaeology are numerous occupation sites found all over the archipelago including Skara Brae, the Ness of Brodgar, Midhowe Broch, the Broch of Gurness, The Knowe of Swandro, The Cairns, Smerquoy, Muckquoy, the Brough of Birsay, Pool, Barnhouse, and Tofts Ness (Wickham-Jones 2015: xxv-xxxii; Hunter and MacSween 1991; Radford 1959: 2-3). These sites show occupation in Orkney from the Mesolithic period through to the Viking Age spanning 5000 years through history (figure 2.1), and have yielded artefacts including pottery, worked stone, burnt bones, metal slags, crucible fragments, hammerscale, iron tools, copper and silver jewellery, and the remains of multiple combustion features (Fojut 2008: 22-23; Owen 2013: 16-17; Dockrill *et al.* 2007: 32-33; Hunter 2007: 287-5; Richards & Ashmore 2005: 34; Richards & Jones 2016: 249; Towers et. Al 2015: 13-17; Card 2010;). The extent of Orkney's archaeological record and the abundance of multi-period sites, make it an ideal location for the study of fuel use (Simpson *et al.* 2003). Among these sites the Ness of Brodgar, the Knowe of Swandro, and Smerquoy/Muckquoy were selected for investigation in this research.

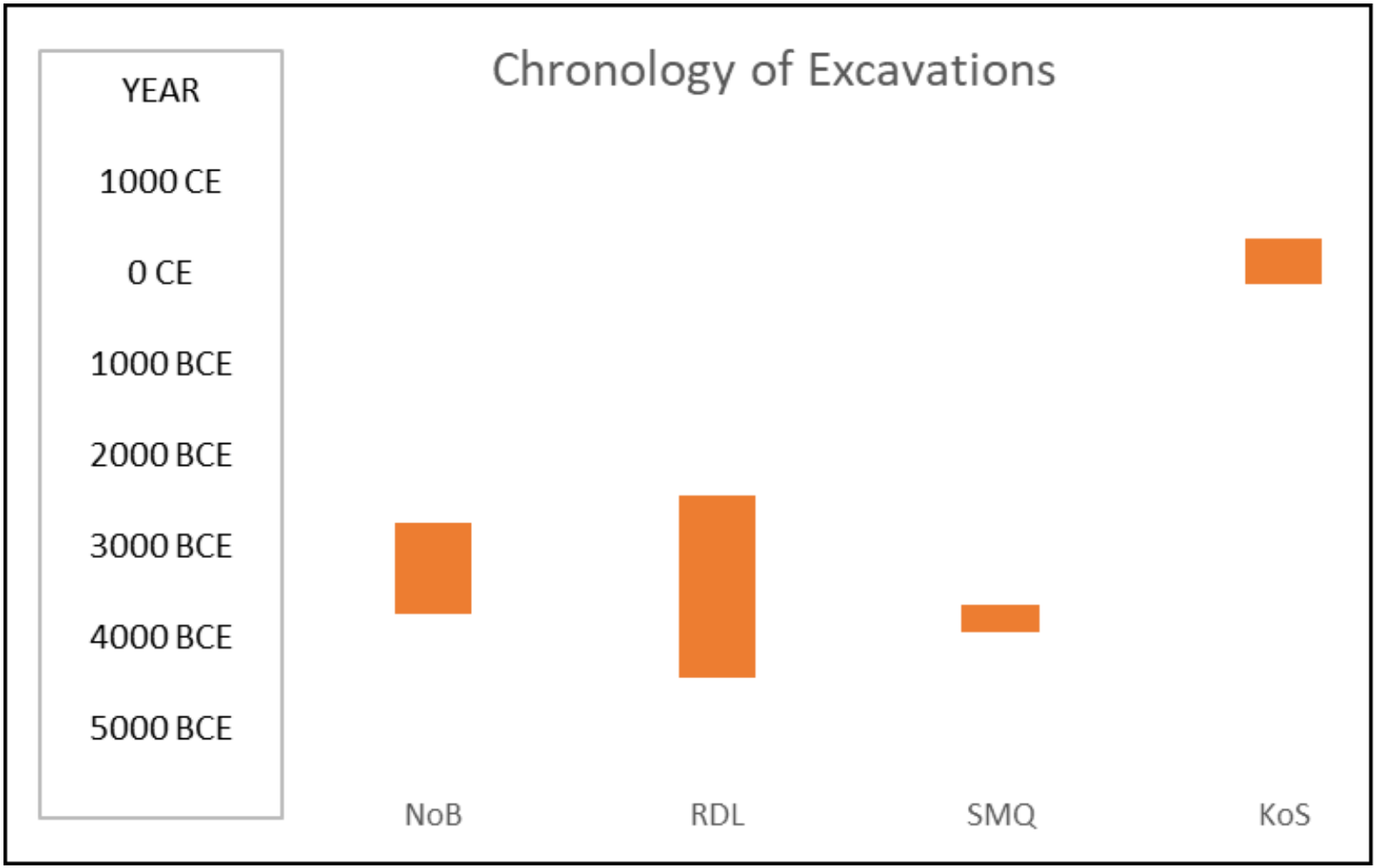

Figure 2.1 A plot showing the time depth for each archaeological site from left to right The Ness of Brodgar, Muckquoy, Smerquoy, and The Knowe of Swandro. Source: Author.

2.3 Review of Orkney's past: Geology, climate, and vegetation

Orkney's geology is comprised of sandstone, flagstone, volcanic ock and granite (Mykura *et al.* 1976: 40; Miller 1976: 20-24; Wickham-Jones 2015: 3-6; Berry 1985: 37-48; McKirdy 2011: 3) (figure 2.2). According to Mykura *et al.* 1976, the archipelago is comprised of sedimentary rocks and subordinate lavas and tuffs of middle and upper argillaceous Old Red Sandstone with a crystalline basement complex made of Moinian metamorphic rocks intruded by Caledonian granite according to Mykura *et al.* (1976: 70). The geology of Orkney is significant to the research, because the parent soil material has a direct effect on what elements find their way into the samples, the magnetic signatures, and the pH of the soils and plant materials. This mix of sandstone, flagstone clay, granite, and volcanic rock create a protolithic material that contains iron, silicon, calcium, carbon, potassium, aluminium, and titanium in various minerals (Pidwirny 2006). These protolithic minerals along with organic material go through a series of processes during weathering and pedogenesis to create compounds such as oxides, carbonates, sulphides, phosphates, and silicates that are present in the soil matrix (Kabata-Pendias & Pendias 1984: 33-39). Sandstone and granite parent material is known to cause low pH or acidic soil. Compounds like haematite (Fe_20_3), siderite ($FeCO_3$), pyrite (FeS_2), and magnetite (Fe_3o_4) can be present from parent rock minerals or form through the weather or diagenetic processes, and have a direct effect on the magnetic properties of soil; this is further affected through anthropogenic intervention like heating (Tarling 1983).

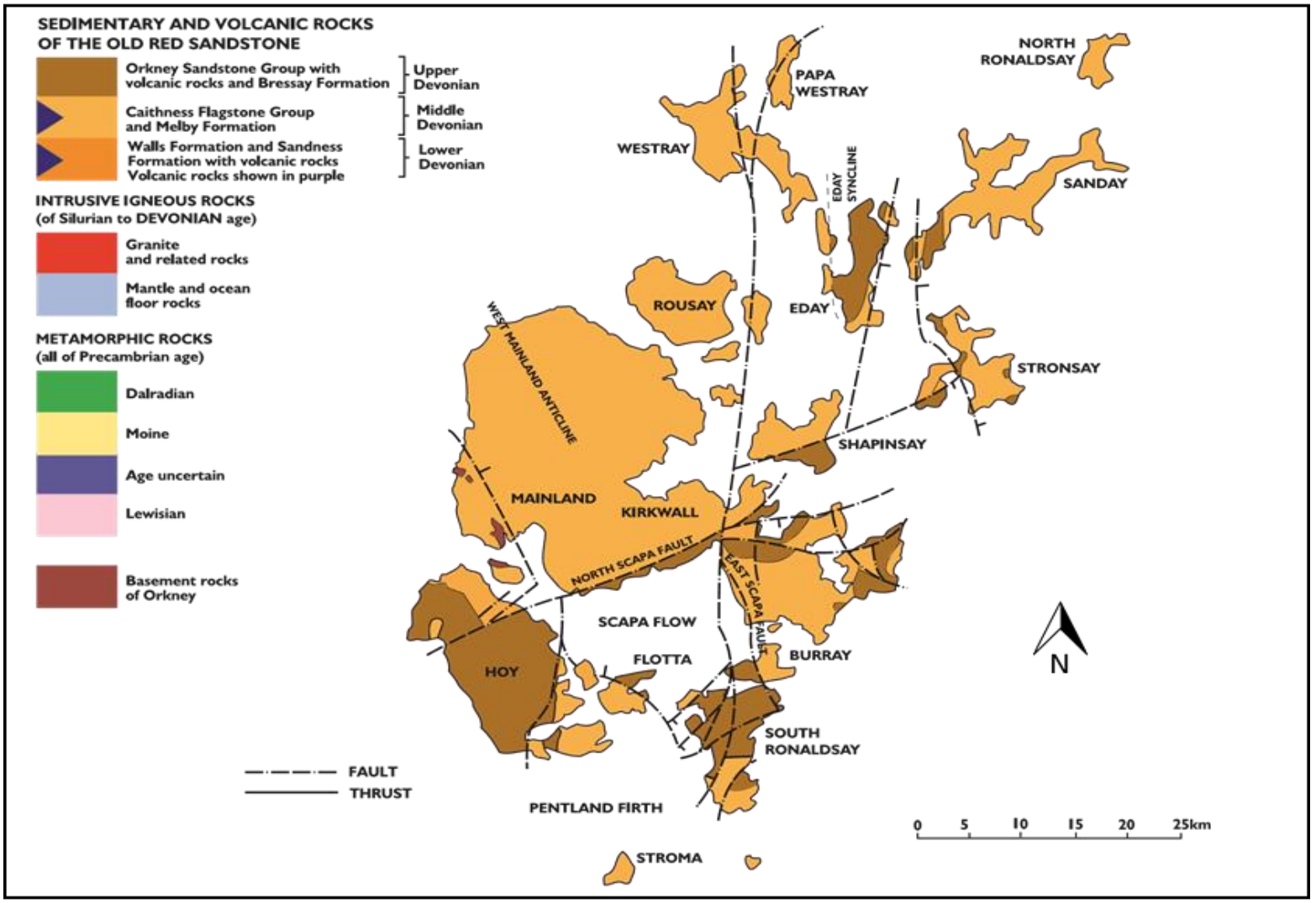

Figure 2.2 A geological map of Orkney. Source: McKirdy (2011: 3) edited by Author.

Orkney has no lush forests, or any forests; woodland is a scarce commodity on the archipelago today, leaving its inhabitants to use alternative fuels even today. The archaeological record of Orkney shows that birch/hazel scrub and willow survived in some capacity demonstrated by the deposition of hazel nuts and charcoals of that taxa into the archaeological record; however, evidence of pine and spruce charcoal on some sites suggests the use of driftwood as a fuel source (Bond 1994: 32; Berry 1985: 32). At the beginning of the late post-glacial period, approximately 5000 BP, Orkney saw a decline in woodland vegetation resulting in the eradication of birch/hazel scrub areas within the archipelago (Bunting 1994) (figure 2.3 & 2.4). This is believed to have been caused by a combination of autogenic and anthropogenic forces including land clearance for grazing and increases in blown sand that varied between vicinities as per Keating and Dickson (1978). The appearance of pastoral vegetation communities coincided with the decline of woodland, suggesting that the lack of trees in Orkney is largely attributed to deliberate anthropogenic activity such as forest clearing for animal grazing (Farell *et al.* 2014). This lack of wood resources is partially responsible for the extensive survival of archaeology; in the absence of timber for construction, the Orkney stone became the medium of choice for the ancient builders (Farell *et al.* 2014). In the western Mainland and the hills of Rousay, peat had begun to form from 6000 BP and 5700 BP respectively (Bunting 1994), and among the rest of Orkney around 3000-3400 BP (Bond 1994: 32; Berry 1985: 32). The loss of trees would have also made the effects of the weather harsher and more damp with no wind breaks or absorption of ground water through the roots of woodland vegetation (Bond 1994: 33).

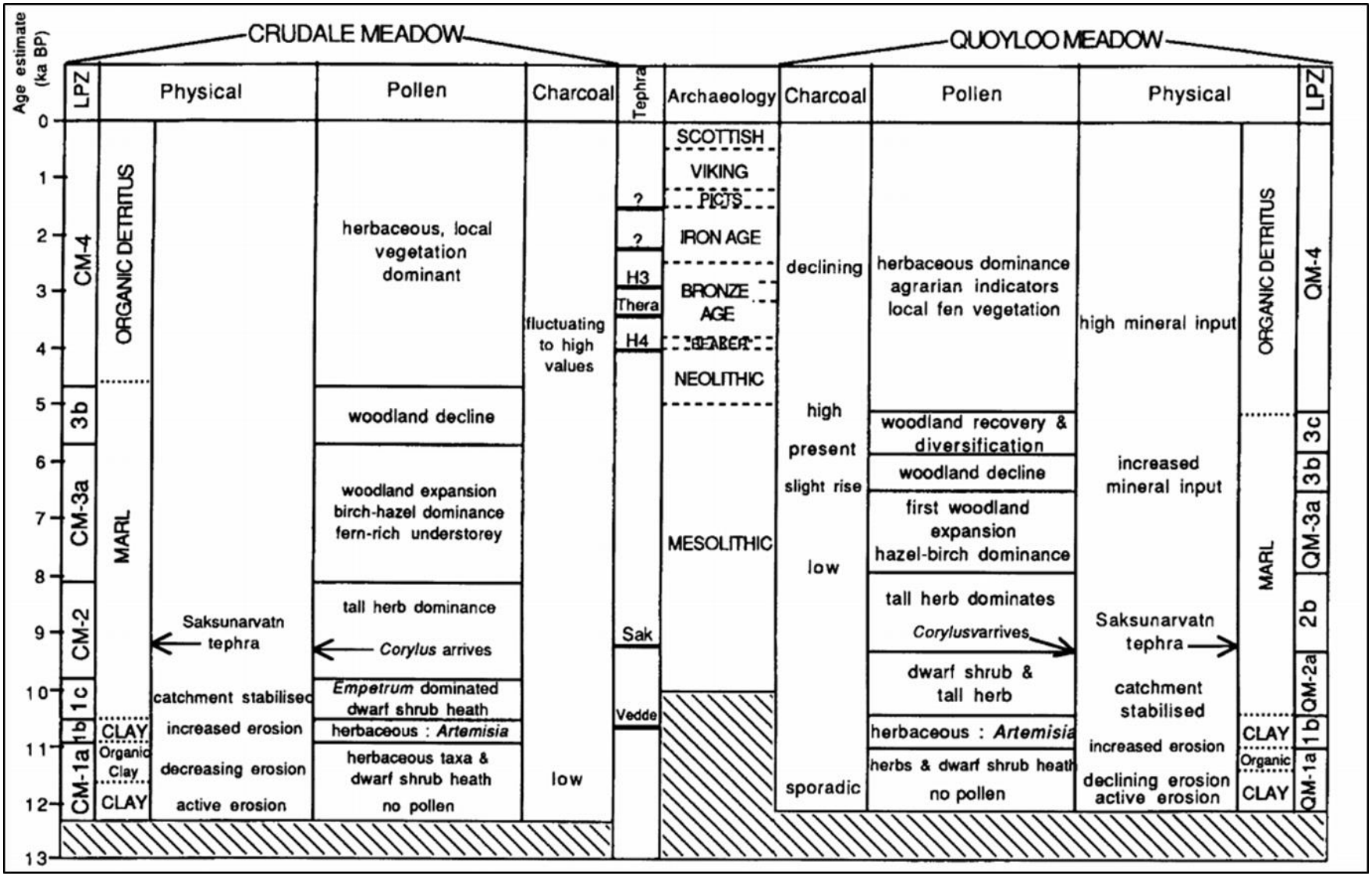

Figure 2.3 The vegetation history of Western Mainland, Orkney. Source: Bunting (1994) edited by Author.

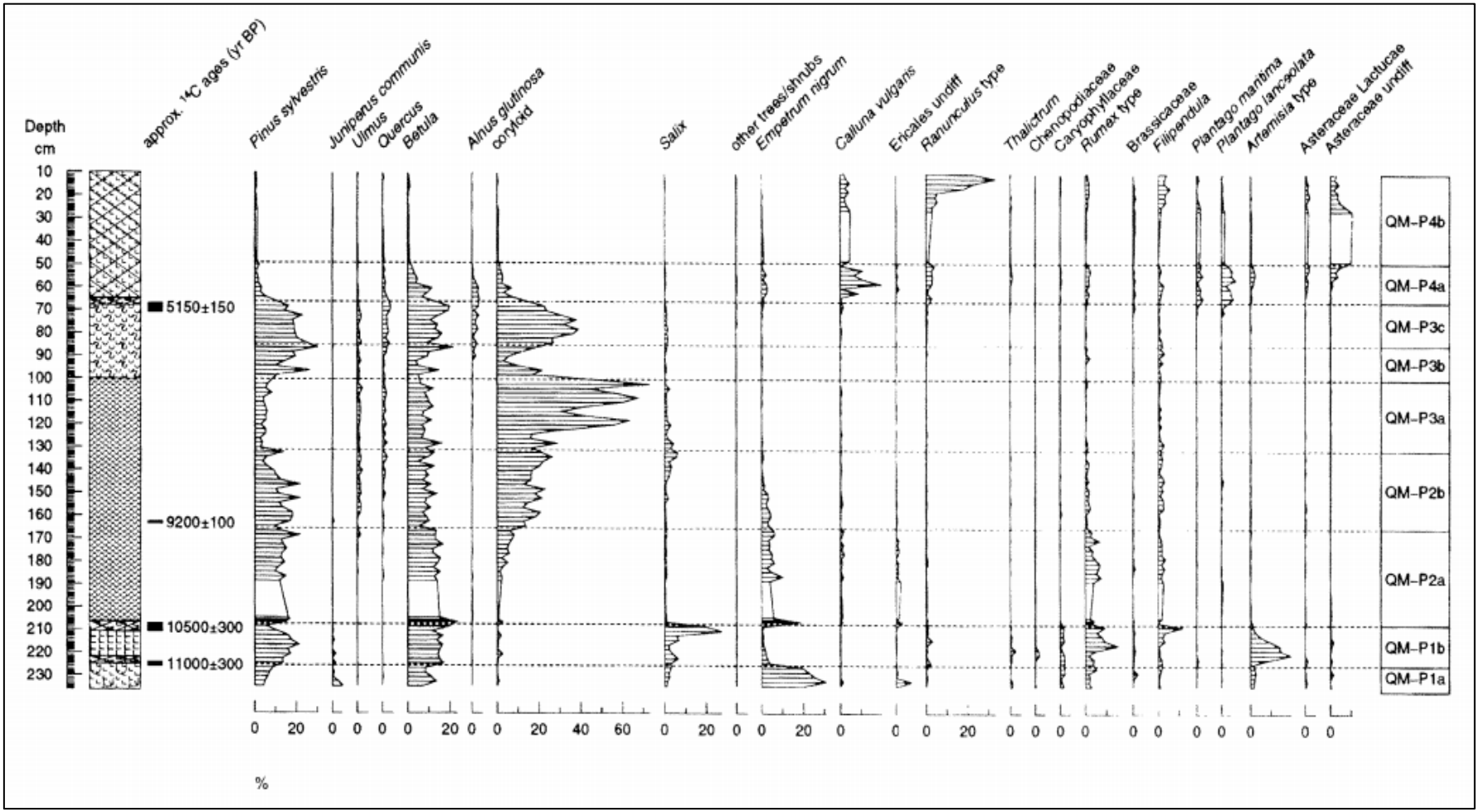

Figure 2.4 The percentage of pollen present at Quoyloo meadow according to time depth and species. Source: Bunting (1994) edited by Author.

2.4 Orkney's relationship with fuel

Both in the historical record and the oral tradition fuel is mentioned, but not wood, the main materials being burned are peat, dung, and seaweed (Muir 2014: 13-22; Pálsson & Edwards 1978: 32). The climate remains unforgiving from the Mesolithic through to today in the winter months with extended darkness, extreme winds, and harsh seas (Wickham-Jones 2015: 8-9). The Summer months were not much better leading to a significantly shorter growing season, there is mention of crops being harvested and stored before they were fully ripened in 18th century accounts (Bond 1994: 30). The need for alternative fuels in the Neolithic gave way to fuels like dung and peat being the standards in the region (Fenton 1997: 208 & 213). In folklore peat is even the unsung hero of the story of Assipattle and the Stoorworm, using smoldering peat to ignite the oil of the Stoorworm's liver (Muir 2014: 13-22). The cutting of peat is also mentioned in the Orkneyinga Saga with Turf-Einarr the Earl of Orkney "introducing" peat as a fuel to the Orcadians due to the scarcity of wood (Pálsson & Edwards 1978: 32). This is also evident in the lyrical insults from across the Pentland firth mocking Orcadians from the isle of Sanday for their use of dung as fuel, 'I have been to Egilsay, and I have been to Wyre, but I've never been in Sanday where the coo dung's fire' and 'The little isle o' Sanday, where the coos shit fire' (Fenton 1997: 208). The alternative fuel tradition in Orkney continued from the Mesolithic through to today. Peat, dung, and seaweed have been the mainstays of fuel resources among the archipelago. The need for fuels to burn hotter was even met by the production of peat charcoal (Fenton 1997: 213).

The fuels available to the Neolithic and Pictish inhabitants of Orkney would have been limited to peat, turf, grasses, animal dung, animal bone, seaweed, driftwood, and the wood from birch/hazel scrub that was not used for other

industries (Farell *et al.* 2014; Bond 1994: 32; Bunting 1994). These fuels were used in the experimental production of modern ash to use in the comparison and subsequent identification of fuels from archaeological deposits.

2.5 The management of fuel resources

Fuel for fire is a universal need for human survival. Every society has utilized fire and by default fuels, given the implied relationship between them that there cannot be fire without fuel. According to Picornell-Gelabert and Servera-Vives (2017), fuel is the central component of subsistence activities among human societies, and in turn the gathering of fuel in the landscape and the consumption of fuels within domestic spaces are a core component of social practices. The gathering of fuel and the tending of the fire would have been a task ubiquitous to everyday life. MacLeod (1925) recounts a letter from a Jesuit missionary having trouble converting the Iroquois to Christianity because they did not believe an eternal fire, as hell is described in Christianity, could exist in the absence of wood. Keeping a stock of fuel and maintaining the fire day and night would have been an important, if not paramount, responsibility within the social constructs of a group (Pyne 2001: 24; Heizer 1963; MacLeod 1925; Conedera *et al.* 2009). As the population and fuel needs increase, so does the industry of fuel collection (Cloud 1969: 33). The practices of fuel procurement can range from gathering dead branches and forest litter, to felling trees in large quantity or large-scale peat cutting operations that can alter the landscape (Heizer 1963). Fuel is needed year-round regardless of climate, yet harsher more extreme climates do create higher demands for fuel, as more fire is needed to counteract a colder, damper, or darker climate (Rotherham 2005; Morris 2015: 29). The need for and consumption of fuel also increases with the sophistication and status of a settlement. Different fuels are suitable to varying uses, for example, peat can

reach higher temperatures than wood or dung fuels, while wood fuel produces more light (Simpson 2003). This is similar to the differences in combustion properties between hardwood and softwood varieties due to the higher lignin content among softwood (pine, cedar, and fir) making it burn hotter, brighter, and significantly faster than hardwood fuels (oak, birch, ash, willow) (Burton 2009). According to Rotherham (2005), the expenditure of fuel for production pottery, metalworking, and food preparation scale on par with the status and size of a site. The fuel needs would also be increased by the gathering of people at higher status sites, swelling the need for fuel to produce light, heat, and cooked food. The fuel needs of a given population can outgrow what the local environment can sustain, forcing people to travel further and further from home to extract fuel sources (MacLeod 1925). In some instances, the over exploitation of fuel resources could lead to the failure of an occupation site due to a lack of fuel resources (Simpson 2003; Heizer 1963). There is evidence of using certain sites seasonally to allow for the regrowth of fuel sources to extend the longevity of a sites viability to sustain life as seen with Pinarbaşi, Anatolia, Turkey and several indigenous tribes in North America (Asouti 2003; Heizer 1963).

2.6 Understanding fire technology: From opportunistic foraging to mastery

The use, creation and manipulation of fire is directly connected to a population's technology level (Clark & Yusoff 2014). The following discusses fire lighting techniques and the various uses of fire to demonstrate the relationship between fire and technology within the chronological scope of the research and illustrate the necessity of fuel to be available for settlements to have existed. Without fuel resources, the failure of a site becomes inevitable (Picornell-Gelabert & Servera-Vives 2017). With no fuel there is no way to heat a home, cook food, and sterilize water (Heizer 1963; MacLeod 1925).

The earliest users of fire, Homo erectus 1.5 million years ago in Africa, did not possess the technology to light a fire; however, they were able to utilize wild fires started by natural processes including lightning in a practice known as fire foraging (Goudsblom 1992: 12-13; Gowlett 2016). This would allow someone the use of fire without having to possess the skills to create it, affording the fire forager access to new food sources from using the fire to cook increasing the amount of edible food materials, the spread of wildfire causing animals to flee the area and be easier to hunt, and the new plants available from the germination promoted by the warmth and smoke of the fire (Burton 2009). Fire foraging gave way to fire nurturing as it was discovered how to fuel the fire with wood and other plant material (Pausus & Keeley 2009; Goudsblom 1992: 24). But this was only prolonging a fire started through natural processes, and not being able to transport the fire or create it at will. The relationship with wildfire culminated with the ability to light and maintain fire on command. This lead to the development of the hearth and the eventual manipulation fire for the means of production (Pyne 2001: 27; Gowlett 2016; Pausus & Keeley 2009; Goudsblom 1992: 58-64).

There are several methods of lighting a fire, friction, percussion, or pressure (McCafferty 2017). Whether it is with a bow drill, fire plow, fire saw, pump drill, or fire piston the principals of primitive fire lighting remain the same (Wescott 1999); a means of creating an ember through the production of heat from friction, percussion, or pressure is applied to a tinder nest to create an ember that generates enough heat to combust small kindling fuel and gradually building up to a heat source that can burn the bulk fuel (Boy Scouts of America 2009; McCafferty 2017) including larger branches, logs, bones, dung cakes, or peat blocks. In modern fires the tinder nest is usually made of dried grasses, fine bark material, nettle fiber, or any fine fibrous material that can be made into a nest shape to accept an ember; kindling is small twigs or small pieces of fuel that can ignite easily to help the fire spread without suffocating it (Wescott 1999). Given that an archaeological fire cannot be observed, there is a need to consider the present-day fires used by primitive survivalists. The materials used in a tinder nest and the kindling to feed the fire are burned away completely, especially fires maintained for prolonged periods in hearths, leaving negligible amounts of ash from these sources in the final ash accumulation within the combustion feature.

The manipulation of fire allowed for humans to implement land management practices such as slash and burn agriculture and to transmute the structure of earthly material including hardening wood for spears by removing moisture and adding carbon to the wood or annealing stone to aid in knapping, and to transform clay and ore into new substances like iron, pottery, glass, and ceramic (Pyne 2001: 24-26; Rehder 200: 46; Clark & Yusoff 2014).

Based on the assemblage of artefacts from Orkney it is known that pottery was being produced, food was being prepared, and stone was being fashioned into tools and weapons during the Neolithic period, and in the Pictish period there is

evidence of metalworking in addition to the industries available in the Neolithic (Pyne 2001: 129-133; Pausus & Keeley 2009; Thér 2004; Heizer 1963; MacLeod 1925). This shows an understanding of how fire can be used to alter the state of an object throughout the Neolithic by using flame to bake clay into pottery, cook food, and remove moisture from stone so it is more prone to crack/flake during knapping (Coles 1973: 111-153; Clark & Yusoff 2014). According to Rehder (2000: 6-7), fuels like dung have a very different burning pattern than charcoal fuels and as a result of this fuel use is directly related to what temperature can be reached and what chemical changes take place during combustion. During the Pictish period the knowledge of fire use has increased to include the practice of transforming materials with temperature in the form of metallurgy (Dockrill & Bond 2013; Berna *et al.* 2007). This demonstrated that the Picts had the knowledge of increasing temperature with bellows or increased understanding of fuel properties, and the ability to craft items using fire that are needed in creating further objects (Wickham-Jones 2015: 92; Pausus and Keeley 2009; Clark & Yusoff 2014). This multiple step crafting shows the expansion on the grasp of knowledge and ability to manipulate fire that has surpassed that of their Neolithic ancestors.

2.7 The formation of ash through combustion

Combustion is an exothermic reaction in which chemical energy is converted into thermal energy (Clark & Yusoff 2014) involving three main components often referred to as the fire triangle fuel, heat, and oxygen (figure 2.5), and flame cannot exist without them. If any of these mechanisms are removed, the fire reduces to

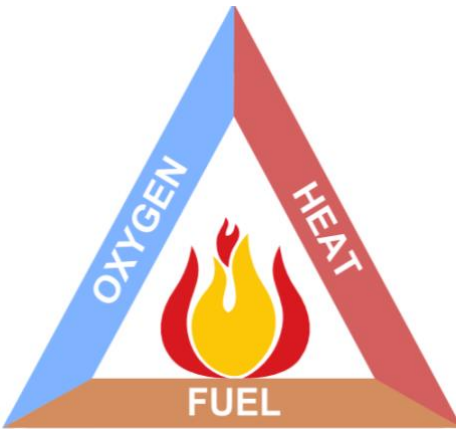

Figure 2.5 The fire triangle. Source: www.firesafetyinfo.co.uk/fire-triangle

a smolder and dies out. Combustion releases the energy held within a fuel's atomic bonds through oxidation in the form of fire (Clark & Yusoff 2014). The term combustion is used to designate the oxidative conversion of unburnt solid fuel into gases, ash, and residues (Sullivan & Ball 2012; Byram 1959). The first process in the chemical reaction of combustion is ignition, this occurs when the heat-release rate is larger than the heat-loss rate at any point below the flame temperature (Hirano 2002); however, pyrolysis must take place to provide a gaseous fuel source to be ignited. Pyrolysis is the releasing of gaseous fuel from a solid fuel source as a response to heating (Panahi *et al.* 2017). There are three stages of combustion, beginning with raw fuel material and ending with ash after complete combustion (Byram 1959). Pre-ignition, where solid fuels are heated, dried, and volatized; flaming combustion of the vaporised volatiles and carbon monoxide; smoldering or glowing, is the combustion of the char residue (table 2.1). These stages of combustion do not occur linearly or in any particular sequence but are all intrinsically linked (Sullivan & Ball 2012).

The Formation of ash through combustion			
Stages of Combustion	**Processes**	**Compounds Formed**	**Elements present**
Preignition/Pyrolysis	The devolatilization of organic material	oxalates, nitrates, chlorides, hydroxides, carbonates, sulphates, and inorganic amorphous (non-glass) material	Al, C, Ca, Cl, Fe, K, Mg, Na, O, P, S, Si, Ti
Flaming combustion	Burning of combustible gases	silicates, phosphates and oxides	
Smoldering	Burning of Char residue		
Ash	Complete combustion		

Table 2.1 A table showing the stages, processes, compounds, and elements present throughout the formation of ash in combustion (Vassilev et al. 2013; Vassilev et al. 2014; Baernthaler et al. 2006). Source: Author

2.8 A background to magnetic susceptibility

Magnetic susceptibility is the measure of a samples potential to be magnetized when placed in an applied magnetic field (Mulay 1963: 1759). The application of magnetic measurements is used to identify the magnetic minerals present among a sample, and to determine if those minerals have been exposed to heat (Tarling 1983: 35; Mulay 1963: 1782). Magnetic minerals are part of the geology of the earth and become incorporated into sediments through the breakdown of parent material and the diagenesis of minerals throughout pedogenesis (Pulley & Rowntree 2016; Tarling 1983: 58-59; Tarling 1971: 21; Kapper *et al.* 2014). There are five forms of magnetism as shown in figure 2.6. Diamagnetism has a negative magnetic susceptibility measurement characterized by repulsion between the sample and the applied field (Mulay 1963: 1761). Diamagnetic materials include water, some organic material, and calcium carbonate. Paramagnetism is a weak positive magnetic susceptibility measurement autonomous of applied field, and occurs commonly among the transition metals group, iron containing minerals, and salts (Mulay 1963: 1761). Antiferromagnetics show a moderate positive magnetic susceptibility that increases with temperature until the Néel point, a temperature that changes the magnetism of the material, beyond this the material behaves like a paramagnet, this is observed among iron oxides such as hematite and goethite. Ferrimagnetic magnetic susceptibility is shown by a strong positive measurement that is independent of temperature until the Curie temperature, a temperature that changes the magnetism of the material, beyond this the material behaves like paramagnet, this is observed among iron oxides such as magnetite maghemite, and iron sulphides such as pyrrhotite and greigite. Ferromagnetism is a very strong positive measurement that is field dependent, this strong magnetism is lost gradually with heat until the curie temperature at which the sample behaves as paramagnetic observed with iron, nickel and

chromium (Mulay 1963: 1761-1765; Tarling 1971: 5-9). Magnetic susceptibility measurements are then converted using formulas to determine the mass specific magnetic susceptibility expressed in units $x10^{-8}(m^3kg^{-1})$, and frequency dependent magnetic susceptibility expressed as a percentage. The mass specific magnetic susceptibility value is the conversion of the measurement into a value that represents the 10 cm^3 sample volume. This is to adjust for sample measurements to be representative of a uniform volume regardless of shape and size, and for samples that did not completely fill the sample pots (Mulay 1963: 1760). The frequency dependent magnetic susceptibility is expressed as a percentage of the relative contributions to magnetism from superparamagnetic grains to the total magnetic susceptibility based upon the ratio between superparamagnetic and stable single domain magnetic particles (Kozhevnikov *et al.* 2014; Hrouda & Pokorný 2011).

Understanding the types of magnetism, their associated minerals, and their changes related to temperature are a vital component to investigating archaeological fuel remains. Some of the previous work using magnetic measurements is discussed in sections 3.2, 3.4, and 3.7 including magnetic susceptibility measurements being used in the field of archaeology in the study of heating activity, interpretation of floor surfaces, and the formation of sediments. (Church *et al.* 2007; Batt & Dockrill 1998; Peters & Batt 2002; Kanu *et al.* 2014; Kapper *et al.* 2014; Peters *et al.* 2001; Peters *et al.* 2002; Blaha et al 2008).

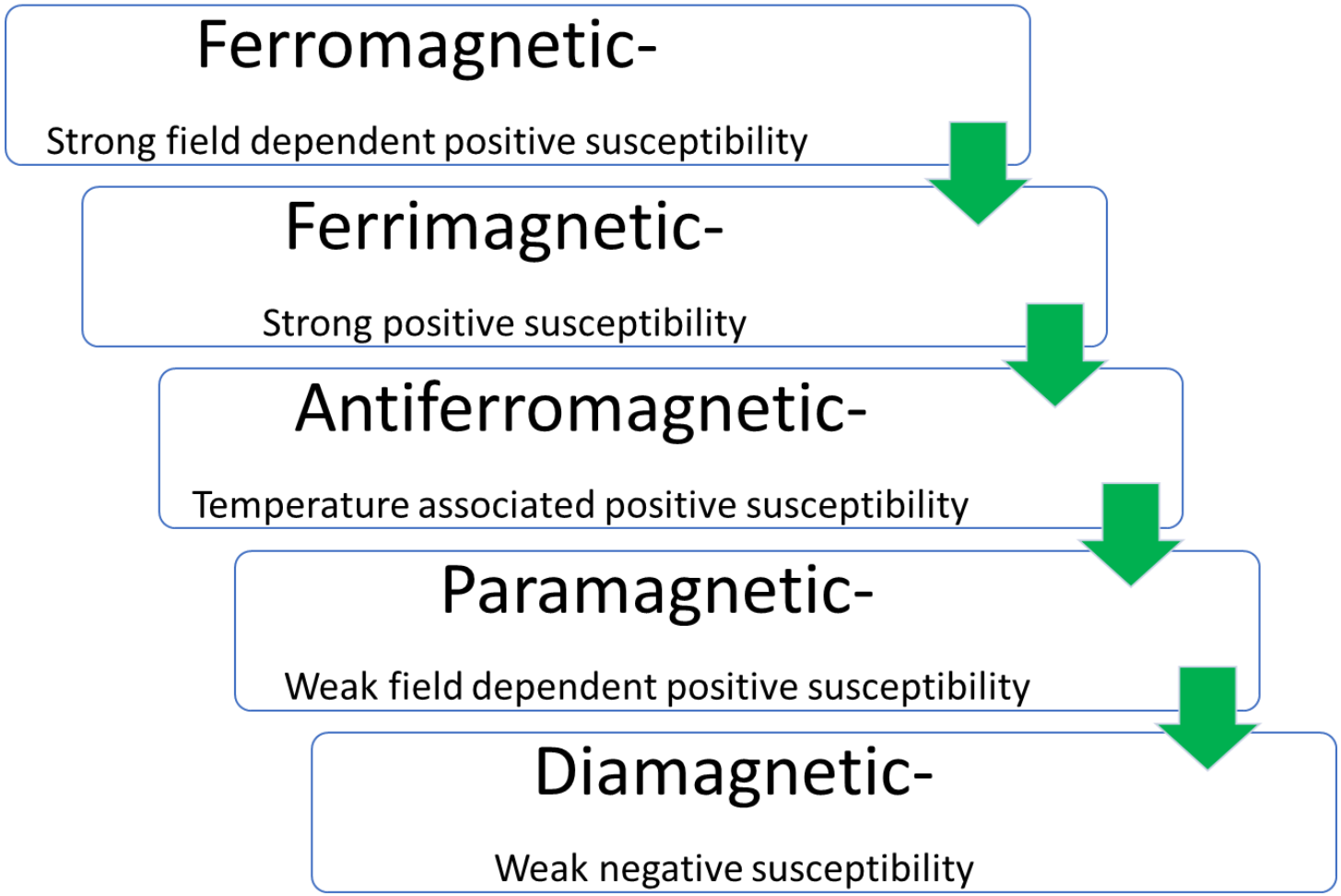

Figure 2.6 A table of the stages of magnetism (Mulay 1963 1760-1762; Tarling 1971: 5-9). Source: Author

2.9 A background to pH

Potential of Hydrogen (pH) is a logarithmic scale, quantified by moles per litre of hydrogen ions, used to specify the acidity or alkalinity of a solution with 0 being the most acidic, 7 being neutral, and 14 being the most alkaline (Bates 1973; Cronyn 1990: 19). pH in sediments is directly affected by interaction with minerals; for example, silica-rich geological material tends to create acidic sediments, and silica poor material produces basic/alkaline sediments according to Tarling (1983: 35). Ashes are known to be alkaline, and to be able to raise the pH of acidic soil, due to the high levels of alkaline carbonates, bicarbonates, and hydroxides of elements including potassium, sodium, phosphorous, and calcium (Etiégni & Campbell 1991; Cronyn 1990: 19; Di Gianfilippo *et al.* 2016; Ohno 1992). Studying the changes in the pH of fuel material and their ashes throughout increasing temperature allows for a more comprehensive interpretation of the results of archaeological combustion residues. Tracking these changes also aid in the identification of fuels and the temperatures that they were exposed to through the comparison of modern analogue ash samples and archaeological materials described in section 5.4.2.

2.10 A background to scanning electron microscopy with energy dispersive X-ray spectroscopy

Scanning electron microscopy with energy dispersive X-ray spectroscopy (SEM/EDX) is a combination of two techniques, an electron microscope that produces images using a focused beam of electrons, and an elemental analysis method that utilizes the X-ray emission spectrum to characterize elements (Goldstein 2003: 21-22). The images obtained using the scanning electron microscope can achieve higher resolution than optical microscopy, and offer the addition of an analytical capacity (Pollard & Heron 1996: 49). Scanning electron

microscopy for this research was performed using a backscatter detector to use the backscatter electron emissions to create an image of the topography of the surface of the sample when exposed to an electron beam (Goldstein 2003: 22). Energy dispersive X-ray spectroscopy works by use of an electron gun to excite the atoms and create inner shell vacancies, and in turn electron promotion which stimulates X-ray emission as shown in figure 2.7 (Ponting 2004). The analytical results of SEM/EDX are presented in both images of the sample, and the emission spectra that quantifies the elements present in units of percentage abundance. For this investigation, the primary use of the SEM/EDX was to obtain the elemental composition of samples. This afforded both the characterization of fuel types by elemental content among the modern analogue samples, and to aid in the identification of fuels from archaeological sample material.

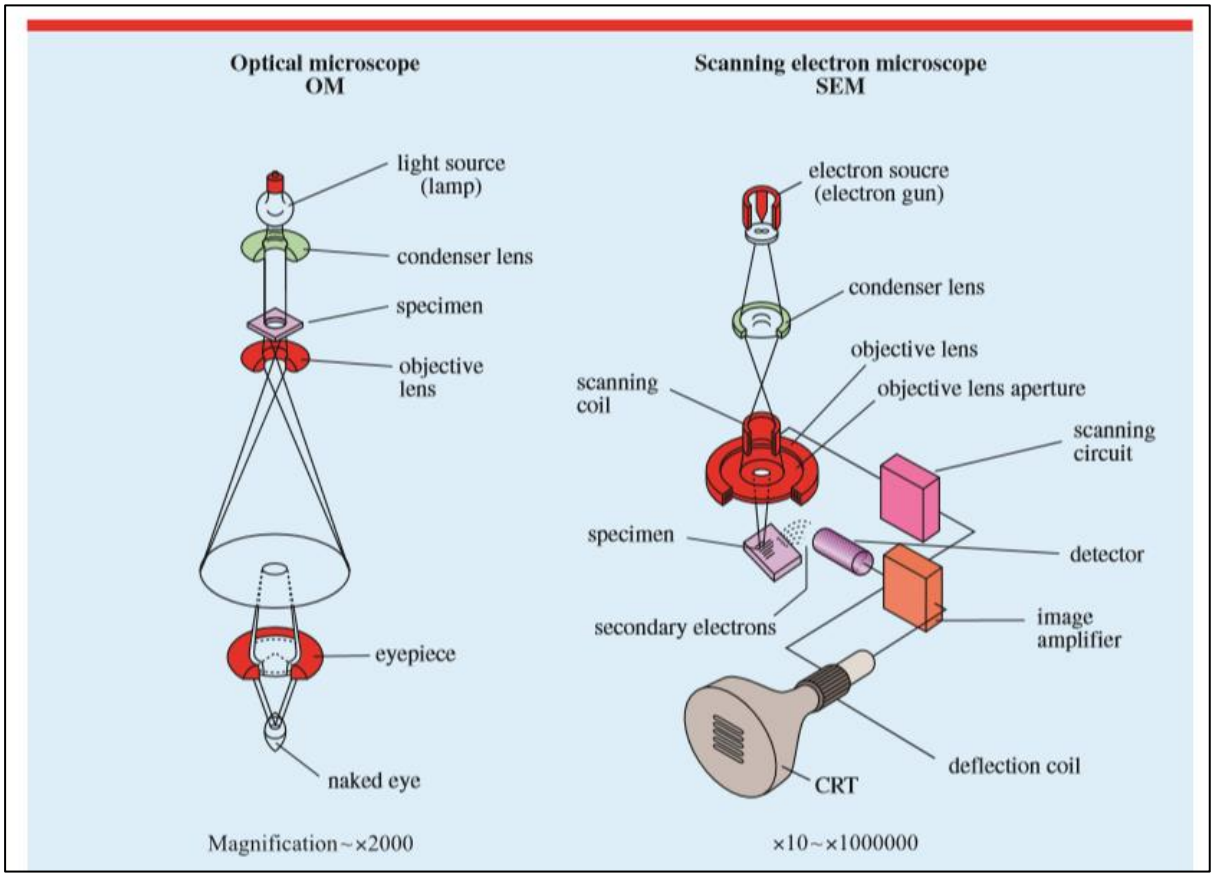

Figure 2.7 A diagram of showing how a SEM/EDX instrument works with a comparison to an optical microscope on the left. Source: Ponting (2004).

2.11 A background to principal components analysis

Principal components analysis is a multi variate statistical method used to examine relationships within a dataset. (Baxter 1995; Baxter 1994). The most common variables used in principal components analysis are the data obtained through trace element or oxide quantification including XRF (X-ray Fluorescence), EDX (energy dispersive X-ray spectroscopy), and AAS (atomic absorption spectrometry) (Baxter 1995; Pizarro *et al.* 2012); however methods of PCA are being implemented to utilise principal components analysis to identify the production region of pottery with examples of provenance, and to aid in the reconstruction of potsherds (Pizarro *et al.* 2012; Zvietcovich 2016). A common use of PCA among archaeological research is determining the provenance of pottery using the chemical structure to determine where and when ceramic was produced, as seen with the work of Bitetto *et al.* (2015).

Principal components analysis examines a dataset of multiple variables (3+), and displays the data 2 dimensionally according to new variables (principal components) that correspond with the variations within the data (Pizarro *et al.* 2012). The principal components are distributed directionally according to their respective level of variation, these are often described with a loading plot showing the various directions and intensity of the variables in the data that affect the eigenvalue of principal components (Baxter 2003) (figure 2.8). Eigenvalues show the intensity of each variable with the orientation being dictated by the eigenvector. The distribution of data according to PCA allows the identification of associations between observational groups, for example Modern vs. Archaeological, and the correlation of variables, such as magnetic susceptibility, pH, and elemental abundance (Baxter 2003; Baxter 1994). This can be seen

through the assignment and subsequent plotting according to the principal components of the dataset shown with a score plot (figure 2.8).

There is debate on the efficacy of using logarithmic scale or data ranking systems to improve the results of principal components analysis (Baxter 1995). The raw data from multiple variables can be problematic if the values are too disparate for example, the values of trace elements near 0.5% abundance versus magnetic susceptibility values ranging from 20 $x10^{-8}(m^3kg^{-1})$ - 3650 $x10^{-8}(m^3kg^{-1})$. This large difference in values can cause the numbers of higher value to hold more weight within the analysis, and potentially skew results in favor of the variables with higher values (Baxter 1994; Baxter 1995). Logarithmic treatment of the data can fix this by distributing the data according to a base 10 number system; ranking the data can also be viable, assigning a rank number 1,2,3,4,5, etc. according to a predetermined scale based on the original values of the data (Baxter 1995; Baxter 2003). The use of either logarithmic treatment or ranking of data can combat the skewing of results due to analysis of greatly varying values from numerous analytical techniques including SEM/EDX, magnetic susceptibility, and pH values. Using a data treatment method such as logarithmic scale or data ranking makes the use of multiple analytical methods possible in principal components analysis with no skewing of data or inaccuracy in interpretation caused by datasets from different techniques with varying values.

For this research, principal components analysis was implemented to visually plot the data from several analytical methods to see the correlations present between modern analogue ash and archaeological hearth, midden, and ash samples. The trace elements were investigated to rule out the use of elements that could be problematic due their presence both among ashes and as common constituents of mineralogical matrix material. This approach was also discussed by Baxter

(1995) when investigating ceramic and glass production with the omission of the data concerning silicon, and the work of Pizarro *et al.* (2012) investigating ceramic production also leaves out any mention of silicon due to its ubiquitous relationship with soils.

The use of principal components analysis is a viable method to aid in the identification of archaeological fuels using comparison to modern analogues based on several analytical techniques, if the precautions for the potential for skewed data discussed by Baxter (1995) are heeded.

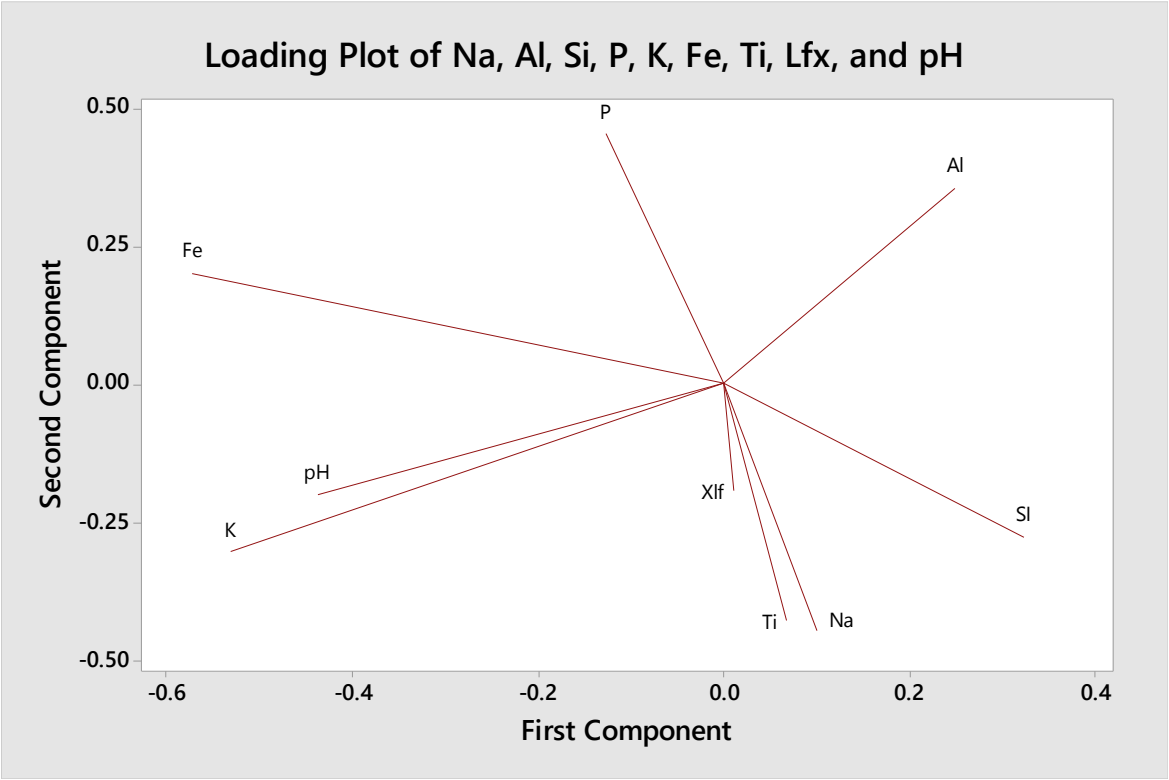

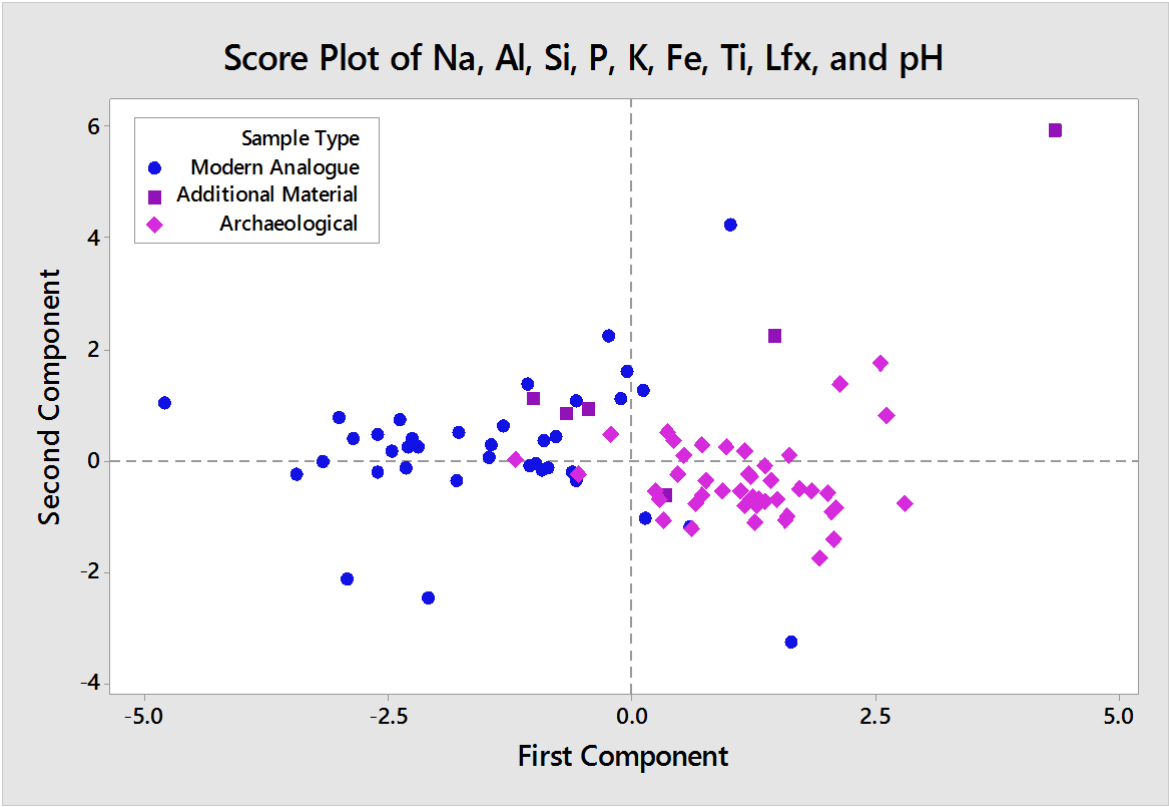

Figure 2.8 From top to bottom. First a loading plot showing the variables and their respective directional pull on the plot, next a score plot showing the data according to nine variables aluminium, silicon, phosphorous, potassium, iron, titanium, MS, and pH. Source: Author.

2.12 Review of archaeological sites selected for this investigation

This section discusses the Ness of Brodgar, the Knowe of Swandro, and Smerquoy/Muckquoy to develop the background of the sites being investigated by this research (figure 2.9). The following focuses on establishing the chronological periods represented by each site, the finds that have been recorded for each site, the local environment around each site, and the previous/ongoing excavation history. Starting with the Ness of Brodgar, then the Knowe of Swandro, and finally Smerquoy/Muckquoy each site being investigated in the research is discussed. As stated in section 1.4, these sites were chosen because of the length of their occupation, their differing locations and fuel availability, and the time periods that they represent.

Figure 2.9 A map of Orkney with a magnified section showing the locations of the archaeological sites used in this research indicated in dots; purple for Ness of Brodgar, Yellow for Knowe of Swandro, red for Smerquoy, and orange for Muckquoy. Source: Google Earth Pro modified by Author.

2.12.1 The Ness of Brodgar

The Ness of Brodgar is located in the 'Heart of Neolithic Orkney' world heritage site, between the largest fresh water loch on mainland Orkney, the Loch of Harray and the brackish Loch of Stenness that flows out to the Hoy sound and Bay of Ireland (Card *et al.* 2007) (figure 2.10). Within one kilometre of the Ness of Brodgar are several other important Neolithic Orcadian archaeological sites. The Stones of Stenness, one of the earliest henge sites in the British Isles located on the southern bank of the stream that connects the Loch of Stenness and the Loch of Harray The Barnhouse Settlement, a Neolithic village site contemporary with Skara Brae located on the southern shore of the Loch of Harray. The Ring of Brodgar, a circular stone henge located on the isthmus between the Loch of Stenness and the Loch of Harray. Finally, the Maeshowe Neolithic passage burial tomb that is the namesake for the tomb type exclusive to Orkney located approximately 1 Km to the east. (Card *et al.* 2007; Card 2010) (figure 2.10). The Ness of Brodgar existed contemporarily with all of the sites during its life span.

The Ness of Brodgar was inhabited from 3300-2300 BCE; however, this site is not the typical occupation site (Towers *et al.* 2015: 2-3). The buildings were in use for a millennium, yet the archaeological evidence suggests that the Ness was a gathering or trading location strategically placed in the epicenter of Orkney's prehistoric monuments (Towers *et al.* 2015: 2-3). According to Card *et al.* (2007), the other occupation sites in Orkney at this time were 'modest' by comparison, suggesting that the Ness of Brodgar was of fundamental importance. Excavations began in 2003 with the discovery of a suspected Bronze age stone slab, geophysical survey, and test trenches. The investigation has continued over a decade with no end in sight to the information this site has to offer. The excavations at the Ness of Brodgar consists of a main trench that contains the

remains of an enclosed settlement with multiple Neolithic structures, and a secondary trench with large middens indicative of long term occupation (Towers *et al.* 2015: 5). The finds from the Ness of Brodgar include coloured and decorated pottery, mace heads, axe heads, carved stone balls, decorated stonework, stone spatulas, and a large number of deer and cattle bone (Towers *et al.* 2015: 12-23). The sample material gathered from the Ness of Brodgar was collected from hearth deposits, hearth rake out, and ash dumps from structures 1, 7, 8, 12, 14, and 19 within the enclosed area of the main trench, and various samples from the large-scale midden in the secondary trench T located approximately 100 m from the main excavation trench (figure 2.11). Structures 1, 8, 12, and 14 are all contemporary to one another, structures 7 and 19 are from an earlier construction. Looking at the fuel evidence from this excavation offers a glimpse into the fuel resource management protocols for a high-status site with over 1000 years of occupation.

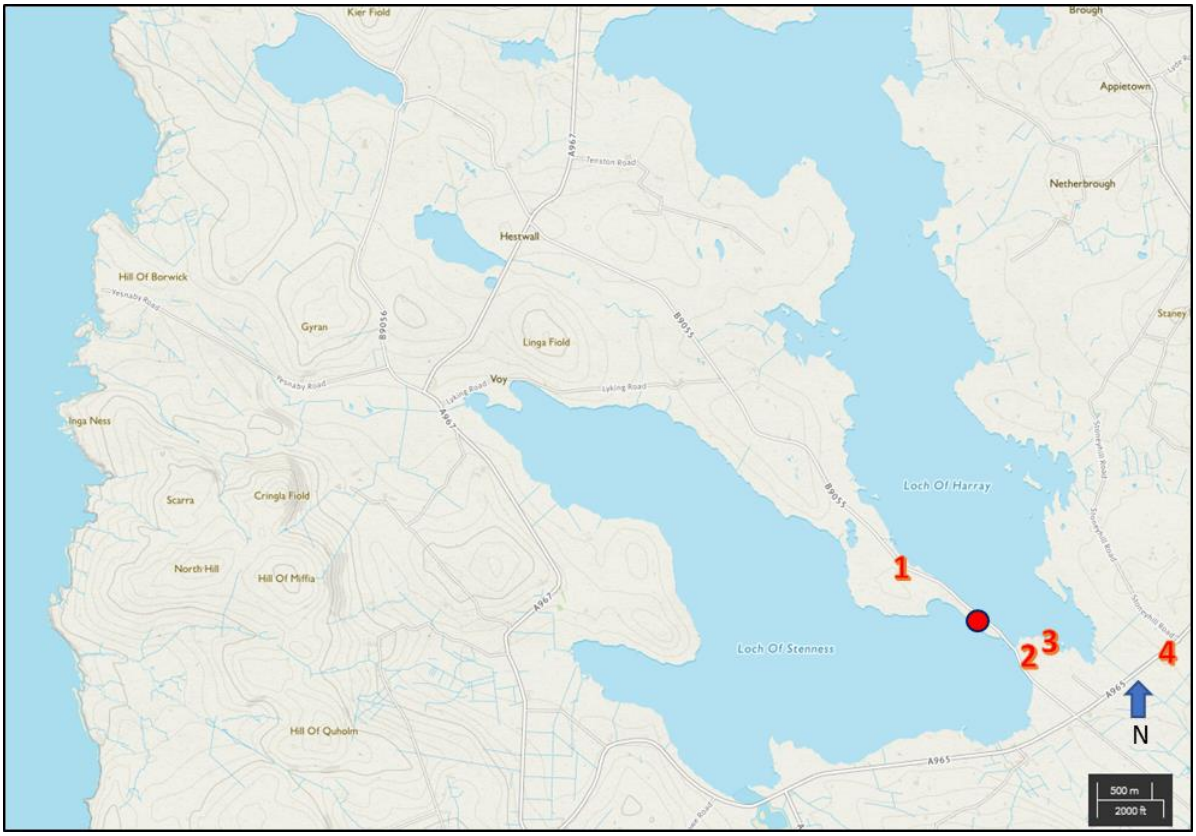

Figure 2.10 A map of the area surrounding the Ness of Brodgar with the excavation area shown by a red dot, and the other sites shown with red numbers 1 the Ring of Brodgar, 2 the Stones of Stenness, 3 the Barnhouse settlement, and 4 Maeshowe chambered tomb. Source: https://osmaps.ordnancesurvey.co.uk modified by Author.

Figure 2.11 an overhead view of the Ness of Brodgar Trench T (left) main excavation trench (right). Structure numbers in yellow
Source: Orkneyjar.com

2.12.2 The Knowe of Swandro

The Knowe of Swandro is located on the coast of the Bay of Swandro, Rousay, Orkney. A multiperiod site spanning from the Neolithic Age through the Viking Age located directly behind a boulder beach, and flanked to the east by the Norse settlement of Westness (Dockrill & Bond 2013) (figure 2.12). The Westness settlement was excavated during the 1970s by Norwegian archaeologist Sigrid Kaland (Kaland 1993: 308-317). The Knowe of Swandro site is situated along the tidally effected area of coastline within the Bay of Swandro across the Eynhallow Sound from Mainland, Orkney, and is a featured section of the Westness walk portion of the Orkneyinga Saga Trail. The Knowe of Swandro is located a kilometre southeast of the Midhowe Broch and Midhowe Chambered Cairn (figure 2.12). Both Midhowe and Swandro are Neolithic burial sites with Iron Age settlement mounds in close proximity. The focus of this investigation is to study and gain understanding into the destruction of coastal archaeological remains in an attempt to better save and preserve remaining sites, while also providing insight into the relationship between various cultures that settled there (Dockrill & Bond 2013). The excavations are very much rescuing the remains of this settlement mound from imminent danger of rising tides and the immense force of the sea.

The site consists of a Neolithic chambered tomb overlaid by a series of Iron Age and subsequent Pictish structures on the western most area of the site, with an adjacent series of structures terraced into levels of early and late Iron Age and pictish ending at the intrusion of early Norse wall construction to the eastern most extremity of the excavation (Dockrill & Bond 2013 B). Although the upper most layers of archaeology show signs of damage from tidal forces, the underlying layers of archaeology show an excellent level of preservation. The excavations

on Swandro have been ongoing since 2010 and have produced numerous small finds ranging from the Neolithic period through the landnám period of Norse Settlement on the Island of Rousay (Dockrill & Bond 2016). The landnám period refers to the Norse settlement and subsequent land clearance of an area.

The finds include worked antler, bone, and whale bone, crucible fragments, slag, hammerscale, a brooch, a roman coin, bone needles, and a number of varied animal bones including cattle, sheep, cat, seal, and a large quantity of limpet shells. The sample material from this site was collected from structure 3, a Pictish structure dating to between 300-800 CE, that has yielded small finds including slag, crucible fragments, furnace lining fragments, small pieces of copper, and other crafting evidence, that suggest this building was used as a workshop/smithy (Dockrill & Bond 2013) (figure 2.13). During the 2018 excavations it was established using magnetic susceptibility and hand held XRF that the earliest occupation surfaces within structure 3 were occupied by a copper smith. The presence of a dedicated coppersmith in such a rural setting is truly a testament to the status and wealth of this site. The abundance of production material evident on this site can also infer a high status to the settlement at the Knowe of Swandro. The samples from structure 3 in the Knowe of Swandro offer a potential look into the fuel use of a high status Pictish site (Dockrill & Bond 2016). Evidence of metal working is indicative of reaching higher heating temperatures than Neolithic populations. Tuyéres discovered in structure 3 indicate that a bellows was in use within the combustion feature to augment the temperature even further with added oxygenation. This increase in technology offers a means to look at archaeological ash created with temperatures at least as high as 900^0 C required to work metals (Berna *et al.* 2007: Clark & Yusoff 2014).

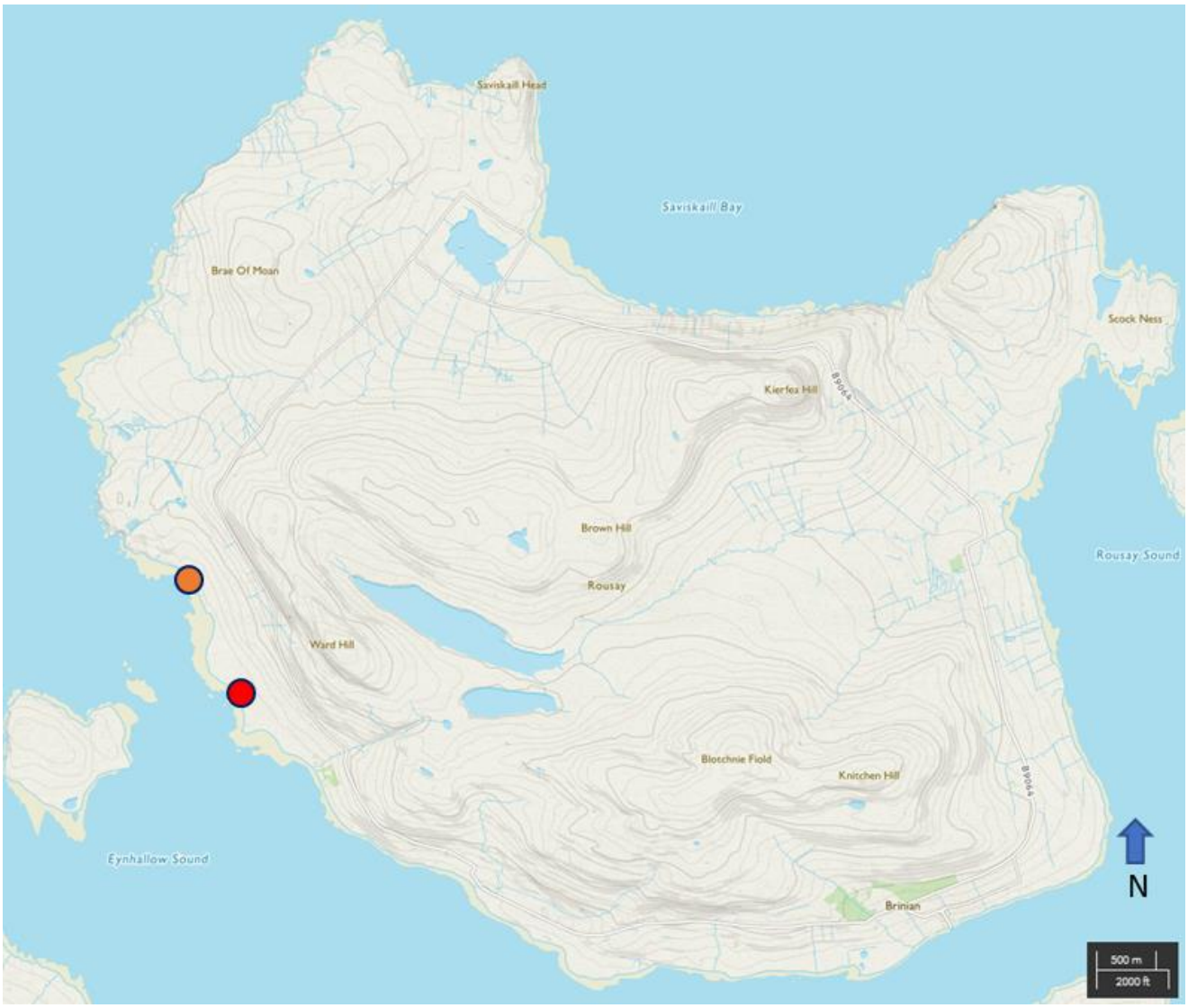

Figure 2.12 A map of the Isle of Rousay with the Knowe of Swandro shown by a red dot and The area of Midhowe shown by an orange dot. Source: https://osmaps.ordnancesurvey.co.uk modified by Author.

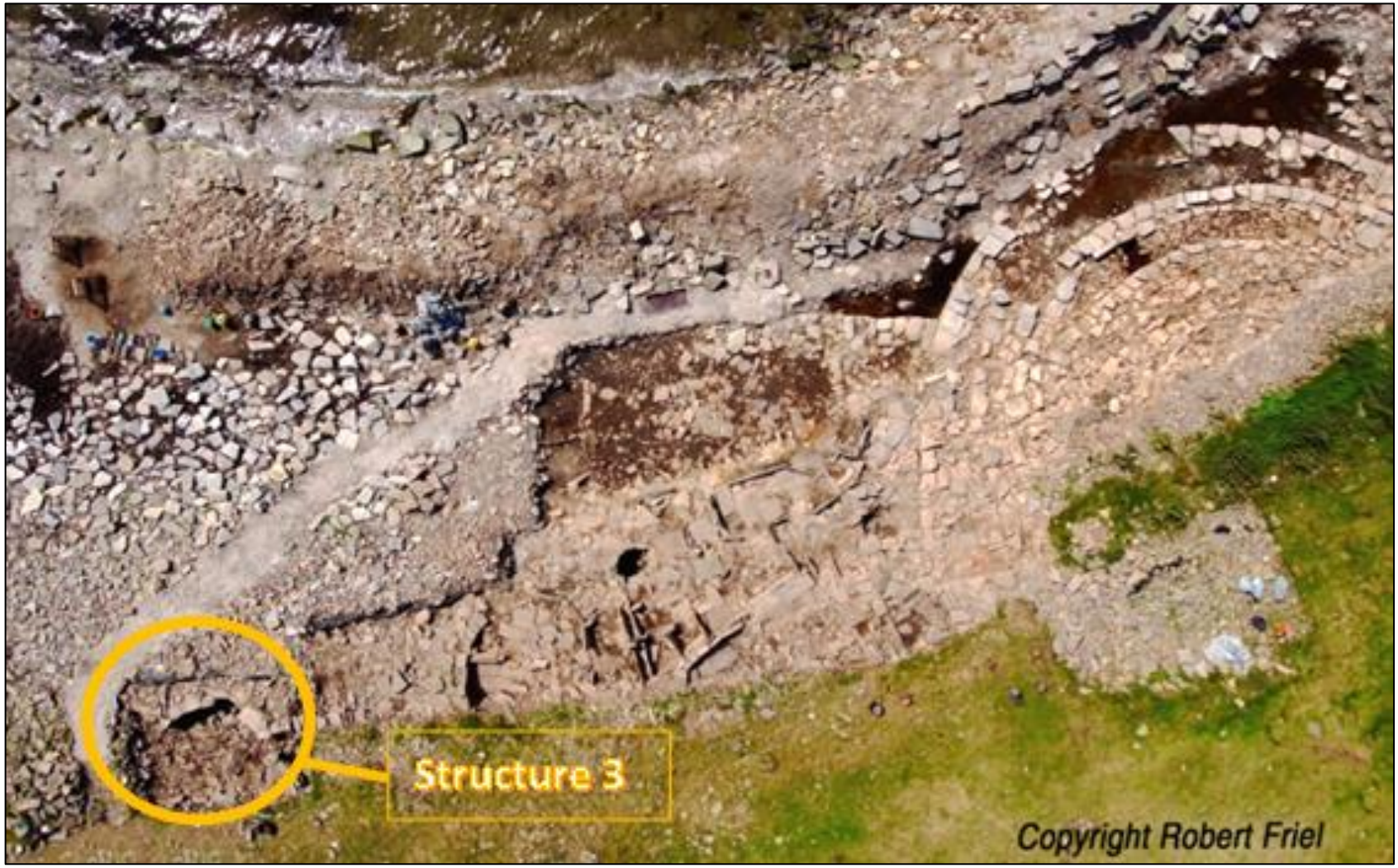

Figure 2.13 Aerial site photograph of the Knowe of Swandro. Source: Robert Friel

2.12.3 Smerquoy and Muckquoy

The sites of Smerquoy and Muckquoy are separate excavations carried out by teams directed by Colin Richards. Both sites are Neolithic settlement sites that are located in similar areas although not adjacent. Both sites are landlocked and not immediately connected to a water source like the Ness of Brodgar and the Knowe of Swandro. Smerquoy and Muckquoy lie approximately 2 Km inland on opposing ends of the Bay of Firth (figure 2.14). These sites were considered as one for the investigation given the similarity in site type, chronology, and excavation techniques.

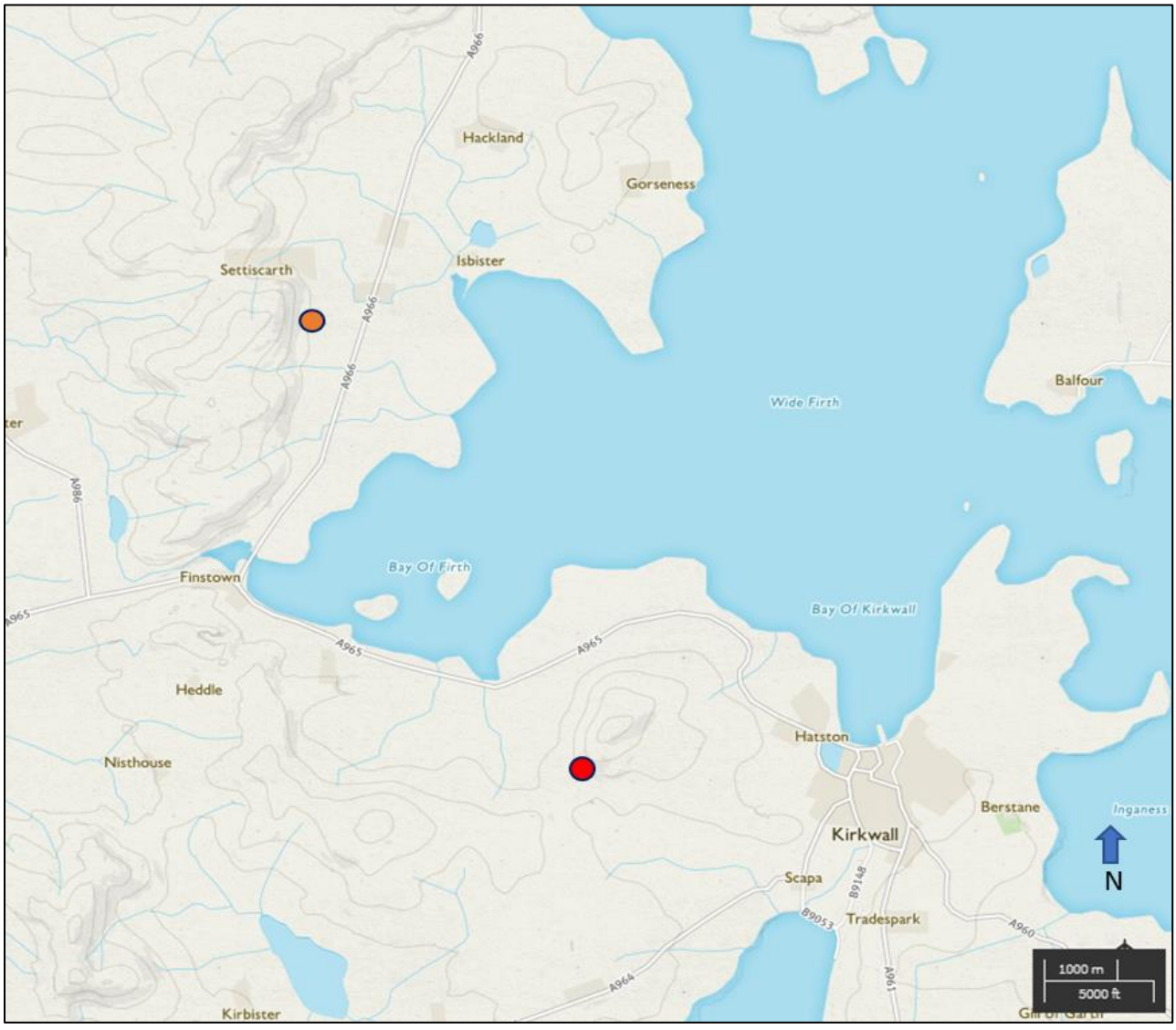

Figure 2.14 A map of the areas around Smerquoy and Muckquoy with the Muckquoy excavation shown by an orange dot and the Smerquoy excavation shown in red. Source: https://osmaps.ordnancesurvey.co.uk modified by Author.

The investigation at Smerquoy began with a field walk in 2010 and initial excavations began in 2013. The deposits near the surface had been disturbed by ploughing, yet the subsequent contexts have yielded in situ remains of structures and numerous finds. The Smerquoy excavation has uncovered the remains of an early Neolithic village over the course of three field seasons in St Ola near Kirkwall, Orkney dating between 3500-3200 BCE. The site contains a number of early Neolithic stone houses situated five to six metres apart on the lower portion of the northwest slope of Wideford Hill a few hundred metres south of the Wideford Hill Cairn (Gee *et al.* 2016). The houses on the site are considered large for the early Neolithic, at approximately 50 m^2 (Lisle 2016). The finds at Smerquoy include pottery sherds, a broken mace head, polished quartz mace fragment, and skaill knives (Gee *et al.* 2016). Of the sites being used for this research, Smerquoy is the highest above sea level and the farthest from a body of water. The samples collected from this site were hearth samples from two of the Neolithic stone houses. The two structures, both within the main excavation trench, were known as Ali's Hoose and Billy's Hoose (figure 2.15). both are stone houses built in similar style to Barnhouse structure 2 (Gee *et al.* 2016). Also, like Barnhouse, the houses at Smerquoy were constructed near a passage grave. The houses both have central scoop hearths, round dugout hearths sometimes lined with clay, and clay floor surfaces (Gee *et al.* 2016). Billy's Hoose overlaps the north end of Ali's Hoose, indicating that Ali's Hoose construction and occupation predate that of Billy's Hoose. Ali's Hoose has a porch feature used to take advantage of ambient sunlight while still within the confines of a structure. It as well has evidence of alterations to internal features, indicating a long period of occupation.

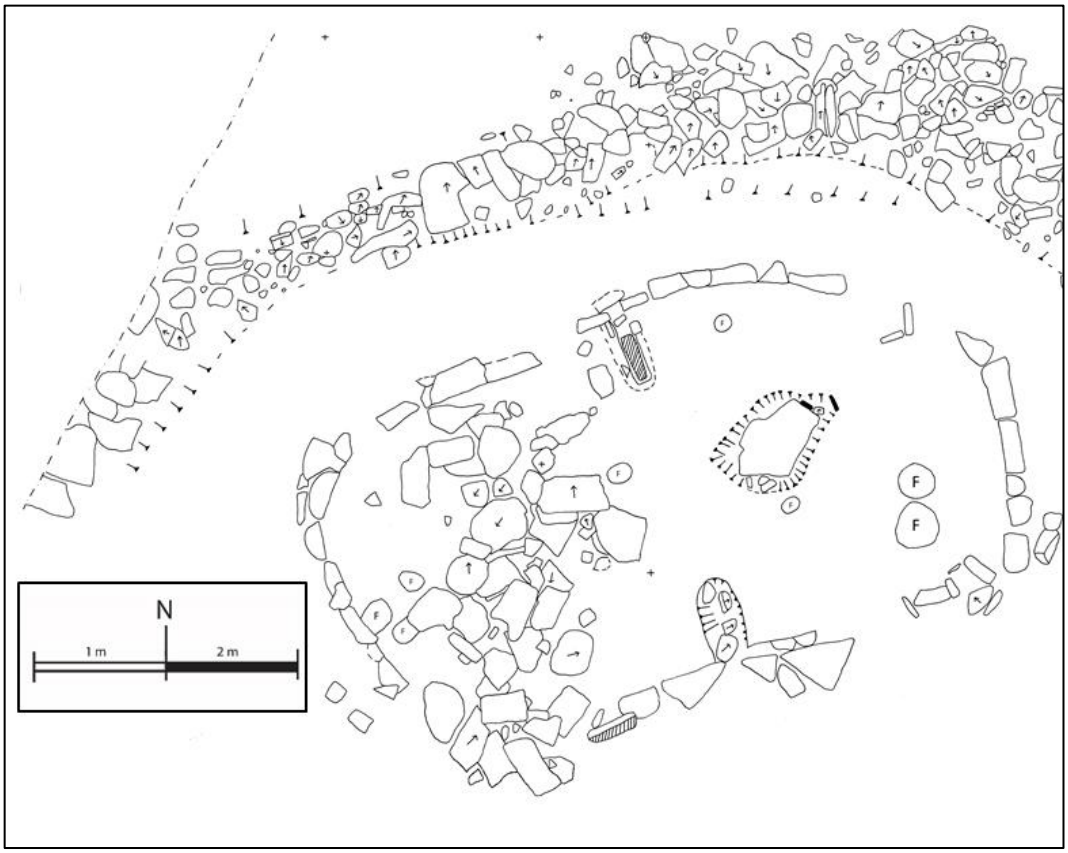

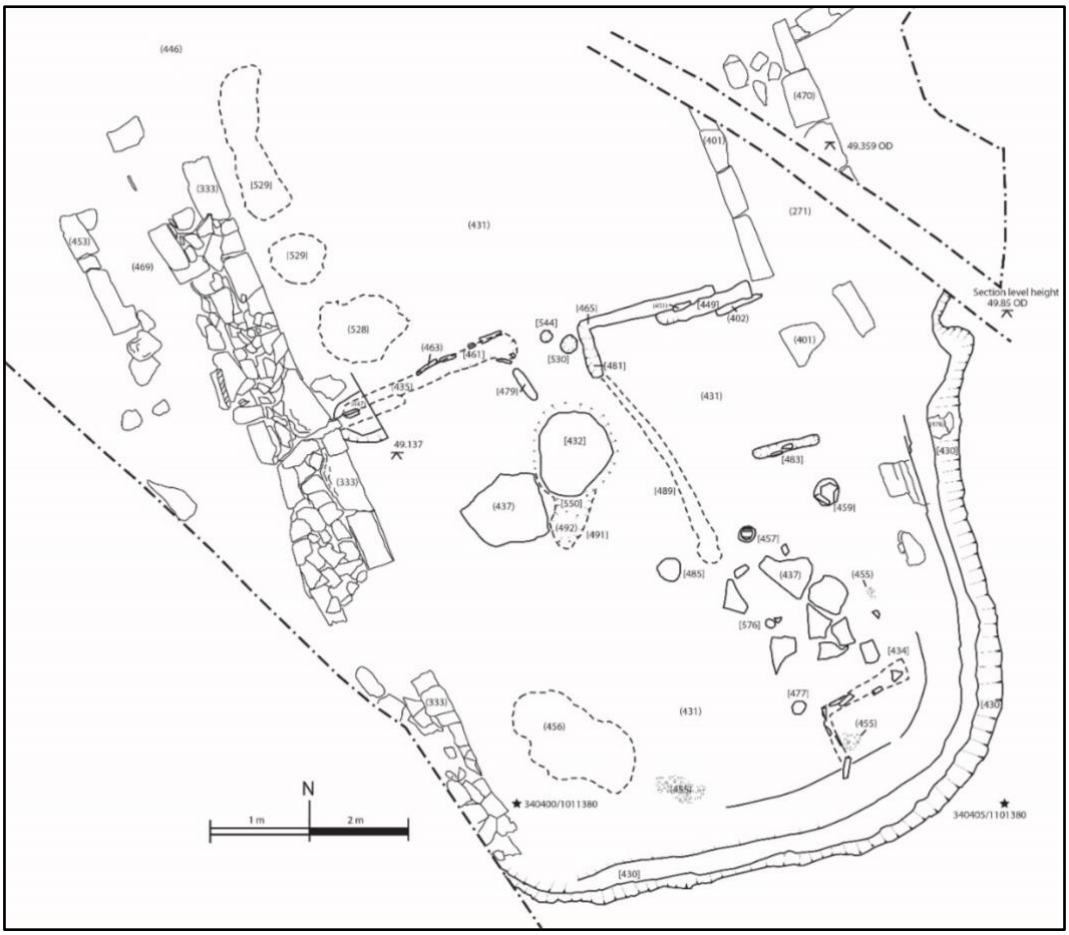

Figure 2.15 Plan drawings for both of the structures samples at Smerquoy. A plan drawing of Billy's Hoose (top) a plan drawing of Ali's Hoose (bottom) Source: Chris Gee

Muckquoy, Redland, Mainland, Orkney was recognized in 2006 with the discovery of flint and stone artifacts from the low mound in the southwest corner of the field adjacent to Finstown-Evie road, Redland. Field walks were organised in 2006, 2013, and a third surface investigation carried out from 2014-2015 (Richards *et al.* 2016). The field walking yielded several finds including sherds of grooved ware pottery, a leaf shaped arrow head, and a broken mace head. Muckquoy is a Neolithic settlement, the excavations have revealed a massive village complex, that is believed to be larger than both Skara Brae and the Ness of Brodgar based upon the size and extent of the midden, the sites occupation spans from 4,000-2,000 BCE (Richards et al 2016). The excavations at Muckquoy have added to the understanding of the development of communities over a 1500-year timeline within Orkney. The site lies on level ground on the western coastal plain near the Bay of Firth and is sheltered from westerly winds by a series of ridges consisting of Cuffie hill, Burrien hill, and Rowamo hill. Muckquoy has an anomalous barrier around the site that is thought to be the remains of a fence or wall, from near the end of the occupation of the site, with ash midden radiating away from them (Richards *et al.* 2016). It is believed that this wrapping of the site is to demonstrate its nucleated settlement status as a symbol of community. The samples from Muckquoy are all ashy midden material collected from the periphery of the settlement mound (figure 2.16). This site provides insight into the fuel use among Neolithic occupation sites.

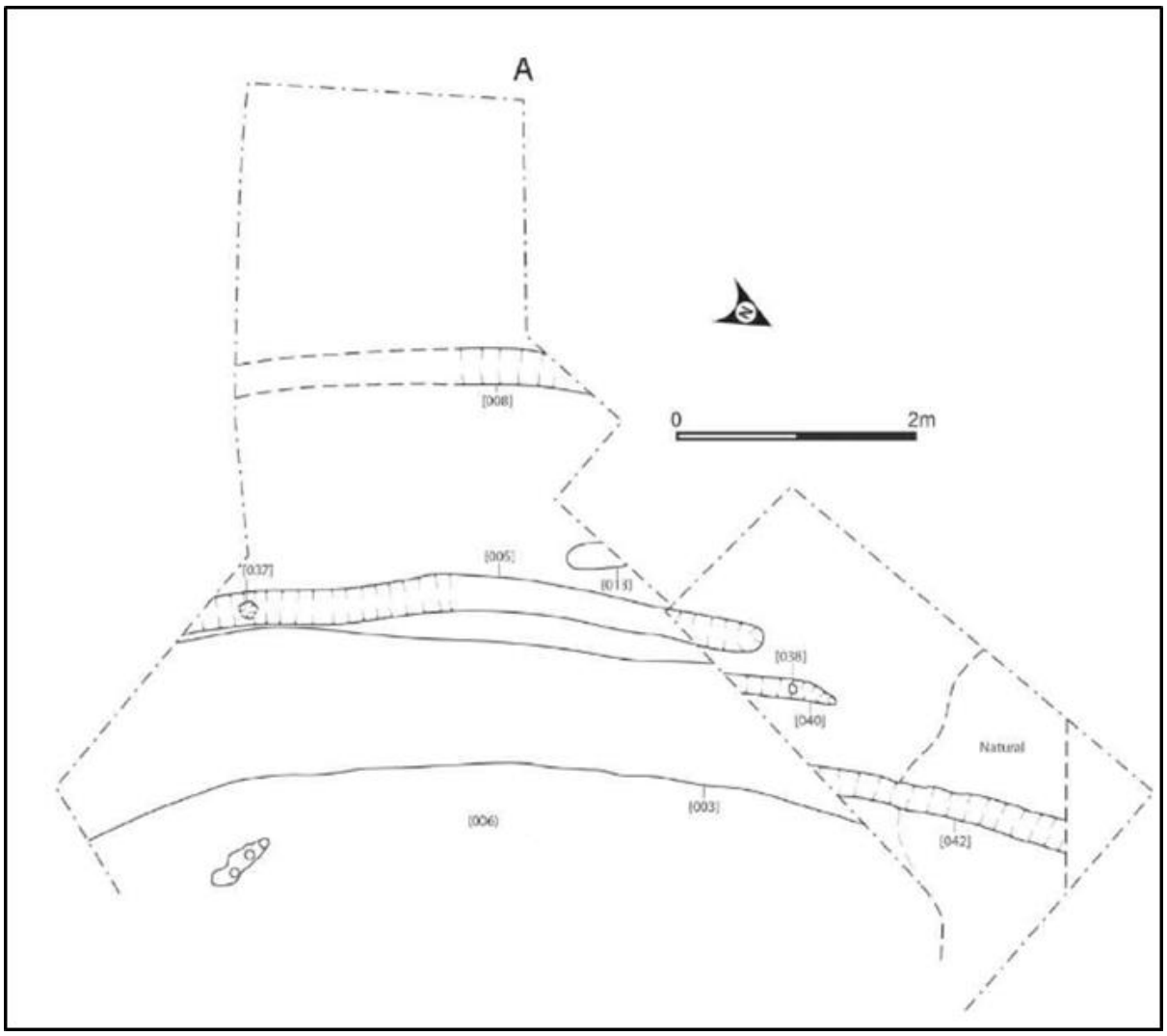

Figure 2.16 A plan drawing of the peripheral midden from the Muckquoy excavation. Source: Gee et al. (2016)

Chapter 3: Fanning the flames (Literature Review)

3.1 Overview

Archaeological research into the use of fuels requires the investigation of many different fields of science including modern research concerning ash disposal/recycling and archaeological research investigating the firing techniques of Neolithic pottery (Blaha *et al.* 2008; Ayswarya *et al.* 2011; Spencer & Sanderson 2012; Eliyahu-Behar *et al.* 2009). This chapter uses existing literature to review previous fuel research methods and archaeological investigation to develop an understanding of the previous research focused on the archaeology of Orkney, the previous archaeological investigations into fuel from other regions of the world, modern analogue experimentation with fuel, and current research with biofuel. Critical review of previous archaeological investigations justifies the chosen methods and illustrates the context and significance of this research.

This chapter is divided into sections to better organize the themes that are relevant to the research. First the key papers ar critically reviewed to show the literary basis for this research and discuss the boons and limitations of the previous work using comparison to modern analogues to identify archaeological fuels. Next, the previous studies carried out within Orkney are reviewed to show the depth of work that has been undertaken in the region, and the types of methods that have been applied to investigate the archaeological deposits. This is followed by a critical review of previous fuel studies from further afield to show the extent of research into archaeological fuels and fire from a broader perspective both geographically and methodologically. Next, modern analogue experimentation from other investigations is discussed to illustrate the scope of previous experimentation with modern analogue fuels. Finally, the methods for the investigation of modern fuels and ash are critically reviewed.

3.2 Critical review of the key papers

This section presents and discusses the key papers that were the literary basis for this research. The previous methods used to investigate fuel use with ash remains have pointed out potential limitations and problematic factors. Using this literature to inform the project helped to provide adaptations to overcome the previous limitations of other projects, and provide answers to questions that were previously left unanswered.

The work of Batt and Dockrill (1998) explains the benefits of archaeological prospection using magnetic measurement techniques such as magnetic susceptibility and remanence in conjunction with archaeological investigation and chemical analysis of P, Ca, and Fe using ICP-AES to determine formation processes and source material of the archaeological deposits including hearths, middens, and soils in Old Scatness Broch, Shetland. The use of magnetic remanence and susceptibility can aid in the determination of function and date of hearths and other combustion features. The magnetic remanence left behind in a material is parallel to the earth's magnetic field, the drift of this magnetic field over time provides a way to date a sample. The variations of mineral behaviors in an applied magnetic field makes it possible to identify minerals within a sample using magnetic susceptibility. Magnetic susceptibility and chemical analyses can aid in the determination of formation processes and source material of middens, and susceptibility in combination with micromorphology and environmental data can aid in the detection and characterization of anthropogenic enhancement of soils (Batt and Dockrill 1998). The methods used in the work performed by Batt and Dockrill (1998) prove to be a useful tool in investigating ash residues as well as source material from combustion events within archaeological contexts. Batt and Dockrill (1998) solidify the legitimacy of multi-method, or toolkit approaches

to archaeological investigation and interpretation. Adapting these methods to focus on the investigation of fuel use aids in creating the methodologies developed for this project.

Dewar *et al.* (2002) aimed to use magnetic measurements such as mass specific magnetic susceptibility, magnetic viscosity, frequency dependent susceptibility, high temperature variation in susceptibility, anhysteric remanent magnetisation, and isothermal remanent magnetisation to measure and aid in the interpretations of fuel use within ash middens inside structure 12 and 21 at the Old Scatness Broch, Shetland. In addition, Dewar *et al.* set out to identify fuel sources from the ash midden samples by comparison to modern fuel ash samples of heather turf, upper and lower peat, commercial peat, seaweed, driftwood, grass, cow dung, moss, and charcoal. There were also additional modern samples drawn from experimental archaeological investigations into iron smelting that included peat ash, clay, bog ore, furnace residues, and slag. The research of Dewar *et al.* (2002) also utilised supporting data from environmental analysis, dating and experimental archaeology to fully understand the results. Dewar *et al.* (2002) was able to determine differences in magnetism and colour among the two middens that is associated to fuel use or heating regime, and areas of the two deposits that appear to be derived from the same fuel or heating regime based upon the high magnetism of turf and lower peat fuels compared to the other modern analogue samples that were considered (figure 3.1). The complexity of the relationship between the ash material and the natural and anthropogenic activities that contribute to fuel derived archaeological deposits is emphasized as a potential limitation of further research. The unknown contributions of mixed materials within deposits could be problematic for the precise identification of fuel materials. The use of additional analytical techniques such as pH and SEM/EDX

offers a broader and more robust dataset to base interpretations on, where Dewar *et al.* (2002) uses only mineral magnetic methods. The preparation of modern ash did not specify a heating temperature, and does discuss discrepancy between the laboratory and open air produced modern analogue ash. To compensate for this potential variation, this research used multiple heating temperatures (200^0C, 400^0C, and 900^0C) to create ash and collected ash from three open air burns. The work of Dewar *et al.* (2002) provided a good base for this research, along with potential limitations to address concerning mixing of materials and variations between modern fuels exposed to different heating regimes. Dewar *et al.* (2002) does identify possible fuel sources that could have created the Old Scatness ash midden deposits despite the limitations caused by mixing of material.

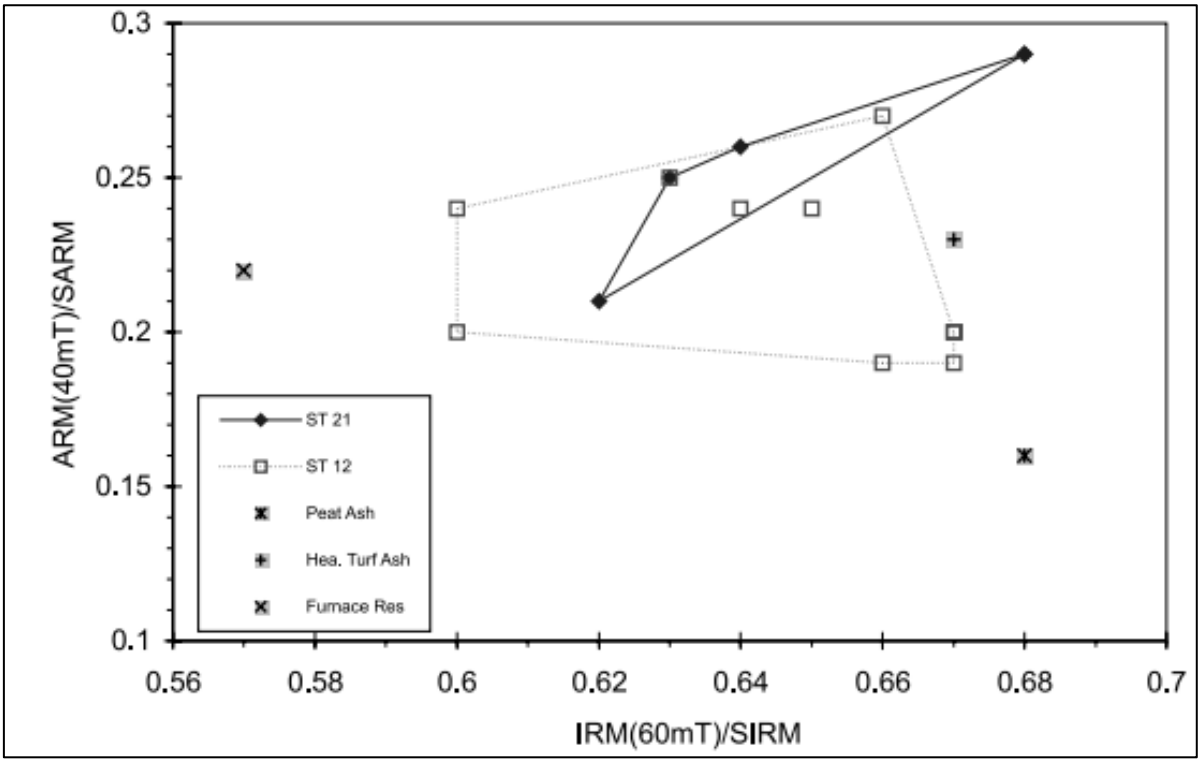

Figure 3.1 Using ratios of ARM at 40 mT/Saturation AR< vs. IRM at 60 mT/Saturation IRM to compare archaeological and modern analogue samples. Source: Dewar et al. (2002).

The work of Church *et al.* (2007) focused on the experimental burning of four fuel sources to determine variations on their mineral magnetic signatures: well-humified peat, fibrous peat, peaty turf and wood to identify fuel ash from nine archaeological sites in the Western Northern Isles of Scotland including Cladh Hallan, Old Scatness, Galson, and Bostadh. The results for Old Scatness are shown in figure 3.2. The results were compared to six room temperature magnetic measurements from sites throughout the North Atlantic to determine fuel type using magnetic signatures. The methods were high and low frequency magnetic susceptibility, direct field and alternating field anhysteric remanent magnetisations and two measurements in different fields created using isothermal remanent magnetisations. Although their research did not investigate the use of more alternative fuels such as seaweed, dung or grasses, they were mentioned as a potential fuel source. The methods used for experimental burning provide a guideline for the work with modern analogues necessary for this project, and combined with the work of Braadbaart *et al.* (2012) and Dewar *et al.* (2002) offers a reliable standard for conducting further experimentation with modern analogues germane to ash and fuel research with a more comprehensive sample set then previously used. The use of inert sand in replica hearths did prevent any variation due to the sediment material of the hearth: however, the fuel ash within hearths is mixed with sediment and this can be problematic if not addressed. The use of soil or samples of the natural soil from excavation sites could have offered answers into the problem of mixed materials within samples. It is also mentioned in the research of Church *et al.* (2007) that fuel type modifies the colour of ash distinguishable through the assignment of Munsell colour designations. Canti and Linford (2000) have also investigated the relationship between temperature and colour of archaeological soils and sediments. Although there is a discernable

difference between the quantity of ash produced by peat fuel and wood fuel, Church *et al.* (2007) does not offer a means of quantifying this difference. Measuring the amount of fuel used, quantified in mass or volume, would aid in the creation of a more accurate means of measuring the ash production of a given fuel source, and subsequently offer yet another means for identifying fuel type or potential burning period for a given combustion feature.

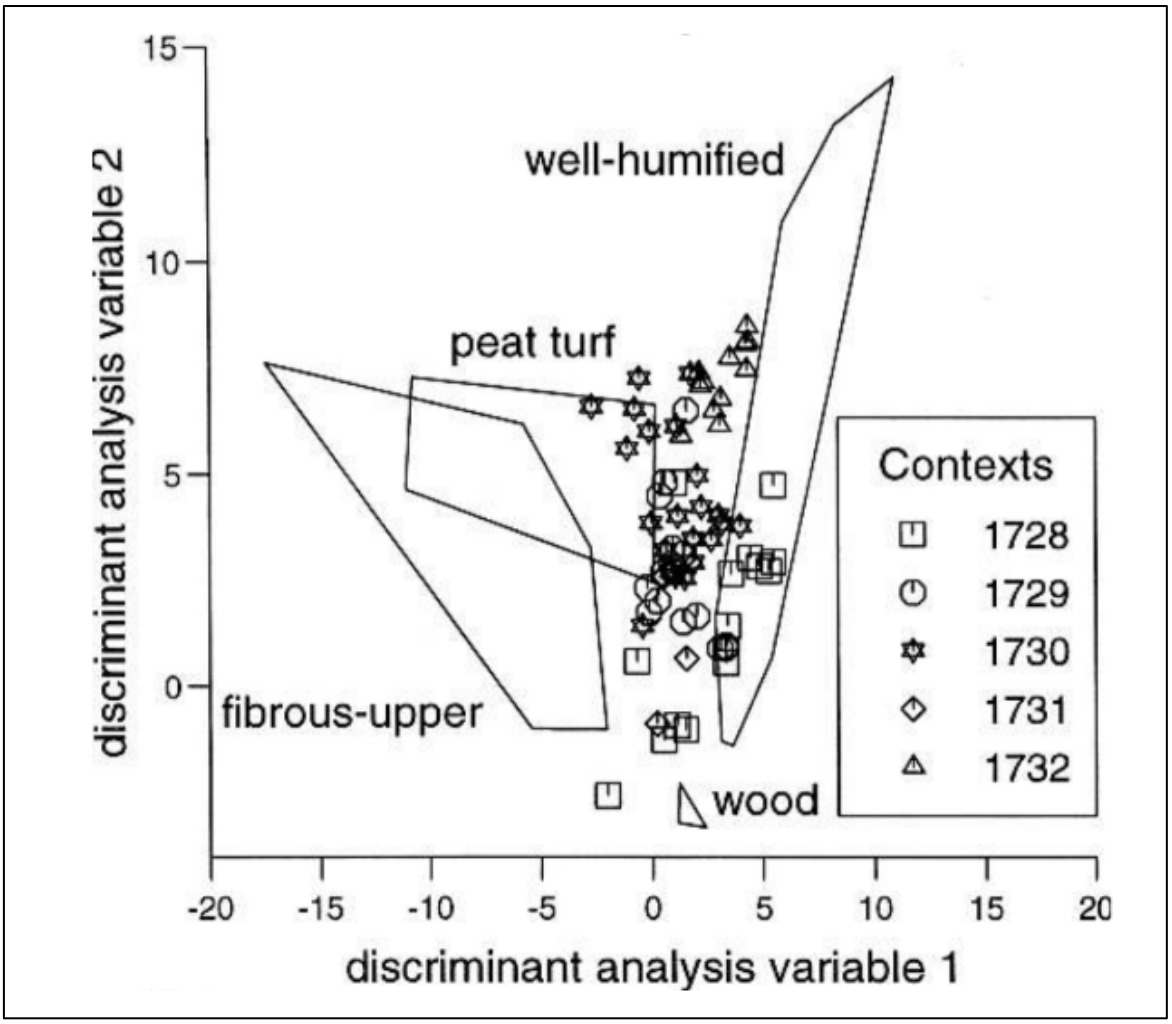

Figure 3.2 Room temperature discriminant biplot of magnetic measurements of experimental ash residues compared to samples from Old Scatness. Source: Church et al. (2007)

The work of Peters *et al.* (2002) utilizes modern analogue samples of peat and wood ash and their magnetic susceptibility measurements and magnetic remanence to identify fuel components within ash samples from excavations in the Northern and Western Isles of Scotland. Using room temperature magnetic susceptibility measurements and calculating the frequency dependence and mass specific magnetic susceptibility, Peters *et al.* (2002) could distinguish between four types of fuel ash from the controlled burns on Calanais Farm, Isle of Lewis, Scotland (Peters *et al.* 2001), including wood, well humified peat, fibrous peat, and peat turf. The results placed the four fuels into two categories well humified peat and wood ash, and fibrous upper peat and peat turf. This method was then applied to samples from three sites; a midden deposit from Old Scatness Broch, Shetland, hearth deposit from Cladh Hallan, South Uist, and hearth deposit from Bostadh, Isle of Lewis (Peters *et al.* 2002). It was determined that the archaeological samples all contained fuel ash that could be identified based upon the methods of Peters *et al.* (2002). Peters *et al.* (2002) documented finding well humified peat and wood ash within the samples from Bostadh and one of the hearths from Cladh Hallan, the remaining samples from Cladh Hallan and Old Scatness contained ashes from both fuel types established by the investigation. This is an example of a single analytical technique being used to identify fuels from ash, but there were limitations. The fuel could only be limited to a fuel category and not by individual type. With the addition of other analytical methods to aid in the interpretation and corroboration of findings such as SEM/EDX and pH this research aims to identify fuels by type and temperature from within archaeological deposits through the application of the methods presented in chapter 5.

Peters and Batt (2002) carried out the examination of a long-term use central hearth within house 401 from the Late Bronze/Early Iron Age at the Cladh Hallan settlement site on South Uist, Scotland. The hearth was sampled from three distinct surfaces separated by ash build-up and floors, associated ceramic evidence suggests that the hearth surfaces date from the Late Bronze Age to the Early Iron Age (Peters & Batt 2002). The investigation into fuel use undertaken by Peters and Batt (2002) used mineral magnetic measurements including archaeomagnetic dating, anhysteric remanant magnetisations, isothermal remanant magnetisations, and magnetic susceptibility measurements to identify fuel sources from within the hearth deposits. The identification of fuels in Peters and Batt (2002) drew from the research of Peters *et al.* (2001) carrying out controlled burns within experimental hearths at Calanais Farm, Isle of Lewis. Peters and Batt (2002) used comparison to the modern ash prepared by Peters *et al.* (2001) to inform the identification of fuels from within the archaeological hearth. The analysis undertaken indicated a shift in fuel sources from well humified peat in the earliest phase of burning, and a mixture of well humified peat, fibrous upper peat, and peat turf in the later phases of the hearth. The methods used by Peters and Batt (2002) are applicable in creating a timeline of fuel sources for a given combustion feature. Data gathered from multiple sources in the region gives a more comprehensive interpretation of the fuel management strategies in place, and the prepared modern analogue ash provides an aid in the identification of fuels from archaeological ash. In addition, the use of more modern analogue fuel types and a multi method analytical approach improves the accuracy and reliability of the identification of archaeological fuel and heating temperature.

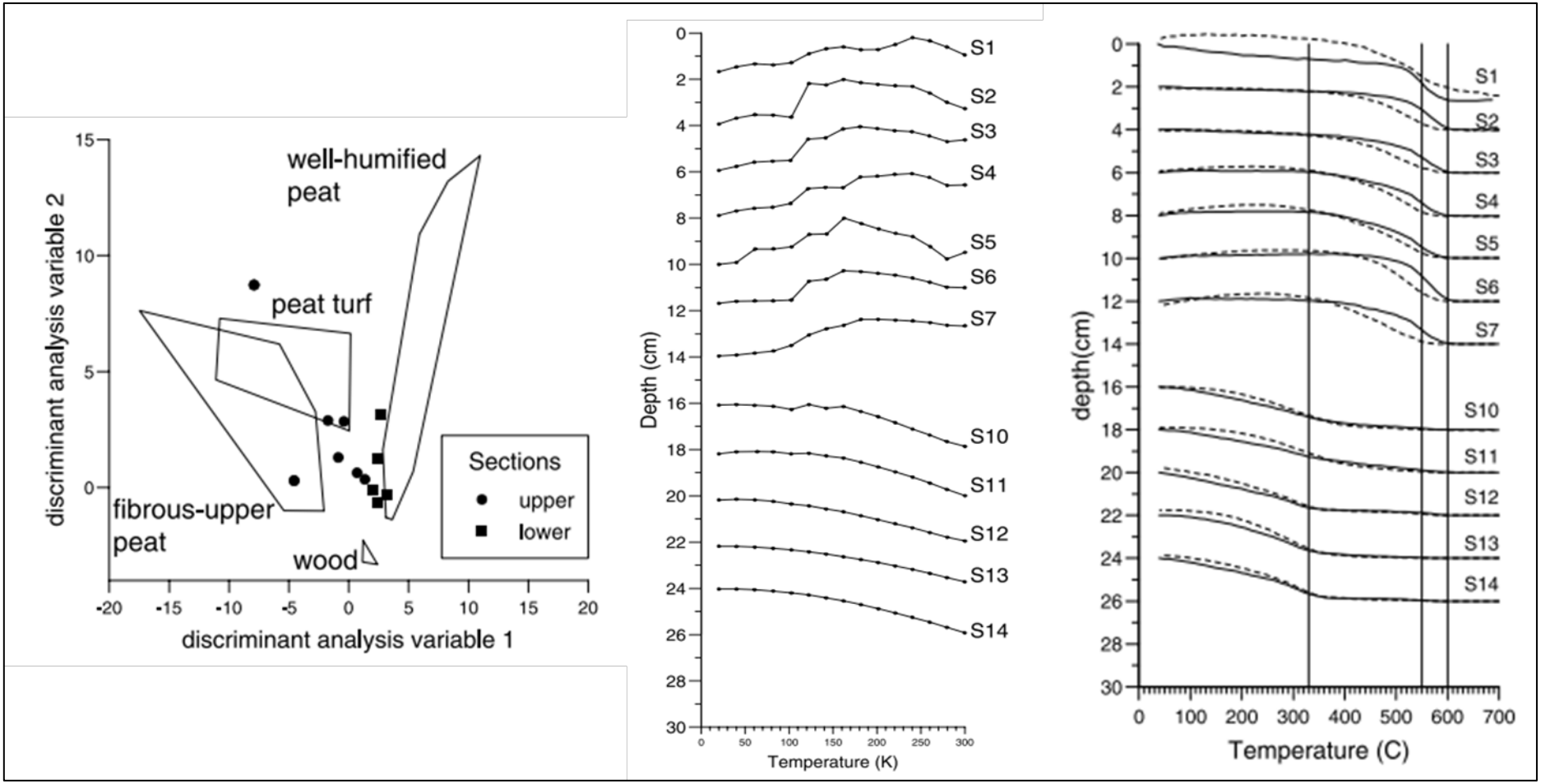

Figure 3.3 Fuel type discriminant biplot of Peters et al. (2001) based on discriminant analysis variables of room temperature measurements of modern ash residues (left) Variation of remanence with low temperatures for the 12 ash samples plotted as a function of depth (middle) Variation of susceptibility with high temperatures for the 12 ash samples plotted as a function of depth (right) Source: Peters and Batt (2002)

Char and ash remains within the soil matrix were examined by Braadbaart *et al.* (2012) using incident light microscopy and DTMS (Direct Temperature-resolved Mass Spectrometry) to gain insight into fuel sources used in archaeological contexts. Braadbaart *et al.* (2012) used a multi-method approach to investigate the end products of fire (char/ash) in the archaeological record, and investigate the heating properties of several fuel sources that would have been utilised by ancient societies. Wood, peat and cow dung were all used to determine efficacy in heat production, and to develop a means for identification. The fuels used by ancient peoples can offer insight into the socio-economic activities associated with fire according to Braadbaart *et al.* (2012) local availability influences the choice of fuels, and their remains are made easily distinguishable using both incident light microscopies to determine structure (figure 3.3), and direct temperature resolved spectrometry for quantifying elemental content. Braadbaart *et al.* (2012) also noted that the molecular content of char and ash remains aid in deciphering the burning temperature with benzenes and alkylated phenols being present in fuel material burned between 300-400°C, and only benzenes remaining in fuels heated to above 400°C. In addition, Braadbaart *et al.* (2012) stated that elemental composition can be used in identifying types of fuels present in archaeological deposits, for example silica phytoliths being indicative of plant material (including peat, dung, grasses, heather and seaweed) as a fuel source. Using microscopy and elemental analysis does appear to be a useful means for identifying fuels; however, using additional methods creates a more robust and reliable dataset. The use of magnetic susceptibility, pH and Munsell colour assignment in addition to elemental analysis and microscopy ensures that the resulting method for fuel identification is reliable. The influence of the elemental

content on the pH and magnetism of a sample also compliments the results, being able to corroborate the findings from each method using the results from another. For example, a sample with high quantities of iron also has high magnetic susceptibility, and a sample with high concentrations of calcium has a higher pH.

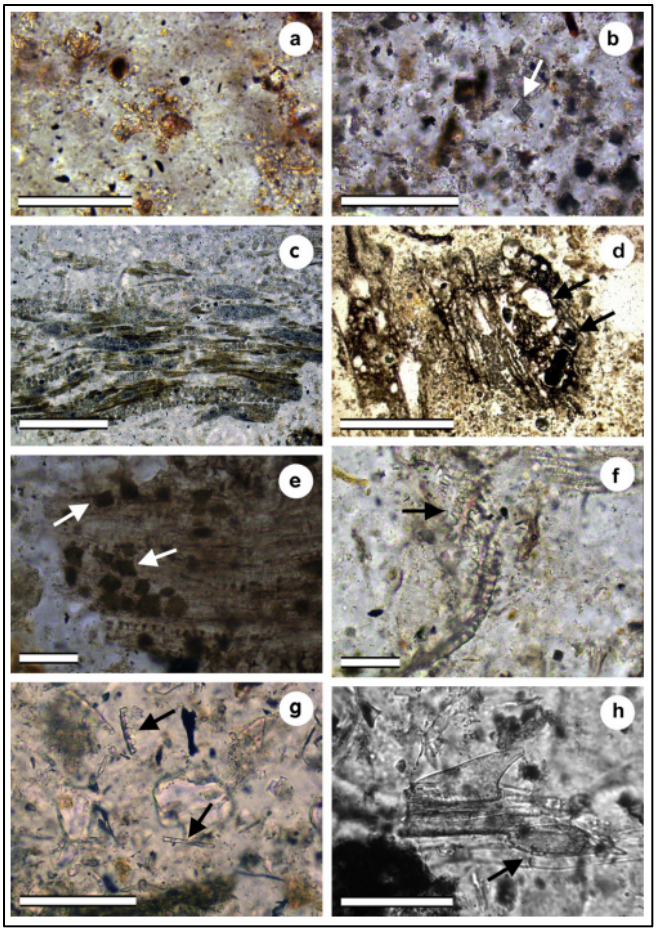

Figure 3.4 Micrographs of the different ash types using plain polarized light (PPL); a. Wood ash with fine grained carbonate crystals, scale bar ¼ 100 mm; b. Wood ash showing lozenge shaped calcitic pseudomorphs after calcium oxalates (arrow), scale bar ¼ 100 mm; c. Wood ash showing many calcitic pseudomorphs after calcium oxalates in bundles of tissue with often dark brown hue, scale bar ¼ 200 mm; d. Wood ash with globular shapes in calcium carbonate, probably caused by gas exudation during combustion (arrows), scale bar ¼ 500 mm; e. Peat ash showing calcitic pseudomorphs after calcium oxalates (arrows) in bundles of tissue, scale bar ¼ 50 mm; f. Peat ash showing fragments of silica phytoliths (arrow), scale bar ¼ 50 mm; g. Cow dung ash showing silica phytoliths (arrows), scale bar ¼ 100 mm; h. Prickles in cow dung ash with the second inserted at right angles to the first,scale bar ¼ 50 mm (photograph by Pearsall) Source: Braadbaart et al. (2012)

The key papers do provide a good basis for the development of a method for the identification of archaeological fuel using comparison to modern analogues; however, there are some limitations to address. The addition of more modern analogue fuel types, and a more comprehensive suite of methods improves the accuracy and the reliability of fuel identification.

3.3 Critical review of Orkney's previous archaeological investigations

While a broad and diverse literature base improves the understanding of fuel research, a more in depth and focused look into the investigations undertaken within Orkney is necessary to fully comprehend the parameters and restrictions for creating an Orkney focused method. The marginal climate and limited fuel availability in Orkney makes it an ideal location for the study of fuel use in the past as discussed in sections 2.3-2.4. Identifying limitations and potential complications experienced by other researchers helps improve the efficacy of the project. Discussing the previous work carried out in Orkney illustrates the need for a method of fuel identification that does not rely on the use of charcoal analysis, given the lack of wood fuels in Orkney and the subsequent lack of charcoal remains in Orkney's archaeological record.

Toolis *et al.* (2007) applied a series of methods in the investigation of a burnt mound excavated at Meur, Sanday, Orkney. The 2005 excavation revealed an open stone structure with a central trough surrounded by a burnt mound (Toolis *et al.* 2007). This mound was associated with cooking based upon the presence of pottery sherds, sheep, cow, gull, haddock, cod, herring, and eel bones within a central trough feature. Although Toolis *et al.* (2007) did not focus on fuel examination, there is evidence of fuel use present within the deposits. The fuel evidence within the burnt mound is demonstrative of several fuel sources according to Toolis *et al.* (2007). The evidence from charcoal is limited because it was only present among two contexts (Toolis *et al.* 2007). This lack of charcoal is also noted in the work of Hunter (2007: 198-199) from the excavations at the multiperiod settlement at Pool, Sanday, Orkney and in the work of Dockrill *et al.* (2007: 158-159) from the excavations at Tofts Ness, Sanday, Orkney. From the two contexts that did contain charcoal, it shows that heather and softwood are

the only charred fuel materials present. In addition, the plant macrofossil content showed the presence of burnt peat, burnt turf, and possibly charred seaweed (Toolis *et al.* 2007). The results of the phytolith extraction carried out by Toolis *et al.* (2007) indicates the plant source material was related to wild grasses, which agrees with the plant macrofossil identification of turf material. Soil chemistry analysis was also applied by Toolis *et al.* (2007), pH analysis indicates the samples were alkaline, and the high levels of phosphate indicate significant burning. Toolis *et al.* (2007) suggests that the burnt mound was a facility used for cooking, and the main fuel used was peat supplemented by heather and possibly seaweed based upon the results from the analysis of the context samples. The work of Toolis *et al.* (2007) uses a multimethod approach to investigate a burnt mound, and does discuss the fuels used within the late Bronze Age and early Iron Age deposits; however, fuel use was not the focus of the research. The investigation of the Meur burnt mound carried out by Toolis *et al.* (2007) does illustrate the limitations of charcoal analysis in regions where wood is not the main fuel source such as Orkney.

Its abundance of settlement sites makes Orkney an ideal location for the study of fuel use due to the longevity of the sites within the landscape as discussed in section 2.2. Due to the large pre-existing body of work from Orkney's numerous archaeological sites, a substantial archive of samples exists from past excavations. This number of readily available samples from previously excavated sites makes it possible to continue researching using newly developed techniques without a need to gather more sample material from newly excavated sites; this is an option that has been commonly used in the Orkney Islands. In addition, it is possible to collect new samples from undisturbed section of previously excavated sites as done by Simpson *et al.* (2006). By using a pre-

existing sample set it is possible to continue to gain data and interpretive information from a site, decades after it has been excavated as seen with sites like Skara Brae and the research of Simpson *et al.* (2006) examining the middens and their relationship/composition in different phases of site formation by characterising their components including shell, bone, quartz, charcoal, and phytoliths. Using thin section micromorphology, total phosphorous and particle size distribution analysis Simpson *et al.* (2006) determined it was evident that the midden material from both early and late phases of the site were dominated by fuel residues. The Ashes to Ashes project used existing sample material from both the Smerquoy, Muckquoy, and the Knowe of Swandro excavations. The extensive existing sample material from excavations within the region make it an ideal location to base a methodology on given the potential availability of sites to examine.

The work undertaken by Bell and Dickson (1989) examined coprolites and midden remains to determine the diet of inhabitants on the Iron Age site of Stromness cemetery broch at Warebeth, Orkney. Using a stereo microscope to examine both the light and heavy fractions of the sieved coprolite samples, and were able to identify deer, sheep, goat, weasel, and fox hair within the faecal matter of both human and domestic animal coprolites; the plant remains identified with the samples included barely, wild turnip, hemp nettle, and linseed. This shows a diverse diet among the inhabitants of the area. It was also noted that there were small inclusions of burnt fuel material both adhered to the coprolites and incorporated into them, this was deemed to be from the preparation of the food. It is suggested by Bell and Dickson (1989) that the meat was prepared by being placed directly onto the embers of the fire, which consisted of peat and small kindling. Although this section of the research conducted by Bell and

Dickson (1989) was focused on coprolites and diet, fuel was discussed due to the relationship between fire and food and the incorporation of fuel material into the fecal matter as a result of cooking. The fuels identified were peat, heather leaves, and bracken kindling according to Bell and Dickson (1989). Due to the complex and opportunistic relationship humans have with the environment, many facets of a population's existence in a region can provide potential data to aid the interpretation of a populations relationship with the environment and the affects that may have on social and economic factors. This again shows the fuel use data from Orkney is a secondary factor to other research, and a method to investigate the use of fuel resources within Orkney is needed to fully interpret the deposits.

Figure 3.5 Images of the coprolites used in the analysis from Stromness. Source: Bell and Dickson (1989)

It is possible to obtain data relevant to fuel resources and firing technology through the analysis of artefacts such as pottery. Spencer and Sanderson (2012) investigated the possibility of fuel scarcity as a potential explanation for poor quality pottery within the archaeological matrix at Pool, Sanday, Orkney using high-temperature thermoluminescence (HTTL). Quantifying the temperature at which pottery samples from different stratigraphic phases were heated to, poorer quality pottery could be attributed to scarcity of fuel or a change in firing technology according to Spencer and Sanderson (2012). The research of Spencer and Sanderson (2012) also utilised previous paleoclimate data to support the interpretation of fuel resource scarcity being the cause of the lower quality of pottery firing within the region. The work of Spencer and Sanderson (2012) also illustrates the value of artefacts from within archaeological contexts being used to aid in the interpretation of deposits. In addition, this affirms the need for research focused into fuel use within Orkney and not as a secondary outcome of other investigations.

It is evident from the existing literature available on the analyses of ash and other combustion residues, that a multi-method approach relying on a suite of analytical techniques is necessary to quantify the organic and inorganic compounds present in combustion residues (Braadbaart *et al.* 2012; Etiégni & Campbell 1991; Photos-Jones 2007). In previous research focusing on cramp found within Bronze Age cremation burials, Photos-Jones *et al.* (2007) used several methods to determine the main constituents of cramp (vitrified material associated with cremation) including petrography, scanning electron microscopy with energy dispersive X-ray analysis (SEM-EDX), X-ray diffraction (XRD), inductively coupled plasma emission spectroscopy (ICPMS), and gas chromatography (GC). Cramp is thought to be a result of sand fusing to dry seaweed during the

cremation process, yet seaweed has not been identified within the archaeological record as a fuel material from funeral pyres based on the existing samples of cremation debris (Photos-Jones 2007). Using cramp samples from Loth, the Knowes of Trotty, Crantit, and Kewing funerary sites in Orkney, Photos-Jones (2007) quantified oxides of Si, Al, Fe, Mg, Ca, Na, K, P, and Sr to determine the major factors in cramp production. Photos-Jones (2007) concluded that the higher percentage of K, Na, and Ca oxides within seaweed ash when combined with silicate materials such as quartz acts as a flux agent and aid in the creation of an alumino-silicate melt (siliceous liquid) containing bone fragments and a glassy appearance when cooled known as cramp (figure 3.5). Although Photos-Jones (2007) does not focus on ash, it is focused on the investigation of a combustion residue. Applying elemental analysis to ash material provides a means to classify samples based upon the concentration of elements. The use of SEM/EDX provides a means to characterise and quantify selected elements, and to capture high magnification images of the sample materials.

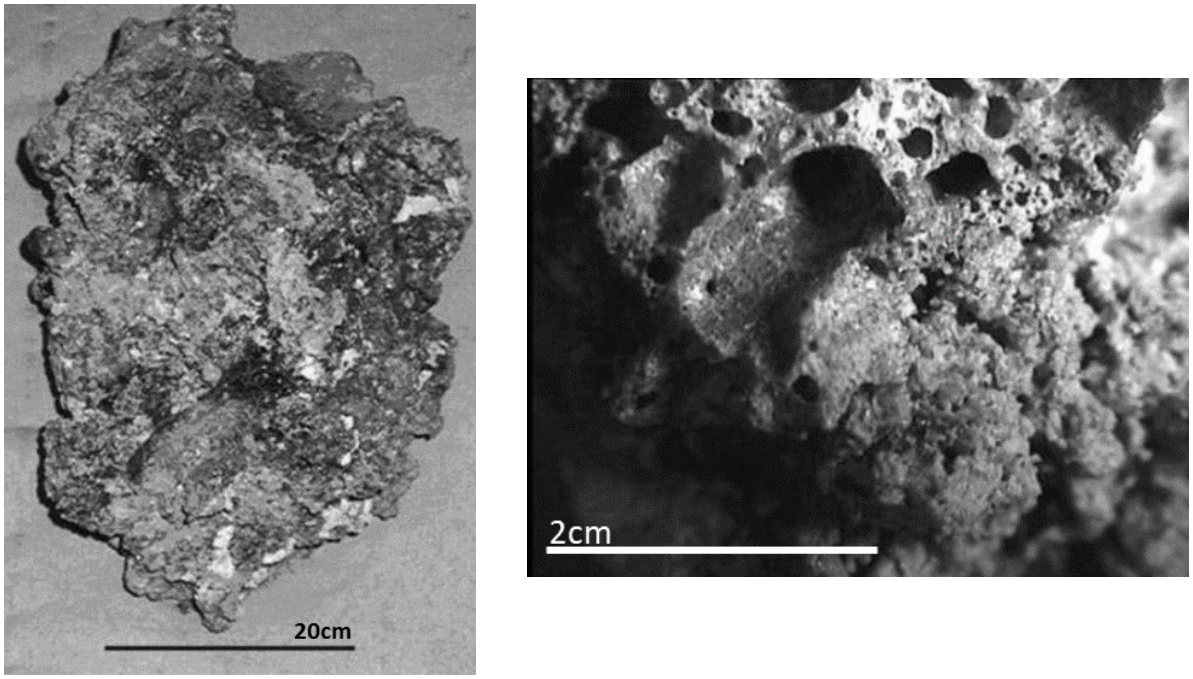

Figure 3.6 Images of cramp a large example from the Kewing cist (left) and a magnified image of cramp from Crantit cist (right). Source: Photos-Jones (2007)

The discussions about fuel use within most of the investigations in Orkney are secondary to the investigation, and those results have focused mainly on charred plant remains, which are scarce, or sediments and not on ash. The discussion of fuel use often arises given the intrinsic relationship with survival and fuel. Ash exists wherever there was combustion unlike charcoal which requires certain parameters such as low O during combustion to be produced (Braadbaart *et al.* 2009; Pierce 1998). A means to identify fuel remains from ash would provide a means to fully interpret the function of combustion features in the absence of charcoal, and further the interpretation of the economy and environmental relationship of populations within Orkney.

3.4 Critical review of previous archaeological fuel investigations from further afield

This section presents and discusses the archaeological investigations into fuel use that were not carried out on material from Orkney, but were still considered when developing a method for the identification of archaeological fuel using comparison to modern analogues.

The use of multiple analyses provides a means to corroborate findings as well as quantify a greater number of constituent materials. Summers (2015) investigated an ash deposit from the Old Scatness excavation in Shetland with the presence of vitrified fuel ash slag, making use of Photos-Jones *et al.* (2007) (section 3.3) previous work with cramp production to identify seaweed ash. The ash deposit was discovered inside of a stone slab-sided box within Structure 8 at Old Scatness; the light and heavy fraction were examined with a binocular microscope to identify the constituents of the material. According to Summers (2015), the deposit contained molluscs, bryozoans, bristle worms, barnacles, and sea urchin; however, the dominant component of the sample's heavy fraction was a pale grey vitreous fuel ash slag. This slab-sided box was interpreted by Summers (2015) as a container to hold seaweed ash that was burned away from the settlement, possibly on the beach where it was harvested, to be used in several methods including food preservation, dairy processing, and wool scouring due to its high alkaline (calcium potassium) and salt (sodium) content. This is an example of being able to further the interpretation of a site's economy and relationship with their environment with a better understanding of the ashes that have been deposited.

Many of the settlement sites throughout the North Atlantic show evidence of a long sequence of occupation from the Neolithic through the Iron Age according to Dockrill and Bond (2009). There is evidence of this from the sites of Tofts Ness,

Sanday, Orkney, and the Jarlshof and Old Scatness excavation sites in Shetland as discussed in Dockrill and Bond's (2009) research. The examination of anthropogenic soils was used to illustrate the economic strategies that were present during the Neolithic and Bronze Age shown through the evidence from Tofts Ness and Jarlshof, and how these practices continued, indicated from the archaeological record within the early Iron Age at Tofts Ness and the middle Iron Age at Old Scatness. Dockrill and Bond (2009) show the success of these sites in providing resources through anthropogenic soil manipulation and the use of a mixed paleoeconomy that utilizes both the land and seascape to aid in multiperiod subsistence of sites (figure 3.6). The availability of fuel has a large impact on the success of a site and its potential influence on the landscape, making the identification of fuel material from archaeological deposits a useful tool in the interpretation of the relationship between the ecology and economy of long term occupation sites.

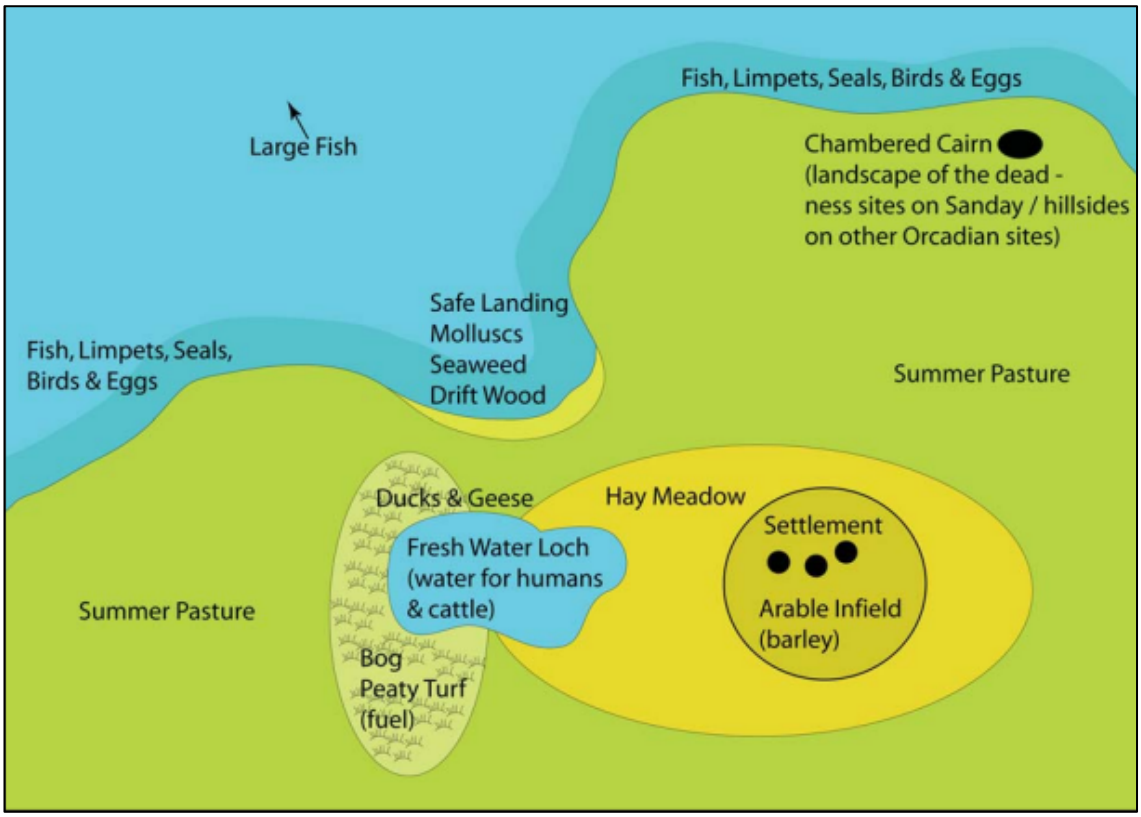

Figure 3.7 A stylised resource and landscape model based on the Tofts Ness data but incorporating the similar locational evidence from two other Neolithic settlements on the island of Sanday, at Pool and Stove. Source: Dockrill & Bond (2009)

The interdisciplinary approach undertaken by Amorosi *et al.* (1997) demonstrates the use of archaeological, historical, ecological, environmental and anthropological data to extrapolate the impact to the North Atlantic region from Norse colonisation of Shetland, Orkney, Caithness, The Hebrides, The Faeroes, Iceland, and Greenland. The research of Amorosi *et al.* (1997) also discusses the use of landscape management practices that are well adapted to northern Europe and The British Isles, not being viable in settings like Greenland and Iceland, showing that local environment is a large factor in the success or failure of subsistence practices. The work draws evidence from archaeological pollen data, zooarchaeological assemblages, paleoenvironmental research and historical sources. This research, although it pertains to a larger geographical area than just Orkney, offers a good example of utilizing source material from various disciplines of research. The use of multiple fields of science, anthropological study, and previous archaeological investigation is vital to fully interpret the data gathered and accurately assess the fuel use within the Knowe of Swandro, the Ness of Brodgar, and Smerquoy/Muckquoy.

Vleminckx *et al.* (2014) experimented with a method for assessing the impact of human disturbance on tropical forests using the abundance of charcoal within the soil to determine past use of slash and burn agriculture in Cameroon, Central Africa. The methods of Vleminckx *et al.* (2014) utilised soil cores taken in a grid pattern, to assess the abundance of charcoal present within stratigraphic layers. A charcoal abundance index number was given according to the system developed by Vleminckx *et al.* (2014) for each core sample. The abundance of charcoal was plotted according to depth, and the trends were then compared between several sites in southeast and southwest Cameroon. The results from Vleminckx *et al.* (2014) indicate a trend among the sites all showing significant

increases in charcoal abundance in two distinct periods c. 80 – 850 BP and c. 1500 – 2800 BP. Statistical analysis was used to determine any correlations between the burning evidence from the soil and the fluctuation in predominant tree species to determine if there was an anthropogenic influence on the present-day tree species assemblage in Central Africa. This research demonstrates the potential for interpretation of landscape change through anthropogenic activity, and the potential for using statistical analyses applied to variables that are not associated chronologically, applied by Vleminckx *et al.* (2014) to charcoal data from the past and the current tree assemblage of Central Africa.

Simpson *et al.* (2003) compares the fuel resource utilisation of two different settlement age sites in Mývatnssveit northern Iceland; one of the sites was a high-status settlement Hofstaðir and the other a low status site Sveigakot that was ultimately abandoned. The investigation by Simpson *et al.* (2003) was carried out using thin section micromorphology and image analysis, along with modern analogue fuel residues for control, to identify fuel ash residues. Modern analogue fuels including peat, mineral-based turf, willow, birch, cow dung, and sheep dung were chosen with consideration to historical records that mention fuel sources (Simpson *et al.* 2003). The comparative modern analogue samples along with archaeological samples of heating activity residues were examined using constant illumination (plane polarised, crossed polars and oblique incident) with an image analysis system comprising of a polarising microscope (Simpson *et al.* 2003). The results suggest variations in exploitation of fuel sources between the sites of divergent status indicated by the Hofstaðir site having more abundance of wood fuels and the Sveigakot site showing more marginal use of fuels such as willow and cow dung. Simpson *et al.* (2003) suggests that the differences in consumption of fuel resources are indicative of social regulation of fuel sources.

The work of Simpson *et al.* (2003) is a good example of using modern analogues to aid in the investigation of archaeological fuels; in addition, it further demonstrates the efficacy of fuel use data aiding in the interpretation of the economy of a site.

Asouti (2003) investigated the exploitation of wood fuel resources through the examination and subsequent identification and quantification of wood charcoal remains in the archaeological record at the Pinarbaşi site in Anatolia, Turkey. The investigation shows that the relationship between the migrant inhabitants was beneficial for the woodland vegetation. According to Asouti (2003), the seasonal occupation of the sites gave the woodlands a chance to replenish, and the 'pruning' style of fuel collection helped the woodland vegetation to grow and produce fruit and nuts. The patterns observed by Asouti (2003) were interpreted as a reflection of the site's fuel exploitation strategies in the context of the local and regional paleoenvironment. 38 flotation samples were selected. From there, 200 charcoal fragments from each float were then examined. Asouti (2003) employed a fragmentation/preservation index in addition to other analytical methods to identify 18 different taxa including almond, terebinth, reeds, and small shrubs.

The work of Mentzer (2014) offers an extensive review of methods applicable to the investigation of fuel use by past people through the use of a methodological approach that utilises multiple analytical techniques to fully examine and interpret the use of combustion features. Mentzer (2014) presented a literature review examining previous research on combustion features and the methodological approaches to their identification in archaeological contexts. According to Mentzer (2014) hearths and heating activity residues provide source material for several analytical methods including micromorphology, scanning electron

microscopy, energy dispersive X-ray spectroscopy, magnetic susceptibility and magnetic mineralogy, stable oxygen and carbon isotope analysis, lipid analysis, and X-ray defraction. In addition to the palaeoecological and palaeoeconomical data that is acquired through the study of heating activity residues, Mentzer (2014) provides a comprehensive review of methods for the identification, recording, analyses and interpretation of combustion features through the critical review of the existing literature on combustion feature investigation.

Alperson-Afil (2012) focused on the characteristics of archaeological large area fires such as burning associated with agriculture as well as natural disasters and wildfires at the Acheulian site of Gesher Benot Ya'aqov, Israel; however, this work also offers useful insight into examining smaller scale industrial and domestic combustion features through the study of fire modified flint samples and review of the palaeoclimate of the region (figure 3.7). The ability to interpret the evidence left within the archaeological record in the form of ash deposits and large stratigraphic ash horizons is extremely useful in gathering acumen germane to formation processes and functional uses of a particular site. The ignition source/point and spreading pattern of a burned area adds to a dataset, furthering interpretation of heat activity residues within archaeological contexts. Both anthropogenic and environmental ignition sources were considered for the scope of the research carried out by Alperson-Afil (2012), and the work comprehensively covers three variables that affect the efficiency of fire- fuel distribution (both oxygen source and what is burning), wind speed and direction, and moisture content of both the fuel source and the area surrounding the combustion zone. Alperson-Afil (2012) states that the intensity of a fire varies vertically, and this is especially useful when considering anthropogenic fires that were ignited within enclosed combustion features. The area of the research that concentrated on

anthropogenic fire, discussed the use of the spatial distribution of burned artefacts such as flint as a means to determine the remains of possible hearths. Alperson-Afil (2012) concluded that the fire evidence from the Gesher Benot Ya'aqov excavation were of anthropogenic origin due to the climate conditions of the region not being conducive to wildfire based on the moisture of the sediments and the ambient climate of the region. The research performed by Alperson-Afil (2012) is a useful resource for understanding the functions of fire and offers expedient techniques to employ in further investigations of ash deposits. This research is also useful due to the approach of the investigation considering the contributions of ignition and combustion in addition to the actual deposits.

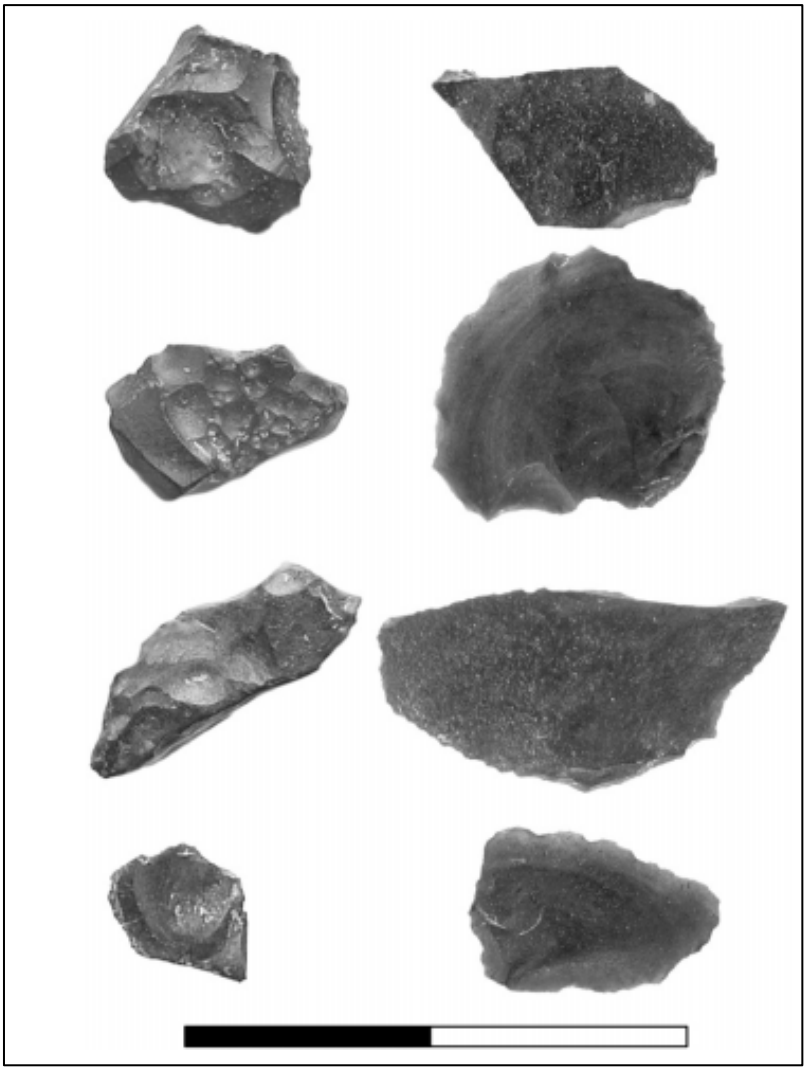

Figure 3.8 Images of flint micro artifacts burnt on the left and unburnt on the right, 2cm scalebar. Source: Alperson-Afil (2012)

The work of Braadbaart *et al.* (2009) provides a means for examining charred plant material and determining the temperature at which it was heated, as well as investigating the exposure of charred plant material to high soil pH using potassium and calcium hydroxide to mimic alkaline soil conditions. The research of Braadbaart *et al.* (2009) expands on the experimental methods of modern analogue preparation in Braadbaart (2004) and Braadbaart and Poole (2008), and discusses the effects of alkaline environments causing the fracture and further breakdown of charred plant materials within archaeological deposits, specifically the pH levels of shell-rich material that is commonly found among coastal archaeological sites that are so frequent in the North Atlantic. The characteristic differences among charcoal heated below 310° and specimens heated to higher temperatures as demonstrated by Braadbaart *et al.* (2009), offer a means of readily deciphering between domestic and industrial ash residue based on the effects of higher temperature exposure on the structure of the deposited material. Braadbaart *et al.* (2009) used oak heartwood heated to several different increasing temperatures followed by exposing each sample to potassium hydroxide and calcium hydroxide (simulating volcanic ash and shell rich soil respectively) for 147 days. Braadbaart *et al.* (2009) stated that charcoal heated below 310° became soft and did not retain its structure, while the samples heated to higher temperatures survived much better and preserved their structure. This further illustrates the need for the development of a method for the identification of fuel materials that does not rely on charcoal but ash.

Cook *et al.* (2005) used geochemical analysis with XRF (X-ray Fluorescence) to detect copper alloy working at the site of a Roman town *Calleva Atrebatum* (Silchester, Hampshire, UK). The site had little evidence of non-ferrous metal working. With the utilization of XRF (X-ray Fluorescence) to detect Pb, Zn and

Cu, followed by ICP-MS (Inductively Coupled Plasma Mass Spectrometry) on the samples of the highest concentrations to test for further evidence of the presence of Au, Ag and Sn (Cook *et al.* 2005). The data collected from the surveys and subsequent analysis suggests the working of copper alloys including brass (Cook *et al.* 2005). The work of Berna *et al.* (2007) investigating late Bronze and Iron Age strata at Tel Dor, Israel in a similar analytical approach to researching a different location and time period. This method would be a useful tool in researching ash residue and hearth material both in situ and in a laboratory setting. Despite the fact that Cook *et al.* (2005) were investigating metalworking and not fuel sources, the methods used are applicable to an examination of ash residues in archaeological deposits due to the differing elemental signatures among fuel established by Braadbaart *et al.* (2009).

Pierce *et al.* (1998) investigates the identification of the constituents of fuel from hearth ash using inductively coupled plasma atomic emission spectra (ICP-AES) analysis applied to both archaeological and modern analogue samples. The archaeological and modern analogue material for the analyses carried out by Pierce *et al.* (1998) were all collected from the same region near Crow Canyon archaeological centre at the base of the Rock Mountains in Southwest Colorado, USA. The methods can accurately identify the type of material (bark, wood, etc.) and taxa from a fuel source for both modern and archaeological material, due to the variation in elemental composition of fuel materials being significant enough to distinguish according to Pierce *et al.* (1998). Pierce *et al.* (1998) digested samples in nitric and hydrochloric acid (HNO3: HCl, 1:3), reduced the solution to 3ml by heating to 1250C, and then collected the remaining solids with a filter prior to ICP-AES analysis. The results presented in Pierce *et al.* (1998) show the concentrations of Al, Ca, Cl, Fe, K, Mg, Na, S, Si, Ti, and Zn among the

archaeological and modern samples; all of these elements with the exception of zinc were established as the main constituents of ash within section 2.4 (Vassilev *et al.* 2013; Vassilev *et al.* 2014; Baernthaler *et al.* 2006). Pierce at al. (1998) additionally discussed the variation between modern and archaeological ash being caused by the mixture of sediment among the archaeological samples; however, the variation is seen with elements that contribute to the sediments make up such as silicon, iron, and aluminium which is to be expected in mixed samples. The use of a multi method approach to analyses by this project adds to the confidence of results and not rely on the use of SEM/EDX analysis alone. Results from magnetic measurements, pH analysis, and Munsell colour assignment provides a robust dataset on which to base interpretations. This work also adds to the understanding of analyzing modern and archaeological samples with consideration to the variations caused by the mixture of archaeological material and sediment within features.

Although the research performed by Bathurst *et al.* (2010) did not focus on the investigation of combustion features or associated fuel sources, the sampling strategy and archiving protocols are a good model. The use of negative samples, or samples known to have no content of diatoms in the case of Bathurst *et al.* (2010), in conjunction with positive samples collected from a 600m radius is an efficient method of validating results, as well as augmenting the dataset. The need to address a demand for additional samples in the contingency of a necessity for further analyses was confronted with the gathering of surplus material (up to 5g) during the collection phase of the work. The benefit of superfluous sample is not limited to subsequent analyses alone. Once the material has dried the additional quantity of sample offsets the effects of loss to mass/volume from drying (Bathurst *et al.* 2010). Archaeological research is often

referred to as “the unrepeatable experiment” due to the severity of limited quantities of material and time. This predicament is often exacerbated by the constant refinement and development of analytical techniques. Retaining surplus sample allows additional analyses as suitable techniques become available.

In archaeological research SEM/EDX has been used extensively in a number of applications from aiding in the interpretation of deposits to reconstruct activities from a site as carried out by Eliyahu-Behar *et al.* (2008), to investigating Iron age metallurgy of bronze alloys to determine interaction with more advanced cultures as performed by Valério *et al.* (2010). The microscopic imaging and analytical capacity of SEM/EDX is a valuable tool in archaeological investigation. The work of Canti (2003) investigated the chemical and microscopic characteristics of plant ashes that are found within archaeological soils to better understand what components of fuel survive into ash within the archaeological record. Using SEM/EDX, Canti (2003) was able to distinguish fuels into several groups including wood, grasses, roots, leaves, seeds, and fruits using the quantified levels of high solubility components, low solubility components, and silica. According to Canti (2003) ashes of high silica-low calcium grass ash is easily distinguishable from low silica-high calcium wood ash; however, the presence of identifiable mineral bodies among plants makes it possible to identify fuels from their ashes.

3.5 Critical review of modern analogue experimentation/experimental archaeology

The use of modern analogues to aid in the interpretation of archaeological deposits is a common practice. This section discusses other research that has utilised modern analogue materials in the investigation into fuels and fire.

Braadbaart and Poole (2008) investigated the alterations that wood fuel sources undergo during the charcoalification process and its importance to archaeological studies due to its ability to endure diagenetic processes in soil. According to Braadbaart and Poole (2008) charcoalification of plant material is the most common mode of survival into the archaeological record due to the retention of structure and increased potential for subsistence through the deteriorating and altering processes of diagenesis. The research of Braadbaart and Poole (2008) created modern analogue combustion residue samples of wood exposed to 19 temperature ranging from 160^0C – 1200^0C and prepared charcoal using oak heated to 450^0C, this was followed by burning to produce charcoal combustion residue samples at 800^0C, 900^0C, 1000^0C, 1100^0C, and 1200^0C; both a low heating and high heating rate were used by placing samples in a furnace at ambient temperature then gradually heating for the low heating rate, and placing the samples in a preheated furnace for the high heating rate. This was done to simulate a fuel used to start a fire (low heating rate) and fuel that was placed on an already ignited fire (high heating rate) (Braadbaart and Poole 2008). The modern samples were then analysed using morphology, reflectance, thermogravimetric elemental analysis, and direct temperature-resolved mass spectrometry (Braadbaart and Poole 2008). Charcoal is ubiquitous and produced inadvertently in regular burning which causes it to be commonly deposited among combustion features and associated ecofacts such as middens. In researching ash residue and related fuel sources, Braadbaart and Poole (2008) offer

invaluable insight into the progressions of combustion, the processes necessary to transmute wood sources into charcoal, as well as the disparities between wood and charcoal as a fuel source based on their analytical signatures. For the purposes of this research, the work performed by Braadbaart and Poole (2008) provides a means to determine function of a combustion feature due to the greatly variable burning temperatures and characteristics of wood and charcoal, functional temperature of combustion features, and function based on the end products left within the archaeological deposits. In addition, the analytical work used in the identification of fuels and functions of combustion features, Braadbaart and Poole (2008) also provide a comprehensive methodology for the creation of modern analogue combustion residue samples.

Braadbaart *et al.* (2017) used comparison to modern analogue material to investigate the fuel use among the Iron Age site at Vlaardingen, the Netherlands. Using alder, ash, *sphagnum* peat*,* reed peat, sedge peat, and cow dung Braadbaart *et al.* (2017) created modern analogue ash samples heated to 500^0C. Granulometry determined by laser diffraction and elemental analysis using XRF were carried out along with the microscopic analysis to record opal phytoliths to compare the modern and archaeological samples. in addition, Braadbaart *et al.* (2017) applied principal components analysis to identify the relationships between the modern and archaeological material according to the levels of CaO and SiO_2 (figure 3.8). Dung and peat fuels are identified as the most likely fuel sources among the Vlaardingen samples based upon the high levels of silicon and low levels of calcium (Braadbaart et al 2017). When considering the frequency of opal phytoliths, the archaeological samples are associated to both cow dung and peat fuel. Braadbaart *et al.* (2017) discusses the potential loss of more friable charred material from peat and dung fuels, and suggests that

avoiding flotation and sieving prevents the loss of some of the more fragile material. The work of Braddbaart *et al.* (2017) uses modern analogues only heated to one temperature limiting the potential for identifying fuels that were heated to higher or lower temperatures to be identified. In addition, the use of more analyses creates more variables and increase the efficacy of principal components analysis for identifying the relationships between modern and archaeological fuels and increase the accuracy of fuel identification.

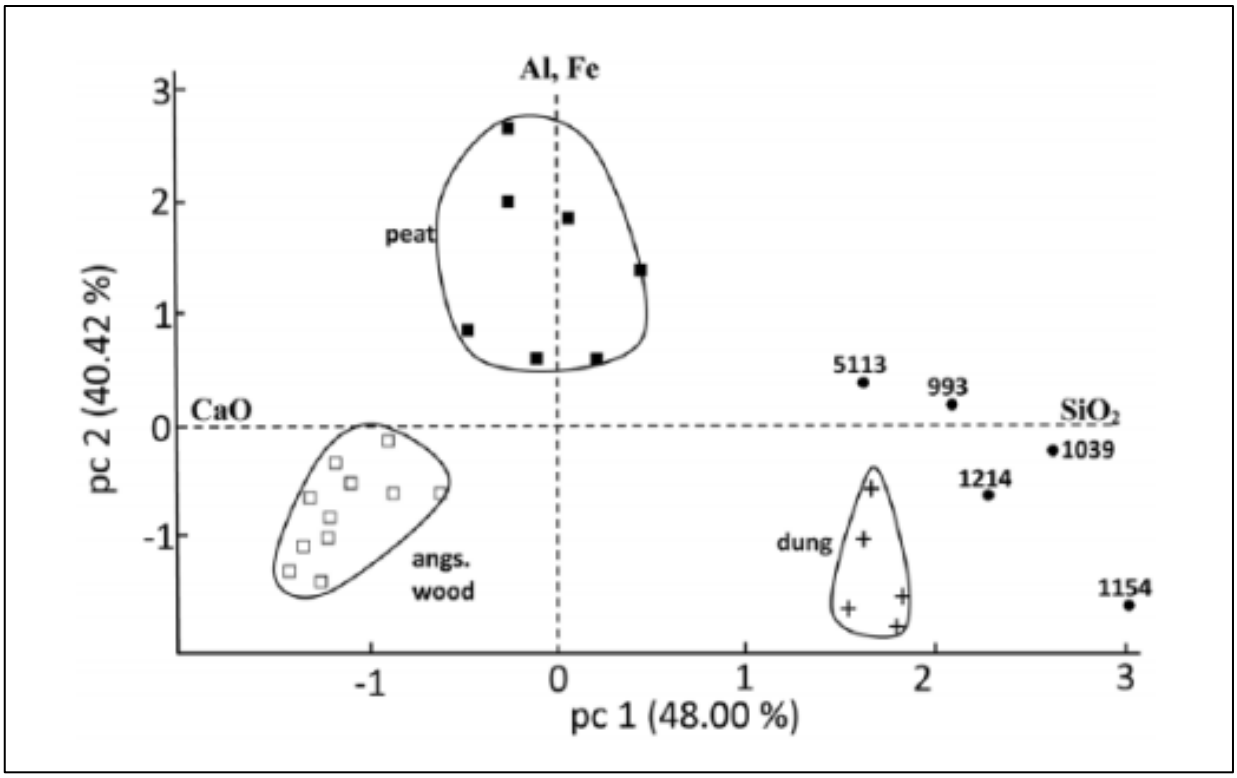

Figure 3.9 Score plot of principal component analysis of the chemical analyses of the reference and archaeological ashes. The archaeological ashes are the mean of five measurements. The horizontal 0-axis shows the directions where CaO (left) and SiO2 (right). Source: Braadbaart (2017).

Hall *et al.* (2008) explored the use of stable carbon isotopes among charcoal from the Middle Stone Age site of Sibudu Cave, KwaZulu-Natal, South Africa and modern charcoal prepared at 450^0C with wood collected from Seaton Park (KwaZulu-Natal) and Kloof (Eastern Cape) South Africa to determine their potential in providing environmental proxies to the past. The modern analogues showed that stems, branches, and charcoal preserve proxy environmental data relevant to rainfall, humidity and temperature which would be indicative of the region the vegetation was grown. Hall *et al.* (2008) additionally investigated the depletion of δ^{13}C isotope abundances in wood due to burning, and it was discovered during experimentation that combustion temperatures between 450^{o}C to 500^{o}C affect the carbon isotope signature of charcoal; however, the seasonal and annual isotopic trends from the growth of the tree are retained (Hall *et al.* 2008). The results presented by Hall *et al.* (2008) show the viability of obtaining proxy environmental data using δ^{13}C isotope values from archaeological charcoal, and the viability of using modern analogue materials to aid in the interpretation of data from archaeological samples.

Kedrowski *et al.* (2009) investigated the use of alternative fuel sources at the Swan Point archaeological site in Alaska through the use of GC/MS analysis of fatty acids via fatty acid methyl ester derivatives within hearth residues. Kedrowski *et al.* (2009) was able to identify the use of animal bone from several species as a fuel source, and show the variation in the formation of combustion features when bone is the primary fuel source with the aid of modern analogue bone used as a fuel on a sand substrate. In marginal climates, the need for alternate fuel sources is a concern, given the unpredictability of conditions. In the instance of Swan Point, the bones of prey animals as well as large mammals contributed not only to the diet of the inhabitants but to the need for a readily

available fuel source. According to Kedrowski *et al.* (2009), bone fires produce residues rich in lipids. The fatty acids can be extracted from lipids and identified through their conversion to methyl esters through GC/MS analysis. Kedrowski *et al.* (2009) states that in addition to identifying bone as a fuel source, this method can also be implemented to discern prey species and diet in areas of poor preservation. Burnt bone is better preserved than unburnt; however, this does complicate the identifications. The research of Kedrowski et al (2009) is not only another example of the utilization of modern analogues to aid in archaeological investigation, it also shows the adaptation by humans when wood fuel is not available.

Bellomo (1993) takes a methodological approach to identify combustion features and determine if they were ignited by natural or anthropogenic sources. The approach utilises both field and laboratory analyses. As a result of the multi-method approach, Bellomo (1993) is able to determine if a combustion feature was used for a prolonged period based on soil characteristics established through a series of methods including macroscopic examination, magnetic susceptibility measurements, isothermal remanent magnetization, alternating field demagnetization characteristics, analyses of magnetometer data, and palaeointensity studies. For this research Bellomo (1993) as well studied 28 fires in a range of sedimentary settings that included Virunga National Park, Zaire; Sibiloi National Park, Kenya; and in the State of Illinois to create modern analogue sediments exposed to heating events; temperature data from the fires was also recorded using a flexible thermocouple (figure 3.9). The analytical signatures and macroscopic characteristics of archaeological hearth features show a similarity to modern sediments exposed to multiple burn instances from the experimentation. Matching archaeological sediments to modern analogues that

were exposed to multiple burns or only a single burn provides a means to readily and systematically identify human generated combustion features from single instance burns which would indicate a wildfire (Bellomo 1993). This provides further evidence to the benefits of using experimentation with modern analogues in the investigation of archaeological deposits and the interpretation of their relationship in the palaeoeconomy and palaeoenvironment.

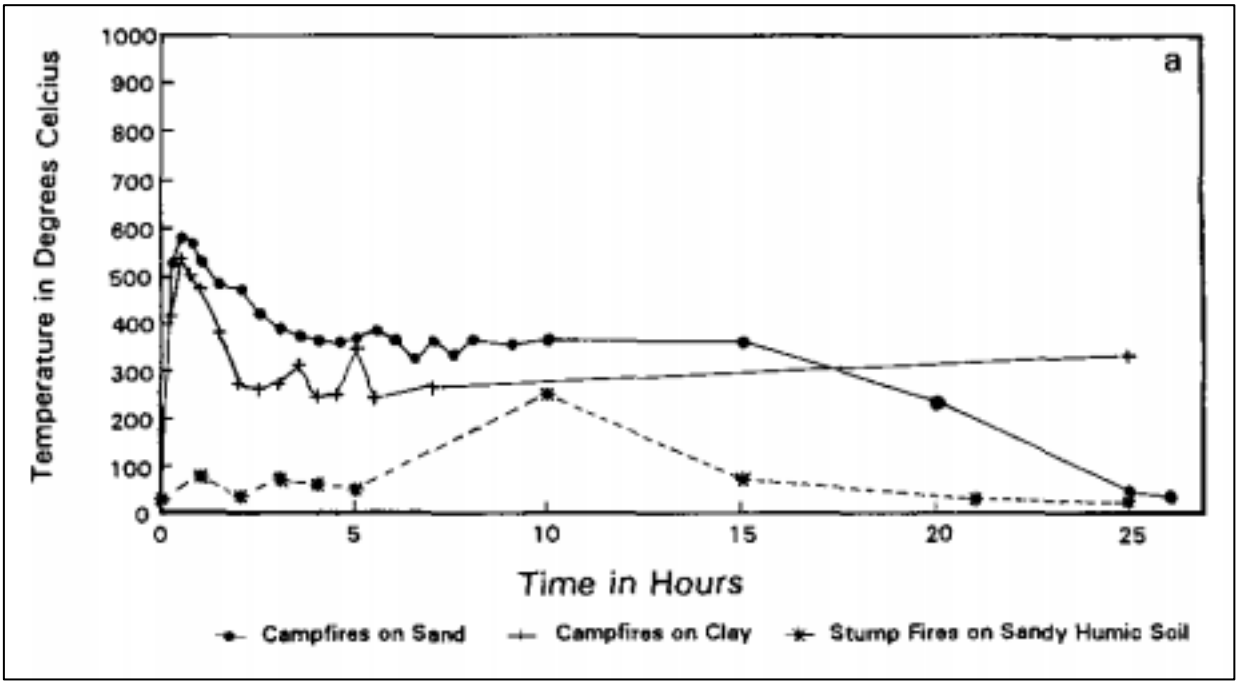

Figure 3.10 Mean surface temperatures for campfires on various sediments. Source: (Bellomo 1993).

3.6 Review of modern ash research

This section discusses the research being carried out on modern ash material. The examination of modern ash can add insight into the development of a method for the identification of archaeological fuels. Modern research that investigates the formation of ash is beneficial in understanding the changes that a fuel goes through during the process of becoming ash (Hagman *et al.* 2013; Maceiras *et al.* 2015; Magdzjarz *et al.* 2016; Du *et al.* 2014).

The work of Etiégni and Campbell (1991) focused on examining the properties of wood ash to aid in the current issue with ash waste. The recycling and disposal

of ash is a growing concern as environmental regulations are becoming increasingly stringent. Investigating the properties of ash has already brought forth recycling ash through its use as an agricultural agent, a binding agent, a base for ceramics glaze, an additive in the production of cement and for the neutralisation of waste (Etiégni and Campbell 1991). Although the research carried out by Etiégni and Campbell (1991) does not cover the analyses of archaeological heating activity residues, the methods used in the study could be beneficial for increasing the reliability of results in archaeological research. The use of homogeneous readily available ash content for the experiments of Etiégni and Campbell (1991) was adapted by using modern analogue samples of ash content to then compare to archaeological samples.The preparation method used by Etiégni and Campbell (1991) is also useful in obtaining quantifiable measurements, and ensuring control over sample size creating more precise datasets. By heating samples over several instances of recurring time and temperature and weighing after each heating and cooling cycle until there is no change in mass, Etiégni and Campbell (1991) ensured that there would be no fluctuation in mass or volume due to exposure to changes in environment such as humidity.

Heikkinen *et al.* (1998) investigates the slagging tendency of peat ash for the power production industry in Finland. The ancient fuel's low energy value makes it a prime fuel in the boilers used to produce power in Finland (Heikkinen *et al.* 1998). The ash produces slag, which can delay or slow down production. By understanding how different peat sources respond to heating, the power suppliers could make more informed and efficacious fuel orders. A multi-method approach was taken to analyse the different peat ash sources including ICP-AES, DCP-AES, X-ray diffraction and scanning electron microscopy. The peat ash

sources and their varying degrees of slagging tendency are then plotted according to the results of the analyses, providing a means of determining which peat fuel sources create the least amount of slag (figure 3.10). The work carried out by Heikkinen *et al.* (1998) can be applied to the analyses of archaeological fuel sources by creating a dataset of characteristics of selected fuels from the region and their associated ash residues.

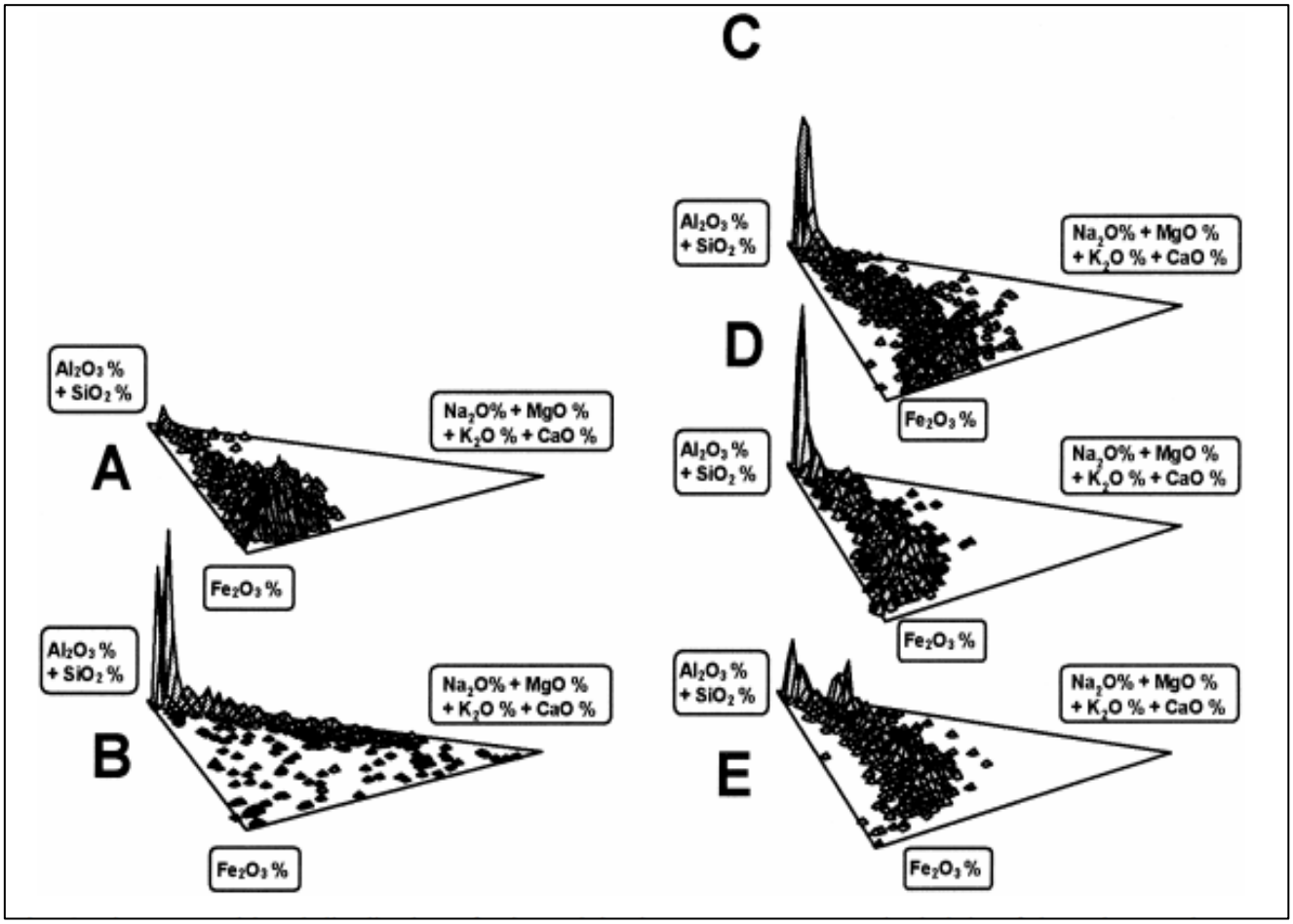

Figure 3.11 The compositional distribution of ash particles in peat types A–E. The height of the column relates to the fraction of particles with the indicated composition. Source: Heikkinen et al. (1998).

The two-part investigation into the behavior of fuel during combustion and the subsequent formation of ash undertaken by Vassilev *et al.* (2013) and Vassilev *et al.* (2014) is a vital resource in understanding the chemical reaction of combustion and its role in the transmutation of fuels into ash and exhaust; the research was carried out to aid in the management of biomass fuel, and inform the designation of uses in different fuel applications. The first part of the research discussed in Vassilev *et al.* (2013) focuses on the behavior of the organic and inorganic matter within fuels during combustion, covering an extensive sample set of 86 varieties of biomass fuels separated into six categories wood and woody biomass, herbaceous and agricultural biomass, aquatic biomass, animal and human waste biomass, contaminated biomass and industrial biomass, and biomass mixtures. With the use of mass spectrometry and laser ablation ICP-MS, Vassilev *et al.* (2013) identified Si, Ca, K, P, Al, Mg, Fe, S, Na, and Ti to observe the transformations in the mineralogy of ashes from different heating temperatures from 500^0C up to 1500^0C. the research concluded that the phase minerals of ash can be classified according to three groups; primary, pre-existing or original minerals that have undergone no transformation during combustion (glass, silicates, and oxyhydroxides) ; secondary, new mineral phases created during combustion from the original minerals with the addition of glass and char (carbonates, oxyhydroxides, glass, silicates, phosphates, and sulphates) ; tertiary, new minerals or mineral phases formed after combustion or during the storage of ash (phosphates, sulphates, chlorides, glass, silicates, and carbonates). According to Vassilev *et al.* (2013), the mineralogy of ash is highly variable between fuel types, and the knowledge of the components of fuel can inform how it performs during combustion. Understanding the behavior of fuel

during combustion and the changes that it undergoes while transforming from raw fuel material to ash is beneficial to the study of archaeological ash and the development of a methodology for the identification of fuel material from ash deposits.

The second part of the work carried out by Vassilev *et al.* (2014) discusses the fusion of ash and the mechanisms responsible for the formation of ash during combustion. In this section of the work, Vassilev *et al.* (2014) used light microscopy, scanning electron microscopy, powder X-ray diffraction, differential-thermal analysis, and thermos-gravimetric analysis to identify the elements and minerals present among ash for the purposes of their classification. The slagging, fouling, fusion of can be detrimental to thermo-chemical conversion equipment, and the work of Vassilev *et al.* (2014) offers a means to identify these potential fuel problems in different fuel types based on their classification using prepared ashes of a variety of fuel types. According to Vassilev *et al.* (2014) this database of ash formation and fuel behaviour during combustion can be used to identify a fuel's potential use based on the characteristics observed such as elemental content and phases of minerals present before during and after combustion; this is a testament to the ability to identify fuels used in the past based on the same markers.

The following example of magnetic research is applied to modern fuels for the purpose of pollution studies (Blaha *et al.* 2008). The examination of coal-fired power plant fly ash demonstrates the application of magnetic measurements to modern samples only, and does not focus on the identification of an unknown fuel source through comparison of modern and archaeological samples (Blaha 2008); however, this investigation does demonstrate the capabilities of magnetic measurements on ash residues to identify mineral content when used in league

with scanning electron microscopy with energy dispersive X-ray spectroscopy. The work of Blaha *et al.* (2008) identified magnetic spherules of magnetite in fly ash which are hazardous to the human respiratory system (figure 3.11). The research of Blaha *et al.* (2008) illustrates the need for filtration systems that eliminate harmful compounds from coal-fired power plants, and also demonstrates the efficacy of magnetic susceptibility measurements used with elemental quantification methods including SEM/EDX and XRF to investigate ash material.

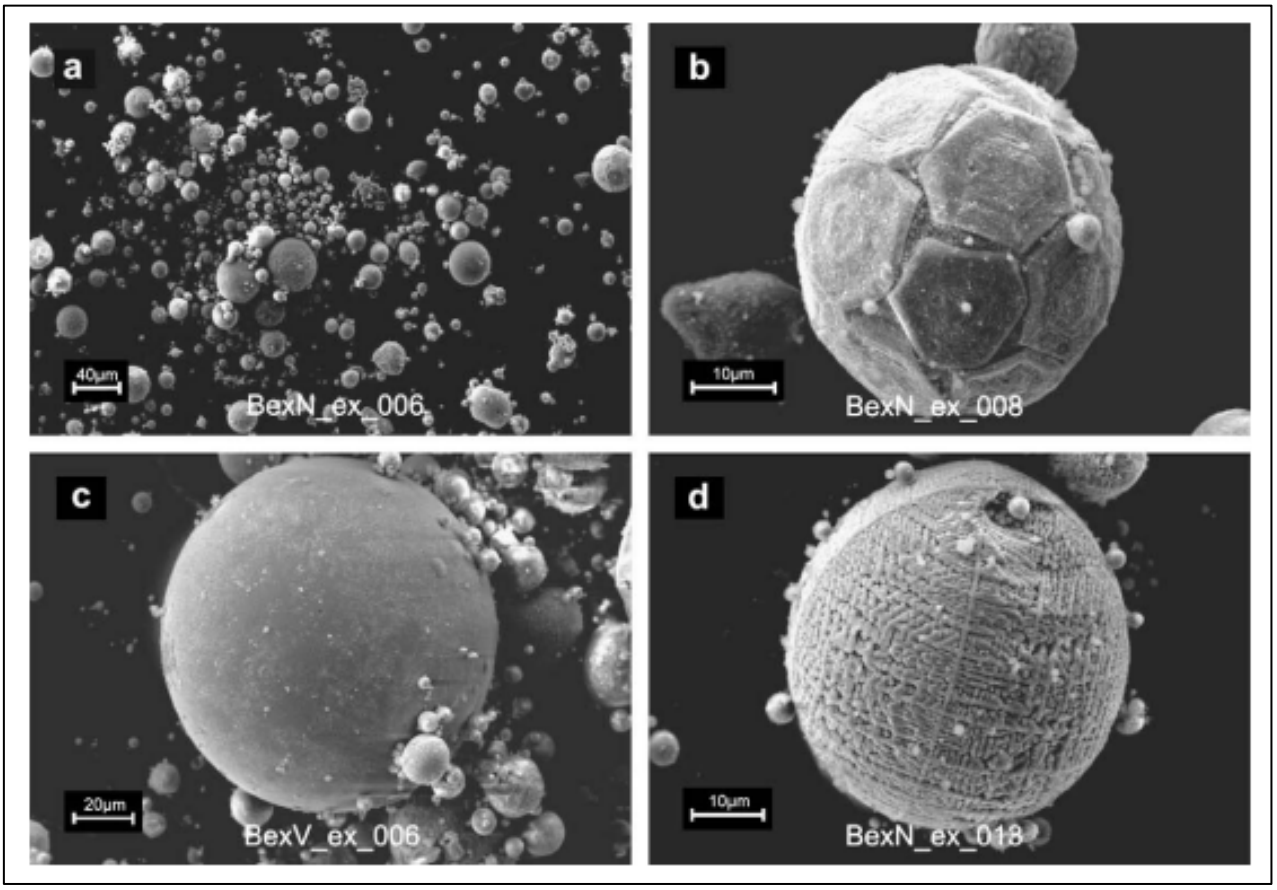

Figure 3.12 (a) Overview of particles from the magnetic extract of fly ash (BexN_ex sample). (b) Magnetic spherule with hexagonal-pattern surface structure (rarely observed). (c) Spherule with smooth orange-peel surface structure (frequently occurring). (d) Spherule with thread-like surface structure (frequently observed).. Source: Blaha (2008).

The work of Ohno (1992) investigated the neutralization of soil acidity and the release of phosphorous and potassium in relation to the application of wood ash. The disposal and recycling/repurposing of ash is a popular area of study as mentioned in section 3.6. The investigation undertaken by Ohno (1992) aimed to discern the chemical properties of a soil that dictates the rate of soil acidity neutralization by wood ash and the release of plant nutrient potassium and phosphorous to determine the efficacy of ash as a fertilizer. The ash was collected from a power plant in New Hampshire, USA that burns 60% hardwood and 40% softwood (Ohno 1992). For the analysis of change to pH of soil, 4 grams of soil was mixed with 40 mL of water and 0.1 g of wood ash, this was repeated for each of the 10 soil samples from local farms and forests (Ohno 1992). The work of Ohno (1992) concluded that there is a relationship between soil pH and rate of wood ash reaction that effects the release of potassium and phosphorous in soils. According to Ohno (1992), the application of wood ash will quickly raise the pH of soils to near neutral, and with monitoring there is little risk to the contamination of water and surface soils with excessive phosphorous or potassium.

In the research of modern fuels SEM/EDX is also a useful technique, being employed by Pedersen and Ottosen (2006) to test the efficacy of electrodialytic extraction in the treatment of copper chromate arsenate treated wood waste ash. The pollution of soil and water from fly ash waste is a common problem near wood burning power plants as mentioned in section 3.6, and the ability to treat waste ash to make it suitable for soil treatment/fertilization is a vital component to waste ash disposal (Etiégni and Campbell 1991; Heikkinen *et al.* 1998). The investigation used samples of both treated and untreated waste ash cast in

epoxy, polished, and coated in carbon. Scanning electron microscopy was used to obtain images of the sample material to assess any differences in the structure of the ash as a result of the electrodialytic remediation. Using EDX spot and area analysis along with element mapping Pedersen and Ottosen (2006) confirmed that arsenic is removed through electrodialytic remediation, but copper and chromium remain unaffected. This is due to the chromium and copper becoming incorporated into the matrix of the ash, while the arsenic is present in calcium arsenate and is almost completely removed from dissolution during electrodialytic remediation (Pedersen & Ottosen 2006). Pedersen and Ottosen (2006) confirm the efficacy of electrostatic remediation in removing arsenic from waste ash, while demonstrating the difficulties with removing copper and chromium due to their association with the formation of ash during combustion.

3.7 Literature review conclusions

This chapter has laid out the literary basis for this investigation through the review of previous archaeological fuel research, modern fuel research, the use of various analytical techniques in archaeological applications, and discussion on the analytical techniques chosen for this project magnetic susceptibility, pH analysis, and SEM/EDX analysis. The numerous investigations into combustion residues and the use of fire by past cultures as discussed throughout this chapter has established the lack of research based on archaeological ash and the identification of fuels. Modern analogues provide a means to investigate the changes fuel undergo throughout combustion, and a multi-method approach to analyses offers a means to accurately identify fuel constituents from ash based on variables from a multitude of factors including elemental components, magnetism, and pH.

The use of magnetic susceptibility data aids both archaeological and modern fuel investigation, and its principles were explained in section 2.8. The minerals present in the fuel material change throughout the process of combustion, just as the minerals in sediments change when exposed to the heat put off by the combustion of fuel (Kanu *et al.* 2014; Kapper *et al.* 2014; Tarling 1999). This enables the use of magnetic measurements to aid in the identification of fuel materials from ash given the unique mineral components of different fuels as shown in the work of Church *et al.* (2007), Dewar *et al.* (2002), Peters and Batt (2002), and Braadbaart *et al.* (2008).

The basic principles of pH and the relevance to this research was discussed in section 2.9. The use of pH in archaeological investigation is almost intrinsically linked to use as part of a suite of methods as seen in Summers (2015). The use of pH analysis is not only valuable for monitoring the changes to fuel exposed to

increasing temperature, but to understanding how the ash reacts within the soil after it is deposited.

The concepts and basic function of the scanning electron microscope and energy dispersive X-ray spectroscopy were discussed in section 2.8 (Goldstein 2003; Pollard & Heron 1996; Pollard *et al.* 2007). Other fuel investigations have used elemental analysis methods including ICPAES, XRF, GCMS, DTMS, and SEM/EDX. For this research, the implementation of SEM/EDX analysis is used to obtain magnified images of samples and elemental analysis to aid in the identification of archaeological fuels from ash samples. The use of SEM/EDX is ideal for this investigation because it is nondestructive and only requires a small sample.

As shown throughout this literature review, the most effective approaches to investigating ash employ multiple analytical methods. Multi method or toolkit approaches provide a comprehensive metric for characterizing ashes by making use of datasets from several techniques. When considering the investigation of ash, there are several methods that provide the best overall dataset for use in the identification of fuels from archaeological ash material. Magnetic measurements such as mass specific magnetic susceptibility and frequency dependence use the minerology and previous heat exposure of the samples to characterise fuel materials and their associated depositional sediments. Elemental analysis techniques such as energy dispersive X-ray spectroscopy show the makeup of the ash material, but also offer a way to corroborate or “ground truth” the findings from other analytical methods. The minerology that is determined through magnetic susceptibility measurements, and the pH of samples that is influenced by certain elements can be confirmed using EDX.

Chapter 4: The ‘fuel’ for the research (Materials)

4.1 Overview

This section discusses the materials that were chosen for analyses focusing first on the modern analogue material then the archaeological samples. Modern analogue material was chosen based on the availability within the Orkneys both today and during the occupation of the archaeological sites where the samples were drawn from as discussed in section 2.2. Collecting the modern analogue material from the same region as the archaeological material being analysed provides the closest replication of the ash deposited within the archaeological matrix (Church *et al.* 2007; Dewar *et al.* 2002; Bellomo 1993). The exposure to the same soil geology provides the closest equivalence for reproducing ash with the same elemental content, magnetic susceptibility, and pH (Pizarro *et al.* 2012).

Where the previous chapters have introduced themes, and developed the background to the research, this chapter focuses solely on presenting the sample materials.

4.2 Modern analogue material:

Modern analogue materials such as seaweed, driftwood, grasses, cow dung, sheep dung, heather, willow, hazel, cow and sheep bone, and various cuts of peat from several sources were collected throughout the Orkney Islands (with the exception of the animal bones due to logistics). The materials were collected from multiple areas of Orkney dictated by the availability of each material and access to collect it (table 4.1). The locations were the Bay of Swandro near the Knowe of Swandro excavation site on Rousay, the cattle byre near the Langstane house on Rousay, the hillside adjacent to the Taversoe Tuick Cairn site on Rousay, and a small patch of scrub/brush in Twatt on Mainland (figure 3.1).

These materials were considered for this research to create a series of ash samples that were representative of the resources available to the inhabitants of the Orkneys within the chronological scope of this research (section 2.2) Grasses, seaweed tangle, and small brush like heather would be used for tinder to accept an ember and ignite into flame, smaller diameter trees such as willow and hazel, and stalks of seaweed would be ideal for kindling and igniting the main fuel sources such as peat, dung, bone, and driftwood (Fenton 1997: 208-213; Wescott 1999; Boy Scouts of America 2009). The materials used for the purposes of igniting the ember, such as grasses and tinder, and feeding the fire to a size that large fuel can be combusted like kindling is burnt until only negligible amounts remain.

Modern Analogue Sample Summary Table		
Sample Type	**Collection Location**	**Year of Collection**
Seaweed	Bay of Swandro	2015
Driftwood	Bay of Swandro	2015
Grasses	Bay of Swandro	2015
Cow Dung	Langstane House	2015
Sheep Dung	Taversoe Tuick Cairn	2015
Heather	Langstane House	2015
Willow	Twatt	2016
Hazel	Twatt	2016
Animal Bone	Not collected in Orkney	2016
Fozzy Peat	Corrigal Farm House	2016
Middle Peat	Corrigal Farm House	2016
Low Peat	Corrigal Farm House	2016
Highland Park Peat	Highland Park Distillery	2016
Rousay Peat	Langstane House	2015

Table 4.1 A table listing where each modern analogue fuel was collected from and the year.
Source: Author

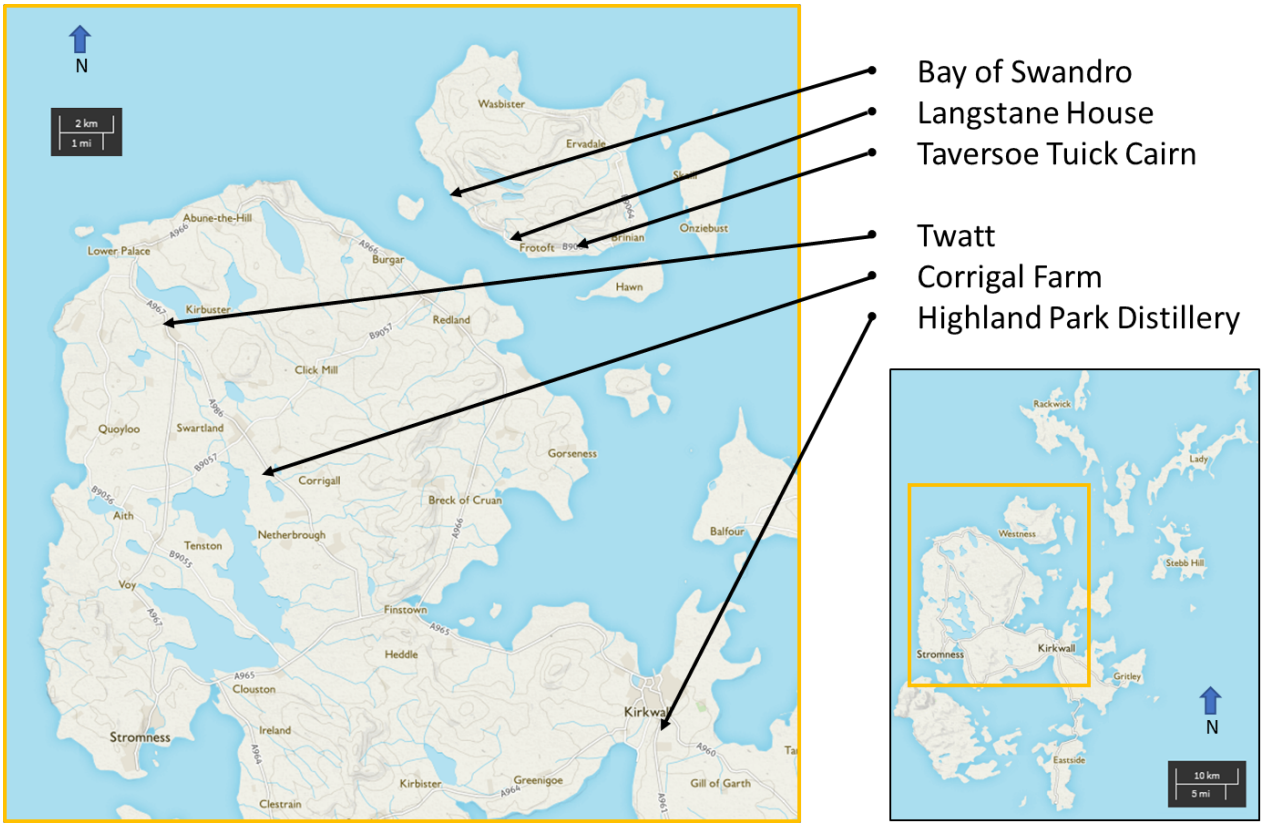

Figure 4.1 Map of Orkney showing the locations where modern analogue fuels were collected.
Source: Google Earth Pro modified by Author

- **Seaweed/Kelp (*Laminaria digitate*)**

The kelp that grows just off the coast of Orkney has a tremendous number of uses including cosmetics, food production, textiles, paper production, dentistry and a fuel once dried (Fenton 1997: 207; Miller 1976: 161). For this project both the leaves and the stalks, or tangle, were collected. This material was harvested by hand from the shores on the Bay of Swandro, Rousay, Orkney.

- **Driftwood (Cedar/*Juniperus virginiana*)**

The driftwood was collected from the beach near the Knowe of Swandro, Bay of Swandro, Rousay, Orkney. The variety of wood that could potentially drift to the North Atlantic could vary quite widely throughout the occupation at some sites; however, this material also shows the attributes of wood soaked in sea water for a prolonged period.

- **Grasses**

The grasses harvested were a combination of holy-grass (*Hierochloe odorata*), brown galingale (*Cyperus fuscus*), bur-reed (*Sparganium eurycarpum*) and branched bur-reed (*Sparganium erectum*). These are all coastal growing grasses that thrive near beeches, and were collected a few meters inland from the Knowe of Swandro, Bay of Swandro, Rousay, Orkney in the fields adjacent to the excavation site.

- **Cow Dung**

The dung was collected from within a byre on a farm adjacent to the Langstane house on Rousay, Orkney. The dung was already mixed with hay which eliminated a step for preparation and made the dung easier to handle. Dung was usually mixed with hay or grass to help it hold shape and be more manageable (Fenton 1997: 208). All of the cattle that produced the dung were fed silage produced using plant material grown on the isle of Rousay.

- **Sheep Dung**

The dung was harvested from sheep that had been grazing on a hill bank near the Taversoe Tuick Cairn, Rousay, Orkney. The sheep are set to graze in different areas of the island throughout the year so their diet is not completely fixed.

The wood fuels were not collected from the small forest located near Finstown due to the restriction to only collect material that had fallen naturally. Although this would have provided a slightly more diverse wood selection, this would have limited the wood samples to only what was available on the ground on the day of collection.

- **Heather (*Calluna vulgaris*)**

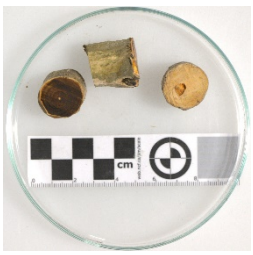

The heather was cut during the pruning of roadside growth, and had been drying for several years. Heather is a very hardy plant and is the vast majority of ground cover in Orkney. Heather grows well in acidic soils, and is an

ideal grazing plant for sheep and cattle. This sample was taken from the pruning of a particularly large heather shrub.

- **Willow (*Salix fragilis*)**

Willow is a deciduous plant that thrives in wet soil conditions, and is known for its resilience and rapid growth. Crack willow was collected for this project near Twatt, Mainland, Orkney. Crack willow produces long straight pliant limbs. This material would be useful in the production of multiple items including fencing, netting, baskets, and skin boat frames in addition to fuel.

- **Hazel (*Corylus avellana*)**

The hazel for this project was collected near Twatt, Mainland, Orkney. Hazel is able to grow in many conditions, it is not as resilient are quick to take root as the willow, but can be cultivated in a similar fashion to produce poles. The hazel also produces nuts which can provide a food source. This material would be useful in the production of multiple items including fencing, netting, baskets, and skin boat frames.

- **Cow and Sheep Bone**

The bones for this project were sourced in Bradford from a local butcher, this was due to the logistics of transporting bones from Orkney to Bradford. Orkney has a long tradition of sheep and cattle grazing. There is abundant evidence among the deposits described subsequently of animal bone and burnt animal bone being present in many of the midden deposits excavated throughout

Orkney. Bone is very dense and saturated with fats that would make it an ideal fuel. The bone obtained in Bradford did not have the same diet as Orkney cattle, and would not have been exposed to the same environment, these differences may be present in the results.

The peat samples are all from the Orkney Islands and consist of three levels from a two-meter peat cutting event at Corrigal Farm House Museum (top, middle, and low), various cuts from the Highland Park Distillery's heather peat field, and middle cuts of peat from Rousay.

- **Fozzy (Fibric)**

Top cut or fibric peat is the material closest to the surface. It still contains a large amount of distinguishable parent plant material, and is soft and springy when dried. Fibric peat is the least dense and lightest in colour, often a shade of medium brown to reddish brown.

- **Middle (Hemic)**

Middle cut or hemic peat is the intermediate layer between the fibric and sapric layers. Some of the parent plant material is distinguishable, yet there is a considerable amount of decomposition. This layer of peat is brittle and hard once dried, yet not as dense as sapric peat.

- **Low (Sapric)**

Low cut or sapric peat is the portion located on the bottom of the peat deposit. It is the densest and darkest of the peat cuts, and has similar characteristics to coal. Sapric peat

consists of the most decomposed plant material, and the parent plant material is unrecognizable to the naked eye.

- **Highland Park Heather Peat**

The Highland Park Distillery in Kirkwall, Orkney provided peat from their heather peat fields. The subsequent preparation and analyses was carried out using a mixture of fibric, hemic and sapric cuts of Highland Park peat due to the amount available and the manner in which it is stored at the distillery.

- **Rousay Peat**

The peat collected on the isle of Rousay, Orkney was cut several years ago, from a field on the island and put into storage at the Langstane house. The cuts consisted only of middle (hemic) cuts of peat.

4.3 Additional modern sample material

In addition to modern analogue fuel material, samples were also collected to examine ashes from uncontrolled modern burning environments like fire pits and hearths. Ash was collected from an open fire pit used as part of a PhD project firing pottery fueled with Caithness peat extracted from the Causymere site and pine (Copper 2015). Peat from two different sources, Caithness and Orkney, burned separately in the hearth at the Corrigall Farm House Museum in Orkney. The Orkney peat ash from the Corrigal museum was collected directly from the hearth, and is the same peat that was collected for producing modern analogue ash. The Caithness peat ash was collected from an ash dump and consists of ash from several different burning events. The peat ash from the museum provides a means to investigate single fuel source ash from an uncontrolled setting.

Figure 4.2 from the left: Modern peat and pine ash, Caithness peat, and Orkney peat. Source: Author

4.4 Archaeological material:

Samples of hearth material, midden, and ash deposit from the Ness of Brodgar, the Knowe of Swandro, and Smerquoy/Muckquoy were chosen for this investigation into fuel use as discussed in section 2.12 (table 4.2). Where the background chapter discussed the sites location and histories, this section focuses on the sample material from the excavations being used for this investigation. Due to the availability of sample material, there is a temporal gap between the Neolithic and the Pictish periods. The Cairns in South Ronaldsay would have been an excellent source of samples to represent the Neolithic through the Iron Age, but samples were not available. In addition, samples from the Bronze age would have been useful as well; however, sites from this period are often burials and not occupation sites.

The following is a detailed description of each archaeological sample with consideration to color, inclusions, structure, and context relationships. The sample descriptions are organized by context number, site and year of collection. A Harris matrix has been generated for each sample set to demonstrate the relationship between materials for each given year of collection and for each site respectively. The ability to view samples stratigraphically aids in the identification of changes to patterns in fuel use with respects to related deposits such as hearths and middens.

The archaeological sample material is presented in stratigraphic order, the Harris matrices created for each archaeological site represent the excavation year the samples were collected and show the associations of only the related sample material and structural features associated to this research. Considering the archaeological data in terms of stratigraphy can provide a means to study the changes, if any, to fuel resource utilization over time, and variations in use

of fuels between functional areas and structures within individual settlement/occupation sites. All of the following context descriptions are taken from the context cards provided by the excavation teams with additional information added by the author when needed.

The archaeological material is all associated with heating activities such as hearth material, hearth rake out, ash dumps, or midden layers with the presence of heating residues. Most of the heating activity associated with housing would be from within a hearth; however, there are also secondary combustion features such as ovens that use embers from the hearth to cook food (figure 4.3). Most Neolithic hearths fall into two categories, either a scoop hearth that is dugout, round, and sometimes lined with clay, or a rectangular hearth that is lined with stone (figure 4.4). The stone lined hearth comes later in the Neolithic, but by the Pictish period it is the standard for hearth construction in Orkney.

Figure 4.3 A photo of a dwelling from the Skara Brae settlement with the hearth indicated in orange sand (top) and a photo of an oven feature from an iron age structure at the Knowe of Swandro (bottom): Source Historic Scotland.

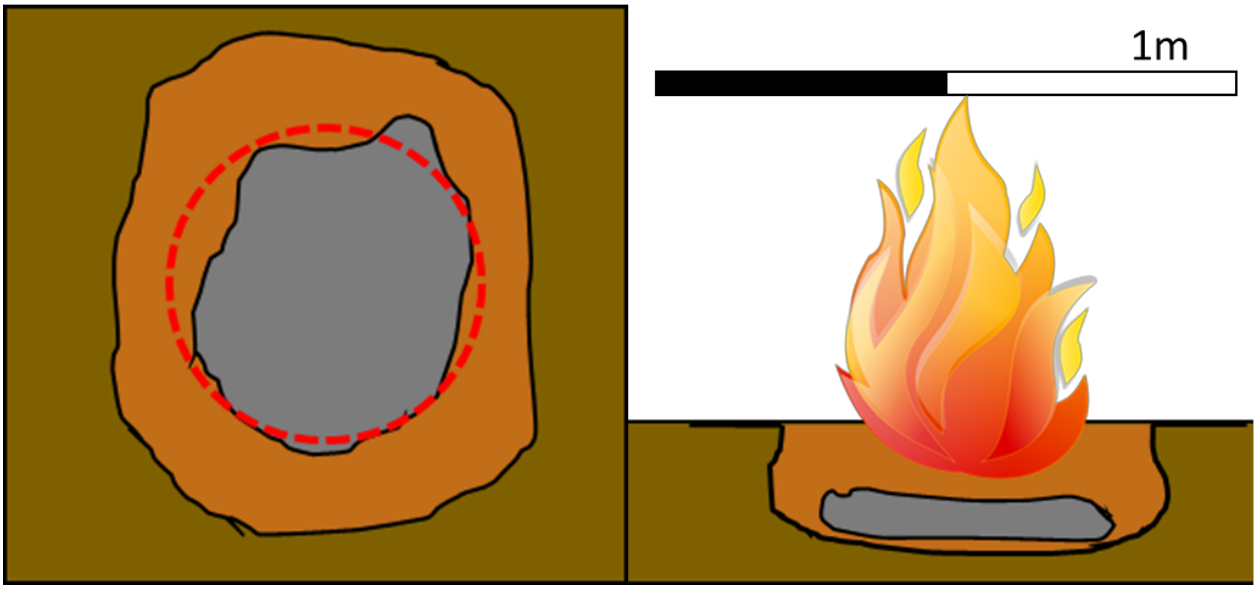

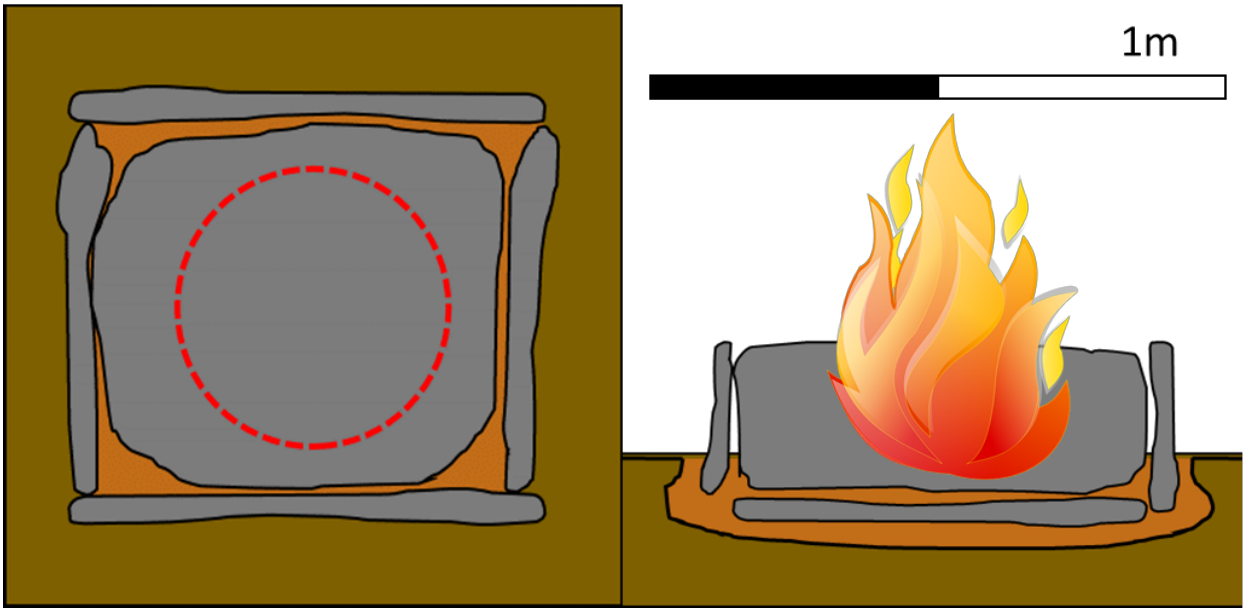

Figure 4.4 Drawing of hearths in elevation perspective on the left and plan perspective on the right. The dashed circles represent the fire in elevation perspective the colours represent grey for stone, brown for soil, and reddish brown for heat effected material. with scoop hearth on the top and a rectangular hearth on the bottom. Source Author.

Archaeological Sample Summary Table		
Site Code & Context	**Sample Type**	**Year of Collection**
NoB 2617	Hearth rake out	2015
NoB 3851	Hearth rake out	2015
NoB 3857	Hearth rake out	2015
NoB 4264	Ash dump	2015
NoB 4656	Hearth	2015
NoB 4674	Hearth	2015
NoB 5332	Ash dump	2015
NoB 6156	Ash dump	2015
NoB 5013	Hearth	2015
NoB 3783	Ash dump	2015
NoB 3851	Hearth rake out	2016
NoB 6339	Hearth	2016
NoB 6346	Hearth	2016
NoB 6348	Hearth	2016
NoB 6351	Hearth	2016
NoB 6354	Hearth	2016
NoB 6355	Hearth	2016
NoB 6356	Hearth	2016
NoB T 4825	Midden	2016
NoB T 4831	Midden	2016
NoB T 4860	Midden	2016
NoB T 5810	Midden	2016
NoB T 5849	Midden	2016
NoB T 5855	Midden	2016
KoS 2039	Hearth	2015
KoS 3081	Midden	2015
KoS 3196	Midden	2015
KoS 3201	Midden	2015
KoS 3217	Midden	2015
KoS 3225	Midden	2015
KoS 3238	Midden	2015
KoS 3255	Midden	2015
RDL 031	Midden	2015
RDL 001	Midden	2015
RDL 004	Midden	2015
RDL 006	Midden	2015
RDL 009	Midden	2015
RDL 007	Midden	2015
RDL 013	Midden	2015
RDL 016	Midden	2015
RDL 023	Midden	2015
RDL 032	Midden	2015
SMQ A	Hearth	2015
SMQ B	Hearth	2015

Table 4.2 A table listing each archaeological sample by context showing the sample type and the year it was collected Source: Author

4.4.1 The Ness of Brodgar 2015 excavations

The Ness of Brodgar 2015 season was the first year that samples were collected for the project. The samples were drawn from the main trench P, and were hearth samples from several structures including structures 1, 7, 8, 12, 14, and 19 (figure 4.4 & 4.6). The samples from the Ness of Brodgar were chosen to show the sites relationship with fuel. To accomplish this, hearth samples were taken in sequence from several areas of in situ burning from hearth features in structures 8 and 14, deposits of ash from deposits in structures 1, 7, 12, and 19, and a series of ash midden deposits in trench T. This provided the opportunity to look at fuel use from within the stratigraphic sequence of a hearth as well as the deposits of ash from other areas of the site to create a comprehensive interpretation of fuel use at the Ness of Brodgar.

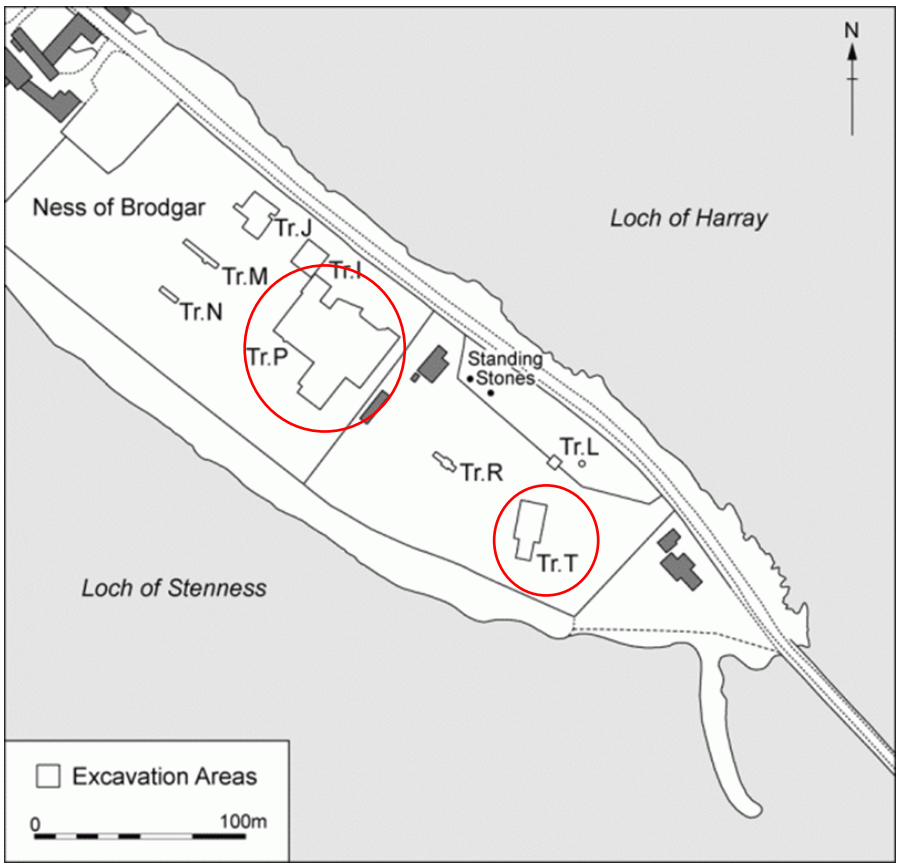

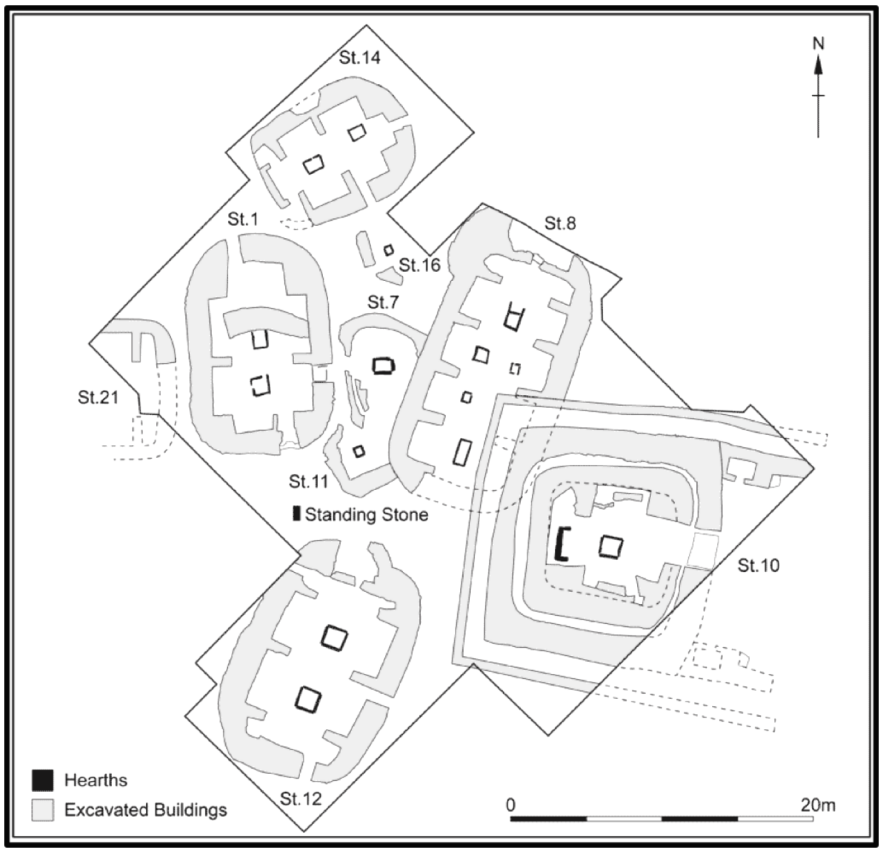

Figure 4.5 left to right: A site plan drawing of the Ness of Brodgar showing all of the excavation trenches, trench P and trench T shown with red circles(top left) next a plan drawing of the Ness of Brodgar excavation trench P (bottom right). Source: Orkneyjar.com

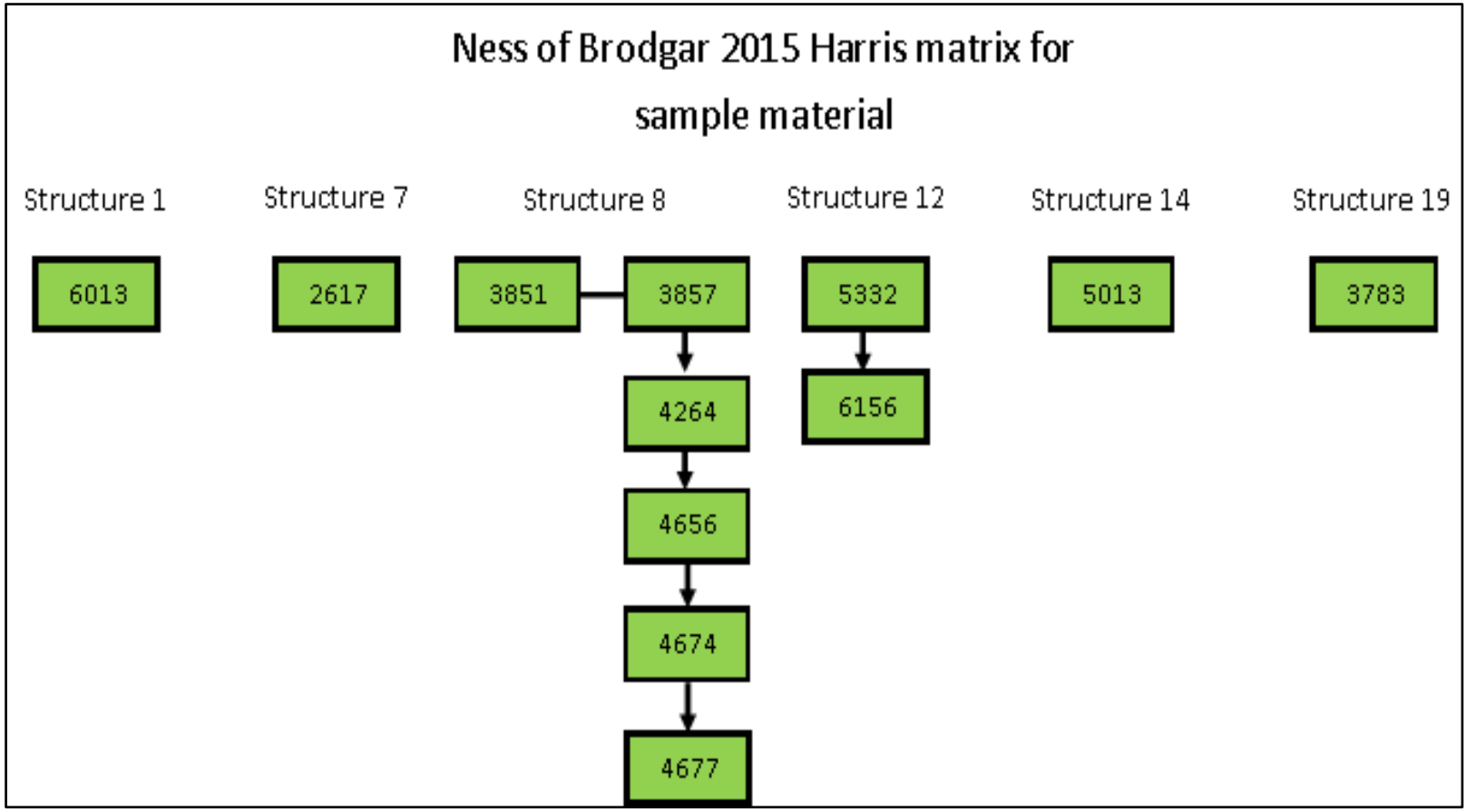

Figure 4.6 Harris Matrix for the 2015 Ness of Brodgar samples. Source: Author

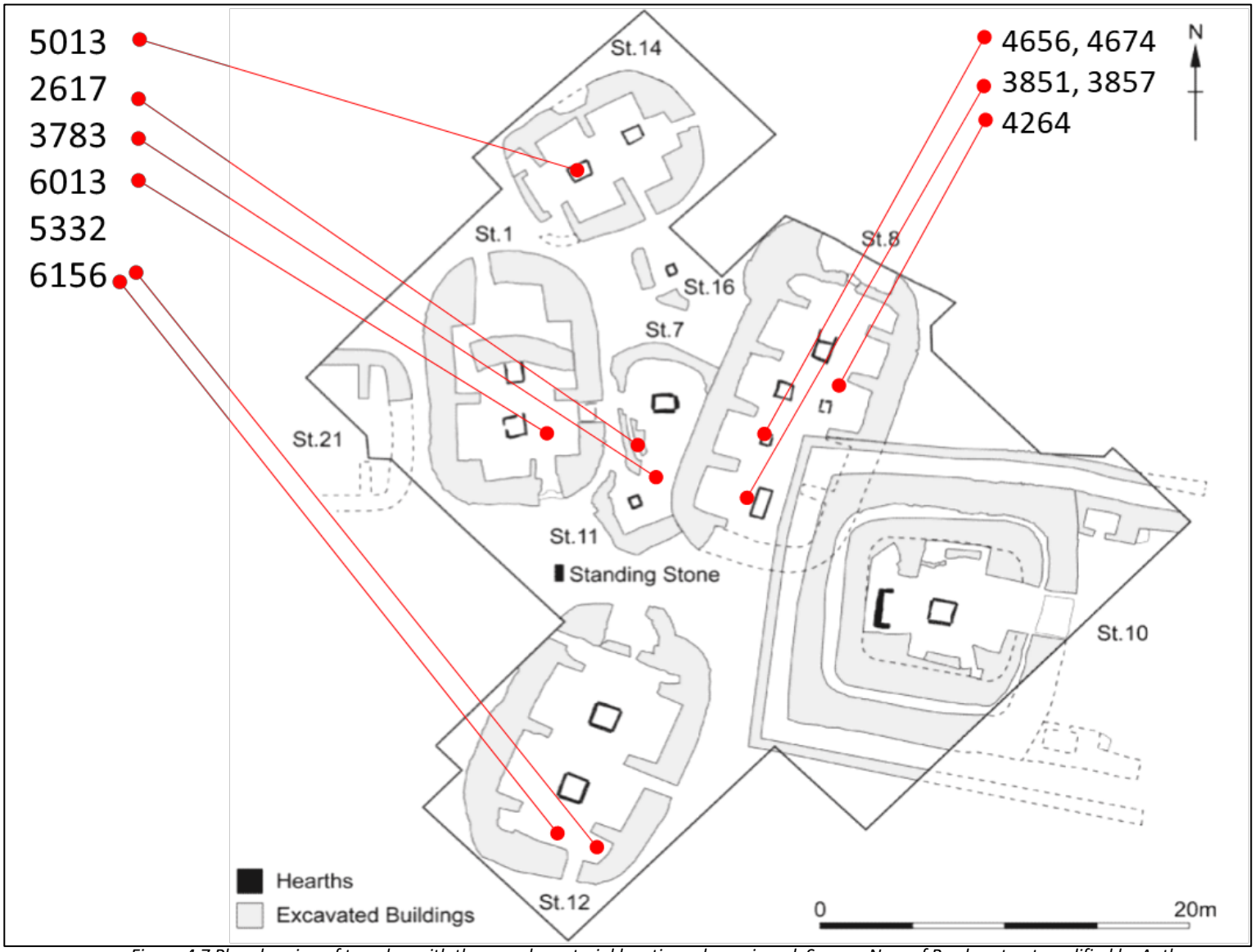

Figure 4.7 Plan drawing of trench p with the sample material locations shown in red. Source :Ness of Brodgar trust modified by Author

- **NoB15 [6013]**

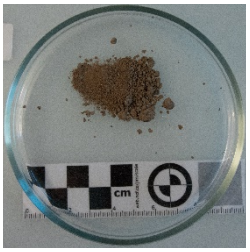

Reddish brown sandy silt with yellow and black mottles and black, red, and yellow flecks in Structure 1. Mixed deposit south and west of pier [1068], likely more than 1 deposit. Occupation layer with mixed ashy deposits, possibly trampled from hearth or a dump of ashy material.

- **NoB15 [2617]**

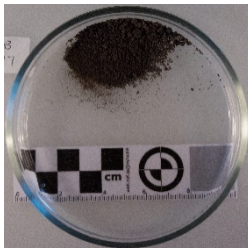

Dark grey/black ashy clay silt with dark grey to black charcoal mottles with frequent flecks of burnt bone <1cm ^{2} + subangular pieces of heat-affected sandstone. Flat, almost triangular slabs set on top of this layer may have been used to perch around the hearth. Floor deposit/ashy hearth rake out in Structure 7.

- **NoB15 [3851]**

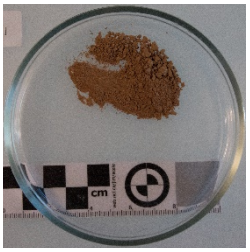

Bright pink-red clayish silt material derived from hearth rake out or spilling out of hearth [3852] within Structure 8. The deposit includes charcoal, burnt stone and burnt red clay in small amounts. Material could be the same as [3857] that is focused on the north eastern orthostats themselves.

- **NoB15 [3857]**

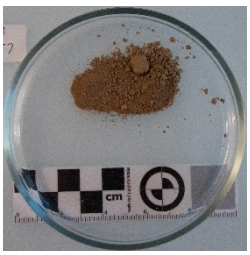

Bright orange pink silty clay deposit located on and spilling over hearth [3852] within Structure 8. This represents heat effected material raked out from the hearth. This material is located below context [3851] in the stratigraphic sequence.

- **NoB15 [4264]**

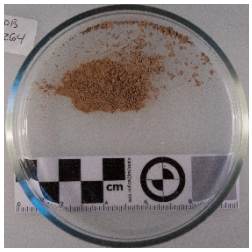

Bright orange pink silty clay with very few tiny fragmented burnt degraded subangular sandstone flecks in Structure 8. Dump or raised deposit of burnt very mixed and patchy material, variegated black charcoal and burnt red silt. The deposit was rather sterile, could be rake out of oven feature associated with firing pottery.

- **NoB15 [4656]**

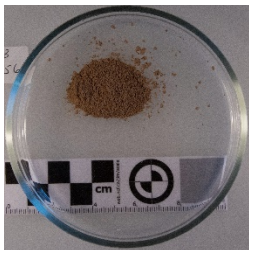

Mid reddish yellow clay silt deposit with little clay and small inclusions of charcoal. In situ burning in west hearth (6309) in Structure 8.

- **NoB15 [4674]**

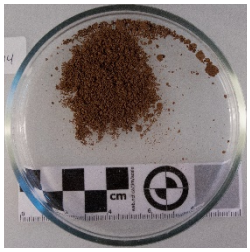

Medium pink and red clay silt burning layer within west hearth (6309) in Structure 8, shows evidence of intense heat.

- **NoB15 [5332]**

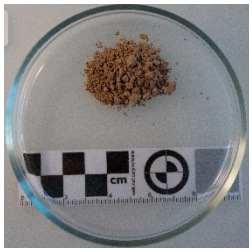

Fairly thick layer of bright orange clayey silt mottled with pale clay and heavily flecked with paler and darker speckles. This suggests this is composed of homogenized peat ash or similar parent material. Further excavation indicates this is the latest layer in a series of bright ashy laminae that range from orange to pale creamy yellow. This deposit was unlike any other located in Structure 12 with extensive deposits.

- **NoB15 [6156]**

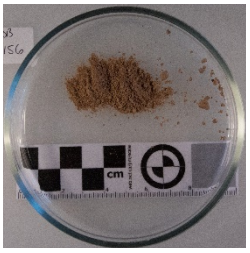

Bright orangey-red deposit in Structure 12, similar to [5332], fairly thick but with more pale brown spots. Part of a series of horizons that alternate between orange and pale yellow. Edges are crisp and un-oxidized, suggesting the material was not due to in-situ burning.

- **NoB15 [5013]**

An oval patch of bright orange and red ashy silt material in Structure 14. The deep colour indicates intense in situ burning this burnt deposit was far more extensive than other higher in the sequence of the west hearth.

- **NoB15 [3783]**

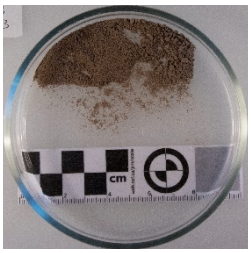

Located in Structure 19. A very mixed, mid-brown pink ashy silty clay deposit that includes frequent flecks of charcoal, burnt stone, bone and peat ash throughout with larger patches of clay + charcoal rich patches, and crumbs of degraded pottery too friable to be small found. Appears to represent a discrete dump along several other contexts ([3775], [3781],[3782]) above it to the south of hearth stone [3707].

4.4.2 The Ness of Brodgar 2016 excavations

The 2016 excavation season at the Ness of Brodgar focused on sampling a series of burnt horizons from two hearths within structure 8. All but 2 of the samples from this field season are from the same hearth feature hearth [6309]. The two remaining samples, 3851 and 5689, were collected from hearth [3852]. Structure 8 has 6 hearths, where every other structure in trench P has one to three hearths (figure 4.7 & 4.8). Structure 8 had a significant relationship with fuel use given the number of hearths, and that is why sampling for this excavation year was focused to this building.

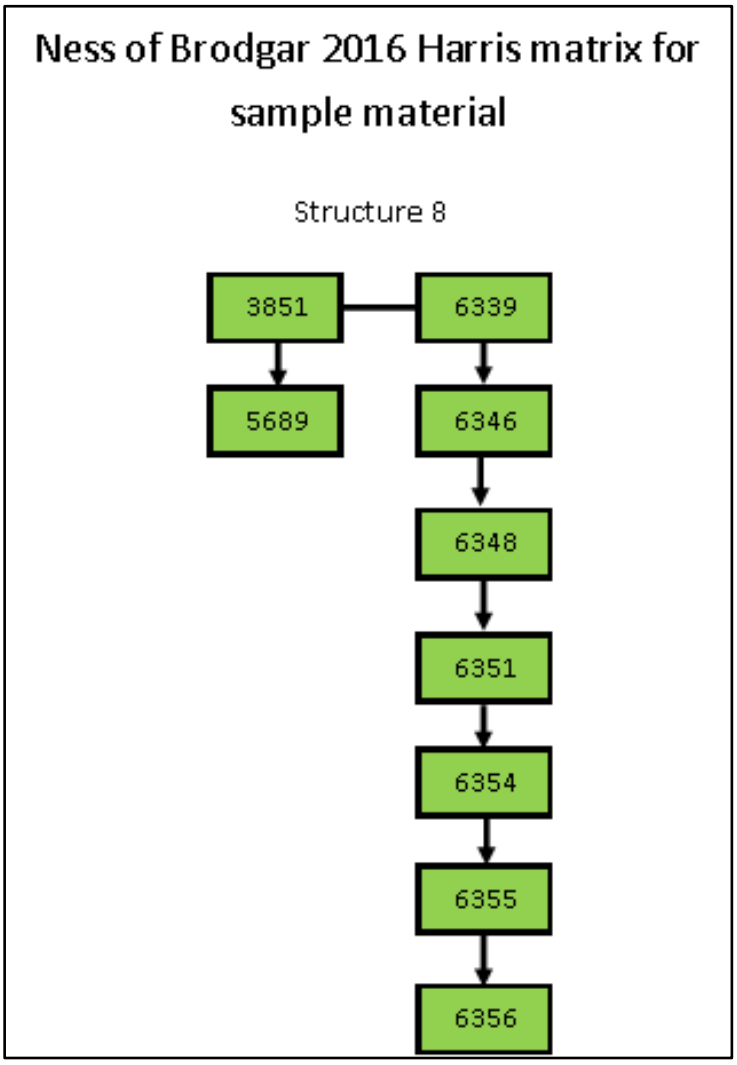

Figure 4.8 Harris matrix for the 2016 Ness of Brodgar samples. Source: Author

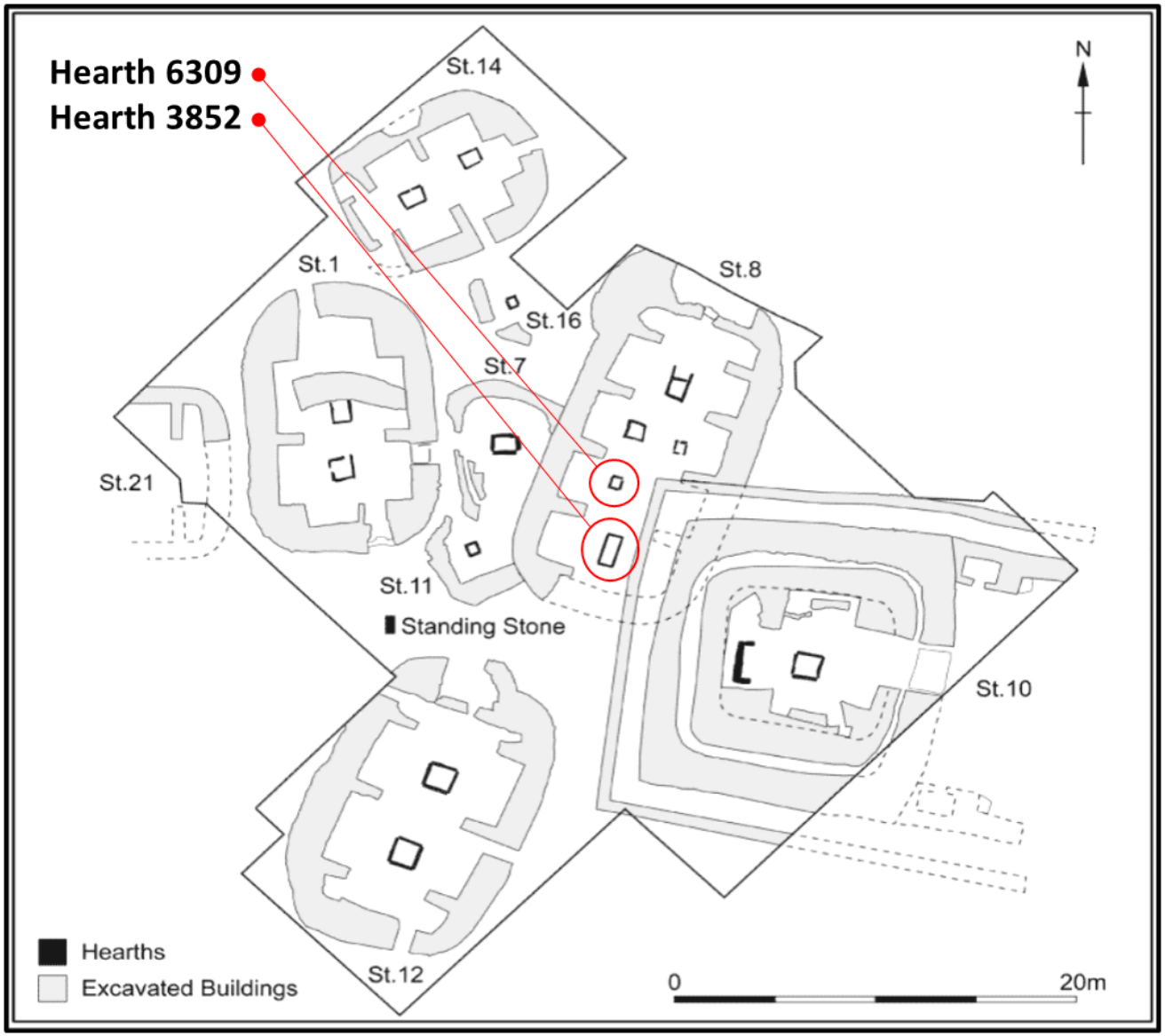

Figure 4.9 A plan of the Ness of Brodgar trench P with the hearths that were sampled from structure 8 indicated in red circles. Source: Ness of Brodgar Trust

- **NoB16 [3851]**

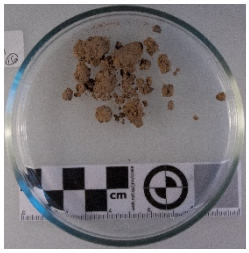

Bright pink-red clayish silt material derived from hearth rake out or spilling out of hearth [3852] within Structure 8. The deposit includes charcoal, burnt stone and burnt red clay in small amounts. Material could be the same as [3857] that is focused on the north eastern orthostats themselves. This context was sampled both in 2015 as well as 2016 to investigate the changes to the samples after a year of exposure to the climate and taphonomic processes in situ.

- **NoB16 [6339]**

Mottled orange brown clayey silt with inclusions of charcoal flecking, ash flecks and fire cracked stone. This deposit is part of hearth [6309] within Structure 8. Deposit contains upper fill of the hearth, and possibly a dump from another hearth. This material is located above context [6346] in the stratigraphic sequence.

- **NoB16 [6346]**

Light grey silty clay with large ash inclusions. This is a small discrete ashy lens within hearth [6309] in Structure 8. A grey ash dump sitting atop in-situ burnt material [6348]. This material is located above context [6348] in the stratigraphic sequence.

- **NoB16 [6348]**

Bright orange red silty clay deposit within Structure 8. The deposit contains inclusions of burnt bone fragments and charcoal flecking. This deposit is an in-situ burnt horizon

from with hearth [6309], and demonstrates evidence of intense burning. This material is located above context [6351] in the stratigraphic sequence.

- **NoB16 [6351]**

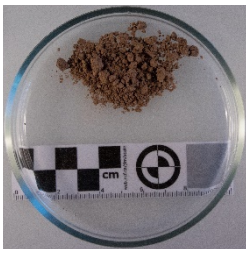

Bright reddish orange clayey sandy silt within Structure 8. In-situ burnt horizon within hearth [6309] notably less heat effected than upper deposits with inclusions of laminated stones likely from the hearth during firing.

- **NoB16 [6354]**

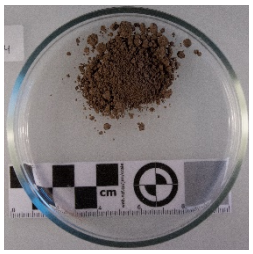

Orangey reddish clay silt with inclusions of ash deposit and charcoal flecking within Structure 8. This material is located below context [6351] and above context [6355] in the stratigraphic sequence. A layer in hearth [6309] potentially in situ burnt horizon or heat effected soil.

- **NoB16 [6356]**

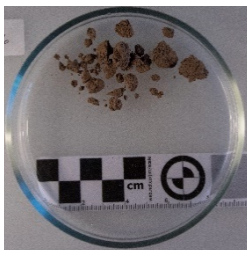

Orange light brown silty clay with inclusions of ash, charcoal and burnt bone flecks. Ashy burnt deposit in hearth [6309] within Structure 8, heavily mottled with varying shades of orange and yellow. This material is located below context [6355] in the stratigraphic sequence.

4.4.3 Ness of Brodgar Trench T excavations 2016

Trench T is located approximately 50 meters to the west of the main excavation and contains a substantial midden as well as an intruding circular structure dating to the Iron Age some 2,000 years ago, this reuse of existing structures is common in the Orkneys (figure 4.9 & 4.10) (Towers *et al.* 2015: 2-3).

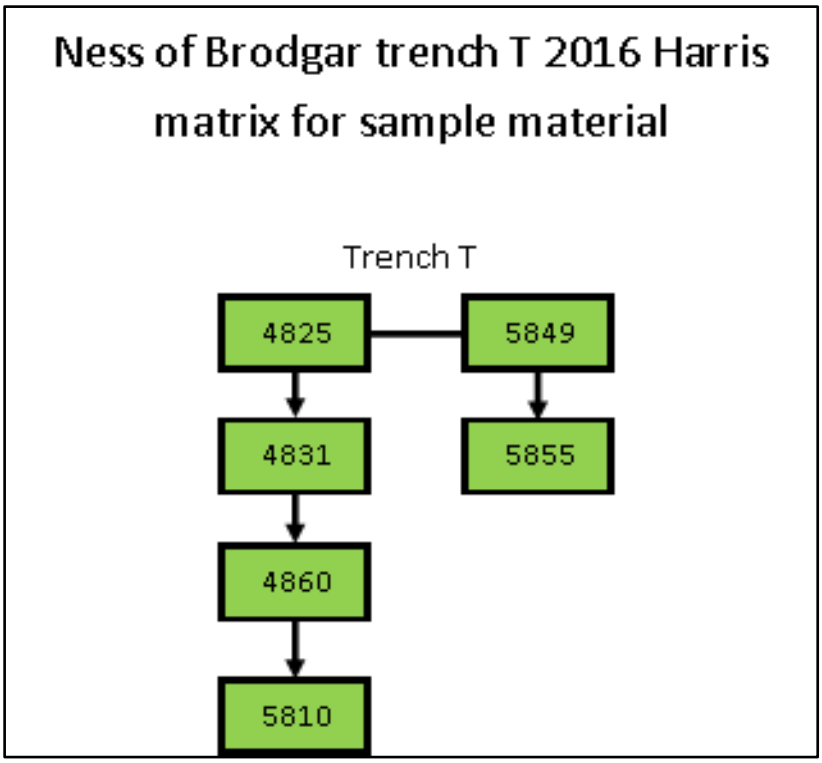

Figure 4.10 Harris matrix for the 2016 Trench T samples. Source: Author

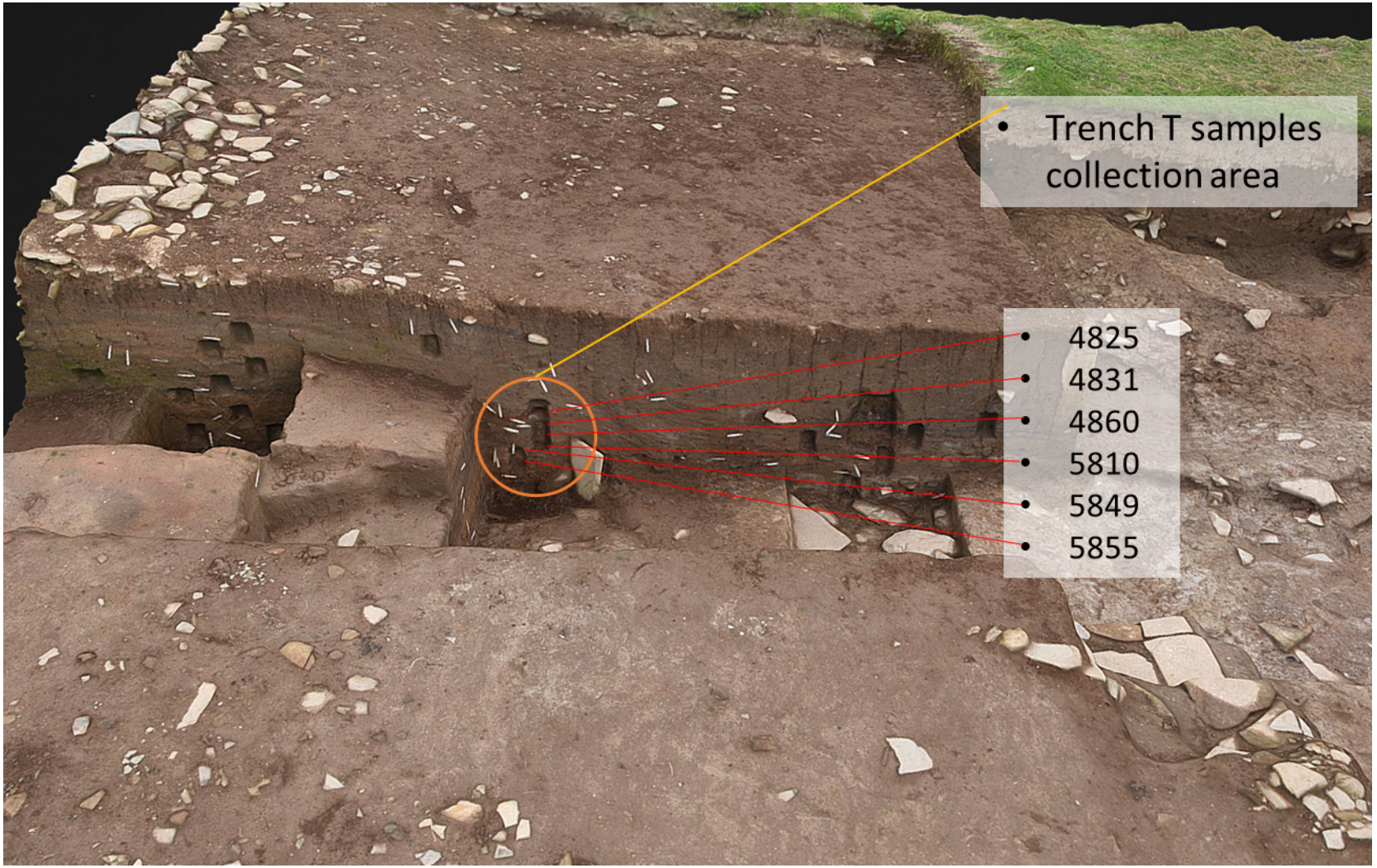

Figure 4.11 A photograph of the Ness of Brodgar Trench T with the area of midden where the samples were collected outlined in orange, and the sample contexts shown with red lines. Source: Ness of Brodgar Trust modified by author.

- **NoBT16 [4825]**

Mid greyish black silt with small amounts of burnt bone flecks. Appears to have large amounts of burnt material. This ashy midden deposit is part of a series of midden deposits laid around the base of the mound near Trench T.

- **NoBT16 [4831]**

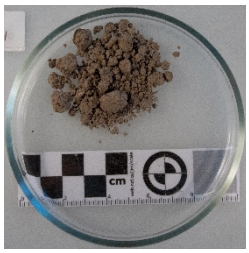

Mottled grey orange brown clayey silt with small inclusions of burnt bone and angular stone. This deposit is extremely heterogeneous, mottled with grey, black, orange and yellow patches, in the center was a ring of concentric circles of different coloured midden deposits. A collection of small dumps of midden material at the base of the mound.

- **NoBT16 [4860]**

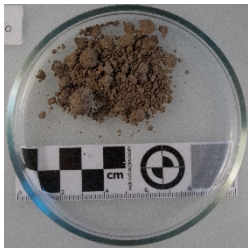

Mid yellowish brown clayey silt with flecks of orange and yellow peat ash and angular sandstone. This is a redeposited midden possibly used to build up the ground level in the area.

- **NoBT16 [5810]**

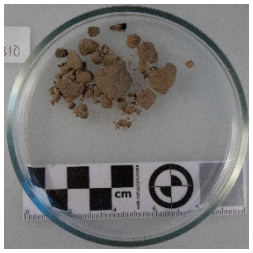

Orange brown clayey silt with inclusions of occasional sub angular flagstone, charcoal, light greyish yellow firm silty clay, sub angular burnt flagstone, and burnt clay. This context was used as a midden from a space nearby for a long period, possible food waste and hearth sweepings. This deposit contained a large amount of pottery and animal bone.

- **NoBT16 [5849]**

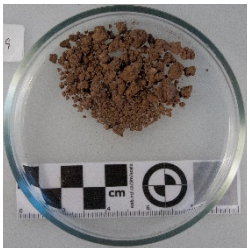

Medium red silty clay with no inclusions. This deposit is part of the series of midden dumps that contributes to overall midden heap accumulation, and represents the top of levelling of midden deposits with group Context [5842].

- **NoBT16 [5855]**

Dark grey brown clay silt deposit with frequent inclusions of burnt bone. The deposit is a thick horizontal band with a high frequency of burnt bone and pottery. This could be midden enhanced soil that separates undisturbed material from the worked material above.

4.4.4 The Knowe of Swandro

The sample material from the Knowe of Swandro was collected from structure 3, with the exception of one hearth sample from structure 2 (figure 4.11). The site and the significance of the structures were discussed in section 2.12.2. These samples consist of midden material rich with limpet shell, ash, and metal working debris. Although the Knowe of Swandro is known for being a coastal excavation and rescue project, structure 3 is located almost completely off the storm beach within the protected area of the Swandro walk (figure 4.12).

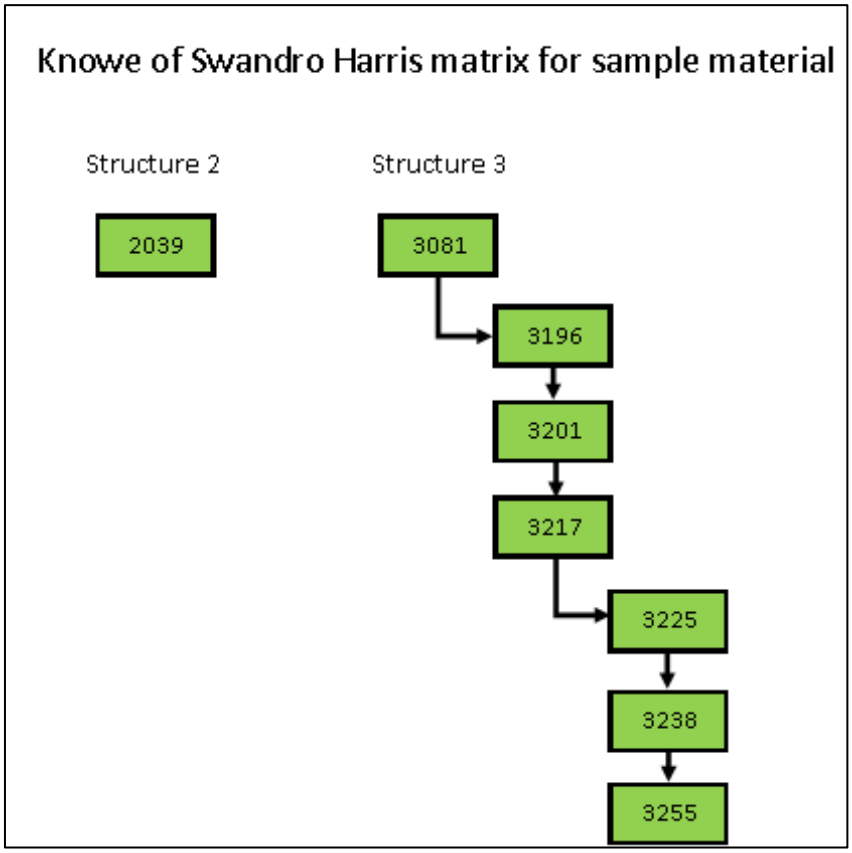

Figure 4.12 Harris matrix for the Know of Swandro samples. Source: Author

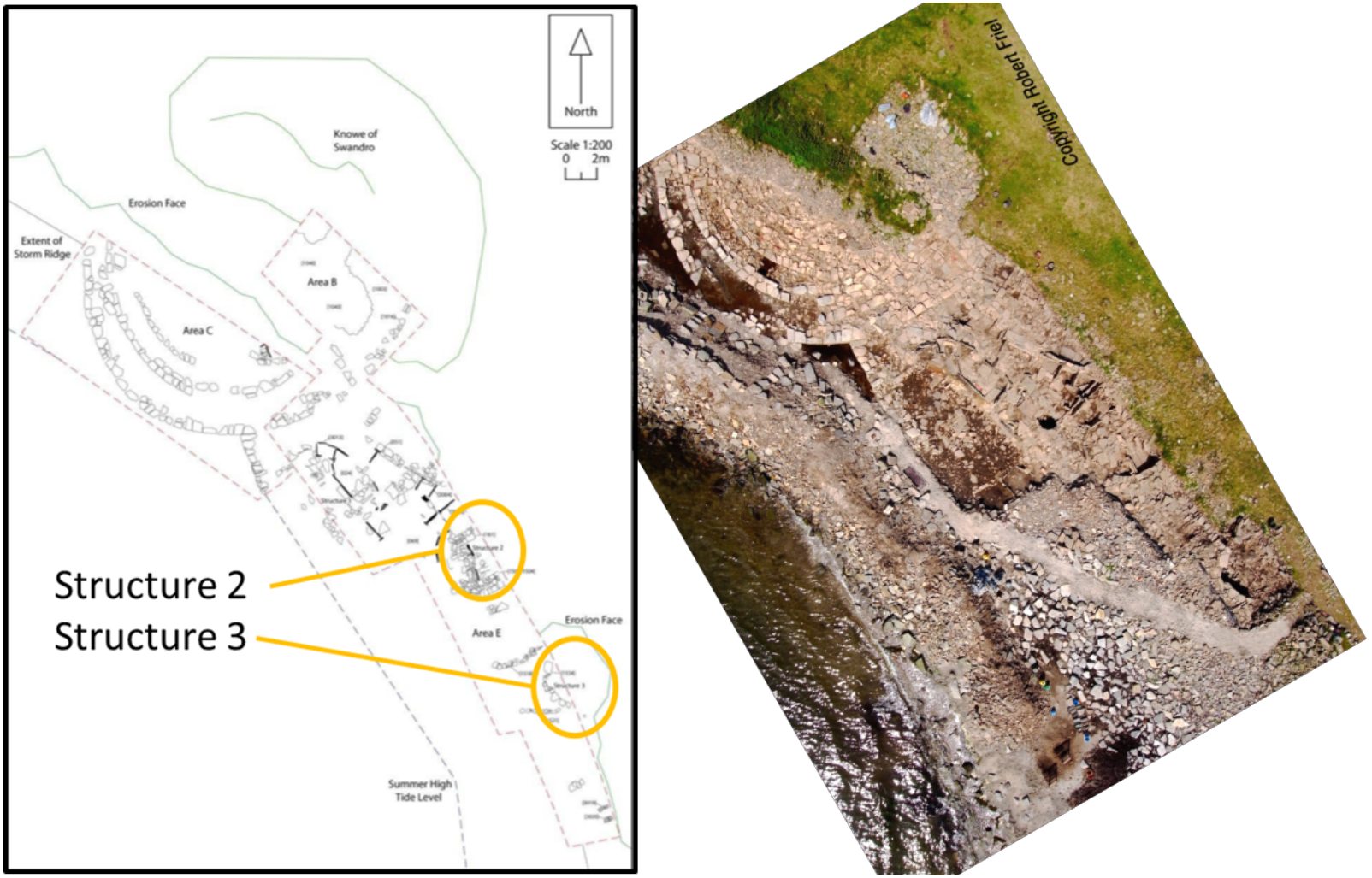

Figure 4.13 A site drawing of the Knowe of Swandro (left) next an overhead view of the Knowe of Swandro (right). Source: Robert Friel

- **KoS15 [3081]**

Small area of rubble that butts orthostat 3069, wall [3080] and wall [3082] in the northeast section of Structure 3. The deposit is brown silty clay loam with varying sizes(1-41cm) of sub-angular inclusions along with limpet shell.

- **KoS14 [3196]**

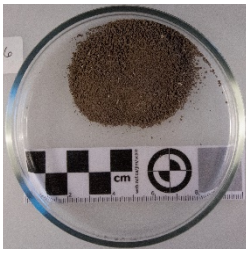

Rubble and dark brown silty clay loam with inclusions of angular, sub-angular, sub-rounded stone (all 9-75cm), and charcoal flecking within Structure 3. This material butts contexts [3195] and [3198], and is sealed by [3197]. Possible fill of kelp burning pit in Structure 3.

- **KoS14 [3201]**

Dark brown silt clay loam with inclusions of angular (4-38cm), 6cm sub-rounded stone and limpet. This context butts orthostat [3202] and walls [3200], [3199], and [3198], and seals context [3217]. Possible midden infill of the annexe/cell/passage to Structure 3.

- **KoS14 [3217]**

Very dark brown silty clay loam material with charcoal flecking and angular inclusions (1-55cm) in annexe/cell/passage to Structure 3. This midden material is sealed by context [3201] and butts wall [3199].

- **KoS14 [3225]**

Brown silty clay loam with inclusions of angular rounded stone (2-20cm) and charcoal flecking. This is part of the midden infill in the annexe/cell/passage to Structure 3.

- **KoS15 [3238]**

Very dark grey silty clay loam with inclusions of angular/sub-angular stone(6-67cm), angular burnt stone(18cm), carbon flecking, limpet and bone. This midden deposit is located in Structure 3.

- **KoS15 [3255]**

Black silty clay loam with yellow mottling and inclusions of sub-angular/angular stone(3-13cm) and limpet (50% of deposit) in Structure 3. This is possibly an equivalent context to [3042]. The material is sealed by contexts [3042], [3096], and [3254]

4.4.5 Smerquoy

The samples collected from the Smerquoy site consisted of hearth samples from two of the Neolithic stone houses as discussed in section 2.12.3 (figure 4.14).

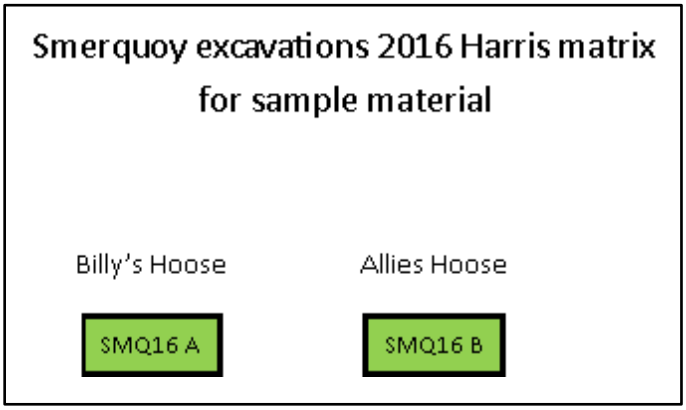

Figure 4.14 Harris matrix for sample from Smerquoy. Source: Author

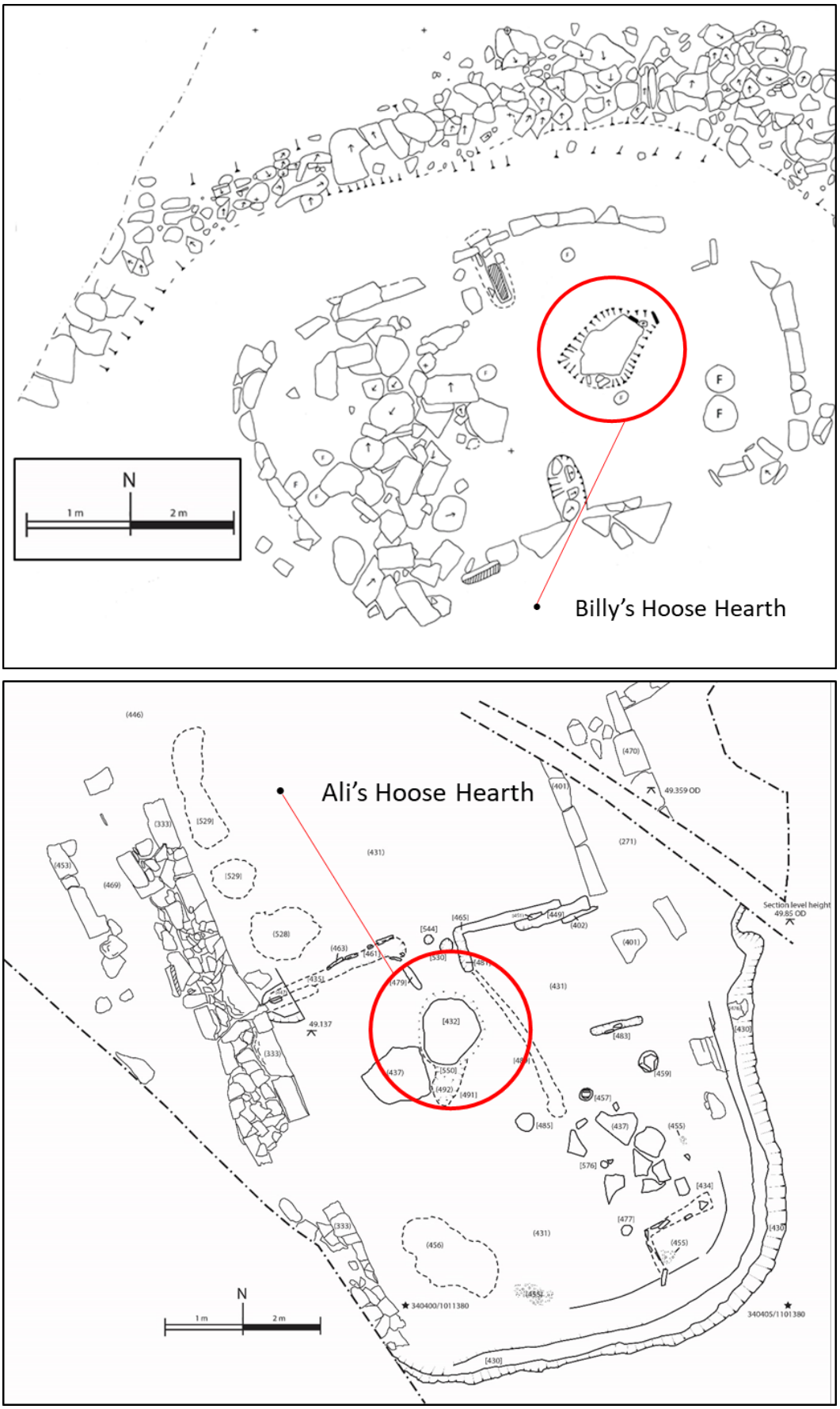

Figure 4.15 Plan drawings of Billy's Hoose (top) and Ali's Hoose (bottom) with the hearth feature shown in red circles. Source: Chris Gee modified by Author.

- **SMQ16 A**

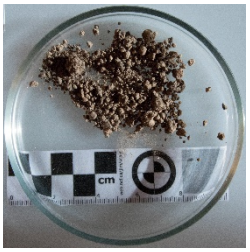

Orange yellow sandy silt with inclusions of charcoal. Hearth feature within the structure called Billy's Hoose. This feature was approximately 1x2 meters in in size.

- **SMQ16 B**

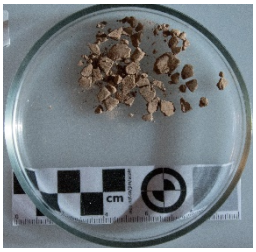

Yellow, red, orange silty material with inclusions of charcoal. Upper ashy layer fill of sloop hearth feature located within Allie's Hoose.

4.4.6 Muckquoy

As discussed in section 2.12.3, Muckquoy is a Neolithic settlement site. The following describes the samples from this excavation (figure 4.15 & 4.16).

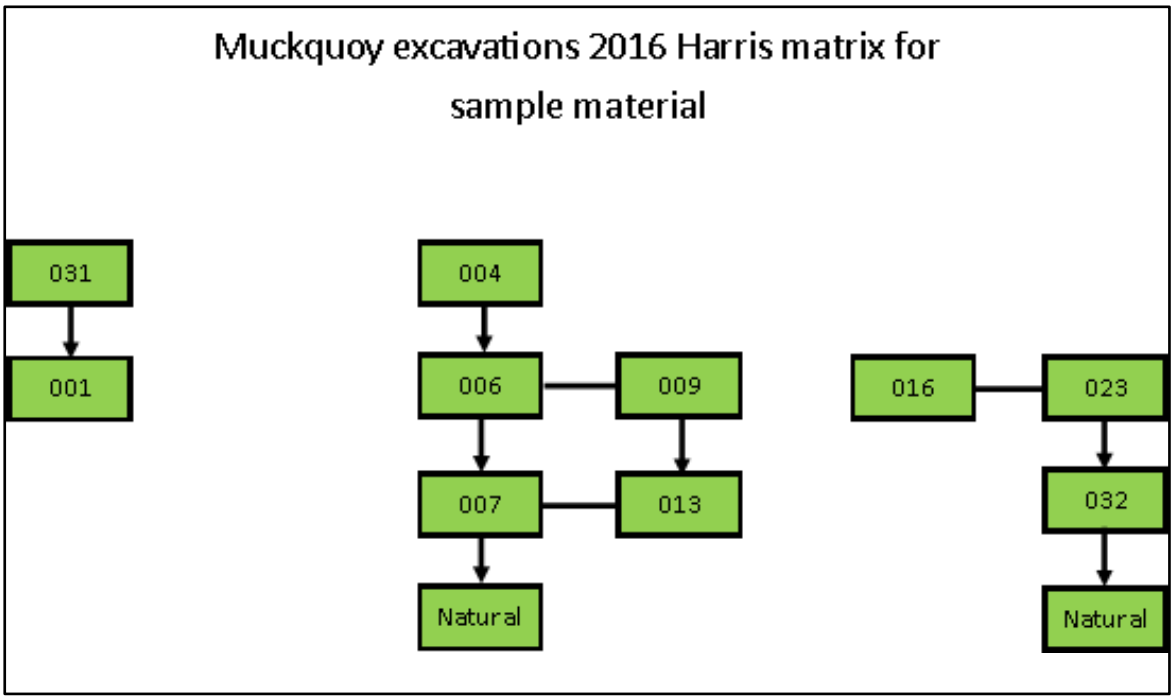

Figure 4.16 Harris matrix for samples from Muckquoy. Source: Author

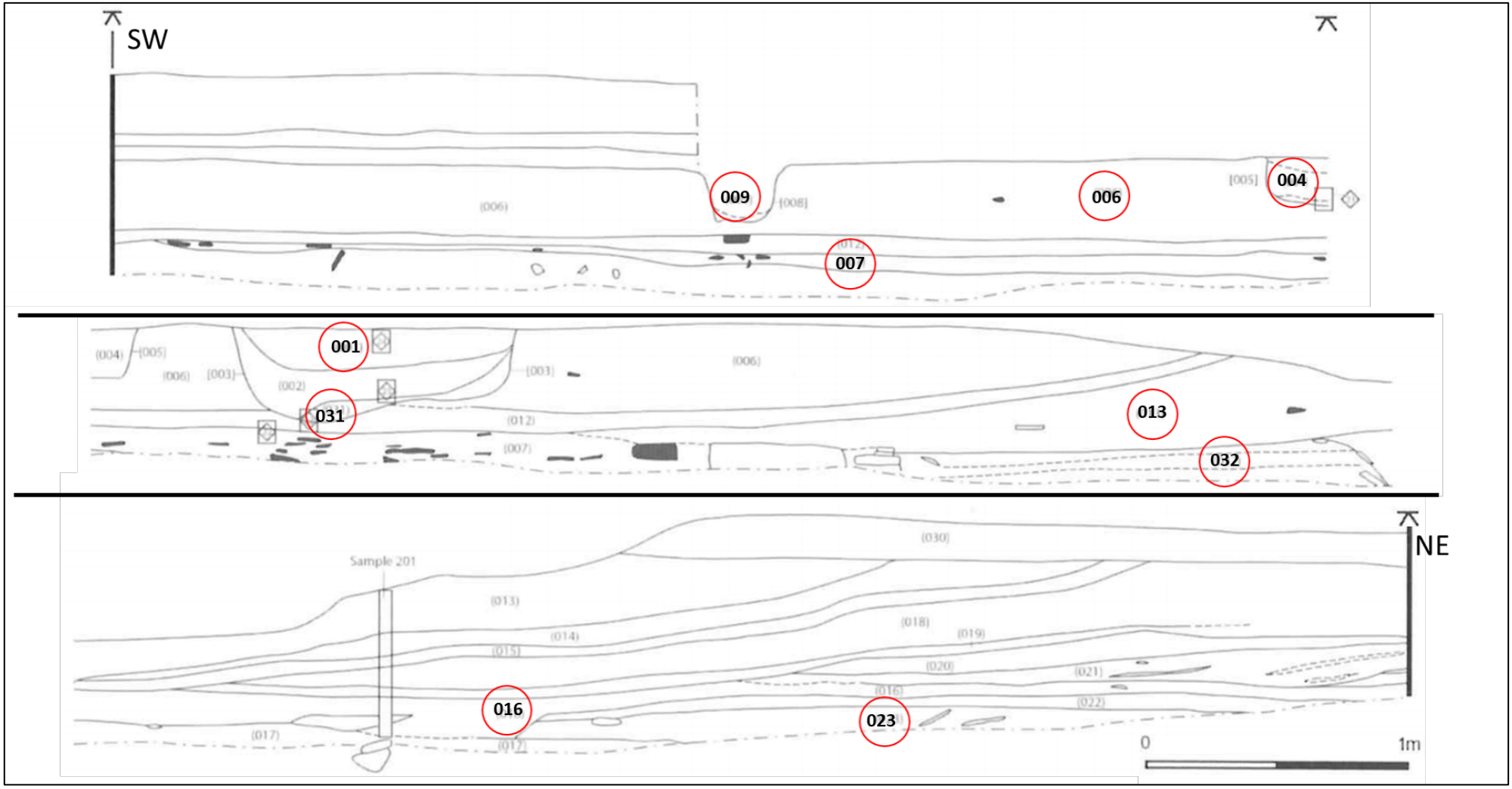

Figure 4.17 Section drawings from Muckquoy with the contexts of the samples shown in red circles Source: Chris Gee modified by Author.

- **RDL16 031**

Dark brown grey slightly sandy silt fill of cut [003] with inclusions of very small rounded flag stones. Possible Late Neolithic or Bronze Age fill. Sealed by context [002] and seals context [003].

- **RDL16 001**

Dark reddish brown sandy silt with dark grey patchy areas. Very few inclusions of rounded fragments of flag and sand stones. Possible organic peaty fill of ditch. Sealed by context [036], seals context [2], fill of ditch [003].

- **RDL16 004**

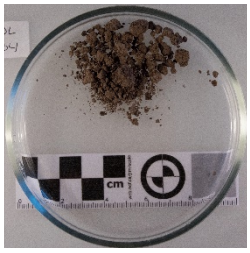

Sandy silt with dark grey and reddish brown particles. Very small inclusions of stone in low abundance. Sealed by [036], seals [005], fill of ditch/cut [005].

- **RDL16 006**

Mid reddish brown sandy silt with rare inclusions of cremated bone fragment, small stones and charcoal flecks. This context is located below context [005] and above context [012].

- **RDL16 009**

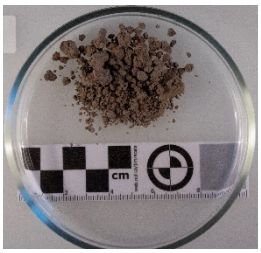

Dark greyish brown sandy silt fill of ditch [008]. Sterile of observable inclusions. Sharp boundary with context [006].

- **RDL16 007**

Light grey brown sandy silt with rare inclusions of small charcoal flecks and small cremated bone, and frequent inclusions of large platey stones. Midden material located below context [013] and above the natural soil matrix.

- **RDL16 013**

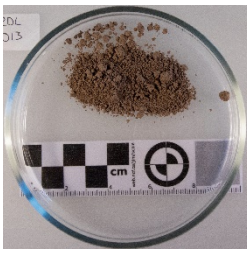

Mid-light orange brown sandy silt with rare inclusions of charcoal flecks and cremated bone fragments. This context has a diffuse boundary with context [032]. This context is a midden.

- **RDL16 016**

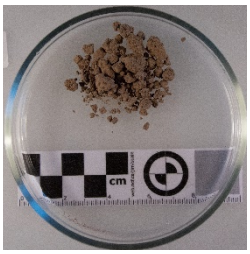

Dark greyish brown silty midden deposit with inclusions of cremated bone, charcoal flecks, small stones, and iron pan flecks. This context is likely a Late Neolithic midden. This context is overlain by context [021] and overlays contexts [022], [017].

- **RDL16 023**

Lighter brown orange sandy silt ashy midden layer with inclusions of fragmented charcoal and burnt and cremated bone fragments. This context is overlain by context [022], and overlays context [017].

- **RDL16 032**

Light brown grey sandy silt midden layer with inclusions of small cremated bone fragments, charcoal flecks and small flagstones (up to 0.15 cm). This context is possibly the same as context [007], is overlain by context [017] and overlays natural material.

4.4.7 Additional archaeological materials

Samples of Archaeological matrix were also collected to examine the effects of heating on sediment material. Archaeological matrix refers to the sediment from several contexts that has been flotted and sorted to remove all material of archaeological significance. This material was used as a proxy for archaeological soil to investigate the changes to the sediments around combustion features that are exposed to heat, and the sediment that is found within middens that would mix with depositional material. This material was analysed both unheated and heated to 900^0C for 6 hours to investigate the changes to soil materials from exposure to heat (figure 4.17). The archaeological matrix was analysed to examine the potential effects heating could have on soils germane to the analyses.

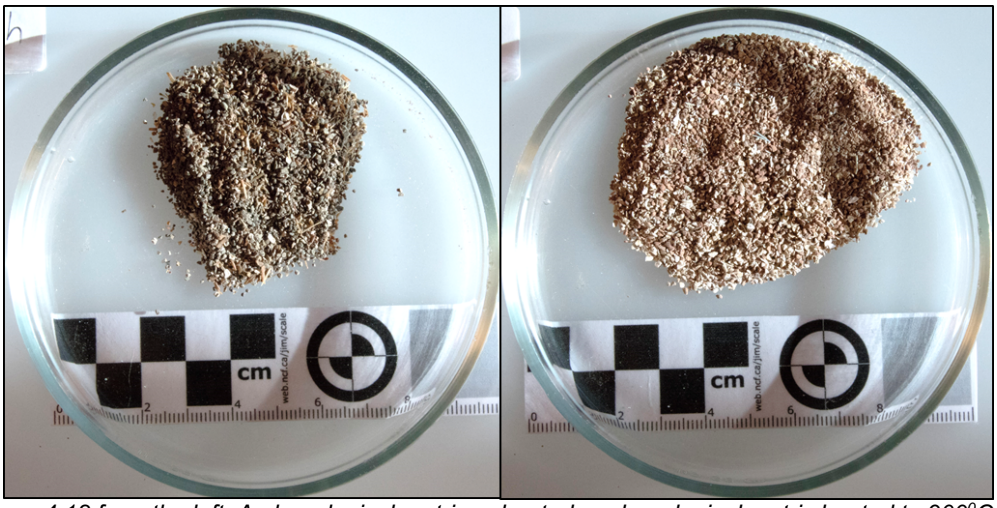

Figure 4.18 from the left: Archaeological matrix unheated, archaeological matrix heated to 900^0C. Source: Author

4.5 Conclusions

This chapter presented the materials that were chosen for this investigation. The modern analogue materials were discussed with respects to their relevance to the research and the locations from which they were collected. The availability of the fuels and the reasoning for their selection was discussed in the background chapter section 2.2.

The modern analogue fuels offer a wide spectrum of fuel materials available within the region of Orkney, and represent fuels used for different stages of building a fire as well as different types of use for the fire itself. By using a series of samples from archaeological excavations focusing on sites in different areas and spanning different periods of occupation, a general and broad understanding of fuel resource utilization within Neolithic Orkney can be developed.

The archaeological sample material was displayed in stratigraphic sequence according to the Harris matrices that were produced for this research. The archaeological samples were discussed in respects to the contextual information from the excavation reports, and the context cards for each excavation site.

Chapter 5: Tending the flames (Methods)

5.1 Overview

The following chapter presents the methodologies used to achieve the objectives of this research stated in section 1.2, and the steps taken to ensure the accuracy and repeatability of the results. The identification of archaeological fuel material from ash requires a multimethod approach with consideration to both modern analogue and archaeological material as established throughout sections 3.2, 3.4 and 3.5. As explained in section 3.7, the chosen methods for analysis are magnetic susceptibility, pH, and SEM/EDX. These methods were chosen due to their ability to characterise the constituents and properties of ash. The preparation of the modern ash material was informed by the previous work with creating modern analogue ash as discussed in sections 3.2 and 3.5, and used the limitations from those experiments to create a more comprehensive dataset with 14 fuels ashed at three temperatures.

The methodologies for this project are broken down into three phases. The first was preparing and burning the modern analogue fuel materials to ash at three temperature intervals (200^0C, 400^0C, and 900^0C) to provide samples of 14 fuel materials at three intervals of ashing temperature. The second was to analyse the modern analogue ash that was created using scanning electron microscopy with energy dispersive X-ray spectroscopy, magnetic susceptibility measurements, and pH measurements. In addition to the analyses, the calculation of mass lost at each ashing temperature and the assignment of Munsell colour numbers was carried out. The final phase was to analyse the archaeological material with the same methods and use comparison corroborated by principal components analysis to try to identify the modern analogue fuels that are associated with the archaeological samples.

5.2 Modern analogue ash preparation

Modern analogue material required preparation to produce ash from the raw fuels. The fuel materials used for this investigation were peat, seaweed, driftwood, cow dung, sheep dung, grasses, heather, willow, hazel, and animal bone as presented in section 4.2. The samples required drying to remove excess moisture, and cutting/breaking to size in some instances before being ashed to ensure the material would burn properly. The steps taken to prepare the 14 modern analogue fuel materials and create ash samples at three temperature intervals are as follows.

- The samples were dried using a drying cabinet set to 50^0C for a period of 4 days to completely remove all moisture from the sample material ensuring that the mass calculations would be as accurate as possible.
- The samples were then cut down or broken up to near uniform sizes, approximately 2.5cm pieces, in an attempt to fit material within the crucible for ashing.
    - During this process smaller pieces are created from snapping and cutting. These should be used to fill spaces left between the 2.5cm material, there are some gaps due to the ununiform shape of the fuel materials.
- For each temperature interval for all modern analogue material, a 250ml crucible was weighed and then filled with material and weighed again to calculate the masses of the modern analogue material before exposure to heat.
- Each 250ml subsample was ashed at 200^0C, 400^0C and 900^0C for 6 hours in a muffle furnace, adapted from the preparation methods used in previous modern analogue experimentation and modern bio fuel research presented in table 5.1. These temperatures emulate both cooking conditions and the outer ember area of a fire at 200^0C (smoldering). According to Rehder (2000: 6), below 255^0C pyrolysis does not take place, and below 250^0C charcoal does not form. This provides a sample that shows just heat effected sample material that has undergone no major chemical changes. The slightly larger fires for light/heat,

hardening wooden spears, working glass, charcoalification, low end pottery firing (Rehder 2000: 46), and the base of a flame 400^0C (burning) (Pausus & Keeley 2009; Rehder 200: 50-52). The minimum temperature for working iron, maximum temperature for firing pottery in antiquity (Jones & Brown 2000: 177; Appleby 2008), making glass and the tip of a flame 900^0C (Rehder 2000: 138-142). This allowed the yield of ash to be calculated systematically, and to track changes directly correlated to temperature increase. Due to the time restraints of this project it was not possible to create modern ash heated to 600^0C to represent an intermediate temperature between 400^0C and 900^0C; however, that temperature range has no associated function. As mentioned in Jones and Brown (2000) and Appleby (2008), pottery fired to less than 800^0C will not be viable and the substandard pottery produced by low firing temperatures would be repeatedly rebaked while in use as cookware at the 200^0C - 400^0C temperature intervals (Jones *et al. 2016).*

- After a burning duration of 6 hours (due to laboratory issues some burns were cut off then continued at a later date) the muffle furnace was switched off with the modern analogue material left to cool overnight while remaining within the controlled environment of the muffle furnace as to not introduce any contamination. Once cooled the sample and crucible were weighed to track the changes in mass caused by burning. The samples were ashed under reducing conditions, which could affect the extent of the oxidising that takes place during ashing. This is addressed with the use of ash samples gathered from open air ashing to investigate the differences between the two.
- The sample material was then homogenised using a mortar and pestle and then put into labelled storage bags for further analyses using SEM/EDX and pH measurement.

Ashing Temperatures and Their Function in Antiquity	
Temperature	**Function**
200^0C	Smoldering, cooking, lower than the charring temperature
400^0C	Working glass, hardening wood, firing pottery, charcoalification
900^0C	Working iron, firing pottery, creating glass,

Table 5.1 A table showing the heating temperatures used to create the modern analogue ash, and some of their respective functions within antiquity. Source: Author with reference to Rehder (2000).

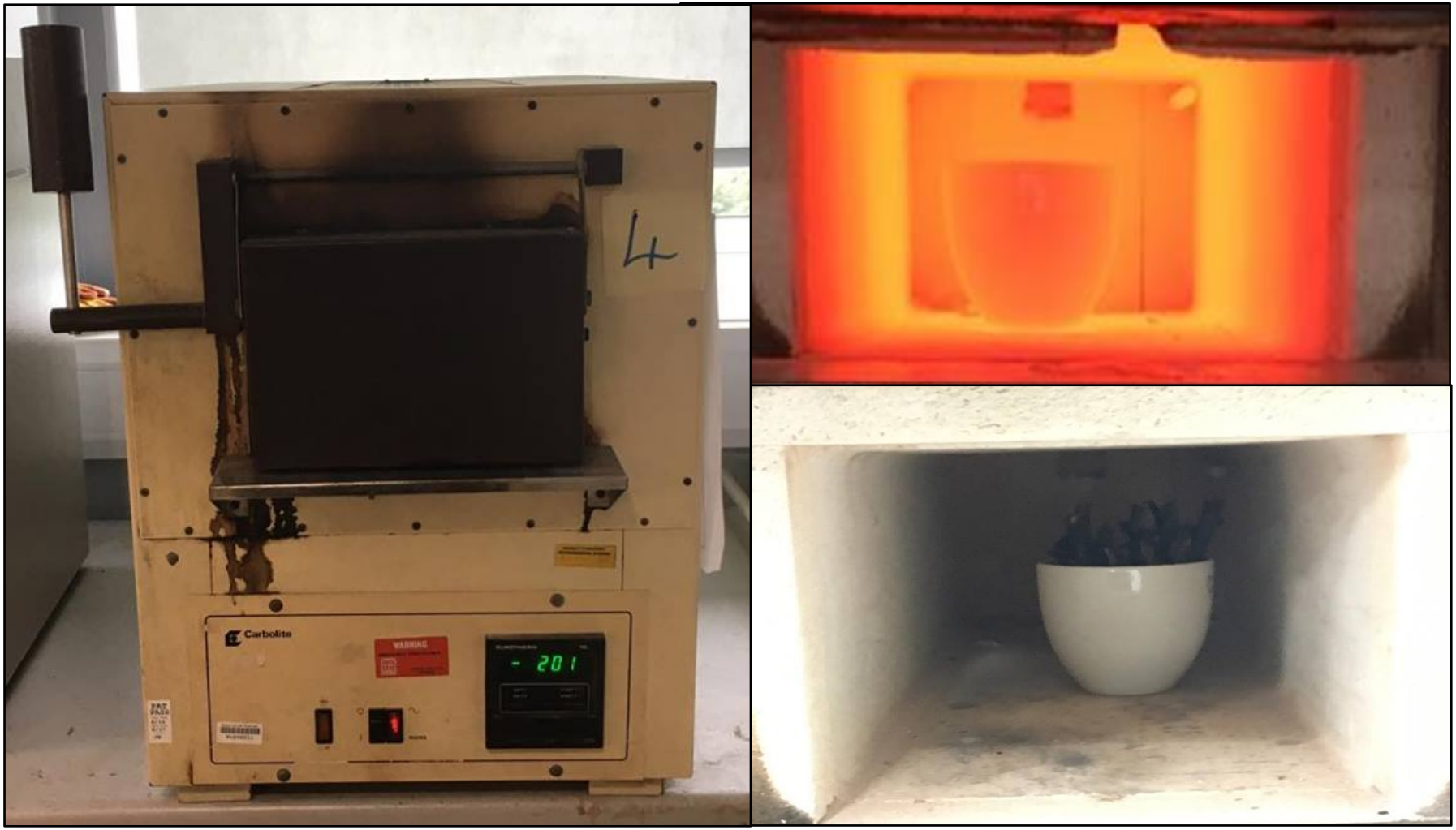

Figure 5.1 Clockwise from left- The muffle furnace used for these experiments. A crucible filled with willow inside the muffle furnace before burning. A crucible heated to 900^{0}C in the muffle furnace. Source: Author

5.3 Methods for the application of analytical techniques

The modern ash produced for this investigation was used to aid in the identification of archaeological material and to develop and refine the analytical processes needed to investigate the fuel constituents present within archaeological ash deposits. This was done to create a more reliable characterisation of fuel constituents.

Any fuel that had a loss of mass 95% or greater was not used in the subsequent analyses. The mass lost within the parameters of the experiment was indicative that no fuel material would be found in greater than trace abundances at a mass lost percentage greater than 95% unless it was the only fuel in use. This is most applicable to tinder and kindling fuels used to start fires as discussed in section 2.6. Even when considering the repeated use of a combustion feature no fuel material would be left at that rate of loss to contribute to any accumulation of combustion residue.

Preliminary analysis methods were used in addition to the suite of detailed analytical methods being used to characterise the properties of combustion residues. The mass lost and Munsell colour for each modern analogue sample at all intervals of temperature was carried out. Munsell colour number assignment was applied to all samples both modern analogue and archaeological to further identify changes among modern analogues, and to offer a means of comparison for later use in the identification of archeological fuel constituents. Munsell colour assignment was also utilised in the investigations into fuels carried out by Church *et al.* (2007) and Canti and Linford (2000) as mentioned in section 3.2. In addition, this research quantified the difference in the mass of ash from different fuels at different temperatures as observed but not systematically recorded by Church *et al.* (2007).

5.3.1 Mass lost

- All of the crucibles were weighed using a 1kg-0.01g precision digital scale before the material was added, and again after to establish the starting mass of all samples before the ashing process.
    - All of the fuel material must be securely placed in the crucible to ensure that nothing is lost transporting the crucibles from the work surface to the muffle furnace and vice versa. Some material can also be lost during ashing by falling out of the crucible if it is precariously placed during filling.
- All materials were then weighed after the burning periods and mass lost was calculated using the formula

  % Mass Lost = $(\frac{(burnt\ mass - unburnt\ mass)}{unburnt\ mass})x100.$

5.3.2 Munsell colour assignment

Unlike the mass lost calculations that can only be applied to the modern material that was ashed for this investigation, Munsell colour assignment is applicable to all samples to add a further means of corroborating the findings (Munsell Colour 2000). The use of colour can aid in the identification of fuel matches between modern ash and archaeological samples using the differences of ash colour and changes in sediment colour based on fuel used and temperature as mentioned in section 3.5 (Church *et al.* 2007; Canti & Linford 2000).

- All of the Munsell colour assignments for this research were carried out in a controlled light setting with the curtains drawn to keep out the variable ambient light from the sun, and using the controlled UV laboratory lights with an additional work lamp and 100-watt incandescent bulb, the settings are as controlled as possible to view all of the samples

under the same conditions. This avoids variation in colour assignment from the influence of different lighting conditions.

- A small portion of the sample was collected using a small, white plastic, laboratory spatula and subsequently held directly against the aperture of the suspected colour matches within the Munsell book.

5.4.1 Magnetic susceptibility

The magnetic susceptibility was measured using the Bartington MS2B magnetic susceptibility bridge (figure 5.2). Magnetic susceptibility was explained in section 2.6 (Mulay 1963; Dearing 1994; Tarling 1999), and examples of its use in previous studies was discussed in sections 3.2, 3.4, and 3.7. The following explains the steps that were taken to prepare the sample material, measure the magnetic susceptibility using both low and high frequency, and to calculate the low frequency mass specific magnetic susceptibility and the frequency dependent magnetic susceptibility using formulas from Mulay (1963: 1760).

All sample material was subjected to magnetic susceptibility measurements to establish the magnetic properties of each sample utilising the low and high frequency measurements to calculate the low frequency mass specific magnetic susceptibility (χlf x10^{-8}(m^3kg^{-1})) and the percentage frequency dependence (%χfd x10^{-8}(m^3kg^{-1})).

- All sample material was distributed into three 10 ml volume plastic containers compatible with the Bartington Instruments MS2B Magnetic Susceptibility Bridge. In the instance that modern analogue ashing left insufficient material for three sample pots, one or two containers were used as appropriate for the amount of material present.
- The mass was recorded minus the weight of the sample pot.

- All samples were then subjected to three measurements at both high and low frequency, zeroing the machine between each measurement. The multiple repeat measurements ensure the reproducibility of the results. The MS2B was allowed 30 minutes to equilibrate upon being switched on and after changing from low field to high field measurements.

After the measurements are compiled and the means have been calculated, the bulk density, mass specific, and frequency dependent magnetic susceptibility can be computed using the formulas in table 5.2. Microsoft Excel was used to process all of the data.

Formulas used	
Bulk density	$\mathrm{P} = Mass/Volume$
Mass specific magnetic susceptibility	$\chi lf = \kappa/\rho$
Frequency dependence	$\chi_{fd}\% = (\kappa_{lf} - \kappa_{hf}/ \kappa_{lf}) \times 100$, $\chi_{fd}\%$

Table 5.2 all of the equations used to calculate the mass specific and frequency dependent magnetic susceptibly. Source: Author

Figure 5.2 A photograph of the Bartington MS2B magnetic susceptibility bridge used for the research, and several tubs filled with 10cc magnetic susceptibility sample pots. Source: Author

5.4.2 pH

The background to pH and a brief explanation behind the science was presented in section 2.9. The use of pH analysis in previous work was discussed in sections 3.4 and 3.6 (Summers 2015; Ohno 1992). The following discusses the use of pH analysis as carried out in this research, and the steps taken to obtain accurate results, and maintain the repeatability of the analysis.

- 1g of each sample was suspended in 10ml-deionized water to standardize mass and dilution effects.
- All samples were then left to settle for 12 hours before being poured through a funnel and filter paper to avoid the bulb sensor of the pH meter being affected by the buoyant material within the ash.
- The Mettler Toledo MP220 pH meter (figure 5.3) is calibrated using two buffer solutions that are purchased for use in the laboratory (pH 4.0 and pH 7.0).
- Readings are taken (three for each sample) at approximately 20°C
- The meter was recalibrated after every five measurements.

Figure 5.3 A photo of the Mettler Toledo pH meter used for the analysis. Source: Author

5.4.3 Scanning electron microscopy/energy dispersive X-ray spectroscopy

The basic concepts behind SEM/EDX were presented section 2.8, and the use of SEM/EDX in fuel research was discussed in sections 3.4 and 3.6. Scanning electron microscopy and energy dispersive x-ray spectroscopy offer the combination of high resolution images at intense magnification along with compositional mapping of a sample in both area selection and spot selection format. For this investigation an FEI Quanta 400 SEM/EDX was used.

Preparation

- 12.5mm specimen stubs are affixed with Leit carbon adhesive discs.
    - All samples are set onto 12.5mm aluminum specimen stubs by attaching the Leit carbon discs and exposing the adhesive surface, and then placing the stub into the sample container and pressing into the material several times to attach as much as possible. To avoid cross contamination and wastage of sample material all excess material that did not adhere to the specimen stub is knocked loose by tapping or 'flicking' the stub before removing it from the sample's container. All of the samples were homogenized using a mortar and pestle to ensure to provide a representative sample.

- All samples are then placed in a vacuum chamber to be coated with carbon using an electrically charged carbon cord to cover the samples.
    - Once coating is completed all the samples are placed in a sample holder to be moved to the SEM/EDX unit.
- Sample stubs are loaded onto the stage of the SEM/EDX machine in a clockwise circular pattern, according to the holes provided for the sample

stubs. The calibration sample of cobalt is oriented at the 12:00 position and all samples following at 2:00, 4:00, 6:00 etc. (figure 5.4).

- Once the samples are loaded onto the stage the door can be closed and the vacuum reinstated.
  - From this point the SEM/EDX standard operation procedures are followed.

Analyses

- Each sample has an image taken at 100x and 400x magnification.
- All samples are subjected to a minimum of 1 area analysis (approximately 2mm^2) and 5 spot analyses for confidence in results, robust dataset, and repeatability of results.
- The results and associated images for each sample are then used to generate a report on INCA software, and subsequently saved to a dedicated USB flash drive.

Figure 5.4 Clockwise from top left- SEM/EDX samples on stubs, samples being carbon coated in the vacuum chamber, sample stubs being loaded into the SEM/EDX observation stage, and finally the FEI Quanta 400 SEM/EDX machine and computer system. Source: Author

This research also focuses on a specific group of elements that was established in section 2.7. This was done to consider the potential fuel markers present among the modern analogue fuel that contained no contamination, and the archaeological sample material that contained soil contamination, other additions from midden fill, and potentially mixed combustion residue from multiple sources in time, purpose, and type of combustion feature (i.e. furnace, kiln, hearth, oven, etc.). This data combined with the elimination of elements due to background noise or contamination from environmental and material sources dictated the elements to focus on during the analyses of archaeological material. The elements that were deemed significant among the materials are sodium, magnesium, aluminium, silicon, phosphorus, calcium, sulfur, potassium, iron, and titanium. The only elements that were not considered for this investigation were oxygen and carbon.

5.5-Methods chapter conclusions

This chapter presented the methods and techniques being used to create a methodology for the identification of archaeological fuel sources from ash sample material. The methods were presented with consideration to their use in past investigations as discussed throughout the literature review chapter. The preparation and analyses methods presented in this chapter were developed to ensure both the accuracy of results and repeatability of the examinations.

Chapter 6: After the fires (Results)

6.1 Overview

This chapter presents the results of the investigations and is divided into two main sections focusing on the modern analogue and then the archaeological sample results. The modern analogue results are presented by fuel type to illustrate the changes that take place within the fuels as ashing temperature is increased. The archaeological sample results are presented according to site and year of sample collection, and organized per the Harris matrices presented in section 3.2. The data is presented utilizing both data tables and graphs to provide both the numerical data as well as a visual representation of the figures. The raw data from the analyses is available in the appendices. The interpretations of the results are discussed in chapter 7.

6.2 Modern analogue results

This section presents the data that was obtained from ashing and subsequently analyzing modern analogue fuel samples of peat, seaweed, driftwood, grasses, sheep dung, cow dung, heather, hazel, willow and animal bone discussed in section 4.2, according to the procedures presented in sections 5.2, 5.3, and 5.4. The modern analogue fuels were chosen with consideration to their availability both contemporarily and within the chronological scope of this research (Neolithic – Iron Age) as presented in sections 2.2 and 4.2. The interpretation of these results and their implications for the identification of archaeological fuels are discussed throughout chapter 7.

The modern analogue data illustrates the changes that fuels undergo during the ashing process for three different temperatures 200^0C, 400^0C, and 900^0C. In addition to the detailed analyses, the modern analogue results include the mass lost data obtained during the ashing process that was described in section 5.2. Using ashes created at three increasing temperatures not only shows the

changes that fuel undergoes throughout the ashing process, but also shows the effects of different functionalities of fire such as cooking (200^0C), pottery firing (400^0-900^0C), stone tool production(400^0C-900^0C), and metal working (900^0C) discussed in section 5.2.

6.2.1 Preliminary analytical method results

The most noticeable and obvious results are the physical changes that each fuel goes through when exposed to increasing temperatures. This is shown through the photographic evidence presented (figure 6.1 & figure 6.2), the mass lost data (figure 6.3), and the Munsell colour assignments (table 6.1). These observations record the changes to mass, colour, size, shape, and texture of each fuel type.

Munsell Colour Number Assignment Table					
200^0 C Samples		**400^0 C Samples**		**900^0 C Samples**	
Seaweed	Gley1 5/N + 10YR 5/8	**Seaweed**	Gley1 6/N	**Seaweed**	Gley1 2.5/N + 10YR 7/4
Cow Dung	2.5Y 6/1	**Cow Dung**	2.5Y 6/1	**Cow Dung**	Gley2 8/5PB W/ Purple incl.
Sheep Dung	7.5YR 3/1	**Sheep Dung**	10R 2.5/1	**Sheep Dung**	5Y 7/1
Grass	Gley1 6/N	**Grass**	Gley1 4/N	**Grass**	7.5YR 7/1
Driftwood	Gley1 3/N + 5YR 3/4	**Driftwood**	5Y 5/1	**Driftwood**	
Heather	Gley1 3/N	**Heather**	Gley2 4/5PB	**Heather**	
Willow	10R 2.5/1	**Willow**	Gley1 4/N	**Willow**	
Hazel	7.5YR 2.5/3	**Hazel**	Gley1 5/N	**Hazel**	
Animal Bone	7.5YR 6/6	**Animal Bone**	Gley1 2.5/N + 7.5YR 5/2	**Animal Bone**	Bright White No Munsell match
Rousay Peat	10YR 2/1	**Rousay Peat**	10YR 2/1	**Rousay Peat**	7.5YR 5/6 + Gley1 2.5/N
Fozzy Peat	Gley1 2.5/N	**Fozzy Peat**	Gley1 2.5/N	**Fozzy Peat**	2.5Y 7/4
Mid Peat	Gley1 2.5/N	**Mid Peat**	10YR 3/1	**Mid Peat**	2.5Y 8/1
Low Peat	Gley1 3/N	**Low Peat**	2.5Y 2.5/1	**Low Peat**	2.5Y 7/3
H.P. Peat	Gley1 2.5/N	**H.P. Peat**	Gley1 2.5/N	**H.P. Peat**	10YR 8/4

Table 6.1 A table showing the Munsell colour number assignment for modern analogue fuels at increasing temperatures. Source: Author

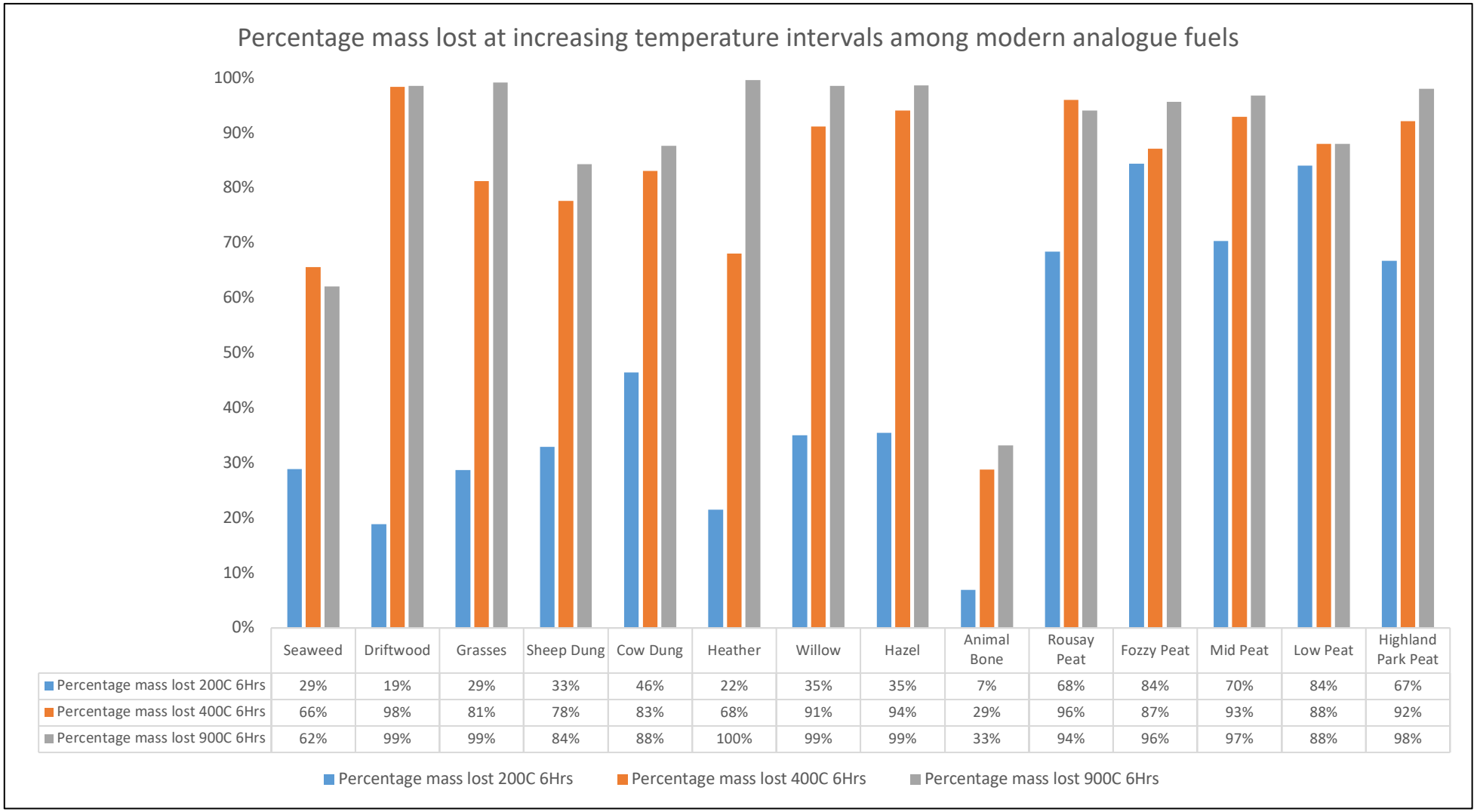

	Seaweed	Driftwood	Grasses	Sheep Dung	Cow Dung	Heather	Willow	Hazel	Animal Bone	Rousay Peat	Fozzy Peat	Mid Peat	Low Peat	Highland Park Peat
Percentage mass lost 200C 6Hrs	29%	19%	29%	33%	46%	22%	35%	35%	7%	68%	84%	70%	84%	67%
Percentage mass lost 400C 6Hrs	66%	98%	81%	78%	83%	68%	91%	94%	29%	96%	87%	93%	88%	92%
Percentage mass lost 900C 6Hrs	62%	99%	99%	84%	88%	100%	99%	99%	33%	94%	96%	97%	88%	98%

Figure 6.1 A chart showing the mass lost among modern analogue fuels at increasing temperatures. Source: Author

From unburnt fuel material, there is a marked change in the appearance and characteristics of the modern analogue samples heated to 200^0C for 6 hours. All the wood fuels and seaweed show a darkening to a deep brown, and become brittle showing signs of charring (figure 6.2 & 6.3 table 6.1). Grasses and cow dung have already begun to ash, retaining their original shape, but losing a majority of mass and turning a medium gray colour (figure 6.3 table 6.1). The peat fuels as well as sheep dung all darken to a very dark brown almost black and have become brittle, all the remaining plant material within the peat has charred to a similar degree as the wood fuels and seaweed (figure 6.2 & 6.3 table 6.1). The cow and sheep bone have become a yellow brown and have hardened significantly (figure 6.3 table 6.1).

As the temperature is increased to 400^0C the wood fuels and seaweed have charred and begun to ash turning a medium grey similar to the grasses and cow dung at 200^0C (figure 6.2 & 6.3 table 6.1). The grasses and cow dung have maintained the gray colour from 200^0C, but no longer retain any of their original shape consisting of mostly ash content after 6 hours (figure 6.2 table 6.1). The peat fuels and sheep dung have continued to darken and char; they have not yet begun to ash, but no longer retain any shape (figure 6.2 & 6.3 table 6.1). The animal bones have significantly darkened to a light brown and dark grey, and have become very brittle (figure 6.3 table 6.1).

The highest temperature interval of 900^0C completely incinerated driftwood, willow, and hazel to more than 95% mass lost (figure 6.1). The grasses have become a fine powder of light grey almost white ash, while the cow dung has become a very hard crystal structure with a purple hue (figure 6.2 table 6.1). The peat fuel produced a fine yellow to orange ash with some chunks of very hard

blackened charred peat; Rousay cut peat being the most orange and Highland Park peat being the most yellow (figure 6.2 & 6.3 table 6.1). The sheep dung produced an ash similar in consistency to the peat ash from the same temperature, yet the colour was grey with very little yellow (figure 6.2 & 6.3 table 6.1).

The mass of the modern analogue fuel materials was affected by increasing temperatures, each fuel type demonstrates specific trends associated with mass and exposure to heat. When exposed to 200^0C the mass of peat fuels was most affected losing 67% - 84% of their mass, the wood fuels 19% - 35%, grasses and seaweed 29%, and the dungs lost between 33% and 46% (figure 6.1).

The largest change to mass occurred at the 400^0C interval with an average of 82% mass lost compared to the 44.8% average mass lost from 200^0C. The wood fuels, dung, and grasses had the largest spike of mass lost at this temperature interval ranging from 68% - 98% (figure 6.1).

The increase in loss of mass according to temperature continued at 900^0C, but to a lesser extent than the large increase seen at 400^0C with an average mass loss of 88.3% at 900^0C. At this temperature, the wood fuels and grasses were burned to almost complete combustion of the material (figure 6.1).

The fuel material least affected by exposure to heat is animal bone. Cow and sheep bone showed little change at 200^0C with only 7% mass lost. At the highest temperature interval, the bone had the least amount of mass lost (figure 6.1).

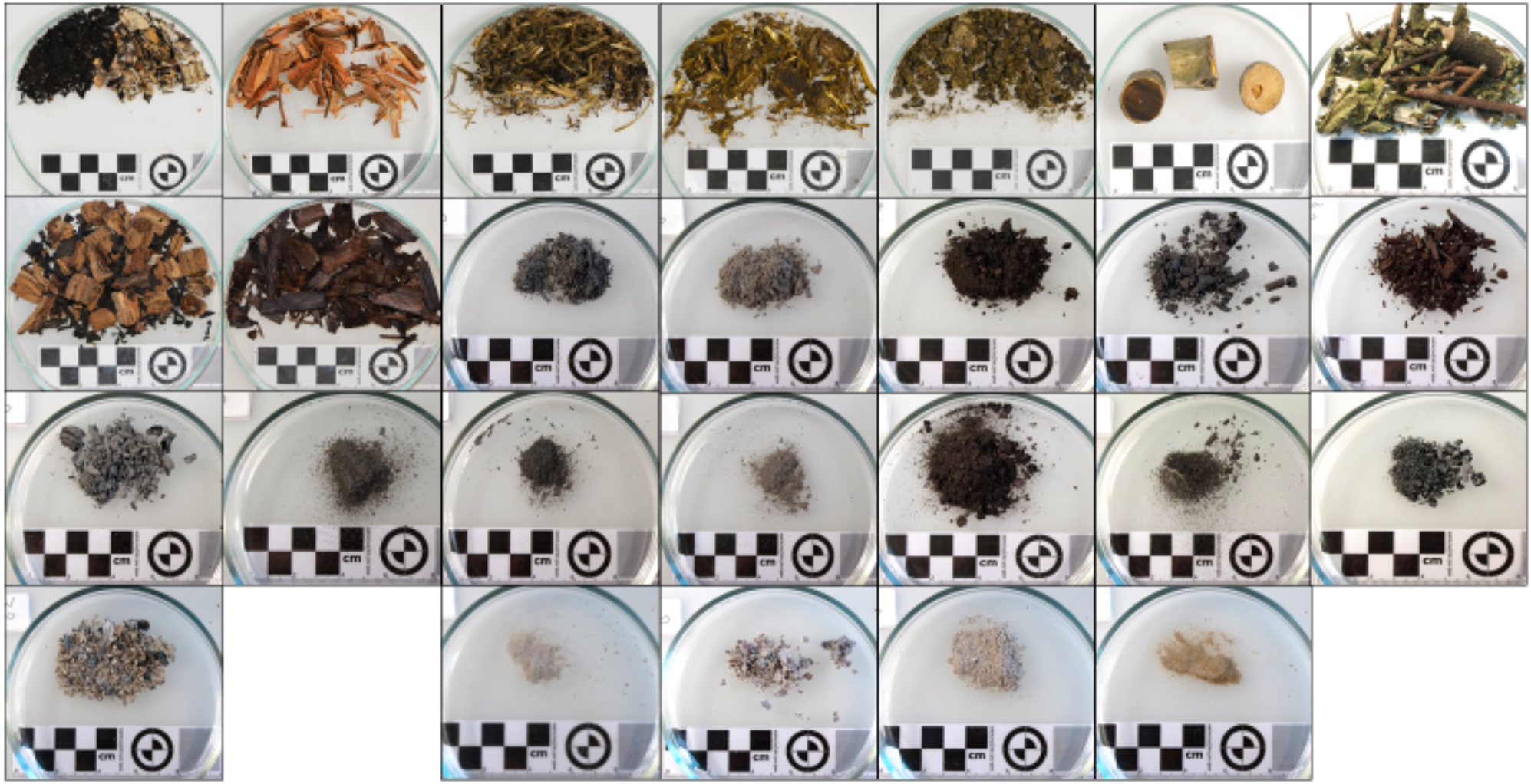

Figure 6.2 An image of modern analogue materials showing unburnt material at the top, and increasing temperatures in descending order down the page 200^{0}C, 400^{0}C, and 900^{0}C. From left to right the modern analogues are seaweed, driftwood, grasses, cow dung, sheep dung, heather, and willow. Source: Author

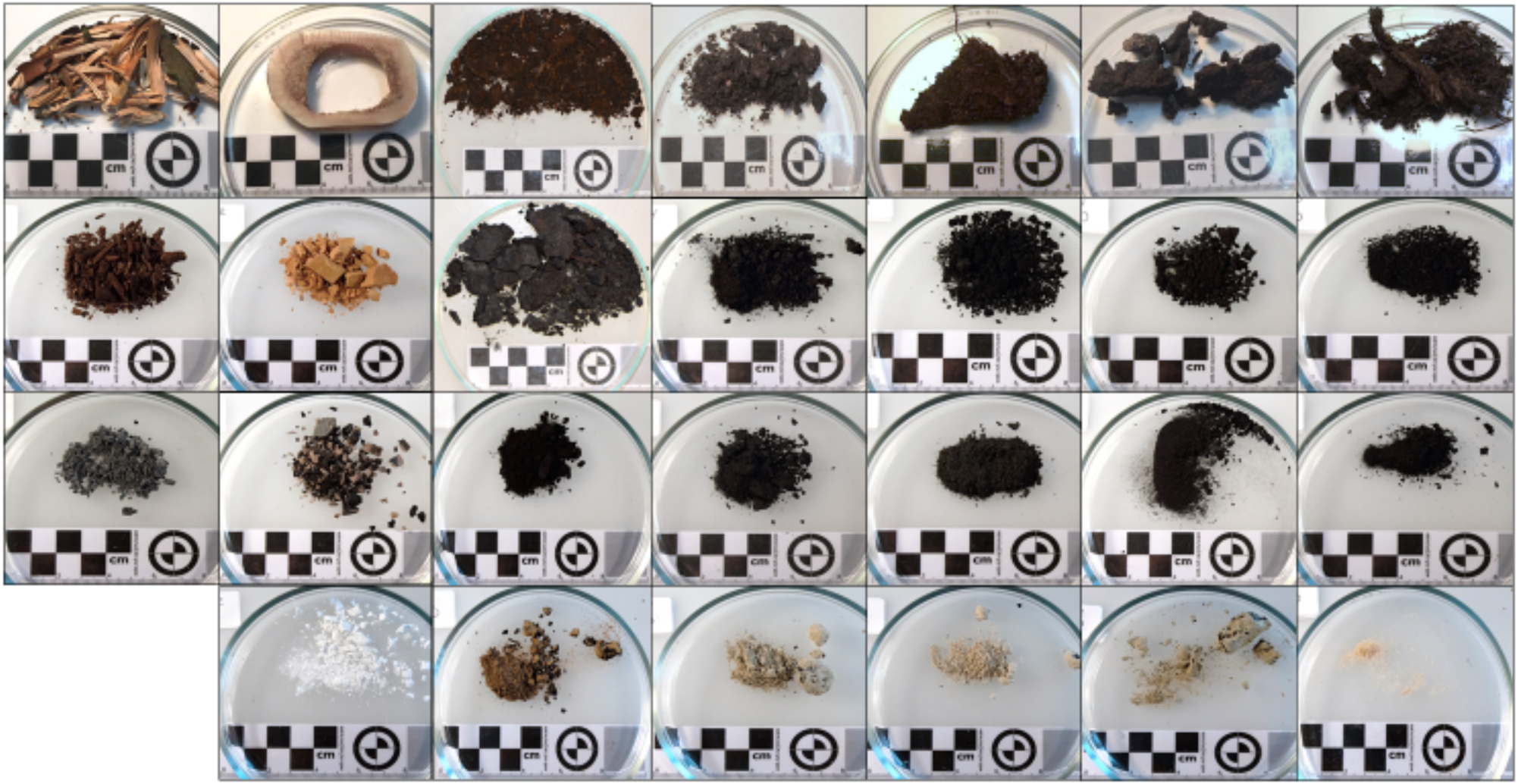

Figure 6.3 An image of modern analogue materials showing unburnt material at the top, and increasing temperatures in descending order down the page 200^{0}C, 400^{0}C, and 900^{0}C. From left to right the modern analogues are hazel, animal bone, Rousay peat, fozzy peat, middle peat, low peat, and Highland Park peat. Source: Author

6.2.2 Detailed analytical method results

The modern analogue analytical results are laid out following each modern analogue fuel type through increasing temperature intervals. This allows a useful platform to demonstrate the relationships between each individual fuel type and establish the patterns that are present as the fuels are exposed to increasing intervals of temperature. The implications of the results and the interpretations are covered in chapters 7 and 8 the discussion and conclusions respectively.

Seaweed

The MS of the seaweed samples show an increase as temperature increases from -1.5×10^{-8} m^3kg^{-1} at 200^0C, 1.6×10^{-8} m^3kg^{-1} at 400^0C, and 30.6×10^{-8} m^3kg^{-1} at 900^0C shown in table 6.2 and figure 6.4. the seaweed started with a diamagnetic measurement which increased as the ashing temperature was increased. The FDMS is not able to be calculated for the diamagnetic value from the 200^0C and 400^0C samples; however, the 900^0C have a FDMS value of 7.8% respectively (table 6.2)

The SEM/EDX results for seaweed show the presence of sodium, magnesium, sulphur, chlorine, potassium, and calcium among all three samples (figure 6.4). There is also aluminium, silicon, and phosphorous within the 200^0C and 400^0C samples. Iron was only found in the 400^0C seaweed sample. The most abundant element among all three samples is calcium as shown in figure 6.4 and table 6.2.

The pH data from the seaweed ash samples shows an intensification in alkalinity as the temperature increases 6.9 at 200^{0}C*, 9.8 at 4*00^{0}C*, and 12.2 at 9*00^{0}C (figure 6.4 table 6.2).

Seaweed 200^{0}C											
Xlf=κ/p x10^{-8} m^{3}kg^{-1}	-1.5										
%X*fd*	N/A										
Atomic % of elements	Na 7.8%	Mg 4.0%	Al 0.6%	Si 3.3%	P 0.8%	S 3.2%	Cl 5.4%	K 4.2%	Ca 1.6%	Fe	Ti
pH	6.9										
Seaweed 400^{0}C											
Xlf=κ/p x10^{-8} m^{3}kg^{-1}	1.6										
%X*fd*	N/A										
Atomic % of elements	Na 3.8%	Mg 4.6%	Al 1.0%	Si 2.4%	P 0.3%	S 2.2%	Cl 0.4%	K 1.7%	Ca 24.7%	Fe 0.3%	Ti
pH	9.8										
Seaweed 900^{0}C											
Xlf=κ/p x10^{-8} m^{3}kg^{-1}	30.6										
%X*fd*	7.8										
Atomic % of elements	Na 14.2%	Mg 4.4%	Al	Si	P	S 3.4%	Cl 12.3%	K 5.1%	Ca 6.5%	Fe	Ti
pH	12.2										

Table 6.2 The analytical data for seaweed showing the results of each analytical method organised by ashing temperature. Source: Author

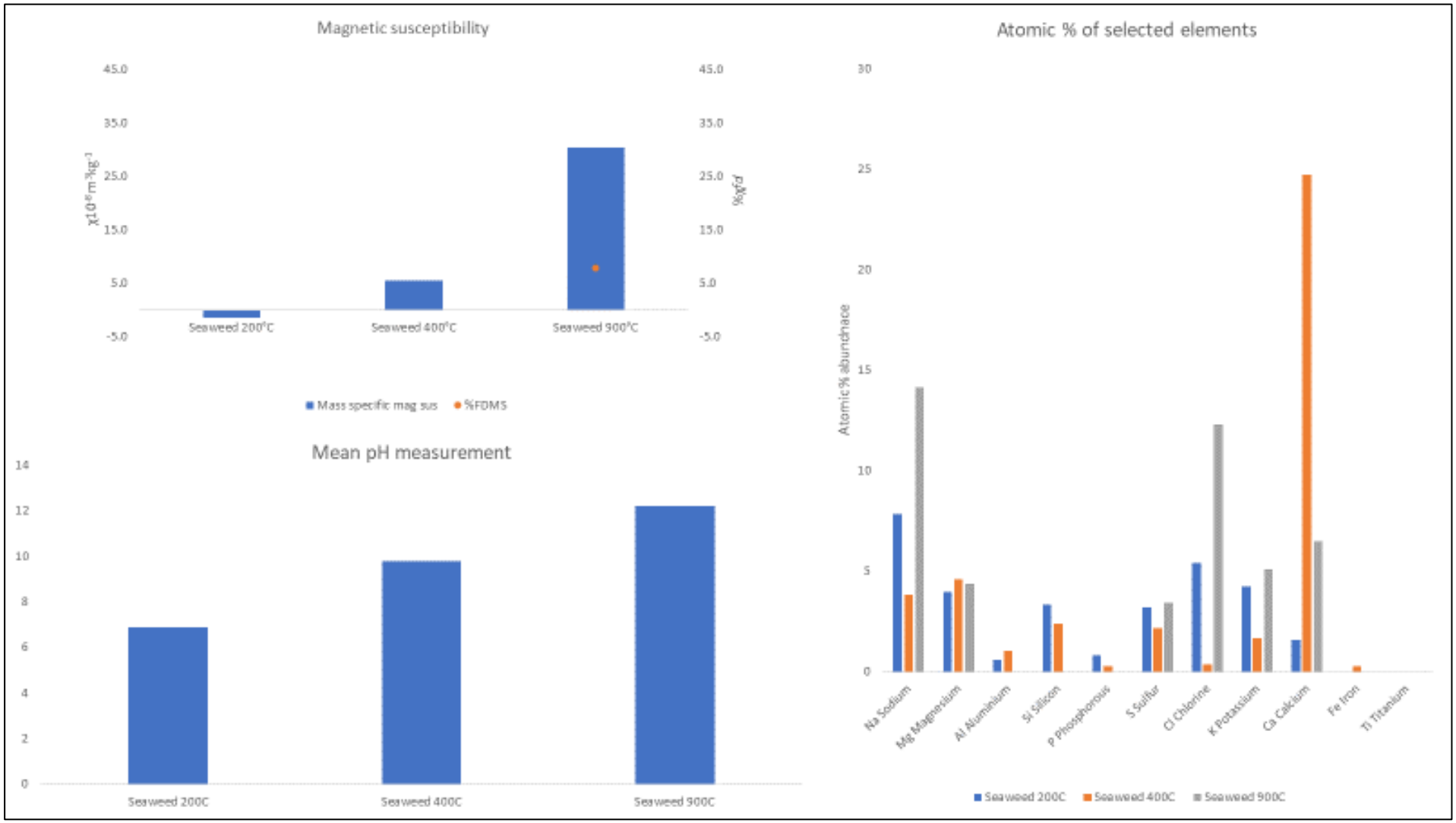

Figure 6.4 Clockwise from top left the low frequency mass specific magnetic susceptibility and percentage frequency dependence, the atomic percentage abundance of selected elements, and the pH of seaweed at increasing temperature. Source: Author

Driftwood

The MS of the driftwood samples shows the sample material has a diamagnetic measurement of -2.0 x10^{-8} m^3kg^{-1} at 200^{0}C, and a value of zero for the 400^{0}C sample. The FDMS was not able to be calculated for either sample given the diamagnetic and zero values of the 2 samples, as shown in figure 6.5 and table 6.3.

The SEM/EDX results for driftwood show the presence of magnesium, aluminium, silicon, potassium, calcium, and iron among both samples, and sodium, phosphorous, sulphur, and chlorine within the 400^{0}C sample (figure 6.5). The most abundant element among all three samples is calcium.

The pH data from the driftwood ash samples shows an increase from the near neutral measurement from the 200^{0}C sample to 9.1 pH for the 400^{0}C sample (table 6.3).

Driftwood 200^{0}C											
Xlf=κ/p x10^{-8} m^3kg^{-1}	-2.0										
%X*fd*											
Atomic % of elements	Na	Mg 1.3%	Al 1.3%	Si 3.9%	P	S	Cl	K 0.7%	Ca 3.5%	Fe 0.7%	Ti
pH	6.9										
Driftwood 400^{0}C											
Xlf=κ/p x10^{-8} m^3kg^{-1}	N/A										
%X*fd*	N/A										
Atomic % of elements	Na 4.6%	Mg 4.3%	Al 0.3%	Si 0.1%	P 0.3%	S 1.6%	Cl 0.1%	K 0.6%	Ca 3.4%	Fe 0.7%	Ti
pH	9.1										

Table 6.3 The analytical data for driftwood showing the results of each analytical method organised by ashing temperature. Source: Author

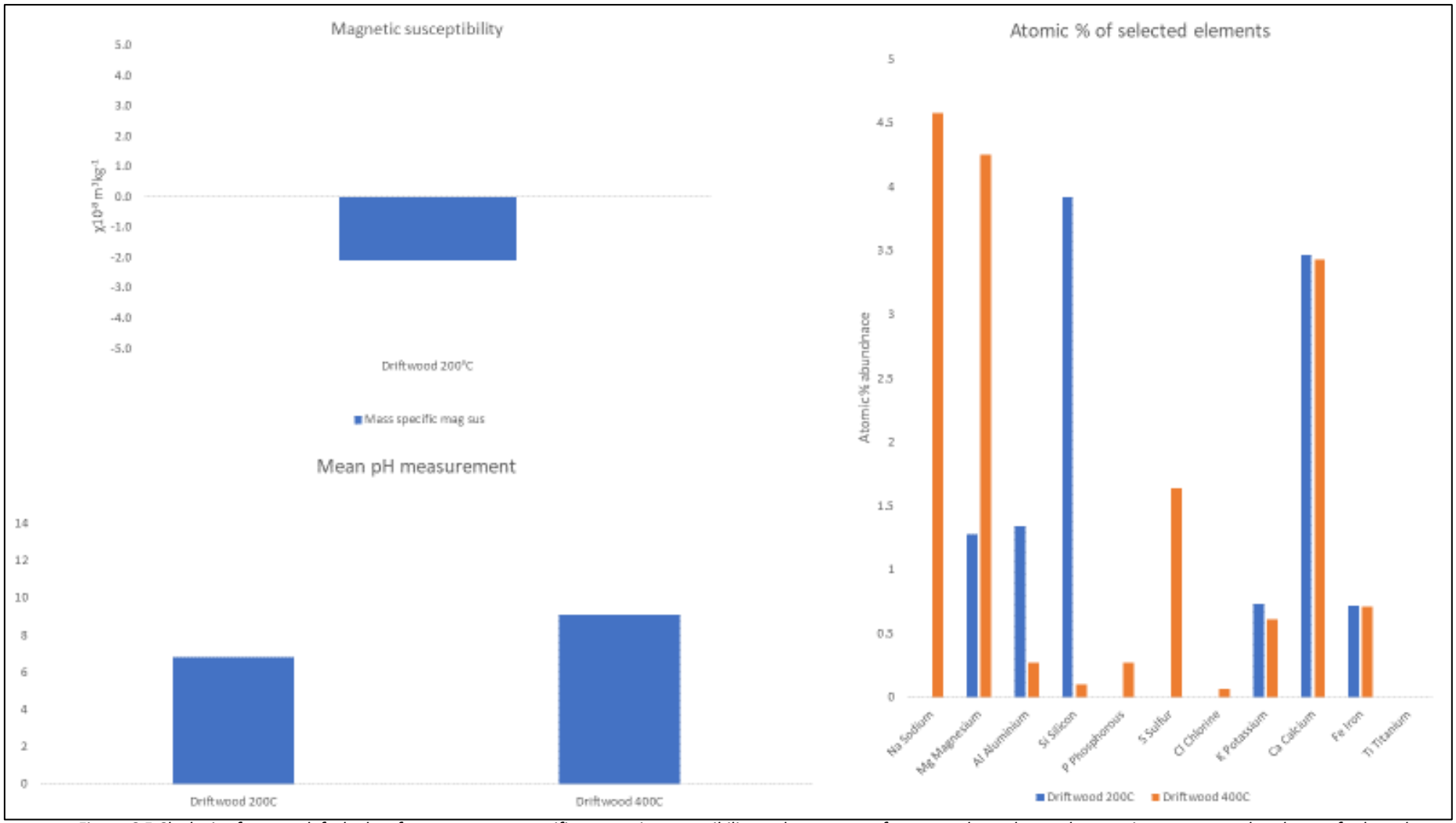

Figure 6.5 Clockwise from top left the low frequency mass specific magnetic susceptibility and percentage frequency dependence, the atomic percentage abundance of selected elements, and the pH of driftwood at increasing temperature. Source: Author

Grasses

The MS of the grasses samples show the material has a diamagnetic measurement of -2.8 x10^{-8} m^3kg^{-1} at 200^{0}C, and a value of 24.6 x10^{-8} m^3kg^{-1} at 400^{0}C as shown in figure 6.6 and table 6.4. The FDMS could not be measured for either sample (table 6.4).

The SEM/EDX results for driftwood show the presence of sodium, magnesium, silicon, phosphorous, chlorine, potassium, and calcium (figure 6.6). The 200^{0}C sample also contains sulphur (table 6.4). The most abundant element among all three samples was potassium.

The pH data from the driftwood ash samples shows an increase from the near neutral measurement from the 200^{0}C sample to 9.6 pH for the 400^{0}C sample (table 6.4).

Grasses 200^{0}C											
Xlf=κ/p x10^{-8} m^3kg^{-1}	-2.8										
%X*fd*	N/A										
Atomic % of elements	Na 1.0%	Mg 1.4%	Al	Si 2.0%	P 1.1%	S 1.1%	Cl 2.1%	K 4.9%	Ca 5.2%	Fe	Ti
pH	6.9										
Grasses 400^{0}C											
Xlf=κ/p x10^{-8} m^3kg^{-1}	24.6										
%X*fd*	N/A										
Atomic % of elements	Na 1.5%	Mg 2.8%	Al	Si 24.1%	P 1.8%	S	Cl 15.4%	K 18.9%	Ca 3.3%	Fe	Ti
pH	9.6										

Table 6.4 The analytical data for grasses showing the results of each analytical method organised by ashing temperature. Source: Author

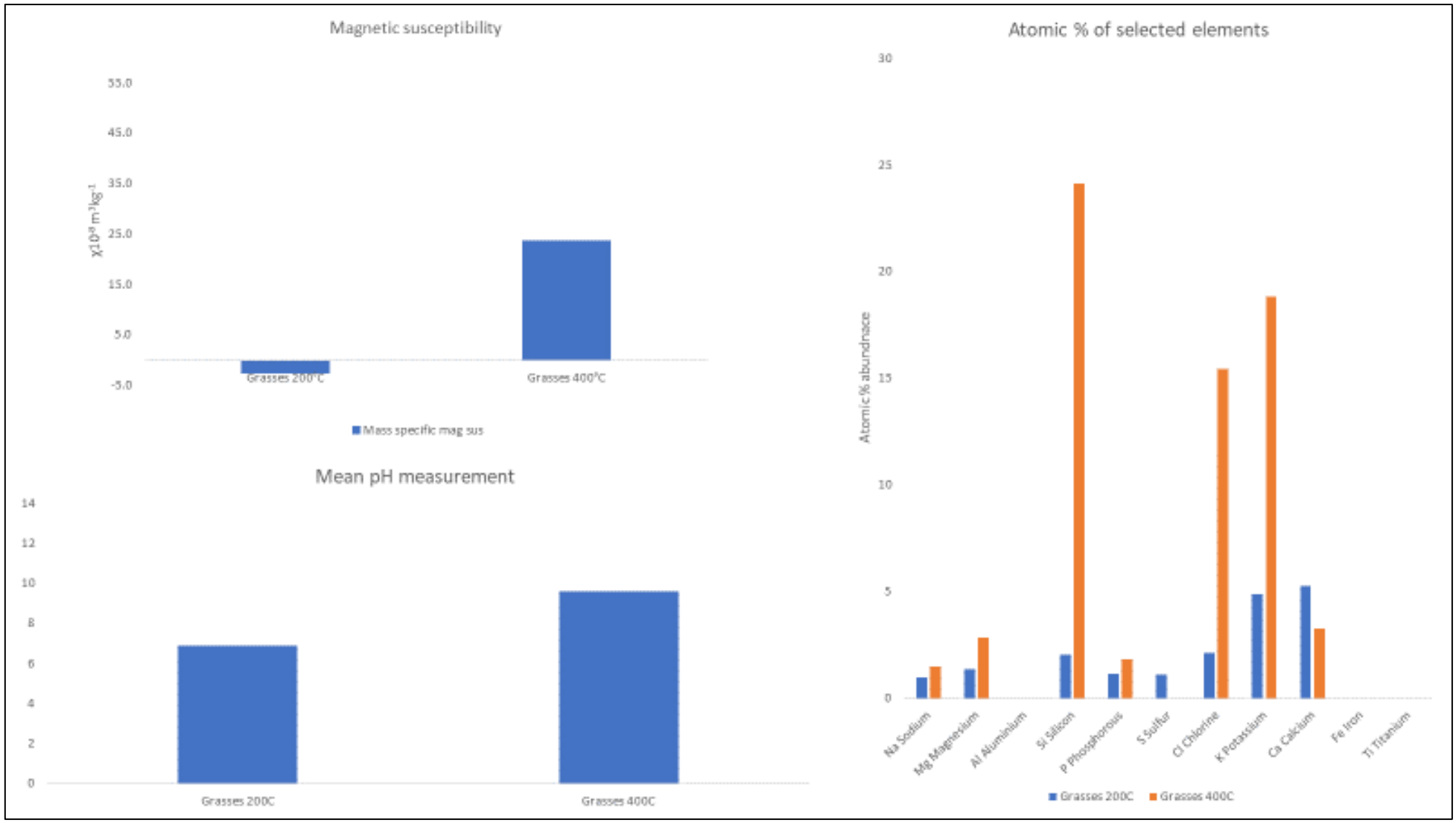

Figure 6.6 Clockwise from top left the low frequency mass specific magnetic susceptibility and percentage frequency dependence, the atomic percentage abundance of selected elements, and the pH of grasses at increasing temperature. Source: Author

Cow dung

The MS of the cow dung samples shows an increase as temperature increases from 2.3 x10^{-8} m^3kg^{-1} at 200^{0}C to 26.7 x10^{-8} m^3kg^{-1} at 400^{0}C, and at 900^{0}C the value drops to 12.9. The FDMS is not able to be calculated for any of the cow dung samples (table 6.5).

The SEM/EDX results for cow dung show the presence of sodium, magnesium, silicon, phosphorous, sulphur, chlorine, potassium, and calcium shown in figure 6.7 and table 6.5. There is also aluminium and iron present within the 200^{0}C and 400^{0}C samples. The most abundant element among all three samples was potassium.

The pH data from the cow dung ash samples shows an intensification of alkalinity as temperature is increased. The cow dung sample rise in pH from neutral at 200^{0}C, 10.0 at 400^{0}C, and 12.2 at 900^{0}C (table 6.5).

Cow dung 200^{0}C											
Xlf=κ/p x10^{-8} m^3kg^{-1}	2.3										
%X*fd*	N/A										
Atomic % of elements	Na 4.2%	Mg 1.5%	Al 0.4%	Si 8.1%	P 2.4%	S 4.3%	Cl 12.8%	K 21.5%	Ca 4.4%	Fe 0.4%	Ti
pH	7.0										
Cow dung 400^{0}C											
Xlf=κ/p x10^{-8} m^3kg^{-1}	26.7										
%X*fd*	N/A										
Atomic % of elements	Na 4.8%	Mg 2.1%	Al 0.2%	Si 4.7%	P 3.6%	S 0.6%	Cl 6.4%	K 6.8%	Ca 5.5%	Fe 0.2%	Ti
pH	10.3										
Cow dung 900^{0}C											
Xlf=κ/p x10^{-8} m^3kg^{-1}	12.9										
%X*fd*	N/A										
Atomic % of elements	Na 5.1%	Mg 2.3%	Al	Si 6.5%	P 0.5%	S 0.4%	Cl 11.9%	K 11.2%	Ca 5.5%	Fe	Ti
pH	12.2										

Table 6.5 The analytical data for cow dung showing the results of each analytical method organised by ashing temperature. Source: Author

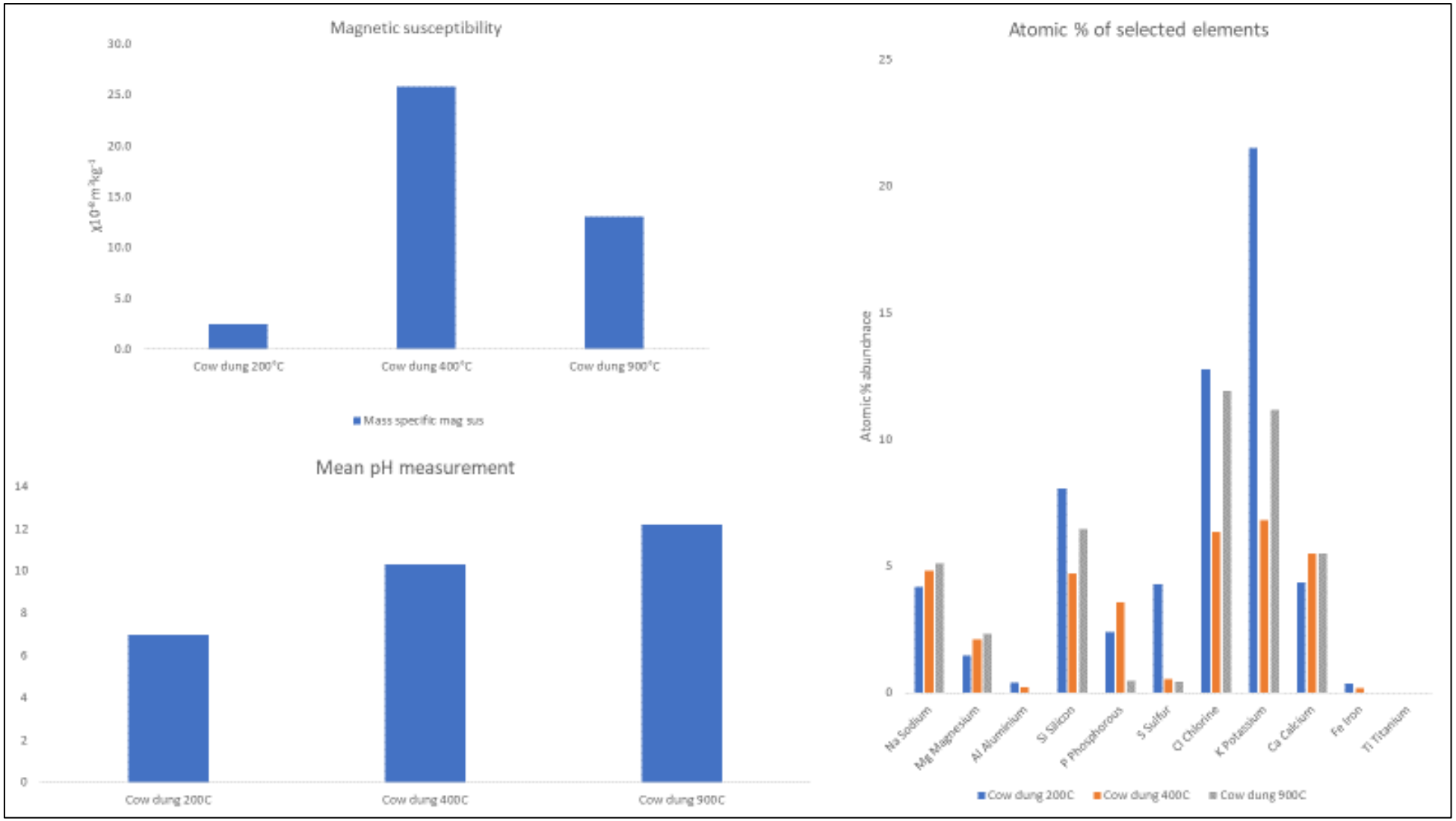

Figure 6.7 Clockwise from top left the low frequency mass specific magnetic susceptibility and percentage frequency dependence, the atomic percentage abundance of selected elements, and the pH of cow dung at increasing temperature. Source: Author

Sheep dung

The MS of the sheep dung samples show an increase as temperature increases from 0.6 x$10^{-8}$$m^3kg^{-1}$ at 200^{0}C, 15.9 x$10^{-8}$$m^3kg^{-1}$ at 400^{0}C, and 214.6 x$10^{-8}$$m^3kg^{-1}$ at 900^{0}C. The FDMS is not able to be calculated for the 200^{0}C sample; however, the value does decrease from 17.8% at 400^{0}C to 6.5% at 900^{0}C (table 6.6).

The SEM/EDX results for sheep dung show the presence of sodium, magnesium, aluminium, silicon, phosphorous, potassium, calcium, and iron (figure 6.8). There is also sulphur present within the 200^{0}C and 400^{0}C samples, chlorine within the 400^{0}C sample, and titanium within the 400^{0}C and 900^{0}C samples. The most abundant element among all three samples is silicon.

The pH data from the sheep dung ash samples shows an intensification of alkalinity as temperature is increased (figure 6.8). The sheep dung samples rise in pH from slightly acidic 6.4 at 200^{0}C, 9.6 at 400^{0}C, and 10.7 at 900^{0}C (table 6.6).

Sheep dung 200^{0}C											
Xlf=κ/p x10^{-8} m^3kg^{-1}	0.6										
%X*fd*	N/A										
Atomic % of elements	Na 0.9%	Mg 2.0%	Al 14.3%	Si 23.1%	P 3.5%	S 1.3%	Cl	K 9.8%	Ca 4.2%	Fe 2.5%	Ti
pH	6.4										
Sheep dung 400^{0}C											
Xlf=κ/p x10^{-8} m^3kg^{-1}	15.9										
%X*fd*	17.8										
Atomic % of elements	Na 1.1%	Mg 5.9%	Al 1.3%	Si 6.6%	P 4.7%	S 1.5%	Cl 0.2%	K 3.3%	Ca 9.7%	Fe 0.8%	Ti 0.2%
pH	9.6										
Sheep dung 900^{0}C											
Xlf=κ/p x10^{-8} m^3kg^{-1}	214.6										
%X*fd*	6.5										
Atomic % of elements	Na 1.8%	Mg 4.5%	Al 3.03%	Si 13.0%	P 3.7%	S	Cl	K 2.6%	Ca 6.6%	Fe 0.6%	Ti 0.2%
pH	10.7										

Table 6.6 The analytical data for sheep dung showing the results of each analytical method organised by ashing temperature. Source: Author

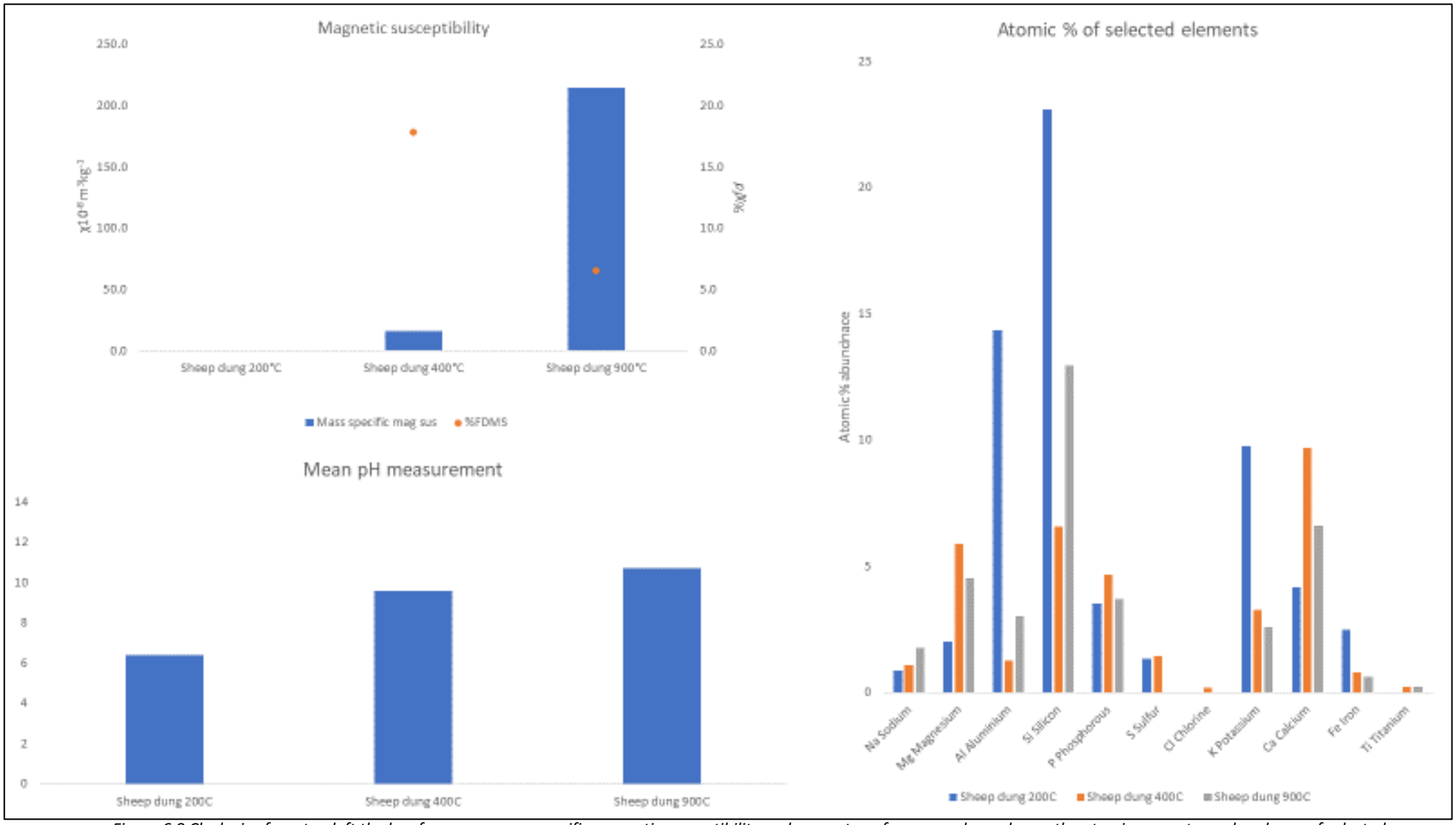

Figure 6.8 Clockwise from top left the low frequency mass specific magnetic susceptibility and percentage frequency dependence, the atomic percentage abundance of selected elements, and the pH of sheep dung at increasing temperature. Source: Author

Heather

The MS of the heather samples show an increase as temperature increases from -2.5 $x10^{-8}m^3kg^{-1}$ at 200^0C to 15.8 $x10^{-8}m^3kg^{-1}$ at 400^0C; the values are not available for the 900^0C sample (figure 6.9). The FDMS is not able to be calculated for any of the samples.

The SEM/EDX results for heather show the presence of sodium, magnesium, silicon, phosphorous, sulphur, potassium, calcium, and iron shown in figure 6.9 and table 6.7. There is additionally aluminium, chlorine, and titanium within the 400^0C sample, and aluminium within the 900^0C sample (figure 6.9). the most abundant element among all three samples is sodium.

The heather samples rise in pH from acidic 5.2 at 200^0C, rise to alkaline 8.8 at 400^0C, and drop back to acidic 6 at 900^0C (table 6.7).

Heather 200^0C											
Xlf=κ/ρ $x10^{-8}$ m^3kg^{-1}	-2.5										
%X*fd*											
Atomic % of elements	Na 6.6%	Mg 1.9%	Al	Si 1.2%	P 1.8%	S 0.6%	Cl	K 3.1%	Ca 1.6%	Fe 0.4%	Ti
pH	5.2										
Heather 400^0C											
Xlf=κ/ρ $x10^{-8}$ m^3kg^{-1}	15.8										
%X*fd*											
Atomic % of elements	Na 4.9%	Mg 3.7%	Al 1.2%	Si 3.0%	P 2.1%	S 2.1%	Cl 0.2%	K 2.4%	Ca 2.9%	Fe 0.6%	Ti 0.1%
pH	8.8										
Heather 900^0C											
Xlf=κ/ρ $x10^{-8}$ m^3kg^{-1}	N/A										
%X*fd*	N/A										
Atomic % of elements	Na 6.8%	Mg 9.3%	Al 1.1%	Si 1.1%	P 0.3%	S 1.0%	Cl	K 1.0%	Ca 12.6%	Fe 2.4%	Ti
pH	6										

Table 6.7 The analytical data for heather showing the results of each analytical method organised by ashing temperature. Source: Author

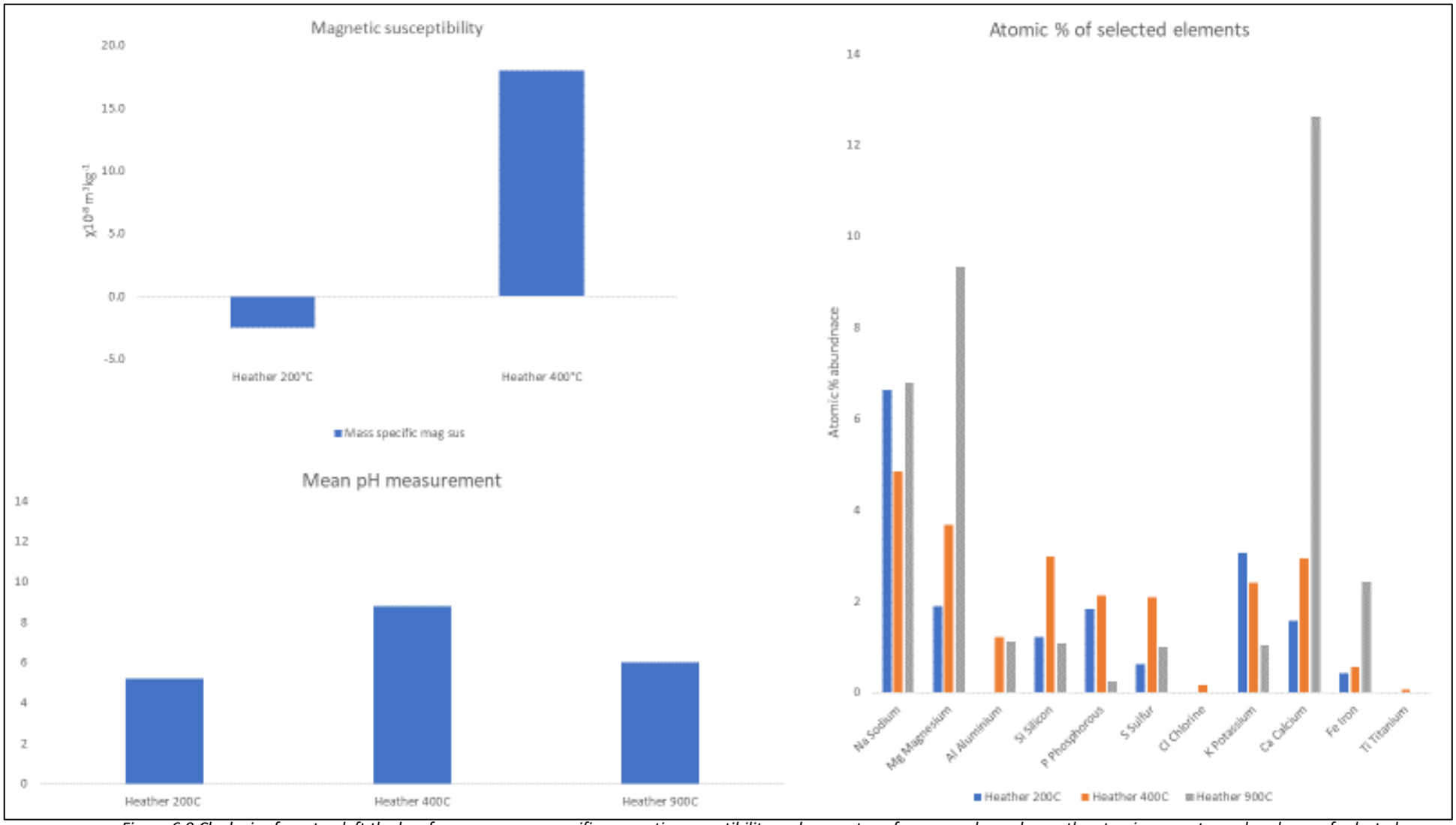

Figure 6.9 Clockwise from top left the low frequency mass specific magnetic susceptibility and percentage frequency dependence, the atomic percentage abundance of selected elements, and the pH of heather at increasing temperature. Source: Author

Willow

The MS of the willow samples show a diamagnetic measurement at 200^0C, and an increase to a value of 4.7 *Xlf*=κ/p $x10^{-8}(m^3kg^{-1})$ at 400^0C (table 6.8). The FDMS is not able to be calculated for either of the samples.

The SEM/EDX results for willow show the presence of aluminium and calcium within the 200^0C sample, and sodium, magnesium, phosphorous, sulphur, chlorine, potassium, and calcium within the 400^0C willow sample (figure 6.10). The most abundant element among the samples is calcium.

The willow samples rise in pH from acidic 6.1 at 200^0C, to alkaline 9.7 at 400^0C (table 6.8)

Willow 200^0C											
Xlf=κ/p $x10^{-8}$ m^3kg^{-1}	-0.1										
%X*fd*											
Atomic % of elements	Na	Mg	Al 10.5%	Si	P	S	Cl	K	Ca 0.1%	Fe	Ti
pH	6.1										
Willow 400^0C											
Xlf=κ/p $x10^{-8}$ m^3kg^{-1}	4.7										
%X*fd*											
Atomic % of elements	Na 0.9%	Mg 0.4%	Al	Si	P 1.8%	S 0.9%	Cl 0.3%	K 5.1%	Ca 14.3%	Fe	Ti
pH	9.7										

Table 6.8 The analytical data for willow showing the results of each analytical method organised by ashing temperature. Source: Author

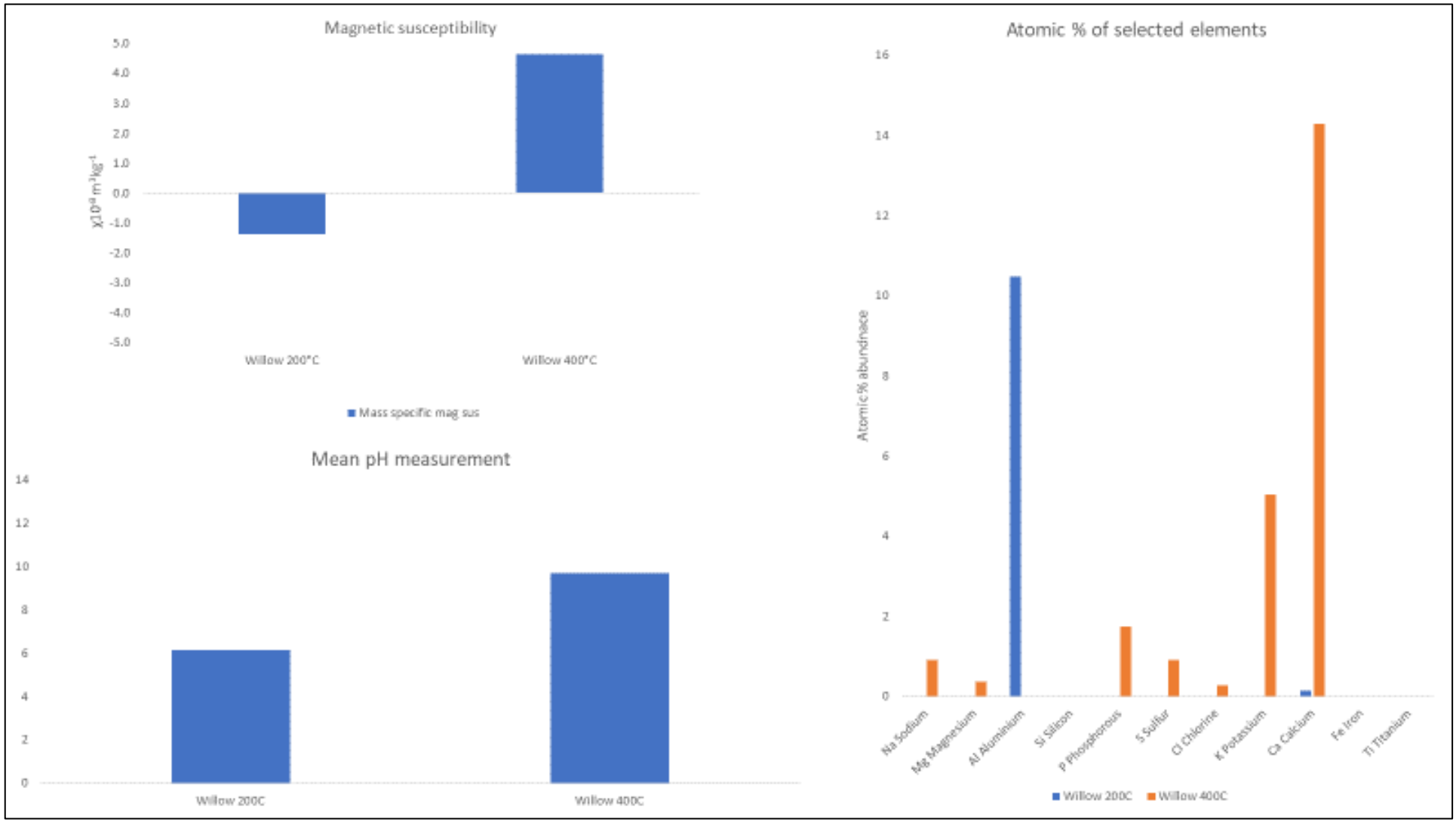

Figure 6.10 Clockwise from top left the low frequency mass specific magnetic susceptibility and percentage frequency dependence, the atomic percentage abundance of selected elements, and the pH of willow at increasing temperature. Source: Author

Hazel

The MS of the hazel samples show a diamagnetic measurement -3.7 $x10^{-8}m^3kg^{-1}$ at 200^0C, and an increase to a value of 9.2 $x10^{-8}m^3kg^{-1}$ at 400^0C (table 6.9). The FDMS is not able to be calculated for either of the samples.

The SEM/EDX results for hazel show the presence of magnesium and sulphur within the 200^0C sample, and sodium, magnesium, aluminium, silicon, phosphorous, sulphur, chlorine, potassium, calcium, and iron within the 400^0C sample (figure 6.11). The most abundant element among the samples is magnesium.

The hazel samples rise in pH from acidic 5.3 at 200^0C, to alkaline 10.1 at 400^0C (table 6.9)

Hazel 200^0C											
Xlf=κ/p $x10^{-8}$ m^3kg^{-1}	-3.7										
%X*fd*											
Atomic % of elements	Na	Mg 0.1%	Al	Si	P	S 0.2%	Cl	K	Ca	Fe	Ti
pH	5.3										
Hazel 400^0C											
Xlf=κ/p $x10^{-8}$ m^3kg^{-1}	9.2										
%X*fd*											
Atomic % of elements	Na 5.1%	Mg 6.1%	Al 1.3%	Si 2.6%	P 2.0%	S 1.6%	Cl 0.2%	K 2.0%	Ca 5.4%	Fe 0.5%	Ti
pH	10.1										

Table 6.9 The analytical data for hazel showing the results of each analytical method organised by ashing temperature. Source: Author

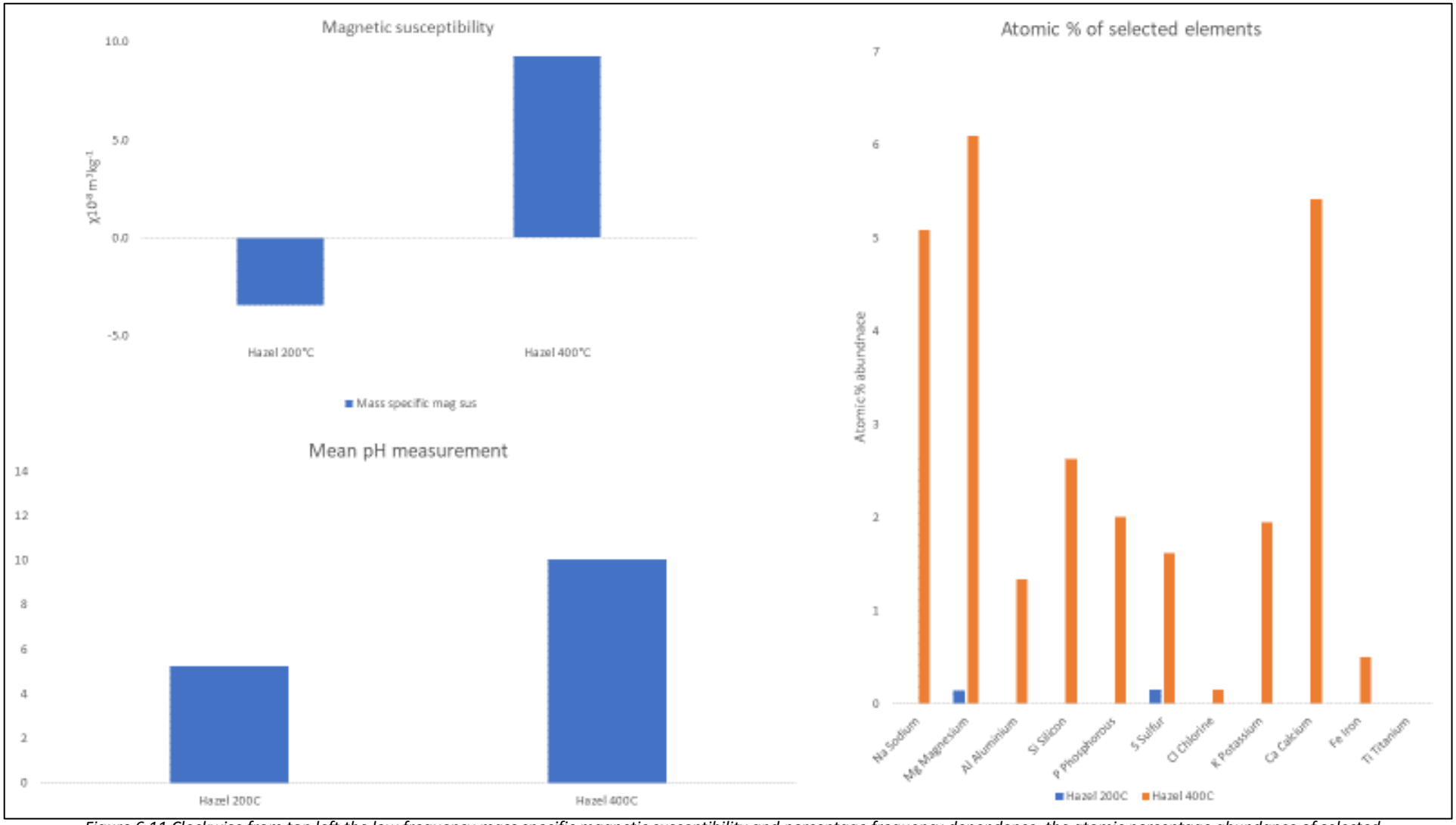

Figure 6.11 Clockwise from top left the low frequency mass specific magnetic susceptibility and percentage frequency dependence, the atomic percentage abundance of selected elements, and the pH of hazel at increasing temperature. Source: Author

Animal bone

The MS of the animal bone samples show a diamagnetic measurement for all temperature intervals (figure 6.12). The FDMS values are not able to be calculated for any of the samples.

The SEM/EDX results for animal bone show the presence of sodium, phosphorous, and calcium among all three samples, and magnesium within the 200^0C sample (table 6.10). The most abundant element among the samples was calcium.

The pH data shows an intensification of alkalinity among all samples, yet the 900^0C is the most intense increase. The 200^0C and 400^0C samples are both neutral, 7.1 and 7.9 respectively, and the 900^0C sample has a pH of 10.5 (table 6.10).

Animal bone 200^0C											
Xlf=κ/p x10^{-8} m^3kg^{-1}	-1.0										
%X*fd*											
Atomic % of elements	Na 0.5%	Mg 0.4%	Al	Si	P 8.0%	S	Cl	K	Ca 12.5%	Fe	Ti
pH	7.1										
Animal bone 400^0C											
Xlf=κ/p x10^{-8} m^3kg^{-1}	-1.1										
%X*fd*											
Atomic % of elements	Na 1.1%	Mg	Al	Si	P 11.1%	S	Cl	K	Ca 17.8%	Fe	Ti
pH	7.9										
Animal bone 900^0C											
Xlf=κ/p x10^{-8} m^3kg^{-1}	-0.8										
%X*fd*											
Atomic % of elements	Na 0.5%	Mg	Al	Si	P 8.9%	S	Cl	K	Ca 14.1%	Fe	Ti
pH	10.5										

Table 6.10 The analytical data for animal bone showing the results of each analytical method organised by ashing temperature. Source: Author

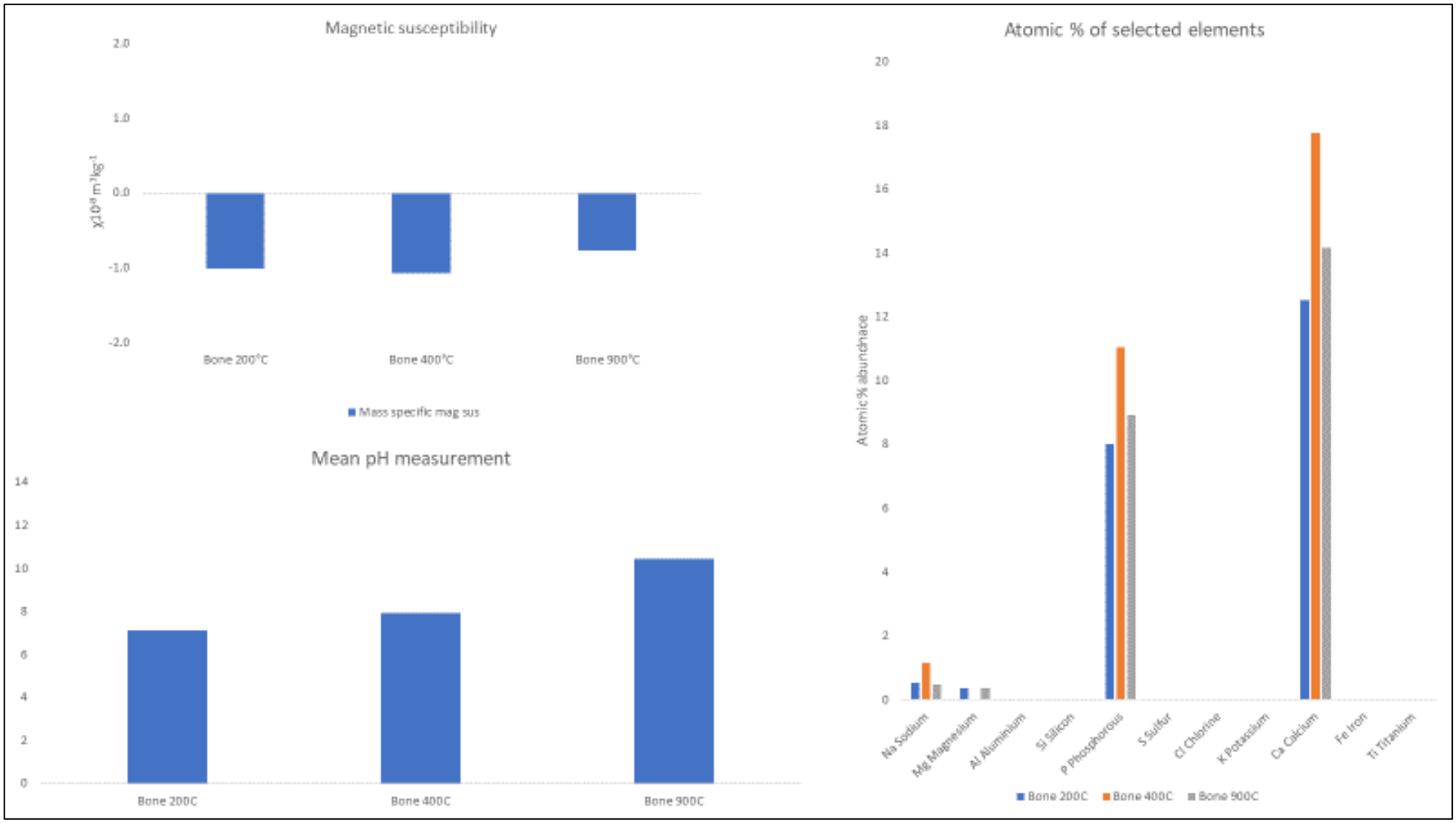

Figure 6.12 Clockwise from top left the low frequency mass specific magnetic susceptibility and percentage frequency dependence, the atomic percentage abundance of selected elements, and the pH of animal bone at increasing temperature. Source: Author

Rousay peat

The MS of the Rousay peat samples show an increase as temperature increases 18.1 x10^{-8} m^3kg^{-1} at 200^{0}C, 331.7 x10^{-8} m^3kg^{-1} at 400^{0}C, and 3559.1 x10^{-8} m^3kg^{-1} at 900^{0}C. The FDMS could not be calculated for the 200^{0}C sample. The 400^{0}C and 900^{0}C samples have FDMS values of 14.3% and 4.6% respectively (table 6.11).

The SEM/EDX spectroscopy results for Rousay peat show the presence of sodium, magnesium, aluminium, sulphur, calcium, and iron throughout all temperature intervals (figure 6.13). There is also silicon present among the 200^{0}C sample, and silicon, phosphorous, potassium, and titanium present in the 900^{0}C sample (table 6.11). the most abundant element among all three sample is magnesium.

pH data from the Rousay peat samples at all three temperature intervals shows an intensification of alkalinity associated with increase in temperature (figure 6.13). The Rousay peat samples start with a pH of 4.3, which increases to 8.9 at 400^{0}C, and peaks at 10.2 at 900^{0}C (table 6.11).

Rousay Peat 200^{0}C											
Xlf=κ/p x10^{-8} m^3kg^{-1}	18.1										
%X*fd*	N/A										
Atomic % of elements	Na 1.9%	Mg 3.6%	Al 2.3%	Si 1.7%	P	S 3.2%	Cl	K	Ca 1.6%	Fe 0.8%	Ti
pH	4.3										
Rousay Peat 400^{0}C											
Xlf=κ/p x10^{-8} m^3kg^{-1}	331.7										
%X*fd*	14.3										
Atomic % of elements	Na 1.9%	Mg 13.4%	Al 1.7%	Si	P	S 13.7%	Cl 1.2%	K	Ca 7.8%	Fe 3.9%	Ti
pH	8.9										
Rousay Peat 900^{0}C											
Xlf=κ/p x10^{-8} m^3kg^{-1}	3559.1										
%X*fd*	4.6										
Atomic % of elements	Na 2.4%	Mg 11.4%	Al 1.4%	Si 2.3%	P 0.7%	S 6.0%	Cl 0.5%	K 0.8%	Ca 5.9%	Fe 6.63%	Ti 0.3%
pH	10.2										

Table 6.11 The analytical data for Rousay peat showing the results of each analytical method organised by ashing temperature. Source: Author.

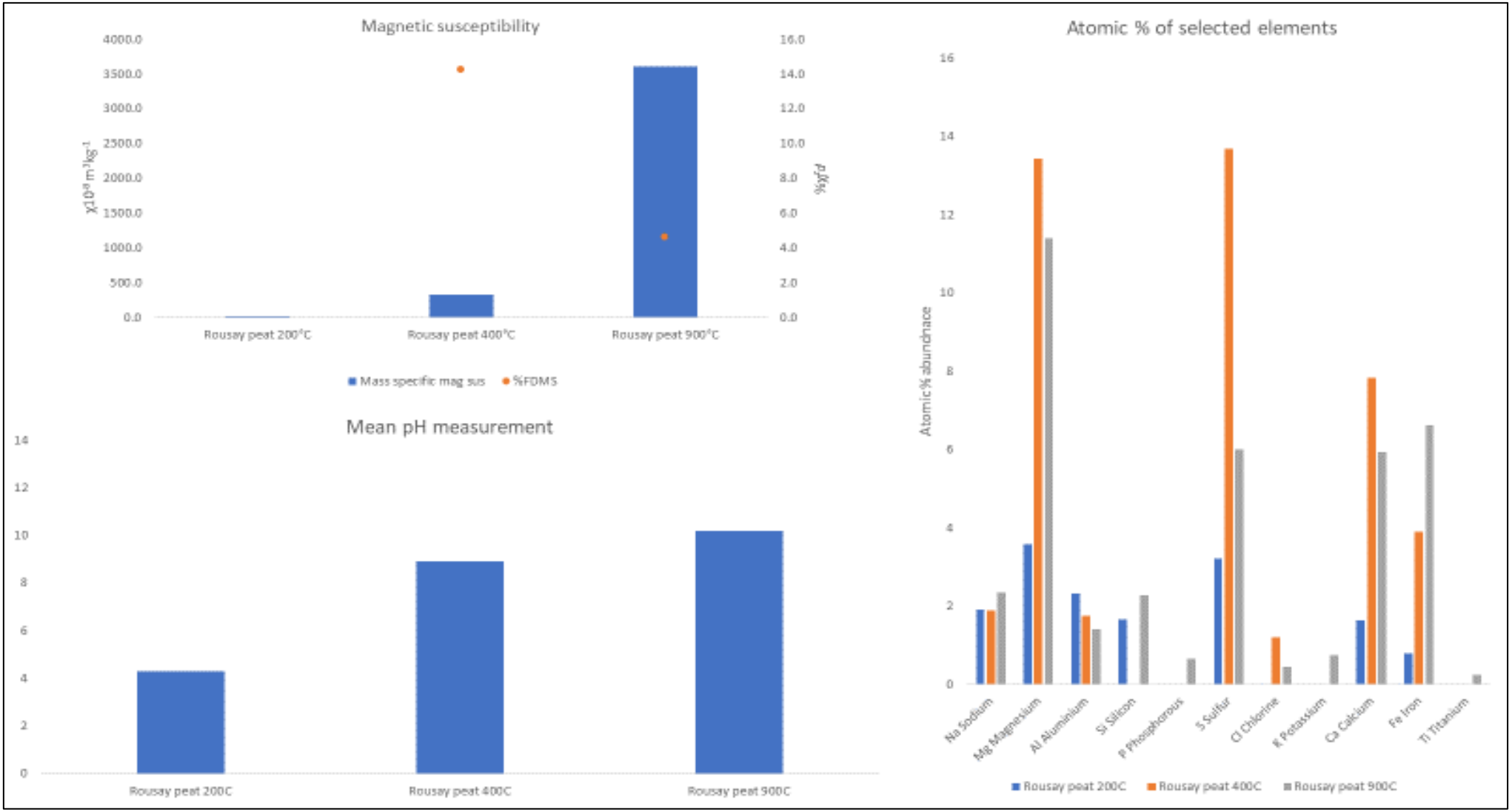

Figure 6.13 Clockwise from top left the low frequency mass specific magnetic susceptibility and percentage frequency dependence, the atomic percentage abundance of selected elements, and the pH of Rousay peat at increasing temperature. Source: Author

Corrigal Peat

Fozzy (fibric)

The MS of the fozzy peat samples show an increase as temperature increases - 1.1 $x10^{-8}m^3kg^{-1}$ at 200^0C, 6.4 $x10^{-8}m^3kg^{-1}$ at 400^0C, and 1135.8 $x10^{-8}m^3kg^{-1}$ at 900^0C (table 6.12). The FDMS value is not able to be calculated for the 200^0C sample, but the 400^0C value is highest at 25.6% and the 900^0C value is lower at 10.7%.

The SEM/EDX results for fozzy peat show the presence of magnesium, aluminium, silicon, sulphur, calcium, and iron within all samples, chlorine within the 200^0C sample, sodium within the 400^0C sample, and sodium, phosphorous, chlorine, potassium, and titanium within the 900^0C sample (table 6.12) the most abundant element among all three samples is magnesium.

The pH results show an increase in pH measeurement as temperature increased, the 200^0C sample is acidic at 5.7, the 400^0C sample is 8.1, and the 900^0C sample is the most alkaline at 9.6 (figure 6.14).

Fozzy peat 200^0C											
Xlf=κ/p $x10^{-8}$ m^3kg^{-1}	-1.1										
%X*fd*	N/A										
Atomic % of elements	Na	Mg 1.6%	Al 0.5%	Si 0.4%	P	S 0.8%	Cl 0.2%	K	Ca 0.7%	Fe 0.3%	Ti
pH	5.7										
Fozzy peat 400^0C											
Xlf=κ/p $x10^{-8}$ m^3kg^{-1}	6.4										
%X*fd*	25.6										
Atomic % of elements	Na 0.4%	Mg 0.8%	Al 0.5%	Si 1.0%	P	S 0.7%	Cl	K	Ca 0.7%	Fe 0.2%	Ti
pH	8.1										
Fozzy peat 900^0C											
Xlf=κ/p $x10^{-8}$ m^3kg^{-1}	1135.8										
%X*fd*	10.7										
Atomic % of elements	Na 2.4%	Mg 11.6%	Al 2.1%	Si 2.5%	P 1.8%	S 4.0%	Cl 0.2%	K 0.3%	Ca 6.3%	Fe 5.6%	Ti 0.2%
pH	9.6										

Table 6.12 The analytical data for fozzy peat showing the results of each analytical method organised by ashing temperature. Source: Author

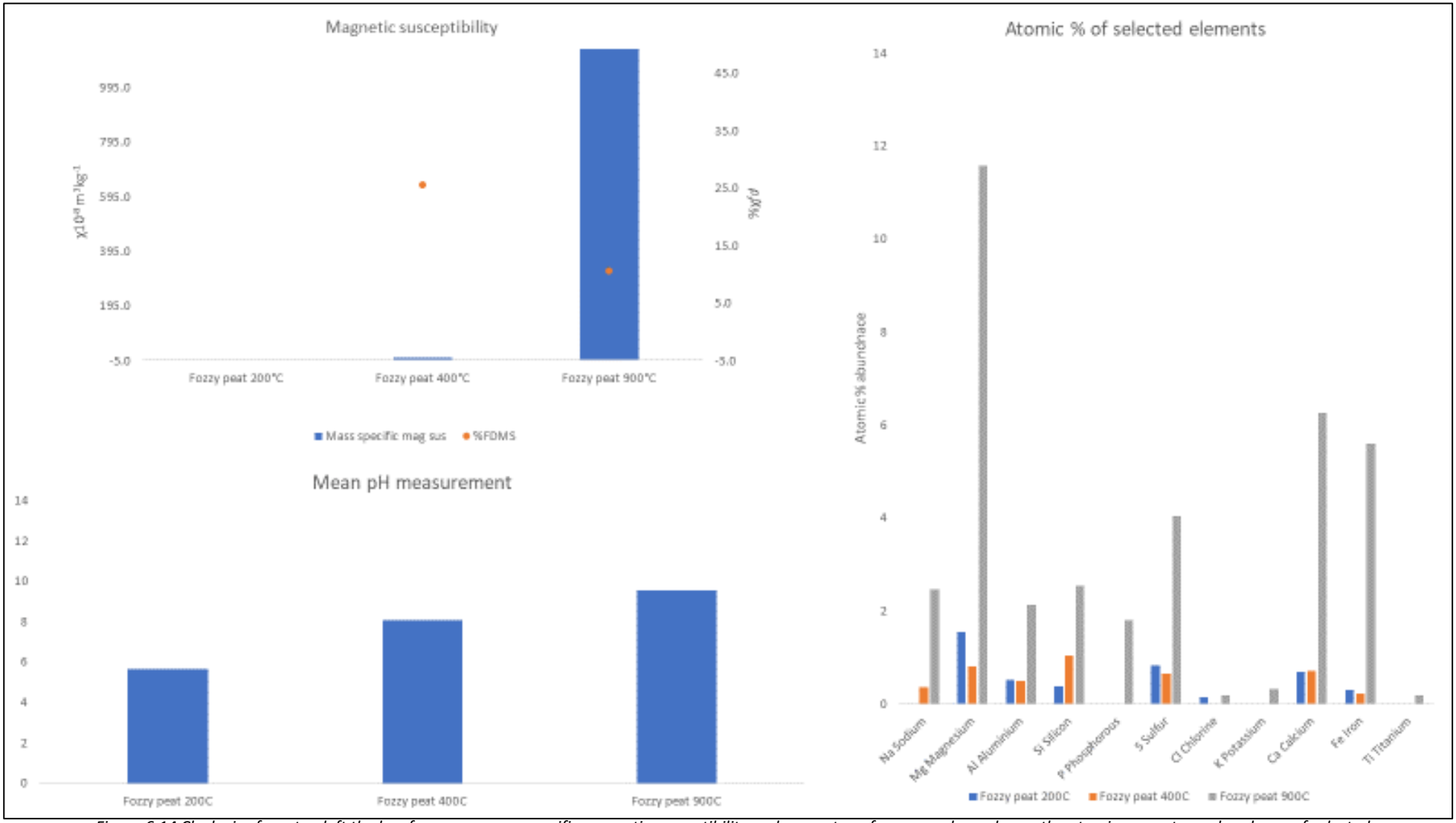

Figure 6.14 Clockwise from top left the low frequency mass specific magnetic susceptibility and percentage frequency dependence, the atomic percentage abundance of selected elements, and the pH of fozzy peat at increasing temperature. Source: Author

Middle (hemic)

The MS of the middle peat samples show an increase as temperature increases 1.4 $x10^{-8}m^3kg^{-1}$ at 200^0C, 90.5 $x10^{-8}m^3kg^{-1}$ at 400^0C, and 823.5 $x10^{-8}m^3kg^{-1}$ at 900^0C (table 6.13). The percentage frequency dependence value is not able to be calculated for the 200^0C sample, but the 400^0C value is highest at 22.4% and the 900^0C value is lower at 11.6%.

The SEM/EDX results for middle peat show the presence of sodium, aluminium, silicon, potassium, calcium, iron, and titanium within all samples, and phosphorous, sulphur, and chlorine within the 200^0C and 400^0C samples (figure 6.15). the most abundant element among all three samples is magnesium.

The pH results show an increase in pH measeurement as temperature increased, the 200^0C sample is acidic at 5.7, the 400^0C sample is 8.8, and the 900^0C sample is the most alkaline at 10.1 shown in figure 6.15 and table 6.13.

Middle peat 200^0C											
Xlf=κ/p $x10^{-8}$ m^3kg^{-1}	1.4										
%X*fd*	N/A										
Atomic % of elements	Na 3.7%	Mg 0.4%	Al 3.7%	Si 15.9%	P	S	Cl	K 0.4%	Ca 0.5%	Fe 0.9%	Ti 0.1%
pH	5.7										
Middle peat 400^0C											
Xlf=κ/p $x10^{-8}$ m^3kg^{-1}	90.5										
%X*fd*	22.4										
Atomic % of elements	Na 1.2%	Mg 4.9%	Al 0.8%	Si 0.9%	P 0.2%	S 4.6%	Cl 0.2%	K 0.1%	Ca 3.6%	Fe 2.9%	Ti 0.3%
pH	8.8										
Middle peat 900^0C											
Xlf=κ/p $x10^{-8}$ m^3kg^{-1}	823.5										
%X*fd*	11.6										
Atomic % of elements	Na 1.9%	Mg 11.7%	Al 3.1%	Si 4.3%	P 0.9%	S 5.2%	Cl 0.3%	K 0.6%	Ca 8.3%	Fe 2.1%	Ti 0.3%
pH	10.1										

Table 6.13 The analytical data for middle peat showing the results of each analytical method organised by ashing temperature. Source: Author

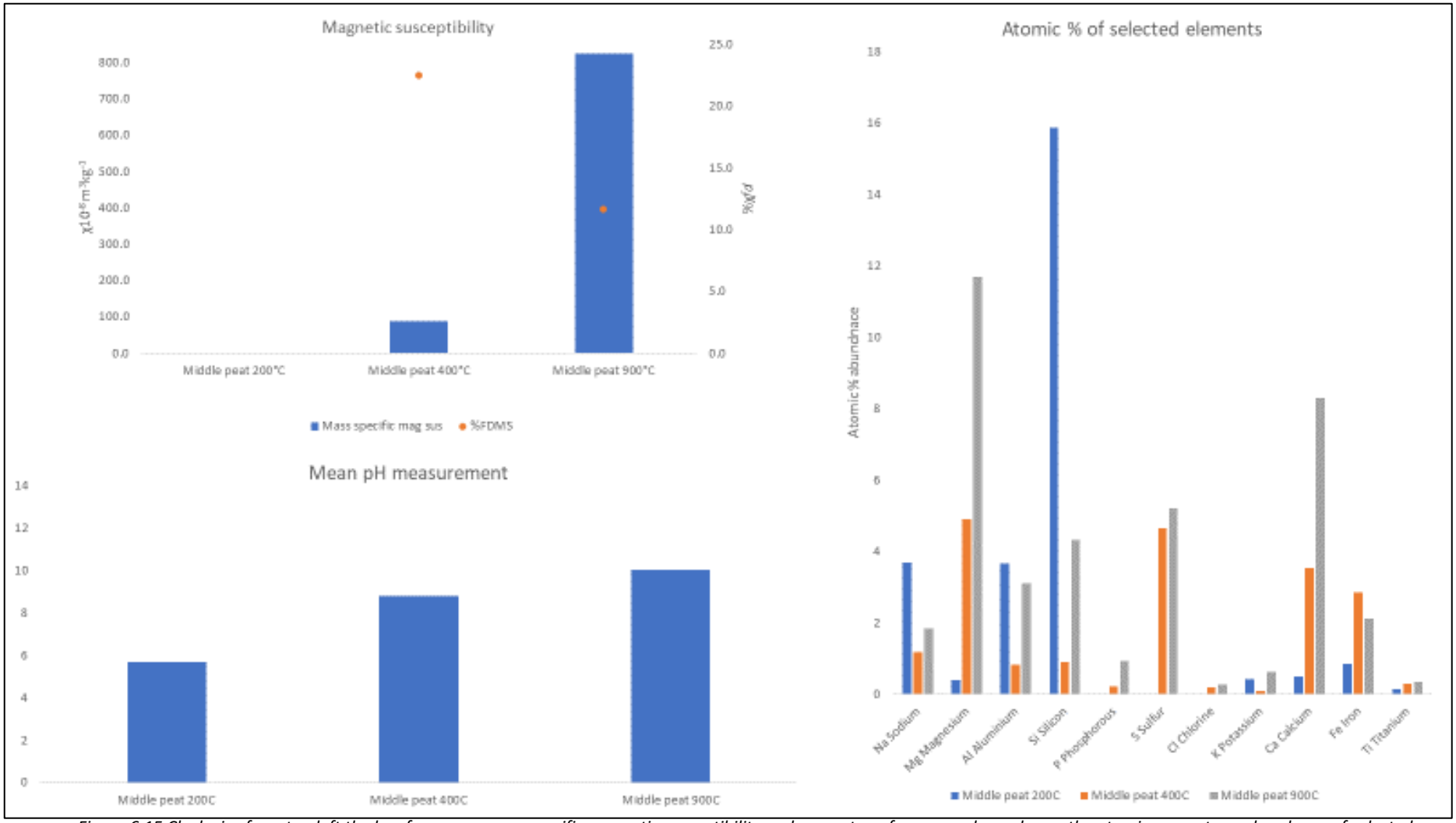

Figure 6.15 Clockwise from top left the low frequency mass specific magnetic susceptibility and percentage frequency dependence, the atomic percentage abundance of selected elements, and the pH of middle peat at increasing temperature. Source: Author

Low (sapric)

The MS of the low peat samples show an increase as temperature increases 12.0 $x10^{-8}m^3kg^{-1}$ at 200^0C, 20.0 $x10^{-8}m^3kg^{-1}$ at 400^0C, and 1006.7 $x10^{-8}m^3kg^{-1}$ at 900^0C (table 6.14). The percentage frequency dependence value is not available for the 200^0C sample, but the 400^0C value and the 900^0C value do show a decrease from 13.3% at 400^0C and 8.2% at 900^0C.

The SEM/EDX results for low peat show the presence of sodium, magnesium, aluminium, silicon, sulphur, calcium, iron, and titanium within all samples, and potassium within the 900^0C sample.

The pH results show an increase in pH measeurement between the 200^0C sample that is neutral at 7.0 and the 400^0C sample that is 8.7. The 900^0C sample has the same pH as the 400^0C sample at 8.7 (table 6.14).

Low peat 200^0C											
Xlf=κ/p $x10^{-8}$ m^3kg^{-1}	12.0										
%X*fd*	N/A										
Atomic % of elements	Na 0.5%	Mg 3.6%	Al 0.7%	Si 1.1%	P 0.2%	S 3.0%	Cl	K	Ca 2.1%	Fe 1.3%	Ti 0.1%
pH	7.0										
Low peat 400^0C											
Xlf=κ/p $x10^{-8}$ m^3kg^{-1}	20.0										
%X*fd*	13.3										
Atomic % of elements	Na 0.3%	Mg 1.4%	Al 0.2%	Si 0.3%	P 0.1%	S 1.8%	Cl	K	Ca 1.4%	Fe 0.8%	Ti 0.1%
pH	8.7										
Low peat 900^0C											
Xlf=κ/p $x10^{-8}$ m^3kg^{-1}	1006.7										
%X*fd*	8.2										
Atomic % of elements	Na 0.4%	Mg 3.6%	Al 2.1%	Si 1.2%	P 0.6%	S 2.6%	Cl	K 0.2%	Ca 4.9%	Fe 1.9%	Ti 0.3%
pH	8.7										

Table 6.14 The analytical data for low peat showing the results of each analytical method organised by ashing temperature. Source: Author

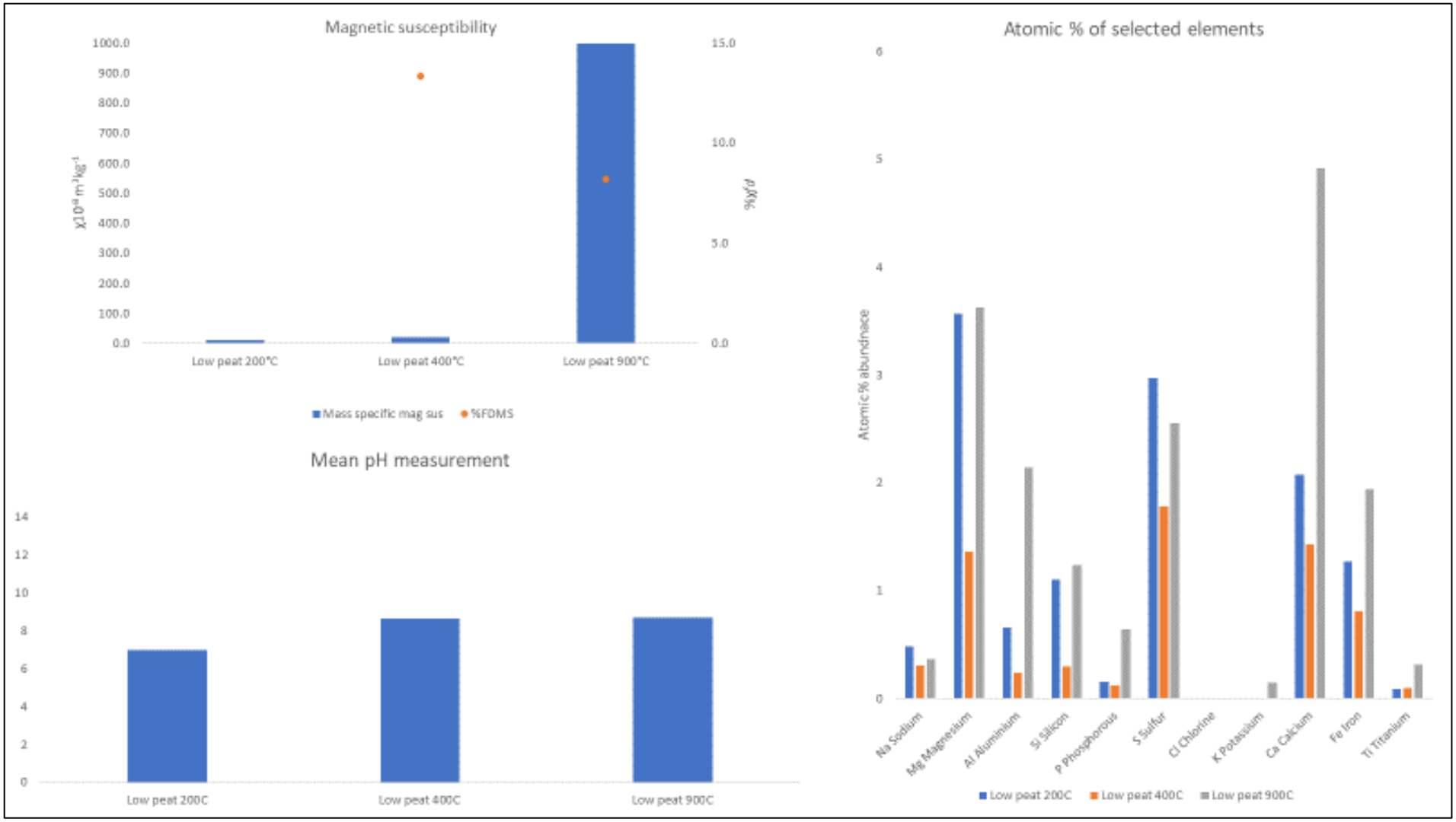

Figure 6.16 Clockwise from top left the low frequency mass specific magnetic susceptibility and percentage frequency dependence, the atomic percentage abundance of selected elements, and the pH of low peat at increasing temperature. Source: Author

Highland Park peat

The MS of the Highland Park peat samples show an increase as temperature increases 4.6 $x10^{-8}m^3kg^{-1}$ at 200^0C, 19.6 $x10^{-8}m^3kg^{-1}$ at 400^0C, and 1748.3 $x10^{-8}m^3kg^{-1}$ at 900^0C (table 6.15). The percentage frequency dependence value is not able to be calculated for the 200^0C sample, but the 400^0C value and the 900^0C value do show a decrease in value from 15.6% at 400^0C and 9.8% at 900^0C.

The SEM/EDX results for Highland Park peat show the presence of sodium, magnesium, aluminium, silicon, sulphur, potassium, calcium, iron, and titanium within all samples, phosphorous within the 400^0C and 900^0C samples, and chlorine within the 900^0C sample (table 6.15). The most abundant element within all three samples is magnesium.

The pH results show an increase in pH measeurement as temperature increased, the 200^0C sample is acidic at 5.2, the 400^0C sample is 7.4, and the 900^0C sample is the most alkaline at 9.7 (figure 6.17).

Highland Park peat 200^0C											
Xlf=κ/p $x10^{-8}$ m^3kg^{-1}	4.6										
%X*fd*	N/A										
Atomic % of elements	Na 0.2%	Mg 0.3%	Al 0.6%	Si 2.0%	P	S 1.2%	Cl	K 0.2%	Ca 0.8%	Fe 0.4%	Ti 0.1%
pH	5.2										
Highland Park peat 400^0C											
Xlf=κ/p $x10^{-8}$ m^3kg^{-1}	19.6										
%X*fd*	15.6										
Atomic % of elements	Na 1.0%	Mg 2.1%	Al 1.6%	Si 1.9%	P 0.2%	S 4.4%	Cl	K 0.2%	Ca 3.1%	Fe 2.1%	Ti 0.1%
pH	7.4										
Highland Park peat 900^0C											
Xlf=κ/p $x10^{-8}$ m^3kg^{-1}	1748.3										
%X*fd*	9.8										
Atomic % of elements	Na 2.3%	Mg 11.8%	Al 3.1%	Si 3.6%	P 0.7%	S 4.4%	Cl 0.2%	K 0.6%	Ca 4.1%	Fe 1.6%	Ti 0.2%
pH	9.7										

Table 6.15 The analytical data for Highland Park peat showing the results of each analytical method organised by ashing temperature. Source: Author

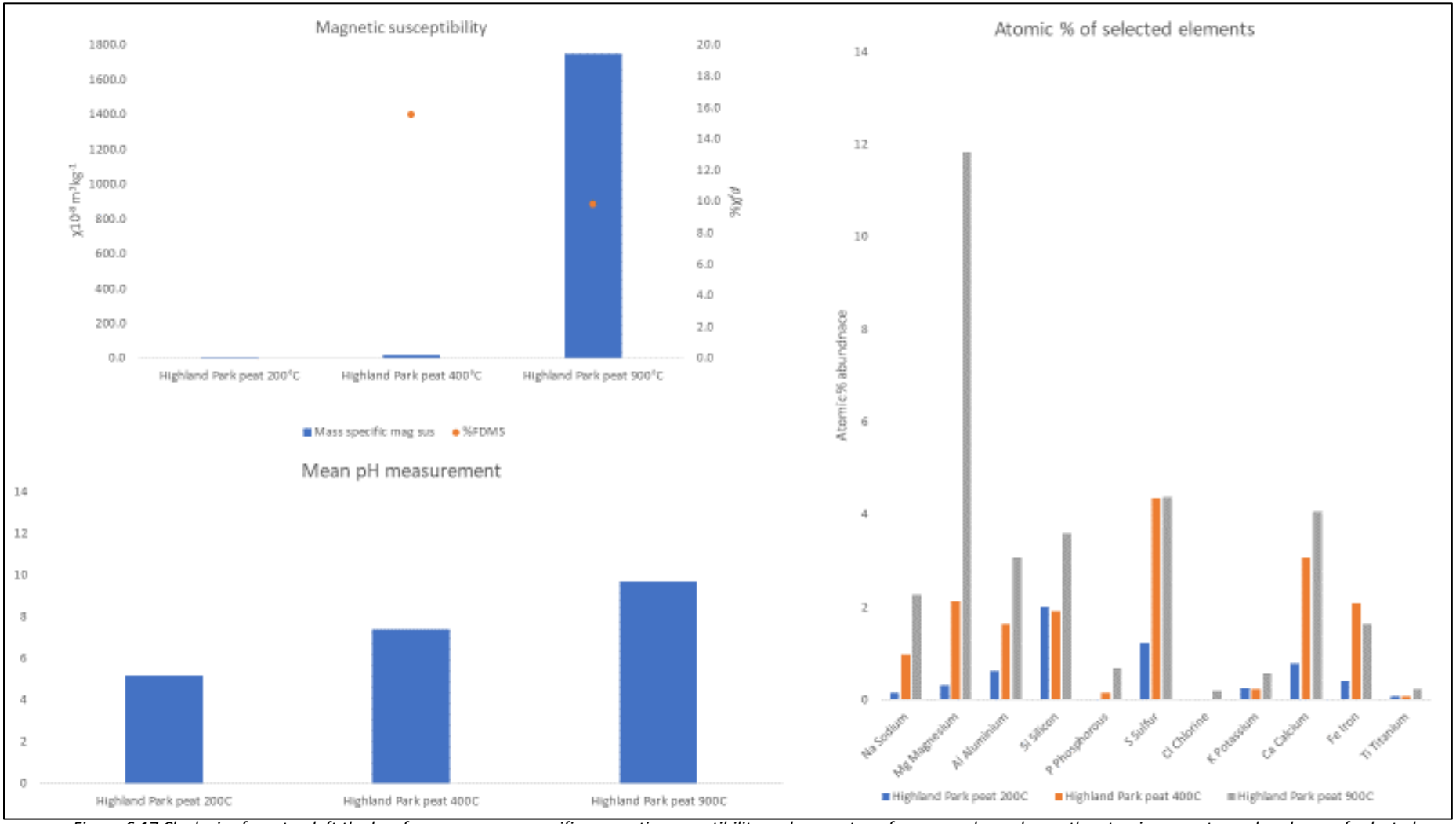

Figure 6.17 Clockwise from top left the low frequency mass specific magnetic susceptibility and percentage frequency dependence, the atomic percentage abundance of selected elements, and the pH of Highland Park peat at increasing temperature. Source: Author

6.2.3 Additional modern ash samples

The additional samples used for this investigation were presented in section 4.3 and include peat ash from the Corrigal farm house museum, peat and wood ash from a fire pit used for pottery firing, sieved and sorted archaeological matrix from the Knowe of Swandro both unheated and exposed to 900^0C for 6 hours, and a mix of all the modern analogue fuels collected for this investigation heated to 500^0C for 6 hours. The interpretation of this data and its implications for this research are discussed in chapter 7.

The sample of modern peat ash both have high MS measurements 4390.0 $x10^{-8}m^3kg^{-1}$ for Caithness peat and 1673.3 $x10^{-8}m^3kg^{-1}$ for Orkney peat. The percentage frequency dependence values of Caithness and Orkney peat are 8.2% and 11.3% respectively (table 6.17). the modern ash samples of peat contain sodium, magnesium, aluminium, silicon, phosphorous, potassium, calcium, iron, and titanium. Only the Orkney peat had a trace amount of chlorine. The Caithness peat had a larger concentration of iron, magnesium, and aluminium while the Orkney peat contained more sodium and silicon as shown in table 6.17 and figure 6.18. Both samples of modern peat ash collected from Corrigal farm have neutral pH measurements (table 6.17). The Caithness peat ash is a very deep reddish brown while the Orkney peat ash is yellowish grey (table 6.16)

The mixed modern analogue fuel ash has a low magnetic susceptibility measurement of 35.6 $x10^{-8}m^3kg^{-1}$ and a percentage frequency dependence value of 8.6% (table 6.17) The mixed sample ashes contain traces of sodium, magnesium, aluminium, silicon, phosphorous, sulphur, chlorine, potassium, calcium, iron, and titanium with the most abundant element being calcium at 6%

(figure 6.18 table 6.17). the pH measurement of the mixed modern analogue ash sample was alkaline at 9.7 (table 6.17). The mixed modern analogue fuels ash is a very dark grey (table 6.16).

The peat and wood ash sample from the open fire pit has a MS measurement of 356.9 $x10^{-8}m^3kg^{-1}$, and a percentage frequency dependence value of 9.7% (table 6.17). the elements present were sodium, magnesium, aluminium, silicon, phosphorous, sulphur, chlorine, potassium, calcium, iron, and titanium (figure 6.18). The most abundant element within the sample is calcium at 13.7% (table 6.17) The peat and wood ash is a pale yellow with dark grey inclusions (table 6.16).

Modern Ash Munsell Colour Assignments	
Caithness peat	10R 4/8
Orkney peat	7.5YR 6/6
Mixed Fuels 500^{0}C	10YR 4/1
Peat and Wood Ash	2.5Y 7/4 + Gley 1 2.5/N

Table 6.16 A table showing the Munsell colour number assignment for modern ash samples. Source: Author

Caithness Peat											
Xlf=κ/p $x10^{-8}$ m^3kg^{-1}	4390.0										
%X*fd*	8.2										
Atomic % of elements	Na 0.5%	Mg 1.8%	Al 3.6%	Si 6.6%	P 0.4%	S 3.8%	Cl	K 0.8%	Ca 6.6%	Fe 16.9%	Ti 0.3%
pH	7.1										
Orkney Peat											
Xlf=κ/p $x10^{-8}$ m^3kg^{-1}	1673.3										
%X*fd*	11.3										
Atomic % of elements	Na 1.3%	Mg 04.6%	Al 2.7%	Si 6.7%	P 0.6%	S 5.5%	Cl 0.3%	K 0.8%	Ca 5.8%	Fe 7.3%	Ti 0.3%
pH	7.3										
Mixed Fuels 500^{0}C											
Xlf=κ/p $x10^{-8}$ m^3kg^{-1}	35.6										
%Xfd	8.6										
Atomic % of elements	Na 2.9%	Mg 4.2%	Al 1.9%	Si 1.0%	P 0.9%	S 3.6%	Cl 2.0%	K 2.9%	Ca 6.0%	Fe 2.9%	Ti 0.5%
pH	9.7										
Peat and Wood Ash											
Xlf=κ/p $x10^{-8}$ m^3kg^{-1}	356.9										
%X*fd*	9.1										
Atomic % of elements	Na 0.8%	Mg 5.3%	Al 2.3%	Si 2.3%	P 0.7%	S 5.0%	Cl 0.5%	K 1.9%	Ca 13.7%	Fe 2.9%	Ti 0.1%
pH	9.7										

Table 6.17 The analytical data for the modern ash samples showing the results of each analytical method. Source: Author

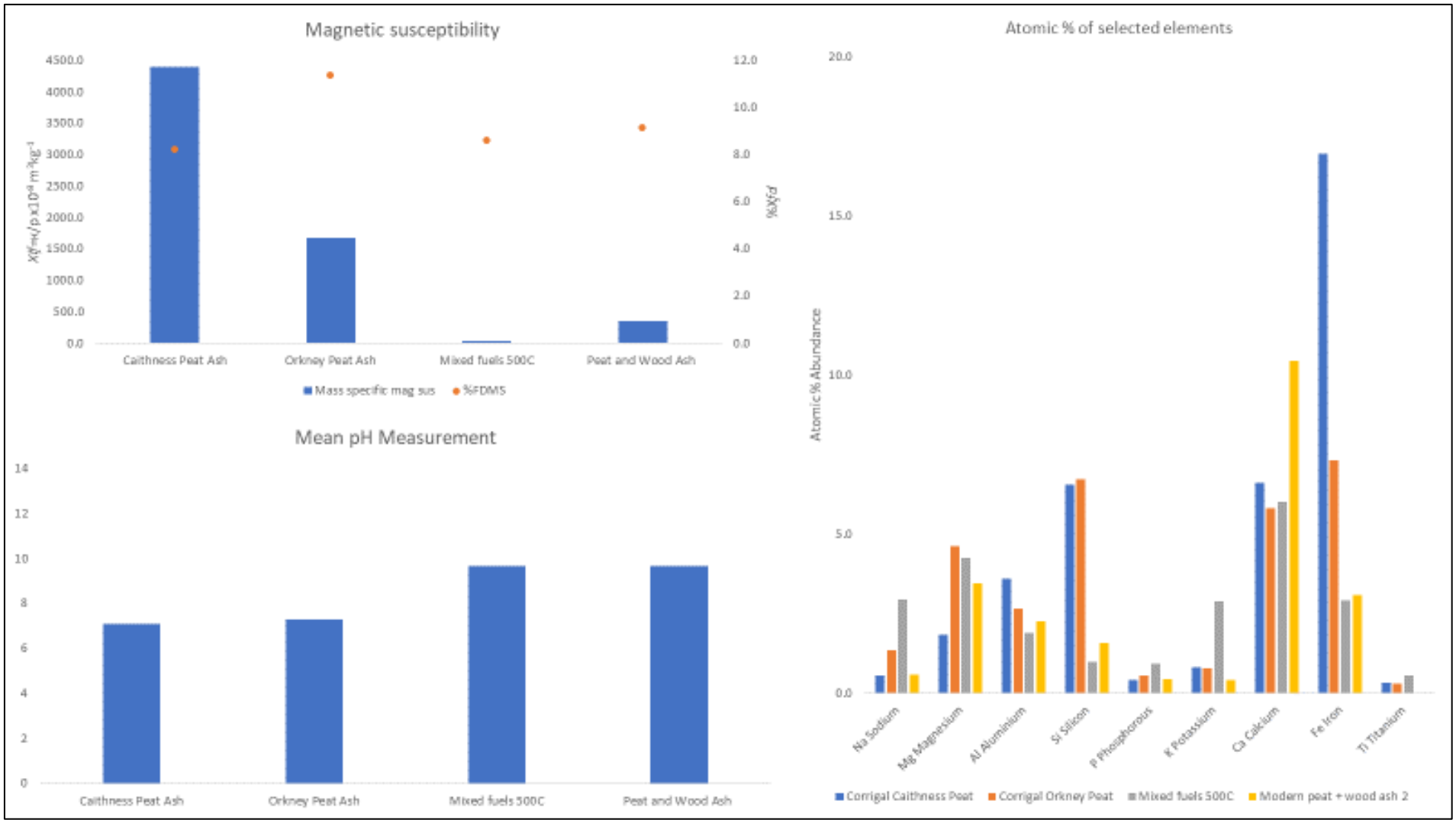

Figure 6.18 Clockwise from top left the low frequency mass specific magnetic susceptibility and percentage frequency dependence, the atomic percentage abundance of selected elements, and the pH of the additional Modern Ash samples. Source: Author

6.3 Archaeological sample analytical results

The analytical results for the archaeological sample material are presented in stratigraphic sequence, according to site code, which structure or trench the samples were obtained from, and the year the samples were collected per the Harris matrices produced for this research and presented in chapter 4.

Ness of Brodgar 2015

The MS for the Ness of Brodgar 2015 samples ranges from 256.4 $x10^{-8}m^3kg^{-1}$ [NoB 3783] – 1328.4 $x10^{-8}m^3kg^{-1}$ [NoB 5013] with an average of 860.2 $x10^{-8}m^3kg^{-1}$ for the 10 samples (figure 6.19). The percentage frequency dependence values ranged from 7.6% [NoB 2617] – 25.8% [NoB 5332] with an average value of 17.1% (table 6.18).

The SEM/EDX results for the Ness of Brodgar 2015 samples show the presence of sodium, magnesium, aluminium, silicon, phosphorous, potassium, calcium, iron, and titanium among all samples with exception of titanium within [NoB 2617] and calcium within [NoB 3857] (table 6.18). The most abundant element among all of the sample material is silicon (figure 6.20).

The pH among the samples material from the Ness of Brodgar 2015 are all neutral or very close to it ranging from 6.7 [NoB 4674] – 7.2 [NoB 3857] & [NoB 5332] with an average pH of 6.9 (table 6.18).

NoB 2617											
Xlf=κ/p x10^{-8} m^{3}kg^{-1}	586.7										
%X*fd*	7.6										
Atomic % of elements	Na 0.7%	Mg 0.5%	Al 4.0%	Si 14.6%	P 0.5%	S	Cl	K 1.3%	Ca 1.1%	Fe 1.2%	Ti
pH	7.0			**Munsell colour number**			2.5Y 2.5/1				
NoB 3851											
Xlf=κ/p x10^{-8} m^{3}kg^{-1}	927.7										
%X*fd*	12.5										
Atomic % of elements	Na 0.9%	Mg 1.0%	Al 6.1%	Si 16.4%	P 0.3%	S	Cl	K 1.7%	Ca 0.3%	Fe 1.6%	Ti 0.4%
pH	7.0			**Munsell colour number**			2.5YR 4/6				
NoB 3857											
Xlf=κ/p x10^{-8} m^{3}kg^{-1}	580.2										
%X*fd*	19.0										
Atomic % of elements	Na 1.1%	Mg 0.7%	Al 5.5%	Si 17.6%	P 0.3%	S	Cl	K 1.6%	Ca	Fe 2.0%	Ti 0.2%
pH	7.2			**Munsell colour number**			5YR 5/4				
NoB 4264											
Xlf=κ/p x10^{-8} m^{3}kg^{-1}	855.2										
%X*fd*	9.1										
Atomic % of elements	Na 0.9%	Mg 0.7%	Al 4.4%	Si 23.0%	P 0.8%	S	Cl	K 1.7%	Ca 1.1%	Fe 1.7%	Ti 0.2%
pH	6.8			**Munsell colour number**			2.5YR 6/4				
NoB 4656											
Xlf=κ/p x10^{-8} m^{3}kg^{-1}	1083.0										
%X*fd*	9.0										
Atomic % of elements	Na 1.2%	Mg 1.1%	Al 7.5%	Si 21.5%	P 0.8%	S	Cl	K 2.5%	Ca 0.5%	Fe 2.3%	Ti 0.3%
pH	6.9			**Munsell colour number**			7.5YR 6/4				
NoB 4674											
Xlf=κ/p x10^{-8} m^{3}kg^{-1}	1309.5										
%X*fd*	9.2										
Atomic % of elements	Na 0.5%	Mg 0.7%	Al 4.7%	Si 14.7%	P 0.5%	S	Cl	K 1.2%	Ca 0.4%	Fe 1.4%	Ti 0.2%
pH	6.7			**Munsell colour number**			5YR 4/3				
NoB 5332											
Xlf=κ/p x10^{-8} m^{3}kg^{-1}	381.4										
%X*fd*	18.7										
Atomic % of elements	Na 0.6%	Mg 0.6%	Al 5.0%	Si 14.5%	P 0.8%	S	Cl	K 1.7%	Ca 0.6%	Fe 2.2%	Ti 0.2%
pH	7.2			**Munsell colour number**			5YR 5/4				
NoB 6156											
Xlf=κ/p x10^{-8} m^{3}kg^{-1}	1293.1										
%X*fd*	8.3										
Atomic % of elements	Na 0.9%	Mg 0.4%	Al 5.0%	Si 17.5%	P 0.4%	S	Cl	K 1.5%	Ca 0.4%	Fe 1.3%	Ti 0.2%
pH	6.7			**Munsell colour number**			7.5YR 6/3				
NoB 5013											
Xlf=κ/p x10^{-8} m^{3}kg^{-1}	1328.4										
%X*fd*	7.6										
Atomic % of elements	Na 0.9%	Mg 0.8%	Al 6.5%	Si 21.5%	P 0.8%	S	Cl	K 1.5%	Ca 0.5%	Fe 1.7%	Ti 0.3%
pH	7			**Munsell colour number**			5YR 4/4				
NoB 3783											
Xlf=κ/p x10^{-8} m^{3}kg^{-1}	256.4										
%X*fd*	25.8										
Atomic % of elements	Na 0.8%	Mg 0.6%	Al 7.2%	Si 21.7%	P 0.5%	S	Cl	K 2.0%	Ca 0.3%	Fe 1.7%	Ti 0.4%
pH	6.9			**Munsell colour number**			5YR 3/1				

Table 6.18 The analytical data for the Ness of Brodgar 2015 samples showing the results of each analytical method organised by stratigraphy. Source: Author

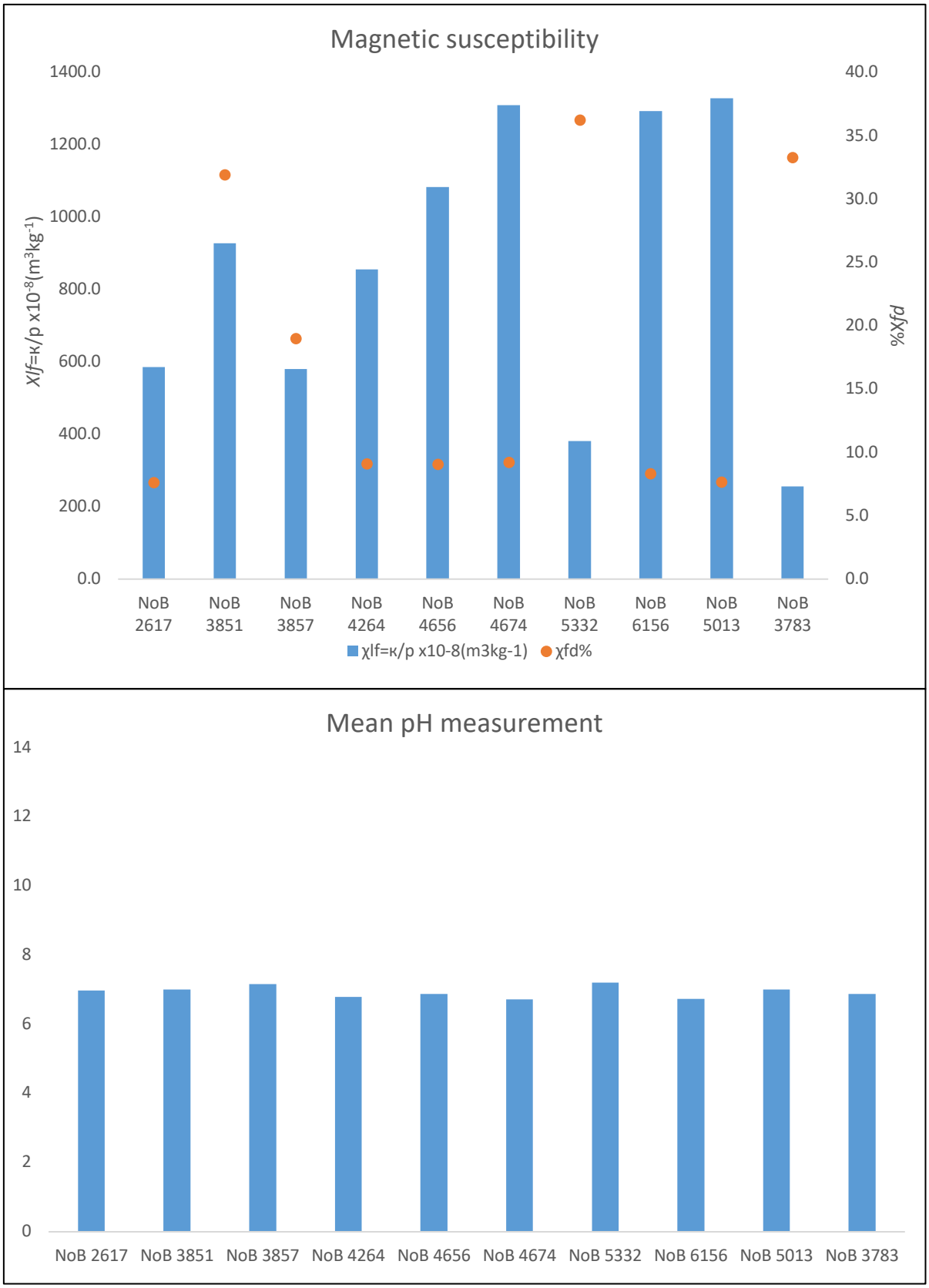

Figure 6.19 The low frequency mass specific magnetic susceptibility and percentage frequency dependence (top) and the pH (bottom) among Ness of Brodgar 2015 excavation samples. Source: Author

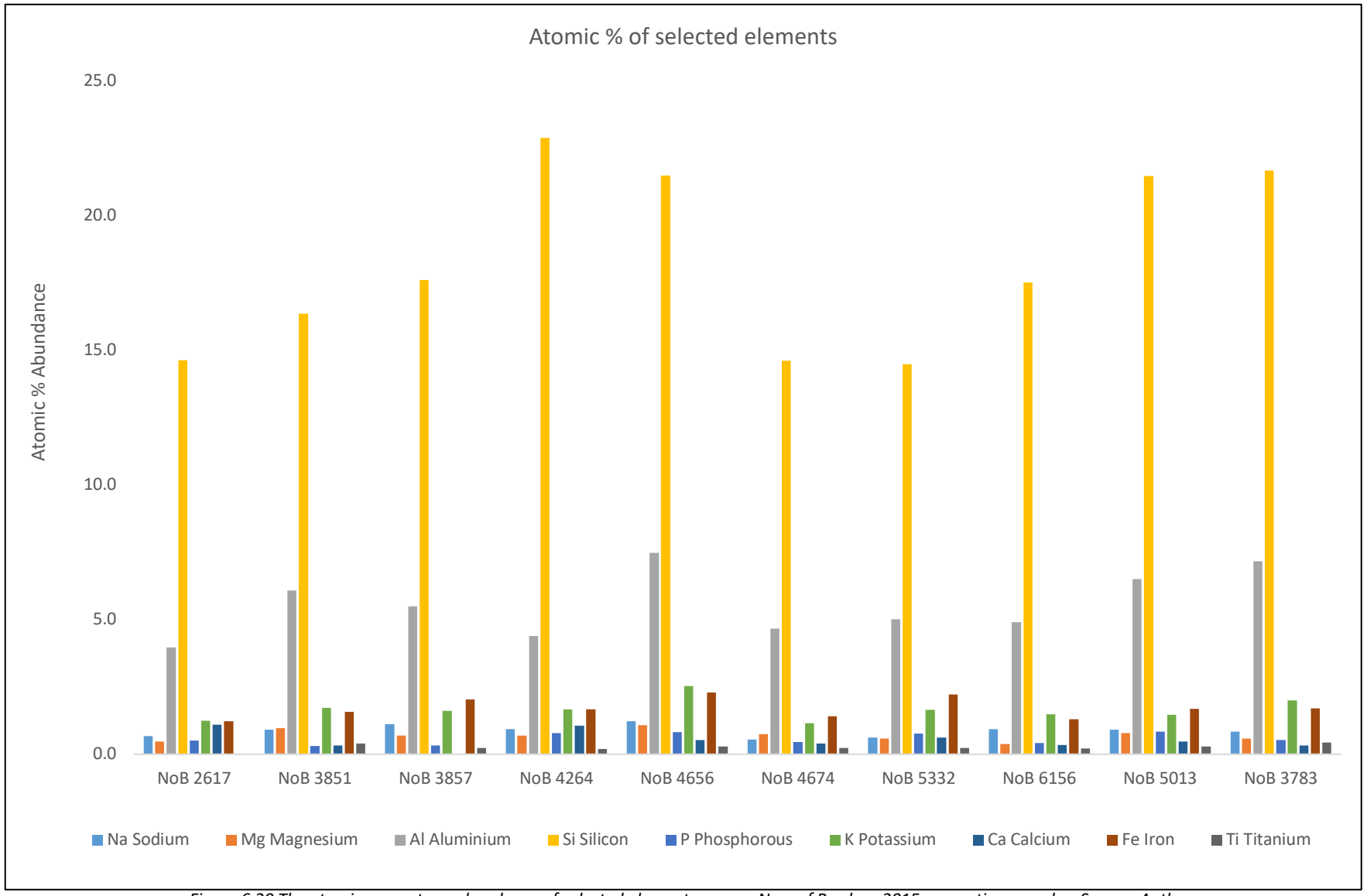

Figure 6.20 The atomic percentage abundance of selected elements among Ness of Brodgar 2015 excavation samples. Source: Author

Ness of Brodgar 2016

The MS for the Ness of Brodgar 2016 samples ranges from 404.2 $x10^{-8}m^3kg^{-1}$ [NoB16 6346] – 1392.1 $x10^{-8}m^3kg^{-1}$ [NoB16 6351] with an average of 947.8 $x10^{-8}m^3kg^{-1}$ for the 8 samples (table 6.19). The percentage frequency dependence values ranged from 7.9% [NoB16 6351] – 10.5% [NoB16 6346] with an average value of 8.8% (table 6.19 & figure 6.21).

The SEM/EDX results for the Ness of Brodgar 2016 samples show the presence of sodium, aluminium, magnesium, silicon, phosphorous, potassium, calcium, iron, and titanium among all samples with the exception of sodium within [NoB16 3851] and phosphorous within [NoB16 6354], and the addition of chlorine within [NoB16 6356]. The most abundant element among all of the sample material is silicon (figure 6.22).

The pH among the samples material from the Ness of Brodgar 2016 are all near neutral ranging from 6.2 [NoB16 6355] – 7.1 [NoB16 6346] with an average pH of 6.6 (table 6.19 & figure 6.21).

NoB16 3851											
Xlf=κ/p x10^{-8} m^{3}kg^{-1}	1129.7										
%X*fd*	9.6										
Atomic % of elements	Na	Mg 1.0%	Al 7.3%	Si 14.2%	P 0.6%	S	Cl	K 1.1%	Ca 0.3%	Fe 7.7%	Ti 0.2%
pH	6.5			**Munsell colour number**			2.5YR 4/6				
NoB16 6339											
Xlf=κ/p x10^{-8} m^{3}kg^{-1}	861.8										
%X*fd*	9.4										
Atomic % of elements	Na 0.7%	Mg 1.5%	Al 4.6%	Si 17.3%	P 1.4%	S	Cl	K 1.2%	Ca 1.5%	Fe 2.6%	Ti 0.2%
pH	6.6			**Munsell colour number**			7.5YR 3/2				
NoB16 6346											
Xlf=κ/p x10^{-8} m^{3}kg^{-1}	404.2										
%X*fd*	10.5										
Atomic % of elements	Na 0.8%	Mg 2.1%	Al 7.9%	Si 17.1%	P 0.6%	S	Cl	K 1.9%	Ca 0.6%	Fe 2.0%	Ti o.3%
pH	7.1			**Munsell colour number**			5YR 2.5/1				
NoB16 6348											
Xlf=κ/p x10^{-8} m^{3}kg^{-1}	1313.9										
%X*fd*	8.6										
Atomic % of elements	Na 0.6%	Mg 3.0%	Al 3.6%	Si 13.8%	P 1.7%	S	Cl	K 1.0%	Ca 2.2%	Fe 2.1%	Ti 0.2%
pH	6.7			**Munsell colour number**			7.5YR 4/4				
NoB16 6351											
Xlf=κ/p x10^{-8} m^{3}kg^{-1}	1392.1										
%X*fd*	7.9										
Atomic % of elements	Na 0.4%	Mg 3.4%	Al 4.0%	Si 13.2%	P 1.9%	S	Cl	K 1.1%	Ca 2.5%	Fe 2.0%	Ti 0.2%
pH	6.3			**Munsell colour number**			5YR 4/6				
NoB16 6354											
Xlf=κ/p x10^{-8} m^{3}kg^{-1}	835.5										
%X*fd*	8.0										
Atomic % of elements	Na 1.2%	Mg 0.6%	Al 3.9%	Si 12.3%	P	S	Cl	K 1.2%	Ca 0.1%	Fe 0.8%	Ti 0.2%
pH	6.4			**Munsell colour number**			7.5YR 3/1				
NoB16 6355											
Xlf=κ/p x10^{-8} m^{3}kg^{-1}	843.0										
%X*fd*	8.1										
Atomic % of elements	Na 0.5%	Mg 0.8%	Al 6.2%	Si 12.5%	P 0.5%	S	Cl	K 1.4%	Ca 0.4%	Fe 0.8%	Ti 0.3%
pH	6.2			**Munsell colour number**			7.5YR 3/2				
NoB16 6356											
Xlf=κ/p x10^{-8} m^{3}kg^{-1}	802.2										
%X*fd*	8.3										
Atomic % of elements	Na 0.6%	Mg 1.7%	Al 3.8%	Si 17.7%	P 1.0%	S	Cl 0.1%	K 1.1%	Ca 1.1%	Fe 2.5%	Ti 0.2%
pH	6.8			**Munsell colour number**			5YR 3/3				

Table 6.19 The analytical data for the Ness of Brodgar 2016 samples showing the results of each analytical method organised by stratigraphy. Source: Author

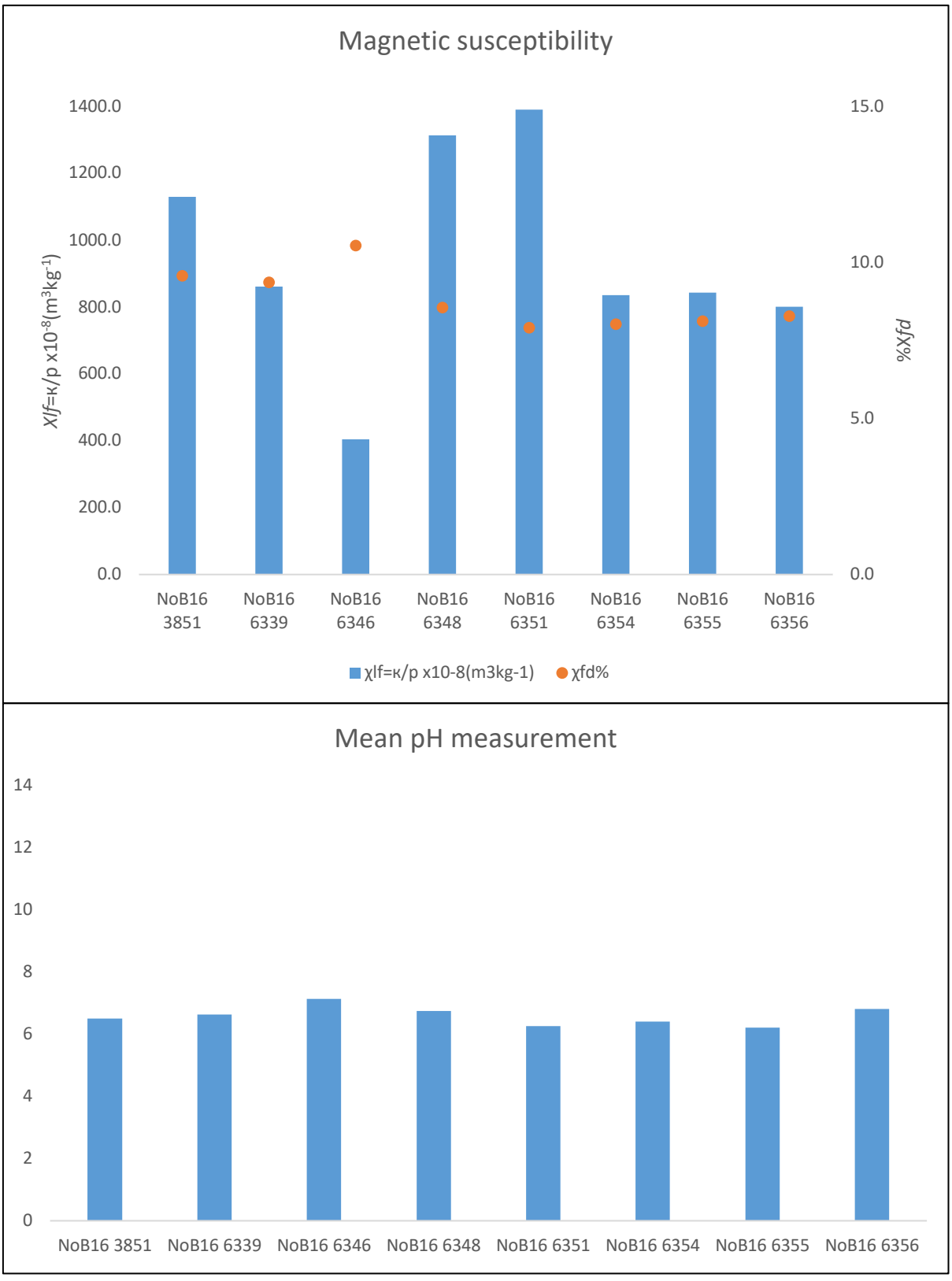

Figure 6.21 The low frequency mass specific magnetic susceptibility and percentage frequency dependence (top) and the pH (bottom) among Ness of Brodgar 2016 excavation samples. Source: Author

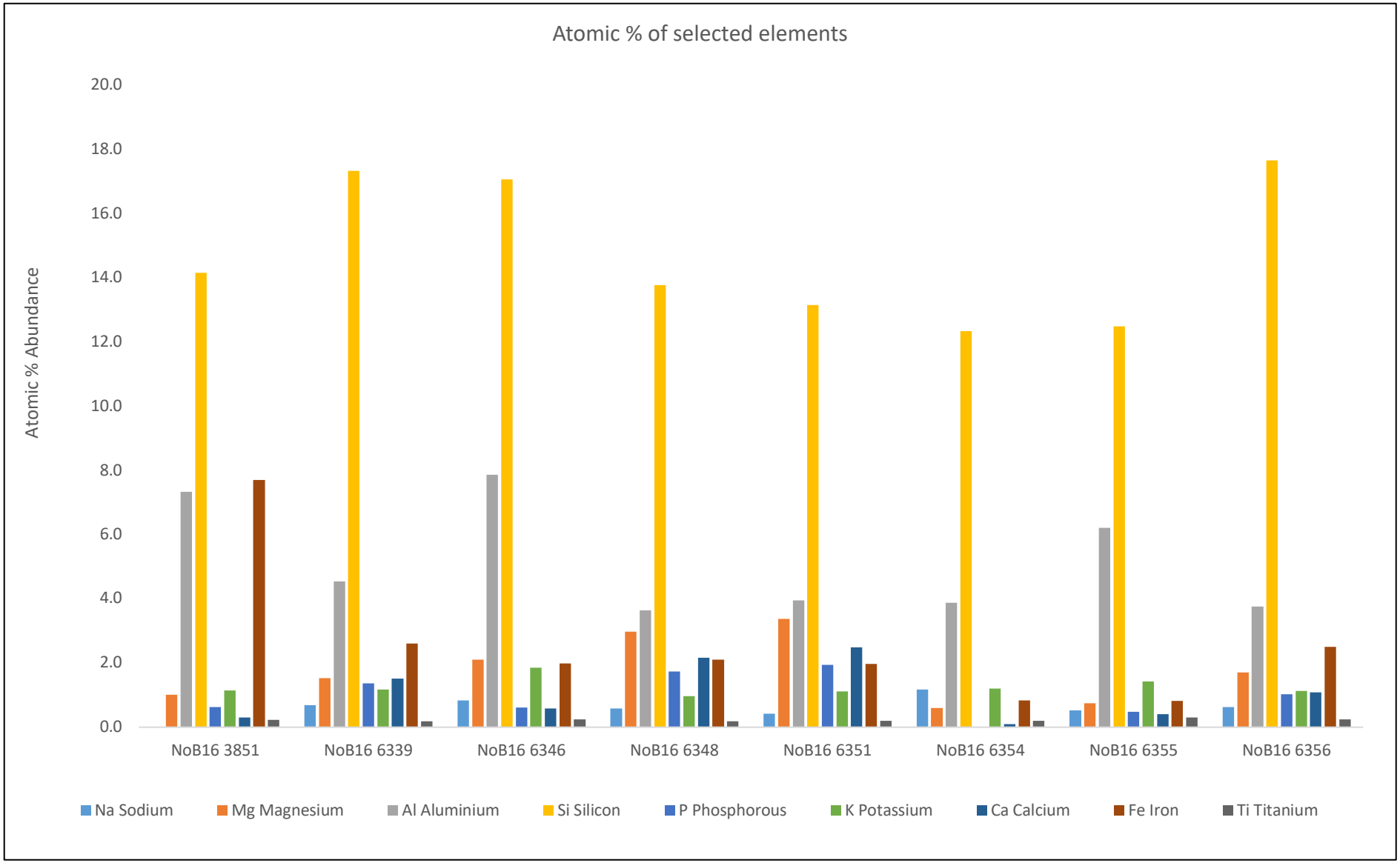

Figure 6.22 The atomic percentage abundance of selected elements among Ness of Brodgar 2016 excavation samples. Source: Author

Ness of Brodgar Trench T 2016

The MS for the Ness of Brodgar trench T 2016 samples ranges from 516.3 x$10^{-8}$$m^3kg^{-1}$ [NoBT 4825] – 2672.7 x$10^{-8}$$m^3kg^{-1}$ [NoBT 5849] with an average of 1122.5 x$10^{-8}$$m^3kg^{-1}$ for the 6 samples (figure 6.23 & table 5.17). The percentage frequency dependence values ranged from 7.0% [NoBT 5849] – 9.9% [NoB16 4825] with an average value of 9.0% (table 6.20).

The SEM/EDX results for the Ness of Brodgar 2016 samples show the presence of sodium, magnesium, aluminium, silicon, phosphorous, potassium, calcium, iron, and titanium among all samples. The most abundant element among all of the sample material is silicon (figure 6.24).

The pH among the samples material from the Ness of Brodgar trench T 2016 are all acidic ranging from 5.2 [NoBT 4860] – 6.3 [NoBT 5849] & [NoBT 4831] with an average pH of 5.9 (table 6.20).

-											
Xlf=κ/ρ x10^{-8} m^{3}kg^{-1}	516.3										
%X*fd*	9.9										
Atomic % of elements	Na 1.0%	Mg 0.4%	Al 5.5%	Si 17.2%	P 0.8%	S	Cl	K 1.6%	Ca 0.8%	Fe 1.3%	Ti 0.4%
pH	6.0			**Munsell colour number**				7.5YR 2.5/1			
NoBT 4831											
Xlf=κ/ρ x10^{-8} m^{3}kg^{-1}	725.9										
%X*fd*	9.5										
Atomic % of elements	Na 0.7%	Mg 0.7%	Al 5.6%	Si 17.9%	P 1.3%	S	Cl	K 1.3%	Ca 1.0%	Fe 3.0%	Ti 0.3%
pH	6.3			**Munsell colour number**				7.5YR 3/3			
NoBT 4860											
Xlf=κ/ρ x10^{-8} m^{3}kg^{-1}	936.2										
%Xfd	9.0										
Atomic % of elements	Na 1.2%	Mg 0.5%	Al 4.6%	Si 14.4%	P 0.8%	S	Cl	K 1.3%	Ca 0.8%	Fe 12.2%	Ti 0.2%
pH	5.2			**Munsell colour number**				7.5YR 4/2			
NoBT 5810											
Xlf=κ/ρ x10^{-8} m^{3}kg^{-1}	890.8										
%Xfd	9.0										
Atomic % of elements	Na 0.8%	Mg 0.5%	Al 3.2%	Si 10.4%	P 0.3%	S	Cl	K 0.9%	Ca 0.4%	Fe 0.7%	Ti 0.1%
pH	6.0			**Munsell colour number**				10YR 3/3			
NoBT 5849											
Xlf=κ/ρ x10^{-8} m^{3}kg^{-1}	2672.7										
%Xfd	7.0										
Atomic % of elements	Na 0.6%	Mg 0.5%	Al 4.0%	Si 14.2%	P 1.1%	S	Cl	K 0.9%	Ca 0.7%	Fe 3.8%	Ti 0.2%
pH	6.3			**Munsell colour number**				2.5YR 3/4			
NoBT 5855											
Xlf=κ/ρ x10^{-8} m^{3}kg^{-1}	993.1										
%X*fd*	9.5										
Atomic % of elements	Na 0.3%	Mg 0.3%	Al 4.0%	Si 5.6%	P 0.9%	S	Cl	K 0.7%	Ca 0.4%	Fe 2.0%	Ti 0.2%
pH	5.7			**Munsell colour number**				7.5YR 3/1			

Table 6.20 The analytical data for the Ness of Brodgar Trench T 2016 samples showing the results of each analytical method organised by stratigraphy. Source: Author

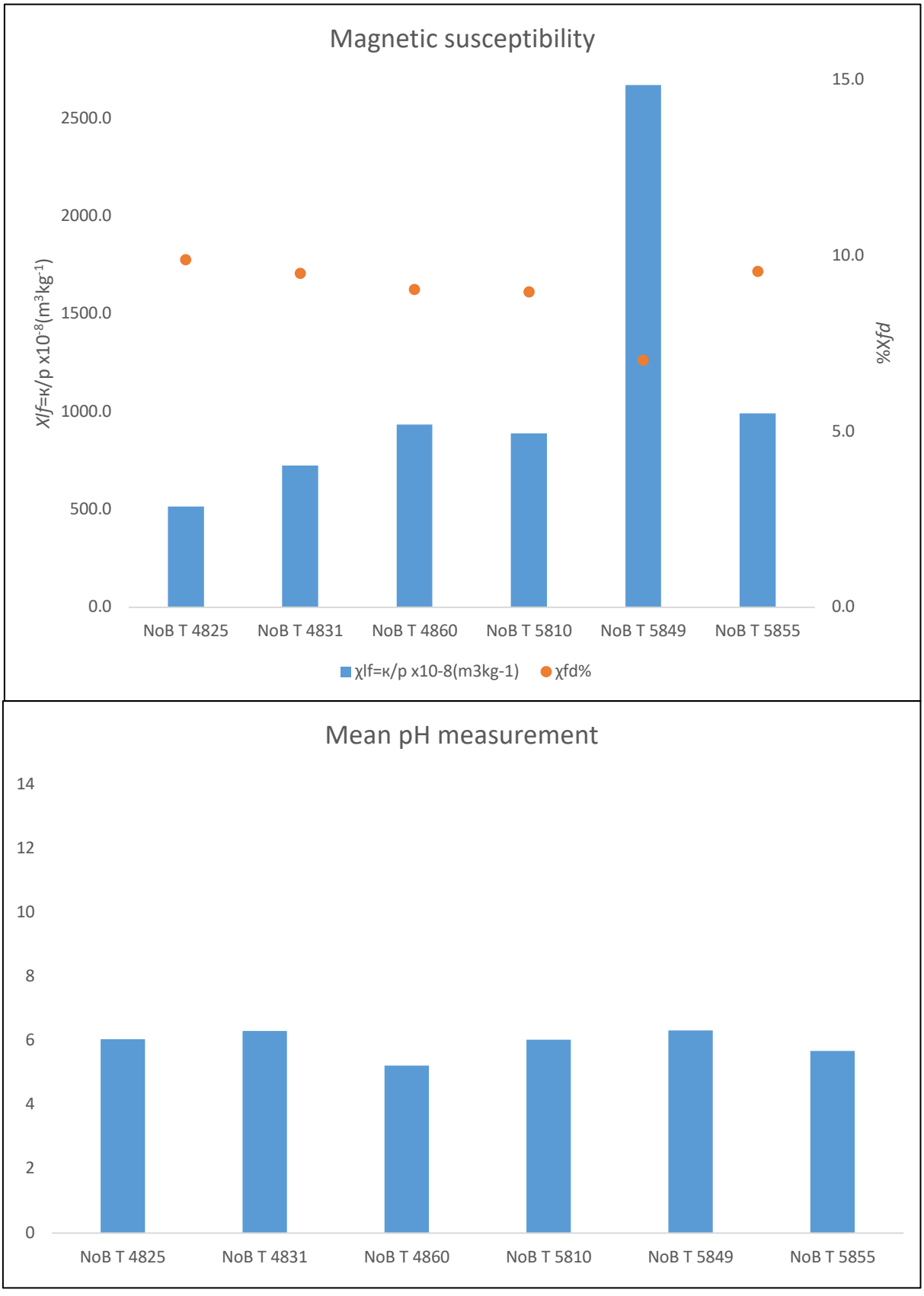

Figure 6.23 The low frequency mass specific magnetic susceptibility and percentage frequency dependence (top) and the pH (bottom) among Ness of Brodgar Trench T 2016 excavation samples. Source: Author

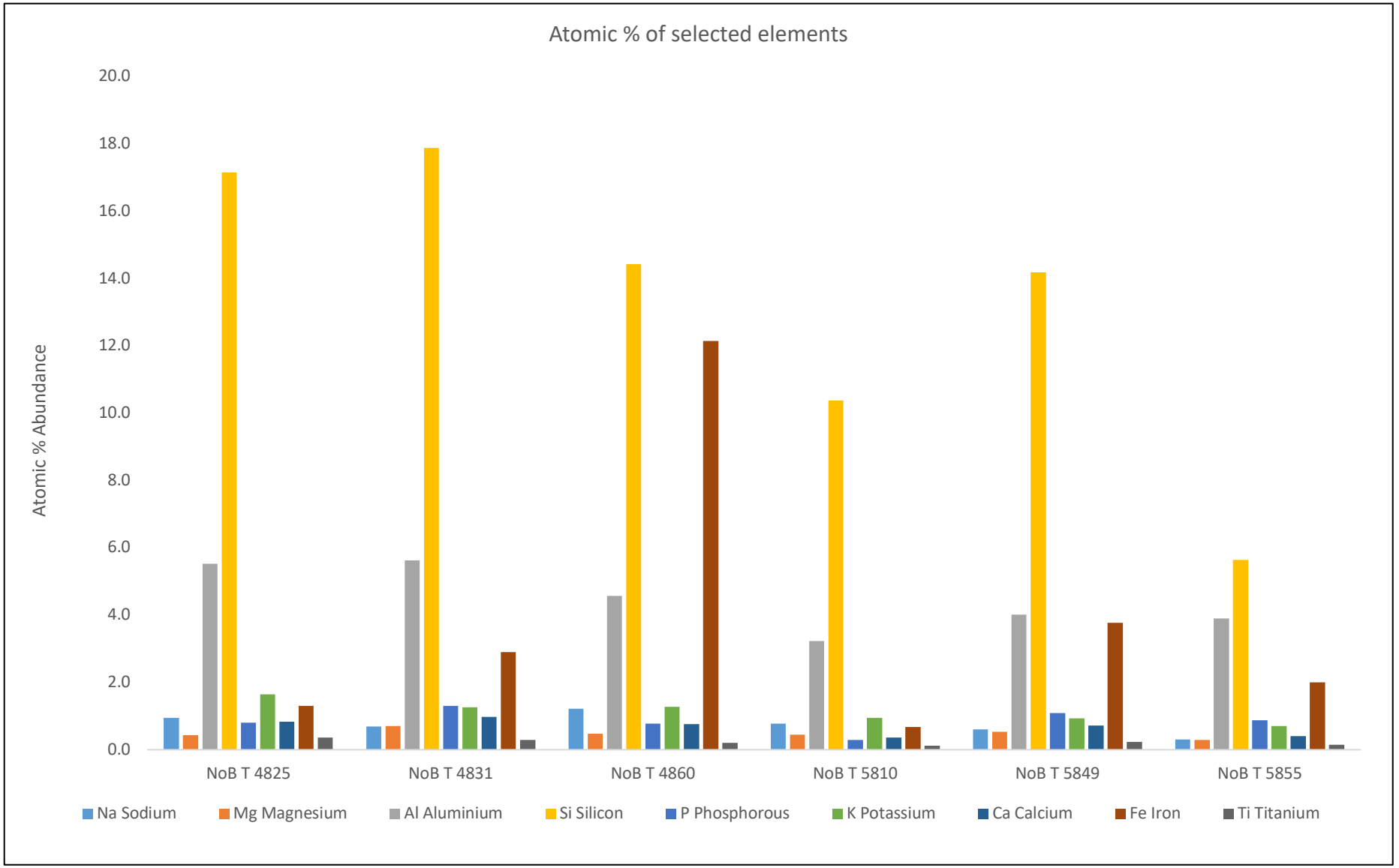

Figure 6.24 The atomic percentage abundance of selected elements among the Ness of Brodgar Trench T 2016 excavation samples. Source: Author

The Knowe of Swandro

The MS for the Knowe of Swandro 2015 samples ranges from 98.3 $x10^{-8}m^3kg^{-1}$ [KoS 3201] – 488.0 $x10^{-8}m^3kg^{-1}$ [KoS 3217] with an average of 334.7 $x10^{-8}m^3kg^{-1}$ for the 8 samples (table 6.21). The percentage frequency dependence values ranged from 7.4% [KoS 3217] – 32.1% [KoS 4825] with an average value of 12.3% (figure 6.25).

The SEM/EDX results for the Knowe of Swandro 2015 samples show the presence of sodium, magnesium, aluminium, silicon, phosphorous, potassium, calcium, and iron among all samples with the exception of sodium and phosphorous within [KoS 2039], sodium, potassium, and iron within [KoS 3201], sodium within [KoS 3225], and phosphorous within [KoS 3255]. In addition, there titanium present within [KoS 2039], [KoS 3196], [KoS 3225], and [KoS 3255]. The most abundant element among all of the sample material is silicon (figure 6.26).

The pH among the samples from the Knowe of Swandro 2015 are all neutral or slightly alkaline ranging from 7.4 [KoS 3217] – 8.1 [KoS 3201], [KoS 3225], and [KoS 3255] with an average pH of 7.9 (table 6.21).

KoS 2039											
Xlf=κ/p x10^{-8} m^{3}kg^{-1}	482.7										
%X*fd*	8.2										
Atomic % of elements	Na	Mg 1.8%	Al 3.8%	Si 5.8%	P	S	Cl	K 0.3%	Ca 0.5%	Fe 0.8%	Ti 0.3%
pH	7.9			**Munsell colour number**				5YR 5/6			
KoS 3081											
Xlf=κ/p x10^{-8} m^{3}kg^{-1}	294.5										
%X*fd*	32.1										
Atomic % of elements	Na 1.0%	Mg 1.1%	Al 1.3%	Si 15.3%	P 1.0%	S	Cl	K 1.1%	Ca 1.6%	Fe 1.5%	Ti
pH	7.8			**Munsell colour number**				10YR 4/2			
KoS 3196											
Xlf=κ/p x10^{-8} m^{3}kg^{-1}	274.4										
%X*fd*	11.2										
Atomic % of elements	Na 1.3%	Mg 0.9%	Al 4.4%	Si 21.0%	P 1.1%	S	Cl	K 1.3%	Ca 1.7%	Fe 1.9%	To 0.4%
pH	7.8			**Munsell colour number**				10YR 4/3			
KoS 3201											
Xlf=κ/p x10^{-8} m^{3}kg^{-1}	98.3										
%X*fd*	9.6										
Atomic % of elements	Na	Mg 2.1%	Al 1.2%	Si 4.6%	P 1.1%	S	Cl	K	Ca 12.6%	Fe	Ti
pH	8.1			**Munsell colour number**				10YR 5/3			
KoS 3217											
Xlf=κ/p x10^{-8} m^{3}kg^{-1}	488.0										
%X*fd*	4.5										
Atomic % of elements	Na 1.0%	Mg 0.7%	Al 3.9%	Si 19.2%	P 1.0%	S	Cl	K 1.5%	Ca 2.4%	Fe 1.7%	Ti
pH	7.4			**Munsell colour number**				10YR 4/3			
KoS 3225											
Xlf=κ/p x10^{-8} m^{3}kg^{-1}	289.6										
%X*fd*	11.4										
Atomic % of elements	Na	Mg 1.2%	Al 4.1%	Si 10.0%	P 1.6%	S	Cl	K 1.0%	Ca 2.0%	Fe 2.5%	Ti 0.7%
pH	8.1			**Munsell colour number**				10YR 5/2			
KoS 3238											
Xlf=κ/p x10^{-8} m^{3}kg^{-1}	302.6										
%X*fd*	9.6										
Atomic % of elements	Na 2.2%	Mg 0.7%	Al 5.6%	Si 21.8%	P 0.6%	S	Cl	K 1.9%	Ca 1.3%	Fe 1.7%	Ti
pH	8			**Munsell colour number**				10YR 4/2			
KoS 3255											
Xlf=κ/p x10^{-8} m^{3}kg^{-1}	447.2										
%X*fd*	9.6										
Atomic % of elements	Na 1.5%	Mg 1.1%	Al 4.3%	Si 20.3%	P	S	Cl	K 1.9%	Ca 2.0%	Fe 1.5%	Ti 0.4%
pH	8.1			**Munsell colour number**				10YR 5/2			

Table 6.21 The analytical data for Knowe of Swandro 2015 samples showing the results of each analytical method organised by stratigraphy. Source: Author

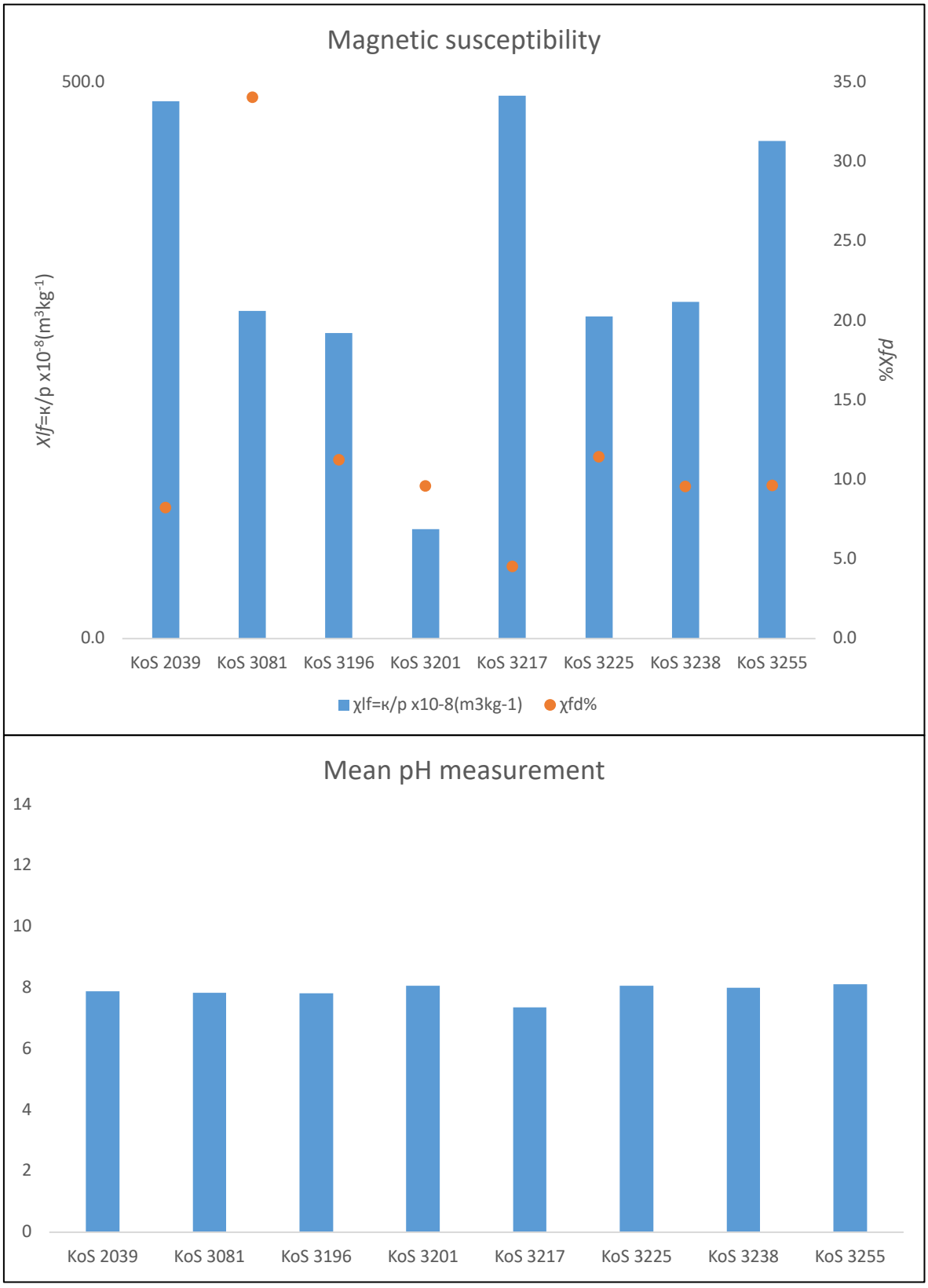

Figure 6.25 The low frequency mass specific magnetic susceptibility and percentage frequency dependence (top) and the pH (bottom) among the Knowe of Swandro excavation samples. Source: Author

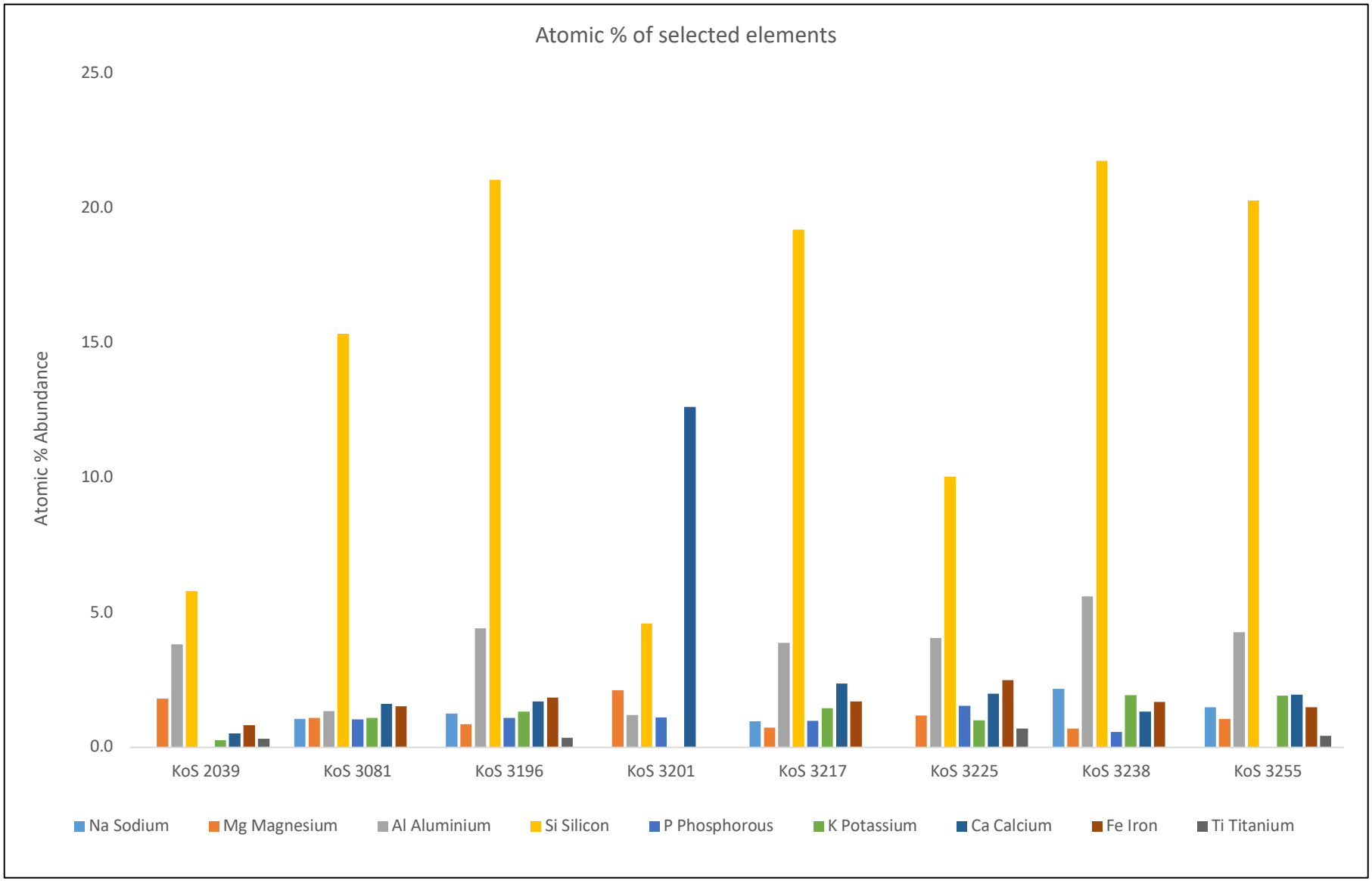

Figure 6.26 The atomic percentage abundance of selected elements among the Know of Swandro excavation samples. Source: Author

Smerquoy/Muckquoy

The MS for the Smerquoy and Muckquoy samples ranges from 33.6 $x10^{-8}m^3kg^{-1}$ [RDL 001] – 1307.9 $x10^{-8}m^3kg^{-1}$ [RDL 023] with an average of 586.0 $x10^{-8}m^3kg^{-1}$ for the 12 samples (table 6.22). The percentage frequency dependence values ranged from 7.5% [SMQ B] – 19.8% [RDL 023] with an average value of 11.3% (figure 6.27).

The SEM/EDX results for the Smerquoy and Muckquoy samples show the presence of sodium, aluminium, silicon, phosphorous, and iron among all samples. The most abundant element among all of the sample material is silicon (figure 6.28).

The pH among the samples material from Smerquoy and Muckquoy are all acidic ranging from 5.9 [RDL 001] – 6.5 [RDL 031] and [SMQ A] with an average pH of 6.2 (table 6.22 & figure 6.27).

RDL 031											
Xlf=κ/p x10^{-8} m^{3}kg^{-1}	57.9										
%X*fd*	14.2										
Atomic % of elements	Na 1.1%	Mg 0.4%	Al 5.8%	Si 24.4%	P 0.3%	S	Cl	K 2.1%	Ca	Fe 0.9%	Ti 0.5%
pH	6.5			**Munsell colour number**				7.5YR 4/1			
RDL 001											
Xlf=κ/p x10^{-8} m^{3}kg^{-1}	33.6										
%X*fd*	10.0										
Atomic % of elements	Na	Mg	Al 2.2%	Si 8.5%	P	S	Cl	K	Ca	Fe 5.7%	Ti
pH	5.9			**Munsell colour number**				7.5YR 3/2			
RDL 004											
Xlf=κ/p x10^{-8} m^{3}kg^{-1}	54.1										
%X*fd*	9.9										
Atomic % of elements	Na 0.6%	Mg	Al 3.3%	Si 14.3%	P 0.2%	S	Cl	K 0.8%	Ca	Fe 2.5%	Ti 0.4%
pH	6.1			**Munsell colour number**				7.5YR 3/1			
RDL 006											
Xlf=κ/p x10^{-8} m^{3}kg^{-1}	833.2										
%X*fd*	10.9										
Atomic % of elements	Na 0.9%	Mg 0.4%	Al 4.9%	Si 18.5%	P 0.4%	S	Cl	K 1.5%	Ca	Fe 1.1%	Ti 0.2%
pH	6.2			**Munsell colour number**				7.5YR 4/3			
RDL 009											
Xlf=κ/p x10^{-8} m^{3}kg^{-1}	65.7										
%X*fd*	19.8										
Atomic % of elements	Na 0.9%	Mg 0.2%	Al 3.8%	Si 16.6%	P 0.2%	S	Cl	K 1.1%	Ca	Fe 0.5%	Ti 0.2%
pH	6.0			**Munsell colour number**				7.5YR 4/2			
RDL 007											
Xlf=κ/p x10^{-8} m^{3}kg^{-1}	324.4										
%X*fd*	11.8										
Atomic % of elements	Na 0.6%	Mg 0.6%	Al 4.5%	Si 12.2%	P 0.8%	S	Cl	K 1.0%	Ca 0.1%	Fe 1.6%	Ti 0.2%
pH	6.2			**Munsell colour number**				10YR 4/4			
RDL 013											
Xlf=κ/p x10^{-8} m^{3}kg^{-1}	746.3										
%X*fd*	11.6										
Atomic % of elements	Na 1.6%	Mg 0.3%	Al 5.3%	Si 21.0%	P 0.5%	S	Cl	K 1.4%	Ca	Fe 1.4%	Ti 0.5%
pH	6.1			**Munsell colour number**				7.5YR 4/3			
RDL 016											
Xlf=κ/p x10^{-8} m^{3}kg^{-1}	628.3										
%X*fd*	10.6										
Atomic % of elements	Na 0.8%	Mg 0.3%	Al 4.3%	Si 21.7%	P 0.2%	S	Cl	K 2.0%	Ca	Fe 0.9%	Ti 0.2%
pH	6.4			**Munsell colour number**				7.5YR 4/2			
RDL 023											
Xlf=κ/p x10^{-8} m^{3}kg^{-1}	1307.9										
%X*fd*	9.4										
Atomic % of elements	Na	Mg 0.4%	Al 3.5%	Si 7.2%	P 5.7%	S	Cl	K 1.7%	Ca 0.2%	Fe 1.4%	Ti 0.3%
pH	6.4			**Munsell colour number**				7.5YR 3/4			
RDL 032											
Xlf=κ/p x10^{-8} m^{3}kg^{-1}	432.2										
%X*fd*	10.6										
Atomic % of elements	Na 0.9%	Mg 0.3%	Al 3.7%	Si 15.2%	P 0.3%	S 0.1%	Cl	K 1.2%	Ca	Fe 0.8%	Ti 0.2%
pH	6.3			**Munsell colour number**				7.5YR 4/3			
SMQ A											
Xlf=κ/p x10^{-8} m^{3}kg^{-1}	1270.7										
%X*fd*	9.1										
Atomic % of elements	Na	Mg	Al 5.8%	Si 25.1%	P 0.7%	S	Cl	K 2.3%	Ca	Fe 2.3%	Ti 0.5%
pH	6.5			**Munsell colour number**				5YR 4/4			
SMQ B											
Xlf=κ/p x10^{-8} m^{3}kg^{-1}	1277.9										
%X*fd*	7.5										
Atomic % of elements	Na 4.9%	Mg	Al 4.2%	Si 7.6%	P 1.2%	S	Cl	K 1.1%	Ca	Fe 2.1%	Ti
pH	6.1			**Munsell colour number**				7.5YR 3/4			

Table 6.22 The analytical data for Smerquoy/Muckquoy samples showing the results of each analytical method organised by stratigraphy. Source: Author

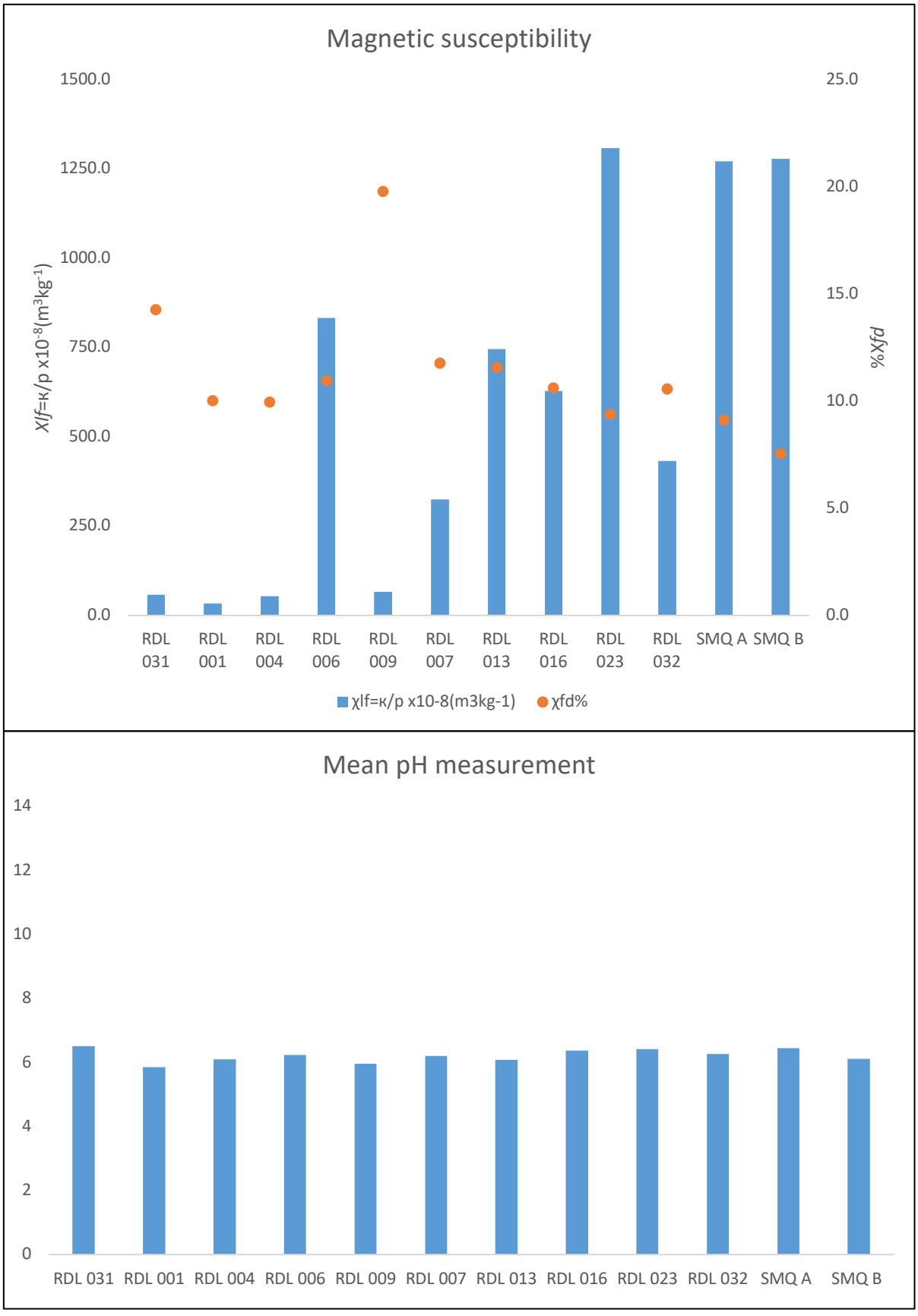

Figure 6.27 The low frequency mass specific magnetic susceptibility and percentage frequency dependence (top) and the pH (bottom) among Smerquoy/Muckquoy excavation samples. Source: Author

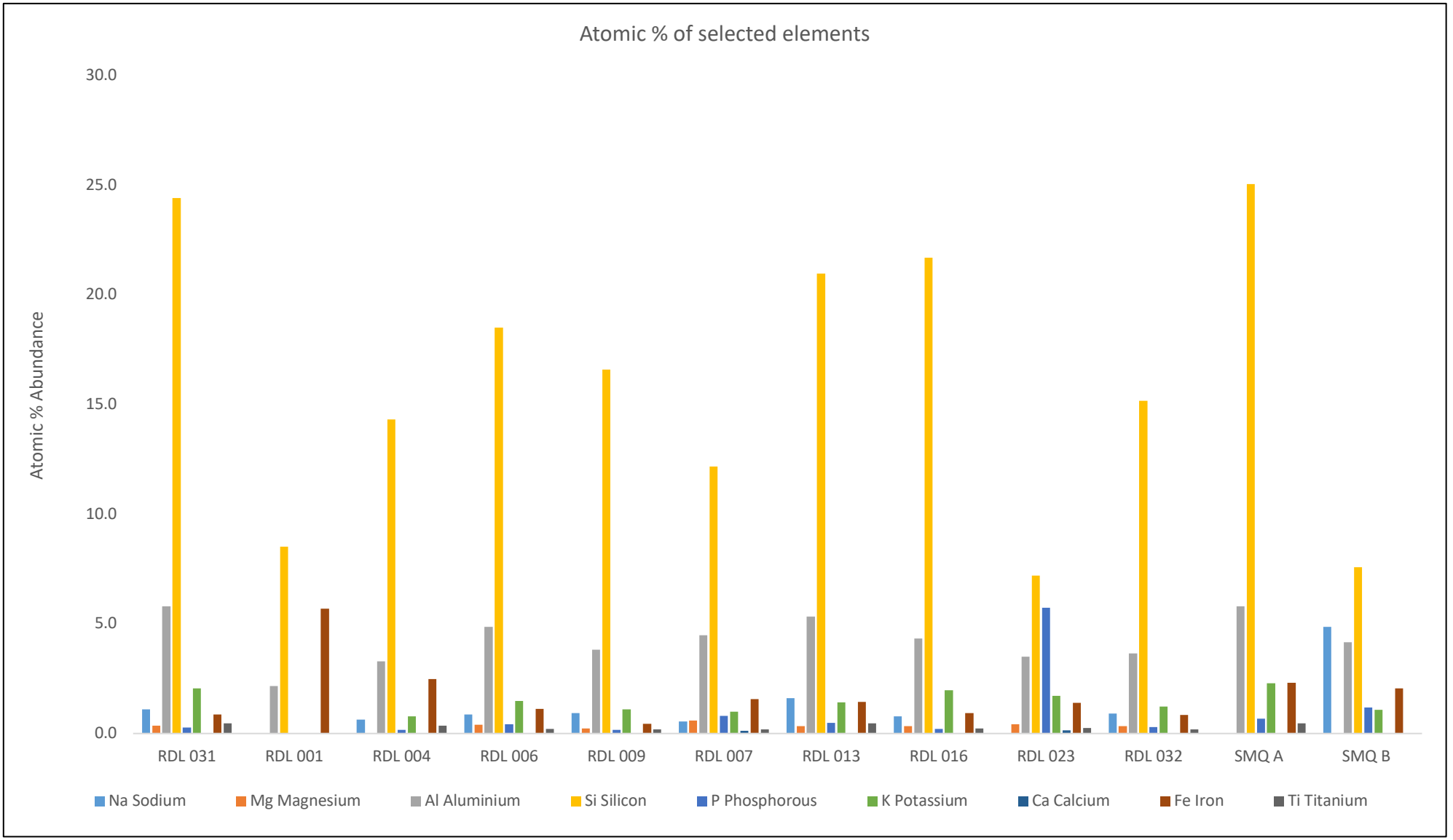

Figure 6.28 The atomic percentage abundance of selected elements among Smerquoy/Muckquoy excavation samples. Source: Author

Additional Archaeological Sample Material	
Archaeological Matrix Unheated	10YR 4/3
Archaeological Matrix 900^{0}C	2.5YR 5/6

Table 6.23 A table showing the Munsell colour number assignment for the additional archaeological sample material. Source: Author

Archaeological Matrix Unheated											
Xlf=κ/p x10^{-8} m^{3}kg^{-1}	87.2										
%Xfd	8.1										
Atomic % of elements	Na 0.7%	Mg 1.7%	Al 4.8%	Si 15.3%	P 1.9%	S	Cl	K 1.8%	Ca 2.5%	Fe 5.0%	Ti 0.4%
pH	5.3										
Archaeological Matrix 900^{0}C											
Xlf=κ/p x10^{-8} m^{3}kg^{-1}	1122.5										
%Xfd	10.3										
Atomic % of elements	Na 1.4%	Mg 1.6%	Al 4.7%	Si 15.3%	P 1.8%	S	Cl	K 2.1%	Ca 6.8%	Fe 5.5%	Ti
pH	10.7										

Table 6.24 The analytical data for the additional archaeological sample material showing the results of each analytical method organised. Source: Author

The archaeological matrix material shows an extreme increase in MS measurement, starting at 87.2 x10^{-8}m^{3}kg^{-1} for the sample that was not heated in the laboratory and rising to 1122.5 x10^{-8}m^{3}kg^{-1} after being exposed to 900^{0}C (table 6.24) (the material could have been exposed to heat before being deposited in the midden). The elements present among the archaeological matrix sample material include sodium, magnesium, aluminium, silicon, phosphorous, potassium, calcium, and iron (figure 6.29). The pH of the archaeological matrix material ranges from 5.3 to 10.7 between the unheated sample and sample of the same material heated to 900^{0}C (table 6.24). The archaeological matrix material appears light brown for the unheated sample and the 900^{0}C sample is red (table 6.23).

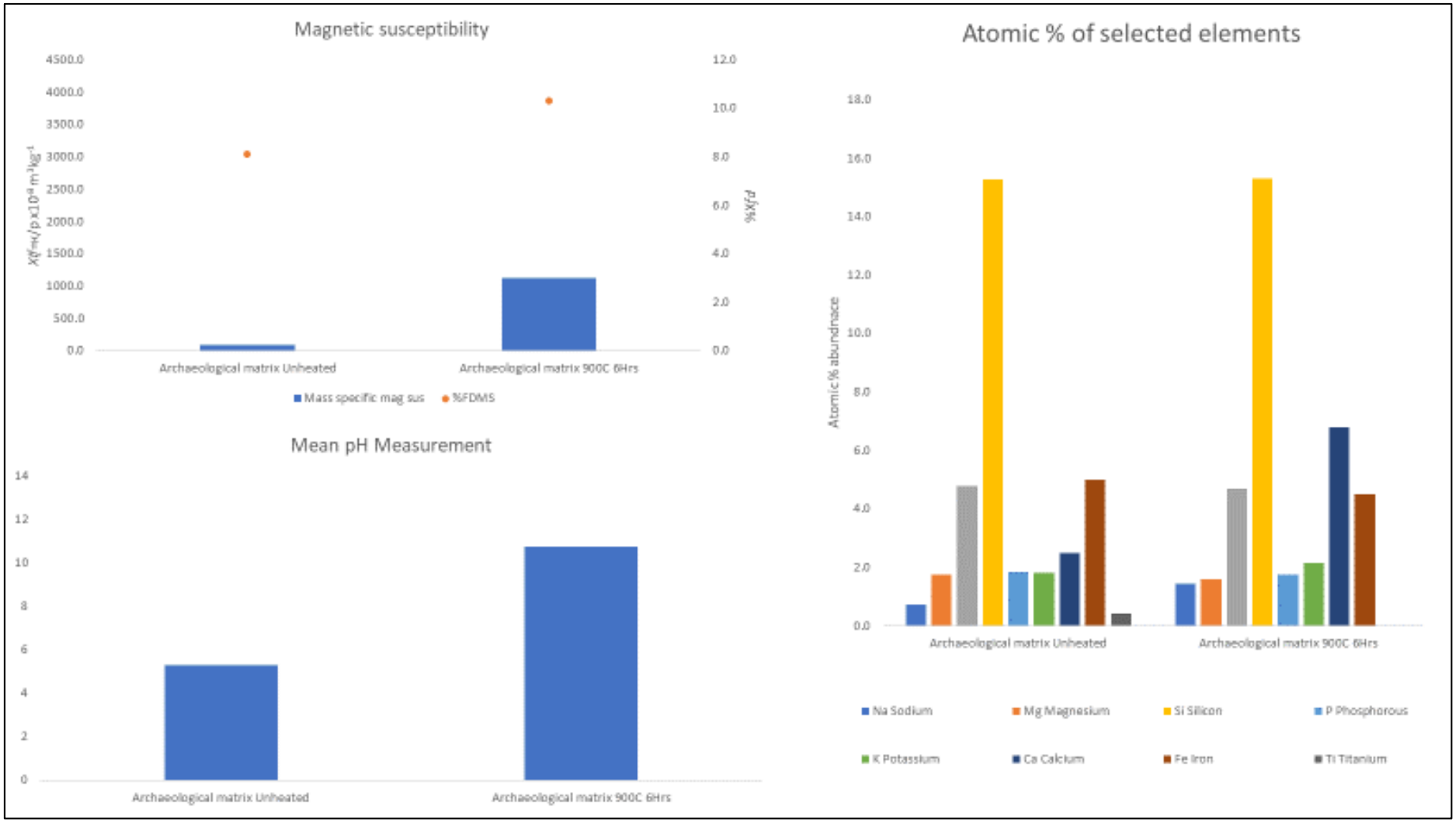

Figure 6.29 Clockwise from top left the low frequency mass specific magnetic susceptibility and percentage frequency dependence, the atomic percentage abundance of selected elements, and the pH among the additional archaeological sample material. Source: Author

6.4 Conclusions

This chapter has presented the initial and detailed analytical data for this investigation. The results of the modern analogue analyses have been presented in section 6.2 to demonstrate the effects of exposing fuels to increasing temperature, and to identify the significant patterns present in the magnetic susceptibility, SEM/EDX, pH, and colour data germane to the identification of fuels from archaeological ash. The archaeological analyses results have been presented in section 6.3 to establish the magnetic susceptibility, SEM/EDX, pH, and colour signatures that are present among the samples. The interpretation and implications of the data gathered from this investigation are discussed in the subsequent discussions chapter. The data presented within this chapter is used to identify the fuels present among the archaeological ash samples, this is discussed and shown using principal components analysis in section 7.3.

The associations between modern fuel and archaeological samples were designated following the variables from the analytical results that best indicate fuel material including MS and the percentage abundance of iron, sodium, titanium, aluminium, potassium, and phosphorous as discussed in sections 2.5 and 3.6. The final results are indicative of what fuel was burned to create the ash, and to what approximate temperature, for each of the archaeological samples.

Chapter 7 Sifting through the ashes (Discussion)

7.1 Overview

The following is a discussion of the results presented in sections 6.2 and 6.3. The discussion has been divided into three sections focusing on the modern analogues, archaeological material, and finally the identification of fuels from archaeological deposits using a comparison with the modern analogue results. This separation allows for the discussion to focus on what was learned from the analyses as they pertain to modern analogue fuels and archaeological material separately before considering the implications of the results on the identification of archaeological fuel material from ash. The identification of fuel from archaeological ash draws from all the analytical data and utilises principal components analysis to present the multivariate data in a way that the associations between the modern analogue and archaeological fuels can be displayed.

7.2 Modern analogues

The significant results from observations of ashing at increasing temperature and subsequent analyses of modern analogue fuel material presented in section 6.2 and their implications for the research are discussed. Understanding how a fuel was used, for cooking, heat, metal working, pottery firing, etc., as discussed in section 2.4, is important to interpretation in addition to the fuel type being used. The Modern analogue fuels are discussed focusing on the implications of each analytical method including magnetic susceptibility, pH, SEM/EDX, mass lost, and Munsell colour assignment throughout this section. The implications of the results as a whole are discussed in section 7.4.

7.2.1 Modern analogue magnetic susceptibility

Low frequency MS

Exposing modern analogue fuel material to increasing intervals of time and temperature increased the magnetic susceptibility of the samples. The modern analogue fuel types all started with diamagnetic readings (apart from grasses) when unburnt samples underwent magnetic susceptibility measurements (figure 7.1). The low and high frequency magnetic susceptibility measurements have an average standard deviation of 0.7 (appendix 1). Rousay peat, seaweed, grasses, heather, willow, hazel, bone, and fozzy peat all retained a diamagnetic magnetic susceptibility measurement when heated to 200^0 Celsius for 6 hours (figure 7.1). Bone was the only sample type that showed no significant change in magnetic susceptibility throughout all increases of temperature, maintaining a diamagnetic magnetic susceptibility measurement throughout all temperature intervals (figure 7.1). This may be due to the abundance of diamagnetic $CaCO_3$ within bone combined with the natural diamagnetism of organic material like collagen (Dearing 1994: 33). Diamagnetism is independent of temperature and applied field as per Mulay (1963: 1761), any significant change in magnetic susceptibility associated with temperature can be attributed to a change in the material's physical or chemical structure. The effect of temperature on the magnetic susceptibility of fuels was most noticeable at 900^0 Celsius. This temperature had the largest increase in MS measurement (figure 7.1). In the case of the peat fuels (Rousay peat, fozzy peat, mid peat, low peat, and highland park peat) this increase was substantial; an increase of over 3,200 $x10^{-8}m^3kg^{-1}$, from 331.5 $x10^{-8}m^3kg^{-1}$ to 3613.6 $x10^{-8}m^3kg^{-1}$ for Rousay peat and a 900 $x10^{-8}m^3kg^{-1}$ to 1700 $x10^{-8}m^3kg^{-1}$ increase among the remaining peat samples. All of the changes in magnetic susceptibility are due to a change in

the mineral concentration and chemical composition of the fuel throughout combustion (Mulay 1963: 1761).

The magnetic minerals are incorporated into the modern analogue fuel material through the soil matrix they were grown in. As discussed in section 2.2, the parent rock material of Orkney is sandstone, flagstone, granite and basalt. These materials all contain magnetic minerals including $FeCO_3$ and FeO_3Si (paramagnetic), Fe_2O_3 and TiO_2, FeS (ferrimagnetic), and haematite and goethite (antiferromagnetic) (Tarling 1983; Land Use Consultants 1998; Dearing 1994; Blundell *et al.* 2009). This material makes way from the soil to the roots and throughout the plant via the vascular system. the organic material from the fuel is burned away through combustion causing a proportional increase in the mineral material within the samples. The magnetic grains were altered by heat throughout the ashing process, resulting in increasing magnetic susceptibility measurements as a result of increase in temperature. Through the processes of deuteric alteration and subsequent oxidizing the structure of magnetic minerals can be altered and create different minerals that have higher or lower magnetic susceptibilities and can be changed further into other magnetic minerals by heating (figure 7.2) (Tarling 1983; Kars *et al.* 2014).

The increase in the MS of modern fuel samples associated with an increase in temperature is due to a combination of a change in the concentration of minerals within the material as the organic material is burned away, and the changing of magnetic minerals through exposure to heat to form more magnetically active minerals. The unburnt materials have diamagnetic measurements due to the majority concentration of organic material that has a diamagnetic value in greater concentration than the magnetic mineral content.

As the fuels are exposed to greater levels of heat more of the organic material and elements of lower melting/flash points are burned away leaving a higher concentration of the magnetic minerals causing an increase in magnetic susceptibility measurements.

The transformation of the antiferromagnetic haematite into the ferrimagnetic magnetite at temperatures greater than 550^0C could explain the increase in magnetic susceptibility demonstrated from 400^0C to 900^0C (Tarling 1983). This is further corroborated by the most marked increase in magnetic susceptibility measurement being reached after temperatures rise above 484.85^0C, established by Zang *et al.* (2017).

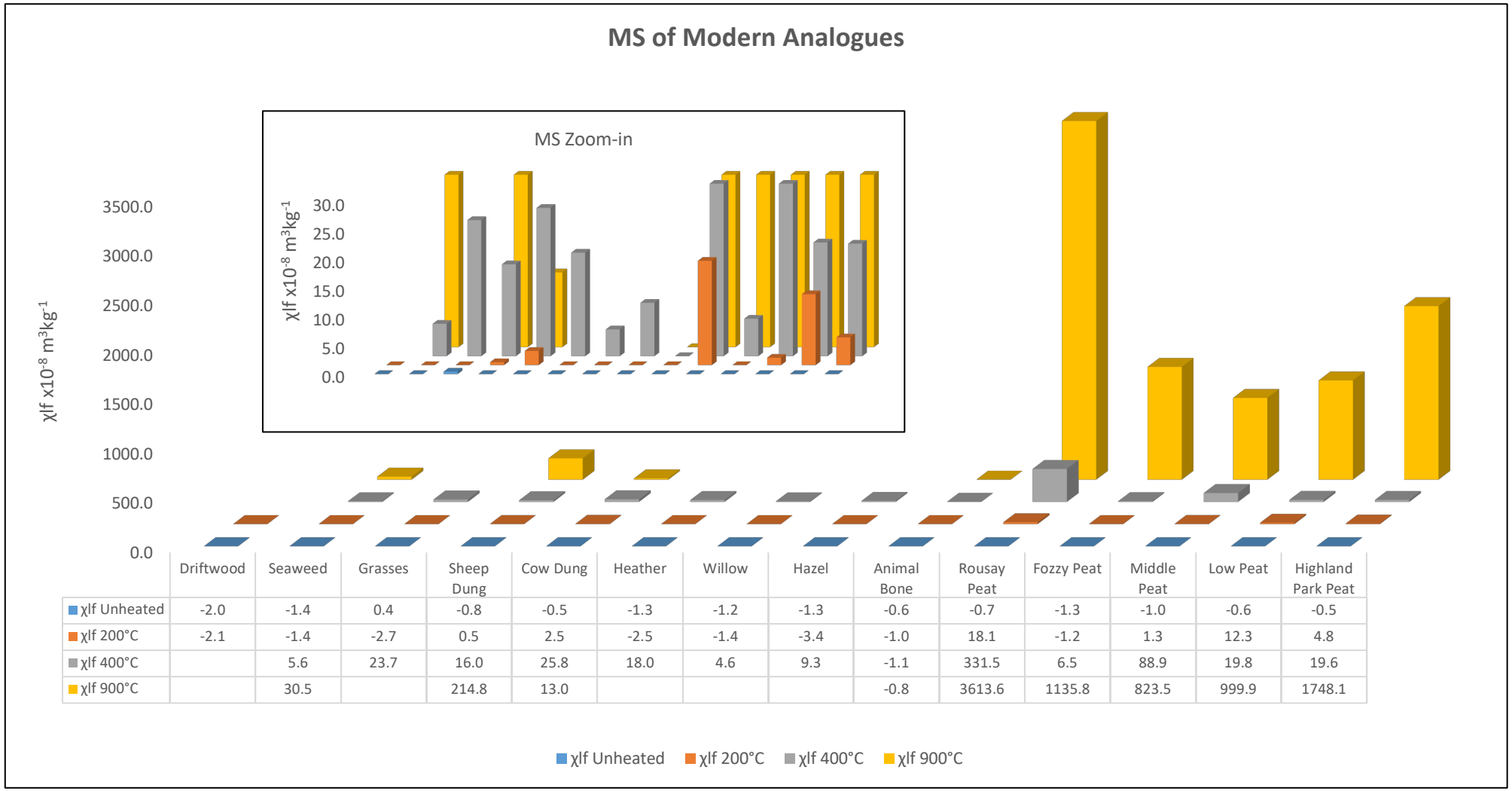

	Driftwood	Seaweed	Grasses	Sheep Dung	Cow Dung	Heather	Willow	Hazel	Animal Bone	Rousay Peat	Fozzy Peat	Middle Peat	Low Peat	Highland Park Peat
χlf Unheated	-2.0	-1.4	0.4	-0.8	-0.5	-1.3	-1.2	-1.3	-0.6	-0.7	-1.3	-1.0	-0.6	-0.5
χlf 200°C	-2.1	-1.4	-2.7	0.5	2.5	-2.5	-1.4	-3.4	-1.0	18.1	-1.2	1.3	12.3	4.8
χlf 400°C		5.6	23.7	16.0	25.8	18.0	4.6	9.3	-1.1	331.5	6.5	88.9	19.8	19.6
χlf 900°C		30.5		214.8	13.0				-0.8	3613.6	1135.8	823.5	999.9	1748.1

Figure 7.1 A 3-dimensional plot showing the low frequency MS organised by fuel type and temperature with a zoom in plot overlayed to show the variation in the smaller values. Source: Author.

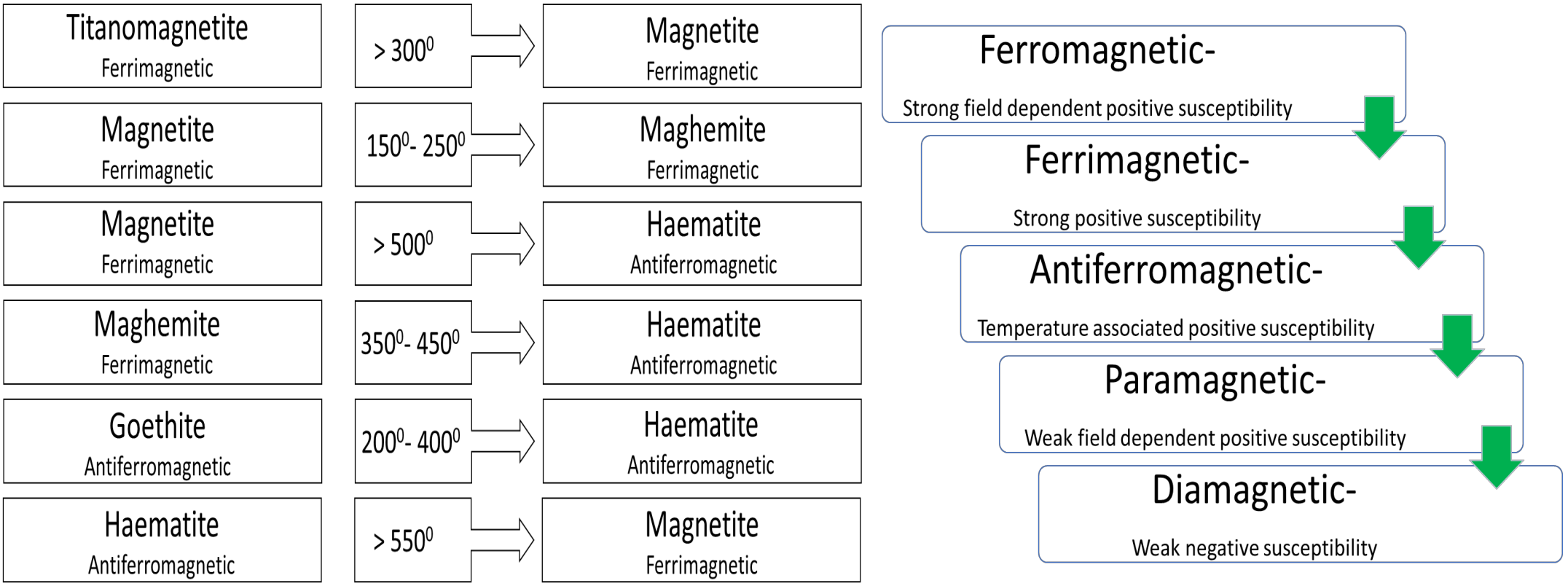

Figure 7.2 Left to right: A table of the changes that magnetic minerals undergo at certain temperatures, and a table of the stages of magnetism (Dearing 1994; Tarling 1983). Source: Author

Frequency dependent magnetic susceptibility

The FDMS was calculated for materials that displayed magnetic susceptibility measurements above 10.0, to avoid complications from the values that fall closer to the instruments level of error. The frequency dependence data is not able to distinguish between fuel types, but can be used to aid in identifying the temperature a fuel was heated to when used in league with other methods such as MS and pH. The fuels heated to 400^0C show the highest values in FDMS ranging from 8.4% - 25.6%, compared to 4.6% - 11.6% at 900^0C (figure 7.3). The peak in the FDMS at 400^0C followed by the drop in the FDMS when heated to 900^0C is indicative of the change that the magnetic minerals present are going through when exposed to increasing temperatures (Kozhevnikov *et al.* 2014; Dearing 1994; Mulay 1963). This as well demonstrates the superparamagnetism in ferromagnetic and ferrimagnetic grains present in lower proportion to the organic material in the samples heated to lower temperatures. This causes the high FDMS due to the higher relative contribution from the ferromagnetic and ferrimagnetic grains to the total magnetic susceptibility (Kozhevnikov *et al.* 2014; Dearing 1994; Mulay 1963; Hrouda & Pokorný 2011).

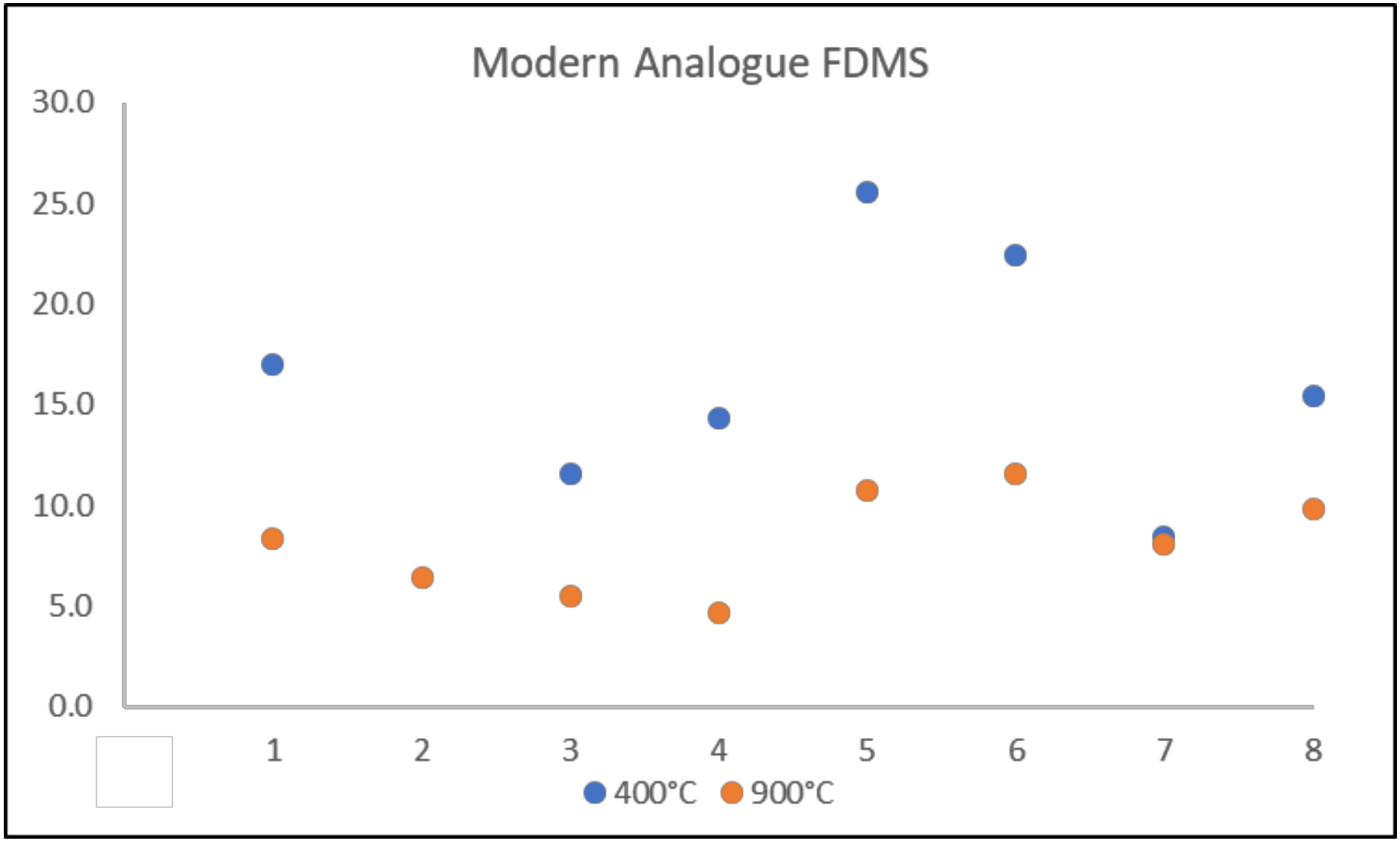

Figure 7.3 The modern analogue FDMS summary, from left to right the samples are 1 seaweed, 2 sheep dung, 3 cow dung, 4 Rousay peat, 5 fozzy peat, 6 middle peat, 7 low peat, and 8 Highland Park peat. Source: Author

7.2.2 pH measurements

The pH values among the fuel types varies greatly from pH 4.3(±0.01) (Rousay peat 200^0C 6Hrs) and pH 12.4 (Driftwood 900^0C 6Hrs), yet the fuels are all within groups based on increase in temperature 4.3-7.1 for fuels exposed to 200^0C, 7.4-10.1 for fuels exposed to 400^0C, and 6-12.4for fuels exposed to 900^0C (figure 7.4). With the exclusion of heather exposed to 900^0C, the grouping based on temperature interval becomes more evident for the other modern analogue fuels 8.8-12.4. The other wood fuels have a mass loss of more than 95%, and were not used in this analysis, this is a trend seen in all wood fuels. All modern analogue fuels show an increase in pH value as they are exposed to increasing temperature (figure 7.4). The differences between the pH of the modern analogue fuel types are not capable of being a standalone method for the characterisation of archaeological fuel types; however, the data can aid in discerning the temperature materials were exposed too when used in conjunction with other analytical methods. The sample pH provides a useful and resource efficient means of strengthening a data set and corroborating findings by showing the relative temperature a sample was heated to, based on the trends observed with the modern analogue ash samples. When combined with the magnetic susceptibility data, the pH can assist in identifying the temperature a sample was exposed to and determine a possible fuel type.

The increase in pH measurement that is associated with increase in ashing temperature can be explained. Throughout the chemical reaction of combustion, the organic material is burned away leaving only the inorganic materials including high concentrations of compounds containing Na, Mg, Ca, and K which makes the ash more alkaline (Etiégni & Campbell 1991; Ohno 1994).

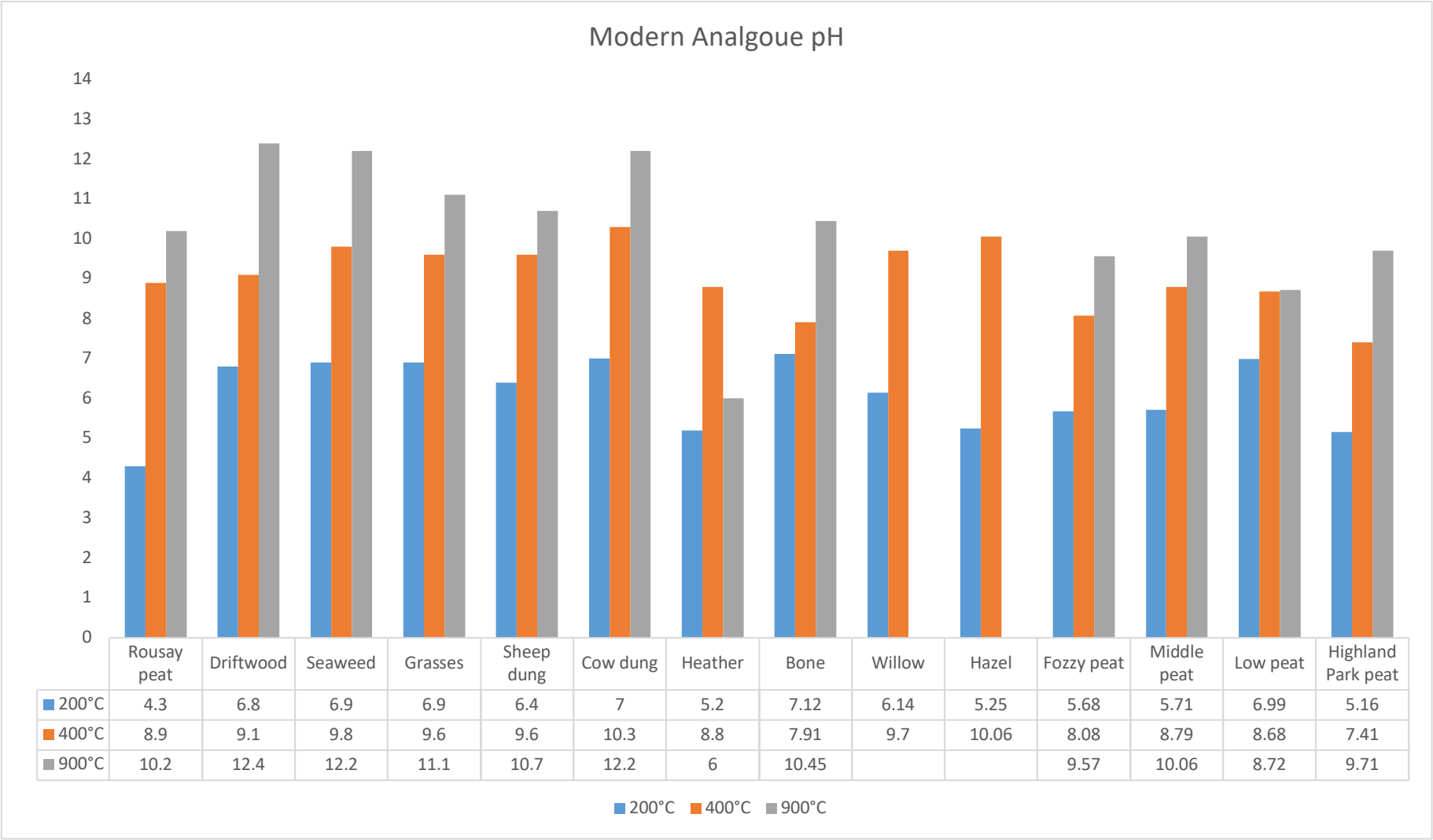

	Rousay peat	Driftwood	Seaweed	Grasses	Sheep dung	Cow dung	Heather	Bone	Willow	Hazel	Fozzy peat	Middle peat	Low peat	Highland Park peat
200°C	4.3	6.8	6.9	6.9	6.4	7	5.2	7.12	6.14	5.25	5.68	5.71	6.99	5.16
400°C	8.9	9.1	9.8	9.6	9.6	10.3	8.8	7.91	9.7	10.06	8.08	8.79	8.68	7.41
900°C	10.2	12.4	12.2	11.1	10.7	12.2	6	10.45			9.57	10.06	8.72	9.71

Figure 7.4 Mean pH measurement among modern analogue samples exposed to increasing intervals of time and temperature. Source: Author

7.2.3 Scanning electron microscopy and energy dispersive X-ray spectroscopy

The following discusses the significant observations from the SEM/EDX analysis of modern analogue fuel materials. The elements being considered for this research Na, Mg, Al, Si, S, Cl, P, K, Ca, Fe, and Ti were predetermined based upon the review of previous fuel examination and explained within section 2.5 (Vassilev *et al.* 2013; Vassilev *et al.* 2014; Baernthaler *et al.* 2006).

Al is very mobile in acidic soils, especially those lower than 5.5 pH, and can be readily available for plants. The presence of Al can be toxic for plants in the absence of Ca and Mg (Kabata-Pendias & Pendias 1985). All of the modern analogue fuel samples that have Al all display a presence of Mg and Ca which are needed to prevent Al toxicity among plants (figures 7.5 & 7.7). The only sample that had a high concentration of Al with a small amount of Ca (0.26%) and no magnesium was willow 200^0C, and this could be an indication as to why the limbs were pruned due to wilting and discoloration that is associated with high levels of Al. It can be expected to see higher abundances of Al among archaeological sample material due to the increased mobility in acidic soils (Kabata-Pendias & Pendias 1985).

The concentration of Fe in the modern analogue fuel samples should have a proportionally lower concentration of Fe than the archaeological samples, similar to Ti and Al. This could be due to the soil material having higher levels of Fe from the geological parent material, and the plant material only having access to Fe through the absorbing of water from the soil. Fe within the samples is present among all modern analogue fuel types except for grasses and willow (figure 7.7). This could be explained through the Fe not being readily transported through plant tissue, causing the newest growth to have lowest

concentrations of Fe and the root area to have the highest (Kabata-Pendias & Pendias 1985). The willow and grasses that were used for this experiment were pruned from new growth and in effect has little to no Fe content, which is shown by the data (figure 7.7).

Ti is not very mobile in plants and is expected to have higher concentrations among the archaeological material that have been mixed with soil that contains larger amounts of Ti (Kabata-Pendias & Pendias 1985). Of the modern analogue fuel materials, the peat samples have the highest frequency and abundance of Ti, out of 15 samples of modern analogue peat ash only 4 do not contain Ti; Rousay peat 200^0C and 400^0C, and fozzy peat 200^0C and 400^0C (figure 7.7). This makes sense due to peat coming from within the soil matrix, and peat soils tend to be acidic which aids in the mobility of Ti and Fe within soils.

There is a relationship between the presence of Ca and the fixation of S during ashing (Obenberger et al 2006). There are only 4 modern analogue fuel samples that contain Ca and do not also contain S; grasses 400^0C, sheep dung 900^0C, willow 200^0C, and middle peat 200^0C. It is also significant to point out that 3 out of the 4 examples are fuels heated to lower temperatures and heating is necessary for this reaction to take place; in addition, this reaction takes place at a greater rate with higher temperature exposure (Obenberger et al 2006).

Magnesium is an element that is essential for plants, and is expected to be in higher concentration among modern analogue fuel material than the archaeological sample material. In acidic or wet soils, Mg, is depleted, but in plant material there should always be an abundance. This would suggest that

modern analogue ash will have a higher concentration of Mg, than the archaeological sample material.

The sample with highest abundance of elements present is Highland Park peat with an average of 5.3% Mg, 2.2% Al, 4.6% S, 0.55% K, 4.2% Ca, 2.8% iron, and 0.24% Ti present between all the temperature variations (figure 7.5-7.7)

The most abundant elements among all modern analogue fuel samples are Mg, Ca and S. Magnesium is present among all samples except for willow 200^0C, Ca is absent from hazel 200^0C and low peat 200^0C, and S was not present among willow 200^0C, middle peat 200^0C, grasses 400^0C, and sheep dung 900^0C (figure 7.7). as would be expected the seaweed samples had the highest presence of Na among all the samples. This is likely due to the salinity of ocean water being absorbed into the plant during growth (Maathuis 2013).

Cow dung demonstrated an anomalous result that is a modern issue with the use of biofuels in commercial applications, researched by Obenberger *et al.* (2006). In the presence of Ca concentration below 15% weight abundance and K concentrations over 7% weight abundance the melting temperature of ash can be affected according to Obenberger *et al.* (2006). This ash melting is present in the modern analogue fuel sample of cow dung heated to 900^0C. The modern analogue fuel Samples of cow dung heated to 400^0C and 900^0C have values within the parameters established by Obenberger *et al.* (2006), 7.9% Ca and 9.7% K, and 7.4% Ca and 14.8% K respectively. The sample of cow dung heated to 900^0C has the appearance and consistency of fuel ash slag or cramp, and is purple in colour, this is further evidence of the physical change of the ash melting at 900^0C and not 400^0C. Although the same potential was there for both fuel samples during ashing, only the sample exposed to the higher temperature

has become vitrified (section 6.1.5). The purple colour could be due to the presence of Mn within the sample from the geological parent material causing the formation of $KMnO_4$ which can produce a pink or purple coloration and a crystal formation in evaporations of solutions. Mn was measured by the SEM/EDX but was not considered for the identification of archaeological fuels due to its' low frequency within the sample material (appendix 3). This could be useful information for modern applications of dung as fuel. If cow dung is to be used as a fuel it must be for functional uses that require temperatures lower than 900^0C to avoid the formation of cramp. The buildup of cramp can cause ash disposal issues, and interfere with heating equipment in modern commercial and industrial applications.

The most obvious outlier of the dataset is animal bone with an average of 0.7% Na, 0.2% Mg, 9.3% P, and 14.8% Ca present between all the temperature variations with the presence of no other elements (figure 7.5-7.7). For the rest of this section bone is not considered for the trends observed due to its variance in content from the remainder of the modern analogue fuel samples.

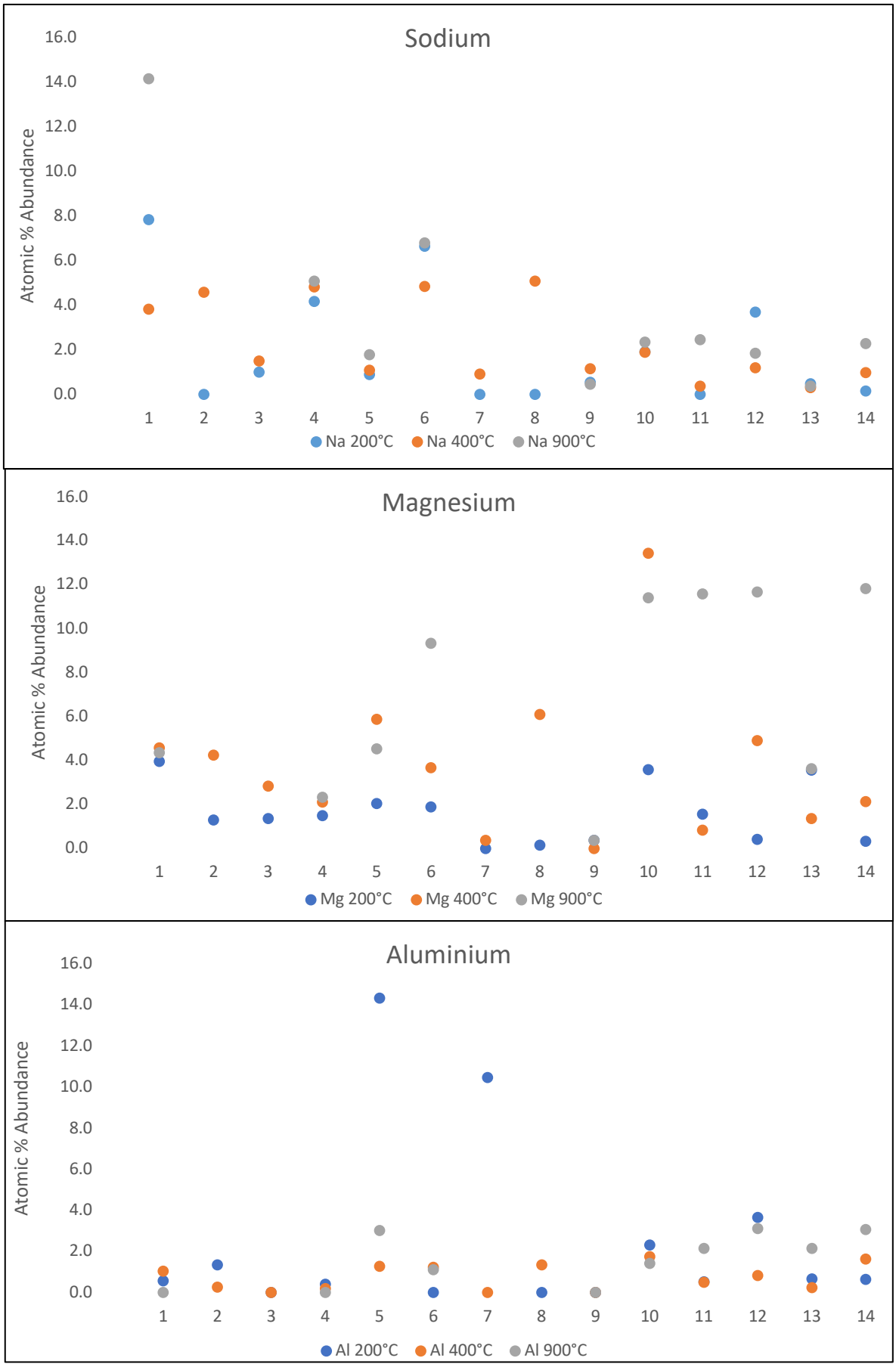

Figure 7.5 a series of plots showing the atomic percentage abundance of individual elements from modern analogue ash samples. In each plot, the samples are organized by temperature and fuel type from left to right: 1 Seaweed, 2 Driftwood, 3 Grasses, 4 Cow dung, 5 Sheep dung, 6 Heather, 7 Willow, 8 Hazel, 9 Bone, 10 Rousay peat, 11 Fozzy peat, 12 Middle peat, 13 Low peat, and 14 Highland Park peat. Source: Author

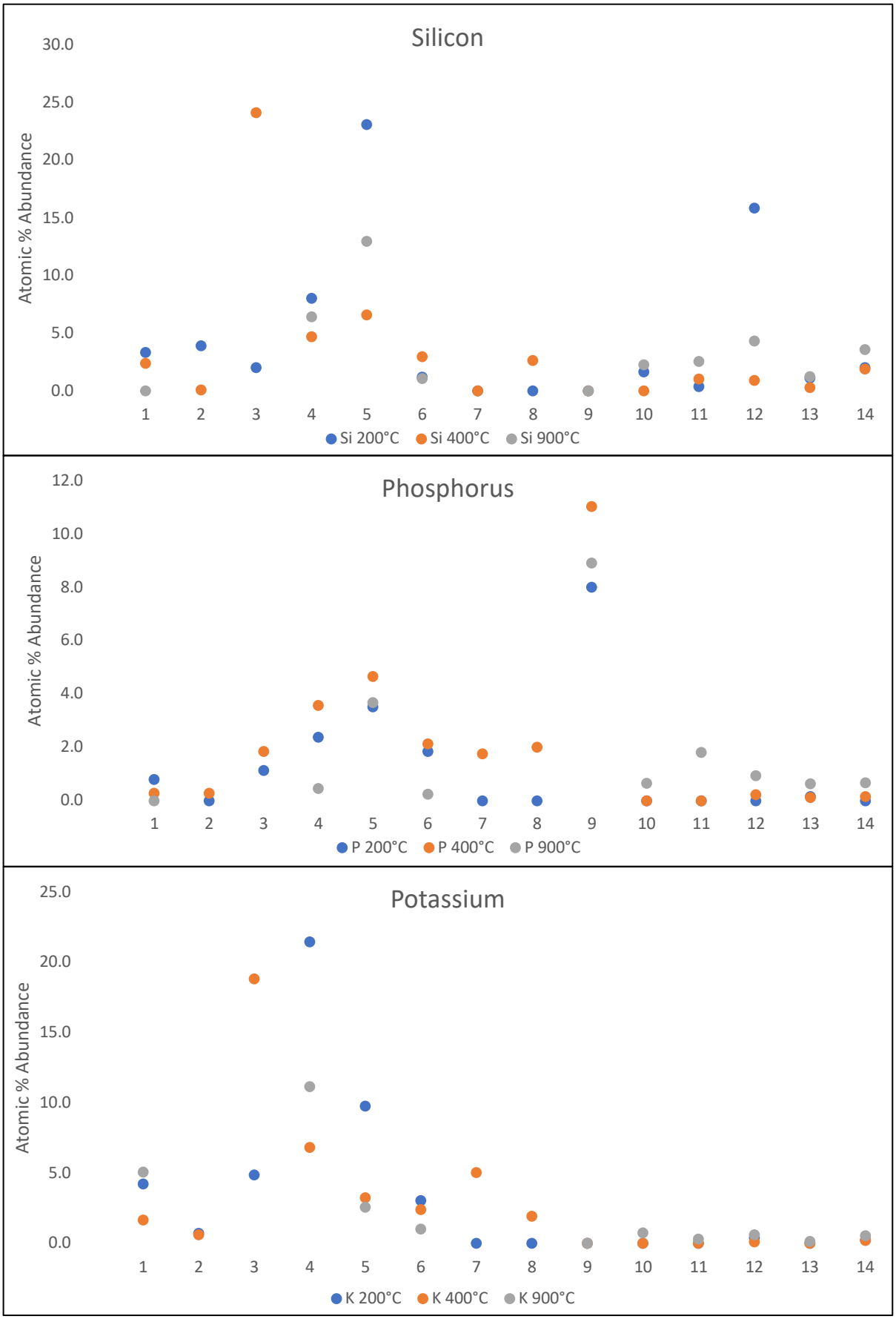

Figure 7.6 a series of plots showing the atomic percentage abundance of individual elements from modern analogue ash samples. In each plot, the samples are organized by temperature and fuel type from left to right: 1 Seaweed, 2 Driftwood, 3 Grasses, 4 Cow dung, 5 Sheep dung, 6 Heather, 7 Willow, 8 Hazel, 9 Bone, 10 Rousay peat, 11 Fozzy peat, 12 Middle peat, 13 Low peat, and 14 Highland Park peat. Source: Author

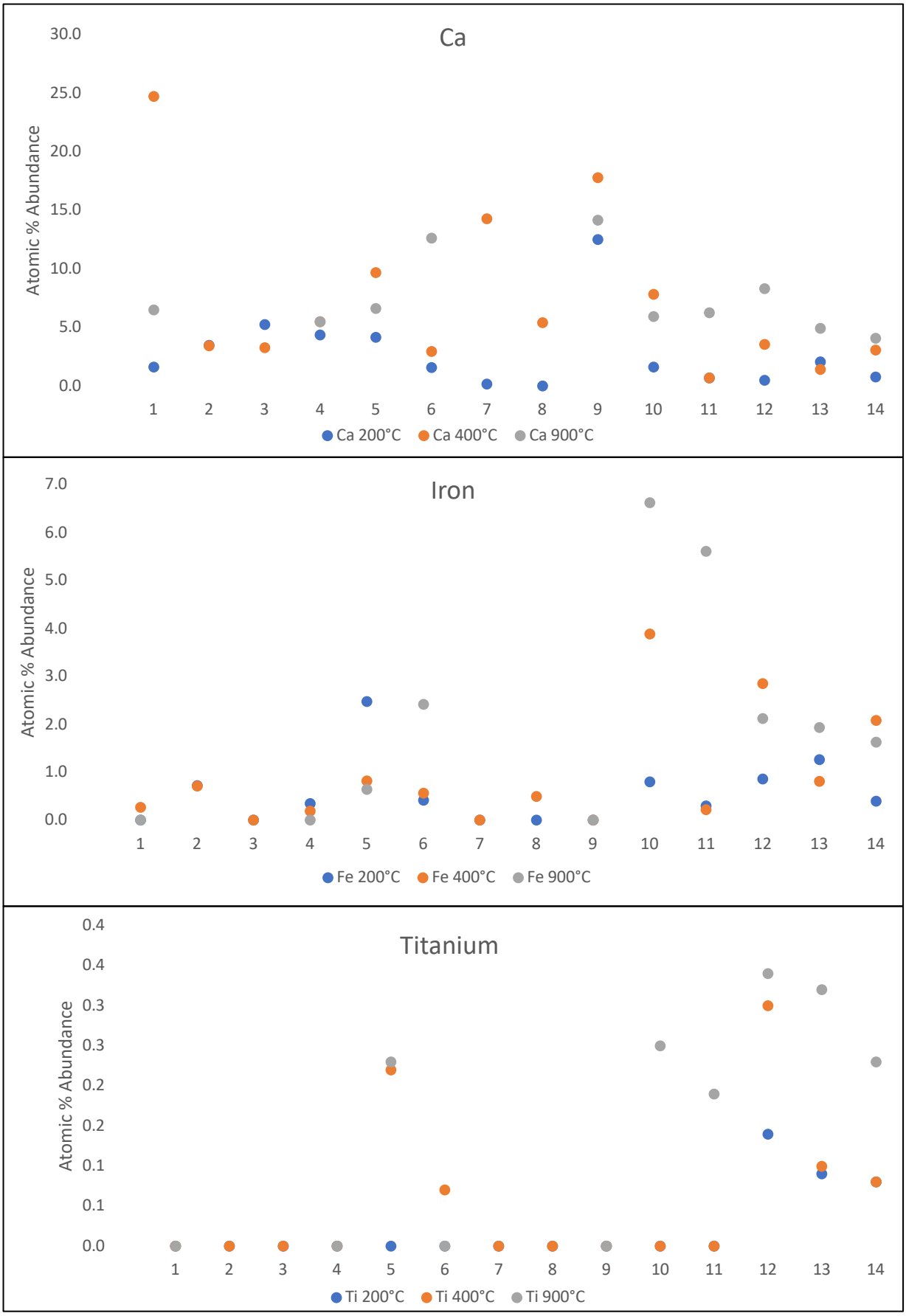

Figure 7.7 a series of plots showing the atomic percentage abundance of individual elements from modern analogue ash samples. In each plot, the samples are organized by temperature and fuel type from left to right: 1 Seaweed, 2 Driftwood, 3 Grasses, 4 Cow dung, 5 Sheep dung, 6 Heather, 7 Willow, 8 Hazel, 9 Bone, 10 Rousay peat, 11 Fozzy peat, 12 Middle peat, 13 Low peat, and 14 Highland Park peat. Source: Author

The SEM/EDX data provides useful insight into what elements are present among different fuel types. The elements being considered for use in the identification of archaeological fuels are Na, Mg,, Al, Si, P, K, Ca, iron, and Ti as explained in section 5.4.3. Some of the elements needed to be excluded based on their abundance in soils versus the abundance in selected fuel materials, which could cause large disparities in the dataset and skew the matching results.

This dataset aids in the identification of archaeological fuel by affording a means to identify fuel material based upon elemental signatures. This data is not able to discern approximate temperature, but provides a potential fuel type based upon the presence or absence of certain elements. For example, Fe and Ti in high concentrations would be indicative of peat fuels.

In addition, the elements present can also be useful in the interpretation of the other analytical methods. The magnetic susceptibility of the samples is affected by the presence of magnetic minerals, mostly oxides of Fe and Ti. The samples with the highest concentrations of those elements also have the highest MS measurements. In the instance of the pH of samples, elements like Ca, Na, Mg, and K influence the acidity/alkalinity of a sample as discussed in section 2.7 (Etiégni & Campbell 1991; Cronyn 1990; Di Gianfilippo *et al.* 2016; Ohno T 1992). The samples with the highest concentration of Ca and magnesium in turn have the highest pH measurements. This makes SEM/EDX not only an additional means to characterise fuel ash, but a means to crosscheck the findings from the remaining methods based on the influence of elemental makeup on magnetism and pH.

7.2.4 Preliminary analytical data

Mass Lost

The mass lost does track a predictable pattern of increased loss of mass as temperature increases (figure 7.6), yet the data is variable enough to offer some aid diagnostically in the instance that an intact ash deposit or combustion feature is sampled. This data set is useful for determining the approximate amount of initial fuel material necessary to produce the known quantity of ash, or how much fuel would have been required to create a particular deposit. The mass lost for the selected modern analogue fuel types show an increase in mass lost associated with increase in temperature (Figure 7.6). Bone's mass is clearly the least affected by heat, only losing 33% of its mass at 900^0C, the only other modern analogue fuel that displayed a resistance to loss of mass through heating was seaweed with 62% mass lost at 900^0C, all other fuels demonstrated a mass loss of 80% or greater with driftwood, grasses, heather, willow and hazel all losing 99% of their mass at 900^0C; driftwood also demonstrated 98% mass lost at 400^0C while all other modern analogue fuels showed a loss ranging from 29% to 96% (figure 7.6).

Munsell colour assignment

The Munsell colour data as described in section 5.3.2 and results presented in section 6.2.1 was used to characterise the changes in colour that modern analogue fuels underwent as a result of exposure to increasing ashing temperature (figure 7.7). This method is very useful for aiding in the identification of archaeological fuels when used with analytical methods for verification and corroboration of findings due to the distinct colours observed among temperature groups and fuel types. This is also an analytical method that can be applied in the field with no equipment needed. The peat fuels start off a very dark brown then to very dark grey and at the highest temperature

yellow to red. Sheep dung is similar to peat for the first two temperature intervals, but differs at 900^0C lacking the yellow to red hue of peat, appearing more light grey (figure 7.7). Cow dung appeared to follow the same trend as grasses turning from grey to a dark grey at 200^0C and 400^0C respectively, at 900^0C cow dung takes on a purple hue due to the presence of manganese, where the grasses are a very light grey (figure 7.7). Bone is distinct at every temperature turning from yellow/brown to dark grey to bright white as temperature was increased (figure 7.7). The wood fuels darken and become a deep brown after being exposed to 200^0C, and turn a dark grey at 400^0C (figure 7.7). Seaweed follows its own trend in colour change, going from light grey with orange inclusions at 200^0C, followed by a medium grey at 400^0, and finally turning very dark grey with yellow inclusions (figure 7.7).

The Munsell colour assignment offers a means to visually identify fuels with no analysis. The colours of fuel ashes from the three temperature intervals demonstrate trends that fuel types, such as wood and peat, displays after exposure to certain levels of heat. This method can be used to identify both the approximate temperature of heating as well as fuel type. Munsell colour assignment used with the analytical methods offer yet another means to corroborate findings when identifying archaeological fuels.

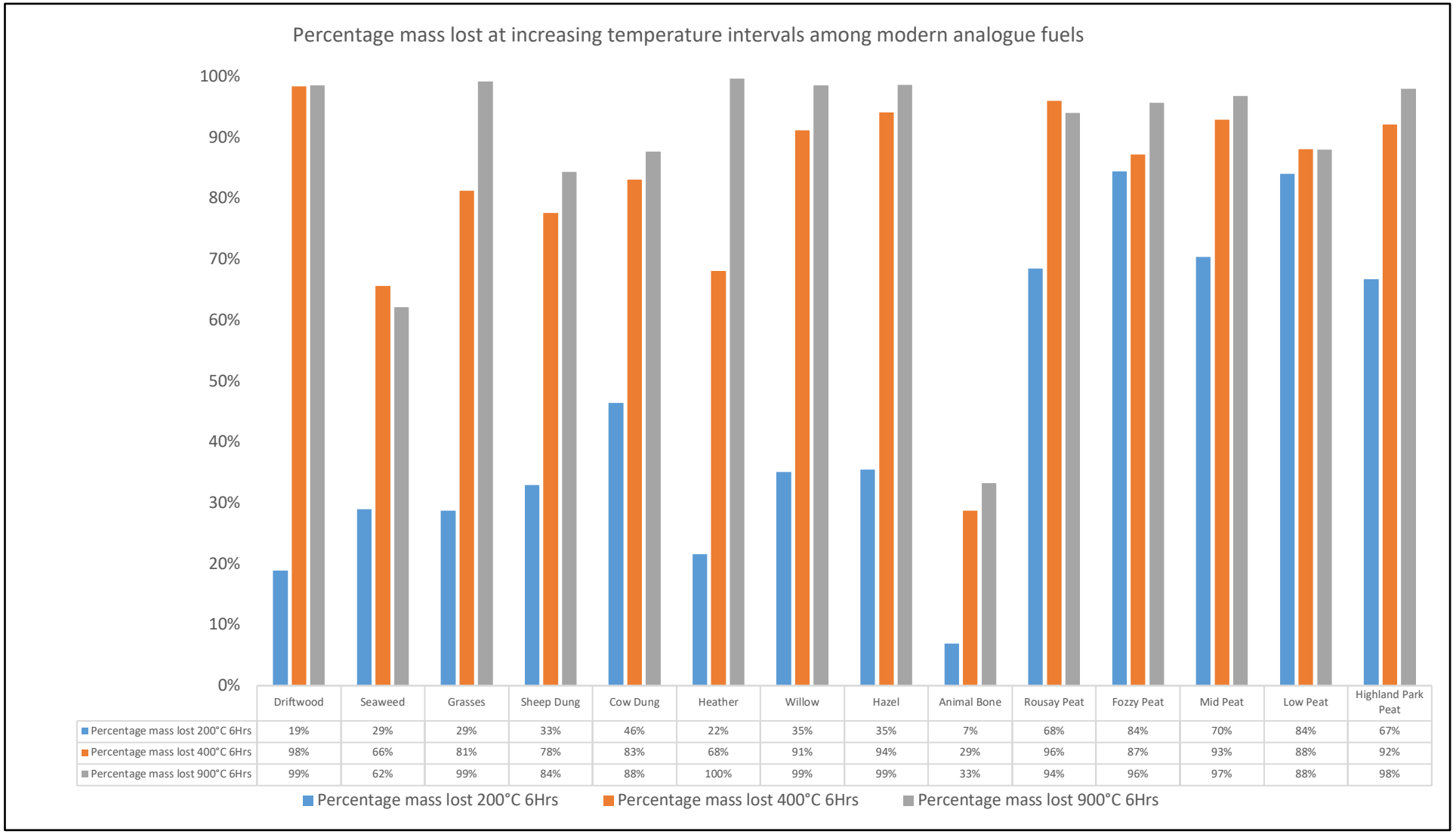

	Driftwood	Seaweed	Grasses	Sheep Dung	Cow Dung	Heather	Willow	Hazel	Animal Bone	Rousay Peat	Fozzy Peat	Mid Peat	Low Peat	Highland Park Peat
Percentage mass lost 200°C 6Hrs	19%	29%	29%	33%	46%	22%	35%	35%	7%	68%	84%	70%	84%	67%
Percentage mass lost 400°C 6Hrs	98%	66%	81%	78%	83%	68%	91%	94%	29%	96%	87%	93%	88%	92%
Percentage mass lost 900°C 6Hrs	99%	62%	99%	84%	88%	100%	99%	99%	33%	94%	96%	97%	88%	98%

Figure 7.8 Percentage mass lost at increasing temperature intervals among modern analogue fuels Source: Author

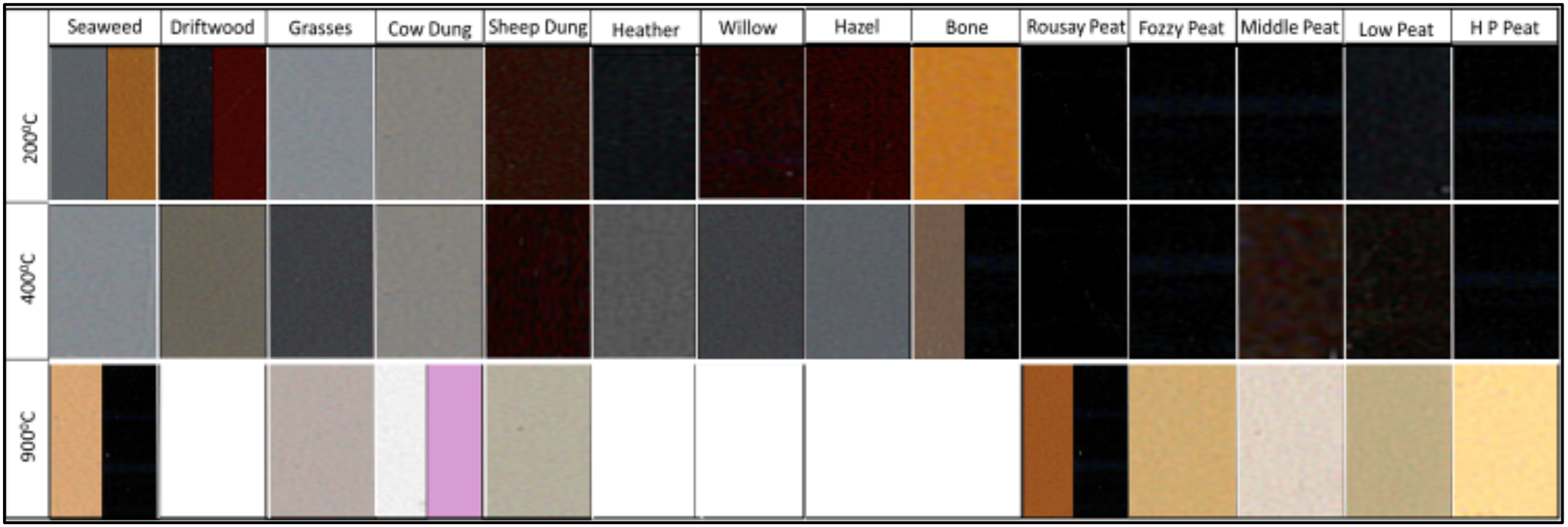

Figure 7.9 Munsell colour assignments chart for each of the modern analogue fuel taken from the Munsell colour book (Munsell Colour 2000). Source: Author

7.2.5 Additional material

The additional sample materials were introduced in Section 4.3, and the results were presented in section 6.2.3. The following discusses the significant findings from the examination carried out for this research and their implications for the identification of archaeological fuels.

Magnetic susceptibility

The additional samples have FDMS values ranging from 8.1% for unheated archaeological matrix to 11.3% for the Orkney peat ash sample collected from the Corrigal farmhouse museum (figure 7.8). The FDMS values of the additional materials are in range with several of the modern analogue samples including sheep dung, seaweed, fozzy peat, middle peat, low peat, and highland park peat at 900^0C, and cow dung heated to 400^0C all between 8% and 12% (figure 7.3 & 7.8).

The archaeological matrix material does show a change to magnetic susceptibility caused by heating shown in figure 7.9. The FDMS values increase from 8.1% to 10.3% after being heated to 900^0C for 6 hours, and the MS values increase from 87.2 $x10^{-8}m^3kg^{-1}$ to 1122.5 $x10^{-8}m^3kg^{-1}$ after being heated to 900^0C for 6 hours (figure 7.8 & 7.9). It is likely that some of the material from within the archaeological matrix samples was already exposed to heat before deposition into the midden.

The magnetic susceptibility data obtained from the additional sample material offers insight that is useful for the identification of archaeological fuels. The changes in magnetism that are present among the archaeological matrix material and the similarity in values between the ash from open air burning and the ash produced in the controlled laboratory setting offer a direct comparison to ash created in both open and controlled settings. This aids in deciphering the

type of fuel used and the approximate functional temperature of the combustion feature. This also suggests that the potential change of magnetism through the application of heat is not affected by combustion environment; using a muffle furnace, open fire pit, or stone hearth all affect the magnetism of the fuels in the same way, only the temperature of the combustion influences the magnetism of

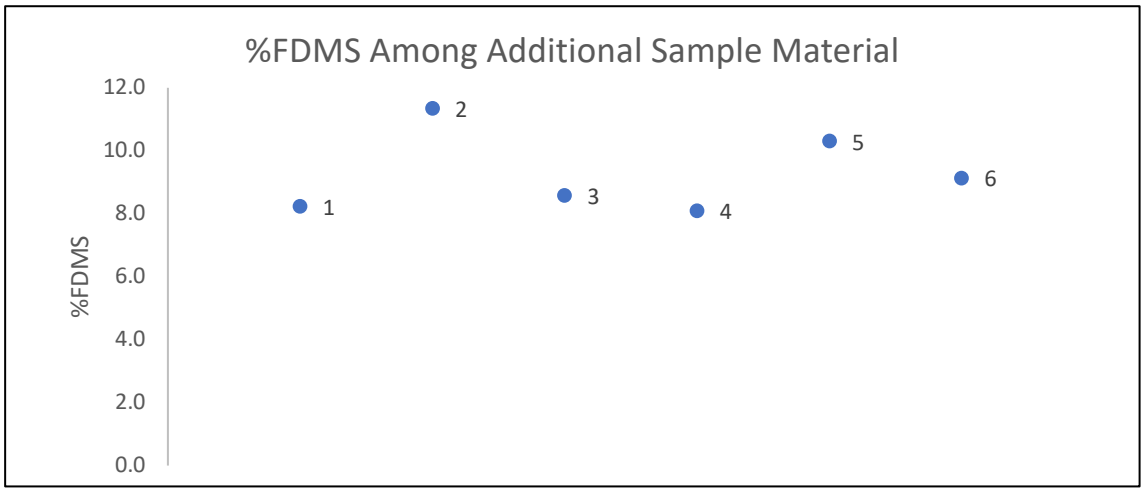

Figure 7.10 The frequency dependent magnetic susceptibility plot for additional sample material. Samples from left to right: 1 Caithness peat, 2 Orkney peat, 3 mixed fuels 500^{0}C, 4 unburnt archaeological matrix, 5 archaeological matrix 900^{0}C, and 6 modern peat and wood ash. Source:

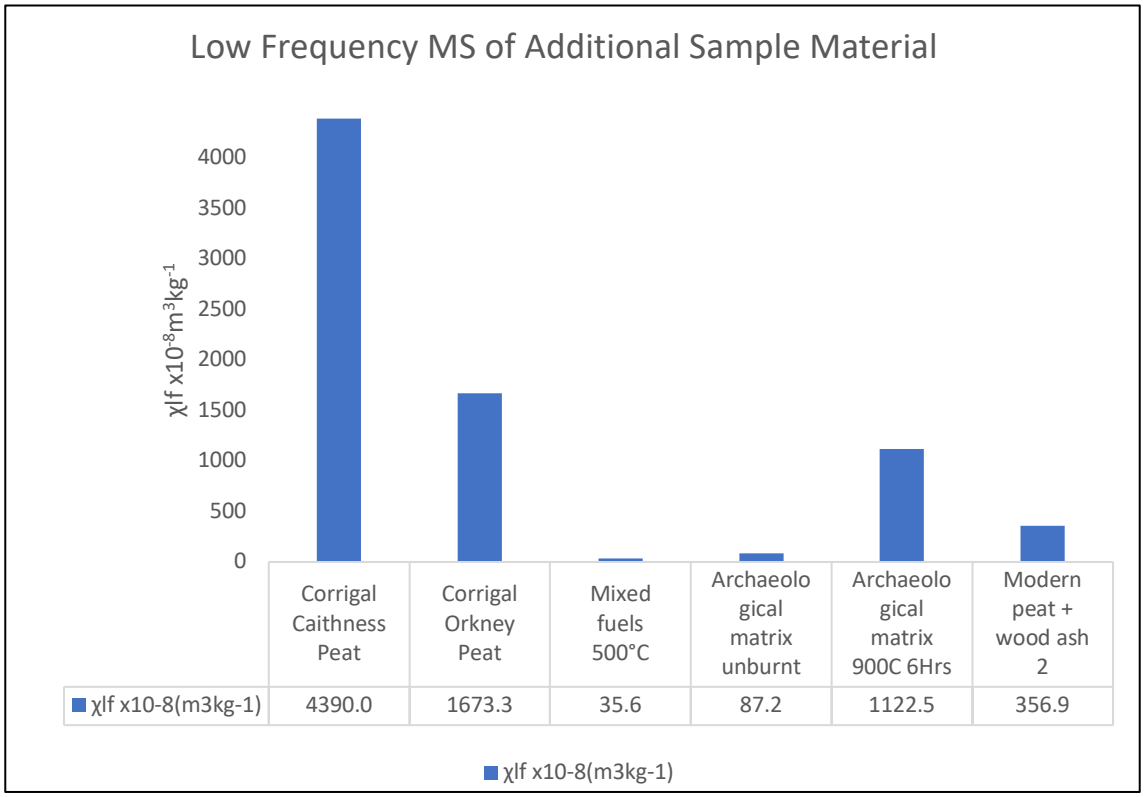

Figure 7.11 Low frequency MS among additional sample material. Samples from left to right: Caithness peat, Orkney peat, mixed fuels 500^{0}C, unburnt archaeological matrix, archaeological matrix 900^{0}C, and modern peat and wood ash Source: Author

pH

The additional sample material shows the pH of various ash and archaeological matrix material. This data provides a means for comparison of pH between the modern analogue ash prepared under controlled settings, and ash from uncontrolled combustion and archaeological matrix material. Drawing insight from the differences among the modern analogue ash and additional material gives further understanding to the relationship between fuels, combustion environment, and resulting ash; and aid in the interpretation and identification of archaeological fuels.

Both of the peat ash samples from the Corrigal farmhouse museum have near neutral pH measurements 7.1 for Caithness peat and 7.3 for Orkney peat. The pH values for the Corrigal peat ash samples does fall within the range of the 200^0C and 400^0C modern analogue peat ash samples, while the pH measurements from the peat and wood ash sample from the pottery firing experiments falls within the ranges of wood fuels at 400^0C and peat fuels at 400^0C and 900^0C. The mixed fuel ash sample has pH values that fall in line with the modern analogue fuel ash from the 400^0C and 900^0C temperature intervals. Exposure to heat raised the pH of the archaeological matrix sample from acidic 5.3 to alkaline 10.7 after heating (figure 7.10).

There is a definite correlation between the additional sample material and the modern analogue ashes that corroborates the ability to identify a possible fuel type and heating temperature based on pH data. This indicates the value of the pH data for the identification of archaeological fuels when used with other analytical methods to verify the findings and strengthen the datasets.

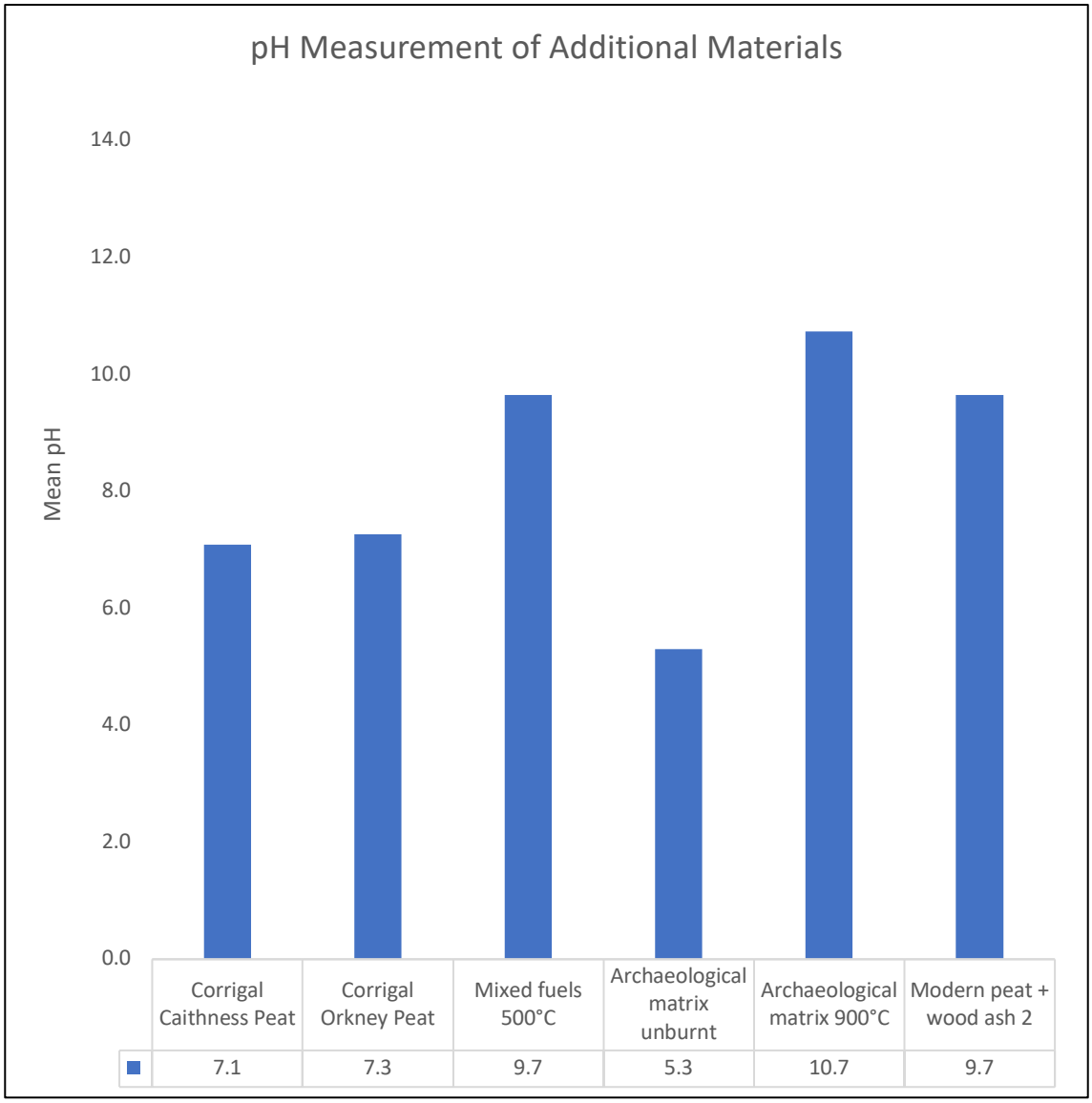

Figure 7.12 pH among additional sample materials. Samples from left to right: Caithness peat, Orkney peat, mixed fuels 500^{0}C, unburnt archaeological matrix, archaeological matrix 900^{0}C, and modern peat and wood ash Source: Author

SEM/EDX

The additional material samples follow the same trends observed per fuel type with the modern analogue material (figure 7.11). The peat samples have the highest levels of Fe and Ti, the archaeological matrix material has the highest concentration of Si, and the sample of peat and wood ash contains the most magnesium and Ca. The levels of Fe and Ti for peat and magnesium and Ca among wood fuels is consistent with the findings from the modern analogue samples (figure 7.5).

Heating does not affect the levels of Si remaining at 15.3% for both archaeological matrix samples, there is also little or no change among the concentrations of Mg, Al, P, K, and Fe (Misra *et al.* 1993). The levels of Na and Ca increase from 0.7% to 1.4% for Na and 2.5% to 6.8% for Ca after exposure to 900^0C (figure 7.11).

The additional material samples confirm that the elemental data can be used to corroborate the findings from the magnetic susceptibility and pH measurement data. The samples with the highest levels of Fe and Ti have the highest low frequency MS values, while the samples with the highest levels of magnesium and Ca have the most alkaline pH measurements.

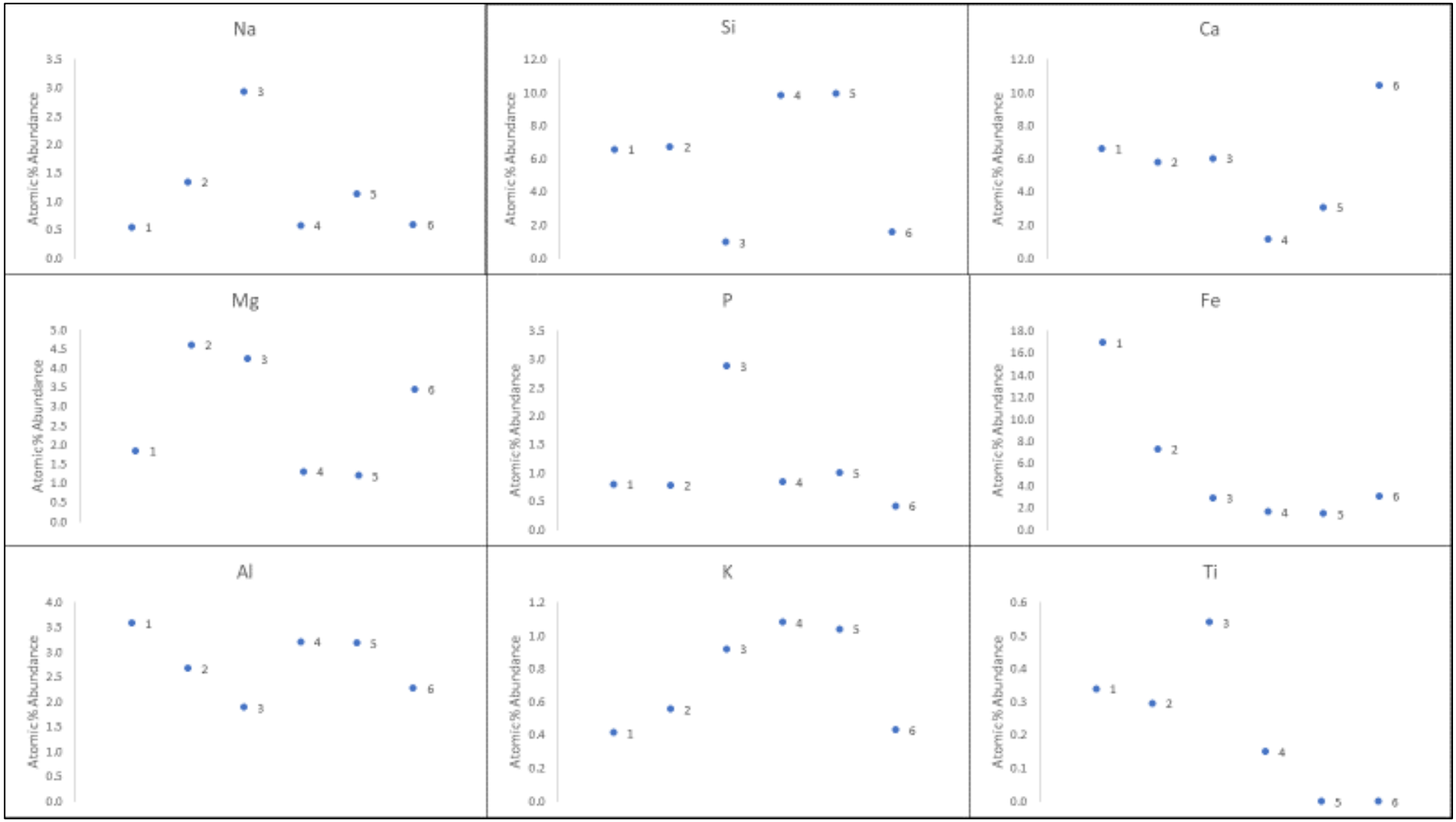

Figure 7.13 Atomic percentage abundance of elements among additional sample material. Samples from left to right: 1 Caithness peat, 2 Orkney peat, 3 mixed fuels 500^{0}C, 4 unburnt archaeological matrix, 5 archaeological matrix 900^{0}C, and 6 modern peat and wood ash Source: Author

Munsell colour assignment

The Munsell colour assignment for the additional sample material shows the colour of ashes from non-controlled combustion environments such as fire pits and hearths, archaeological matrix material, and all the modern analogue fuels mixed together and heated to 500^0C.

The additional sample material demonstrates the changes to colour that a fuel undergoes when burned in an uncontrolled combustion environment like a firepit or hearth (figure 7.12). The difference in combustion environment such as availability of oxygen, changes in wind, and contamination from soil material or preexisting ash could affect the colour of the samples. This is evident in the more vivid tones of red and yellow reached by the peat samples burnt in open settings compared to the modern analogue peats that have more subdued hues of red and yellow (figures 7.7 & 7.12). The mixed modern analogue fuels show the colour of ash from mixed fuel sources. The archaeological matrix material shows the change in colour between unheated soils and soils that have been heated either directly in a hearth surface, or indirectly near a hearth. The data provided by this sample set is a useful tool in interpretation of the analytical results and the subsequent identification of archaeological fuels, by providing examples of fuel ash that were produced in both the uncontrolled settings and with a functionality that was analogous to the archaeological ash. Providing a means to further understand the associations between combustion and ash.

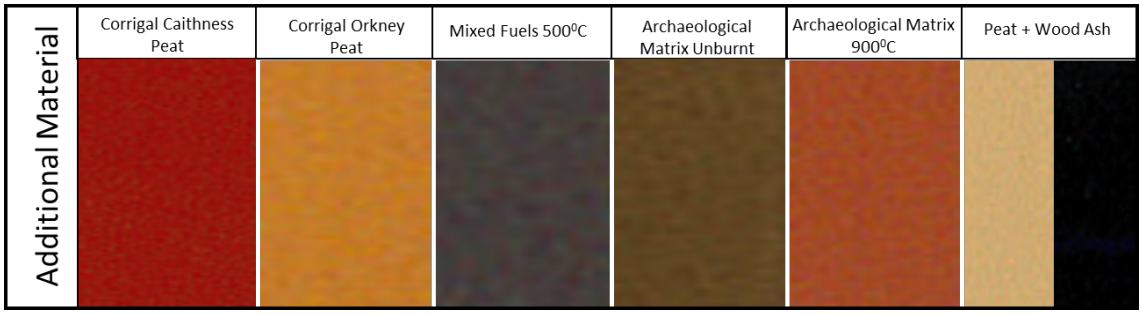

Figure 7.14 Munsell colour assignments for additional sample materials. Samples from left to right: Caithness peat, Orkney peat, mixed fuels 500^0C, unburnt archaeological matrix, archaeological matrix 900^0C, and modern peat and wood ash Source: Author

7.2.6 What was learned from the modern analogue experimentation?

The modern analogue experimentation offers a tremendous amount of data observed from heating 14 modern analogue fuels to 3 temperature intervals. Throughout the process the changes to magnetism, pH, elemental content, colour, and mass were measured and recorded. It is abundantly clear from this data that fuel undergoes changes at different temperature intervals. The changes to the characteristics of the fuel material are mostly seen as increases in the intensity of the changes relative to increase in temperature. For example, as the temperature increases the magnetic susceptibility measurements increase making the highest temperature the highest in magnetism and the unburnt material the lowest as discussed in section 7.2.1. This trend of increase in change relative to increase in temperature was observed with magnetic susceptibility, pH, and mass lost. The elemental content and colour do change with temperature as well, but not in a readily discernable pattern like that observed with the other analytical methods.

The colour change associated with heating does create a means for the identification of fuel based on the observed changes to fuel types including peat, wood, or dung (section 7.2.4), but there is not an incremental pattern that can be plotted. The elemental content of the samples is not only able to discern between fuel types based upon the quantities measured, but can also aid in the interpretation of other analytical methods as discussed in section 7.2.3.

The peat fuels all behaved in a similar way throughout heating and displayed similar results according to temperature. The low frequency MS, pH, and mass lost all increase with the increase of temperature. FDMS shows its highest values when heated to 400^0C with the values at 900^0C being lower, and the 200^0C samples the lowest (section 7.2.1). the Munsell colour assignment goes

from very dark brown at 200^{0}C, to dark brown at 400^{0}C, and finally goes to a range of yellow and red at 900^{0}C. the elemental content of peat also contains similar data between samples, the levels of Fe and Ti are both high compared to the other fuel types. The additional material samples of peat ash show similar results. Both samples have high magnetic susceptibility measurements, pH levels that are consistent with the modern analogue peat ash samples, similar levels of Fe and Ti, and red to yellow colouring.

The wood fuels also follow similar trends to each other. The magnetic susceptibility of wood fuels does increase with temperature, but not to same extent as peat or dung fuels. The pH also increases with heating temperature, and is more alkaline then the peat fuels at all temperatures. The elemental data from the wood fuels shows that the most significant trend is the lack of any particular element in high concentration. Unlike the high levels of Fe and Ti associated with wood, the high levels of P and Ca associated with bone, or the high level of Na found in seaweed, the wood fuels have no significant elemental concentration associated with them. The colour of wood fuels differs from peat but is similar to dung and grasses. The wood fuels turn dark red brown at 200^{0}C, and grey at 400^{0}C.

The dung fuels do share some similarities as a fuel type such as higher levels of P then all other samples apart from bone, high levels of Si, and high alkalinity, yet the dung fuels share more similarities with other fuel groups. The sheep dung follows similar trends to peat only on a smaller scale, while the cow dung shares many similarities to grasses. The sheep dung has the same increase in magnetic susceptibility that was seen with peat; however, the increase is on a smaller scale. The highest magnetic susceptibility value for dung is 214.8 x10^{-8}m^{3}kg^{-1} at 900^{0}C, while the average for the peat fuels is 1664.2 x10^{-8}m^{3}kg^{-1} at

900^{0}C. The colour of sheep dung is very similar to the colours of peat at 200^{0}C and 400^{0}C, the only variation is that sheep dung does not have any red or yellow hue at 900^{0}C, turning a light grey. Cow dung has a similar magnetic susceptibility to grasses. The cow dung also follows a similar trend to grasses in colour change, at 200^{0}C and 400^{0}C both fuels are grey. At 900^{0}C grasses turns light grey while cow dung turns very light grey with purple inclusions.

Seaweed has similar magnetic susceptibility and pH trends to wood fuels. The levels of Na in seaweed set it apart from other fuels elemental content. The colour trend observed in seaweed has parallels to both peat and wood fuels, sharing the grey colouring of wood ash with yellow to red inclusions that are similar in colour to peat.

Bone stands alone in all categories. It remains diamagnetic at all temperature intervals. The pH remains near neutral until heated to 900^{0}C when it becomes alkaline. Bone has the highest concentration of P and Ca. The colour changes that bone undergoes during heating are also not paralleled by any other fuels.

The data gained from the observations of the ashing experiments provide an excellent understanding of the changes that fuels undergo during the process of being converted from fuel to ash. This dataset provides the means to identify archaeological fuels based upon the various unique identifiable attributes of the fuel groups observed in the experiment.

7.3 Archaeological material

The significant findings observed during the analyses of archaeological sample materials are discussed. The interpretation of the archaeological sample data is informed by the findings and interpretations of the modern analogue fuels and additional sample material. By using what was learned from the modern analogue and additional sample material analysis, it is attempted to determine what fuels make up the archaeological samples and to what temperatures these fuels were heated to. The fuels and temperatures suggested by the individual analyses are confirmed using statistical analysis in section 7.4.

There are 43 archaeological samples; 23 from The Ness of Brodgar, 8 from the Knowe of Swandro, and 12 from Smerquoy/Muckquoy. Of the 43 samples there are 8 from ash dumps/hearth rake out, 24 midden samples, and 11 drawn from hearths. The following discusses the relationships observed amongst excavation sites, sample types, and between the modern analogue and archaeological samples.

7.3.1 Magnetic susceptibility

The archaeological samples all fall within the ranges established by the modern analogue magnetic susceptibility measurements observed between 400^0C and 900^0C (table 7.1 and figure 7.13), the lowest measurement 33.5 $x10^{-8}m^3kg^{-1}$ (RDL 001) and the highest 2666.8 $x10^{-8}m^3kg^{-1}$ (NOBT 5849) with no diamagnetic measurements among the archaeological material (figure 7.13). Each archaeological site displays its own trends with individual ranges and means (table 7.1). The Magnetic susceptibility data suggests that the Ness of Brodgar samples were exposed to higher temperatures than the Knowe of Swandro and Smerquoy/Muckquoy samples, or have a proportionally higher concentration of paramagnetic and ferrimagnetic minerals present due to the

differences in soil geology between the sites based on the mean MS and FDMS values (Fialová *et al.* 2006).

The archaeological material does have a slightly lower mean FDMS value than the modern analogue fuels, 11.9% for modern analogues and 10.8% among archaeological samples. This could be accounted for by the presence of soil material within the combustion residue, which has very high magnetic susceptibility when heated due to the presence of minerals from the soils parent material. Feand other ferromagnetic minerals increase the magnetic susceptibility of sample materials and this is exacerbated when those materials are heated because of grain refinement that take place at temperatures above 485^0C (Zang et al 2017).

MS Summary Table				
Excavation Site	**Minimum & Maximum MS**	**MS Range**	**MS Mean**	**MS Standard Deviation**
NoB 15	256.4 – 1328.4	1072.0	867.3	395.9
NoB 16	405.7 – 1415.8	1010.1	999.6	336.0
NoB T	516.3 – 2666.8	2150.5	1121.0	776.5
KoS	98.6 – 488.0	398.4	335.1	132.4
SMQ/RDL	33.5 – 1307.9	1274.4	585.9	503.3

FDMS Summary Table				
Excavation Site	**Minimum & Maximum FDMS**	**FDMS Range**	**FDMS Mean**	**FDMS Standard Deviation**
NoB 15	7.6 – 25.8	18.2	12.7	6.3
NoB 16	7.9 – 10.5	2.6	8.8	0.9
NoB T	7.0 – 9.9	2.9	9.0	1.0
KoS	4.5 – 32.1	27.6	12.0	8.4
SMQ/RDL	7.5 – 19.8	12.3	11.3	3.2

Table 7.1 Summary table of MS and FDMS of archaeological sample material organised by site. Source: Author

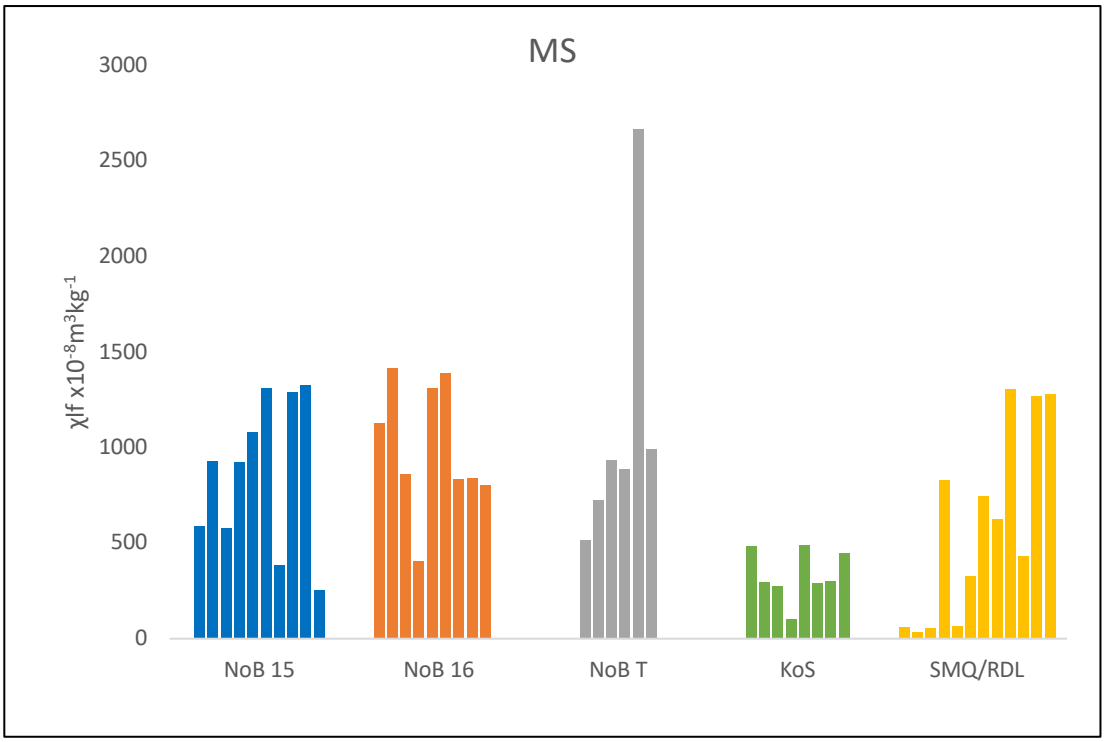

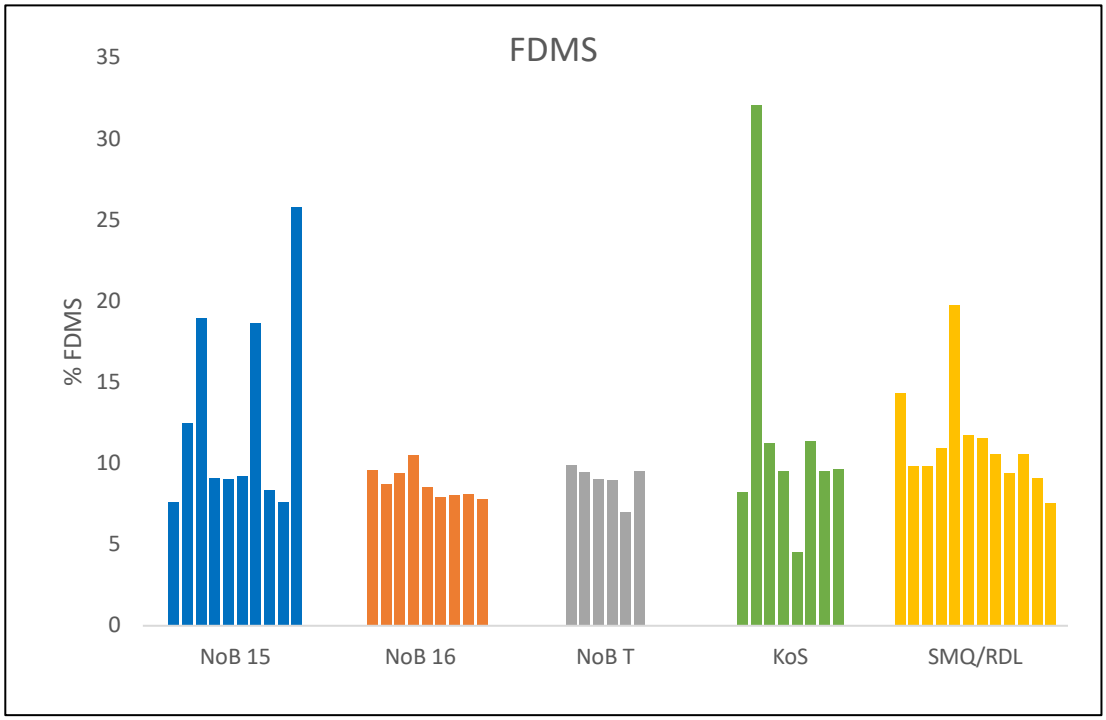

Figure 7.15 The MS and FDMS of archaeological samples organised by site and year of excavation shown with Ness of Brodgar 2015 in blue, Ness of Brodgar 2016 in orange, Ness of Brodgar trench T in grey, Knowe of Swandro in green, and Smerquoy/Muckquoy in yellow. Source: Author

The high MS measurements suggest that the fuels present among the archaeological deposits is possibly peat. The values that fall in the lower ranges of between 0-100 $x10^{-8}m^3kg^{-1}$ and 100-250 $x10^{-8}m^3kg^{-1}$ suggest the fuels present are wood or dung respectively (figure 7.14). The frequency dependence ranges suggest that the heating temperatures were in both the 400^0C range for samples with FDMS values above 15% and 900^0C for samples in the 5-15% FDMS range.

The MS data shows that there are similarities between the archaeological samples and the modern analogue fuel ashes. The Ness of Brodgar samples have magnetic susceptibility values within the range of peat fuels heated to 400^0C and 900^0C, and dung fuels heated to 900^0C. The Knowe of Swandro had the lowest range of MS this is similar to peat fuels heated to 400^0C and 900^0C. The MS from Ness of Brodgar trench T had the most variation, and is in range with peat fuels heated from 200^0C to 900^0C. Trends are also found among sample types (figure 7.14). The samples drawn from hearths had the highest mean MS at 1015.7 $x10^{-8}m^3kg^{-1}$ ash samples had the second highest average at 707.4 $x10^{-8}m^3kg^{-1}$, and the midden samples had the lowest average at 582.8 $x10^{-8}m^3kg^{-1}$ (table 7.2). It is expected that hearth surface material would be exposed to heat on a regular basis while the feature was in use, and contain the most soil material that is made up of the geological parent material, causing those samples to have the highest magnetism as discussed in sections 7.2.1 and 7.2.3.

The archaeological material ranges in FDMS from 4.5% to 32.1%, and the modern analogue material ranged between 6.1% to 25.6% at 400^0C and 4.6% to 11.6% at 900^0C (figure 7.14). The archaeological sample with the highest FDMS 32.1% is a midden sample from the infill of a smithy (KoS 3081) as

discussed in section 4.4.4. There is a large possibility that this sample could contain contamination from small amounts of hammerscale causing the increase in FDMS (the FDMS of Fe hammerscale is 30.3% (appendix 1)).

When considering the data by sample type it shows hearth samples have the lowest mean FDMS at 8.6%, followed by the midden samples at 11.3%, and the ash samples have the highest FDMS at 14.4% (table 7.2). Again, as discussed in sections 7.2.1 and 7.2.3, the sustained exposure to heating that the hearth material went through caused the alteration of the mineral grains resulting in the lowest values of frequency dependence among the archaeological material.

MS Summary Table				
Sample Type	**Minimum & Maximum MS**	**MS Range**	**MS Mean**	**MS Standard Deviation**
Hearth	405.7 – 1392.1	986.4	1015.7	334.0
Ash Dump/Hearth Rake Out	256.4 – 1289.7	1033.3	707.4	359.5
Midden	33.5 – 2666.8	2633.3	582.8	571.6

FDMS Summary Table				
Sample Type	**Minimum & Maximum FDMS**	**FDMS Range**	**FDMS Mean**	**FDMS Standard Deviation**
Hearth	7.5 – 10.5	3.0	8.6	0.8
Ash Dump/Hearth Rake Out	7.6 – 25.8	18.2	14.4	6.9
Midden	4.5 – 32.1	27.6	11.3	5.3

Table 7.2 Summary table of MS and FDMS of archaeological sample material organised by sample type. Source: Author

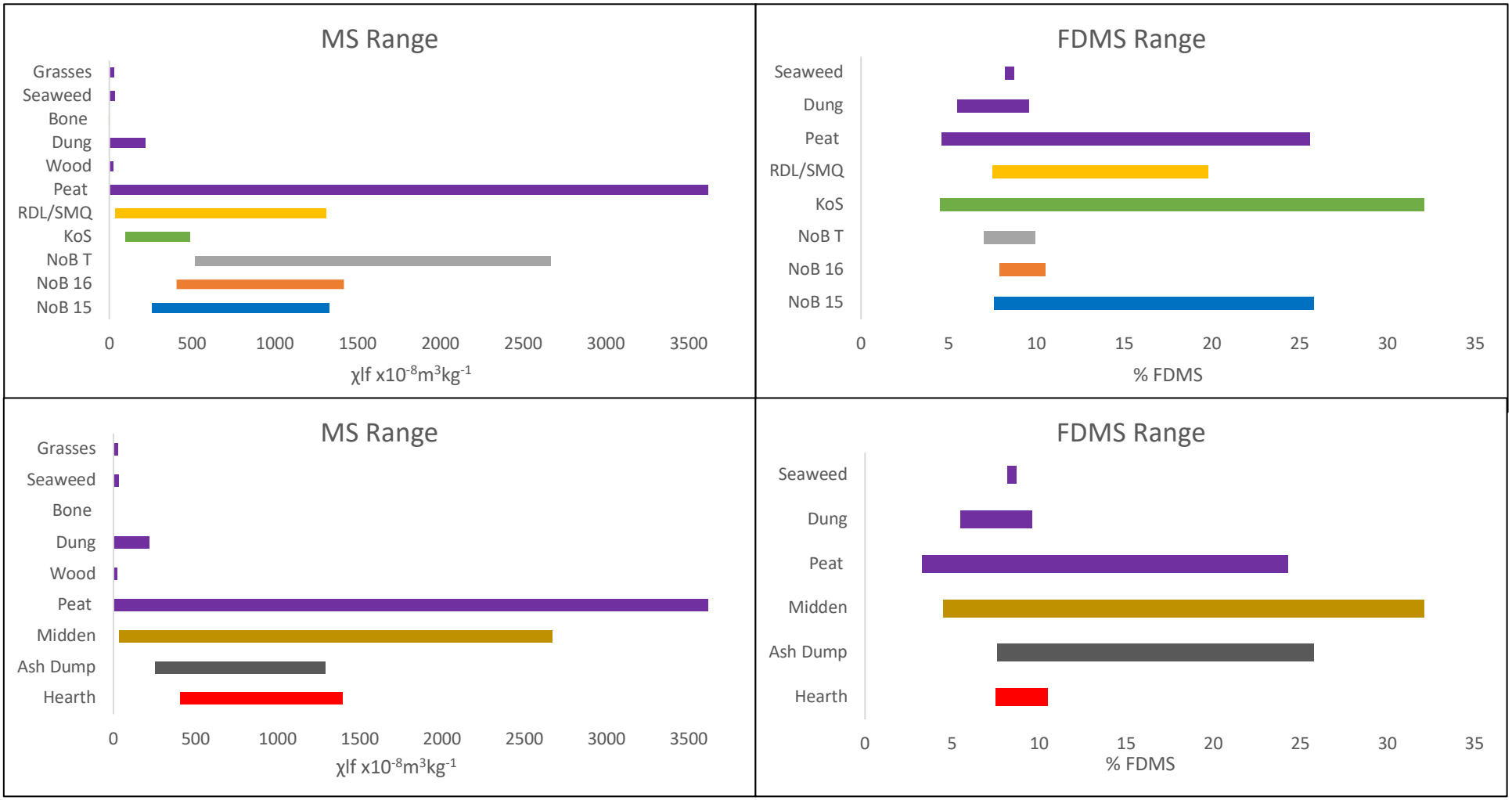

Figure 7.16 The MS and FDMS range of archaeological samples organised by site shown with Ness of Brodgar 2015 in blue, Ness of Brodgar 2016 in orange, Ness of Brodgar trench T in grey, Knowe of Swandro in green, and Smerquoy/Muckquoy in yellow and by sample type shown with hearth samples in red, ash dump and hearth rake out samples in dark grey, and midden samples in brown compared with modern analogues organised by fuel type shown in purple. Source: Author

7.3.2 pH readings

The pH measurements among the archaeological material were all near neutral with some slightly acidic or alkaline, and never more than 1.8 away from neutral (table 7.3). the highest archaeological sample pH was 8.1 and the lowest was 5.2 (figure 7.15). This is possibly due to the mixing of alkaline fuel ash with acidic soil material causing a measurement to be near neutral. The chemical reactions that effect pH are not linear and are complex, but this does offer an explanation for what is happening when the ash is deposited into the archaeological matrix. The burial environment of the sample heavily influences the overall pH of the archaeological matrix, with the inclusions of ash and other midden materials influencing the pH of their immediate surroundings within the burial environment, as seen with using ash in agricultural application to neutralize or raise acidic soils (Demeyer *et al.* 2001).

The pH of the archaeological sample suggests that the fuels in use were peat or wood ashes at 200^0C for archaeological material with a pH between 5 and 7, peat or wood ashes at 400^0C for samples with measurements between 7 and 8, and peat at 400^0 for the samples that measured between 8 and 9.

pH Summary Table				
Excavation Site	**Minimum & Maximum pH**	**pH Range**	**Mean pH**	**Standard Deviation**
NoB 15	6.5 – 7.2	0.7	6.9	0.2
NoB 16	6.2 – 7.1	0.9	6.6	0.3
NoB T	5.2 – 6.3	1.1	5.9	0.4
KoS	7.4 – 8.1	0.7	7.9	0.2
SMQ/RDL	5.9 – 6.5	0.6	6.2	0.2
Sample Type	**Minimum & Maximum pH**	**pH Range**	**Mean pH**	**Standard Deviation**
Hearth	6.2 – 7.9	1.7	6.7	0.5
Ash Dump/Hearth Rake Out	6.7 – 7.2	0.5	7.0	0.2
Midden	5.2 – 8.1	2.9	6.6	0.9

Table 7.3 Summary table of pH of archaeological sample material organised by site and by sample type. Source: Author

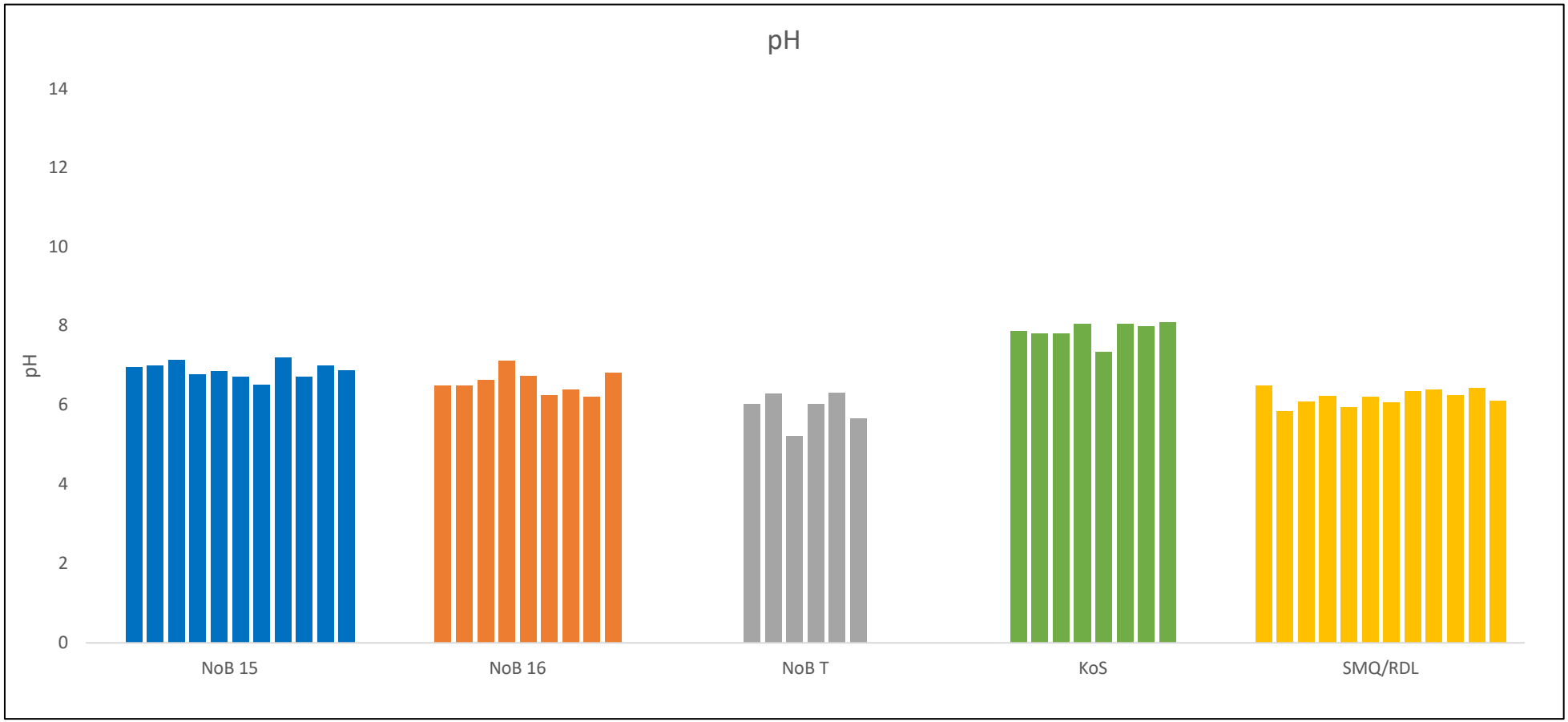

Figure 7.17 Mean pH measurement among archaeological samples organised by site and year of excavation shown with Ness of Brodgar 2015 in blue, Ness of Brodgar 2016 in orange, Ness of Brodgar trench T in grey, Knowe of Swandro in green, and Smerquoy/Muckquoy in yellow. Source: Author

When compared to the modern analogues, the pH ranges from each site fall within the established ranges of different fuel groups and functional temperatures. The samples from The Ness of Brodgar are all in the same pH range (5.2-7.2) this falls within the ranges established by the modern analogue peat fuels heated to 200^{0}C (4.3-7.2). The Knowe of Swandro has pH measurements ranging from 7.4 to 8.1, this is similar to the modern analogue peat fuels heated to 400^{0}C (7.4 to 8.9). The samples from Smerquoy/Muckquoy have a pH range of 5.9 to 6.5 that is similar to wood fuels heated to 200^{0}C (5.2 to 6.8). There is no significant trend among the pH measurements when considering the data by sample type.

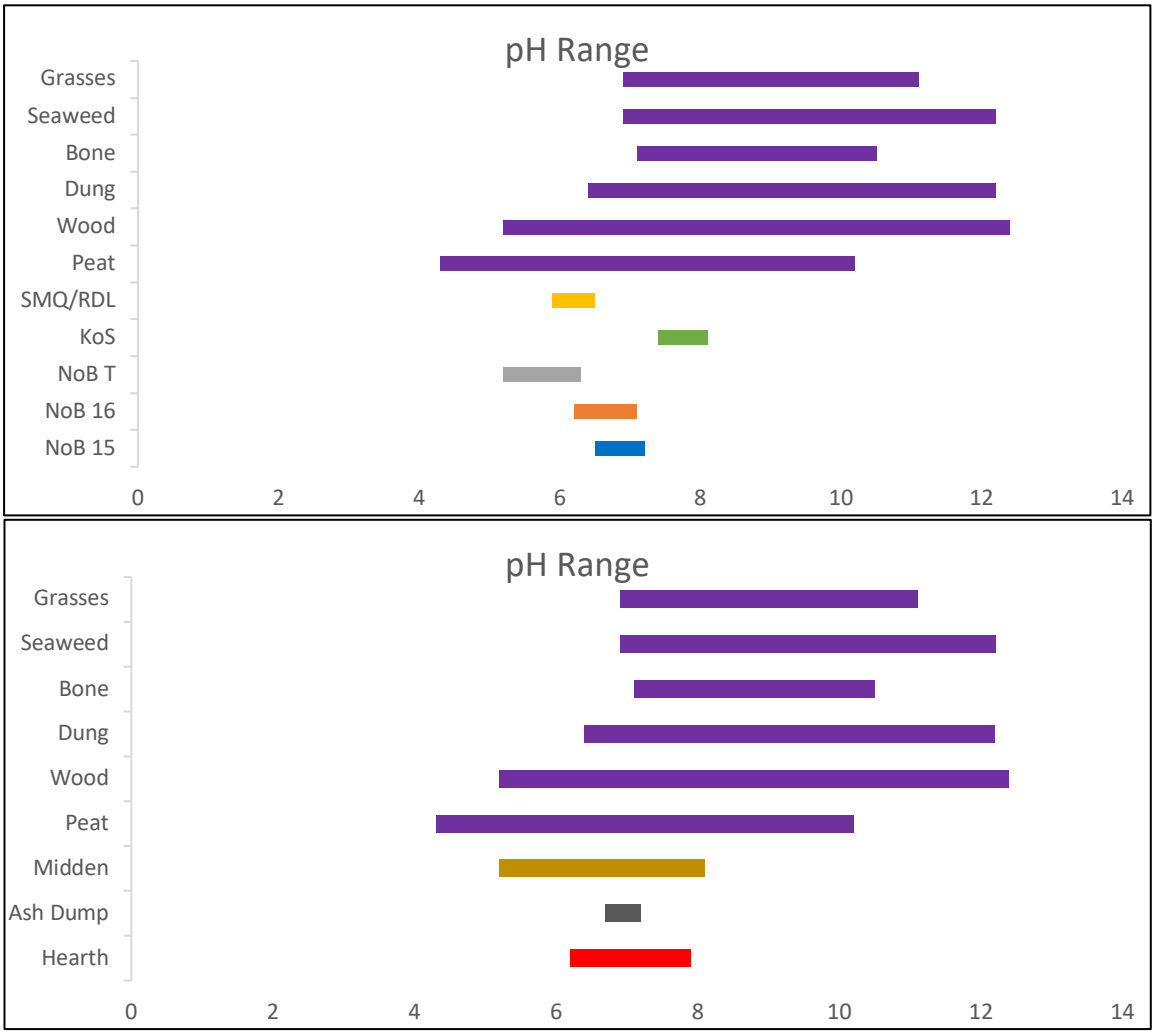

Figure 7.18 The pH range of archaeological samples organised by site shown with Ness of Brodgar 2015 in blue, Ness of Brodgar 2016 in orange, Ness of Brodgar trench T in grey, Knowe of Swandro in green, and Smerquoy/Muckquoy in yellow and by sample type shown with hearth samples in red, ash dump and hearth rake out samples in dark grey, and midden samples in brown compared with modern analogues organised by fuel type shown in purple. Source: Author

7.3.3 Scanning electron microscopy and energy dispersive X-ray spectroscopy

The following discusses the significant observations for the analyses of archaeological sample material and the associations with modern analogue fuel material for each of the nine elements being considered from the SEM/EDX data Na, Mg,, Al, Si, P, K, Ca, Fe, and Ti (The elements being considered for this research were predetermined and explained within sections). The archaeological material presents not only the constituents of fuel within the deposit, but all the inclusions that make up the archaeological matrix (figure 7.17). The elements present in soil, midden deposit, other combustion events, and fuel material are all combined within the archaeological sample material as discussed in section 3.2.

The archaeological material does differ slightly to the modern analogue fuel material which was expected as mentioned in section 7.1.3. It was anticipated that the modern analogue fuel material would have a lower mean concentration of Al, Ti, and Fe due to the differences in the minerals mobility in soils and plants. The archaeological samples have a mean percentage weight abundance of 6.6% ±1.4 Al, 5.4% ±2.0 Fe and 0.59% ±0.2 Ti, and the modern analogue fuel samples have a mean weight percentage of 2.5% ±2.6 Al, 2.7% ±2.9 iron, and 0.3% ±0.1 Ti.

Magnesium was observed at higher abundance among modern analogue fuel materials than in archaeological sample material which was expected due to the difference in the function of magnesium in plants and soil, as well as the mobility of magnesium within acidic soils. The mean percentage abundance of magnesium in archaeological sample material was 0.88% compared to 4.4% abundance among the modern analogue fuel materials.

Only one of the archaeological samples contains S, RDL15-032 0.2% S. This is probably due to the extreme mobility of S within soils causing fluctuations on a seasonal, and sometimes daily, basis dependent upon changes in environmental factors. The modern analogue fuel material contains plant material that would have absorbed and retained S over time, leading to the variation among the two sample types (Brady & Weil 2000).

The only significant difference when comparing the archaeological material by site is that the samples from Smerquoy/Muckquoy contain almost no Ca. Of the 12 samples from Smerquoy/Muckquoy only two (RDL 007 and RDL 023) contain Ca in 0.2% abundance or less (figure 7.17). In contrast, the samples from The Ness of Brodgar and The Knowe of Swandro combined only have one sample that has no detectable quantity of Ca (NoB15 3857).

The SEM/EDX data suggests that peat was the predominant fuel in use among the samples based on the similar elemental levels in Fe and Ti, along with low levels of magnesium and Ca which were markers for wood fuels in high concentrations. The SEM/EDX data does not offer aid in determining functional temperature; however, it does lend itself to corroborate the findings from the magnetic susceptibility and pH analysis.

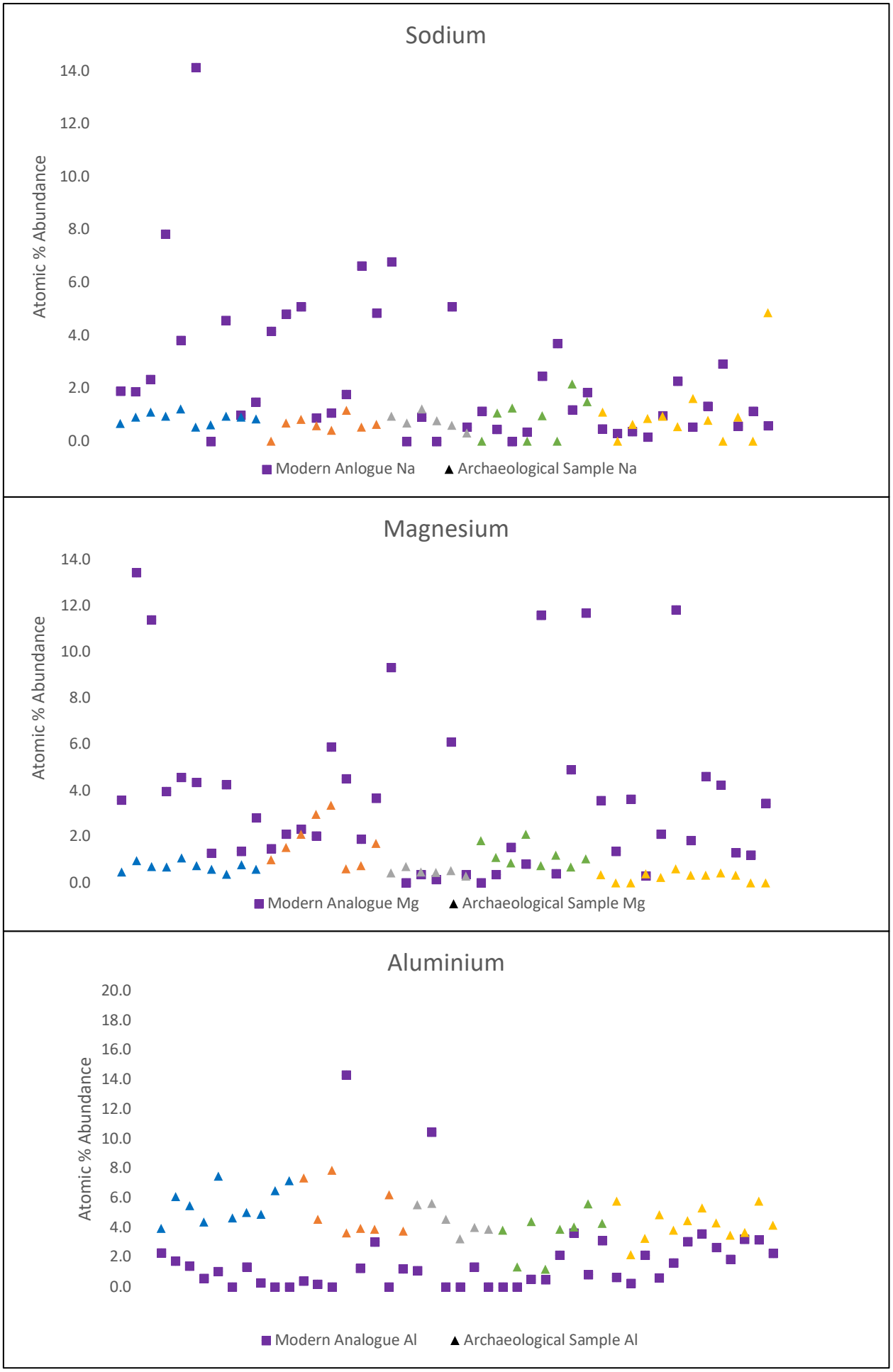

Figure 7.19 The atomic percentage abundance values for selected elements among archaeological sample material organized by site and year of excavation shown with Ness of Brodgar 2015 in blue, Ness of Brodgar 2016 in orange, Ness of Brodgar trench T in grey, Knowe of Swandro in green, Smerquoy/Muckquoy in yellow, and modern analogues organised by fuel type shown in purple. Source: Author

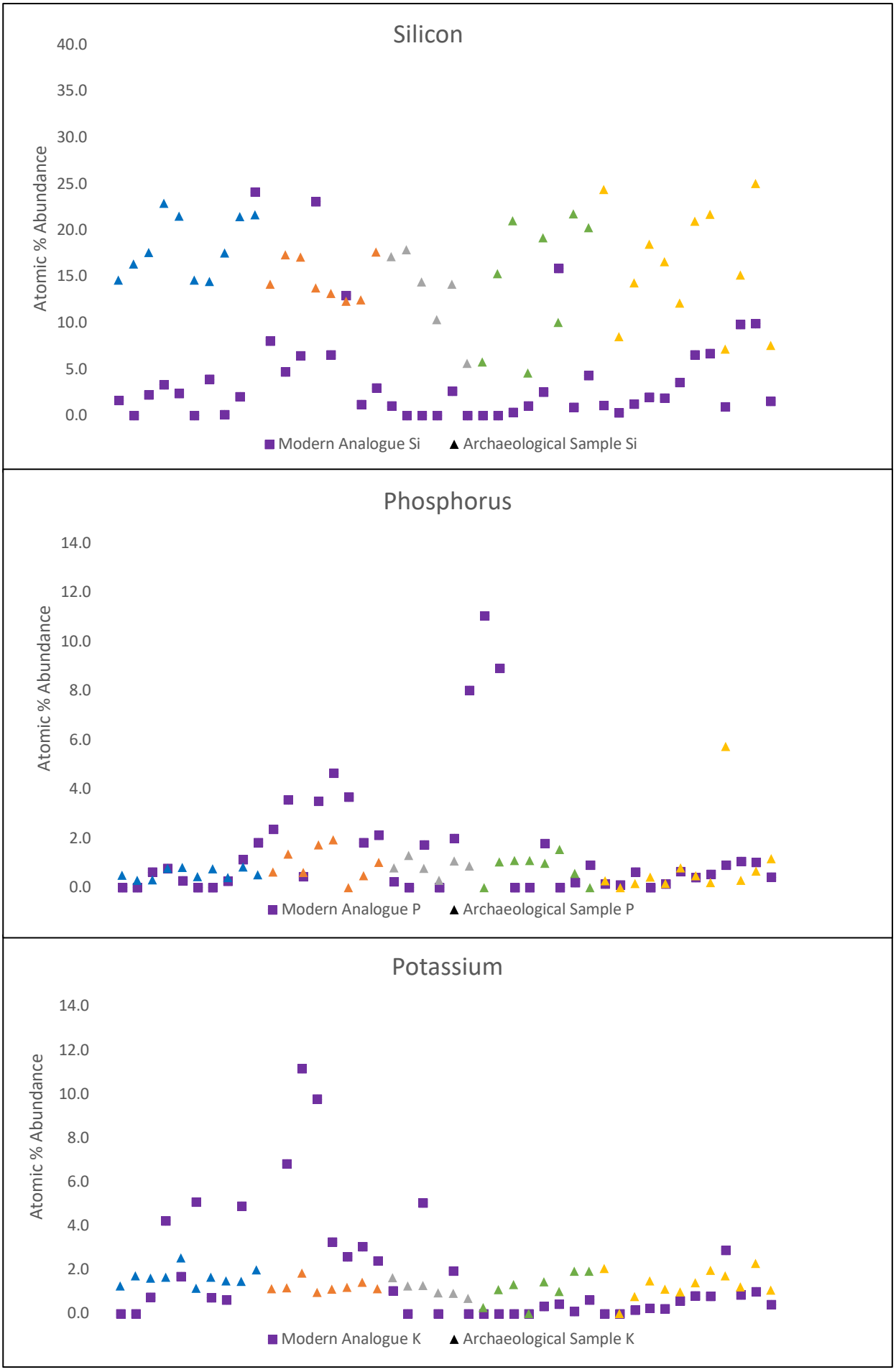

Figure 7.20 The atomic percentage abundance values for selected elements among archaeological sample material organized by site and year of excavation shown with Ness of Brodgar 2015 in blue, Ness of Brodgar 2016 in orange, Ness of Brodgar trench T in grey, Knowe of Swandro in green, Smerquoy/Muckquoy in yellow, and modern analogues organised by fuel type shown in purple. Source: Author

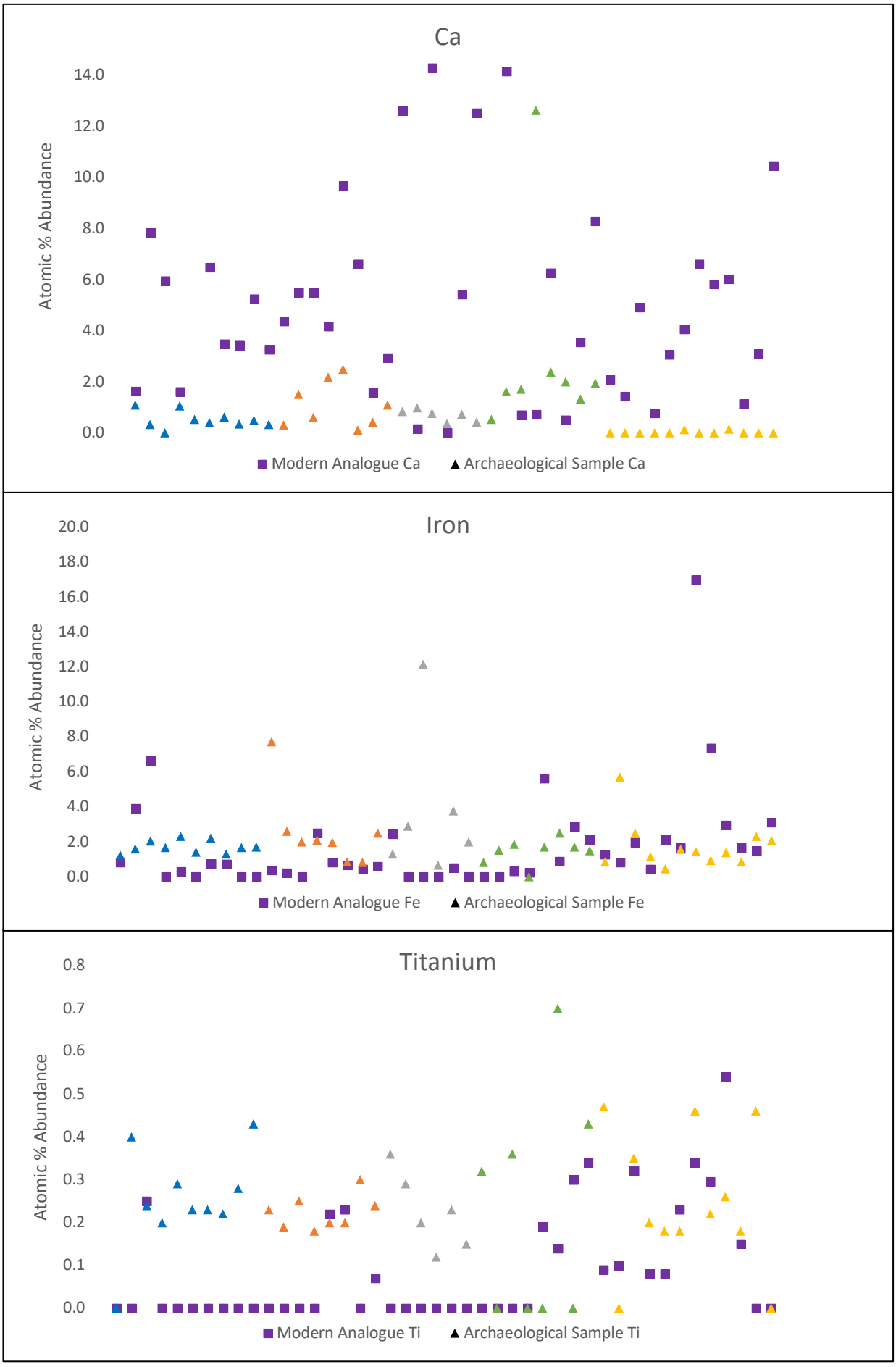

Figure 7.21 The atomic percentage abundance values for selected elements among archaeological sample material organized by site and year of excavation shown with Ness of Brodgar 2015 in blue, Ness of Brodgar 2016 in orange, Ness of Brodgar trench T in grey, Knowe of Swandro in green, Smerquoy/Muckquoy in yellow, and modern analogues organised by fuel type shown in purple. Source: Author

The most noticeable difference between the modern analogue material and the archaeological samples elemental content is the higher levels of Si, Al, and Fewhich are known to be ubiquitous in soil matrices as discussed in section 3.4 (Pierce *et al.* 1998). The additional material sample of archaeological matrix shows that the abundance of Mg, Al, Si, P, and Feare not affected by heating up to 900^0C as shown in section 7.2.5.

Given that the modern analogue SEM/EDX results presented no visible pattern associated to heating, only the fuel type can be identified using this analytical technique; however, the elemental content can aid in the understanding of both the magnetic susceptibility and pH data as discussed in sections 3.3 and 7.2.3. The archaeological material all shares similarities with peat fuels except for four samples (NoB15 3783, KoS 3081, KoS 3196, and KoS 3217) that were similar to both sheep dung and peat. When reviewing the data by sample type, the average levels of Na and Ti are the same among hearth, ash, and midden material (figure 7.18). Ash samples have the highest average level of Al, Si, K, and iron. Hearth samples have the highest average abundance of Mg, and P. Midden materials have the highest levels of Ca.

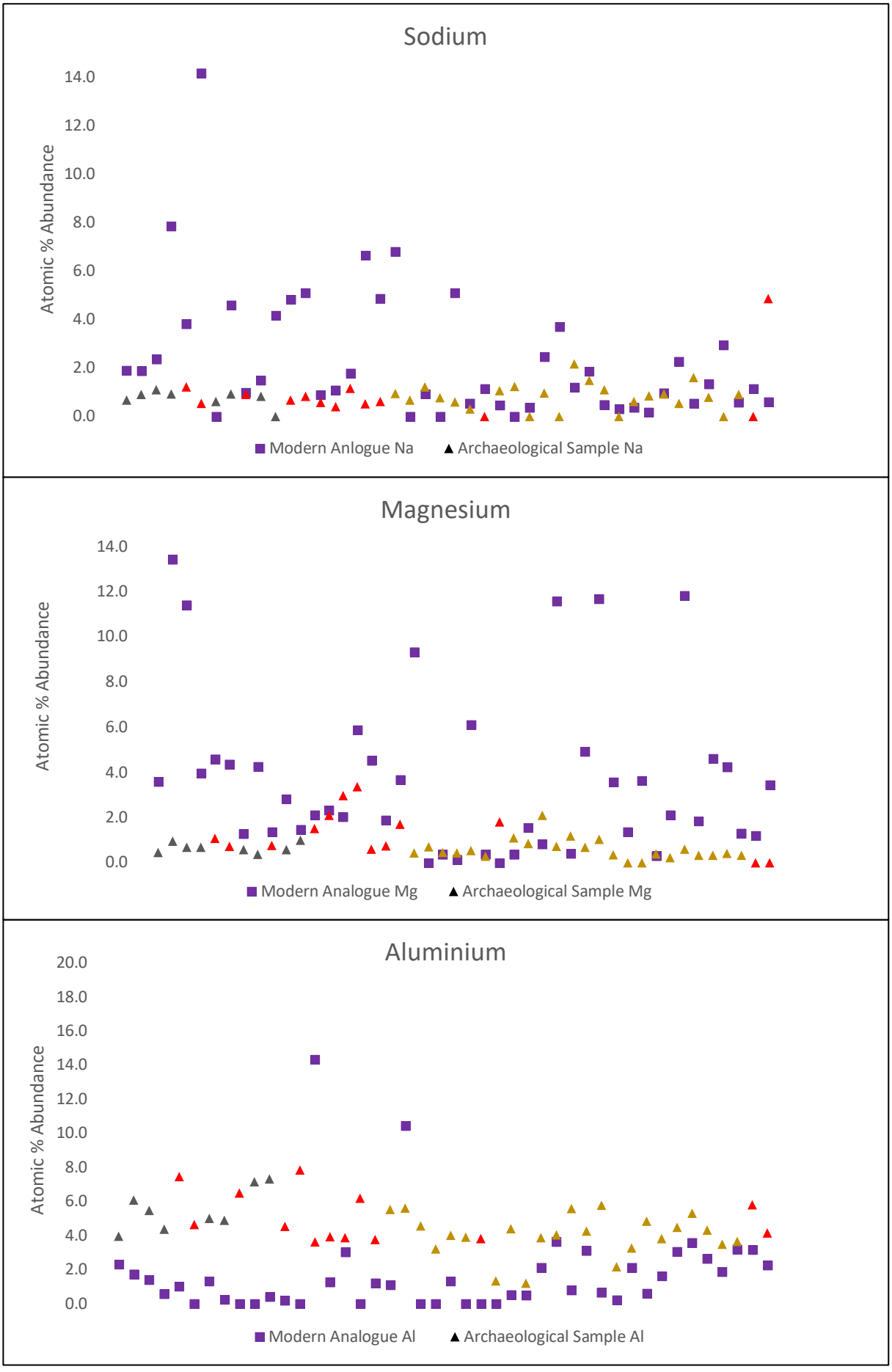

Figure 7.22 The atomic percentage abundance values for selected elements among archaeological sample material organized by sample type shown with hearth samples in red, ash dump and hearth rake out samples in dark grey, and midden samples in brown compared with modern analogues organised by fuel type shown in purple. Source: Author

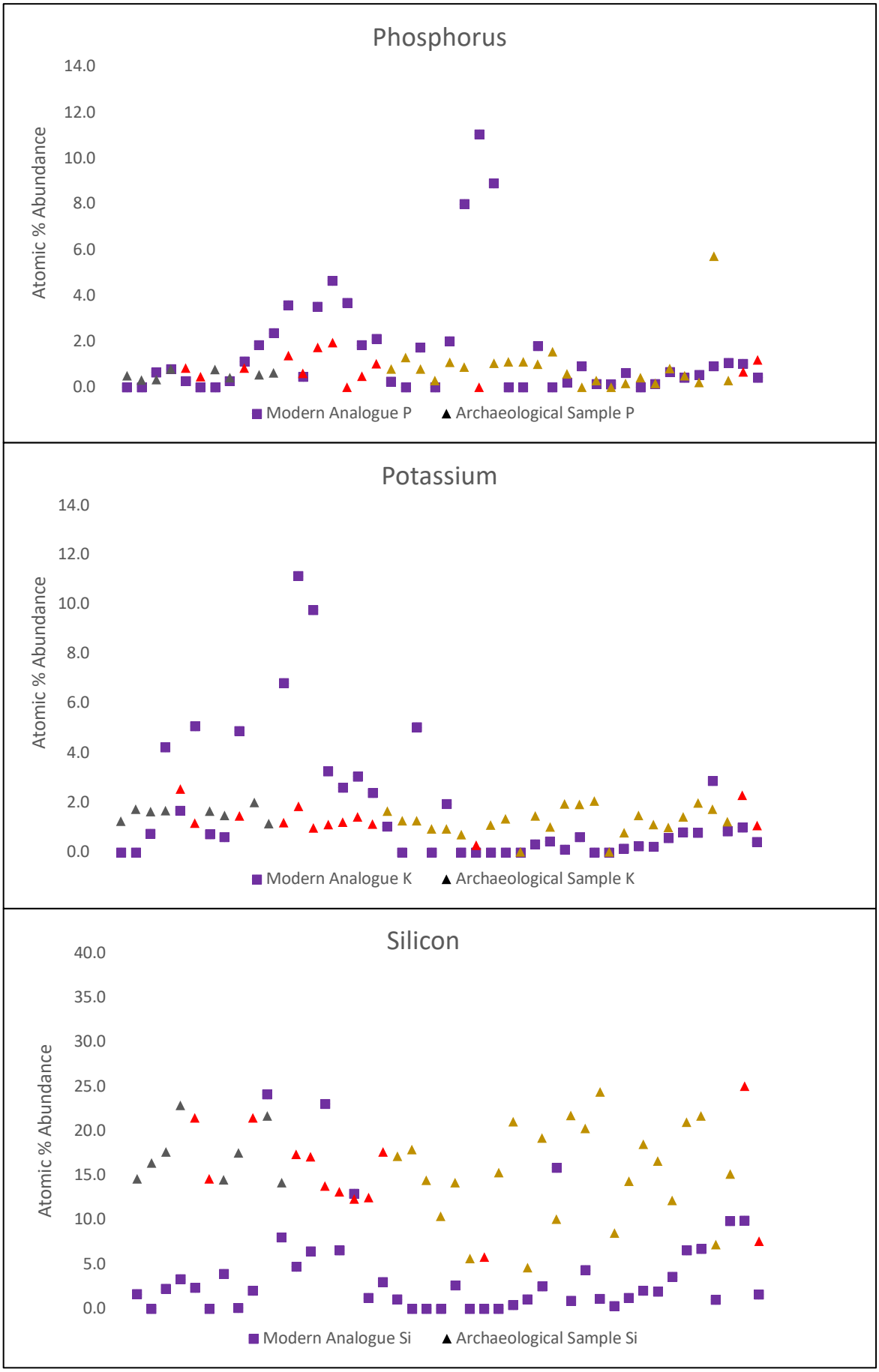

Figure 7.23 The atomic percentage abundance values for selected elements among archaeological sample material organized by sample type shown with hearth samples in red, ash dump and hearth rake out samples in dark grey, and midden samples in brown compared with modern analogues organised by fuel type shown in purple. Source: Author

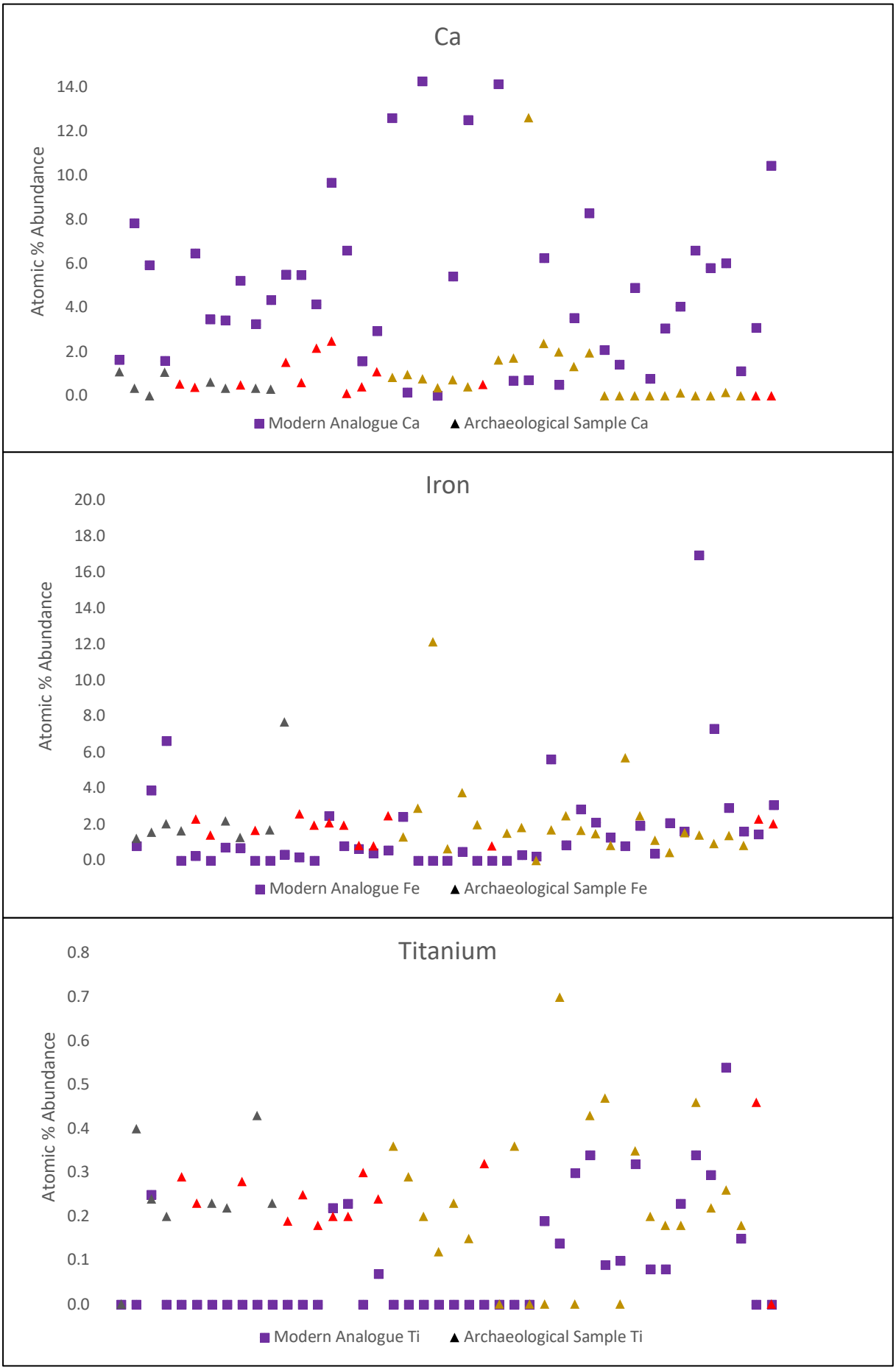

Figure 7.24 The atomic percentage abundance values for selected elements among archaeological sample material organized by sample type shown with hearth samples in red, ash dump and hearth rake out samples in dark grey, and midden samples in brown compared with modern analogues organised by fuel type shown in purple. Source: Author

7.3.4 Munsell colour assignment

The archaeological sample Munsell colour data provides information on both the fuel types in use and the functional temperatures based on the interpretations of the modern analogue and additional sample materials. The dark browns suggest peat heated to approximately 200^0C to 400^0C (figure 7.16 & 7.17). The dark reddish brown suggests wood or dung fuels heated to 200^0C to 400^0C (figure 7.16 & 7.17). The hues of red and yellow suggest peat fuels heat to 900^0C. The extreme redness of some of the samples is indicative of hearth material that contain heated matrix from the combustion feature in addition to fuel residue, as observed with the additional sample material archaeological matrix. The unheated sample is light brown and after being exposed to 900^0C for 6hrs, the sample was a bright orange red. The lighter brown could be due to mixing with matrix material causing the colour to lighten. In addition, the observation of colour is subjective and the colours are a suggestion based on the similarity observed between the colouring of two samples.

The samples from The Ness of Brodgar range in colour from brown, dark brown, red, red brown, dark red brown, and yellow brown. These samples share similarities in colour with all temperature peat ashes, wood 200^0C, bone 400^0C, and seaweed 900^0C. The Knowe of Swandro samples have less colour variation ranging from brown, orange, and yellow brown and share similarities with peat heated to 400^0C and 900^0C and sheep dung. Of all the sites, the Smerquoy/Muckquoy samples have the most colour variation including grey, brown, dark brown, red brown, yellow brown, and dark red brown. The Smerquoy/Muckquoy samples are similar in colour to peat heated to 400^0C and 900^0C and wood fuels heated to 200^0C and 400^0C.

Figure 7.25 The Munsell colour assignment data among archaeological sample material organized by site and year of excavation. Source: Author

Figure 7.26 The Munsell colour assignment data among archaeological sample material organized by site and year of excavation. Source: Author

7.4 Identifying fuels

Using the ashes produced in controlled settings allowed for the changes to the magnetism, pH, elemental content, and colour of fuel material to be tracked through increasing intervals of heating temperature. Understanding the changes that fuels go through during the heating process, as observed in the experiments, makes it possible to attempt to identify fuel type and functional temperature of archaeological samples. Through comparison of the results, matches in trends between five variables (MS and FDMS, pH, SEM/EDX, and Munsell colour assignment) can be assessed to identify matches between modern analogue fuels and archaeological samples. The identification of archaeological fuels based upon the comparison to modern analogue fuels are tested using principal components analysis. The statistical analysis method provides a means of testing the identification of fuels based not only upon review of the data using comparison.

The following discusses the identification of fuels based on comparison, and then the identification of fuels using principal components analysis. The comparison utilizes all datasets from the analyses. Due to the inability to calculate FDMS values for certain samples and the inability to plot Munsell colour assignment, the final principal component analysis did not use this data; however, there were attempts made to use this data in the analysis (appendix 4). Finally, the findings from both means of fuel identification and their implications are discussed.

7.4.1 Identifying fuel from within archaeological deposits using comparison

As shown in section 7.3.5, the archaeological samples share similarities with the modern analogue fuels when considered by excavation site and sample type. The following discusses the relationships between modern analogue fuels and individual archaeological samples in more detail. The trends between sites suggest differences in the type of fuel used as well as the functional temperature for each archaeological site. The trends among sample types show the potential differences between modern and archaeological ash caused by both the burning and post depositional environments.

Fires in open settings utilise multiple fuels (tinder, kindling, and bulk fuel) for different stages of building a fire as discussed in section 2.4. The ash from the fire is eventually discarded in a midden where other ashes can be present as well as soil material (Miller at al. 2009). This creates the need to consider the additional material within midden deposits in addition to the soil matrix, and the potential for multiple fuel sources to be present within a sample. Hearth samples may also have mixed fuels as well as the incorporation of heat exposed soil material and previous ash within the sample material for each hearth layer/burnt horizon.

As shown by the experiments, fuels used for tinder and kindling such as grasses, and wood are almost completely burned away at temperatures above 400^0C for 6 hours (sections 6.2.1 and 7.2.4). In fires that burned for any length of time this would leave only negligible amounts of any material other than the bulk fuel used as discussed in section 2.4. Within Neolithic Orkney, hearths would have been a central feature to the changing populations and developing crafts, and in turn almost constantly in use (Richards 1998). This would mean that the fires would be burning bulk fuels instead of kindling or tinder, and the

accumulations of these ashes over time would end up in ash dumps and middens. the variations between archaeological and modern analogue samples are most likely due to fluctuations in the heating temperature from within the archaeological combustion feature caused by changes in humidity and wind along with inclusions from the post-depositional environment. Factors such as soil geology, bioturbation, flooding, and leaching of elements can all effect the archaeological ash material over time.

It is reasonable to expect contamination of the archaeological samples. Contamination, in this case meaning anything that is not ash material from a single bulk fuel material, can come from the soil matrix, midden material, and ashes or residues from other burning events. The higher concentration of mineral content within the soil matrix likely causes the archaeological sample material to have slightly higher magnetic susceptibility measurements than the modern analogue fuel material that was ashed in a controlled setting (sections 7.2.1&7.3.1). This is shown in the data with the archaeological samples having higher concentrations of magnetic minerals such as iron, Ti, and Al (sections 7.2.3 & 7.3.3). The pH of the archaeological samples is predominantly near neutral measurements contrasted by the alkaline modern analogue ash samples, this can be explained by the chemical reaction of the alkaline fuel ash being incorporated into the acidic soil matrix creating reactions in the material and causing the changes in the pH of the archaeological sample material (sections 7.2.2&7.3.2). The analytical data shows that the modern analogue samples have higher concentrations of K, Ca, and magnesium which also causes higher pH measurements (sections 7.2.3 & 7.3.3). The variations in elemental content between archaeological samples and modern analogue fuel material are caused by the contamination of the archaeological ash samples

from many factors; soil matrix leaching elements away and introducing others, as well as separate ash dumping events causing contamination of the archaeological samples (Akar *et al.* 2012). This also includes the differences in how elements interact within plants versus soil matrices as shown in the abundances of magnesium among modern analogues, and Al, iron, and Ti among archaeological sample material sections 7.2.3 and 7.3.3. The colour variation between the modern and archaeological samples maybe caused by the differences between the levels of available oxygen between the muffle furnace used in the lab and the open fires in which the archaeological ash was produced. The greater availability of oxygen in open fires causes the oxidation of minerals to occur at a more rapid rate resulting in the more pronounced red and yellow colouring among archaeological samples. This is evident with the difference in colour between the modern analogue and the additional material samples of peat fuel ashes shown in sections 7.2.4 and 7.2.5.

The use of multiple samples of similar fuel materials allowed the investigation of fuel types reacting to heat instead of just individual fuels. The fuel types all displayed different ranges for each of the analytical methods as discussed throughout section 7.2. Matches can be assigned with consideration to the changes fuels undergo at different heating temperatures as an explanation for the variations between the modern and archaeological fuels. By assigning the match that is most appropriate for each analytical method it is possible to discern the most likely fuel type and heating temperature that was in use. Between each analytical method the match may vary by temperature but a clear relationship between modern analogue and archaeological sample is established. Due to the results of the modern analogue analysis showing the relationship between FDMS and heating temperature, the temperature match

from that method is given the most weight. The following table shows the matches of fuel type and temperature for each archaeological sample by analytical method and overall best match based on the comparison of the data used for visually identifying the closest matches (table 7.4).

The most predominant match to the archaeological sample material is peat at 900^0C. Of the 43 samples, 27 match peats at 900^0C, 11 match peats at 400^0C, 2 match peat and sheep dung at 900^0C, 2 match peat and sheep dung at 400^0C, and one sample had no definitive fuel match but was likely heated to 900^0C (table 7.4). As no ash heated to 600^0C was used for this research, the 900^0C matches are also representative of fuels heated above 400^0C. As mentioned by Appleby (2008) and Jones and Brown (2000), the material from Neolithic deposits was likely not heated to more than 920^0C given the lack of bellows to augment temperature that would have been in use during the Pictish period. But fires fuelled with peat and mixed fuels used in Applebys experiments reached temperatures above 800^0C with no bellows (Appleby 2008). In addition, the poorly fired pots that would have been refired during cooking would have been exposed to a maximum of 400^0C during cooking as discussed in section 5.2, making the 600^0C temperature interval moot when considering functional fuel use. The lack of modern analogue material heated to a temperature between 400^0C and 900^0C, created a slight gap in the dataset; however, matching is still possible taking into account the lack of functional use of heating temperatures between 400^0C and 900^0C.

Using this method, it is possible to suggest what fuels and functional temperatures were in use to create the archaeological sample; however, with the potential for contamination there is margin for error. That is why it is necessary to use the findings from all the analytical methods and determine the

closest match by identifying the modal fuel type and functional temperature. The ranges established per fuel type in section 7.2.6 allowed the fluctuations among fuel types to be identified. The ranges are then used as a guideline to determine the closest matches. The variations from contamination among archaeological samples can be accounted for in the slight variations of matching among analytical results in table 7.4, for example, the higher MS, lower pH, and colour variation among the archaeological sample material. Taking all of the data into account, considering changes caused by temperature, and being aware of potential contamination it is possible to attempt to identify archaeological fuels using comparison to modern analogues.

Modern Analogue Fuel Matches to Archaeological Samples by Comparison						
Sample	***χlf***	**%χfd**	**pH**	**SEM/EDX**	**Munsell Colour**	**Match**
NoB 2617	Peat 400^{0}C to 900^{0}C	900^{0}C	Peat 200^{0}C	Peat	Peat 200^{0}C to 900^0	Peat 900^{0}C
NoB 3851	Peat 900^{0}C	400^{0}C	Peat 200^{0}C	Peat	Peat 900^{0}C	Peat 400^{0}C
NoB 3857	Peat 400^{0}C to 900^{0}C	400^{0}C	Peat 200^{0}C	Peat	Peat 900^{0}C	Peat 400^{0}C
NoB 4264	Peat 900^{0}C	900^{0}C	Peat 200^{0}C	Peat	Peat 900^{0}C	Peat 900^{0}C
NoB 4656	Peat 900^{0}C	900^{0}C	Peat 200^{0}C	Peat	Peat, Seaweed 900^{0}C	Peat 900^{0}C
NoB 4674	Peat 900^{0}C	900^{0}C	Peat 200^{0}C	Peat	Peat 400^{0}C to 900^{0}C	Peat 900^{0}C
NoB 5332	Peat 400^{0}C to 900^{0}C	400^{0}C	Peat 400^{0}C	Peat	Peat 900^{0}C	Peat 400^{0}C
NoB 6156	Peat 900^{0}C	900^{0}C	Peat 200^{0}C	Peat	Peat 900^{0}C, Bone 400^{0}C	Peat 900^{0}C
NoB 5013	Peat 900^{0}C	900^{0}C	Peat 200^{0}C	Peat	Peat 900^{0}C	Peat 900^{0}C
NoB 3783	Peat 400^{0}C Sheep dung 400^{0}C	400^{0}C	Peat, Sheep dung 200^{0}C	Peat, Sheep dung	Peat, Dung 400^{0}C	Peat & Sheep dung 400^{0}C
NoB16 3851	Peat 900^{0}C	400^{0}C	Peat 200^{0}C	Peat	Peat 900^{0}C	Peat 400^{0}C
NoB16 6339	Peat 900^{0}C	900^{0}C	Peat 200^{0}C	Peat	Peat 400^{0}C, Wood 200^{0}C	Peat 900^{0}C
NoB16 6346	Peat 400^{0}C to 900^{0}C	900^{0}C	Peat 400^{0}C	Peat	Peat 400^{0}C	Peat 900^{0}C
NoB16 6348	Peat 900^{0}C	900^{0}C	Peat 200^{0}C	Peat	Peat 400^{0}C to 900^{0}C	Peat 900^{0}C
NoB16 6351	Peat 900^{0}C	900^{0}C	Peat 200^{0}C	Peat	Peat 900^{0}C	Peat 900^{0}C
NoB16 6354	Peat 900^{0}C	900^{0}C	Peat 200^{0}C	Peat	Peat 400^{0}C	Peat 900^{0}C
NoB16 6355	Peat 900^{0}C	900^{0}C	Peat 200^{0}C	Peat	Peat 400^{0}C	Peat 900^{0}C
NoB16 6356	Peat 400^{0}C to 900^{0}C	900^{0}C	Peat 200^{0}C	Peat	Wood 200^{0}C	Peat 900^{0}C
NoB T	Peat 400^{0}C to	900^{0}C	Peat 200^{0}C	Peat	Peat 400^{0}C	Peat 900^{0}C

4825	900^{0}C					
NoB T 4831	Peat 400^{0}C to 900^{0}C	900^{0}C	Peat 200^{0}C	Peat	Wood 200^{0}C	Peat 900^{0}C
NoB T 4860	Peat 900^{0}C	900^{0}C	Peat 200^{0}C	Peat	Peat 400^{0}C to 900^{0}C	Peat 900^{0}C
NoB T 5810	Peat 900^{0}C	900^{0}C	Peat 200^{0}C	Peat	Wood 200^{0}C	Peat 900^{0}C
NoB T 5849	Peat 900^{0}C	900^{0}C	Peat 200^{0}C	Peat	Wood 200^{0}C	Peat 900^{0}C
NoB T 5855	Peat 900^{0}C	900^{0}C	Peat 200^{0}C	Peat	Peat 400^{0}C	Peat 900^{0}C
KoS 2039	Peat 400^{0}C to 900^{0}C	900^{0}C	Peat 400^{0}C	Peat	Peat 900^{0}C	Peat 900^{0}C
KoS 3081	Peat 400^{0}C Sheep dung 900^{0}C	400^{0}C	Peat 400^{0}C	Peat, Sheep dung	Peat, Dung 900^{0}C	Peat & Sheep dung 400^{0}C
KoS 3196	Peat 400^{0}C Sheep dung 900^{0}C	900^{0}C	Peat 400^{0}C	Peat, Sheep dung	Peat 400^{0}C to 900^{0}C	Peat & Sheep dung 900^{0}C
KoS 3201	Peat 400^{0}C	900^{0}C	Peat 400^{0}C	Peat	Peat 400^{0}C to 900^{0}C	Peat 900^{0}C
KoS 3217	Peat 400^{0}C to 900^{0}C	900^{0}C	Peat 400^{0}C	Peat, Sheep dung	Peat 400^{0}C to 900^{0}C	Peat & Sheep dung 900^{0}C
KoS 3225	Peat 400^{0}C Sheep dung 900^{0}C	900^{0}C	Peat 400^{0}C	Peat	Peat 400^{0}C to 900^{0}C	Peat 900^{0}C
KoS 3238	Peat 400^{0}C	900^{0}C	Peat 400^{0}C	Peat	Peat 400^{0}C to 900^{0}C	Peat 900^{0}C
KoS 3255	Peat 400^{0}C to 900^{0}C	900^{0}C	Peat 400^{0}C	Peat	Peat 400^{0}C to 900^{0}C	Peat 900^{0}C
RDL 031	Peat 400^{0}C	400^{0}C	Peat 200^{0}C	Peat	Peat 400^{0}C, Wood 400^{0}C	Peat 400^{0}C
RDL 001	Seaweed 900^{0}C	900^{0}C	Peat 200^{0}C	Peat	Peat 400^{0}C, Wood 200^{0}C	Unidentifiable
RDL 004	Peat 400^{0}C	400^{0}C	Peat 200^{0}C	Peat	Peat 400^{0}C	Peat 400^{0}C
RDL 006	Peat 900^{0}C	900^{0}C	Peat 200^{0}C	Peat	Peat 400^{0}C to 900^{0}C	Peat 900^{0}C
RDL 009	Peat 400^{0}C	400^{0}C	Peat 200^{0}C	Peat	Peat 400^{0}C to 900^{0}C	Peat 400^{0}C
RDL 007	Peat 400^{0}C	400^{0}C	Peat 200^{0}C	Peat	Peat 400^{0}C to 900^{0}C	Peat 400^{0}C
RDL 013	Peat 400^{0}C to 900^{0}C	400^{0}C	Peat 200^{0}C	Peat	Peat 400^{0}C to 900^{0}C	Peat 400^{0}C
RDL 016	Peat 400^{0}C to 900^{0}C	400^{0}C	Peat 200^{0}C	Peat	Peat 400^{0}C to 900^{0}C	Peat 400^{0}C
RDL 023	Peat 900^{0}C	900^{0}C	Peat 200^{0}C	Peat	Peat 900^{0}C, Wood 200^{0}C	Peat 900^{0}C
RDL 032	Peat 400^{0}C to 900^{0}C	400^{0}C	Peat 200^{0}C	Peat	Peat 900^{0}C	Peat 400^{0}C
SMQ A	Peat 900^{0}C	900^{0}C	Peat 200^{0}C	Peat	Peat 400^{0}C to 900^{0}C	Peat 900^{0}C
SMQ B	Peat 900^{0}C	900^{0}C	Peat 200^{0}C	Peat	Peat 900^{0}C, Wood 200^{0}C	Peat 900^{0}C

Table 7.4 Table of the modern analogue fuel matches to archaeological samples by comparison. Showing the matches according to MS, FDMS, pH, SEM/EDX, and Munsell colour assignment. Source: Author

7.4.2 Confirming fuel identifications with statistical analysis

The associations among archaeological samples and modern analogue fuels were examined using principal components analysis carried out with Minitab17 software. The following discusses the assignment of matches through PCA that makes use of multiple variables including Na, Al, Si, P, K, Fe, Ti, MS, and pH (table 7.2). These variables were chosen because of their relation to ash formation, magnetism and pH as discussed in sections 7.2 and 7.3. The PCA results show clear associations between modern analogue fuels and the archaeological sample material; however, there is a need to consider the potential for contamination within the archaeological material (figures 7.21-7.33). The first and second component account for 43% of the variation in the data.

The modern analogue material is shown to plot in groups dictated by fuel type as shown in figures 7.22-7.33. The peat fuels are the most associated with the archaeological fuels while seaweed is the least related according to the PCA score plots (figures 7.22 & 7.26-7.28).

The archaeological material is plotted completely on the right hemisphere of the PCA score plot with the exception of 2 samples, while the modern analogue material lies mostly on the left except for 8 of the samples (figures 7.21-7.33). According to the loading plot (figure 7.21), this disparity between the modern and archaeological datasets is attributed to the levels of Al, iron, K, Si, and pH. Al, iron, K, and Si are all known to be part of the soil matrix due to the geology of the area as discussed in section 2.3. The levels of K are linked with alkaline pH as discussed in section 2.9. This further illustrates the need to adjust the data to account for the presence of contamination within the archaeological samples.

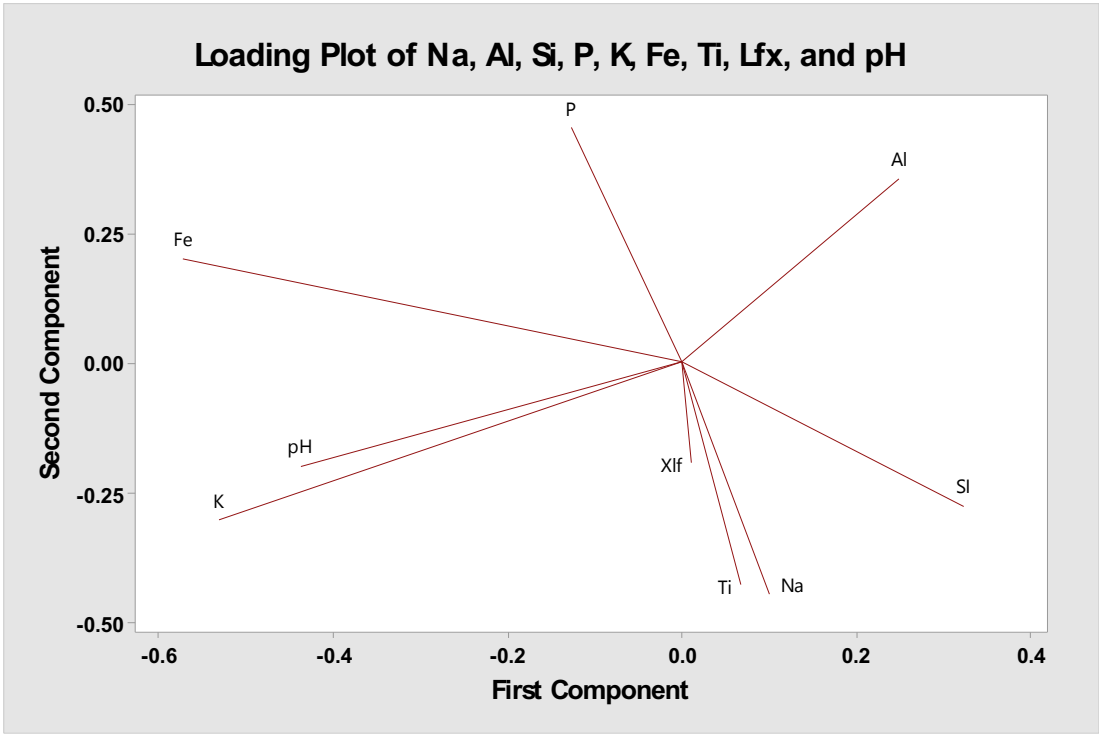

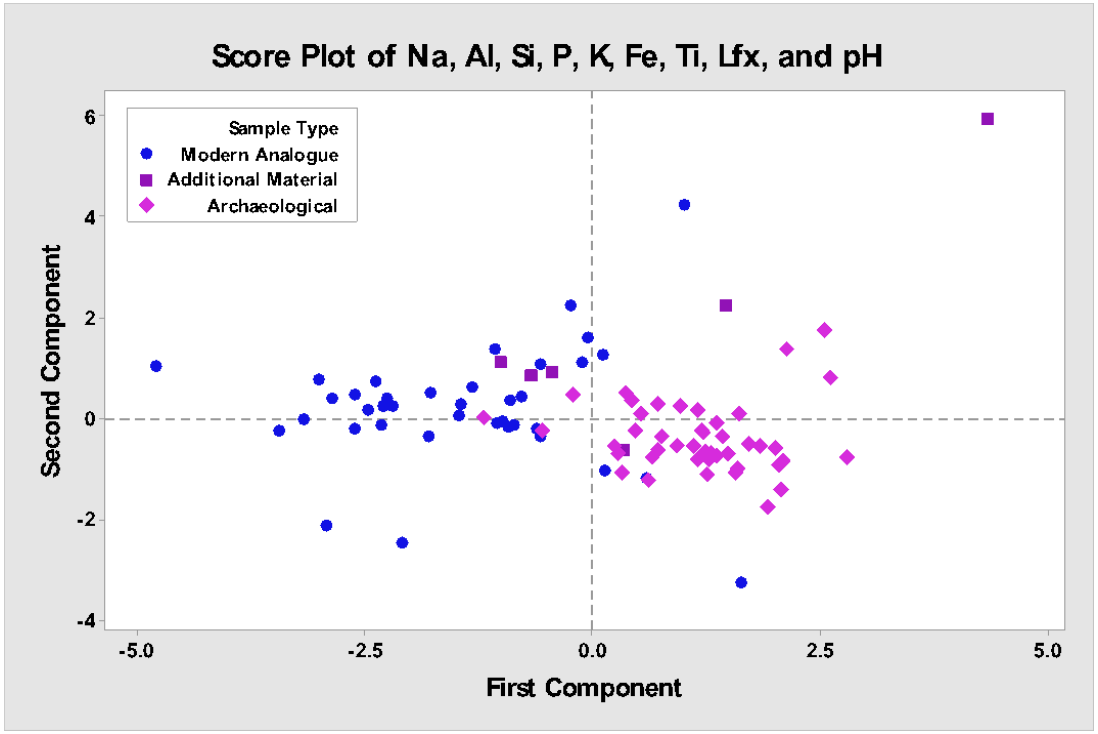

Figure 7.27 The results of principal components analysis considering all modern analogue and archaeological sample material rendering nine variables sodium, aluminium, silicon, phosphorous, potassium, iron, titanium, MS and pH. According to the unadjusted data with ellipses highlighting fuel types yellow for peat, grey for wood, and green for dung. Loading plot on the left and score plot to the right. Source: Author

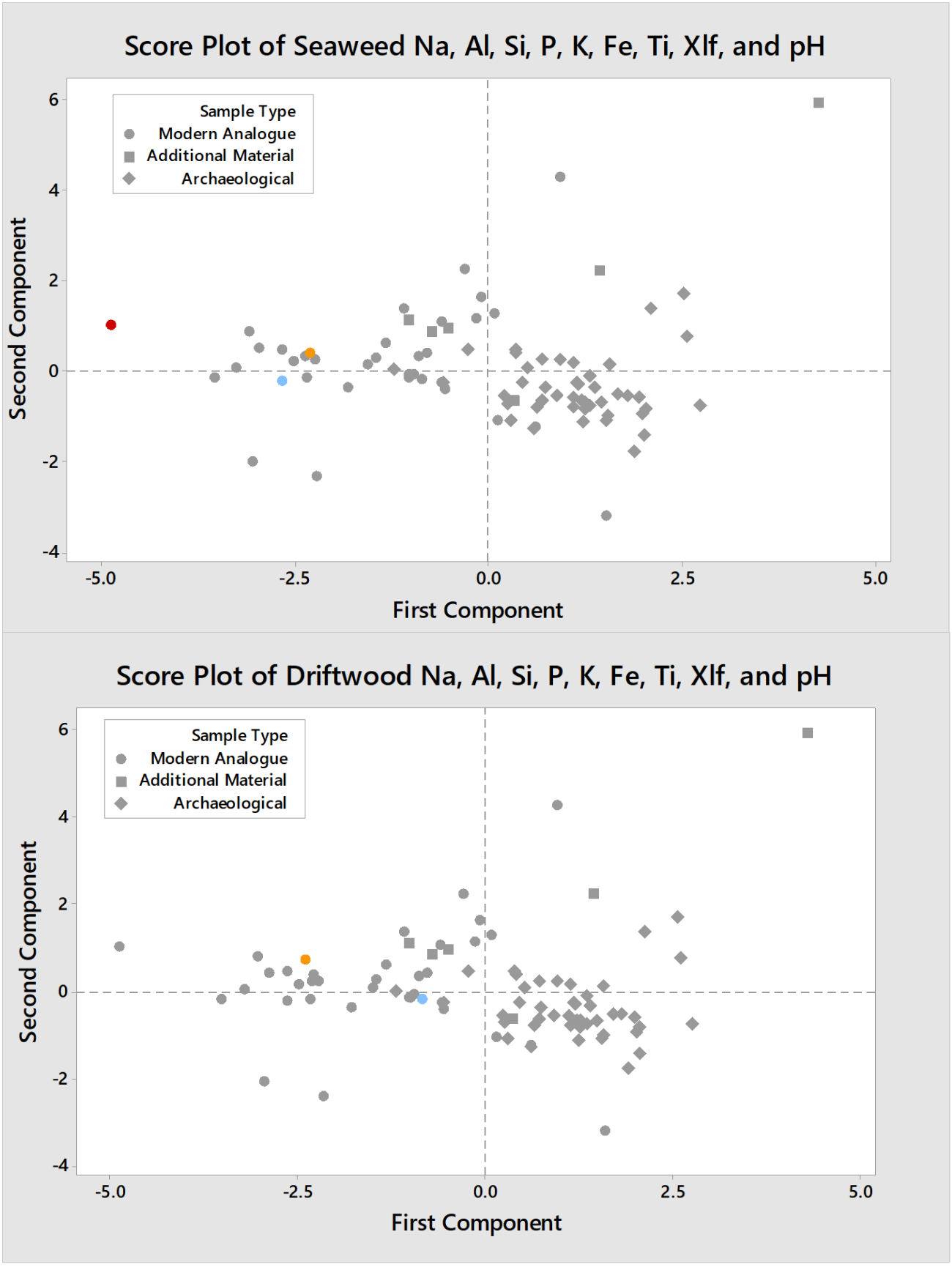

Figure 7.28 The results of the unadjusted principal components analysis considering all modern analogue and archaeological sample material according to nine variables sodium, aluminium, silicon, phosphorous, potassium, iron, titanium, MS and pH. The plots shown from the top: seaweed and driftwood. The heating temperature is indicated as blue for 200^{0}C, yellow for 400^{0}C, and red for 900^{0}C. Source: Author

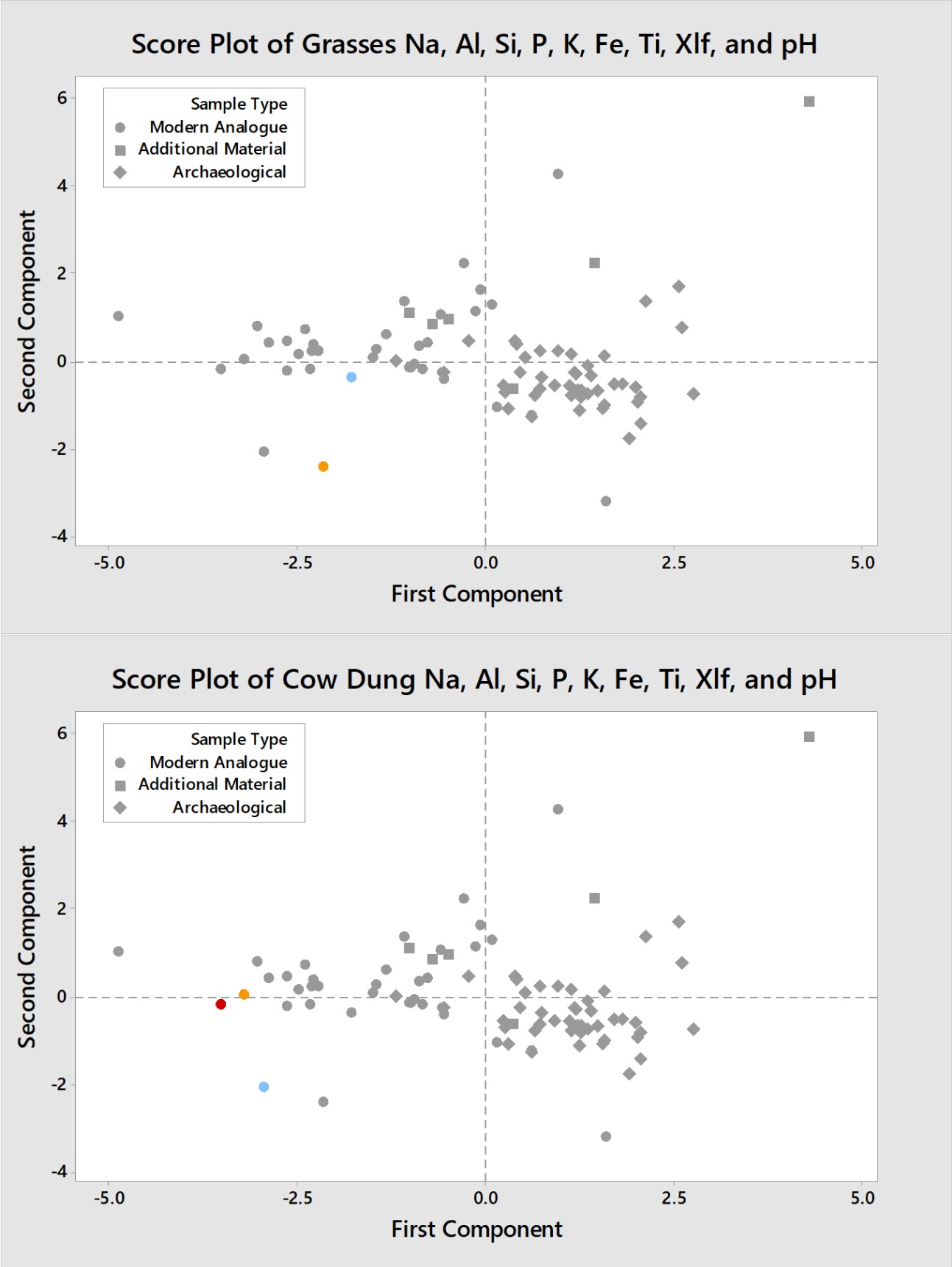

Figure 7.29 The results of the unadjusted principal components analysis considering all modern analogue and archaeological sample material according to nine variables sodium, aluminium, silicon, phosphorous, potassium, iron, titanium, MS and pH. The plots shown are from the top: grasses and cow dung. The heating temperature is indicated as blue for 200^{0}C, yellow for 400^{0}C, and red for 900^{0}C. Source: Author

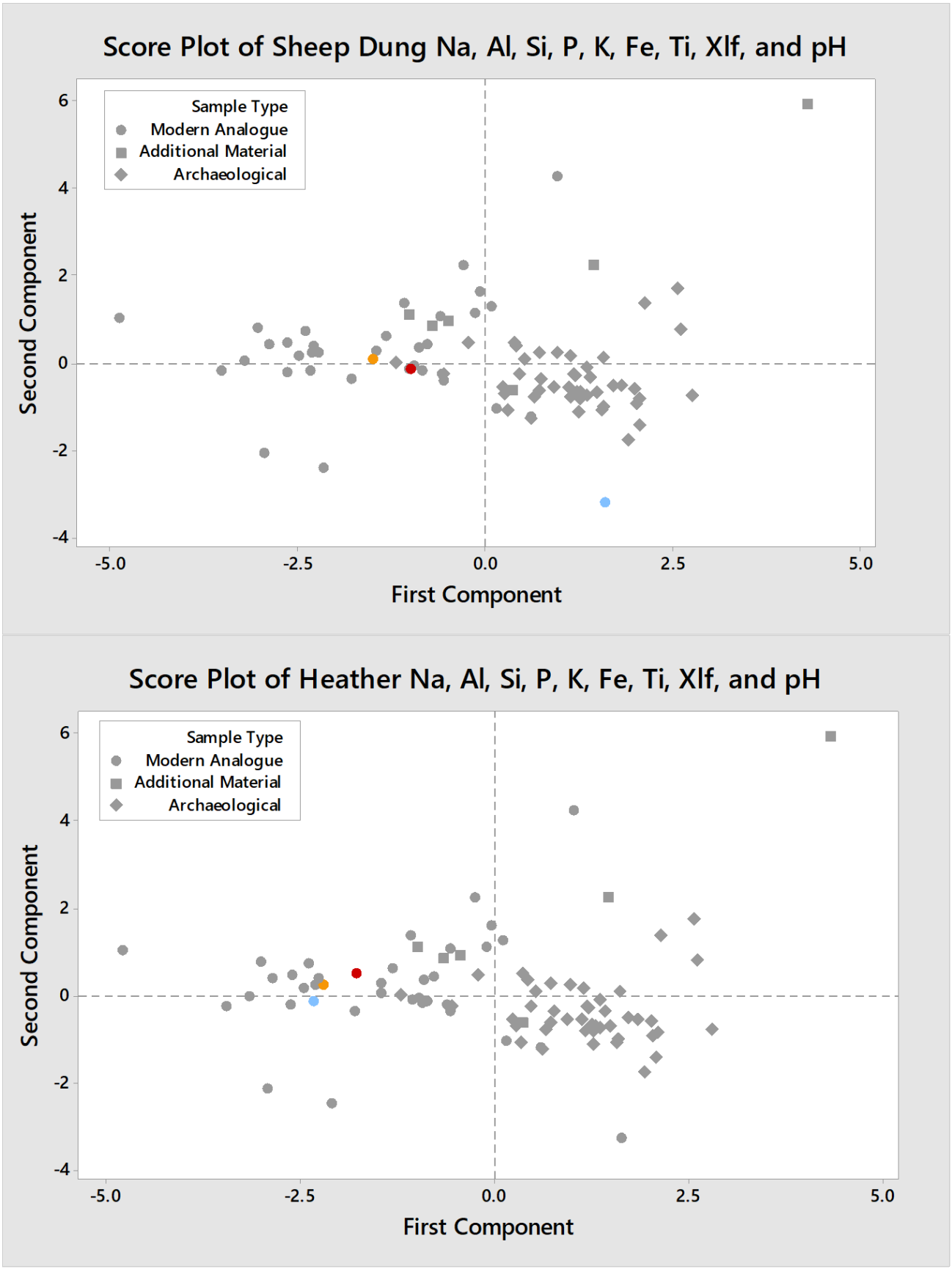

Figure 7.30 The results of the unadjusted principal components analysis considering all modern analogue and archaeological sample material according to nine variables sodium, aluminium, silicon, phosphorous, potassium, iron, titanium, MS and pH. The plots shown are from the top: sheep dung and heather. The heating temperature is indicated as blue for 200^{0}C, yellow for 400^{0}C, and red for 900^{0}C. Source: Author

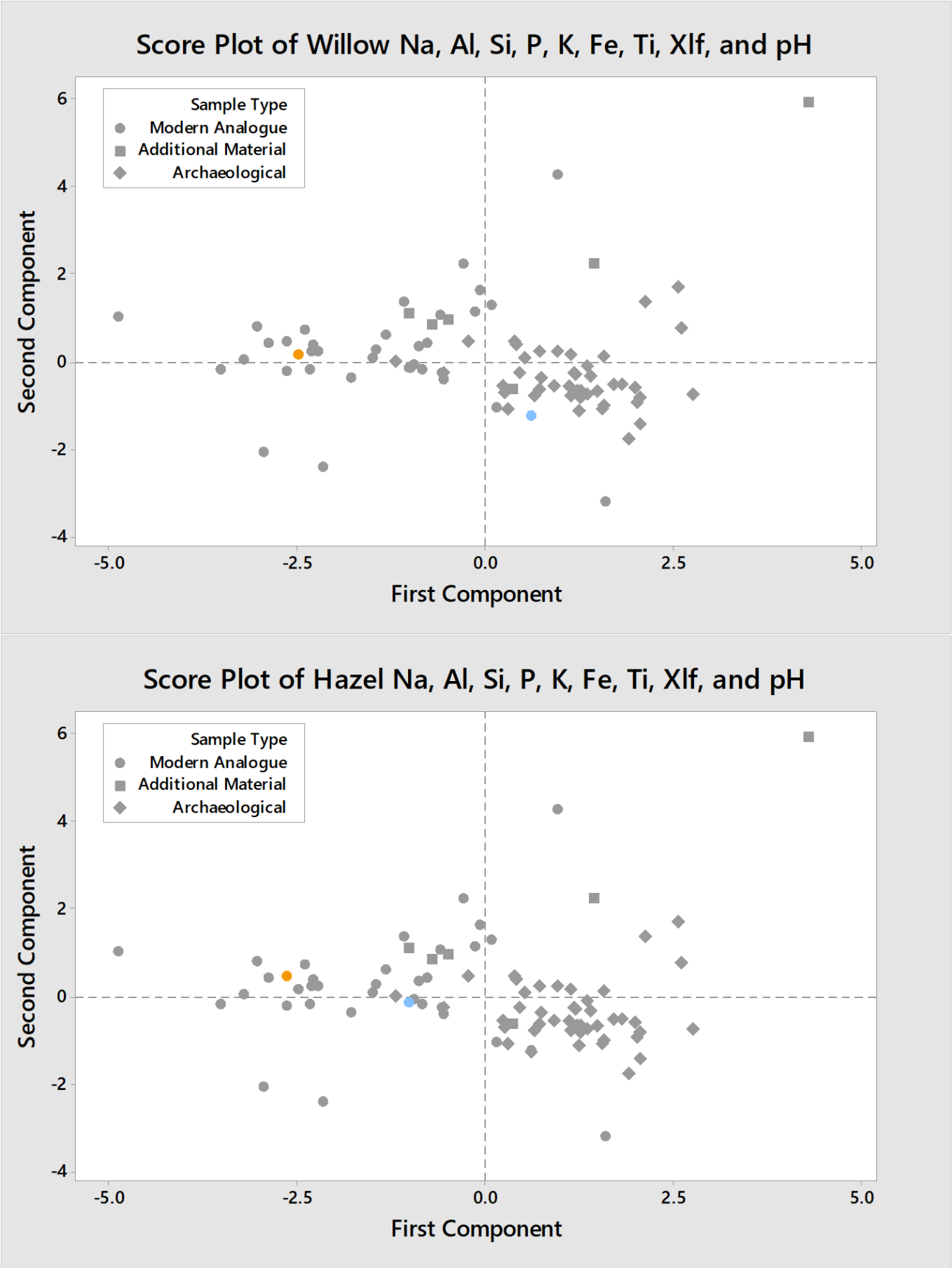

Figure 7.31 The results of the unadjusted principal components analysis considering all modern analogue and archaeological sample material according to nine variables sodium, aluminium, silicon, phosphorous, potassium, iron, titanium, MS and pH. The plots shown are from the top: willow and hazel. The heating temperature is indicated as blue for 200^{0}C, yellow for 400^{0}C, and red for 900^{0}C. Source: Author

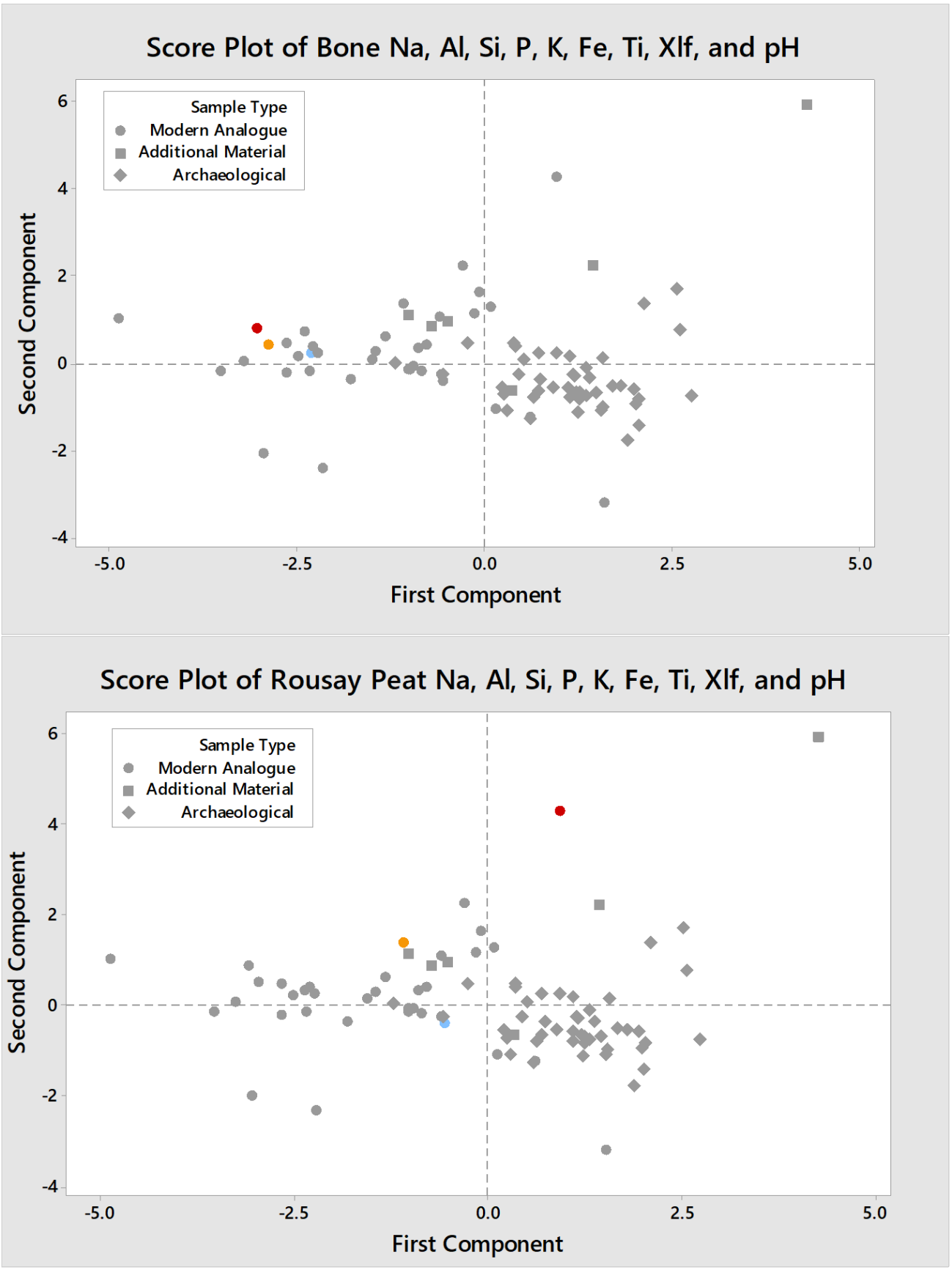

Figure 7.32 The results of the unadjusted principal components analysis considering all modern analogue and archaeological sample material according to nine variables sodium, aluminium, silicon, phosphorous, potassium, iron, titanium, MS and pH. The plots shown are from the top: animal bone and Rousay peat. The heating temperature is indicated as blue for 200^{0}C, yellow for 400^{0}C, and red for 900^{0}C. Source: Author

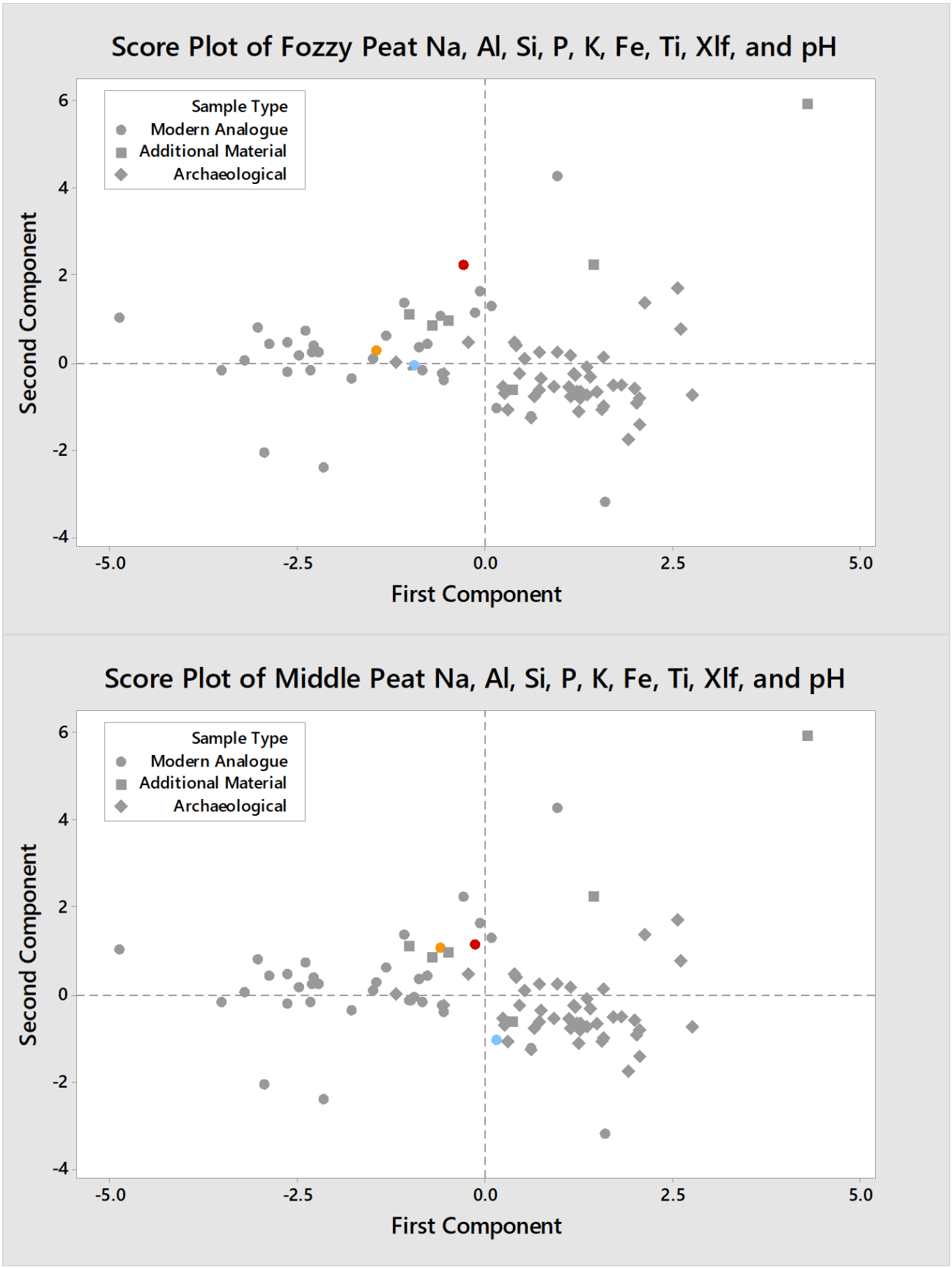

Figure 7.33 The results of the unadjusted principal components analysis considering all modern analogue and archaeological sample material according to nine variables sodium, aluminium, silicon, phosphorous, potassium, iron, titanium, MS and pH. The plots shown are from the top: fozzy peat and middle peat. The heating temperature is indicated as blue for 200^{0}C, yellow for 400^{0}C, and red for 900^{0}C. Source: Author

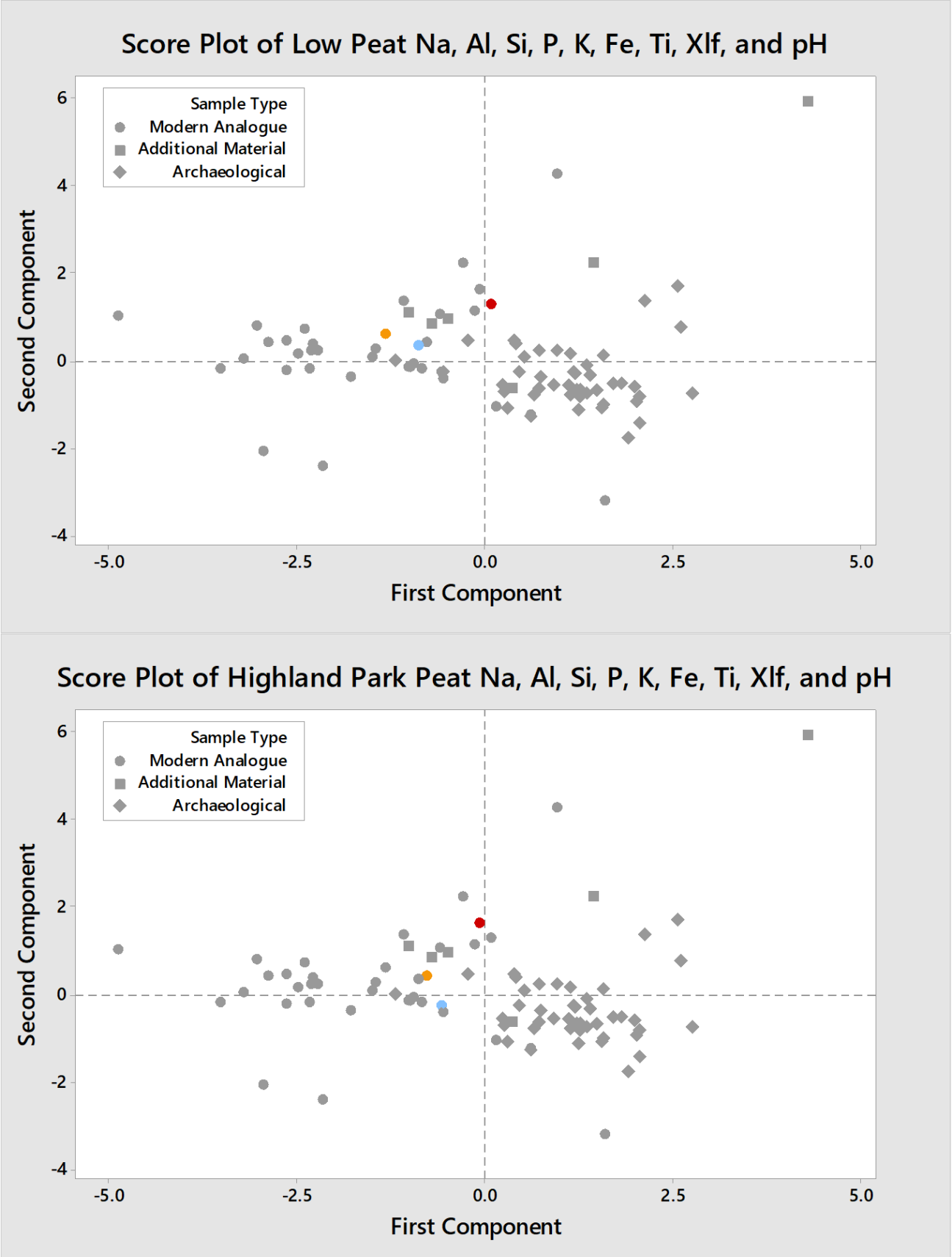

Figure 7.34 The results of the unadjusted principal components analysis considering all modern analogue and archaeological sample material according to nine variables sodium, aluminium, silicon, phosphorous, potassium, iron, titanium, MS and pH. The plots shown are from the top: low peat and Highland Park peat, additional sample material, all peat fuels, all wood fuels, and all dung fuels. The heating temperature is indicated as blue for 200^{0}C, yellow for 400^{0}C, and red for 900^{0}C. Source: Author

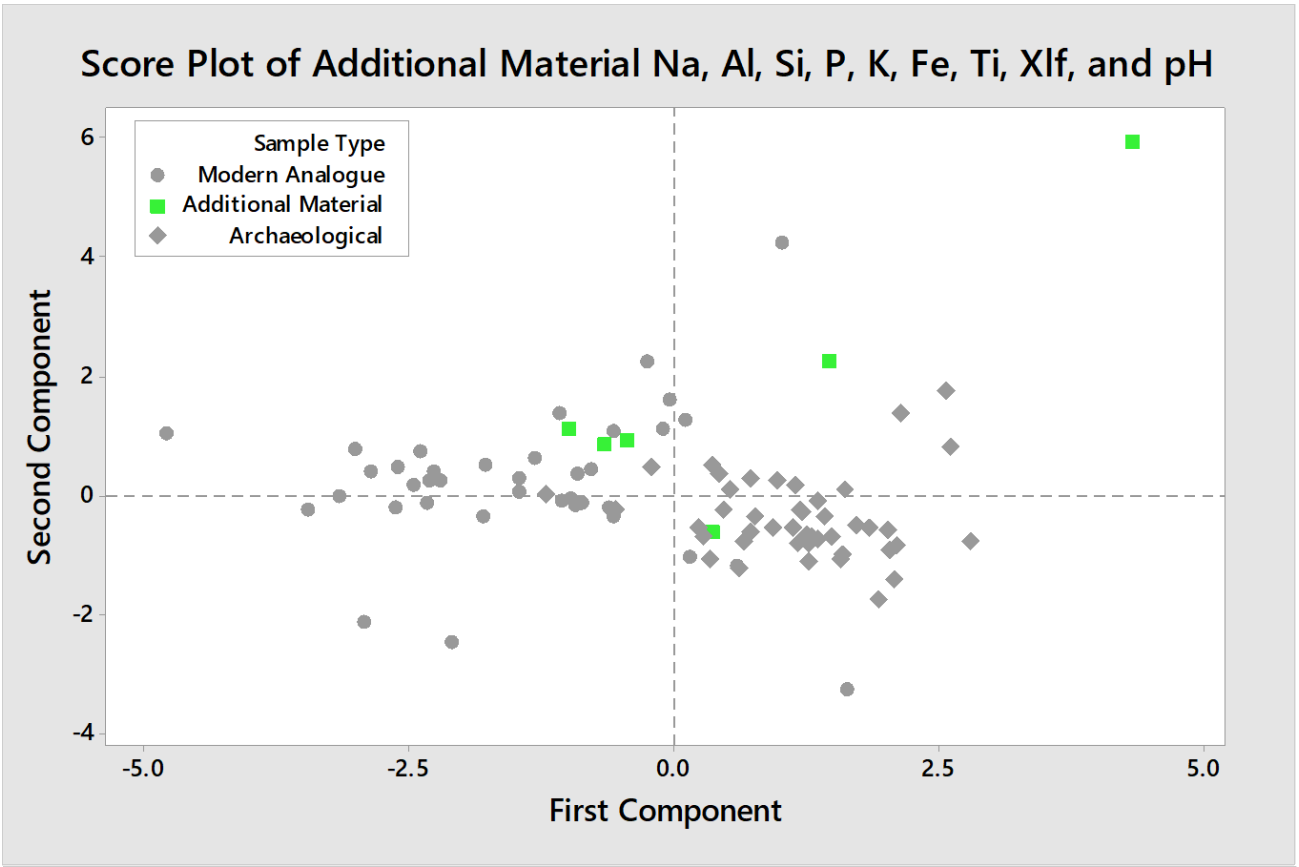

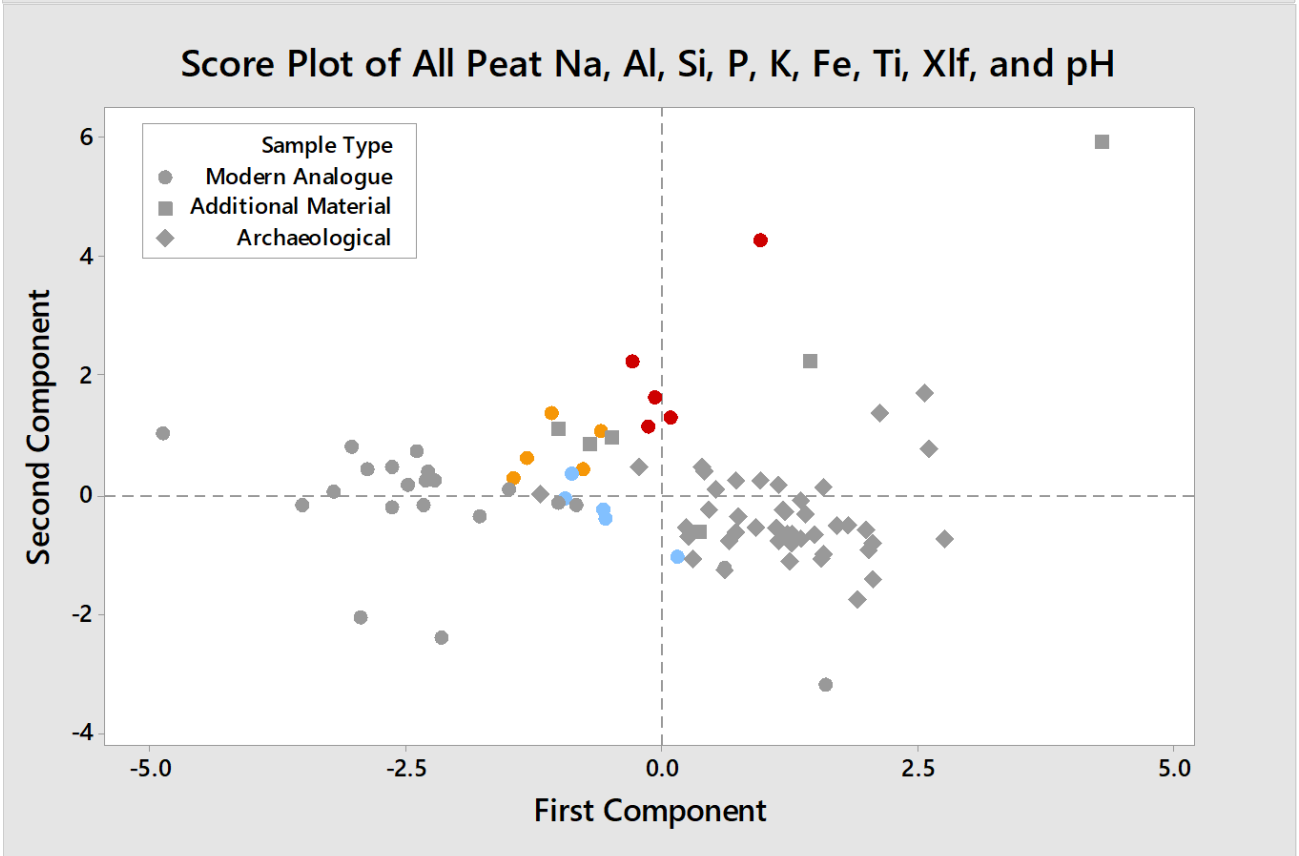

Figure 7.35 The results of the unadjusted principal components analysis considering all modern analogue and archaeological sample material according to nine variables sodium, aluminium, silicon, phosphorous, potassium, iron, titanium, MS and pH. The plots shown are from the top: additional sample material and all peat fuels. The heating temperature is indicated as blue for 200^{0}C, yellow for 400^{0}C, and red for 900^{0}C. Source: Author

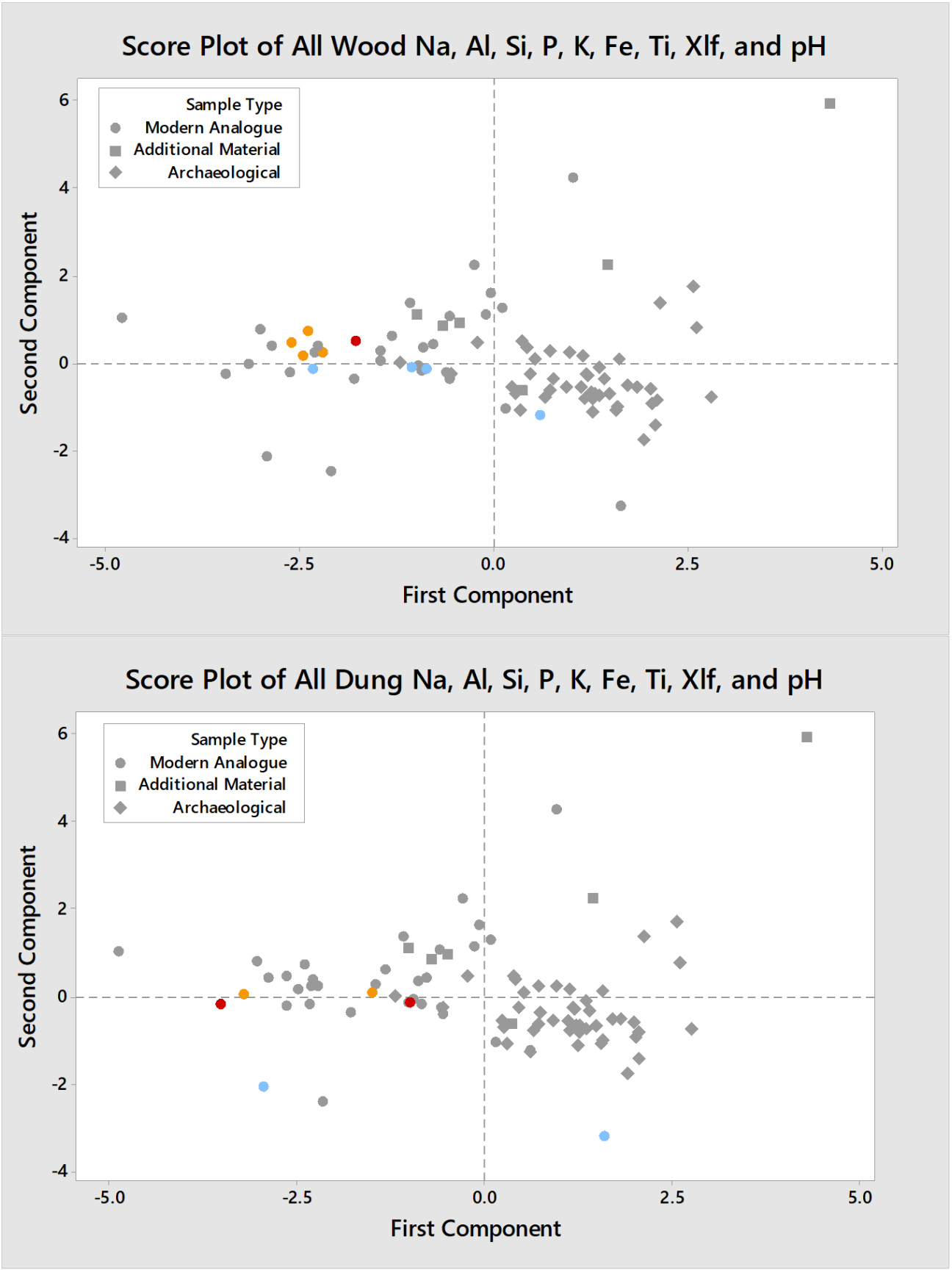

Figure 7.36 The results of the unadjusted principal components analysis considering all modern analogue and archaeological sample material according to nine variables sodium, aluminium, silicon, phosphorous, potassium, iron, titanium, MS and pH. The plots shown are from the top: all wood fuels and all dung fuels. The heating temperature is indicated as blue for 200^{0}C, yellow for 400^{0}C, and red for 900^{0}C. Source: Author

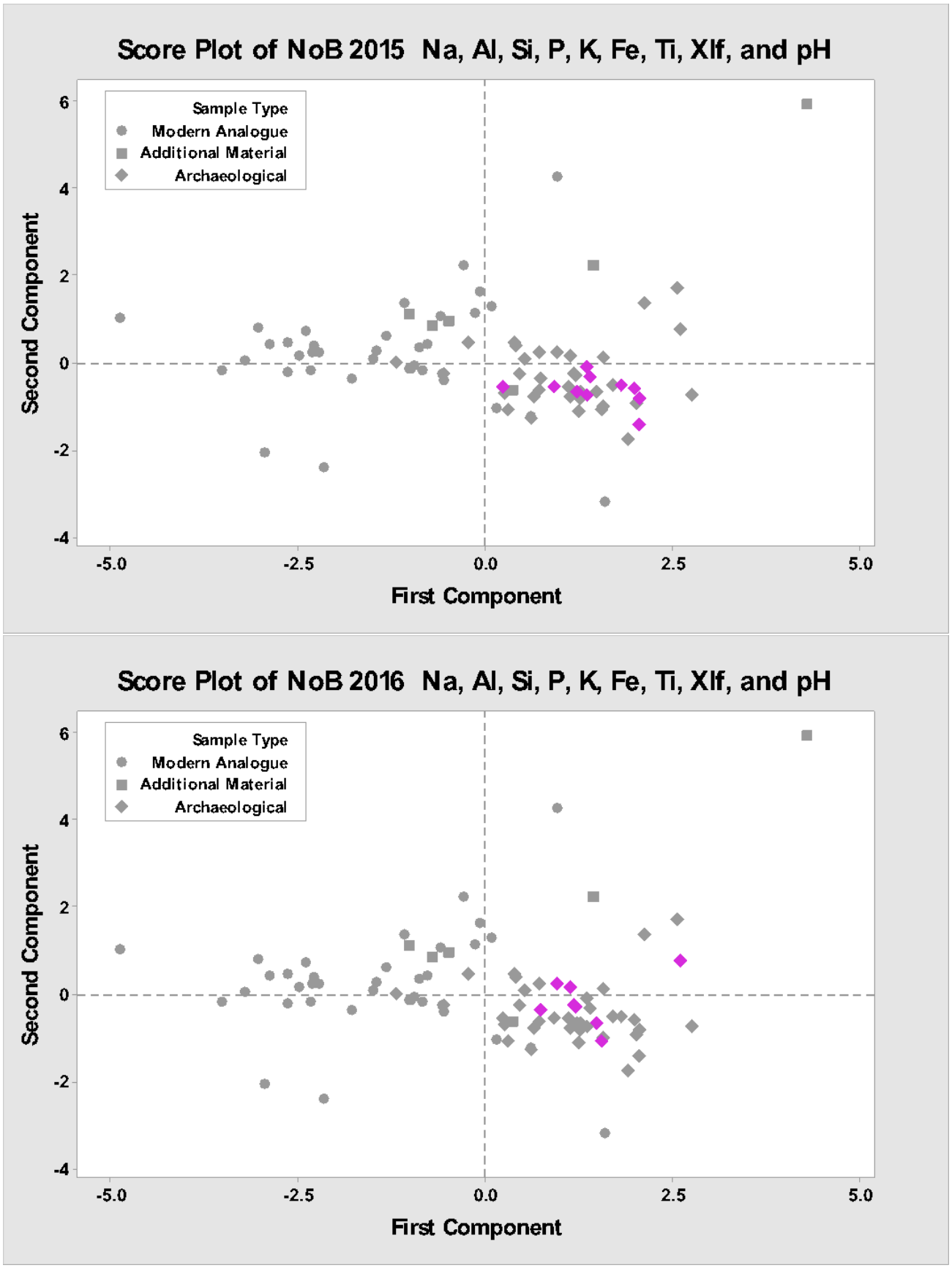

Figure 7.37 The results of the unadjusted principal components analysis considering all modern analogue and archaeological sample material according to nine variables sodium, aluminium, silicon, phosphorous, potassium, iron, titanium, MS and pH. The plots shown are from the top: The Ness of Brodgar 2015, The Ness of Brodgar 2016 highlighted in pink. Source: Author

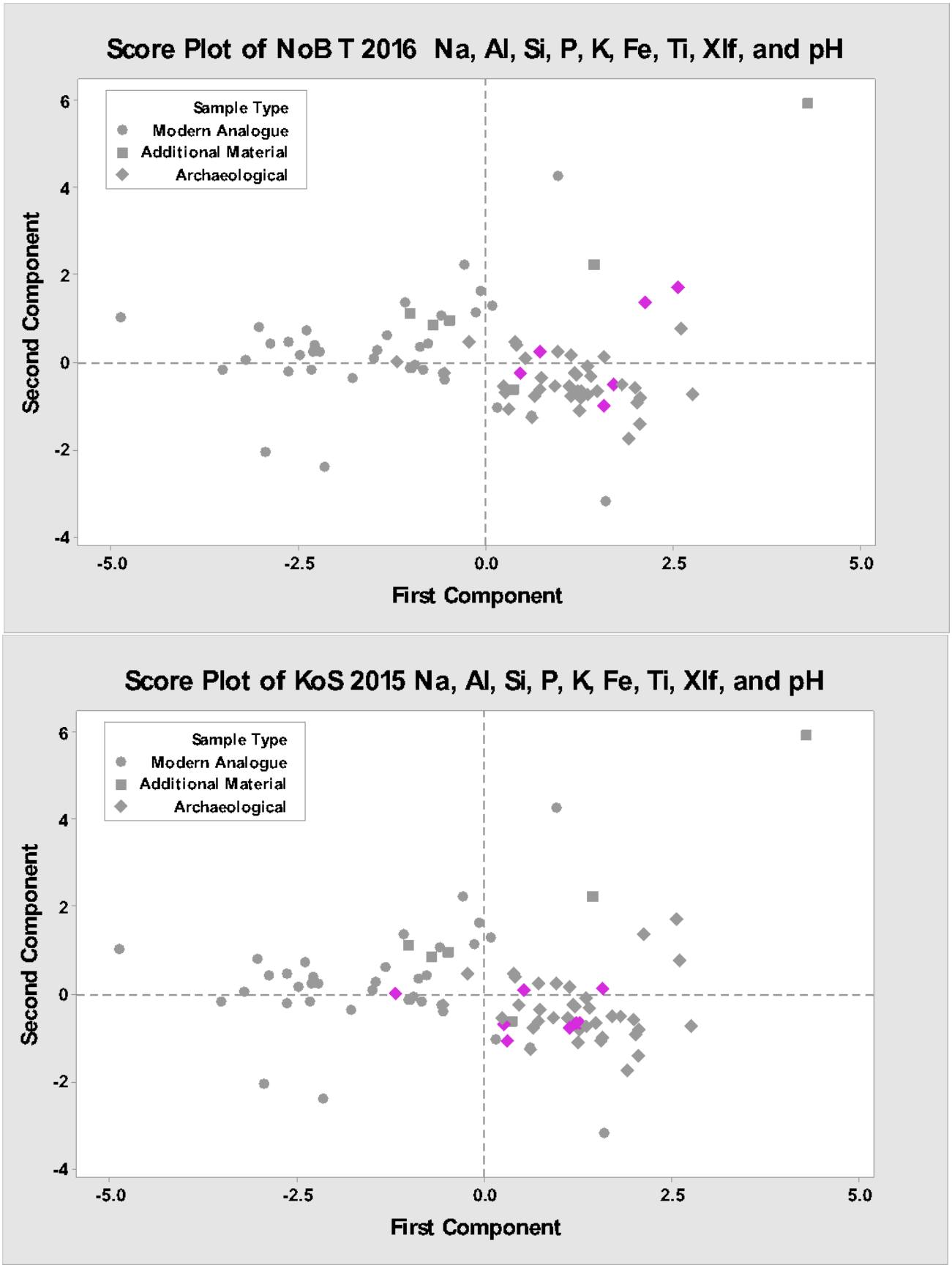

Figure 7.38 The results of the unadjusted principal components analysis considering all modern analogue and archaeological sample material according to nine variables sodium, aluminium, silicon, phosphorous, potassium, iron, titanium, MS and pH. The plots shown are from the top: The Ness of Brodgar Trench T 2016 highlighted in pink. Source: Author

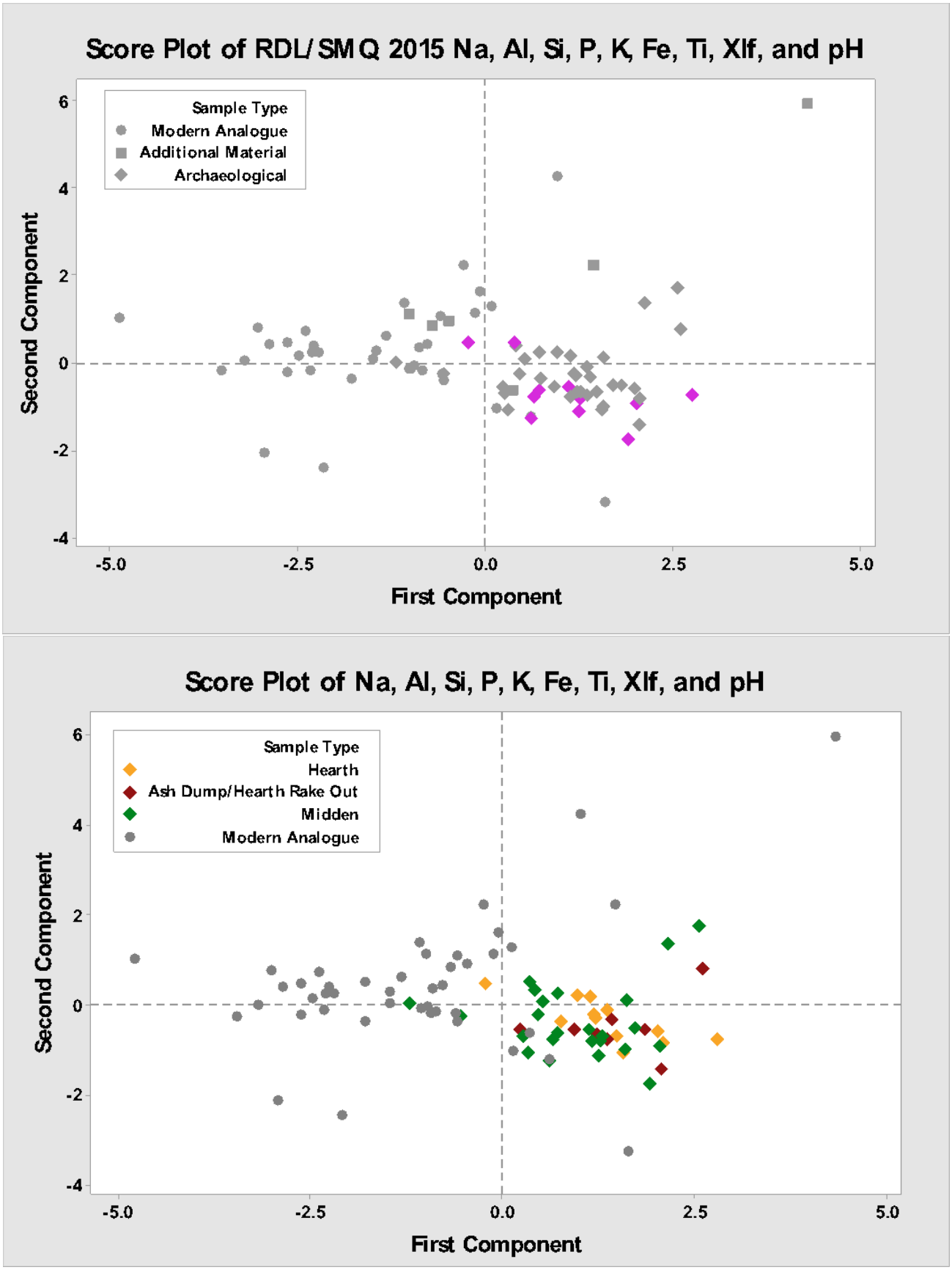

Figure 7.39 The results of the unadjusted principal components analysis considering all modern analogue and archaeological sample material according to nine variables sodium, aluminium, silicon, phosphorous, potassium, iron, titanium, MS and pH. The plots shown are from the top: Smerquoy/Muckquoy 2015 highlighted in pink, and all archaeological samples considered by sample type shown in yellow for hearth, red for ash dump/hearth rake out, and green for midden. Source: Author

To combat the potential threat of contamination altering results or causing inaccurate matching, the need to adjust the modern analogue fuel material to account for a possible inclusion of soil material became apparent. This is just one possible approach to adjust the data to account for soil mixing or other potential sources of contamination. To deal with this issue, all of the modern analogues were adjusted to simulate a 50/50 mix with soil. The data for this was taken directly from the additional sample material unburnt archaeological matrix. To calculate this, the original modern analogue data and the archaeological matrix data were averaged to simulate a mixing of soil material and ash as could potentially be seen among the archaeological samples. This mixing simulation was repeated to represent a 2:1, 3:1, and 4:1 ratio of unheated archaeological matrix to modern ash (appendix 4). The 1:1 ratio of modern ash to archaeological matrix had the best results for simulating a mix with soil as seen with the archaeological samples. This caused the data to group in a much tighter cluster as opposed to the table of the unadjusted data that shows the modern analogue material widely distributed around the archaeological material with only occasional crossover. This shows that there were some similarities between modern and archaeological samples that suggested matches before the data was adjusted; however, after the adjustment the archaeological and modern analogue datasets merge, and demonstrate strong relationships as shown in figure 7.26. The remainder of the PCA plots show the data after the adjustment using the unburnt archaeological matrix.

The adjusting of the modern values brings the data tighter together and shows an interesting change to the associations between archaeological sample and modern ash. Peat is still the most closely related to the archaeological data; however, the adjusted data shows a closer association between archaeological

fuel and driftwood, willow, sheep dung, and bone than previously observed. There is still no evident association between the archaeological material and seaweed, grasses, or cow dung (figure 7.35 & 7.36). The most extreme outliers to the dataset are the Corrigal farm house museum samples of Caithness peat ash and sheep dung heated to 200^0C shown in figures 7.37 and 7.42.

The additional sample materials show the difference in association of the samples between the heated and unheated samples of archaeological matrix material (figure 7.42). The unheated archaeological matrix material is almost dead center of the plot showing the relationship between it and the rest of the sample materials, while the archaeological matrix material heated to 900^0C is only closely associated to the mixed fuels sample heated to 500^0C (figure 7.42). This does remove some of the uncertainty associated with mixed ash samples. If a sample is extremely mixed it does not fall within the ranges established by the modern analogue fuels and remains unidentifiable. However, some mixing with the soil matrix or other fuel materials in small amounts, as suggested in sections 2.2 and 2.4, do not affect the identification according to the variables chosen. Mixing changes the values slightly, but does not completely remove them from the ranges for fuel types established by the modern analogue data. A mixed sample could potentially fall within the ranges of two fuel types as seen with KoS 3217 matching peat heated to 200^0C and sheep dung at 400^0C, and KoS 3081 and SMQ B matching with matching both driftwood at 400^0C and bone at 200^0C.

The archaeological data is evenly distributed, and the modern analogue data shows trends among fuel types yet enough variety to be able to provide insight into fuel matching based on PCA analysis. Grasses, cow dung, seaweed, and driftwood all show similarities according to the PCA plots in figure 7.35 & 7.36.

the Peat fuels share a relationship with sheep dung which is shown in figures 7.37 & 7.39-7.41. Wood fuels plot in a distinct group that is adjacent to peat on the left and dung on the right. Bone is plotted in a tight group outlying the main concentration of data, but is still in very close proximity to two archaeological samples (KoS 3018 & SMQ B) and the samples of driftwood heated to 400^0C (figures 7.35 & 7.39). The archaeological material is distributed in a way that is indicative of a relationship to modern analogue fuels, and with a concentration of data showing trends among excavation sites (figure 7.44-7.46). Each site is distributed in a way that is unique following the differences between the characteristics of each site discussed throughout section 7.3. This is demonstrated in the PCA loading plot which shows the directional pull of each variable (figure 7.34). The Knowe of Swandro and Smerquoy/Muckquoy data show evenly distributed patterns on the PCA score plot (figure 7.44-7.46). The Ness of Brodgar samples are concentrated toward the negative portion of both the first and second component axes which is indicative of the high MS values and large quantities of Al, iron, and Ti among those samples as discussed in section 7.3 (figure 7.44 & 7.45).

When considering the archaeological material according to sample type, there are trends present in the corresponding fuel matches. The hearth samples had the highest frequency of unidentified samples, out of 12 hearth samples 3 were unable to be matched NoB 4656, NoB 5013, and SMQ A (table 7.5). Out of 24 midden samples only 2 were unidentified (KoS 3201 & RDL 013), and 1 out of 8 ash samples were unable to be matched (NoB 4264). The hearth, ash dump, and hearth rake out samples match predominantly to peat fuels heated to 900^0C. The midden material shows the most variability in fuel matches. In addition to matching peat fuels at 900^0C, the midden material also

demonstrates matches to wood at 200^{0}C and 400^{0}C, bone at 200^{0}C, and dung heated to 400^{0}C and 900^{0}C. Where the ash dump and hearth rake out samples only have one sample, NoB 3783, that matches to wood at 200^{0}C, and the hearth samples have one sample matching to wood at 200^{0}C and one sample that is a match for wood at 400^{0}C and bone heated to 200^{0}C (table 7.5).

There is a strong association between the modern analogue samples of peat and the archaeological material, and a few instances of a relationship between archaeological sample and sheep dung, driftwood, willow, and bone. The samples of seaweed, cow dung, grasses, heather and hazel show no definitive associations with the archaeological ash. Out of the 44 archaeological samples, 22 match peat fuels heated to 900^{0}C according to the principal components analysis. In addition, 5 samples match peat fuels heated to 400^{0}C and 2 samples match 200^{0}C peat samples (table 7.5). There are four samples that match with wood fuels heated to 200^{0}C, and one sample that matches sheep dung heated to 900^{0}C. Among the archaeological material, five samples match to two fuels, and five samples were not able to be identified. The matches of archaeological samples to modern analogue fuels is displayed in table 7.5. The matches were assigned based on the proximity of archaeological samples to individual modern analogue samples on the PCA score plots shown in figures 7.35 to 7.46. The matches assigned using PCA are compared with the matching results from the analytical data (table 7.1) and discussed in section 7.4.3.

PCA fuel Match Table	
Sample number and type	**Fuel Match**
NoB 2617 hearth rake out	Peat 200^{0}C
NoB 3851 hearth rake out	Peat 900^{0}C
NoB 3857 hearth rake out	Peat 900^{0}C
NoB 4264 ash dump	Unidentifiable
NoB 4656 hearth	Unidentifiable
NoB 4674 hearth	Peat 900^{0}C
NoB 5332 ash dump	Peat 900^{0}C
NoB 6156 ash dump	Peat 900^{0}C
NoB 5013 hearth	Unidentifiable
NoB 3783 ash dump	Willow 200^{0}C
NoB16 3851 hearth rake out	Peat 900^{0}C
NoB16 6339 hearth	Peat 900^{0}C
NoB16 6346 hearth	Willow 200^{0}C
NoB16 6348 hearth	Peat 900^{0}C
NoB16 6351 hearth	Peat 900^{0}C
NoB16 6354 hearth	Peat 900^{0}C
NoB16 6355 hearth	Peat 900^{0}C
NoB16 6356 hearth	Peat 900^{0}C
NoB T 4825 midden	Peat 900^{0}C
NoB T 4831 midden	Peat 900^{0}C
NoB T 4860 midden	Peat 900^{0}C
NoB T 5810 midden	Peat 400^{0}C
NoB T 5849 midden	Peat 900^{0}C
NoB T 5855 midden	Peat 900^{0}C
KoS 2039 hearth	Peat 400^{0}C
KoS 3081 midden	Driftwood 400^{0}C and Bone 200^{0}C
KoS 3196 midden	Peat 900^{0}C
KoS 3201 midden	Unidentifiable
KoS 3217 midden	Peat 200^{0}C & Sheep Dung 400^{0}C
KoS 3225 midden	Peat 900^{0}C
KoS 3238 midden	Sheep dung 900^{0}C
KoS 3255 midden	Peat 900^{0}C
RDL 031 midden	Willow 200^{0}C
RDL 001 midden	Peat 400^{0}C
RDL 004 midden	Peat 900^{0}C
RDL 006 midden	Peat 900^{0}C
RDL 009 midden	Peat 200^{0}C
RDL 007 midden	Peat 200^{0}C & Peat 400^{0}C
RDL 013 midden	Unidentifiable
RDL 016 midden	Willow 200^{0}C
RDL 023 midden	Peat 400^{0}C
RDL 032 midden	Peat 200^{0}C & Driftwood 400^{0}C
SMQ A hearth	Unidentifiable
SMQ B hearth	Driftwood 400^{0}C and Bone 200^{0}C

Table 7.5 The results of the unburnt archaeological matrix adjusted principal components analysis considering all modern analogue and archaeological sample material according to nine variables sodium, aluminium, silicon, phosphorous, potassium, iron, titanium, MS and pH. Source: Author

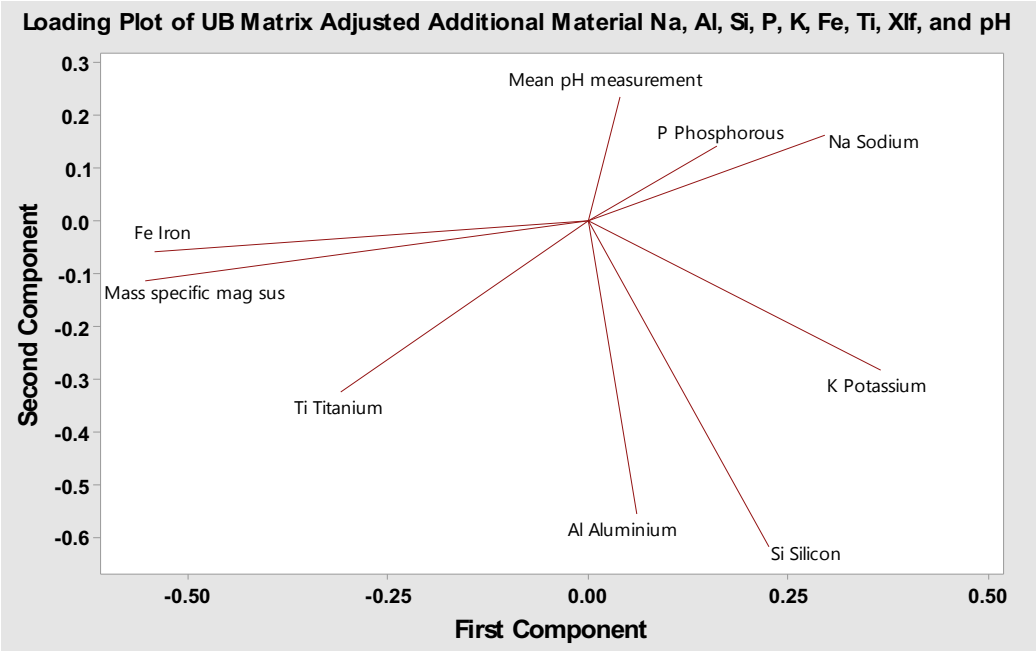

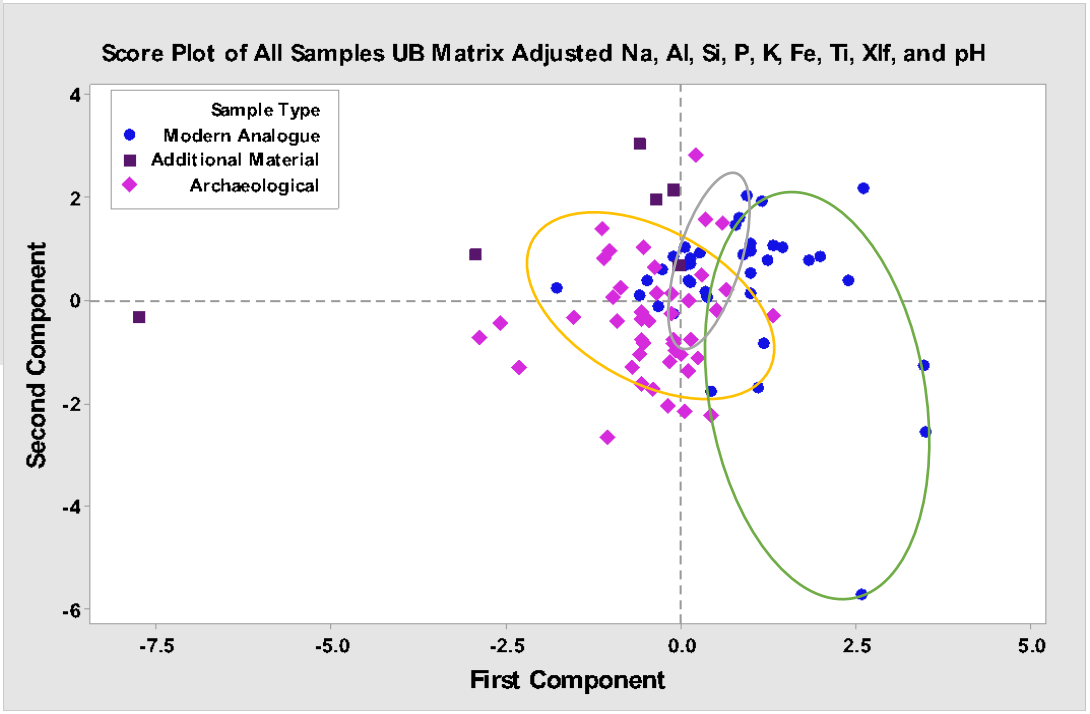

Figure 7.40 The results of principal components analysis considering all modern analogue and archaeological sample material rendering nine variables sodium, aluminium, silicon, phosphorous, potassium, iron, titanium, MS and pH. According to the unburnt archaeological matrix adjusted data modern analogues shown in blue dots, additional samples in purple squares, and archaeological samples in pink diamonds with ellipses highlighting fuel types yellow for peat, grey for wood, and green for dung. Loading plot on the left and score plot to the right. Source: Author

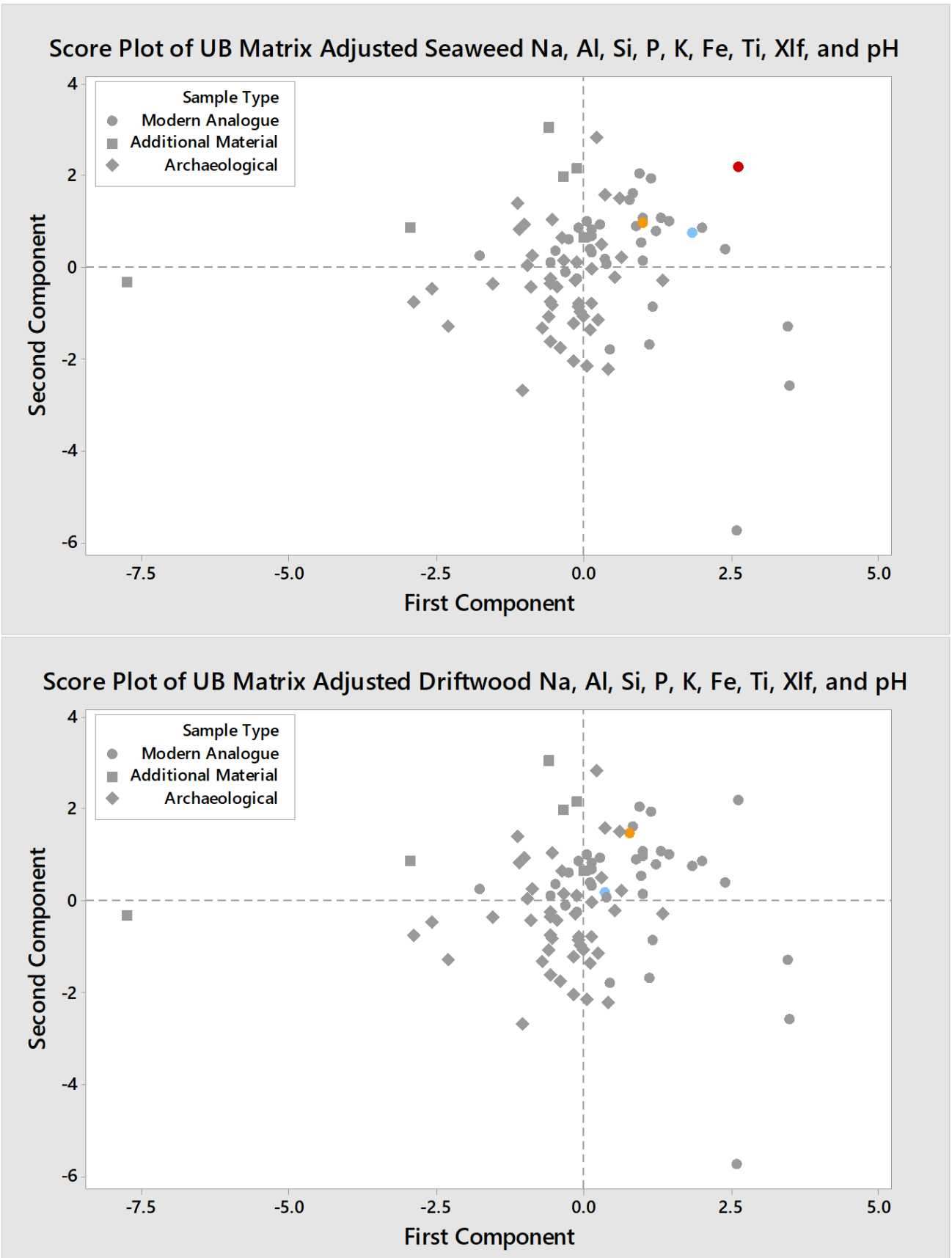

Figure 7.41 The results of the unburnt archaeological matrix adjusted principal components analysis considering all modern analogue and archaeological sample material according to nine variables sodium, aluminium, silicon, phosphorous, potassium, iron, titanium, MS and pH. The plots shown are from the top: seaweed and driftwood. The heating temperature is indicated as blue for 200^{0}C, yellow for 400^{0}C, and red for 900^{0}C. Source: Author

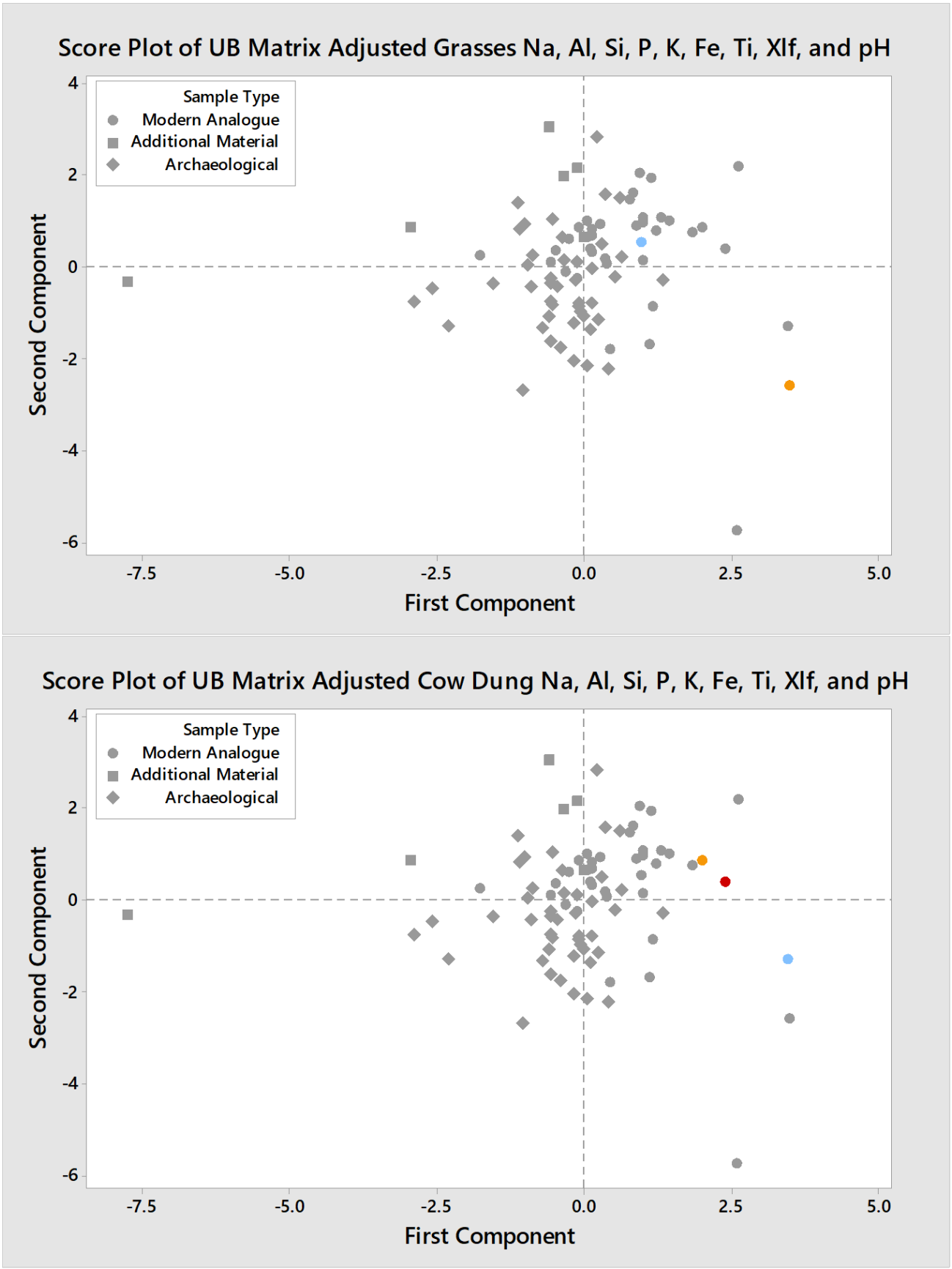

Figure 7.42 The results of the unburnt archaeological matrix adjusted principal components analysis considering all modern analogue and archaeological sample material according to nine variables sodium, aluminium, silicon, phosphorous, potassium, iron, titanium, MS and pH. The plots shown are from the top: grasses and cow dung. The heating temperature is indicated as blue for 200^{0}C, yellow for 400^{0}C, and red for 900^{0}C. Source: Author

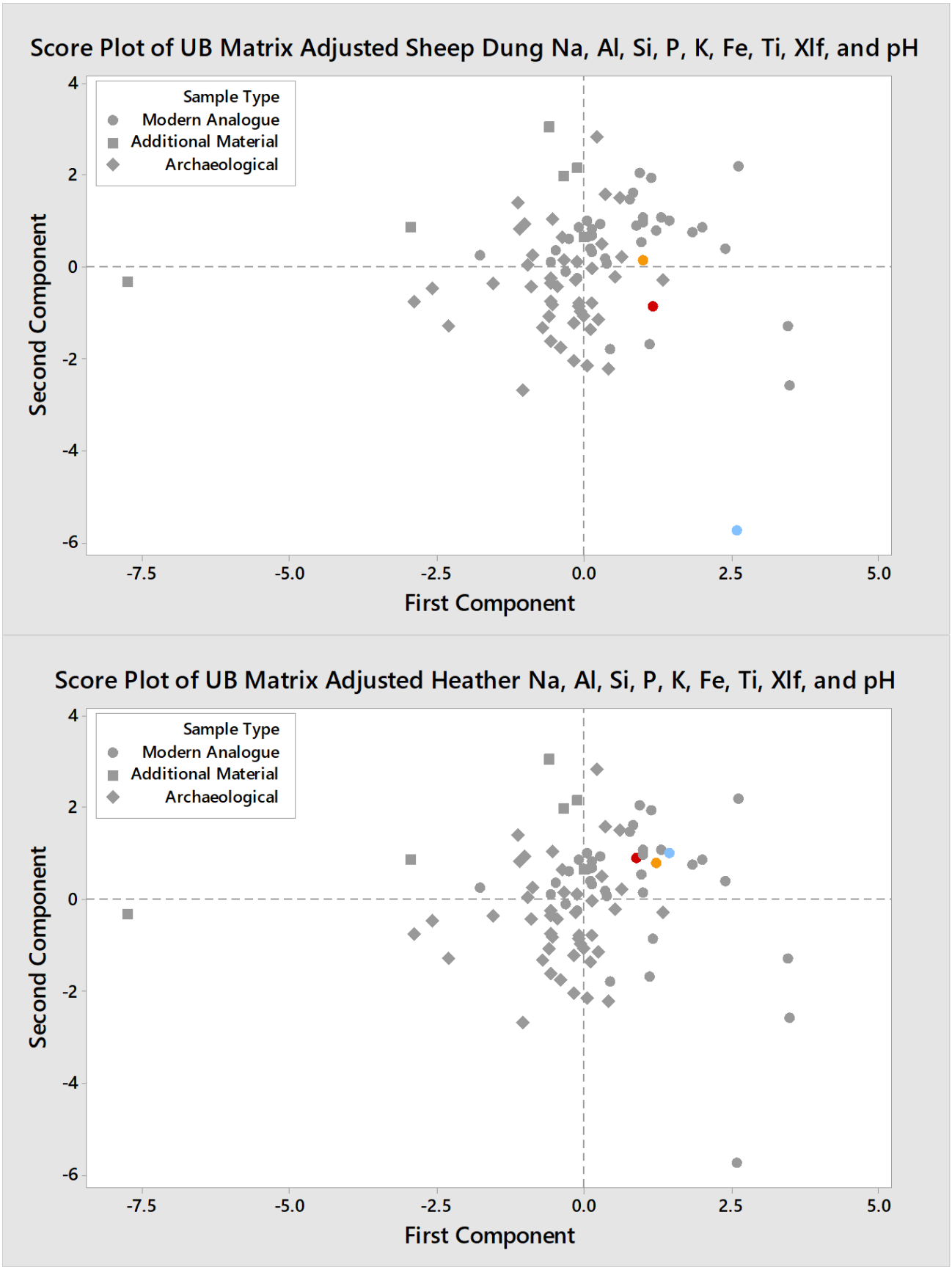

Figure 7.43 The results of the unburnt archaeological matrix adjusted principal components analysis considering all modern analogue and archaeological sample material according to nine variables sodium, aluminium, silicon, phosphorous, potassium, iron, titanium, MS and pH. The plots shown are from the top: sheep dung and heather. The heating temperature is indicated as blue for 200^{0}C, yellow for 400^{0}C, and red for 900^{0}C. Source: Author

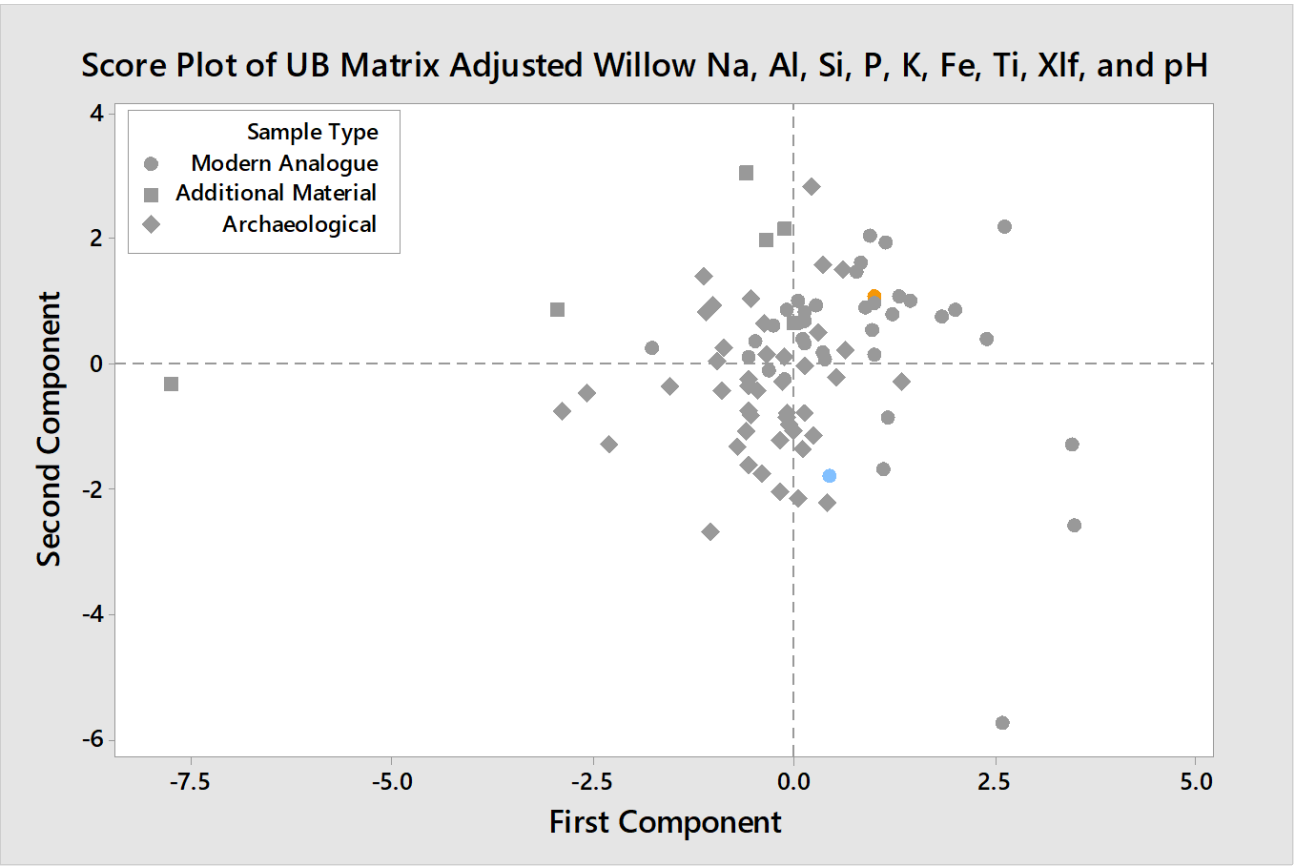

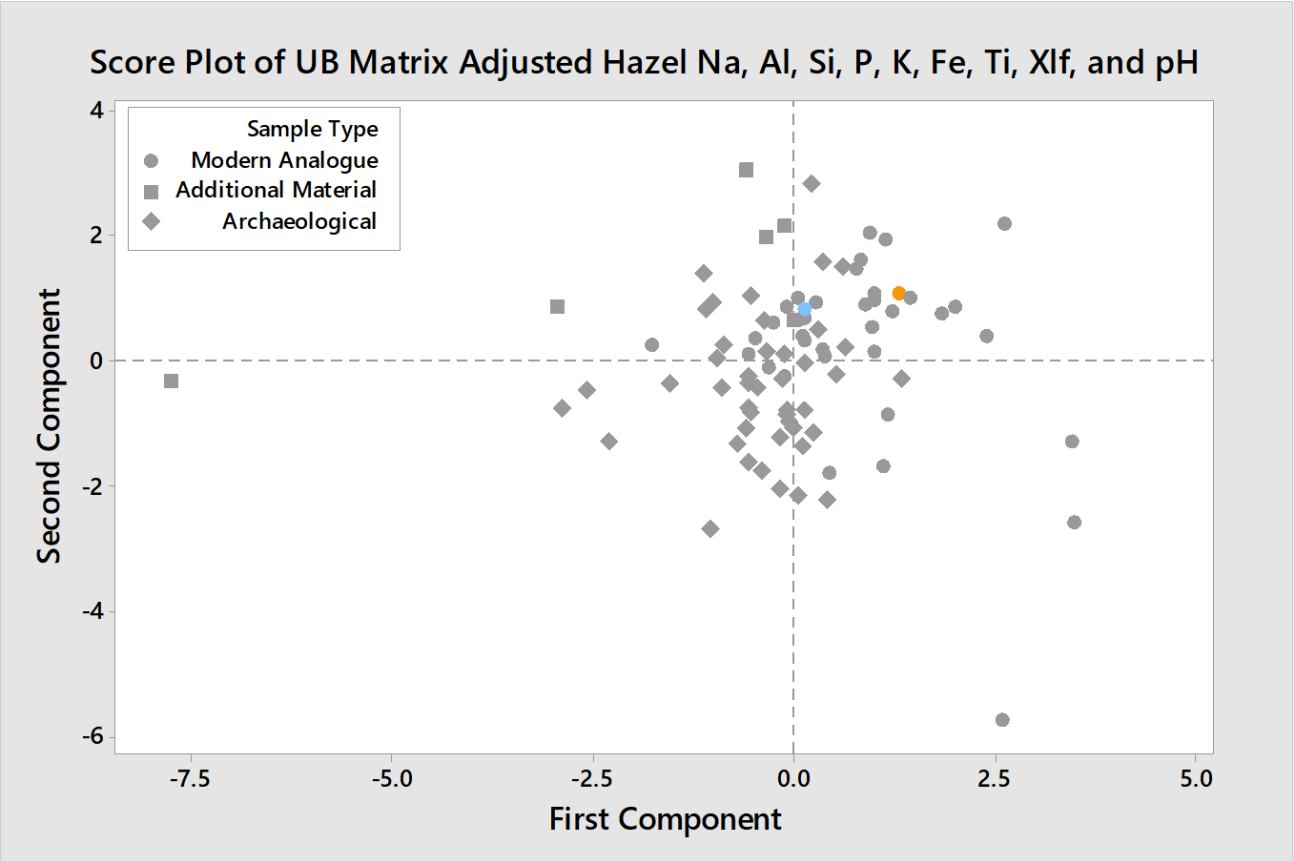

Figure 7.44 The results of the unburnt archaeological matrix adjusted principal components analysis considering all modern analogue and archaeological sample material according to nine variables sodium, aluminium, silicon, phosphorous, potassium, iron, titanium, MS and pH. The plots shown are from the top: willow and hazel. The heating temperature is indicated as blue for 200^{0}C, yellow for 400^{0}C, and red for 900^{0}C. Source: Author

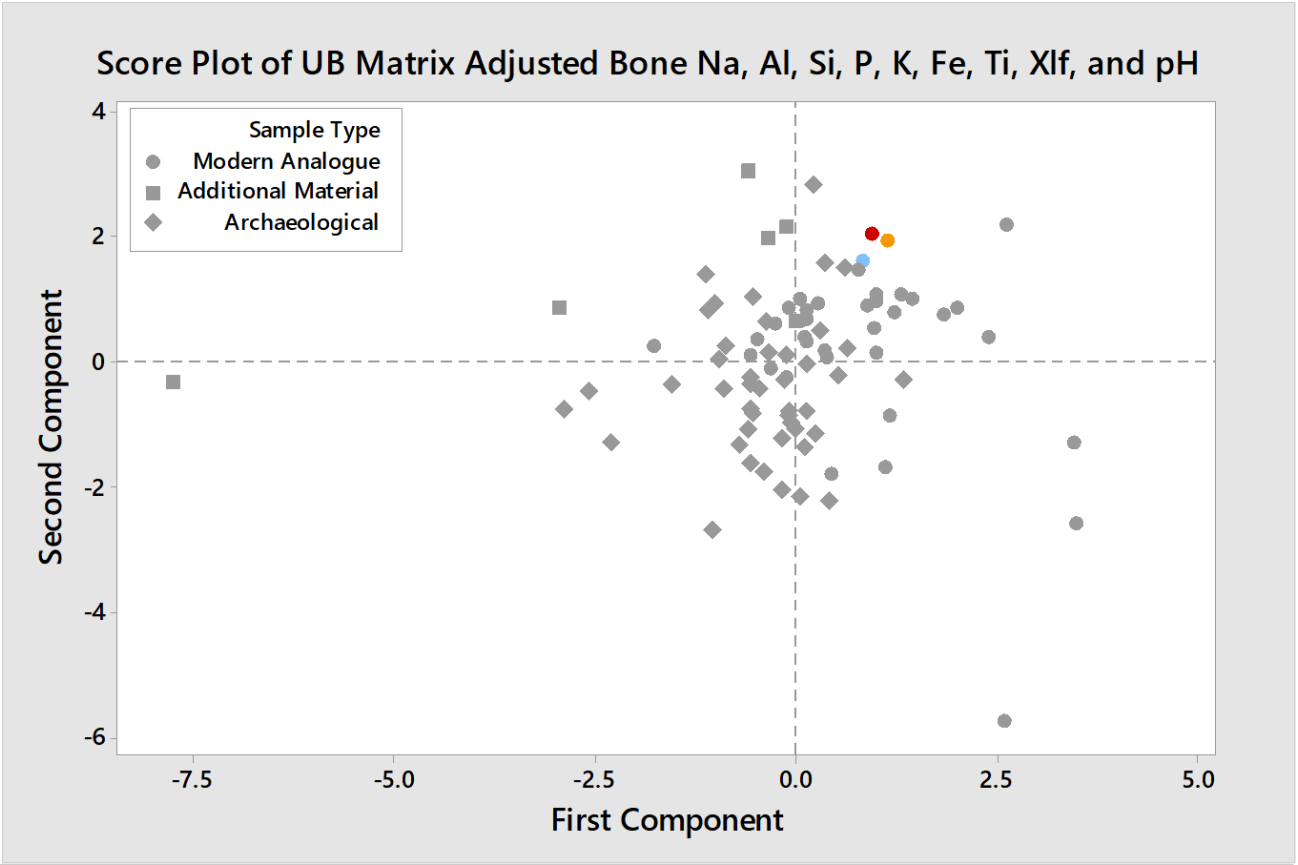

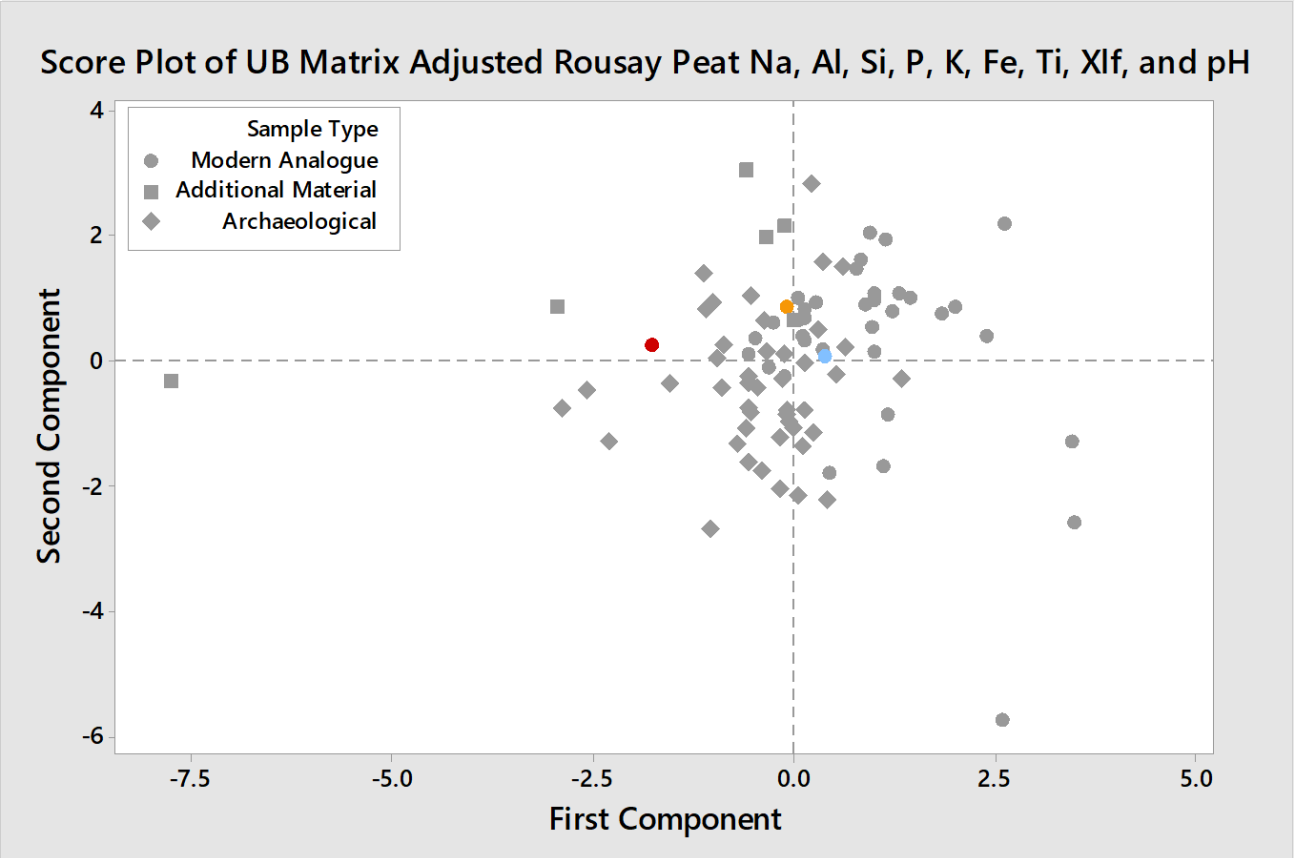

Figure 7.45 The results of the unburnt archaeological matrix adjusted principal components analysis considering all modern analogue and archaeological sample material according to nine variables sodium, aluminium, silicon, phosphorous, potassium, iron, titanium, MS and pH. The plots shown are from the top: bone and Rousay peat. The heating temperature is indicated as blue for 200^{0}C, yellow for 400^{0}C, and red for 900^{0}C. Source: Author

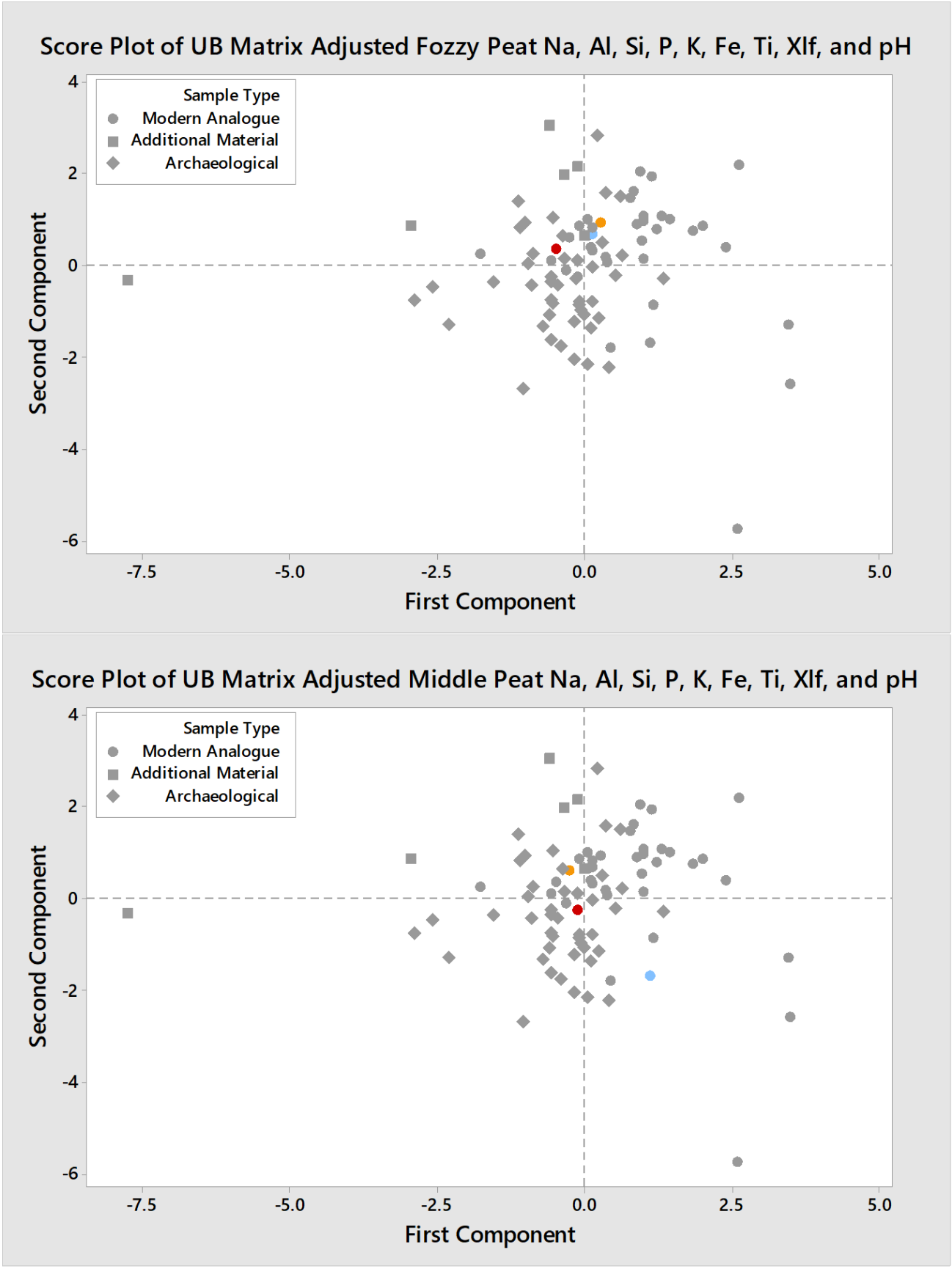

Figure 7.46 The results of the unburnt archaeological matrix adjusted principal components analysis considering all modern analogue and archaeological sample material according to nine variables sodium, aluminium, silicon, phosphorous, potassium, iron, titanium, MS and pH. The plots shown are from the top: fozzy peat and middle peat. The heating temperature is indicated as blue for 200^{0}C, yellow for 400^{0}C, and red for 900^{0}C. Source: Author

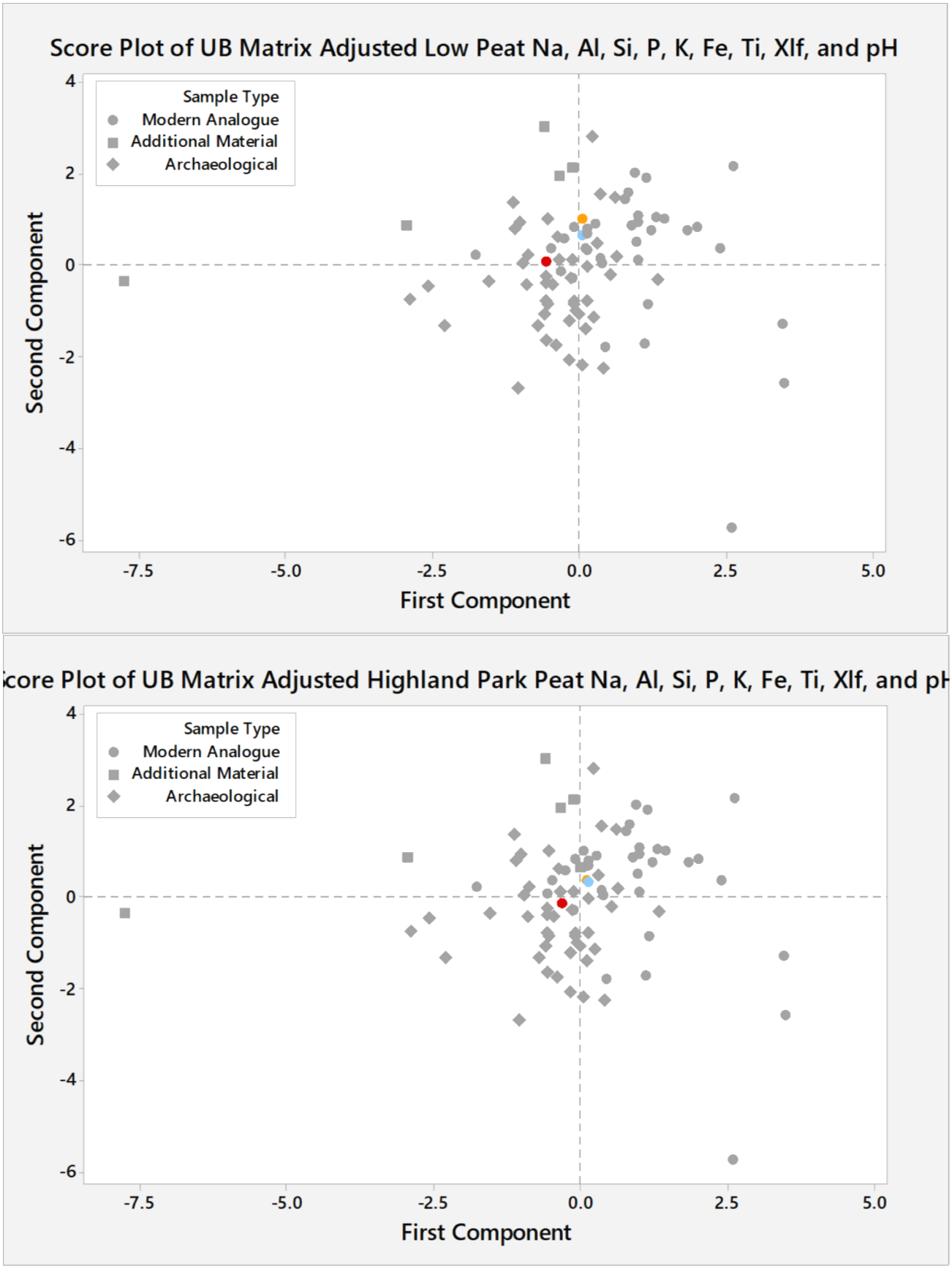

Figure 7.47 The results of the unburnt archaeological matrix adjusted principal components analysis considering all modern analogue and archaeological sample material according to nine variables sodium, aluminium, silicon, phosphorous, potassium, iron, titanium MS and pH. The plots shown are from the top: low peat and Highland Park peat. The heating temperature is indicated as blue for 200^{0}C, yellow for 400^{0}C, and red for 900^{0}C. Source: Author

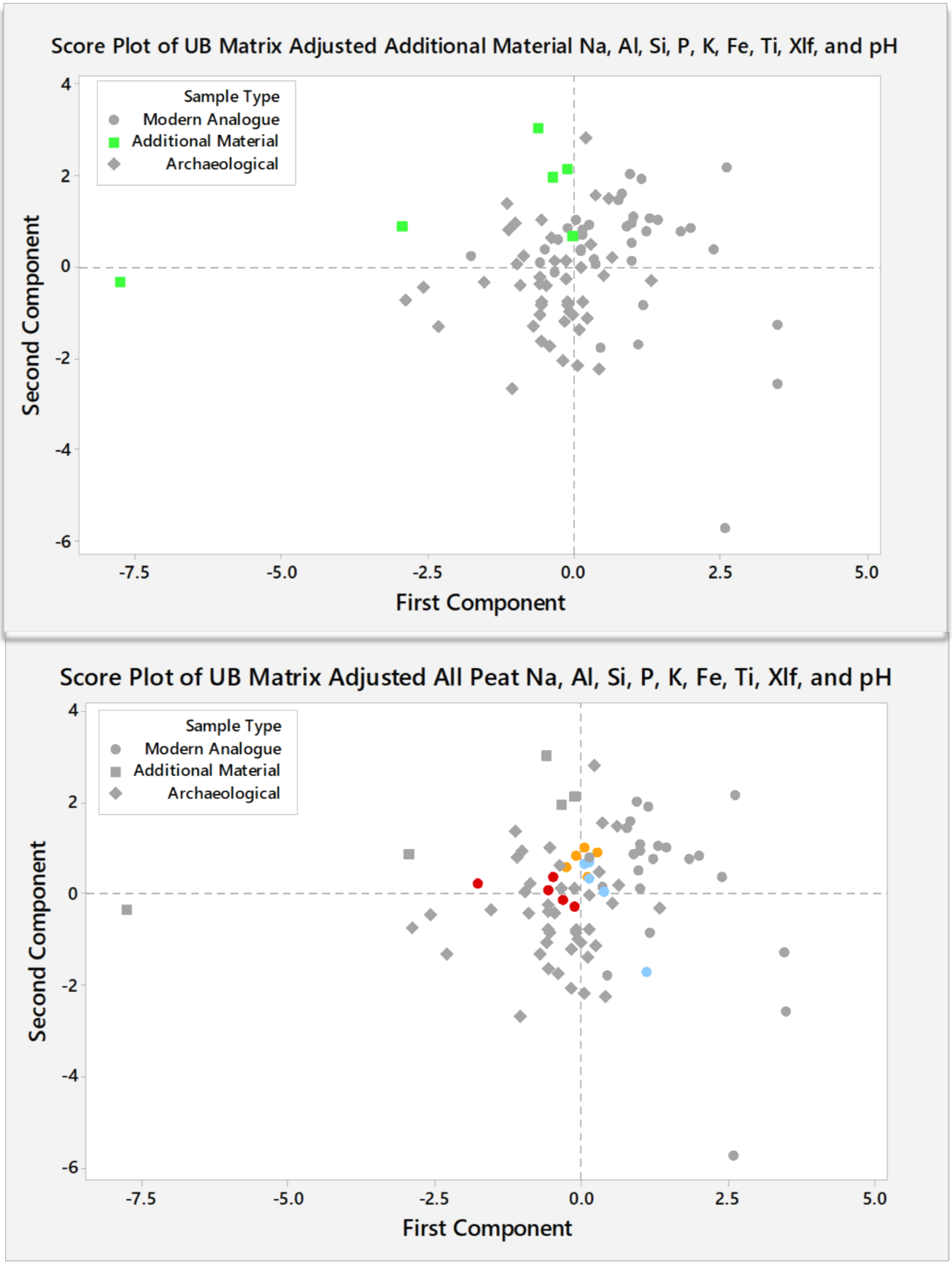

Figure 7.48 The results of the unburnt archaeological matrix adjusted principal components analysis considering all modern analogue and archaeological sample material according to nine variables sodium, aluminium, silicon, phosphorous, potassium, iron, titanium MS and pH. The plots shown are from the top: additional material and all peat. The heating temperature is indicated as blue for 200^{0}C, yellow for 400^{0}C, and red for 900^{0}C. Source: Author

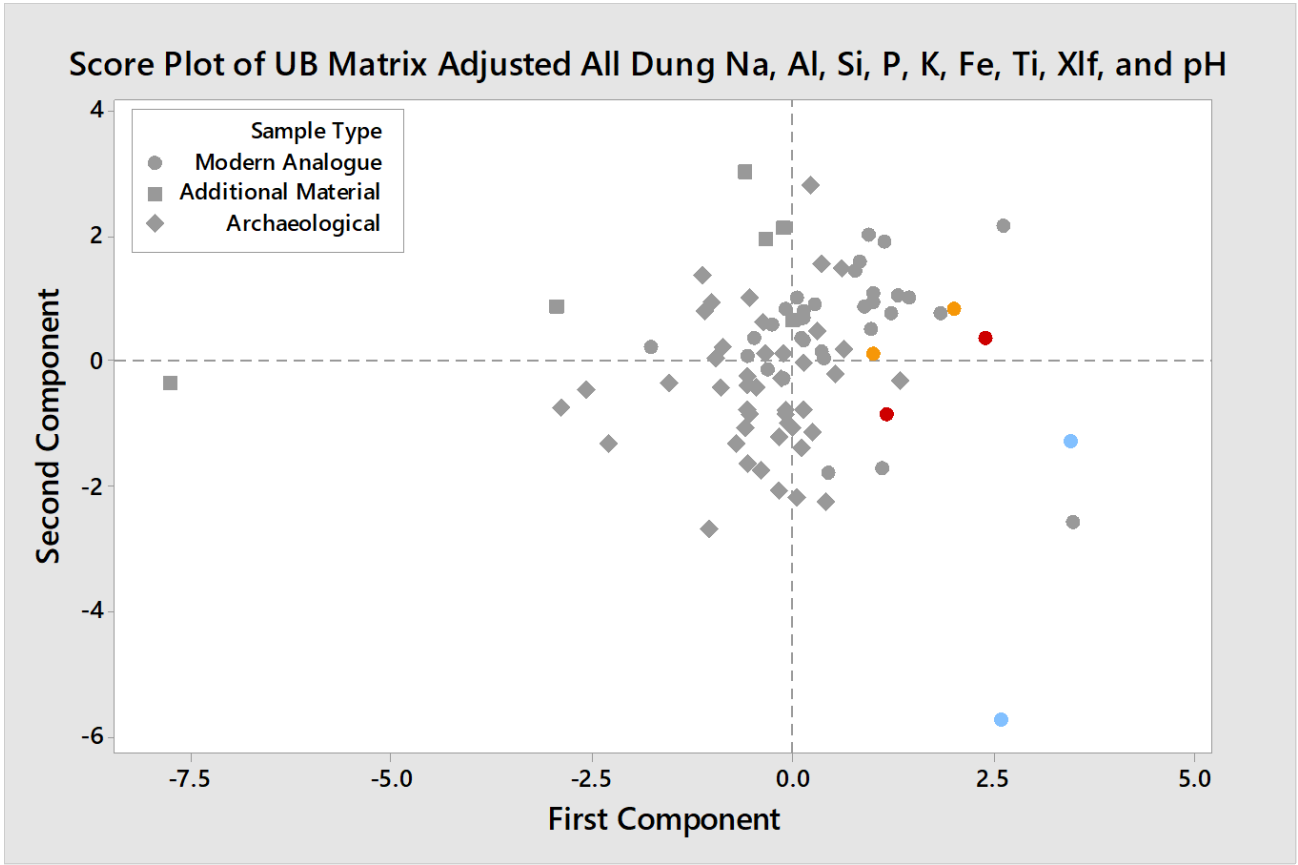

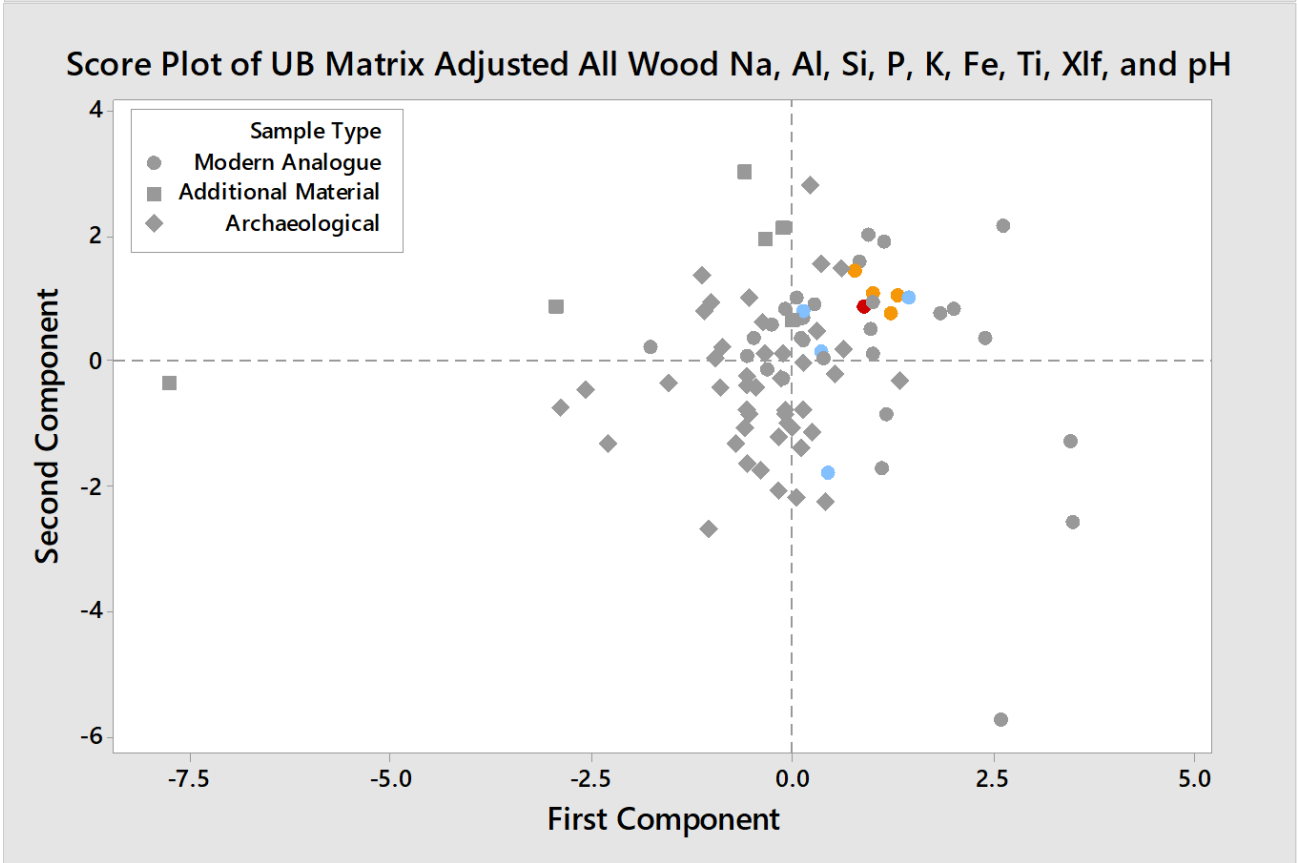

Figure 7.49 The results of the unburnt archaeological matrix adjusted principal components analysis considering all modern analogue and archaeological sample material according to nine variables sodium, aluminium, silicon, phosphorous, potassium, iron, titanium MS and pH. The plots shown are from the top: all dung and all wood. The heating temperature is indicated as blue for 200^{0}C, yellow for 400^{0}C, and red for 900^{0}C. Source: Author

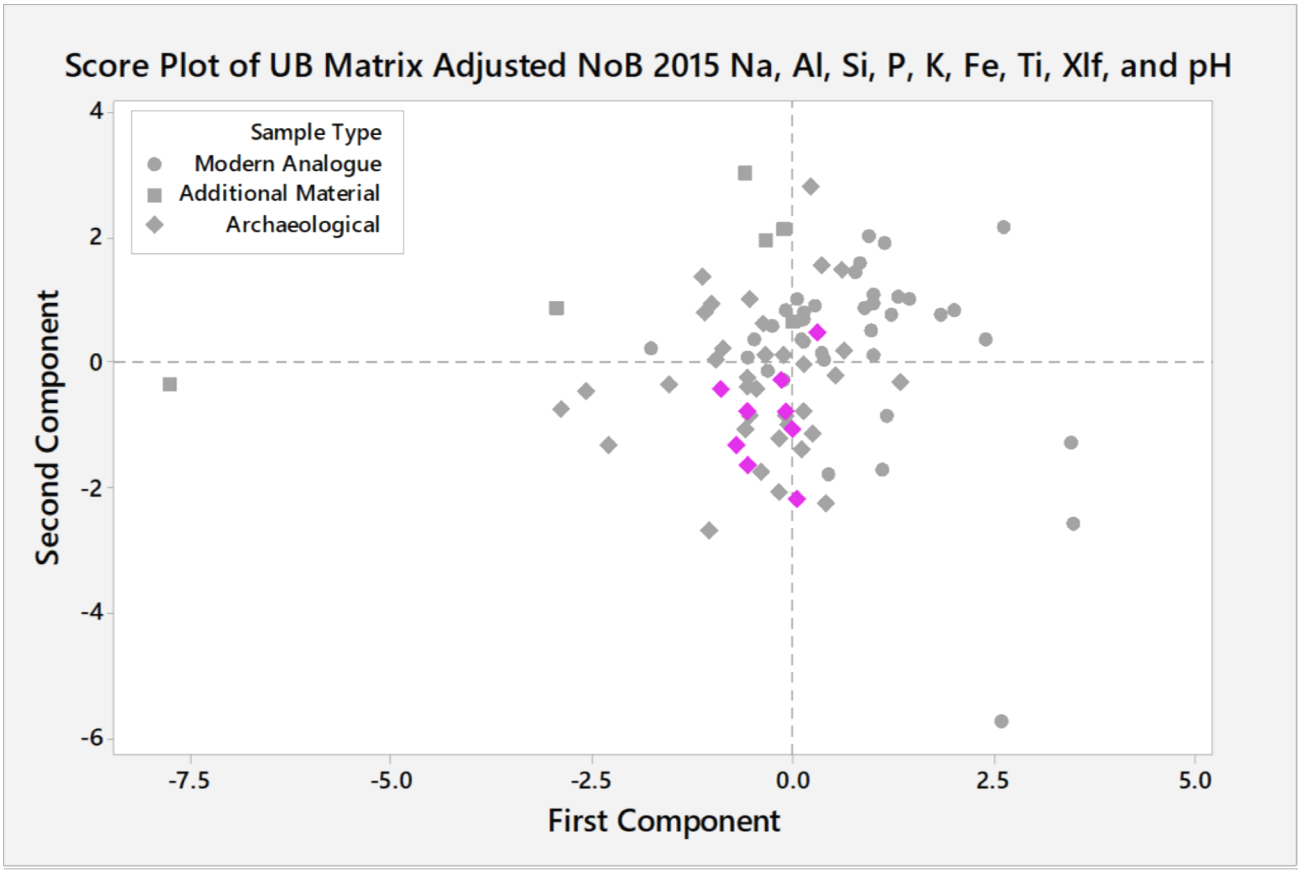

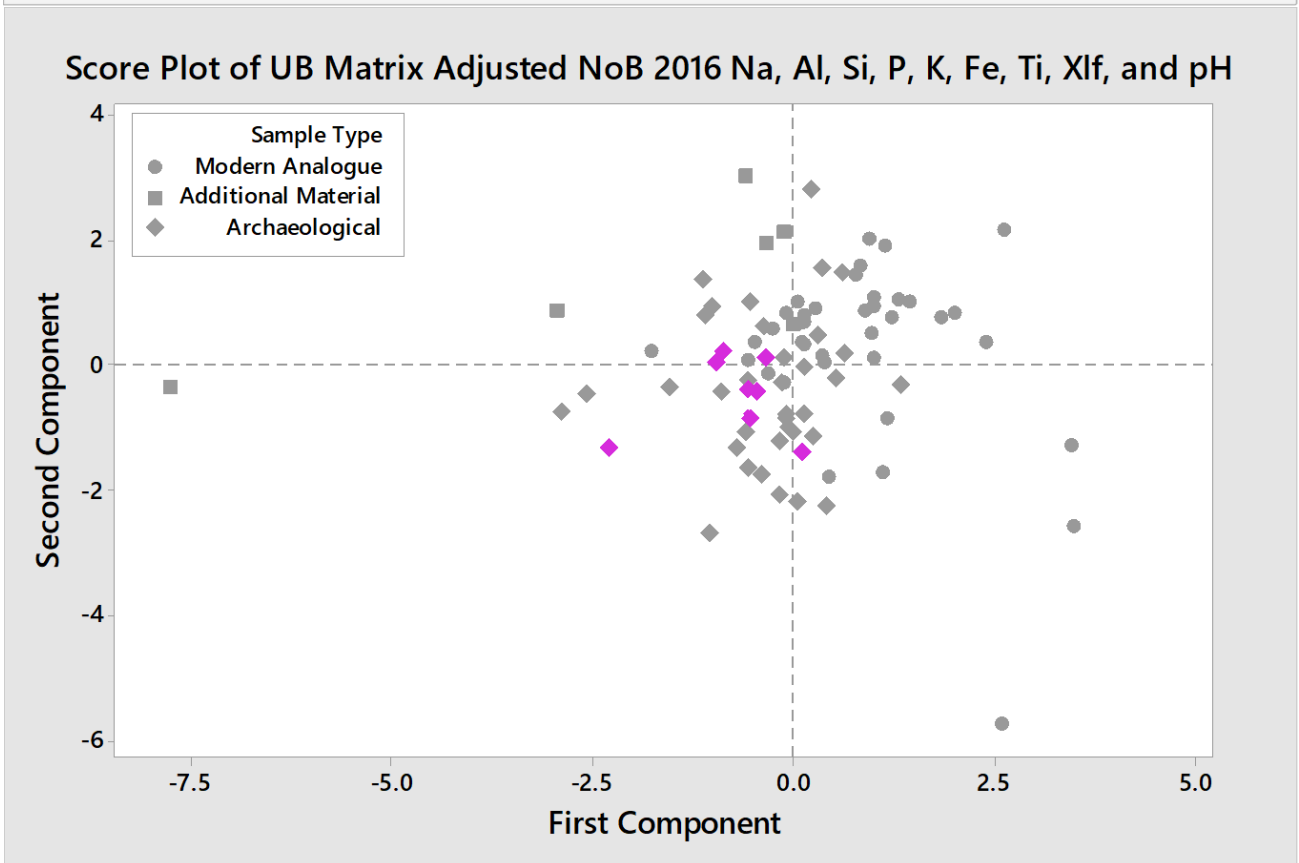

Figure 7.50 The results of the unburnt archaeological matrix adjusted principal components analysis considering all modern analogue and archaeological sample material according to nine variables sodium, aluminium, silicon, phosphorous, potassium, iron, titanium, MS and pH. The plots shown are from the top: The Ness of Brodgar 2015, The Ness of Brodgar 2016 shown in pink. Source: Author

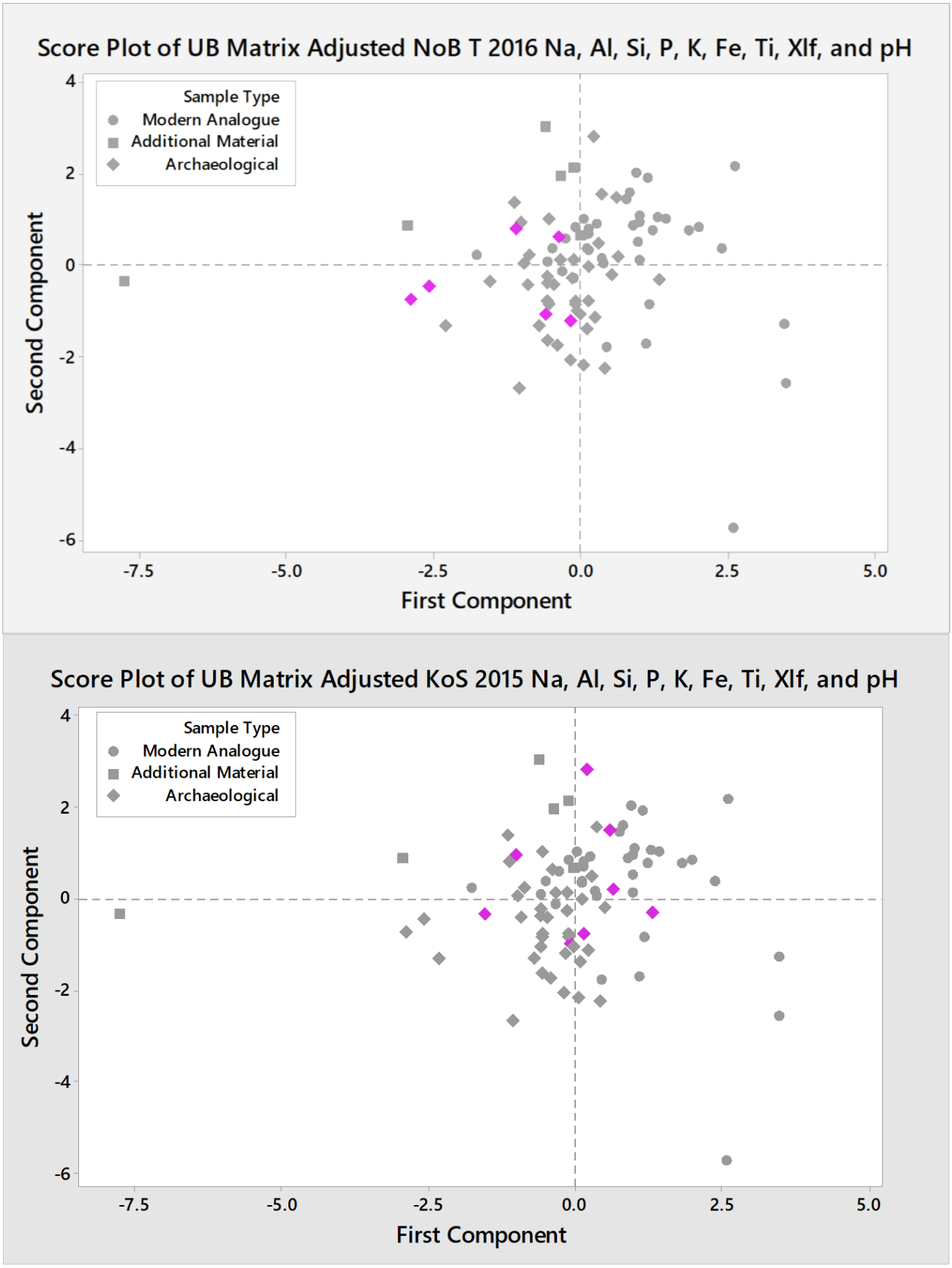

Figure 7.51 The results of the unburnt archaeological matrix adjusted principal components analysis considering all modern analogue and archaeological sample material according to nine variables sodium, aluminium, silicon, phosphorous, potassium, iron, titanium, MS and pH. The plots shown are from the top: The Ness of Brodgar Trench T 2016 and The Knowe of Swandro 2015 shown in pink. Source: Author

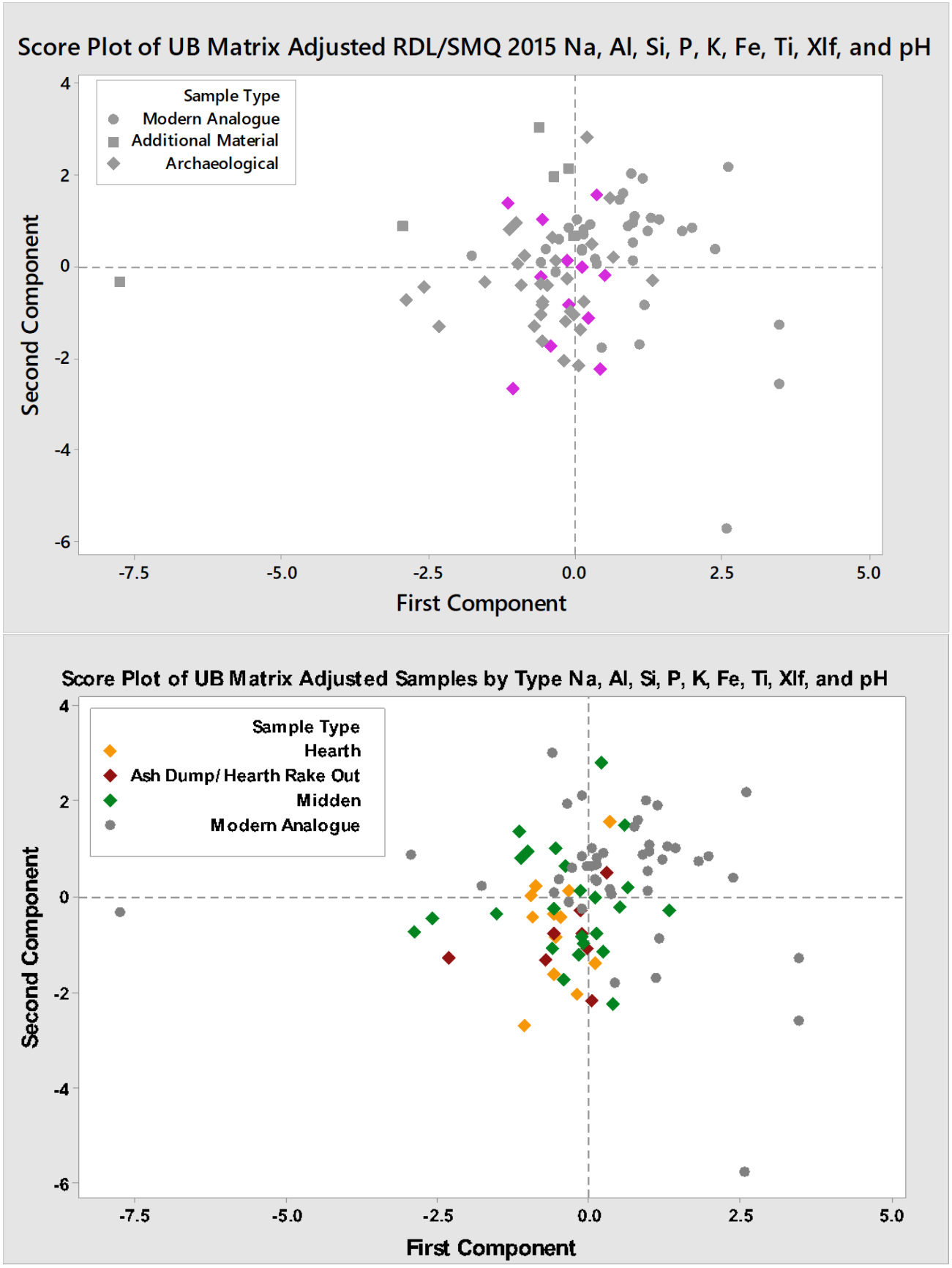

Figure 7.52 The results of the unburnt archaeological matrix adjusted principal components analysis considering all modern analogue and archaeological sample material according to nine variables sodium, aluminium, silicon, phosphorous, potassium, iron, titanium, MS and pH. The plots shown are from the top: Smerquoy/Muckquoy 2015 shown in pink , and all archaeological samples considered by sample type shown in yellow for hearth, red for ash dump/hearth rake out, and green for midden. Source: Author

7.4.3 Considering the SEM images to confirm fuel matches

The SEM images allow comparison of the samples in great detail, but are limited to a monochromatic format. The samples structures can be compared to add further corroboration to the PCA fuel match assignments. From the SEM images it appears that the samples do show visual similarities to the PCA assigned matches. With the samples that only match to one fuel it is still evident that the archaeological samples bear more similarity to one of the compared modern samples; this is seen with NoB 3851 and fozzy peat 900^{0}C and NoB 4674 and middle peat 900^{0}C (figure 8.5). There are very clear differences visually between different samples of the same fuel type as seen with the images of Rousay peat, fozzy peat, middle peat and Highland Park peat. This is due to the levels of formation explained in section 4.2 and the different plant materials that formed the peat from different areas such as heather for the highland park peat and turf for the peat collected from the Corrigall farm house museum. The samples that match to more than one fuel show similarities to attributes of both modern fuels when compared visually. This is evident in KoS 3217 that matches to fozzy peat 900^{0}C and sheep dung 900^{0}C and RDL 032 that matches Rousay peat 200^{0}C and driftwood 400^{0}C. The samples that match to animal bone and driftwood (KoS 3201 & SMQ B) have much more resemblance to driftwood 400^{0}C, and only have one or two inclusions that look like the animal bone. Although there are also limitations to what the magnified images can definitively say, they are still useful for comparing samples in much finer detail than with using a traditional microscope.

SEM images summary plot		
Rousay peat 900^{0}C	NoB 3851	Fozzy peat 900^{0}C
Highland park peat 900^{0}C	NoB 4674	Fozzy peat 900^{0}C
Fozzy peat 900^{0}C	KoS 3217	Sheep dung 900^{0}C
Animal bone 200^{0}C	KoS 3081	Driftwood 400^{0}C
Rousay peat 200^{0}C	RDL 032	Driftwood 400^{0}C
Animal bone 200^{0}C	SMQ B	Driftwood 400^{0}C

Table 7.6 Summary table of SEM images of archaeoligcal and modern analogue materials compared in figure 7.31. Source: Author.

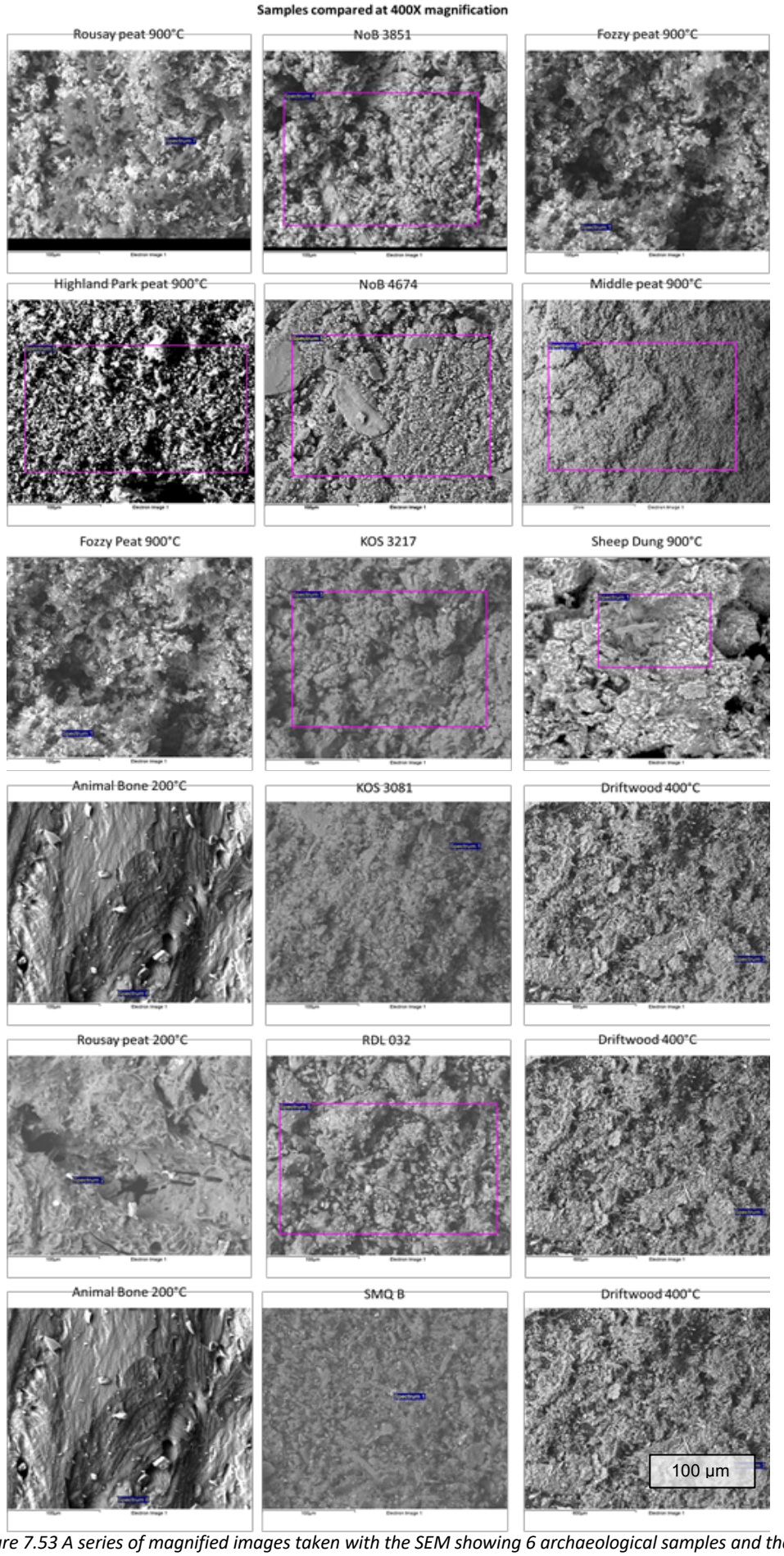

Figure 7.53 A series of magnified images taken with the SEM showing 6 archaeological samples and their possible matches assigned with PCA. The archaeological samples are in the center column flanked by the possible modern fuel matches on either side. 100 µm scale (bottom right) Source: Author.

7.4.4 Conclusions

It is abundantly clear that the archaeological sample material has a strong association with the ashes from modern analogue peat fuels. There are also several samples that show similarities to sheep dung, willow, driftwood, and bone. There are some discrepancies between the matches according to the analytical results and the matches assigned through PCA. These differences in fuel match assignment can be caused by the varying degree of contamination in the archaeological material or the methods used to account for it as discussed in sections 2.2, 2.4, and 7.4.2. Out of 43 samples, 31 of the matches are concurrent between the two matching methods. There are 6 matches that are not in agreement between the 2 datasets NoB 3783, NoB16 6346, KoS 3081, RDL 031, RDL 016, and SMQ B (table 7.6). In addition, 6 samples are unidentified by one of the methods making comparison impossible for those results.

There are unique fuel use trends among each site according to the results of the matching. The Ness of Brodgar samples show matches to predominantly peat fuels heated to 900^0C except for NoB 3783 and NoB16 6346 that match willow at 200^0C. The Knowe of Swandro material matches to both peat and sheep dung at 400^0C and 900^0C, driftwood at 400^0C, and bone heated to 200^0C. The Smerquoy/Muckquoy samples match peat between 200^0C and 900^0C, driftwood at 400^0C, and willow and bone heated to 200^0C (table 7.7). There are some changes in fuel use within archaeological sites, but these differences are between different structures and features not within them. This could be indicative of different fuels being used for different functional purposes or different time periods of use. Fires used for different purposes require

different fuels and burn at varying temperatures as discussed in sections 2.3 and 2.4.

PCA and Analytical Method Fuel Match Table		
Sample number and type	**Analytical Fuel Match**	**PCA Fuel Match**
NoB 2617 hearth rake out	Peat 900^{0}C	Peat 200^{0}C
NoB 3851 hearth rake out	Peat 400^{0}C to 900^{0}C	Peat 900^{0}C
NoB 3857 hearth rake out	Peat 400^{0}C to 900^{0}C	Peat 900^{0}C
NoB 4264 ash dump	Peat 900^{0}C	Unidentifiable
NoB 4656 hearth	Peat 900^{0}C	Unidentifiable
NoB 4674 hearth	Peat 900^{0}C	Peat 900^{0}C
NoB 5332 ash dump	Peat 400^{0}C to 900^{0}C	Peat 900^{0}C
NoB 6156 ash dump	Peat 900^{0}C	Peat 900^{0}C
NoB 5013 hearth	Peat 900^{0}C	Unidentifiable
NoB 3783 ash dump	Peat & Sheep dung 400^{0}C	Willow 200^{0}C
NoB16 3851 hearth rake out	Peat 400^{0}C to 900^{0}C	Peat 900^{0}C
NoB16 6339 hearth	Peat 900^{0}C	Peat 900^{0}C
NoB16 6346 hearth	Peat 900^{0}C	Willow 200^{0}C
NoB16 6348 hearth	Peat 900^{0}C	Peat 900^{0}C
NoB16 6351 hearth	Peat 900^{0}C	Peat 900^{0}C
NoB16 6354 hearth	Peat 900^{0}C	Peat 900^{0}C
NoB16 6355 hearth	Peat 900^{0}C	Peat 900^{0}C
NoB16 6356 hearth	Peat 900^{0}C	Peat 900^{0}C
NoB T 4825 midden	Peat 900^{0}C	Peat 900^{0}C
NoB T 4831 midden	Peat 900^{0}C	Peat 900^{0}C
NoB T 4860 midden	Peat 900^{0}C	Peat 900^{0}C
NoB T 5810 midden	Peat 900^{0}C	Peat 400^{0}C
NoB T 5849 midden	Peat 900^{0}C	Peat 900^{0}C
NoB T 5855 midden	Peat 900^{0}C	Peat 900^{0}C
KoS 2039 hearth	Peat 900^{0}C	Peat 400^{0}C
KoS 3081 midden	Peat & Sheep dung 400^{0}C to 900^{0}C	Driftwood 400^{0}C and Bone 200^{0}C
KoS 3196 midden	Peat & Sheep dung 900^{0}C	Peat 900^{0}C
KoS 3201 midden	Peat 400^{0}C to 900^{0}C	Unidentifiable
KoS 3217 midden	Peat & Sheep dung 900^{0}C	Peat 200^{0}C & Sheep Dung 400^{0}C
KoS 3225 midden	Peat 900^{0}C	Peat 900^{0}C
KoS 3238 midden	Peat 400^{0}C to 900^{0}C	Sheep dung 900^{0}C
KoS 3255 midden	Peat 400^{0}C to 900^{0}C	Peat 900^{0}C
RDL 031 midden	Peat 400^{0}C	Willow 200^{0}C
RDL 001 midden	Unidentifiable	Peat 400^{0}C
RDL 004 midden	Peat 400^{0}C	Peat 900^{0}C
RDL 006 midden	Peat 900^{0}C	Peat 900^{0}C
RDL 009 midden	Peat 400^{0}C	Peat 200^{0}C
RDL 007 midden	Peat 400^{0}C	Peat 200^{0}C & Peat 400^{0}C
RDL 013 midden	Peat 400^{0}C	Unidentifiable
RDL 016 midden	Peat 400^{0}C	Willow 200^{0}C
RDL 023 midden	Peat 900^{0}C	Peat 400^{0}C
RDL 032 midden	Peat 400^{0}C	Peat 200^{0}C & Driftwood 400^{0}C
SMQ A hearth	Peat 900^{0}C	Unidentifiable
SMQ B hearth	Peat 900^{0}C	Driftwood 400^{0}C and Bone 200^{0}C

Table 7.7 A table comparing the analytical fuel matches and the PCA fuel matches between modern analogue and archaeological samples. Source: Author

Chapter 8 Conclusions

8.1 Introduction

This research has produced and analysed modern ash to develop an approach for identifying archaeological fuels. The framework of this research was introduced in chapter 1, and the background to the key concepts were discussed in chapter 2. The analytical methods and the parameters chosen were done so with consideration to extensive literature review of multiple fields of science including archaeology, fuels, and soil pollution as presented in chapter 3. This approach was then tested by investigating the fuel use among the archaeological excavation sites at Ness of Brodgar, Knowe of Swandro, and Smerquoy/Muckquoy in Orkney using the data from the modern analogue analysis to inform the identification of archaeological fuels that was presented in chapter 4. The methods used to carry out the ash production and subsequent analyses were explained in chapter 5. The results of the modern analogue and archaeological sample analyses have been presented in chapter 6, and the implications of these findings and the matches between archaeological samples and modern analogue fuels have been discussed throughout chapter 7.

The following presents the conclusions of this investigation with consideration to the initial research questions presented in section 1.3. The research questions were used to guide this investigation and provide the most effective approach for identifying archaeological fuels using comparison to modern analogues. Answering the research questions will not only provide a comprehensive conclusion to the research, but will also demonstrate that the objectives of this project have been met. The objectives were set to ensure that the aims were realised.

8.2 What changes do fuels go through during the burning process?

Observing and recording the changes to fuels through increasing temperature intervals demonstrates the characteristic differences that are related to heating temperature. At different temperatures and durations of burning, fuels are affected differently as shown in section 6.2. At lower temperatures the organic material is not completely burned away during combustion, leaving higher concentrations of organic material in fuel ash exposed to lower temperatures. As the temperature is intensified the chemical reaction of combustion consumes more of the organic material producing heat, light, and exhaust as they are burned leaving a higher proportion of minerals among the ash. The main constituents of the ash are sodium, magnesium, aluminium, silicon, potassium, calcium, iron, and titanium. The minerals that remain contribute heavily to the magnetic susceptibility and pH measurements. The iron, titanium, and aluminium contribute to the magnetism of the ash, and the sodium, magnesium, potassium, and calcium contribute to the pH of the ash material. This is evident with the rise of MS and pH that is shown to be associated with increase in heating temperature (figure 8.1).

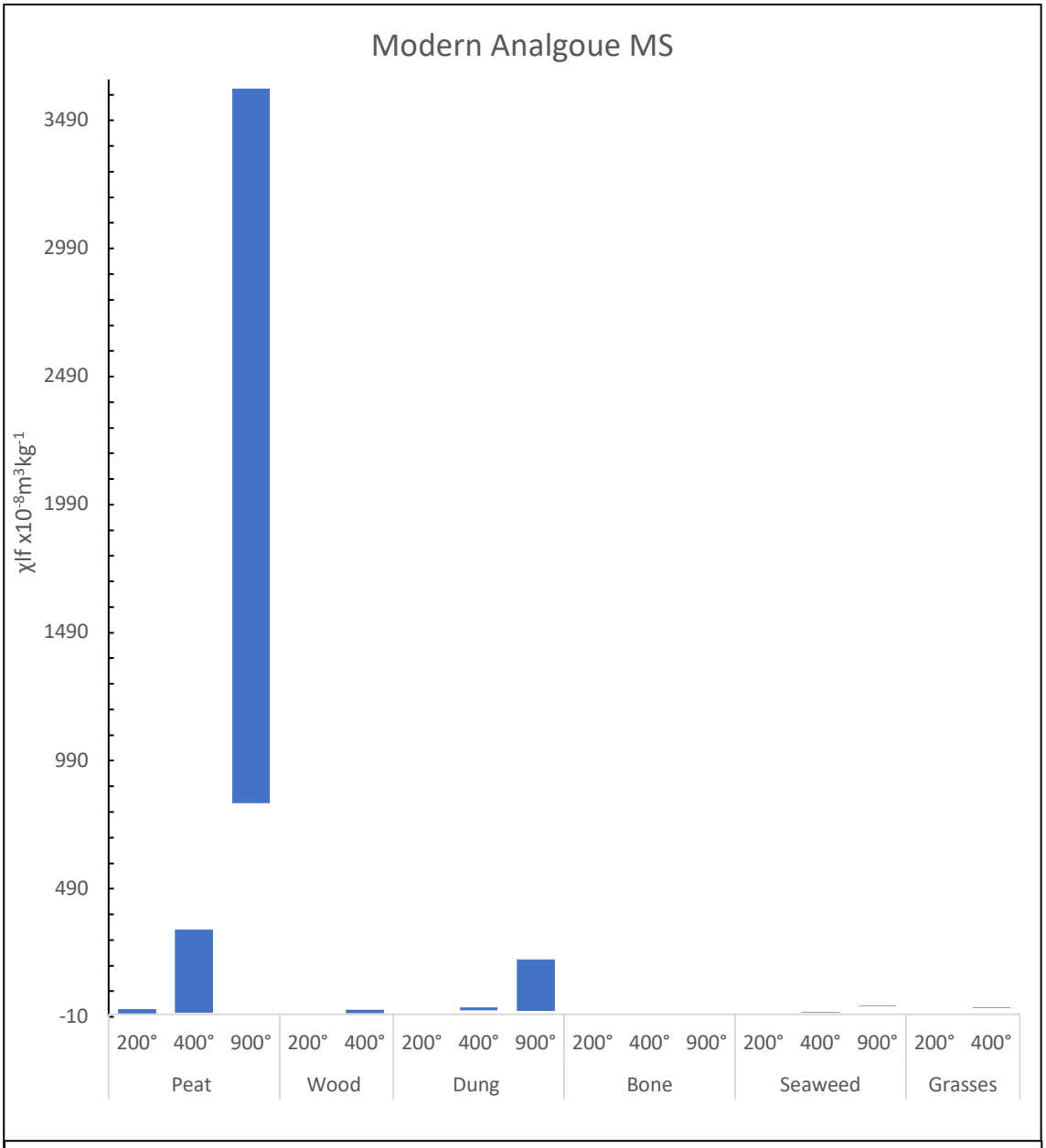
Modern Analgoue MS
3490
2990
2490
1990
1490
990
490
-10
χlf x10-8m3kg-1
200° 400° 900° 200° 400° 200° 400° 900° 200° 400° 900° 200° 400° 900° 200° 400°
Peat
Wood
Dung
Bone
Seaweed
Grasses

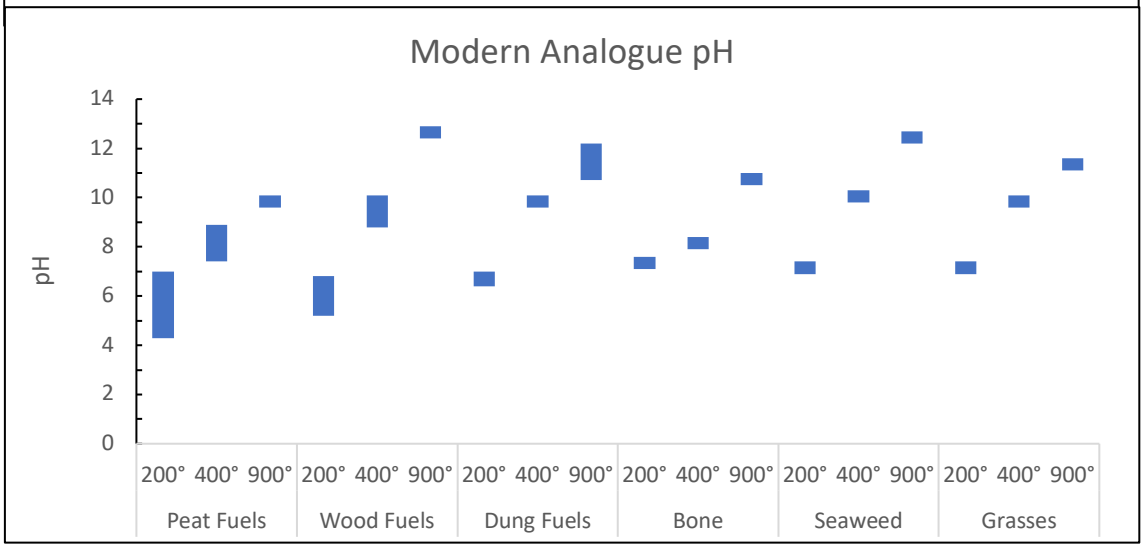
Modern Analogue pH
14
12
10
8
6
4
2
0
pH
200° 400° 900° 200° 400° 900° 200° 400° 900° 200° 400° 900° 200° 400° 900° 200° 400° 900°
Peat Fuels
Wood Fuels
Dung Fuels
Bone
Seaweed
Grasses

8.3 What markers present in modern analogue ash are indicative of fuel sources within archaeological deposits?

As discussed in section 7.2, as the heating temperature increases more of the organic material within the fuel is burned away causing the mineral content to be altered which increases the magnetism and alkalinity associated with elements such as iron, titanium, and aluminium, and sodium, calcium, potassium, and magnesium respectively. The levels of these elements are characteristic for identifying fuel types seen in the results with the peat fuels having high magnesium, iron and titanium levels, the bone having high calcium and phosphorous, the seaweed and driftwood having high sodium, the dung having high levels of aluminium, silicon, and potassium; and the wood fuels having low abundances of elements overall (figure 8.2). This is also evident with the colour of samples, with red and yellow colouring of ashes being indicative of peat and brown and grey being an identifier of wood fuels (table 8.1). The elemental data is not as useful when considering functional temperature as magnetic susceptibility and pH measurements.

Summery table of fuel type identification characteristics				
Fuel type	**MS**	**pH**	**Elements**	**Colour**
Peat	High MS	Alkaline	Mg, Fe, Ti,	Yellow - Red
Wood	Low MS	High alkaline	Low abundance	Brown - Grey
Dung	Medium MS	Alkaline	Al, Si, K	Red – Brown - Grey
Bone	Diamagnetic	Alkaline	Ca, P	Yellow – Brown - Grey – White
Seaweed	Low MS	High alkaline	Na	Brown – Yellow - Grey
Grasses	Low MS	Alkaline	Si, K	Grey

Table 8.1 Summary table of the identification characteristics of modern analgoues organised by fuel type. Source: Author.

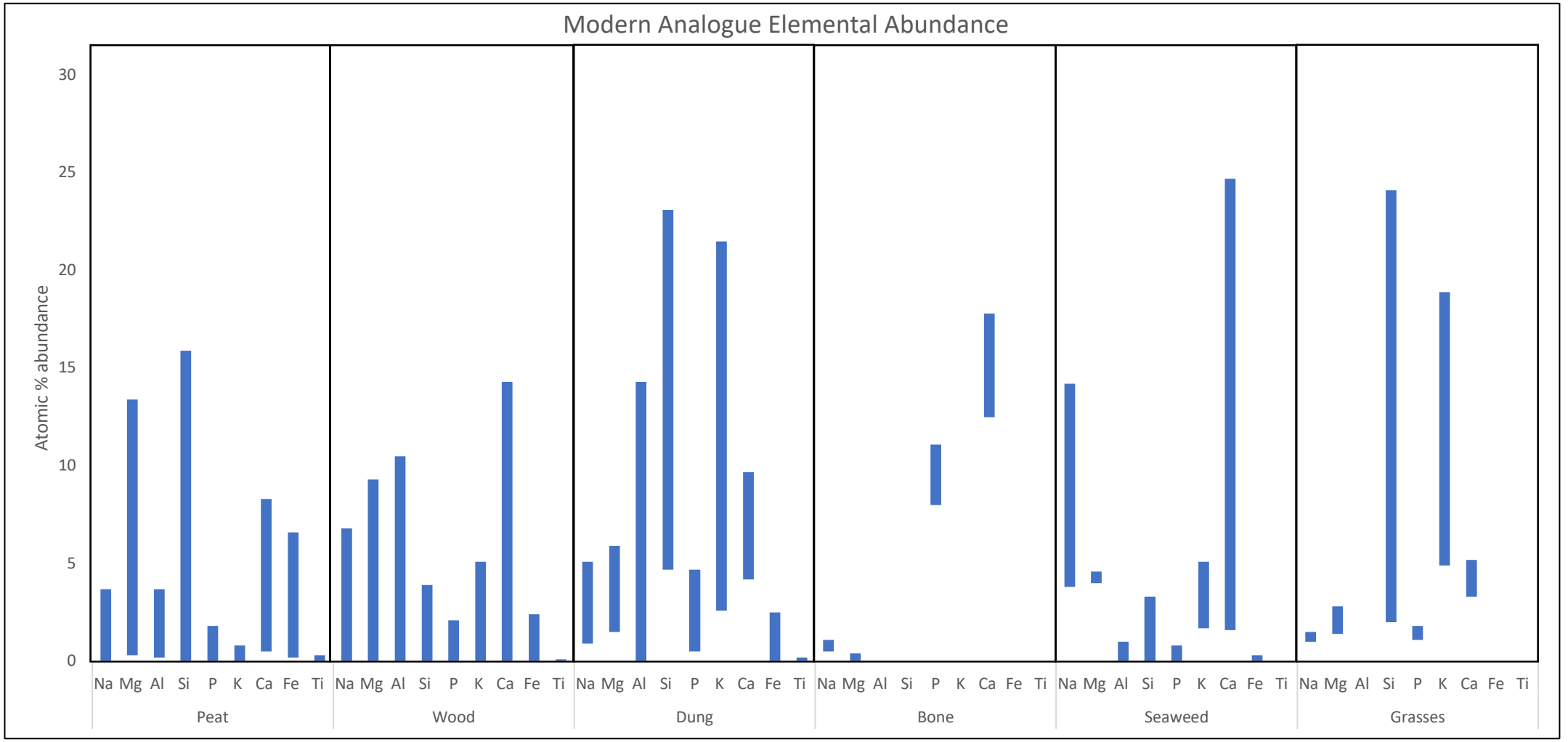

Figure 8.2 Summary plots of the ranges of elemental abundance of modern analogue fuels at 200^{0}C, 400^{0}C, and 900^{0}C organised by fuel type. Source: Author.

8.4 Can changes in fuel use be detected? between sites, within sites, and over time?

Different fuels and functional temperatures can be identified using this method of comparison between archaeological and modern analogue samples. As seen with the matching results from this research, each site investigated has a distinct pattern of fuel use. High temperature exposed peat (900^0C) is the predominant match among the Ness of Brodgar samples. Peat, sheep dung, driftwood, and bone heated between 400^0C and 900^0C is identified among the Knowe of Swandro samples. Peat, willow, driftwood, and bone heated between 200^0C and 400^0C match the Smerquoy/Muckquoy samples (figure 8.3). The differences in fuel type and functional temperature matches between sites, and in some instances between structures or features within sites, shows that changes in fuel use are identifiable using this method. This is evident in the fuel matches from The Knowe of Swandro structure 3 samples transitioning from wood and bone to peat to an unidentifiable sample to peat then to dung and finally back to peat again, and the Smerquoy samples that match to wood and then to peat in the next context.

Hearth samples provide the best means to investigate changes in fuel use within a site, given that hearth samples are sequential when considered in stratigraphic order. Any difference in fuel match within the sequence of hearth deposits would indicate a change in fuel use. This is shown within the data, among the Ness of Brodgar material there are 9 samples from the same western hearth in structure 8 as described in section 4.4. Within the stratigraphic sequence of this hearth feature, the upper most horizon NoB15 4656 is unidentifiable according to the PCA, and NoB16 6346 which is in the middle of the stratigraphic sequence within the hearth feature matches to willow heated to 200^0C. This shows that of the samples from this hearth 78% match

the same fuels. This would indicate that within the sequence of the deposits there are two horizons associated to burning instances using fuels other than peat. This would indicate a change in fuel use for those two samples within the hearth feature. The samples from Smerquoy show a difference in fuel use between structures, SMQ A is unidentifiable according to the PCA and SMQ B matches in between two modern analogues indicating a mix of the two fuels driftwood heated to 400^0C and bone heated to 200^0C.

To confidently identify changes in fuel use among discrete features within sites, it is necessary to use hearth samples. Midden samples are of unknown origin concerning where and how the ash was produced making it impossible to determine changes within a distinct combustion feature. Midden samples can offer insight into fuel use among the site as a whole, but cannot be used to identify fuel use trends in chronologic sequence regarding a single combustion feature.

The results of this examination show that it is possible to not only identify fuels from archaeological samples, but it is possible to infer changes to the fuel resource regimes based on changes to fuel matches. It is possible to identify differences in fuel use within a hearth feature and between hearths in different structures within a site as shown with the results from the Ness of Brodgar and Smerquoy respectively. In addition, it is possible to identify differences in fuel use patterns between different excavation sites. This is shown in the results with the Ness of Brodgar matching mostly 900^0C peat samples, the Knowe of Swandro matching peat, dung, driftwood, and bone samples heated between 400^0C and 900^0C, and Smerquoy/Muckquoy matching peat, driftwood, willow, and bone heated between 200^0C and 400^0C (figure 8.3).

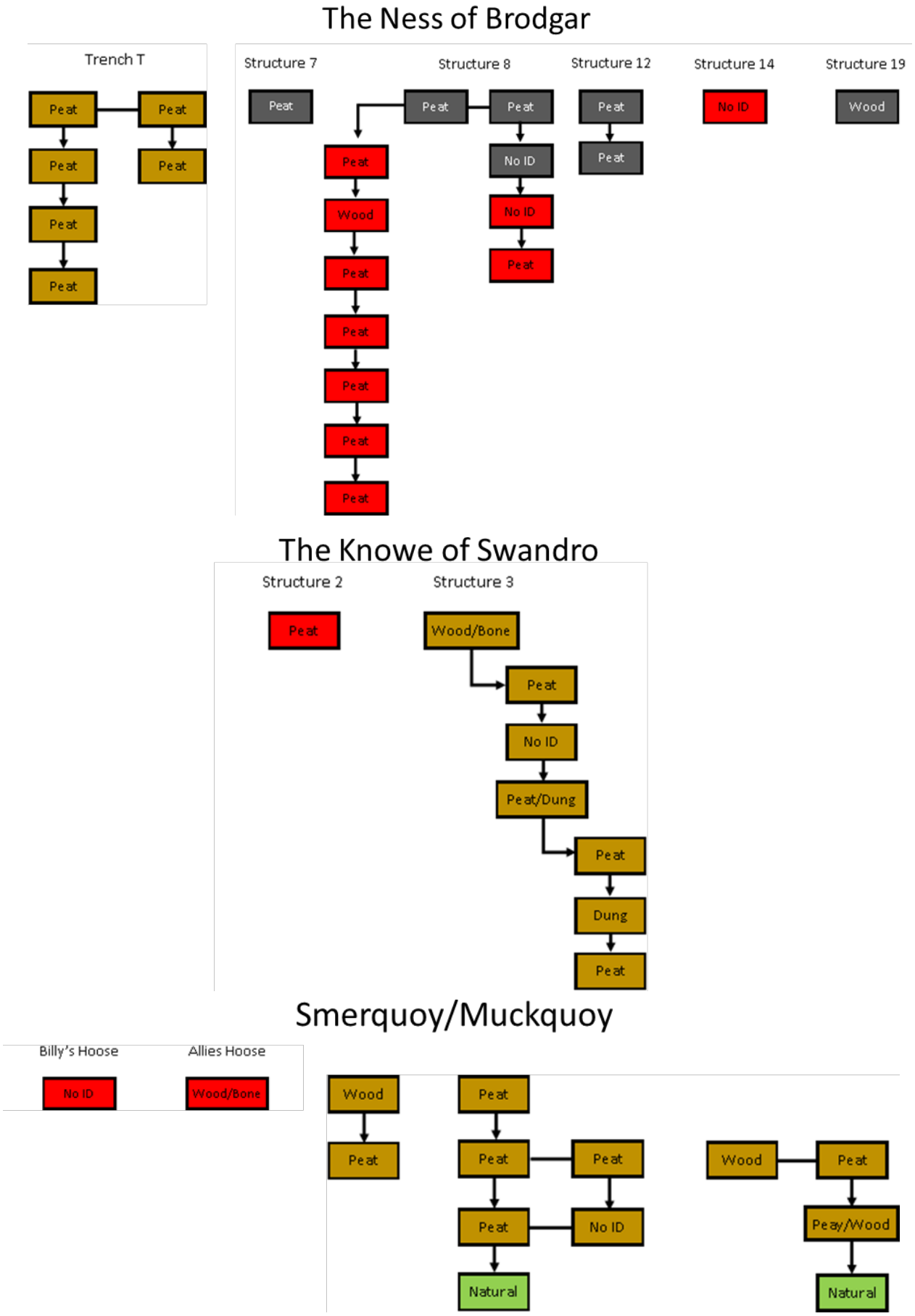

Figure 8.3 Harris matrices for each archaeological site showing modern fuel matches and indicating sample type with red for hearth, dark grey for ash dump/hearth rake out, and brown for midden. Source: Author.

Looking at the different excavations chronologically shows trends linked to fuel use and time period. Peat is the most common fuel match among all of the sites; however, there is a difference in the fuel matches between the Pictish and Neolithic sites fuel use. According to the investigation, The Knowe of Swandro samples are taken from a Pictish area of the site and are the most recent samples by almost 3000 years (figure 8.4). The other sites are all Neolithic period sites. Figure 8.4 shows the chronology of the sites investigated in relation to other contemporary well-known sites in Orkney. The contemporary Neolithic sites include Barnhouse, Skara Brae, the Maeshowe chambered tomb, and the ceremonial site the Ring of Brodgar (Downes and Richards 2005; Downes *et al.* 2013; Card 2010). A Pictish site contemporary to the Knowe of Swandro is shown in the Brough of Birsay. Orkney's archaeological monuments show a people who had reverence to the sea and water, many of the cairn entrances on Rousay face the sea and the area most densely populated with ceremonial monuments is a small isthmus at the junction of a fresh and brackish water source. Proximity to the sea means access to a greater number of resources. There appears to be a correlation with a sites proximity to the sea and its status. The Ness of Brodgar appears to be a high-status ceremonial site in the 'capitol' of Orkney's ceremonial sites. The Knowe of Swandro is a very high-status site in the Pictish period, based on the extensive material evidence of metalworking, and is located on the coast of Rousay. This trend of high status or wealthy sites being near water seems to have endured from the Neolithic through to the Pictish period based on the sites examined for this research (Wickham-Jones 2015).

When it comes to fuels, status seems to have been a factor in the Neolithic. The fuel match evidence shows that earlier in the period a mix of wood and peat

fuels were in use, and as the woodlands are depleted (Bond 1994: 30; Bunting 1994) peat becomes the predominant fuel. At the Ness of Brodgar, peat is the only fuel used in the upper hearth layers from structure 8. In contrast to this the evidence from Smerquoy and Muckquoy show peat in use with a combination of driftwood, bone, and willow to meet their fuel needs. The biggest difference is that between the Neolithic sites there are no samples that match to dung. Dung is only found within the later Pictish period samples from The Knowe of Swandro. As explained by Fenton (1997) the use of dung as a fuel on Sanday and Wyre was looked down on by people on the mainland during the 18th & 19th century. It does not appear that this opinion came from a historical basis. The high status Knowe of Swandro site that appears to have been wealthy enough to employ a copper smith and was using dung fuels. This would mean that either the scarcity of fuel was ubiquitous to life in Pictish Orkney and even the richest farmsteads were unable to escape it, or that the efficacy of dung as a

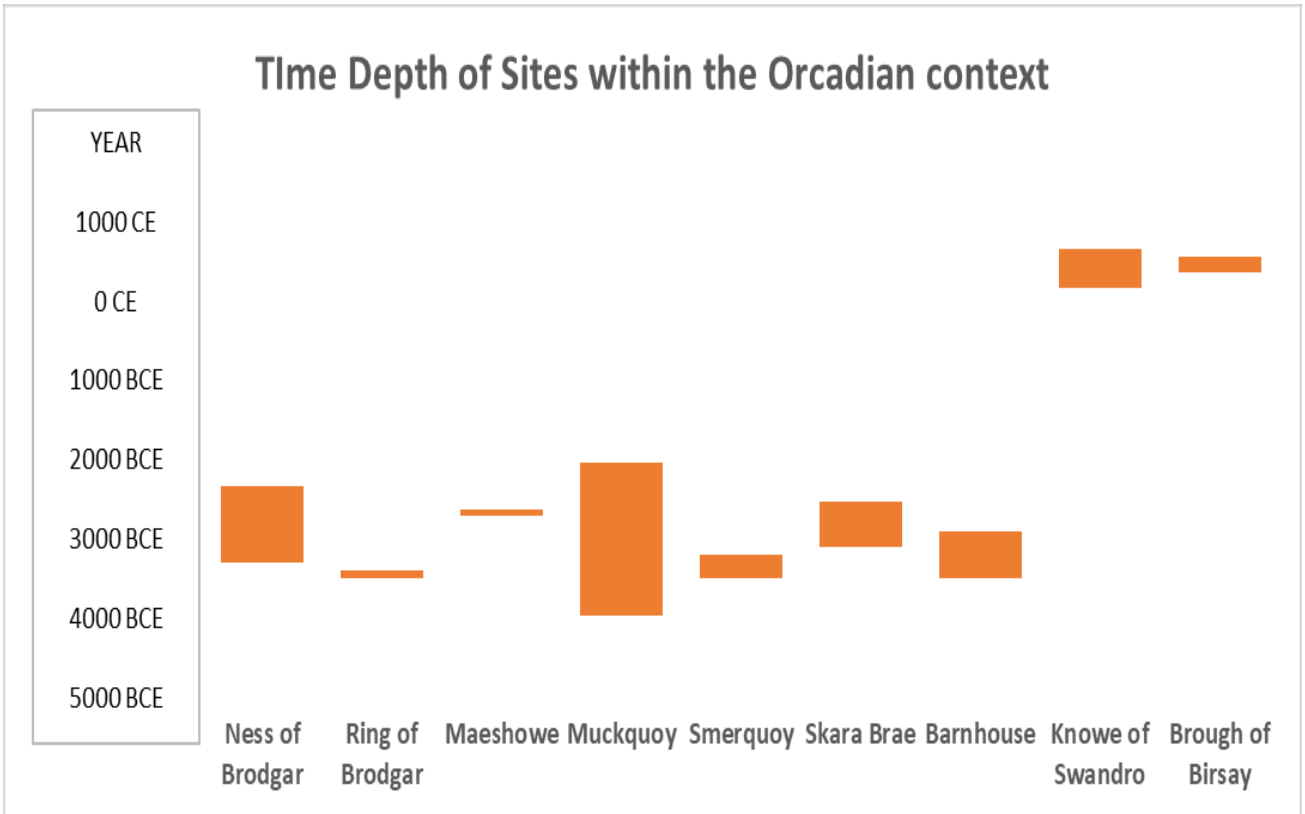

Figure 8.4 A plot showing the time depth for each archaeological site investigated with other notable sites from the time period. from left to right Ness of Brodgar, Ring of Brodgar, Maeshowe, Muckquoy, Smerquoy, Skara Brae, Barnhouse, Knowe of Swandro, and Brough of Birsay. Source: Author.

8.5 What fuels are being used?

The matches of archaeological samples corresponded to modern analogue fuel ash samples principally of peat and some sheep dung heated to both 400^0C and 900^0C according to the analytical methods matching results discussed in section 7.4. When considering the results of the PCA matching the archaeological material still predominantly matches to peat with several instances of matching to sheep dung, driftwood, willow, and animal bone. The samples from these sites do have limitations. The sample material is limited and may not be completely representative of all of the fuel use on a particular site. The data offers glimpses at portions of the fuel use for each site, based upon what features were sampled and in what quantity. To completely understand the fuel use for the entire occupation of a site would require extensive sampling from every combustion feature, ash dump, and midden. This dataset offers discrete indications of the fuel use for the periods directly associated with the archaeological sample material used for this investigation.

The contamination that is incorporated into the sample material from the surface of the combustion feature and the post depositional environment can present problems for the identification of fuels from within archaeological deposits as discussed in sections 7.3 and 7.4. This investigation tried to combat this issue by simulating a 50/50 mix with soil matrix material to demonstrate the need to apply some form of correction for soil contamination, and a means to adjust the data to compensate for the limitations associated with it. This is one possibility to address the issue of contamination of ash material within archaeological contexts.

Ness of Brodgar

The Ness of Brodgar data represents 24 samples from four structures and two excavation trenches. The most common fuel match is peat heated to 900^0C, with only 2 samples matching to willow heated 200^0C. Of the excavation sites, the Ness of Brodgar is the only site examined that did not have fuel matches to bone or driftwood.

The high heating temperatures (900^0C) could indicate some sort of production using heat as mentioned in section 2.4, and this is corroborated by the multiple pottery finds from the site (Card *et al.* 2007; Towers *et al.* 2015). The hearth material matching to willow heated to 200^0C (NoB16 6346) could indicate a fire used for cooking represented by one burnt horizon within the hearth. In addition to the hearth sample, there is one ash dump sample that also matches to the low temperature ash from modern analogue willow heated to 200^0C (NoB15 3783). The Ness of Brodgar samples show that wood was in limited use earlier within the chronology of the sample material within structure 19 and an early layer in hearth 6039 from structure 8, but peat is the only fuel in the later deposits. This could show the decline in woodland vegetation causing the transition to peat fuels as the woodlands depleted.

Knowe of Swandro

The samples from this multiperiod site are Late Iron Age in chronology. The majority of the sample material matches to fuels heated to a high functional temperature of 900^0C. The samples KoS 3081 and KoS 3217 show relationships to fuels heated between 200^0C and 400^0C. KoS 3081 matches to driftwood heated to 400^0C and animal bone heated to 200^0C, and KoS 3217 matches with peat heated to 200^0C and sheep dung heated to 400^0C (section

7.4). The Knowe of Swandro samples all come from structure 3 with the exception of KoS 2039 a hearth sample from structure 2 that matches to peat heated to 400^0C. The samples from the smithy are the only ones that match with dung, the Neolithic material from the Ness of Brodgar and Smerquoy/Muckquoy was produced during the decline of woodlands within Orkney as discussed in section 2.3. This would imply that wood fuels were still available in some capacity during the Neolithic period, but by the Pictish period the wood fuels were almost non-existent. This is evident with peat and sheep dung being the most predominant fuels found within the Pictish samples from the Knowe of Swandro. It is also evident that peat and dung were capable of meeting the needs for fuel at Swandro within the Pictish period. Even though contact and trade were established with mainland Scotland (Fojut 1993), there is no evidence that wood fuels were being imported at Swandro.

The high functional temperatures (900^0C) of the sample material suggest production of pottery or metalwork was taking place (section 2.4). The artefactual evidence adds credence to this with finds consisting of pottery sherds, furnace lining fragments, small pieces of copper, crucible fragments, slag, and hammerscale being found in structure 3 as well (Dockrill & Bond 2013). It has been suggested by Dockrill and Bond (2013) that structure 3 contains the remains of a Pictish smithy (section 2.10.2). The fuel and functional temperature matches from this research corroborate those findings. The lower functional temperature fuel matches could be indicative of fires used for cooking or heating. The sample at the most recent position stratigraphically (KoS 3081) is the last deposit in the sequence chronologically, and could indicate an instance of fuel scarcity, matching to a combination of driftwood heated to

400^{0}C and animal bone heated to 200^{0}C. The use of driftwood and bone could indicate the severity of fuel shortage and using anything possible to fuel the fire.

Smerquoy/Muckquoy

The samples from the Muckquoy excavations are predominantly matches to low functional temperature modern analogue ash samples with the exception of RDL 004 and RDL 006 both matching to peat heated to 900^{0}C. The majority of the samples match to peat heated between 200^{0}C and 400^{0}C. Two of the samples, RDL 031 and RDL 016 match with willow heated to 200^{0}C, and one sample matches with a combination of peat heated to 200^{0}C and driftwood heated to 400^{0}C.

The fuel match data from Smerquoy and Muckquoy could be a further indication of the peat fuels becoming the predominant fuel source as woodlands decline. This is further corroborated with the earlier structures at Smerquoy being of timber construction with the later buildings transitioning to stone (Gee *et al.* 2016). Ali's Hoose showed evidence of being constructed out of timbers in its initial construction and being rebuilt out of stone in a later iteration (Gee *et al.* 2016). The construction evidence combined with the fuel data makes a good case for the transition away from the use of timber resources as the woodlands decline. More research would be required to determine if this transition was by choice to make room for grazing animals or by force as a result of pressure from climate change.

In contrast to the other excavations that suggest sites of production, Muckquoy potentially had limited pottery production based upon the fuel matches. Pottery sherds were found during the excavation that was suggested to be an Early Neolithic village according the Richards *et al.* (2016) (section 2.10.3). The

samples from Muckquoy represent the Late Neolithic in Orkney (Richards *et al.* 2016). The site showed evidence of being enclosed with a series of palisades to form a thick fence or wall. This could be evidence of the motivation for the transition to smaller nucleated groups as resources become scarce and the end of the Neolithic. The majority of the fuel matches from this site suggest that the fuels were used for heating and cooking, with limited production based on the functional temperatures of the fuel matches (section 2.4). The two samples that show no presence of peat (RDL 031 & RDL 016) are not related stratigraphically, and suggest two different burning events at different times using willow as fuel. This could suggest that the fuel was used for a specific purpose.

The hearth samples from two of the houses found at the Smerquoy excavation show two different fuels being used in the two Neolithic houses found within a village complex (section 2.10.3). Sample SMQ A is unidentified by the PCA, while SMQ B matches to a combination of driftwood heated to 400^0C and bone heated to 200^0C. Driftwood and bone could indicate severe scarcity of peat as seen at Smerquoy/Muckquoy, resources as stated regarding the similar fuel match with KoS 3081. Based on the functional temperature match for this sample it is likely that this fuel was used for cooking or heating (section 2.4).

8.6 What potential factors affect the selection of resources?

Based upon the fuel match results, some insight can be gained into the fuel resource management among the different archaeological sites. For instance, the coastal settlement site the Knowe of Swandro has archaeological samples that match to modern peat, sheep dung, driftwood, and bone. The other sites within 2 km of the coast, Smerquoy/Muckquoy, both also have fuel matches to driftwood, showing that this is an opportunistic fuel available when in proximity to the coastline.

The sites on Mainland Orkney are the only sites that show indications of willow being used as a fuel. The Knowe of Swandro has samples that match to driftwood but none that match to willow, hazel, or heather. This is perhaps indicative that except for the opportunistic driftwood on the shores, wood fuels were not available at all on Rousay during the Iron Age, as suggested by Bunting (2017, Keating and Dickson (1978), Farell *et al.* (2014), and Bond (1994). This is perhaps why dung fuel is in use among the Iron Age Knowe of Swandro samples and not the Neolithic samples from the Mainland excavations. Sheep fuel is a renewable and readily available supplement to fuel needs. Pockets of scrub brush plants like willow could still have been available in limited supply on mainland Orkney during the Neolithic when The Ness of Brodgar and Smerquoy/Muckquoy were occupied. The use of driftwood and animal bone together as a fuel could potentially indicate severe scarcity of peat fuel, as it is seen in both the Iron Age sample KoS 3081 and the much earlier Neolithic sample SMQ B, both near the latest stratigraphic layers of the respective excavations chronologically. The most recent deposits are the ones nearest to the end of a sites occupation. Perhaps the shortage of fuel lead to these sites being abandoned, due to an inability to sustain the needs for fire which is ubiquitous to human activity in these chronological periods.

8.7 Final thoughts

The fuel that was most prolific among the sites was peat, there are also matches to sheep dung, willow, driftwood, and bone. It appears that the most viable fuel source was peat, a solid fossil fuel that requires both labour to harvest and time to dry. In the Neolithic period when the development of community was taking shape and the nucleation of kinship groups was happening, it is fitting that a fuel like peat would be predominant (Richards 1998). Peat requires a community effort to harvest and prepare for burning to acquire enough for use as an effective fuel. As woodland resources grow scarcer throughout the Neolithic (Bond 1994:30; Bunting 1994), there is evidence that the expansion of communities starts a reversion back to more closed off kinship groups. This is evident from the 'fencing off' of Muckquoy (Richards *et al.* 2016). The trend of the Picts to dwell in farmsteads and not villages, could be an indication of the continuation of this trend from the Neolithic. Groups were neither getting larger than the resources could support, nor getting smaller than the size needed to harvest the labour-intensive fuels like peat. This practice of neighbours coming together to gather fuel was prevalent within the Northern Isles until the 19th century CE (Fenton 1997: 211).

The sustainable fuel sheep dung was in use among the Iron Age site the Knowe of Swandro in a supplementary role to peat. While the Neolithic sites, the Ness of Brodgar and Smerquoy/Muckquoy, peat was the dominant fuel, it is evident that the needs for fuel were supplemented by willow in small quantities when it was still available. An alternative interpretation to this would be when the ashes were needed for other uses such as spreading on the floor the repel insects (Wahedi *et al.* 2017), as fertiliser, or to filter water.

This conundrum of using finite fossil fuels versus renewable bio fuels demonstrates correlation to contemporary debate surrounding issues of sustainability and environmental impact of fuel resources. In the absence of traditional wood fuel resources as discussed in section 2.2, the evidence of this investigation shows that peat becomes the predominant fuel source, and in times of scarcity sheep dung, driftwood, willow, and animal bone could be used to supplement fuel needs.

8.8 Further work (short and long term)

This investigation focused on Orkney; however, these methods are transferable to any region of the world. The fuel selection research would need to be repeated to ensure collection of the correct fuels for the given region. In addition, the technology level of the population being investigated would need to be evaluated to be sure the heating temperatures have parallels to the functional temperatures in use for the area and chronological period. Then the methodology for the analyses and comparison of fuels would need to be followed to carry out the investigation, keeping in mind the need to address the limitations and problems associated with the contamination of archaeological material.

This research will be written up for publication, and the modern analogue ash preparation and analyses methods are already preapproved to publish with EXARC.net, a global experimental archaeology group, in the Fall of 2018. It is planned to submit the entire project for publication as well.

When the chronology of the sites is available it would be very helpful to use dates associated with the archaeological contexts to provide even more accurate interpretations to the changes to fuel use within archaeological sites, between the archaeological sites, and within Orkney.

There are plans to apply for post-doctoral fellowship funding to continue this research. To expand the archaeological samples to fill in the temporal gaps that are left by a lack of material from the Bronze and Iron Ages. This method can be expanded upon with more modern fuels, different ashing techniques, more temperature increments to fill in the gaps at 600^0C and 1200^0C, and even transferred to other regions of the world. Carrying out ashing of modern fuels in uncontrolled open settings would expand on the reliability of this method and the ability to further understand and compensate for the contamination of ash material within archaeological contexts. An uncontrolled setting would allow the fuels to burn with no influence on the combustion temperature, and be affected by changes to ambient environment conditions. This is a closer recreation than a laboratory setting can achieve. This would also allow for the fuels to be mix with hearth material while burning, and provide a means to investigate one aspect of the contamination issue further. Ideally these experiments could be carried out in reconstructed buildings to represent both Neolithic and Pictish structures found in Orkney. Burning the fuels in replica buildings would afford the ability to monitor a fuels ability to heat a space, light output, effect on air quality, and monitor the efficiency of fuels in practical settings. This would be an approach to create modern analogue ash that is as close to its archaeological counterpart as possible, and hopefully, create an even more accurate method for identifying archaeological fuel.

Bibliography

Akar G, Polar M, Galecki G and Ipekoglu U (2012) Leaching behaviour of selected trace elements in coal fly ash samples from Yenikoy coal-fired power plants. *Fuel Processing Technology* 104: 50-56.

Alperson-Afil N (2012) Archaeology of fire: methodological aspects of reconstructing fire history of prehistoric archaeological sites. *Earth-Science Reviews* 113: 111-119.

Amorosi T, Buckland P, Dugmore A, Ingimundarson J and McGovern T (1997) Raiding the landscape: human impact in the Scandinavian north Atlantic. *Human Ecology* 25, 3: 492-518.

Appleby A (2008) Neolithic pottery firings. Accessed from http://orkneypottery.co.uk/prehistoric-pottery/neolithic-pottery-firings/ (23/10/2018).

Asouti E (2003) Woodland vegetation and fuel exploitation at the prehistoric campsite of Pinarbasi, south-central Anatolia, Turkey: the evidence from the wood charcoal macro-remains. *Journal of Archaeological Science* 30: 1185-1201.

Ayswarya E Abraham B and Thachil E (2011) HDPE-ash nanocomposites. *Journal of Applied Polymer Science* 124: 1659-1667.

Baernthaler G, Zischka M, Haraldsson C and Obernberger I (2006) Determination of major and minor ash-forming elements in solid biofuels. *Biomass & Bioenergy* 30: 983-997.

Bartington Instruments (1995) Operation manual for bartington MS2 magnetic susceptibility system. Oxford: Bartington Instruments.

Bates R (1973) *Determination of pH; Theory and Practice.* New York: Wiley.

Bathurst R, Zori D, Byock J (2010) Diatoms as bio-indicators of site use: locating turf structures from the Viking age. *Journal of Archaeological Science* 37: 2920-2928.

Batt C and Dockrill S (1998) Magnetic moments in prehistory: Integrating magnetic measurements with other archaeological data from the Scatness multiperiod settlement. *Archaeological Prospection* 5: 217-227.

Baxter M (1995) Standardization and transformation in principal components analysis, with applications to archaeometry. *Journal of the Royal Statistical Society. Series C (Applied Statistics)* 44, 4: 513-527.

Baxter M (1994) *Exploratory Multivariate Analysis in Archaeology.* Edinburgh: Edinburgh University Press.

Baxter M (2003) *Statistics in Archaeology.* London: Arnold Publishers.

Bell B and Dickson C (1989) Excavations at Warbeth (Stromness cemetery) broch, Orkney. *Society of Antiquaries, Scotland* 119: 101-131.

Bellomo R (1993) A methodological approach to identifying archaeological evidence of fire resulting from human activities. *Journal of Archaeological Science,* 17: 1-11.

Berna F, Behar A, Shahack-Gross R, Berg J, Boaretto E, Gilboa A (2007) Sediments exposed to high temperatures: Reconstructing pyrotechnological processes in late Bronze and Iron Age strata at Tel Dor (Israel). *Journal of Archaeological Science* 34, 3: 358-373.

Berry R (1985) *The Natural History of Orkney.* Collins: London.

Bitetto A, Mangone A, Mininni R, Gianossa L (2016) A nonlinear principal component analysis to study archaeometric data. *Journal of Chemometrics* 30: 405-415.

Blaha U, Sapkota B, Appel E, Stanjek H and Rösler W (2008) Micro-scale grain-size analysis and magnetic properties of coal-fired power plant fly ash and its relevance for environmental magnetic pollution studies. *Atmospheric Environment* 42: 8359-8370.

Blundell A, Dearing J, Boyle J and Hannam J (2009) Controlling factors for the spatial variability of soil magnetic susceptibility across England and Wales. *Earth Science Reviews* 95: 158-188.

Bond J (1994) Changes and continuity in an island system: the paleoeconomy of Sanday, Orkney. PhD thesis University of Bradford.

Boy Scouts of America (2009) *Boy Scout handbook*. Irving, Texas: Boys Scouts of America.

Braadbaart F (2004) Carbonisation of peas and wheat. A laboratory study. Leiden, The Netherlands. Available from: www.amolf.nl. Accessed 15/10/2017.

Braadbaart F and Poole I (2008) Morphological, chemical and physical changes during charcoalification of wood and its relevance to archaeological contexts *Journal of Archaeological Science* 35: 2434-2445.

Braadbaart F, Poole I and van Brussel A (2009) Preservation potential of charcoal in alkaline environments: an experimental approach and implications for the archaeological record. *Journal of Archaeological Science* 36: 1672-1679.

Braadbaart F, Poole I, Huisman H and van Os B (2012) Fuel, fire and heat: An experimental approach to highlight the potential of studying ash and char remains from archaeological contexts. *Journal of Archaeological Science* 39: 836-847.

Braadbaart F, van Brussel T, van Os B, Eijskoot Y (2017) Fuel remains in archaeological contexts: Experimental and archaeological evidence for

recognizing remains in hearths used by Iron Age farmers who lived in peatlands. *The Holocene* 27, 11: 1682-1693.

Brady N and Weil R (2000) *Elements of The Nature and Properties of Soils.* Prentice Hall: Upper Saddle River.

Bunting J (2017) Holocene vegetation accessed from http://www.landforms.eu/orkney/holocene%20vegetation.htm (10/15/2016).

Bunting M (1994) Vegetation history of Orkney, Scotland; pollen records from two small basins in west Mainland. *New Phytologist* 128, 4: 771-792.

Burton F (2009) Fire the spark that ignited human evolution. University of New Mexico Press: Albuquerque.

Byram G (1959) Combustion of forest fuels. In: Davis K (ed.), Forest Fire Control and Use. New York. McGraw-Hill. (Chapter 3).

Canti M & Linford N (2000) The effects of fire on archaeological soils and sediments. Temperature and colour relationships. *Proceedings of the Prehistoric Society,* 66: 385-395.

Canti M (2003) Aspects of the chemical and microscopic characteristics of plant ashes found in archaeological soils. *Catena* 54: 339-361.

Card N, Downes J, Gibson J, Ovenden S (2007) Bringing a landscape to life? Researching and managing 'The Heart of Neolithic Orkney' world heritage site. *World Archaeology* 39, 3: 417-435.

Card N (2010) Neolithic temples of the Northern Isles: stunning new discoveries in Orkney. *Current Archaeology 241: 12-19.*

Church M, Peters C and Batt C (2007) Sourcing fire ash on archaeological sites in the western northern isles of Scotland, using mineral magnetism. *Geoarchaeology* 22: 747-774.

Clark J and Harris J (1985) Fire and its role in early hominid lifeways. *The African Archaeological Review* 3: 3-27.

Clark N and Yusoff K (2014) Combustion and society: a fire-centered history of energy use. *Theory, Culture & Society* 31, 5: 203-226.

Cloud P (1969) *Resources and Man a Study and Recommendations.* National Academy of Sciences: San Francisco.

Coles J (1973) *Archaeology by Experiment.* London: Hutchinson & CO Publishers.

Conedera M, Tinner W, Neff C, Meurer M, Dickens A, and Krebs P (2009) Reconstructing past fire regimes: methods, applications, and relevance to fire management and conservation. *Quaternary Science Reviews* 28: 555-576.

Cook S, Clarke A, Fulford M (2005) Soil geochemistry and detection of early Roman precious metal and copper alloy working at the Roman town of *Cavella Atrebatum* (Silchester, Hampshire, UK). *Journal of Archaeological Science* 32: 805-812.

Copper, M. (2015) The same but better: understanding ceramic variation in the Hebridean Neolithic. Unpublished PhD thesis. Unpublished: University of Bradford.

Costa Vaz F, Tereso J, Martín-Seijo M, Pereira S, Gaspar R, Seabra L and Sastre-Blanco J (2017) Iron age ovens and hearths from the hilltop of Quinta de Crestelos, Sabor valley (NE Portugal): an archaeobotanical approach on typology, functionality and firewood use. *Quaternary International:* 1-19.

Courty M (2017) Fuel origin and firing product preservation in archaeological occupation contexts. *Quaternary International* 431: 116-130.

Cronyn J (1990) *The Elements of Archaeological Conservation*. London: Routledge.

Dearing J (1994) Environmental magnetic susceptibility: using the bartington MS2 system (pp. 16-18). Kenilworth: Chi Publishing.

Demeyer A, Voundi Nkana JC, Verloo MG (2001). "Characteristics of wood ash and influence on soil properties and nutrient uptake: an overview". *Bioresource Technology* 77 (3): 287–95.

Dewar I, Batt C, Peters C (2002) A mineral magnetic investigation into fuel derived deposits from Old Scatness Broch, Shetland. *Physics and Chemistry of the Earth* 27: 1343-1348.

Di Gianfilippo M, Costa G, Verginelli I, Gavasci R, Lombardi F (2016) Analysis and interpretation of the leaching behavior of waste thermal treatment bottom ash by batch and column tests. *Waste Management* 56: 216-118.

Dockrill S and Bond J (2009) Sustainability and resilience in prehistoric north Atlantic Britain: the importance of a mixed paleoeconomic system. *Journal of the North Atlantic* 2: 33-50.

Dockrill S and Bond J (A) (2013) Rousay: racing against sea and tide. *Current Archaeology* 275: 34-40.

Dockrill S and Bond J (B) (2013) Data structure report: the Knowe of Swandro.

Dockrill S and Bond J (2016) Data structure report: the Knowe of Swandro.

Dockrill S, Bond J, Smith A, Nicholson R (2007) *Investigations in Sanday, Orkney* (vol. 2) *Tofts ness, Sanday and island landscape through 3000 years of prehistory.* Kirkwall: Historic Scotland.

Downes J, Richards C (2005) The dwellings at Barnhouse. In Richards C, and Ashmore, P (Eds.). (2005). *Dwelling among the monuments: the Neolithic*

village of Barnhouse, Maeshowe passage grave and surrounding monuments at Stenness, Orkney (p. 1). McDonald Institute monographs. Cambridge: McDonald Institute for Archaeological Research.
Downes J, Richards C, Brown J, Cresswell AJ, Ellen R, Davies AD, Hall A, McCulloch R, Sanderson DCW, and Simpson IA (2013) Investigating the great Ring of Brodgar, Orkney in Raichards C (Ed.) *Building the Great Stone Circles of the North*. Oxford: Windgather Press: 90-118.

Eliyahu-Behar A, Shilstein S, Raban-Gerstel N, Goren Y, Gilboa A, Sharon I and Weiner S (2008) An integrated approach to reconstructing primary activities from pit deposits: iron smithing and other activities at Tel Dor under Neo-Assyrian domination. *Journal of Archaeological Science* 35: 2895-2908.

Etiégni L and Campbell A (1991) Physical and chemical characteristics of wood ash. *Bioresource Technology* 37: 173-178.

Farrell M, Bunting J, Lee D and Thomas A (2014) Neolithic settlement at the woodland's edge: palynological data and timber architecture in Orkney, Scotland. *Journal of Archaeological Sciences* 51: 225-236.

Fenton A (1997) *The Northern Isles: Orkney and Shetland.* Cromwell Press: Wiltshire.

Fialová H, Maier G, Petrovský E, Kapička A, Boyko T and Scholger R (2006) Magnetic properties of soils from sites with different geological and environmental settings. *Journal of Applied Geophysics* 59: 273-283.

Fojut N (1993) The Brochs of Gurness and Midhowe. Historic Scotland: Dundee.

Gee C, Richards C, and Robertson M (2016) Local histories of passage grave building communities: Brae of Smerquoy. *In:* Richards C and Jones R (Eds.) (2016) *The Development of Neolithic House Societies in Orkney.* Windgather Press: Oxford.

Giles M (2007) Making metal and forging relations: ironworking in the British Iron Age. *Oxford Journal of Archaeology* 26: 395-413.

Goldstein J, Newbury D, Joy D and Lyman C (2003) *Scanning Electron Microscopy and X-Ray Microanalysis.* New York: Springer.

Goudsblom J (1992) *Fire and Civilization.* The Penguin Press: London.

Gowlett J (2006) The early settlement of northern Europe: fire history in the context of climate change and the social brain. *C.R. Palevol* 5: 299-310.

Hagman H, Backman R and Boström D (2013) Co-combustion of animal waste, peat, waste wood, forest residues and industrial sludge in a 50 MWth circulating fluidized-bed boiler: ash transformation, ash/deposit characteristics, and boiler failures. *Energy Fuels* 27: 5617-5627.

Hall G, Woodborne S and Scholes M (2008) Stable carbon isotope ratios from archaeological charcoal as palaeoenvironmental indicators. *Chemical Geology* 247: 384-400.

Heikkinen R, Laitinen R, Patrikainen T, Tiainen M and Virtanen M (1998) Slagging tendency of peat ash. *Fuel Processing Technology* 56: 69-80.

Heizer R (1963) Domestic fuel in primitive society. *The Journal of the Royal Anthropological Institute of Great Britain and Ireland* 93, 2: 186-194.

Hirano T (2002) Combustion science for safety. *Proceedings of the Combustion Institute* 29: 167-180.

Hunter J and MacSween A (1991) A sequence for the Orcadian Neolithic. *Antiquity* 65: 911-914.

Hunter J (2007). *Investigations in Sanday, Orkney* (vol. 1) excavation at Pool. Kirkwall: Orcadian in association with Historic Scotland.

Hrouda F and Pokorný J (2011) Modelling accuracy limits for frequency-dependent anisotropy of magnetic susceptibility of rocks and soils. *Studia Geophysica et Geodaetica* 55: 789-802.

Jones R & Brown B (2000). Neolithic pottery-making on Orkney: A new look. Neolithic Orkney in Its European Context. In: Ritchie A (Ed) *Neolithic Orkney in its European Context.* McDonald Institute Monographs: Cambridge*. 169-184.*

Jones A, Jones R, Tully G, Maritan L, Mukherjee A, Evershed R, MacSween A, Richards C and Towers R (2016) Prehistoric pottery from sites within the Bay of Firth: Stonehall, Crossiescrown, Wideford Hill, Brae of Smerquoy, Muckquoy, Ramberry and Knowes of Trotty. In: Richards C and Jones R (Eds.) *The Development of Neolithic House Societies in Orkney.* Windgather Press: Oxford 303-412.

Kabata-Pendias, A., & Pendias, H. (1984). *Trace elements in soils and plants* Boca Raton, Fla.: CRC Press.

Kaland S H H 1993. *The settlement of Westness, Rousay. In Batey C E, Jesch J and Morris C D (eds.) The Viking Age in Orkney, Caithness and the North Atlantic*. 308-317, Edinburgh.

Kanu M, Meludu O and Oniku S (2014) Comparative study of top soil magnetic susceptibility variation based on some human activities. *Geofísica Internacional* 53-4: 411-423.

Kapper K, Anesin D, Donadini F, Angelucci D, Cavulli F, Pedrotti A and Hirt A (2014) Linking site formation processes to magnetic properties. Rock and archaeomagnetic analysis of the combustion levels at Riparo Gaban, Italy. *Journal of Archaeological Science 41: 836-855.*

Kars M, Auborg C, Labaume P, Berquó and Cavailhes T (2014) Burial diagenesis of magnetic minerals: new insights from the Grés d'Annot transect (SE France). *Minerals* 4: 667-689.

Keating T and Dickson J (1978) Mid-flandrian changes in vegetation on mainland Orkney. *New Phytol 82:* 585-612.

Kedrowski B, Crass B, Behm J, Luetke J, Nichols A, Moreck A and Holmes C (2009) GC/MS analysis of fatty acids from ancient hearth residues at the Swan Point archaeological site. *Archaeometry* 51, 1: 110-122.

Kozhevikov N, Kamnev Ya, Kazansky A (2014) Error analysis of frequency-dependent magnetic susceptibility measurements: magnetic viscosity studies with the Bartington MS2 system. *Russian Geology and Geophysics* 55: 508-514.

Laing L (1974) *Orkney and Shetland: An Archaeological Guide.* David & Charles: Newton Abbot.

Land Use Consultants 1998. Orkney landscape character assessment. Scottish Natural Heritage Review No 100.

Lisle S (2016) Surprise at Smerquoy – an early Neolithic village is unearthed. Accessed from https://archaeologysaga.com/2016/09/01/surprise-at-smerquoy-an-early-neolithic-village-is-unearthed/ (23/4/2017).

Maathuis F (2013) Sodium in plants: perception, signaling, and regulation of sodium fluxes. *Journal of Experimental Botany* 65, 3: 849-858.

MacLeod W (1925) Fuel and early civilization. *American Anthropologist* 27: 344-346.

McCafferty K (2006) Seven way to light a fire without a match. *Field & Stream.* Accessed 13 October 2017.

McKirdy A (2011) *Orkney and Shetland a Landscape Fashioned by Geology*. Scottish Natural Heritage: Battleby.

Mentzer S (2014) Microarchaeological approaches to the identification and interpretation of combustion features in prehistoric archaeological sites. *Journal of Archaeological Method and Theory* 21: 616-668.

Miller C, Conrad N, Goldberg P and Berna F (2009) Dumping, sweeping and trampling: experimental micromorphological analysis of anthropogenically modified combustion features. *P@lethnologie 25-37.*

Miller R (1976) *Orkney.* London: B. T. Batsford Ltd.

Misra M, Ragland K and Baker A (1993) Wood ash composition as a function of furnace temperature. *Biomass and Bioenergy* 4: 103-116.

Morris I (2015) *Foragers, Farmers, and Fossil Fuels How Humans Evolved.* Princeton University Press: Princeton.

Muir T (2014) *Orkney Folk Tales*. Brimscombe Port Stroud: The History Press.

Mulay L (1963) *Magnetic Susceptibility.* John Wiley & Sons: New York.

Munsell Colour (Firm) (2000) *Munsell Soil Colour Charts.* GretagMacbeth: New Windsor.

Mykura W, Flinn D, and May F (1976) *British Regional Geology Orkney and Shetland.* Institute of Geological Sciences: Edinburgh.

Obenberger I, Brunner T and Bärnthaler G (2006) Chemical properties of solid biofuels – significance and impact. *Biomass & Bioenergy* 30: 973-982.

Ohno T (1992). Neutralization of Soil Acidity and Release of Phosphorus and Potassium by Wood Ash. *Journal of Environmental Quality*. 21: 433-438.

Owen K (2016) The Brough of Birsay. Historic Scotland: Dundee.

Panahi A, Levendis Y, Vorobiev N and Schiemann (2017) Direct observations on the combustion characteristics of *Miscanthus* and Beechwood biomass including fusion and spherodization. *Fuel Processing Technology* 166: 41-49.

Pálsson H and Edwards P (1978) *Orkneyinga saga* Penguin Books: Suffolk.

Pausas J and Keeley J (2009) A burning story: the role of fire in the history of life. *Bioscience* 59: 593-601.

Pedersen J and Ottosen L (2006) Elemental analysis of ash residue from combustion of CCA treated wood waste before and after electrodialytic extraction. *Chemosphere* 65: 110-116.

Peters C and Batt C (2002) Dating and source fuel ash residues from Cladh Hallan, South Uist, Scotland, using magnetic techniques. *Physics and Chemistry of the Earth* 27: 1349-1353.

Peters C, Church M and Mitchell C (2001) Investigation of domestic fuel sources on Lewis using mineral magnetism. *Archaeological Prospection,* 8: 227-237.

Peters C, Thompson R, Harrison A and Church M (2002) Low temperature magnetic characterization of fire ash residues. *Physics and Chemistry of the Earth* 27: 1355-1361.

Photos-Jones E, Smith B, Hall A and Jones R (2007) On the intent to make cramp: an interpretation of vitreous seaweed cremation “waste” from prehistoric burial sites in Orkney, Scotland. *Oxford Journal of Archaeology* 26: 1-23.

Picornell-Gelabert L and Servera-Vives G (2017) Landscape practices and everyday life in domestic spaces in bronze age Mallorca (Balearic Islands): perspectives for and archaeology of fuel and firewood. *Quaternary International* 431: 73-89.

Pidwirny, M. (2006). "Composition of Rocks". *Fundamentals of Physical Geography, 2nd Edition*. Accessed on 06/11/2017. http://www.physicalgeography.net/fundamentals/10d.html

Pierce C, Adams K and Stewart J (1998) Determining the fuel constituents of ancient hearth ash via ICP-AES analysis. *Journal of Archaeological Science* 25: 493-503.

Pizarro C, Pérez-Del-Notario N, Sáenz-González C, Rodríguez-Tecedor S, González-Sáiz J (2012) Matching past and present ceramic production in the Banda areh (Ghana): improving the analytical performance of neutron activation analysis in archaeology using multivariate analysis techniques. *Archaeometry* 54: 101-113.

Pollard M, Batt C, Stern B and Young S (2007) *Analytical chemistry in archaeology.* Cambridge: Cambridge University Press.

Pollard, A. M., and Heron, C. (1996). *Archaeological chemistry*. RSC paperbacks. Cambridge: Royal Society of Chemistry.

Ponting M (2004) The scanning electron microscope and the archaeologist. *Physics Education 39*: 166-170.

Pulley S and Rowntree K (2016) Stages in the life of a magnetic grain: sediment source discrimination, particle size effects and spatial variability in the South African Karoo. *Gederma* 271: 134-143.

Pyne S (2001) *Fire A Brief History.* London: The British Museum Press.

Radford C (1959) *The Early Christian and Norse Settlements at Birsay.* Edinburgh: H.M.S.O.

Rehder J (2000) *The Mastery and Uses of Fire in Antiquity*. McGill-Queens University Press: London.

Richards C (1998) Centralizing tendencies: social evolution in Neolithic Orkney. In M Edmonds and C Richards (Eds.) *Understanding the Neolithic of Northwest Europe*. Glasgow: Cruithne Press, 516–32.

Richards, C., and Ashmore, P. J. (Eds.). (2005). *Dwelling among the monuments: the Neolithic village of Barnhouse, Maeshowe passage grave and surrounding monuments at Stenness, Orkney* (p. 1). McDonald Institute monographs. Cambridge: McDonald Institute for Archaeological Research.

Richards C and Jones R (Eds.) (2016) *The Development of Neolithic House Societies in Orkney.* Windgather Press: Oxford.

Richards C, Downes J, Gee C, and Carter S (2016) Materializing Neolithic house societies in Orkney: introducing Varme Dale and Muckquoy. *In:* Richards C and Jones R (Eds.) *The Development of Neolithic House Societies in Orkney.* Windgather Press: Oxford 224-253.

Rotherham I (2005) Fuel and landscape – exploitation, environment, crisis and continuum. *Landscape Archaeology and Ecology* 5: 65-81.

Simpson I, Guttman E, Cluett J and Shepherd A (2006) Characterising anthropic sediments in north European Neolithic settlements: an assessment from Skara Brae, Orkney. *Geoarchaeology: an International Journal* 21, 3: 221-235.

Simpson I, Vésteinsson O, Adderley W and McGovern T (2003) Fuel Resource Utilization in Landscapes of Settlement. *Journal of Archaeological Science* 30: 1401–1420.

Spencer J and Sanderson D (2012) Decline in firing technology or poorer fuel resources? High-temperature thermoluminescence (HTTL) archaeothermometry of Neolithic ceramics from Pool, Sanday, Orkney. *Journal of Archaeological Science* 39: 3542-3552.

Sullivan A and Ball R (2012) Thermal decomposition and combustion chemistry of cellulosic biomass. *Atmospheric Environment* 47: 133-141.

Summers J (2015) Marine fauna from an ash deposit in Structure 8. From Old Scatness broch excavations vol 2.

Tacitus C, (2014) *Agricola*. Cambridge University Press: Cambridge.

Tarling D (1983) *Palaeomagnetism Principles and Applications in Geology, Geophysics, and Archaeology. Chapman and Hall: New York.*

Tarling D (1971) *Principles and Applications of Palaeomagnetism.* Chapman and Hall: New York.

Tarling D and Turner P (eds) (1999) *Palaeomagnetism and Diagenesis in Sediments.* The Geological Society: London.

Thér R (2004) Experimental pottery firing in closed firing devices from the Neolithic – Hallstatt period in Central Europe. *EuroREA* 1: 35-82.

Toolis R, Cerón-Carrasco R, Engl R, Hall A, Hunter F, Inglis R, MacSween A, McLaren D, Madella M, O'Connor T and Smith C (2007) Excavation of a burnt mound at Meur, Sanday, Orkney. *Scottish Archaeological Journal* 29: 31-49.

Towers R, Card N and Edmonds M (2015) The Ness of Brodgar. The Ness of Brodgar Trust: Kirkwall.

Valério P, Silva R, Monge Soares A, Araújo M, Fernandes F, Silva A and Berrocal-Rangel L (2010) Technological continuity in Early Iron Age bronze metallurgy at the southwestern Iberian Peninsula – a sight from Castro dos Ratinhos. *Journal of Archaeological Science* 37: 1811-1819.

Vassilev S, Baxter D and Vassileva C (2013) An overview of biomass during combustion: part I. phase-mineral transformations of organic and inorganic matter. *Fuel* 112: 391-449.

Vassilev S, Baxter D and Vassileva C (2014) An overview of biomass during combustion: part II. Ash fusion and ash formation mechanisms of biomass types. *Fuel* 117: 152-183.

Vassilev S, Vassileva C, Song Y, Li W and Feng J (2017) Ash contents and ash-forming elements of biomass and their significance for solid biofuel combustion. *Fuel* 208: 377-409.

Vleminckx J, Morin-Rivat J, Biwolé A, Daïnou K, Gillet J, Doucet J, Drouet T and Hardy O (2014) Soil charcoal to assess the impacts of past human disturbances on tropical forests. *PLoS ONE* 9(11): 1-8.

Wahedi J, Zakariya R, Elkanah O, Ishuwa M, Vincent V, Enoch T (2017) Activities of neem and wood ash as biopesticides in the control of insect pests on vegetable crops in Mubi. *GSC Biological and Pharmaceutical Sciences* 01, 01: 06-10.

Wescott D (1999) *Primitive Technology a Book of Earth Skills*. Gibbs-Smith Publisher: Salt Lake City.

Wickham-Jones C (2015) *Orkney a Historical Guide*. Birlinn Limited: Edinburgh.

Zang B, Parsons R, Onodera K, Kishimoto H, Kato A, Liu A and Suzuki K (2017) Effect of heating rate during primary crystallization on soft magnetic properties of melt-spun Fe-B alloys. *Scripta Materialia* 132: 68-72.

Zvietcovich F, Navarro L, Saldana J, Castillo L, Castaneda B (2016) A novel method for estimating the complete 3D shape of pottery with axial symmetry from single potsherds based on principal component analysis. *Digital Applications in Archaeology and Cultural Heritage* 3: 42-54.

Appendix 1 Complete Magnetic Susceptibility Data Tables

The following tables show the complete datasets for the modern analogue and archaeological sample materials respectively. These tables include the raw data; standard deviations and averages of the measurements that were used to calculate the figures used within the results and discussions chapters of the thesis. The summaries of these tables are shown in the results chapter for each sample. This data is also used within the discussion chapter to create the plots that show the MS and FDMS values

Modern Analogue Magnetic Susceptibility Dataset

Sample	Sample + Container mass	Container mass	Sample mass	Bulk Density	κ*lf* 1	κ*lf* 2	κ*lf* 3	Standard Deviation	κ*hf* 1	κ*hf* 2	κ*hf* 3	Standard Deviation	Average κ*lf*	Average κ*hf*	χlf =κ/p x10-8 m3kg-1	FDMS = (κlf-κhf/κlf) x 100
Driftwood 1 Unburnt	7.1	4.2	2.9	0.3	-0.7	-0.2	-0.4	0.3	-0.5	-0.4	-0.4	0.1	-0.4	-0.4	-1.5	
Driftwood 2 Unburnt	6.9	4.2	2.7	0.3	-0.8	-0.9	-0.3	0.3	-0.4	-0.5	-0.3	0.1	-0.7	-0.4	-2.5	
Driftwood 3 Unburnt	6.5	4.2	2.3	0.2	-0.3	-0.5	-0.7	0.2	-0.5	-0.5	-0.4	0.1	-0.5	-0.5	-2.2	
Driftwood 1 200^{0}C 3Hrs	6.5	4.2	2.3	0.2	-0.5	-0.6	-0.5	0.1	-0.1	-0.0	-0.1	0.1	-0.5	-0.1	-2.3	
Driftwood 2 200^{0}C 3Hrs	6.9	4.2	2.7	0.3	-0.4	-0.9	-0.5	0.3	-0.0	-.0.	-0.1	0.1	-0.6	-0.1	-2.2	
Driftwood 3 200^{0}C 3Hrs	6.4	4.2	2.2	0.2	-0.6	-0.4	-0.3	0.2	-0.3	-0.1	-0.1	0.1	-0.4	-0.2	-2.0	
Driftwood 1 200^{0}C 6Hrs	6.9	4.2	2.7	0.3	-0.7	-0.5	-0.5	0.1	-0.5	-0.4	-0.3	0.1	-0.6	-0.4	-2.1	
Driftwood 2 200^{0}C 6Hrs	6.6	4.2	2.4	0.2	-0.6	-0.5	-0.5	0.1	-0.5	-0.3	-0.2	0.2	-0.5	-0.3	-2.2	
Driftwood 3 200^{0}C 6Hrs	6.7	4.2	2.5	0.3	-0.5	-0.4	-0.6	0.1	-0.5	-0.4	-0.2	0.2	-0.5	-0.4	-2.0	
Seaweed 1 Unburnt	12.6	4.2	8.4	0.8	-0.8	-0.1	-0.7	0.4	-0.5	-.0.	-0.6	0.1	-0.5	-0.6	-0.6	
Seaweed 2 Unburnt	10.1	4.2	5.9	0.6	-2.1	-0.8	-1.1	0.7	-0.5	-0.6	-0.6	0.1	-1.3	-0.6	-2.3	
Seaweed 3 Unburnt	9.4	4.2	5.2	0.5	-1	-1	-0.7	0.2	-0.6	-0.6	-0.4	0.1	-0.9	-0.5	-1.7	
Seaweed 1 200^{0}C 3Hrs	9.6	4.2	5.4	0.5	-0.6	-0.3	-0.4	0.2	-0.3	-0.1	-0.2	0.1	-0.4	-0.2	-0.8	
Seaweed 2	9.4	4.2	5.2	0.5	-	-	-	0.2	-	-	-	0.1	-0.5	-0.4	-1.0	

200^{0}C 3Hrs					0.7	0.5	0.3		0.4	0.4	0.3					
Seaweed 3 200^{0}C 3Hrs	9.2	4.2	5.0	0.5	-0.5	-0.4	-0.5	0.1	-0.4	-0.4	-0.5	0.1	-0.5	-0.4	-0.9	
Seaweed 1 200^{0}C 6Hrs	8.9	4.2	4.7	0.5	-0.7	-0.6	-0.7	0.1	-0.2	-0.4	-0.4	0.1	-0.7	-0.3	-1.4	
Seaweed 2 200^{0}C 6Hrs	9.2	4.2	5.0	0.5	-0.4	-0.6	-0.6	0.1	-0.3	-0.4	-0.3	0.1	-0.5	-0.3	-1.1	
Seaweed 3 200^{0}C 6Hrs	8.8	4.2	4.6	0.5	-0.7	-0.9	-0.8	0.1	-0.5	-0.5	-0.4	0.1	-0.8	-0.5	-1.7	
Seaweed 1 400^{0}C 6Hrs	9.4	4.2	5.2	0.5	1.3	1.8	1.5	0.3	3.5	2.6	2.7	0.5	1.5	2.9	2.9	
Seaweed 2 400^{0}C 6Hrs	8.8	4.2	4.6	0.5	0.2	0.3	0.5	0.2	2.7	2.0	2.4	0.4	0.3	2.4	0.7	
Seaweed 3 400^{0}C 6Hrs	7.2	4.2	3.0	0.3	0.1	0.2	0.1	0.1	1.6	2.3	2.0	0.4	0.1	2.0	0.4	
Seaweed 1 900^{0}C 6Hrs	8.6	4.2	4.4	0.4	11	13.2	14.2	1.6	11.9	11.2	11.4	0.4	12.8	11.5	29.1	10.2
Seaweed 2 900^{0}C 6Hrs	9.5	4.2	5.3	0.5	18.2	17.7	17.7	0.3	17.4	15.7	16.4	0.9	17.9	16.5	33.7	7.6
Seaweed 3 900^{0}C 6Hrs	9.6	4.2	5.4	0.5	14.1	16.5	15.5	1.2	13.2	14.5	15.1	1.0	15.4	14.3	28.5	7.2
Grasses 1 Unburnt	6.3	4.2	2.1	0.2	0.3	1.4	0.1	0.7	-0.3	-0.3	-0.3	0.0	0.6	-0.3	2.9	
Grasses 2 Unburnt	6.4	4.2	2.2	0.2	1	0.3	-4.9	3.2	-0.3	-0.3	-0.2	0.1	-1.2	-0.3	-5.5	
Grasses 3 Unburnt	6.2	4.2	2.0	0.2	0.7	0.2	1.7	0.8	-0.3	-0.3	-0.4	0.1	0.9	-0.3	4.3	
Grasses 1 200^{0}C 3Hrs	6.0	4.2	1.8	0.2	0.2	0.1	0.1	0.1	0.5	0.4	0.3	0.1	0.1	0.4	0.7	
Grasses 2 200^{0}C 3Hrs	6.0	4.2	1.8	0.2	0.1	0.2	0.2	0.1	0.1	0.2	0.2	0.1	0.2	0.2	0.9	
Grasses 3 200^{0}C 3Hrs	6.2	4.2	2.0	0.2	0.3	0.4	0.2	0.1	0.3	0.5	0.2	0.2	0.3	0.3	1.5	
Grasses 1 200^{0}C 6Hrs	6.0	4.2	1.8	0.2	-0.3	-0.7	-0.4	0.2	-0.6	-1.1	-0.4	0.4	-0.5	-0.7	-2.6	

Grasses 2 200^{0}C 6Hrs	5.9	4.2	1.7	0.2	-0.4	-0.3	-0.6	0.2	-0.3	-0.2	-0.5	0.2	-0.4	-0.3	-2.5	
Grasses 3 200^{0}C 6Hrs	6.1	4.2	1.9	0.2	-0.3	-0.6	-0.8	0.3	-0.6	-0.5	-0.7	0.1	-0.6	-0.6	-3.0	
Grasses 1 400^{0}C 6Hrs	5.2	4.2	1.0	0.1	2	2.5	2.3	0.3	1.2	0.5	0.8	0.4	2.3	0.8	22.7	
Grasses 2 400^{0}C 6Hrs	5.8	4.2	1.6	0.2	5.1	3	4.1	1.1	1.3	1.5	1.5	0.1	4.1	1.4	25.4	
Grasses 3 400^{0}C 6Hrs	5.6	4.2	1.4	0.1	2.4	3.9	3.1	0.8	1.7	1.7	1.6	0.1	3.1	1.7	22.4	
Sheep Dung 1 Unburnt	8.3	4.2	4.1	0.4	-0.4	-0.4	-0.2	0.1	-0.2	-0.2	-0.3	0.1	-0.3	-0.2	-0.8	
Sheep Dung 2 Unburnt	7.3	4.2	3.1	0.3	-0.3	-0.3	-0.4	0.1	-0.4	-0.1	-0.2	0.2	-0.3	-0.2	-1.1	
Sheep Dung 3 Unburnt	7.1	4.2	2.9	0.3	-0.3	-0.1	0	0.2	0.0	-0.1	-0.1	0.1	-0.1	-0.1	-0.5	
Sheep Dung 1 200^{0}C 3Hrs	7.3	4.2	3.1	0.3	0.4	0.4	0.8	0.2	0.1	0.2	0.4	0.2	0.5	0.2	1.7	
Sheep Dung 2 200^{0}C 3Hrs	7.8	4.2	3.6	0.4	0.7	0.5	0.8	0.2	0.1	0.4	0.0	0.2	0.7	0.2	1.9	
Sheep Dung 3 200^{0}C 3Hrs	7.7	4.2	3.5	0.4	0.7	0.5	0.6	0.1	0.3	0.3	0.3	0.0	0.6	0.3	1.7	
Sheep Dung 1 200^{0}C 6Hrs	7.2	4.2	3.0	0.3	0.2	0.2	0.2	0.0	0.0	0.1	0.0	0.1	0.2	0.0	0.7	
Sheep Dung 2 200^{0}C 6Hrs	7.4	4.2	3.2	0.3	0.1	0.3	0.2	0.1	-0.2	0.0	0.2	0.2	0.2	0.0	0.6	
Sheep Dung 3 200^{0}C 6Hrs	7.3	4.2	3.1	0.3	0.1	0	0.1	0.1	-0.1	-0.1	-0.1	0.0	0.1	-0.1	0.2	
Sheep Dung 1 400^{0}C 6Hrs	7.1	4.2	2.9	0.3	3.3	4.1	3.5	0.4	3.1	3.3	3.2	0.1	3.6	3.2	12.5	11.9
Sheep Dung 2 400^{0}C 6Hrs	7.8	4.2	3.6	0.4	4.9	5	4.8	0.1	4.3	4.5	4.2	0.2	4.9	4.3	13.6	11.6
Sheep Dung 3 400^{0}C 6Hrs	7.3	4.2	3.1	0.3	6.9	6.7	6.8	0.1	5.0	4.7	5.1	0.2	6.8	4.9	21.9	27.5
Sheep Dung 1	7.0	4.2	2.8	0.3	62.	62.	62.	0.2	56.	58.	59.	1.4	62.5	58.1	223.3	7.0

900^{0}C 6Hrs					4	7	5		7	3	4					
Sheep Dung 2 900^{0}C 6Hrs	7.0	4.2	2.8	0.3	51.2	53.6	52.6	1.2	49.1	48.6	50.1	0.8	52.5	49.3	187.4	6.1
Sheep Dung 3 900^{0}C 6Hrs	7.0	4.2	2.8	0.3	65.4	65.1	65.7	0.3	62.0	61.3	60.7	0.7	65.4	61.3	233.6	6.2
Cow Dung 1 Unburnt	6.4	4.2	2.2	0.2	-0.4	-0.3	-0.3	0.1	0.2	0.1	0.3	0.1	-0.3	0.2	-1.5	
Cow Dung 2 Unburnt	6.4	4.2	2.2	0.2	-0.3	-0.4	-0.2	0.1	0.2	0.3	0.2	0.1	-0.3	0.2	-1.4	
Cow Dung 3 Unburnt	6.2	4.2	2.0	0.2	0.2	0.3	0.4	0.1	0.3	0.3	0.2	0.1	0.3	0.3	1.5	
Cow Dung 1 200^{0}C 3Hrs	6.0	4.2	1.8	0.2	0.7	0.6	0.5	0.1	0.2	0.3	0.3	0.1	0.6	0.3	3.3	
Cow Dung 2 200^{0}C 3Hrs	6.4	4.2	2.2	0.2	0.4	0.2	0.5	0.2	0.1	0.3	0.2	0.1	0.4	0.2	1.7	
Cow Dung 3 200^{0}C 3Hrs	6.5	4.2	2.3	0.2	0.7	0.5	0.5	0.1	0.2	0.2	0.2	0.0	0.6	0.2	2.5	
Cow Dung 1 200^{0}C 6Hrs	6.4	4.2	2.2	0.2	0.6	0.6	0.4	0.1	0.4	0.3	0.4	0.1	0.5	0.4	2.4	
Cow Dung 2 200^{0}C 6Hrs	6.3	4.2	2.1	0.2	0.6	0.3	0.6	0.2	0.3	0.1	0.4	0.2	0.5	0.3	2.4	
Cow Dung 3 200^{0}C 6Hrs	6.4	4.2	2.2	0.2	0.6	0.4	0.7	0.2	0.2	0.5	0.5	0.2	0.6	0.4	2.6	
Cow Dung 1 400^{0}C 6Hrs	6.0	4.2	1.8	0.2	4	4.1	4.3	0.2	3.5	3.6	3.7	0.1	4.1	3.6	23.0	
Cow Dung 2 400^{0}C 6Hrs	5.1	4.2	0.9	0.1	4.1	4.2	4	0.1	3.6	3.6	3.6	0.0	4.1	3.6	45.6	
Cow Dung 3 400^{0}C 6Hrs	6.1	4.2	1.9	0.2	3.9	3.8	3.9	0.1	3.6	3.4	3.5	0.1	3.9	3.5	20.4	
Cow Dung 1 900^{0}C 6Hrs	9.3	4.2	5.1	0.5	6.5	6.7	6.7	0.1	6.2	6.4	6.2	0.1	6.6	6.3	13.0	
Heather 1 Unburnt	9.2	4.2	5.0	0.5	-0.6	-0.5	-0.7	0.1	-0.5	-0.5	-0.6	0.1	-0.6	-0.5	-1.2	
Heather 2 Unburnt	8.7	4.2	4.5	0.5	-0.7	-0.6	-0.5	0.1	-0.5	-0.5	-0.4	0.1	-0.6	-0.5	-1.3	

Heather 3 Unburnt	8.6	4.2	4.4	0.4	-0.6	-0.5	-0.6	0.1	-0.6	-0.5	-0.6	0.1	-0.6	-0.6	-1.3
Heather 1 200^{0}C 3Hrs	6.2	4.2	2.0	0.2	-0.3	-0.3	-0.9	0.3	-0.3	-0.2	-0.3	0.1	-0.5	-0.3	-2.5
Heather 2 200^{0}C 3Hrs	6.1	4.2	1.9	0.2	-0.2	-0.6	-0.5	0.2	-0.4	-0.4	-0.1	0.2	-0.4	-0.3	-2.3
Heather 3 200^{0}C 3Hrs	6.2	4.2	2.0	0.2	-0.2	-0.6	-0.1	0.3	-0.1	-0.1	-0.1	0.0	-0.3	-0.1	-1.5
Heather 1 200^{0}C 6Hrs	6.4	4.2	2.2	0.2	-0.5	-0.6	-0.9	0.2	-0.6	-0.2	-0.5	0.2	-0.7	-0.4	-3.0
Heather 2 200^{0}C 6Hrs	6.7	4.2	2.5	0.3	-0.5	-0.7	-0.5	0.1	-0.2	-0.4	-0.5	0.2	-0.6	-0.4	-2.3
Heather 3 200^{0}C 6Hrs	6.7	4.2	2.5	0.3	-0.5	-0.7	-0.5	0.1	-0.4	-0.4	-0.4	0.0	-0.6	-0.4	-2.3
Heather 1 400^{0}C 6Hrs	5.5	4.2	1.3	0.1	1.1	0.8	1	0.2	2.8	2.5	2.9	0.2	1.0	2.7	7.4
Heather 2 400^{0}C 6Hrs	5.4	4.2	1.2	0.1	1.7	1.9	1.8	0.1	2.1	1.8	1.9	0.2	1.8	1.9	15.0
Heather 3 400^{0}C 6Hrs	5.2	4.2	1.0	0.1	3.1	2.9	3.2	0.2	1.5	1.3	1.7	0.2	3.1	1.5	30.7
Willow Unburnt	5.3	3.3	2.0	0.2	-0.2	-0.3	-0.2	0.1	-1.3	-1.1	-0.9	0.2	-0.2	-1.1	-1.2
Willow 1 200^{0}C 6Hrs	5.5	3.1	2.4	0.2	-0.3	-0.4	-0.3	0.1	-0.2	-0.1	-0.2	0.1	-0.3	-0.2	-1.4
Willow 2 200^{0}C 6Hrs	5.5	3.0	2.5	0.3	-0.3	-0.3	-0.5	0.1	-0.7	-0.3	-0.1	0.3	-0.4	-0.4	-1.5
Willow 3 200^{0}C 6Hrs	5.6	3.2	2.4	0.2	-0.3	-0.3	-0.3	0.0	-0.5	-0.5	-0.3	0.1	-0.3	-0.4	-1.3
Willow 1 400^{0}C 6Hrs	4.8	3.0	1.8	0.2	0.9	0.6	0.5	0.2	0.4	0.5	0.3	0.1	0.7	0.4	3.7
Willow 2 400^{0}C 6Hrs	4.5	3.0	1.5	0.2	0.9	0.9	0.8	0.1	0.7	0.5	0.5	0.1	0.9	0.6	5.8
Hazel Unburnt	4.6	3.1	1.5	0.2	-0.1	-0.4	-0.1	0.2	-0.4	-0.8	-0.6	0.2	-0.2	-0.6	-1.3
Hazel 1 200^{0}C	4.9	3.0	1.9	0.2	-	-	-	0.3	-	-	-	0.1	-0.6	-0.2	-3.2

6Hrs					0.3	0.8	0.7		0.2	0.2	0.3				
Hazel 2 200^{0}C 6Hrs	5.0	2.9	2.1	0.2	-0.3	-0.7	-0.5	0.2	-0.4	-0.2	-0.2	0.1	-0.5	-0.3	-2.4
Hazel 3 200^{0}C 6Hrs	4.9	3.1	1.8	0.2	-0.7	-0.4	-1.6	0.6	-0.2	-0.1	-0.1	0.1	-0.9	-0.1	-5.0
Hazel 1 400^{0}C 6Hrs	4.2	3.0	1.2	0.1	1.1	1.2	1.3	0.1	0.8	0.8	0.7	0.1	1.2	0.8	10.0
Hazel 2 400^{0}C 6Hrs	4.1	3.0	1.1	0.1	1.1	0.9	0.8	0.2	0.8	0.8	0.7	0.1	0.9	0.8	8.5
Bone Unburnt	12.5	3.0	9.5	1.0	-0.7	-0.9	-0.8	0.1	-0.5	-0.5	-0.5	0.0	-0.8	-0.5	-0.8
Bone 1 200^{0}C	14.3	3.3	11.0	1.1	-1.1	-0.9	-1.3	0.2	-0.5	-0.6	-0.5	0.1	-1.1	-0.5	-1.0
Bone 2 200^{0}C	14.3	3.0	11.3	1.1	-1.9	-0.9	-1.1	0.5	-0.4	-0.5	-0.5	0.1	-1.3	-0.5	-1.2
Bone 3 200^{0}C	13.0	3.1	9.9	1.0	-0.7	-1	-0.9	0.2	-0.4	-0.4	-0.6	0.1	-0.9	-0.5	-0.9
Bone 1 400^{0}C	10.7	3.3	7.4	0.7	-0.7	-0.8	-0.9	0.1	-0.5	-0.3	-0.4	0.1	-0.8	-0.4	-1.1
Bone 2 400^{0}C	10.4	3.2	7.2	0.7	-0.7	-0.6	-1	0.2	-0.2	-0.3	-0.5	0.2	-0.8	-0.3	-1.1
Bone 3 400^{0}C	11.2	3.2	8.0	0.8	-1.1	-0.9	-0.6	0.3	-0.5	-0.5	-0.5	0.0	-0.9	-0.5	-1.1
Bone 1 900^{0}C	14.3	3.1	11.2	1.1	-0.7	-1	-0.9	0.2	-0.4	-0.7	-0.4	0.2	-0.9	-0.5	-0.8
Bone 2 900^{0}C	14.1	3.3	10.8	1.1	-1	-0.8	-0.9	0.1	-0.4	-0.5	-0.5	0.1	-0.9	-0.5	-0.8
Bone 3 900^{0}C	14.6	3.3	11.3	1.1	-0.9	-0.7	-0.8	0.1	-0.6	-0.6	-0.5	0.1	-0.8	-0.6	-0.7
Rousay Peat 1 Unburnt	10.1	4.2	5.9	0.6	-0.2	-0.3	-0.4	0.1	-0.2	-0.0	-0.2	0.1	-0.3	-0.1	-0.5
Rousay Peat 2 Unburnt	8.3	4.2	4.1	0.4	-0.3	-0.4	-0.3	0.1	-0.1	-0.3	-0.2	0.1	-0.3	-0.2	-0.8
Rousay Peat 3 Unburnt	7.8	4.2	3.6	0.4	-0.3	-0.3	-0.4	0.1	-0.3	-0.1	-0.2	0.3	-0.3	0.0	-0.9

Rousay Peat 1 200^{0}C 3Hrs	8.0	4.2	3.8	0.4	0.5	0.5	0.6	0.1	0.3	0.5	0.3	0.1	0.5	0.4	1.4	
Rousay Peat 2 200^{0}C 3Hrs	7.3	4.2	3.1	0.3	0.4	0.5	0.5	0.1	0.5	0.3	1.1	0.4	0.5	0.6	1.5	
Rousay Peat 3 200^{0}C 3Hrs	8.0	4.2	3.8	0.4	0.6	0.5	0.6	0.1	0.5	0.9	0.6	0.2	0.6	0.7	1.5	
Rousay Peat 1 200^{0}C 6Hrs	7.6	4.2	3.4	0.3	7	6.7	6.1	0.5	6.2	3.1	5.9	1.7	6.6	5.1	19.4	
Rousay Peat 2 200^{0}C 6Hrs	8.0	4.2	3.8	0.4	6.4	7	6.1	0.5	6.1	2.9	6.0	1.8	6.5	5.0	17.1	
Rousay Peat 3 200^{0}C 6Hrs	7.8	4.2	3.6	0.4	7.1	6.4	6	0.6	6.3	3.2	5.8	1.7	6.5	5.1	18.1	
Rousay Peat 1 400^{0}C 6Hrs	5.5	4.2	1.3	0.1	34.5	34.1	34.2	0.2	27.9	29.4	28.4	0.8	34.3	28.6	263.6	16.6
Rousay Peat 2 400^{0}C 6Hrs	5.3	4.2	1.1	0.1	38.9	38.9	36.8	1.2	31.7	32.6	32.4	0.5	38.2	32.2	347.3	15.6
Rousay Peat 3 400^{0}C 6Hrs	5.4	4.2	1.2	0.1	45.2	46.8	46.1	0.8	41.5	41.2	40.6	0.5	46.0	41.1	383.6	10.7
Rousay Peat 1 900^{0}C 6Hrs	6.4	4.2	2.2	0.2	790.2	800	789	6.0	747.2	742.1	753.4	5.7	793.1	747.6	3604.8	5.7
Rousay Peat 2 900^{0}C 6Hrs	6.4	4.2	2.2	0.2	806	798	843	24.0	781.6	778.1	781.2	1.9	815.7	780.3	3707.6	4.3
Rousay Peat 3 900^{0}C 6Hrs	6.3	4.2	2.1	0.2	739	749	734	7.6	712.5	709.6	714.3	2.4	740.7	712.1	3527.0	3.9
Fozzy Peat Unburnt	6.1	3.0	3.1	0.3	-0.4	-0.3	-0.5	0.1	-0.3	-0.2	-0.4	0.1	-0.4	-0.3	-1.3	
Fozzy Peat 1 200^{0}C	5.6	3.1	2.5	0.3	-0.6	-0.4	-0.5	0.1	-0.1	-0.1	0.0	0.1	-0.5	-0.1	-2.0	
Fozzy Peat 2 200^{0}C	5.9	3.0	2.9	0.3	-0.5	-0.1	-0.2	0.2	-0.1	-0.1	-0.1	0.0	-0.3	-0.1	-0.9	
Fozzy Peat 3 200^{0}C	5.7	3.0	2.7	0.3	-0.1	-0.1	-0.4	0.2	0.0	0.0	-0.1	0.1	-0.2	0.0	-0.7	
Fozzy Peat 1 400^{0}C	5.7	3.0	2.7	0.3	1.7	2.1	1.7	0.2	0.7	0.9	1.1	0.2	1.8	0.9	6.8	
Fozzy Peat 2	6.2	3.3	2.9	0.3	1.9	2	1.7	0.2	1.4	1.4	1.2	0.1	1.9	1.3	6.4	28.6

400^{0}C																
Fozzy Peat 3 400^{0}C	5.9	3.1	2.8	0.3	2	1.4	1.9	0.3	1.6	1.3	1.2	0.2	1.8	1.4	6.3	22.6
Fozzy Peat 900^{0}C	5.5	3.1	2.4	0.2	27 3.1	27 2	27 2.7	0.6	24 5.5	24 1.2	24 3.7	2.2	272.6	243.5	1135.8	10.7
Middle Peat Unburnt	6.6	3.0	3.6	0.4	- 0.3	- 0.4	- 0.4	0.1	- 0.2	- 0.2	- 0.2	0.0	-0.4	-0.2	-1.0	
Middle Peat 1 200^{0}C	7.3	3.0	4.3	0.4	0.8	0.6	0.7	0.1	0.8	0.9	0.7	0.1	0.7	0.8	1.6	
Middle Peat 2 200^{0}C	7.4	3.1	4.3	0.4	0.5	0.4	0.6	0.1	0.8	0.8	0.9	0.1	0.5	0.8	1.2	
Middle Peat 3 200^{0}C	7.7	3.0	4.7	0.5	0.5	0.7	0.3	0.2	0.7	0.5	0.6	0.1	0.5	0.6	1.1	
Middle Peat 1 400^{0}C	5.5	3.0	2.5	0.3	18. 5	17. 1	16. 9	0.9	11. 1	9.2	10. 5	1.0	17.5	10.3	70.0	41.3
Middle Peat 2 400^{0}C	5.4	3.3	2.1	0.2	19. 1	19. 2	18. 7	0.3	17. 9	17. 2	16. 3	0.8	19.0	17.1	90.5	9.8
Middle Peat 3 400^{0}C	4.9	3.1	1.8	0.2	19. 3	20. 8	21	0.9	16. 5	17. 2	17. 6	0.6	20.4	17.1	113.1	16.0
Middle Peat 900^{0}C	5.6	3.0	2.6	0.3	21 3.5	21 4	21 4.8	0.7	18 9.4	18 8.5	18 9.8	0.7	214.1	189.2	823.5	11.6
Low Peat Unburnt	7.1	3.1	4.0	0.4	- 0.1	- 0.2	- 0.4	0.2	- 0.2	- 0.1	- 0.2	0.1	-0.2	-0.2	-0.6	
Low Peat 1 200^{0}C	7.3	3.2	4.1	0.4	8.3	7.4	7.7	0.5	7.5	7.3	7.4	0.1	7.8	7.4	19.0	
Low Peat 2 200^{0}C	7.5	3.1	4.4	0.4	3.4	3.2	3.3	0.1	3.9	3.9	3.9	0.0	3.3	3.9	7.5	
Low Peat 3 200^{0}C	7.1	3.2	3.9	0.4	3.8	3.5	3.6	0.2	4.1	4.0	3.9	0.1	3.6	4.0	9.3	
Low Peat 1 400^{0}C	7.6	3.3	4.3	0.4	9.2	8.7	9.3	0.3	7.8	7.9	7.7	0.1	9.1	7.8	21.1	
Low Peat 2 400^{0}C	7.6	3.1	4.5	0.5	8.5	7.7	7.1	0.7	6.5	6.3	6.4	0.1	7.8	6.4	17.3	
Low Peat 3 400^{0}C	7.6	3.1	4.5	0.5	9.3	9.7	9.5	0.2	8.7	8.6	8.8	0.1	9.5	8.7	21.1	8.4

Low Peat 1 900^{0}C	7.9	3.1	4.8	0.5	58 6.7	58 5.4	58 1.4	2.8	53 5.7	53 3.5	53 6.2	1.4	584.5	535.1	1217.7	8.4
Low Peat 2 900^{0}C	8.1	3.2	4.9	0.5	64 8.7	65 1.4	65 1.4	1.6	60 1.8	59 2.7	59 5.7	4.6	650.5	596.7	1327.6	8.3
Low Peat 3 900^{0}C	8.2	3.1	5.1	0.5	24 5.3	24 1	24 8.5	3.8	22 7.9	22 5.3	22 6.3	1.3	244.9	226.5	480.3	7.5
Highland Park Peat Unburnt	6.9	3.1	3.8	0.4	- 0.1	- 0.3	- 0.2	0.1	- 0.1	- 0.1	- 0.1	0.0	-0.2	-0.1	-0.5	
Highland Park Peat 1 200^{0}C	6.8	3.0	3.8	0.4	2.3	2.3	2.3	0.0	2.5	2.6	2.4	0.1	2.3	2.5	6.1	
Highland Park Peat 2 200^{0}C	6.9	3.2	3.7	0.4	1.3	1.3	1.2	0.1	1.5	1.5	1.3	0.1	1.3	1.4	3.4	
Highland Park Peat 3 200^{0}C	7.0	3.3	3.7	0.4	1.6	1.2	1.4	0.2	1.6	1.5	1.3	0.2	1.4	1.5	3.8	
Highland Park Peat 1 400^{0}C	5.6	3.0	2.6	0.3	4.4	4.7	4.5	0.2	3.7	4.1	3.7	0.2	4.5	3.8	17.4	
Highland Park Peat 2 400^{0}C	5.0	3.0	2.0	0.2	4.6	4.4	4.6	0.1	3.8	4.0	3.7	0.2	4.5	3.8	22.7	15.4
Highland Park Peat 900^{0}C	5.1	3.3	1.8	0.2	31 5.1	31 4.2	31 4.7	0.5	28 2.2	28 4.7	28 4.3	1.3	314.7	283.7	1748.1	9.8
Mix Fuel 1 500^{0}C	7.0	3.0	4.0	0.4	13. 5	14. 1	14	0.3	12. 6	12. 6	12. 2	0.2	13.9	12.5	34.7	10.1
Mix Fuel 2 500^{0}C	6.1	3.0	3.1	0.3	11. 4	11. 3	11. 2	0.1	10. 5	10. 5	10. 5	0.0	11.3	10.5	36.5	7.1
Orkney Peat 1	6.8	3.3	3.5	0.4	48 2.3	48 6.7	48 4.5	2.2	43 1.2	42 8.7	42 9.1	1.3	484.5	429.7	1384.3	11.3
Orkney Peat 2	5.7	3.1	2.6	0.3	51 9.2	51 5.5	51 8.7	2.0	45 5.4	45 6.1	45 5.9	0.4	517.8	455.8	1991.5	12.0
Orkney Peat 3	6	3.1	2.9	0.3	47 6.9	47 6.8	47 6.6	0.2	42 5.5	42 6.7	42 4.6	1.1	476.8	425.6	1644.0	10.7
Caith Peat 1	17.2	3	14.2	1.4	67 54	67 25. 7	67 37. 4	14.2	61 53. 4	61 26. 5	61 37. 8	13.5	6739. 0	6139. 2	4745.8	8.9
Caith Peat 2	17.5	3.3	14.2	1.4	62 60.	62 58.	62 61.	1.6	57 79.	57 64.	57 69.	7.6	6260. 1	5770. 8	4408.5	7.8

					7	3	4		1	3	1				
Caith Peat 3	18	3.1	14.9	1.5	5995.3	5997.8	5956.7	23.0	5510.4	5501.8	5509.3	4.7	5983.3	5507.2	4015.6	8.0
Archaeological Matrix 1 900^{0}C	14.5	4.2	10.3	1.0	1156.8	1154.4	1155	1.2	1036.9	1038.5	1037.6	0.8	1155.4	1037.7	1121.7	10.2
Archaeological Matrix 2 900^{0}C	13.9	4.2	9.7	1.0	1089.9	1088.8	1089.7	0.6	974.9	976.9	975.8	1.0	1089.5	975.9	1123.2	10.4
Archaeological Matrix UB	14.4	4.2	10.2	1.0	88.3	89.1	89.4	0.6	80.3	82.9	81.9	1.3	88.9	81.7	87.2	8.1
Peat + Pine ash 1	9.5	4.2	5.3	0.5	189.5	191.9	190.6	1.2	179.8	176.4	177.3	1.8	190.7	177.8	359.7	6.7
Peat + Pine ash 2	8.4	4.2	4.2	0.4	155.4	154.8	155	0.3	142.7	141.9	143	0.6	155.1	142.5	369.2	8.1
Peat + Pine ash 3	9.4	4.2	5.2	0.5	178.1	177.3	177.4	0.4	154.9	155.8	155.5	0.5	177.6	155.4	341.5	12.5
Hammerscale	4.4	4.2	0.2	0.0	187.6	195.9	191.4	4.2	133.6	134.4	132.7	0.9	191.6	133.6		30.3
Sand + Hammerscale	12.9	4.2	8.7	0.9	691.6	695.9	698.8	3.6	551.9	552.3	550.8	0.8	695.4	551.7		20.7
Sand	17.7	4.2	13.5	1.4	2.7	2.7	2.7	0.0	2.8	2.7	2.8	0.1	2.7	2.8		
Burnt Sand	18.3	4.2	14.1	1.4	33.4	32.7	33.3	0.4	32	31.9	31.9	0.1	33.1	31.9		3.6
Means	7.7	3.8	4.0	0.4	179.4	179.3	179.3	0.8	163.8	165.3	163.6	0.5	179.3	163.5	260.7	11.9

Archaeological Sample Magnetic Susceptibility Dataset

Sample	Sample + Container mass	Container mass	Sample mass	Bulk Density	κlf 1	κlf 2	κlf 3	Standard Deviation	κhf 1	κhf 2	κhf 3	Standard Deviation	Average κlf	Average κhf	χlf =κ/p x10-8 m3kg-1	FDMS = (κlf-κhf/κlf) x 100
NoB 2617-1	16.9	4.2	12.7	1.3	678.3	678.3	678.4	0.06	633.1	626.2	625.2	4.30	678.3	628.2	534.1	7.4
NoB 2617-2	17.0	4.2	12.8	1.3	746.6	747.8	746.6	0.69	688.4	688.2	688.4	0.12	747.0	688.3	583.6	7.9
NoB 2617-3	15.5	4.2	11.3	1.1	739.5	739.5	739.5	0.00	683.0	683.4	683.1	0.21	739.5	683.2	654.4	7.6
NoB 5332-1	18.6	4.2	14.4	1.4	471.7	453.3	452.0	11.02	372.5	371.4	372.7	0.70	459.0	372.2	318.8	18.9
NoB 5332-2	19.4	4.2	15.2	1.5	673.1	667.9	717.7	27.37	560.5	559.4	560.1	0.56	686.2	560.0	451.5	18.4
NoB 5332-3	19.2	4.2	15	1.5	557.7	562.8	558.4	2.76	455.9	454.9	454.0	0.95	559.6	454.9	373.1	18.7
NoB 3783-1	17.8	4.2	13.6	1.4	254.1	252.5	262.0	5.09	165.8	171.9	172.0	3.55	256.2	169.9	188.4	33.7
NoB 3783-2	16.3	4.2	12.1	1.2	543.3	567.1	551.1	12.13	457.2	457.4	455.4	1.10	553.8	456.7	457.7	17.5
NoB 3783-3	17.8	4.2	13.6	1.4	198.0	197.8	197.3	0.36	142.3	148.3	146.5	3.08	197.7	145.7	145.4	26.3
NoB 5013-1	19.8	3.0	16.8	1.7	221 7.6	221 8.2	221 7.8	0.31	204 2.1	204 3.9	204 2.9	0.90	2217.9	2043.0	1320.2	7.9
NoB 5013-2	18.8	3.0	15.8	1.6	211 7.6	211 4.6	211 8.2	1.93	195 3.8	197 4.1	195 2.3	12.18	2116.8	1960.1	1339.7	7.4
NoB 5013-3	20.3	3.1	17.2	1.7	228 2.6	227 9.4	228 0.7	1.61	211 8.2	210 0.4	210 3.4	9.53	2280.9	2107.3	1326.1	7.6
NoB 4674-1	19.7	3.1	16.6	1.7	220 7.8	220 8.0	220 8.0	0.12	202 2.5	202 9.2	203 4.2	5.87	2207.9	2028.6	1330.1	8.1
NoB 4674-2	19.2	3.4	15.8	1.6	210 6.7	210 5.4	210 6.1	0.65	194 0.3	193 6.2	193 8.3	2.05	2106.1	1938.3	1333.0	8.0
NoB 4674-3	20.7	3.1	17.6	1.8	224 7.0	224 5.6	224 6.9	0.78	198 4.0	199 9.4	198 5.6	8.47	2246.5	1989.7	1276.4	11.4

NoB 4667-1	18.9	3.3	15.6	1.6	242.6	241.8	241.9	2.33	222.3	222.1	222.0	0.15	2420.1	2228.1	1551.3	7.9
NoB 4667-2	19.1	3.1	16	1.6	235.8	235.4	235.4	0.30	216.8	219.3	217.2	12.71	2354.1	2178.1	1471.3	7.5
NoB 4667-3	18.0	3.1	14.9	1.5	239.1	239.6	239.7	3.80	222.3	220.5	220.8	8.98	2393.8	2212.1	1606.6	7.6
NoB 4656-1	18.3	3.1	15.2	1.5	158.4	157.9	157.0	4.72	143.9	142.2	143.7	2.95	1578.4	1431.6	1038.4	9.3
NoB 4656-2	19.8	3.1	16.7	1.7	188.9	188.5	188.6	1.98	172.4	171.8	172.4	3.31	1887.3	1721.7	1130.1	8.8
NoB 4656-3	17.8	3.1	14.7	1.5	156.9	157.0	157.0	0.30	142.1	142.5	143.1	2.38	1570.0	1427.5	1068.0	9.1
NoB 6013-1	17.5	3.1	14.4	1.4	121.8	122.1	122.0	1.39	111.5	111.6	111.4	0.70	1220.3	1115.6	847.5	8.6
NoB 6013-2	17.7	3.3	14.4	1.4	117.5	117.2	117.4	1.51	108.2	107.6	108.1	3.53	1174.3	1080.2	815.5	8.0
NoB 6013-3	15.8	3.1	12.7	1.3	111.5	112.1	111.6	3.04	102.4	102.8	102.3	2.86	1117.9	1025.2	880.3	8.3
NoB 4264-1	18.6	3.1	15.5	1.6	141.6	141.8	141.6	0.06	129.5	129.3	129.4	0.75	1416.7	1294.6	914.0	8.6
NoB 4264-2	17.5	3.3	14.2	1.4	125.2	125.2	125.3	0.10	113.6	113.5	113.6	1.06	1252.9	1137.3	882.3	9.2
NoB 4264-3	17.6	3.3	14.3	1.4	140.2	140.2	140.2	0.10	126.7	127.2	126.9	2.41	1402.1	1269.9	980.5	9.4
NoB 6156-1	16.2	3.1	13.1	1.3	170.9	171.3	170.9	0.56	157.2	157.3	157.1	0.55	1709.7	1573.1	1305.1	8.0
NoB 6156-2	16.2	3.3	12.9	1.3	165.3	165.3	165.3	0.45	151.9	151.2	151.5	3.84	1653.4	1515.7	1281.7	8.3
NoB 6156-3	16.5	3.1	13.4	1.3	172.3	171.7	171.5	4.22	156.9	157.1	156.7	2.07	1718.5	1569.6	1282.4	8.7
NoB 3851-1	20.9	3.1	17.8	1.8	189.6	189.6	189.6	0.31	171.5	172.1	171.9	3.36	1896.3	1718.7	1065.3	9.4
NoB 3851-2	20.4	3.1	17.3	1.7	101.6	101.6	101.6	0.15	822.9	827.6	825.1	2.35	1016.5	825.2	587.6	18.8
NoB	20.4	3.1	17.3	1.7	195	195	195	2.22	177	176	177	4.80	1957.	1772.	1131.4	9.4

3851-3					6.7	9.8	5.5		7.2	7.6	2.4		3	4		
NoB 3857-1	21.1	3.3	17.8	1.8	966 .9	966 .6	966 .9	0.17	778 .5	775 .3	776 .9	1.60	966.8	776.9	543.1	19.6
NoB 3857-2	20.7	3.1	17.6	1.8	110 2.2	109 8.5	110 1.1	1.90	902 .1	900 .2	901 .7	1.00	1100. 6	901.3	625.3	18.1
NoB 3857-3	20.5	3.1	17.4	1.7	996 .7	995 .7	996 .2	0.50	807 .2	800 .6	805 .3	3.40	996.2	804.4	572.5	19.3
NoB30 6354-1	17.8	3.3	14.5	1.5	116 1.4	115 9.0	115 6.3	2.55	107 1.4	106 9.0	107 0.8	1.25	1158. 9	1070. 4	799.2	7.6
NoB30 6354-2	17.8	3.3	14.5	1.5	125 7.8	124 8.6	125 4.1	4.63	115 4.3	115 1.3	115 2.8	1.50	1253. 5	1152. 8	864.5	8.0
NoB30 6354-3	18.1	3.3	14.8	1.5	124 9.9	124 5.3	124 6.1	2.46	114 3.7	114 1.1	114 1.9	1.33	1247. 1	1142. 2	842.6	8.4
NoB28 6348-1	16.6	3.1	13.5	1.4	174 9.7	174 7.1	174 9.3	1.40	160 3.3	159 8.6	160 0.7	2.35	1748. 7	1600. 9	1295.3	8.5
NoB28 6348-2	17.0	3	14	1.4	191 8.6	192 3.6	191 6.2	3.78	175 6.0	174 9.9	175 3.4	3.06	1919. 5	1753. 1	1371.0	8.7
NoB28 6348-3	17.0	3	14	1.4	176 6.4	178 4.0	176 4.3	10.82	162 0.4	161 8.7	162 0.1	0.91	1771. 6	1619. 7	1265.4	8.6
NoB16 6355-1	17.5	3.3	14.2	1.4	113 6.3	113 5.8	113 3.8	1.32	104 3.9	103 8.6	104 0.5	2.69	1135. 3	1041. 0	799.5	8.3
NoB16 6355-2	17.7	3	14.7	1.5	122 5.6	122 2.4	122 3.0	1.70	112 4.3	112 2.8	112 2.0	1.17	1223. 7	1123. 0	832.4	8.2
NoB16 6355-3	17.9	3.2	14.7	1.5	131 0.2	130 8.7	130 5.5	2.40	120 4.8	120 5.0	120 5.3	0.25	1308. 1	1205. 0	889.9	7.9
NoB33 5689-1	18.4	3.1	15.3	1.5	213 0.9	213 0.4	212 7.4	1.89	194 6.1	193 6.7	194 2.5	4.74	2129. 6	1941. 8	1391.9	8.8
NoB33 5689-2	18.3	3.1	15.2	1.5	211 7.1	211 9.0	210 8.6	5.54	193 6.4	193 1.1	193 4.7	2.71	2114. 9	1934. 1	1391.4	8.6
NoB33 5689-3	18.8	3	15.8	1.6	231 2.2	230 9.1	231 1.4	1.61	211 1.1	210 6.3	210 9.8	2.48	2310. 9	2109. 1	1462.6	8.7
NoB31 6356-1	18.3	3.1	15.2	1.5	121 6.3	121 4.3	122 0.1	2.95	111 7.8	111 5.9	111 6.3	1.00	1216. 9	1116. 7	800.6	8.2
NoB31 6356-2	15.9	3	12.9	1.3	104 4.5	104 3.4	104 3.0	0.78	954 .7	951 .8	953 .6	1.46	1043. 6	953.4	809.0	8.6

NoB31 6356-3	17.9	3.1	14.8	1.5	118 2.5	118 2.0	117 7.6	2.70	108 6.9	108 5.1	108 6.4	0.93	1180. 7	1086. 1	797.8	8.0
NoB29 6351-1	17.5	3.1	14.4	1.4	198 3.3	197 0.0	198 0.7	7.05	182 3.2	182 2.6	182 0.7	1.31	1978. 0	1822. 2	1373.6	7.9
NoB29 6351-2	16.1	3.2	12.9	1.3	175 8.6	175 4.0	175 0.3	4.16	161 6.4	161 1.8	161 3.9	2.30	1754. 3	1614. 0	1359.9	8.0
NoB29 6351-3	16.6	3.1	13.5	1.4	195 2.4	194 4.0	194 6.2	4.36	179 6.5	179 0.3	179 4.7	3.19	1947. 5	1793. 8	1442.6	7.9
NoB27 6339-1	18.1	3	15.1	1.5	127 1.4	125 6.1	126 8.1	8.05	114 3.6	115 9.1	114 9.6	7.82	1265. 2	1150. 8	837.9	9.0
NoB27 6339-2	18.4	3.1	15.3	1.5	135 1.4	134 0.2	134 2.0	6.01	121 9.8	121 4.6	121 7.3	2.60	1344. 5	1217. 2	878.8	9.5
NoB27 6339-3	17.9	3.1	14.8	1.5	129 6.0	129 2.9	129 3.5	1.64	117 1.3	116 8.7	116 9.5	1.33	1294. 1	1169. 8	874.4	9.6
NoB16 3851-1	19.0	3	16	1.6	178 4.1	178 0.0	177 6.8	3.66	160 4.5	160 1.8	160 3.2	1.35	1780. 3	1603. 2	1112.7	9.9
NoB16 3851-2	18.0	3	15	1.5	163 0.0	162 2.8	161 8.3	5.90	146 6.2	147 1.5	146 9.8	2.71	1623. 7	1469. 2	1082.5	9.5
NoB16 3851-3	19.1	3	16.1	1.6	192 9.3	190 8.5	191 3.8	10.81	174 0.0	173 8.2	173 8.5	0.96	1917. 2	1738. 9	1190.8	9.3
NoB16 6346-1	15.8	3	12.8	1.3	570 .6	568 .0	564 .6	3.01	512 .0	510 .6	510 .9	0.74	567.7	511.2	443.5	10.0
NoB16 6346-2	16.7	3	13.7	1.4	509 .0	507 .1	506 .1	1.47	455 .7	444 .9	451 .3	5.43	507.4	450.6	370.4	11.2
NoB T 5855-1	16.5	3.3	13.2	1.3	131 0.8	130 7.5	131 1.2	2.03	119 0.5	118 7.3	118 8.9	1.60	1309. 8	1188. 9	992.3	9.2
NoB T 5855-2	14.9	3	11.9	1.2	113 8.2	113 7.0	113 6.5	0.87	102 6.2	102 3.7	102 5.6	1.31	1137. 2	1025. 2	955.7	9.9
NoB T 5855-3	14.9	3.3	11.6	1.2	118 8.2	118 6.9	118 7.9	0.68	107 6.5	107 1.3	107 2.8	2.68	1187. 7	1073. 5	1023.9	9.6
NoB T 4825-1	16.8	3	13.8	1.4	588 .5	588 .1	586 .6	1.00	528 .3	531 .0	527 .9	1.69	587.7	529.1	425.9	10.0
NoB T 4825-2	16.5	3.1	13.4	1.3	776 .2	774 .8	775 .7	0.71	700 .1	698 .7	699 .9	0.76	775.6	699.6	578.8	9.8
NoB T	18.2	3.1	15.1	1.5	821	820	820	0.40	740	738	740	0.87	820.8	739.8	543.6	9.9

4825-3					.3	.6	.6		.2	.8	.4					
NoB T 4831-1	17.2	3	14.2	1.4	104 2.2	102 3.7	102 2.3	11.11	930 .2	925 .8	928 .6	2.23	1029. 4	928.2	724.9	9.8
NoB T 4831-2	17.3	3.1	14.2	1.4	106 3.7	106 1.3	106 3.7	1.39	963 .4	958 .9	960 .7	2.26	1062. 9	961.0	748.5	9.6
NoB T 4831-3	19	3.1	15.9	1.6	113 1.8	112 9.9	113 0.3	1.00	102 9.3	102 6.7	102 8.1	1.30	1130. 7	1028. 0	711.1	9.1
NoB T 4860-1	14.9	3.3	11.6	1.2	116 5.0	116 2.4	116 3.9	1.31	105 8.6	105 5.5	105 7.3	1.56	1163. 8	1057. 1	1003.2	9.2
NoB T 4860-2	15.9	3.2	12.7	1.3	111 5.9	111 5.6	111 5.7	0.15	101 9.7	102 0.1	102 0.3	0.31	1115. 7	1020. 0	878.5	8.6
NoB T 4860-3	16.5	3	13.5	1.4	125 8.0	125 6.3	126 3.4	3.71	114 1.0	114 2.3	114 1.8	0.66	1259. 2	1141. 7	932.8	9.3
NoB T 5810-1	18.9	3	15.9	1.6	144 0.6	144 1.0	143 7.6	1.86	131 2.4	130 9.7	130 8.9	1.83	1439. 7	1310. 3	905.5	9.0
NoB T 5810-2	20.1	3.2	16.9	1.7	131 1.9	130 6.7	131 2.1	3.06	119 2.7	119 1.9	119 2.0	0.44	1310. 2	1192. 2	775.3	9.0
NoB T 5810-3	19.8	3	16.8	1.7	166 0.3	165 7.1	166 0.5	1.91	151 4.6	150 7.8	151 1.8	3.42	1659. 3	1511. 4	987.7	8.9
NoB T 5849-1	17.6	3	14.6	1.5	399 3.4	398 9.4	398 0.5	6.60	370 8.1	370 3.5	370 6.9	2.39	3987. 8	3706. 2	2731.3	7.1
NoB T 5849-2	19	3.1	15.9	1.6	433 1.4	431 2.0	431 8.7	9.85	401 5.3	401 7.4	401 5.9	1.08	4320. 7	4016. 2	2717.4	7.0
NoB T 5849-3	17.6	3	14.6	1.5	372 1.6	372 0.1	371 4.5	3.74	346 2.3	345 9.8	346 0.7	1.27	3718. 7	3460. 9	2547.1	6.9
KoS 3081-1	15.4	4.2	11.2	1.1	370 .5	372 .6	375 .5	2.51	253 .2	254 .3	262 .2	4.91	372.9	256.6	332.9	31.2
KoS 3081-2	14.7	4.2	10.5	1.1	184 .4	182 .3	191 .6	4.88	112 .5	118 .2	119 .9	3.88	186.1	116.9	177.2	37.2
KoS 3081-3	15.6	4.2	11.4	1.1	413 .3	415 .0	410 .1	2.49	304 .3	294 .1	294 .4	5.80	412.8	297.6	362.1	27.9
KoS 2039-1	17.7	4.2	13.5	1.4	757 .0	757 .8	757 .1	0.44	693 .5	696 .8	696 .8	1.91	757.3	695.7	561.0	8.1
KoS 2039-2	19.4	4.2	15.2	1.5	643 .6	637 .2	637 .9	3.51	583 .6	589 .4	589 .0	3.24	639.6	587.3	420.8	8.2

KoS 2039-3	18.3	4.2	14.1	1.4	673.5	673.9	673.5	0.23	617.7	617.9	617.0	0.47	673.6	617.5	477.8	8.3
KoS 3238-1	15.5	3.0	12.5	1.3	414.9	415.6	415.3	0.35	376.3	372.1	377.1	2.69	415.3	375.2	332.2	9.7
KoS 3238-2	15.4	3.0	12.4	1.2	370.7	370.9	370.8	0.10	333.3	336.2	334.3	1.47	370.8	334.6	299.0	9.8
KoS 3238-3	15.5	3.0	12.5	1.3	349.1	348.2	347.9	0.62	316.4	316.3	316.4	0.06	348.4	316.4	278.7	9.2
KoS 3255-1	14.2	3.0	11.2	1.1	493.1	493.6	492.7	0.45	442.4	444.3	447.4	2.52	493.1	444.7	440.3	9.8
KoS 3255-2	14.0	3.1	10.9	1.1	475.6	475.1	475.3	0.25	432.8	430.0	429.8	1.68	475.3	430.9	436.1	9.4
KoS 3255-3	14.7	3.3	11.4	1.1	534.1	533.9	534.3	0.20	482.2	483.2	481.8	0.72	534.1	482.4	468.5	9.7
KoS 3217-1	12.0	3.0	9	0.9	447.7	446.3	446.9	0.70	411.4	412.0	413.6	1.14	447.0	412.3	496.6	7.7
KoS 3217-2	12.6	3.0	9.6	1.0	415.5	415.0	415.3	0.25	385.8	390.2	394.9	4.55	415.3	390.3	432.6	6.0
KoS 3217-3	12.6	3.0	9.6	1.0	454.9	539.5	547.5	51.31	510.8	511.1	511.0	0.15	514.0	511.0	535.4	0.6
KoS 3196-1	12.0	3.0	9	0.9	228.0	227.7	228.3	0.30	202.2	202.1	202.1	0.06	228.0	202.1	253.3	11.3
KoS 3196-2	11.1	3.0	8.1	0.8	232.2	231.7	231.9	0.25	205.4	206.3	205.6	0.47	231.9	205.8	286.3	11.3
KoS 3196-3	11.3	3.0	8.3	0.8	239.6	239.3	240.0	0.35	212.8	213.0	213.1	0.15	239.6	213.0	288.7	11.1
KoS 3225-1	11.7	3.0	8.7	0.9	271.3	274.4	271.1	1.85	240.0	240.9	241.1	0.59	272.3	240.7	313.0	11.6
KoS 3225-2	12.2	3.0	9.2	0.9	247.7	247.4	247.1	0.30	219.0	219.3	219.1	0.15	247.4	219.1	268.9	11.4
KoS 3225-3	11.8	3.0	8.8	0.9	254.7	252.4	253.0	1.19	225.3	224.8	225.1	0.25	253.4	225.1	287.9	11.2
KoS 3201-1	12.0	3.0	9	0.9	92.6	92.7	92.5	0.10	82.9	83.0	82.7	0.15	92.6	82.9	102.9	10.5
KoS	11.9	3.0	8.9	0.9	76.	76.	75.	0.15	69.	67.	67.	1.44	76.0	68.1	85.4	10.4

3201-2					1	0	8		7	0	5					
KoS 3201-3	11.7	3.0	8.7	0.9	96.2	92.7	92.5	2.08	86.1	86.7	86.5	0.31	93.8	86.4	107.8	7.9
RDL 001-1	15.9	3.3	12.6	1.3	38.7	37.2	38.2	0.76	34.0	33.5	33.9	0.26	38.0	33.8	30.2	11.1
RDL 001-2	16.4	3.3	13.1	1.3	53.2	51.8	50.4	1.40	47.8	48.0	48.4	0.31	51.8	48.1	39.5	7.2
RDL 001-3	16.0	3.2	12.8	1.3	39.1	38.5	39.5	0.50	34.2	34.5	34.3	0.15	39.0	34.3	30.5	12.0
RDL 004-1	12.4	3.2	9.2	0.9	38.4	38.4	39.1	0.40	34.1	33.8	34.0	0.15	38.6	34.0	42.0	12.1
RDL 004-2	14.6	3.2	11.4	1.1	42.6	42.5	43.4	0.49	38.2	38.1	38.2	0.06	42.8	38.2	37.6	10.9
RDL 004-3	13.7	3.1	10.6	1.1	88.2	86.7	87.3	0.75	79.9	80.3	80.1	0.20	87.4	80.1	82.5	8.4
RDL 006-1	16.8	3.1	13.7	1.4	1167.4	1168.2	1184.0	9.36	1055.3	1048.7	1050.6	3.40	1173.2	1051.5	856.4	10.4
RDL 006-2	15.7	3.0	12.7	1.3	1083.3	1085.8	1084.7	1.25	968.8	968.0	967.1	0.62	1084.6	967.3	854.0	10.8
RDL 006-3	16.3	3.0	13.3	1.3	1039.3	1043.7	1041.8	2.21	920.1	917.1	921.3	2.16	1041.6	919.5	783.2	11.7
RDL 007-1	16.2	3.0	13.2	1.3	461.3	459.0	459.9	1.16	403.6	405.5	404.7	0.95	460.1	404.6	348.5	12.1
RDL 007-2	16.4	3.0	13.4	1.3	435.2	434.0	434.5	0.60	382.0	382.2	382.0	0.12	434.6	382.1	324.3	12.1
RDL 007-3	17.4	3.3	14.1	1.4	431.3	426.2	429.6	2.60	381.7	381.0	381.3	0.35	429.0	381.3	304.3	11.1
RDL 009-1	15.5	3.0	12.5	1.3	78.4	77.6	78.3	0.44	72.6	56.5	71.5	8.99	78.1	66.9	62.5	14.4
RDL 009-2	15.4	3.0	12.4	1.2	86.0	85.6	86.2	0.31	74.5	75.5	75.0	0.50	85.9	75.0	69.3	12.7
RDL 009-3	16.2	3.1	13.1	1.3	86.7	86.3	86.5	0.20	75.2	43.6	58.6	15.81	86.5	59.1	66.0	31.6
RDL 013-1	15.2	3.3	11.9	1.2	896.9	900.7	898.3	1.92	800.0	797.3	799.8	1.50	898.6	799.0	755.2	11.1

RDL 013-2	16.0	3.0	13	1.3	977.2	974.0	979.2	2.62	861.9	859.6	860.4	1.17	976.8	860.6	751.4	11.9
RDL 013-3	16.4	3.0	13.4	1.3	992.9	988.2	989.7	2.40	877.2	871.4	875.6	3.00	990.3	874.7	739.0	11.7
RDL 016-1	13.9	3.0	10.9	1.1	705.1	703.2	712.5	4.91	629.5	629.5	630.0	0.29	706.9	629.7	648.6	10.9
RDL 016-2	16.5	3.1	13.4	1.3	904.3	894.5	897.8	4.99	826.5	793.1	793.4	19.20	898.9	804.3	670.8	10.5
RDL 016-3	15.6	3.2	12.4	1.2	694.9	692.9	693.7	1.01	622.8	621.0	621.7	0.91	693.8	621.8	559.5	10.4
RDL 023-1	17.9	4.2	13.7	1.4	179 5.6	178 9.5	179 4.6	3.27	163 3.6	164 0.0	163 4.1	3.56	1793.2	1635.9	1308.9	8.8
RDL 023-2	20.6	4.2	16.4	1.6	209 0.5	207 8.3	209 8.2	10.03	189 1.7	188 8.7	188 5.9	2.90	2089.0	1888.8	1273.8	9.6
RDL 023-3	20.0	4.2	15.8	1.6	212 2.6	211 9.7	212 1.3	1.45	192 2.4	191 1.8	191 2.6	5.90	2121.2	1915.6	1342.5	9.7
RDL 031-1	15.1	3.0	12.1	1.2	51.1	50.9	51.5	0.31	44.1	44.1	44.0	0.06	51.2	44.1	42.3	13.9
RDL 031-2	15.3	3.0	12.3	1.2	76.1	75.8	76.3	0.25	65.8	57.1	65.0	4.81	76.1	62.6	61.8	17.7
RDL 031-3	14.8	3.1	11.7	1.2	81.2	81.2	81.7	0.29	74.5	69.2	72.3	2.66	81.4	72.0	69.5	11.5
RDL 032-1	15.9	3.0	12.9	1.3	678.1	680.0	679.9	1.07	603.0	604.2	603.7	0.60	679.3	603.6	526.6	11.1
RDL 032-2	16.4	3.2	13.2	1.3	549.6	549.8	546.0	2.14	494.0	494.0	494.0	0.00	548.5	494.0	415.5	9.9
RDL 032-3	16.0	3.0	13	1.3	459.5	457.6	456.9	1.35	410.6	409.9	410.2	0.35	458.0	410.2	352.3	10.4
SMQ A 1	19.8	3.2	16.6	1.7	208 5.1	208 0.0	207 9.6	3.07	189 3.8	189 1.0	188 8.8	2.51	2081.6	1891.2	1254.0	9.1
SMQ A 2	20.2	3.1	17.1	1.7	222 7.5	222 5.4	222 3.8	1.86	202 8.7	202 4.5	202 8.0	2.25	2225.6	2027.1	1301.5	8.9
SMQ A 3	19.1	3.0	16.1	1.6	202 3.0	202 0.7	201 9.2	1.91	183 4.6	183 4.0	183 4.4	0.31	2021.0	1834.3	1255.3	9.2
SMQ B	16.4	3.1	13.3	1.3	171	170	170	3.84	158	158	158	1.40	1708.	1584.	1284.7	7.3

1					2.1	9.3	4.5		5.5	2.7	3.9		6	0		
SMQ B 2	16.5	3.1	13.4	1.3	162 5.7	162 1.4	162 3.7	2.15	150 0.0	149 9.8	150 0.1	0.15	1623. 6	1500. 0	1211.6	7.6
SMQ B 3	17.2	3.1	14.1	1.4	188 2.3	188 0.7	188 2.7	1.06	173 8.1	173 6.7	173 6.1	1.03	1881. 9	1737. 0	1334.7	7.7
Means	16.9	3.2	13.6	1.4	112 3.3	112 2.1	112 2.8	2.8	101 8.4	101 6.9	101 7.5	2.4	1122. 7	1017. 6	779.4	10.8

Appendix 2 Complete pH Datasheets

The following presents the complete pH datasheets for the modern analogue and archaeological sample material. The modern analogue material is presented organised by fuel type and temperature, followed by the archaeological material organised site and year of excavation. This data was used to generate the pH plots used within the main body of the thesis.

Modern Analogue Samples pH Data				
Sample Type	Mass of Sample	Distilled Water Volume	Mean pH Measurement	Solution Temperature
Driftwood Unburnt	Approximately 0.1g	10 ml	6.5	20.5
Driftwood 200^{0}C 3Hrs	Approximately 0.1g	10 ml	7	20.5
Driftwood 200^{0}C 6Hrs	Approximately 0.1g	10 ml	6.8	20.5
Driftwood 400^{0}C 6Hrs	Approximately 0.1g	10 ml	9.1	20.5
Driftwood 900^{0}C 6Hrs	Approximately 0.1g	10 ml	12.4	20.6
Blank (Distilled Water)	Approximately 0.1g	10 ml	6.5	20.4
Buffer 1	N/A	N/A	4.2 (cal. pH4)	20.4
Buffer 2	N/A	N/A	6.9 (cal. pH7)	20.5
Buffer 3	N/A	N/A	9.0(cal. pH9)	20.4
Seaweed Unburnt	Approximately 0.1g	10 ml	7.2	20.4
Seaweed 200^{0}C 3Hrs	Approximately 0.1g	10 ml	7.2	20.4
Seaweed 200^{0}C 6Hrs	Approximately 0.1g	10 ml	6.9	20.6
Seaweed 400^{0}C 6Hrs	Approximately 0.1g	10 ml	9.8	20.5
Seaweed 900^{0}C 6Hrs	Approximately 0.1g	10 ml	12.2	20.5
Blank (Distilled Water)	Approximately 0.1g	10 ml	6.4	20.5
Buffer 1	N/A	N/A	4.2 (cal. pH4)	20.5
Buffer 2	N/A	N/A	7.0 (cal. pH7)	20.3
Buffer 3	N/A	N/A	9.0 (cal. pH9)	20.4
Grasses Unburnt	Approximately 0.1g	10 ml	7.1	20.5
Grasses 200^{0}C 3Hrs	Approximately 0.1g	10 ml	6.5	20.5
Grasses 200^{0}C 6Hrs	Approximately 0.1g	10 ml	6.9	20.7
Grasses 400^{0}C 6Hrs	Approximately 0.1g	10 ml	9.6	20.6
Grasses 900^{0}C 6Hrs	Approximately 0.1g	10 ml	11.1	20.5
Blank (Distilled Water)	Approximately 0.1g	10 ml	6.4	20.6
Buffer 1	N/A	N/A	4.5 (cal. pH4)	20.7
Buffer 2	N/A	N/A	7.1 (cal. pH7)	*20.6*
Buffer 3	N/A	N/A	9.1 (cal. pH9)	20.4

Sheep Dung Unburnt	Approximately 0.1g	10 ml	8.6	20.5
Sheep dung 200^{0}C 3Hrs	Approximately 0.1g	10 ml	7.2	20.5
Sheep dung 200^{0}C 6Hrs	Approximately 0.1g	10 ml	6.4	20.6
Sheep dung 400^{0}C 6Hrs	Approximately 0.1g	10 ml	9.6	20.5
Sheep dung 900^{0}C 6Hrs	Approximately 0.1g	10 ml	10.7	20.5
Blank (Distilled Water)	Approximately 0.1g	10 ml	6.4	20.5
Buffer 1	N/A	N/A	4.5 (cal. pH4)	20.5
Buffer 2	N/A	N/A	7.0 (cal. pH7)	20.4
Buffer 3	N/A	N/A	8.9 (cal. pH9)	20.5
Cow Dung Unburnt	Approximately 0.1g	10 ml	9.2	20.5
Cow dung 200^{0}C 3Hrs	Approximately 0.1g	10 ml	7.5	20.5
Cow dung 200^{0}C 6Hrs	Approximately 0.1g	10 ml	7	20.5
Cow dung 400^{0}C 6Hrs	Approximately 0.1g	10 ml	10.3	20.5
Cow dung 900^{0}C 6Hrs	Approximately 0.1g	10 ml	12.2	20.6
Blank (Distilled Water)	Approximately 0.1g	10 ml	6.3	20.5
Buffer 1	N/A	N/A	4.1 (cal. pH4)	20.4
Buffer 2	N/A	N/A	7.0 (cal. pH7)	20.5
Buffer 3	N/A	N/A	9.1 (cal. pH9)	20.5
Heather Unburnt	Approximately 0.1g	10 ml	5.1	20.6
Heather 200^{0}C 3Hrs	Approximately 0.1g	10 ml	5.7	20.5
Heather 200^{0}C 6Hrs	Approximately 0.1g	10 ml	5.2	20.5
Heather 400^{0}C 6Hrs	Approximately 0.1g	10 ml	8.8	20.7
Heather 900^{0}C 6Hrs	Approximately 0.1g	10 ml	6	20.6
Blank (Distilled Water)	Approximately 0.1g	10 ml	6.2	20.5
Buffer 1	N/A	N/A	4.3 (cal. pH4)	20.5
Buffer 2	N/A	N/A	7.0 (cal. pH7)	20.5
Buffer 3	N/A	N/A	9.0 (cal. pH9)	20.6
Animal Bone 200^{0}C 6Hrs	Approximately 0.1g	10 ml	7.12	20.5
Animal Bone 400^{0}C 6Hrs	Approximately 0.1g	10 ml	7.91	20.5

Animal Bone 900^{0}C 6Hrs	Approximately 0.1g	10 ml	10.45	20.4
Willow 200^{0}C 6Hrs	Approximately 0.1g	10 ml	6.14	20.4
Willow 400^{0}C 6Hrs	Approximately 0.1g	10 ml	9.7	20.4
Hazel 200^{0}C 6Hrs	Approximately 0.1g	10 ml	5.25	20.4
Hazel 400^{0}C 6Hrs	Approximately 0.1g	10 ml	10.06	20.3
Rousay Peat Unburnt	Approximately 0.1g	10 ml	5.8	20.5
Rousay Peat 200^{0}C 3Hrs	Approximately 0.1g	10 ml	5.8	20.6
Rousay Peat 200^{0}C 6Hrs	Approximately 0.1g	10 ml	4.3	20.5
Rousay Peat 400^{0}C 6Hrs	Approximately 0.1g	10 ml	8.9	20.5
Rousay Peat 900^{0}C 6Hrs	Approximately 0.1g	10 ml	10.2	20.5
Blank (Distilled Water)	Approximately 0.1g	10 ml	6.7	20.7
Buffer 1	Approximately 0.1g	N/A	4.5 (cal. pH4)	20.3
Buffer 2	Approximately 0.1g	N/A	7.1 (cal. pH7)	20.4
Buffer 3	Approximately 0.1g	N/A	9.2 (cal. pH9)	20.4
Fozzy Peat 200^{0}C 6Hrs	Approximately 0.1g	10 ml	5.68	20.4
Fozzy Peat 400^{0}C 6Hrs	Approximately 0.1g	10 ml	8.08	20.4
Fozzy Peat 900^{0}C 6Hrs	Approximately 0.1g	10 ml	9.57	20.3
Middle Peat 200^{0}C 6Hrs	Approximately 0.1g	10 ml	5.71	20.3
Middle Peat 400^{0}C 6Hrs	Approximately 0.1g	10 ml	8.79	20.3
Middle Peat 900^{0}C 6Hrs	Approximately 0.1g	10 ml	10.06	20.3
Low Peat 200^{0}C 6Hrs	Approximately 0.1g	10 ml	6.99	20.3
Low Peat 400^{0}C 6Hrs	Approximately 0.1g	10 ml	8.68	20.2
Low Peat 900^{0}C 6Hrs	Approximately 0.1g	10 ml	8.72	20.2
Highland Park Peat 200^{0}C 6Hrs	Approximately 0.1g	10 ml	5.16	20.2
Highland Park Peat 400^{0}C 6Hrs	Approximately 0.1g	10 ml	7.41	20.2
Highland Park Peat	Approximately	10 ml	9.71	20.2

900^{0}C 6Hrs	0.1g			
Mixed Fuel 500^{0}C 6Hrs	Approximately 0.1g	10 ml	9.65	20.1
Corrigal Orkney Peat	Approximately 0.1g	10 ml	7.27	20.1
Corrigal Caith Peat	Approximately 0.1g	10 ml	7.09	20.1
Peat and Wood Ash	Approximately 0.1g	10 ml	9.65	20.1
Archaeological Matrix Unburnt	Approximately 0.1g	10 ml	5.3	20.1
Archaeological matrix 900C 6Hrs	Approximately 0.1g	10 ml	10.74	20.0

Archaeological Material pH Data					
Sample Type	**Mass of Sample**	**Distilled Water Volume**		**Mean pH Measurement**	**Solution Temperature**
KOS 2039	Approximately 0.1g	10 ml		7.88	20.4
KOS 3081	Approximately 0.1g	10 ml		7.83	20.4
KOS 3196	Approximately 0.1g	10 ml		7382	20.5
KOS 3201	Approximately 0.1g	10 ml		8.07	20.4
KOS 3217	Approximately 0.1g	10 ml		736	20.4
KOS 3225	Approximately 0.1g	10 ml		8.06	20.4
KOS 3238	Approximately 0.1g	10 ml		8	20.6
KOS 3255	Approximately 0.1g	10 ml		8.11	20.5
RDL 001	Approximately 0.1g	10 ml		5.86	20.5
RDL 004	Approximately 0.1g	10 ml		6.1	20.5
RDL 006	Approximately 0.1g	10 ml		6.24	20.5
RDL 007	Approximately 0.1g	10 ml		6.21	20.3
RDL 009	Approximately 0.1g	10 ml		5.96	20.4
RDL 013	Approximately 0.1g	10 ml		6.08	20.5
RDL 016	Approximately 0.1g	10 ml		6.37	20.5

RDL 023	Approximately 0.1g	10 ml	6.41	20.7
RDL 031	Approximately 0.1g	10 ml	6.5	20.6
RDL 032	Approximately 0.1g	10 ml	6.27	20.5
SMQ1	Approximately 0.1g	10 ml	6.45	20.6
SMQ2	Approximately 0.1g	10 ml	6.11	20.7
NOB15 2617	Approximately 0.1g	10 ml	6.97	*20.6*
NOB15 5332	Approximately 0.1g	10 ml	7.21	20.4
NOB15 3783	Approximately 0.1g	10 ml	6.88	20.5
NOB15 5013	Approximately 0.1g	10 ml	7	20.5
NOB15 4674	Approximately 0.1g	10 ml	6.72	20.6
NOB15 4667	Approximately 0.1g	10 ml	6.53	20.5
NOB15 4656	Approximately 0.1g	10 ml	6.87	20.5
NOB15 6013	Approximately 0.1g	10 ml	6.79	20.5
NOB15 4264	Approximately 0.1g	10 ml	6.79	20.5
NOB15 6156	Approximately 0.1g	10 ml	6.73	20.4
NOB15 3851	Approximately 0.1g	10 ml	7	20.5
NOB15 3857	Approximately 0.1g	10 ml	7.16	20.5
NOB T 5855	Approximately 0.1g	10 ml	5.68	20.5
NOB T 4825	Approximately 0.1g	10 ml	6.04	20.5
NOB T 4831	Approximately 0.1g	10 ml	6.31	20.5
NOB T 4860	Approximately 0.1g	10 ml	5.23	20.6
NOB T 5810	Approximately 0.1g	10 ml	6.03	20.5
NOB T 5849	Approximately 0.1g	10 ml	6.32	20.4
NOB16 6354	Approximately 0.1g	10 ml	6.41	20.5
NOB16 6348	Approximately 0.1g	10 ml	6.74	20.5

NOB16 6355	Approximately 0.1g	10 ml	6.22	20.6
NOB16 5689	Approximately 0.1g	10 ml	6.5	20.5
NOB16 6356	Approximately 0.1g	10 ml	6.82	20.5
NOB16 6351	Approximately 0.1g	10 ml	6.26	20.7
NOB16 6339	Approximately 0.1g	10 ml	6.64	20.6
NOB16 3851	Approximately 0.1g	10 ml	6.51	20.5
NOB16 6346	Approximately 0.1g	10 ml	7.13	20.5

Appendix 3 Scanning Electron Microscopy with Energy Dispersive X-ray Spectroscopy Datasheets

The following presents the full results for the SEM/EDX analysis of the modern analogue and archaeological sample materials. These results are produced using INCA software and show all of the elements present within the sample material. The results used within the thesis only consider the elements that were deemed germane to the investigation, as discussed within the section 2.7. The modern analogue data is organized by fuel type and heating temperature, and the archaeological samples are organized by site and year of excavation. These results show both the percentage mass abundance and the percentage atomic abundance, a peak plot, and include a 400x magnified image of the sample material. The datasheets also indicate which what compounds the elements were likely present within based on comparison to laboratory standards within the INCA database. All samples are labeled in the bottom left corner of the INCA datasheet.

Ashes to ashes

26-Apr-16 11:33:38 AM

Spectrum processing :
No peaks omitted

Processing option : All elements analyzed (Normalised)
Number of iterations = 4

Standard :
O SiO2 1-Jun-1999 12:00 AM
Na Albite 1-Jun-1999 12:00 AM
Mg MgO 1-Jun-1999 12:00 AM
Al Al2O3 1-Jun-1999 12:00 AM
Si SiO2 1-Jun-1999 12:00 AM
P GaP 1-Jun-1999 12:00 AM
S FeS2 1-Jun-1999 12:00 AM
Cl KCl 1-Jun-1999 12:00 AM
K MAD-10 Feldspar 1-Jun-1999 12:00 AM
Ca Wollastonite 1-Jun-1999 12:00 AM
I Not defined 1-Jun-1999 12:00 AM
W W 1-Jun-1999 12:00 AM

Element	Weight%	Atomic%
O K	50.81	68.19
Na K	8.40	7.84
Mg K	4.48	3.96
Al K	0.73	0.58
Si K	4.36	3.34
P K	1.16	0.80
S K	4.79	3.21
Cl K	8.89	5.39
K K	7.70	4.23
Ca K	2.98	1.60
I L	4.03	0.68
W M	1.67	0.19
Totals	100.00	

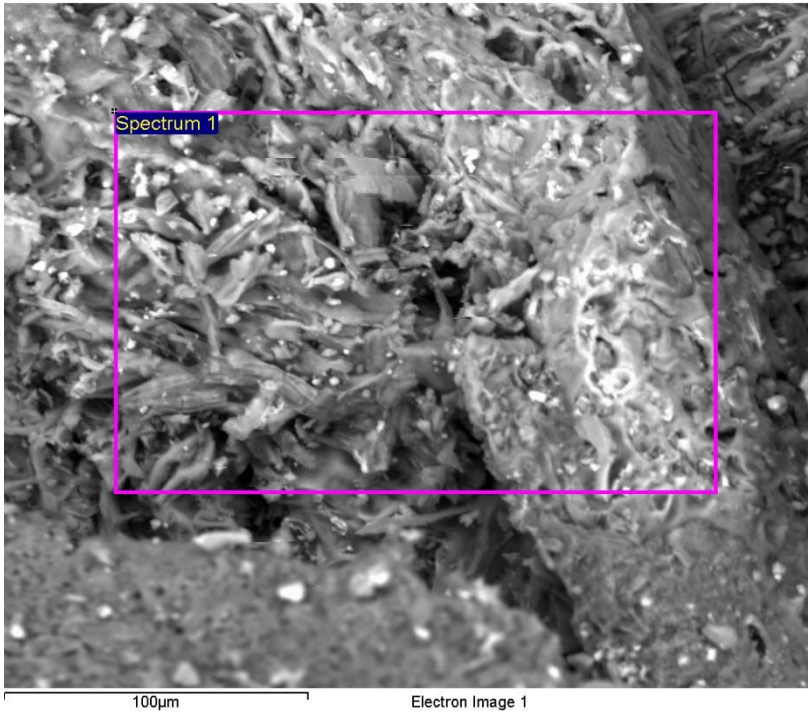

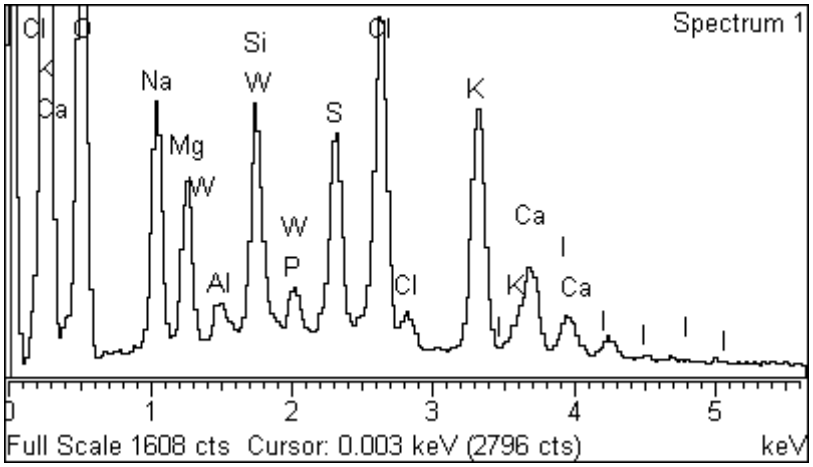

Comment:Seaweed 200 6Hrs

INCA

Ashes to ashes

03-Jun-16 11:41:46 AM

Spectrum processing :
No peaks omitted

Processing option : All elements analyzed (Normalised)
Number of iterations = 4

Standard :
O SiO2 1-Jun-1999 12:00 AM
Na Albite 1-Jun-1999 12:00 AM
Mg MgO 1-Jun-1999 12:00 AM
Al Al2O3 1-Jun-1999 12:00 AM
Si SiO2 1-Jun-1999 12:00 AM
P GaP 1-Jun-1999 12:00 AM
S FeS2 1-Jun-1999 12:00 AM
Cl KCl 1-Jun-1999 12:00 AM
K MAD-10 Feldspar 1-Jun-1999 12:00 AM
Ca Wollastonite 1-Jun-1999 12:00 AM
Fe Fe 1-Jun-1999 12:00 AM

Element	Weight%	Atomic%
O K	39.19	58.69
Na K	3.67	3.82
Mg K	4.65	4.58
Al K	1.17	1.04
Si K	2.79	2.38
P K	0.36	0.28
S K	2.91	2.17
Cl K	0.54	0.37
K K	2.74	1.68
Ca K	41.36	24.72
Fe K	0.62	0.27
Totals	100.00	

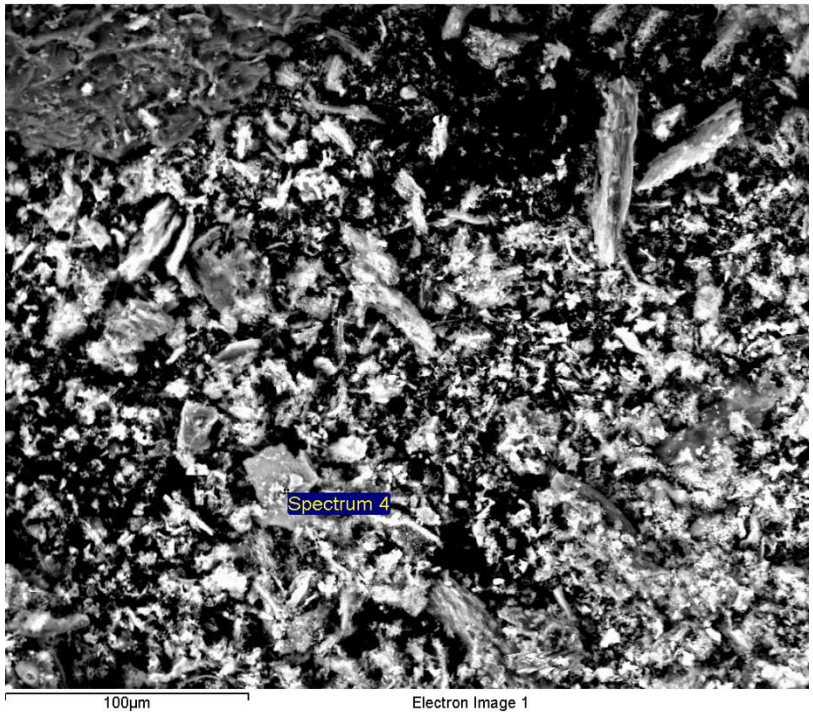

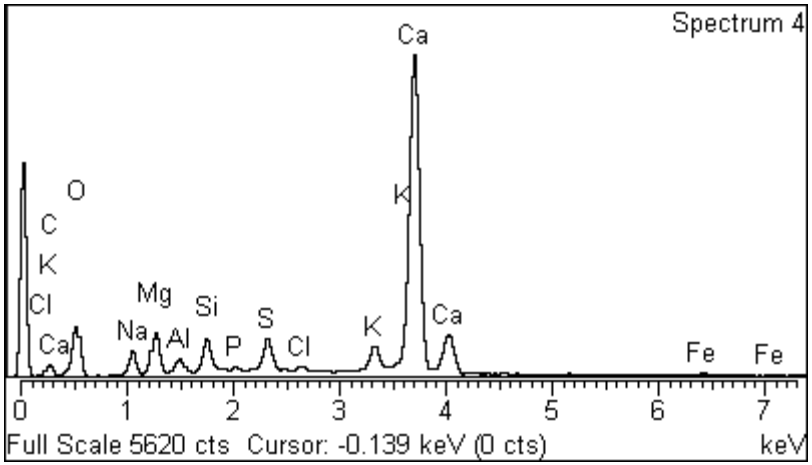

Comment:Seaweed 400 6hrs

INCA

Ashes to ashes

Spectrum processing :
Peak possibly omitted : 10.460 keV

Processing option : All elements analyzed (Normalised)
Number of iterations = 4

Standard :
O SiO2 1-Jun-1999 12:00 AM
Na Albite 1-Jun-1999 12:00 AM
Mg MgO 1-Jun-1999 12:00 AM
S FeS2 1-Jun-1999 12:00 AM
Cl KCl 1-Jun-1999 12:00 AM
K MAD-10 Feldspar 1-Jun-1999 12:00 AM
Ca Wollastonite 1-Jun-1999 12:00 AM
Sr SrF2 1-Jun-1999 12:00 AM

Element	Weight%	Atomic%
O K	36.03	53.29
Na K	13.74	14.15
Mg K	4.48	4.36
S K	4.66	3.44
Cl K	18.42	12.29
K K	8.41	5.09
Ca K	10.98	6.48
Sr L	3.28	0.89
Totals	100.00	

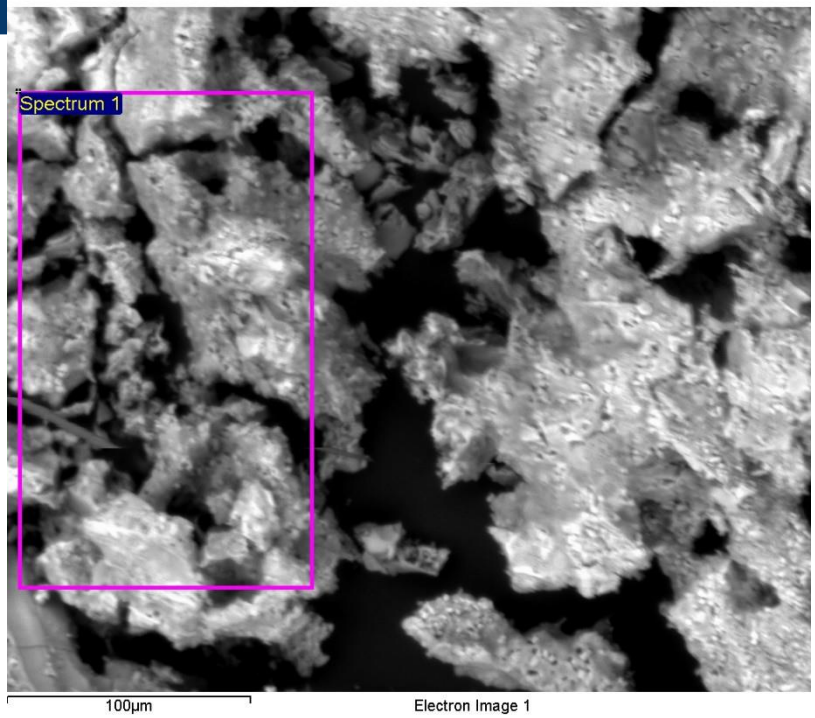

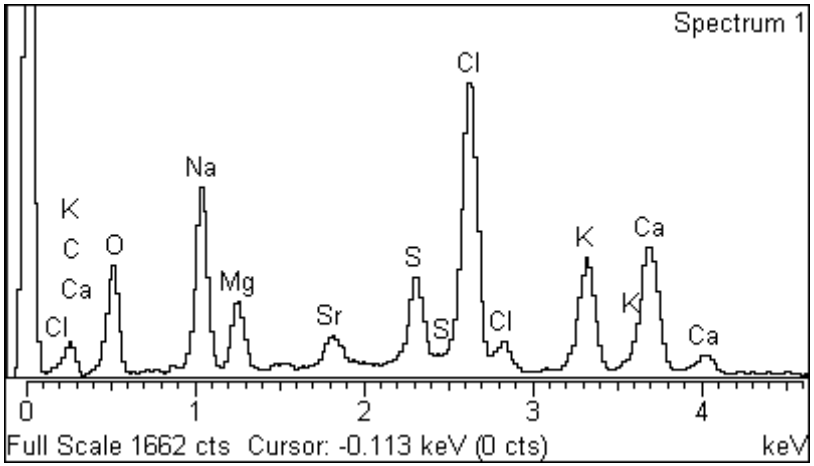

Comment: Seaweed 900 6Hrs

Ashes to ashes

26-Apr-16 11:56:35 AM

Spectrum processing :
No peaks omitted

Processing option : All elements analyzed (Normalised)
Number of iterations = 6

Standard :
O SiO2 1-Jun-1999 12:00 AM
Mg MgO 1-Jun-1999 12:00 AM
Al Al2O3 1-Jun-1999 12:00 AM
Si SiO2 1-Jun-1999 12:00 AM
S FeS2 1-Jun-1999 12:00 AM
K MAD-10 Feldspar 1-Jun-1999 12:00 AM
Ca Wollastonite 1-Jun-1999 12:00 AM
Fe Fe 1-Jun-1999 12:00 AM

Element	Weight%	Atomic%
O K	78.51	88.34
Mg K	2.18	1.62
Al K	2.18	1.46
Si K	5.49	3.52
S K	0.63	0.35
K K	0.73	0.34
Ca K	8.43	3.79
Fe K	1.84	0.59
Totals	100.00	

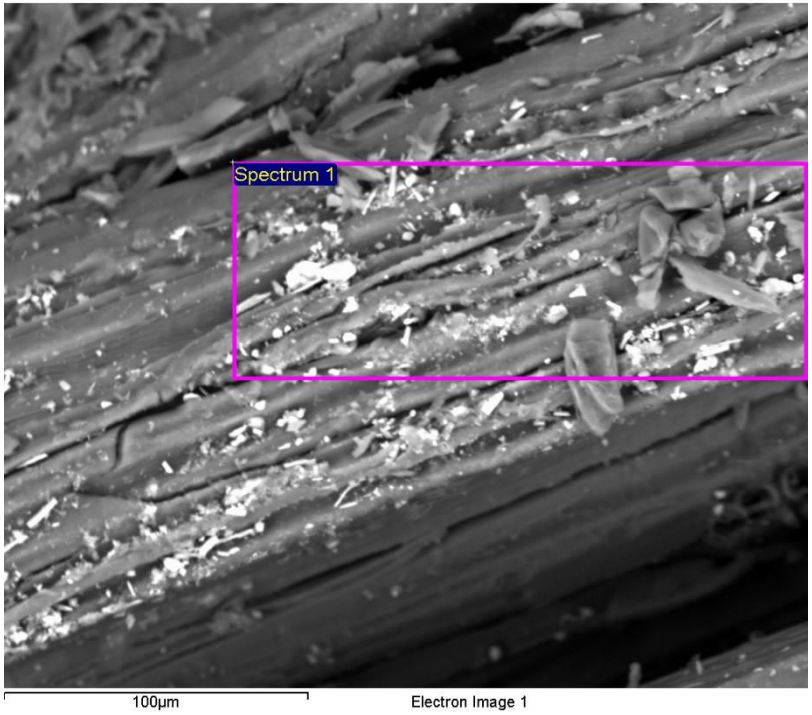

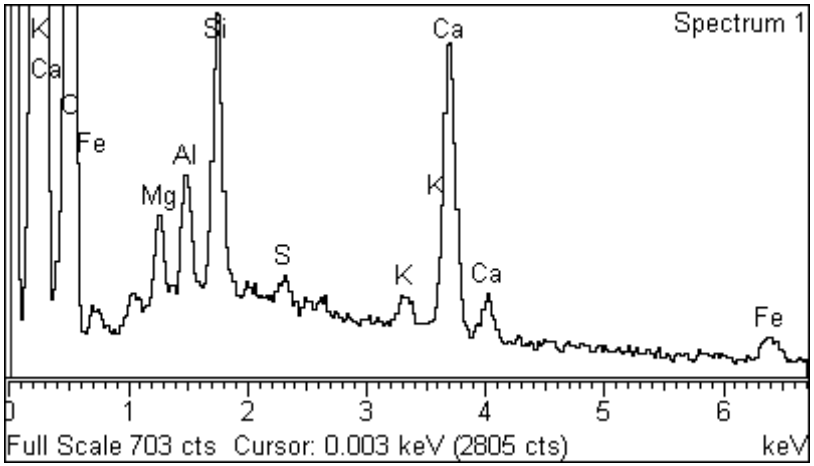

Comment:Driftwood 200 6Hrs area 2

Ashes to ashes

12-Dec-16 11:02:59 AM

Spectrum processing :
Peak possibly omitted : 14.350 keV

Processing option : All elements analyzed (Normalised)
Number of iterations = 5

Standard :
C CaCO3 1-Jun-1999 12:00 AM
O SiO2 1-Jun-1999 12:00 AM
Na Albite 1-Jun-1999 12:00 AM
Mg MgO 1-Jun-1999 12:00 AM
Al Al2O3 1-Jun-1999 12:00 AM
Si SiO2 1-Jun-1999 12:00 AM
P GaP 1-Jun-1999 12:00 AM
S FeS2 1-Jun-1999 12:00 AM
Cl KCl 1-Jun-1999 12:00 AM
K MAD-10 Feldspar 1-Jun-1999 12:00 AM
Ca Wollastonite 1-Jun-1999 12:00 AM
Fe Fe 1-Jun-1999 12:00 AM
W W 1-Jun-1999 12:00 AM

Element	Weight%	Atomic%
C K	32.75	45.10
O K	37.68	38.95
Na K	6.37	4.58
Mg K	6.24	4.25
Al K	0.43	0.27
Si K	0.17	0.10
P K	0.50	0.27
S K	3.18	1.64
Cl K	0.15	0.07
K K	1.43	0.61
Ca K	8.30	3.43
Fe K	2.41	0.71
W M	0.39	0.04
Totals	100.00	

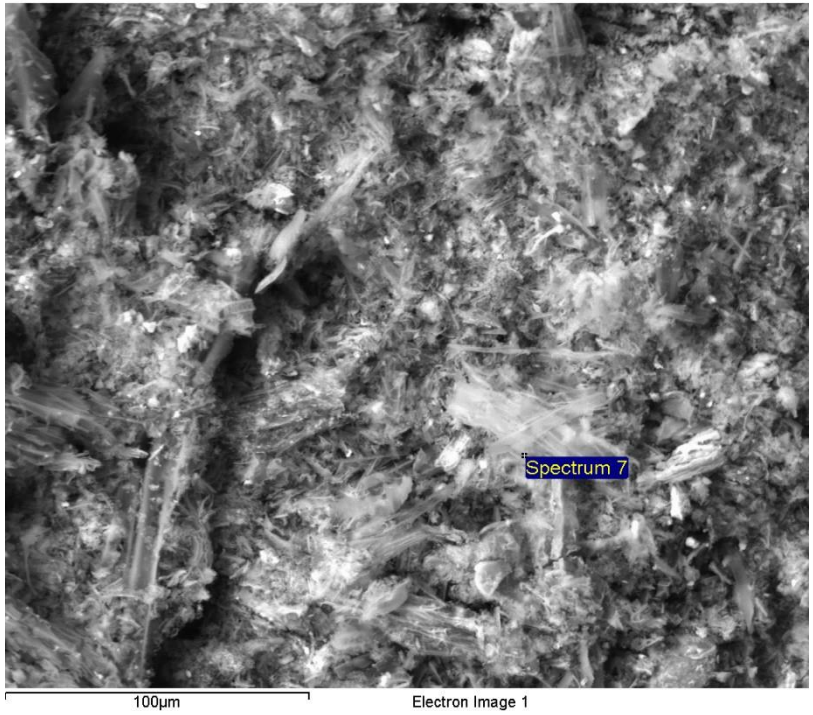

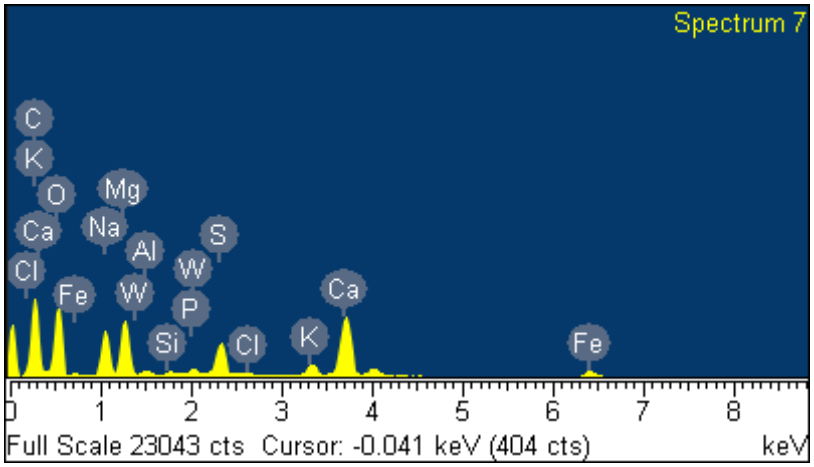

Comment:Driftwood 400 6Hrs

INCA

Ashes to ashes

26-Apr-16 10:53:15 AM

Spectrum processing :
No peaks omitted

Processing option : All elements analyzed (Normalised)
Number of iterations = 4

Standard :
O SiO2 1-Jun-1999 12:00 AM
Mg MgO 1-Jun-1999 12:00 AM
Si SiO2 1-Jun-1999 12:00 AM
S FeS2 1-Jun-1999 12:00 AM
Cl KCl 1-Jun-1999 12:00 AM
K MAD-10 Feldspar 1-Jun-1999 12:00 AM
Ca Wollastonite 1-Jun-1999 12:00 AM

Element	Weight%	Atomic%
O K	50.92	65.36
Mg K	0.37	0.31
Si K	42.10	30.79
S K	0.37	0.23
Cl K	0.86	0.50
K K	4.00	2.10
Ca K	1.39	0.71
Totals	100.00	

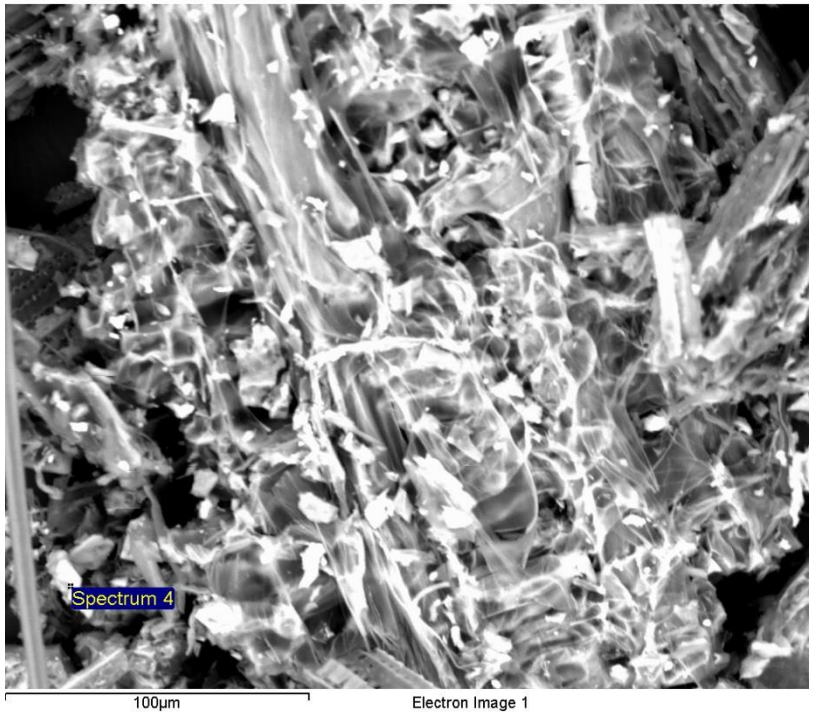

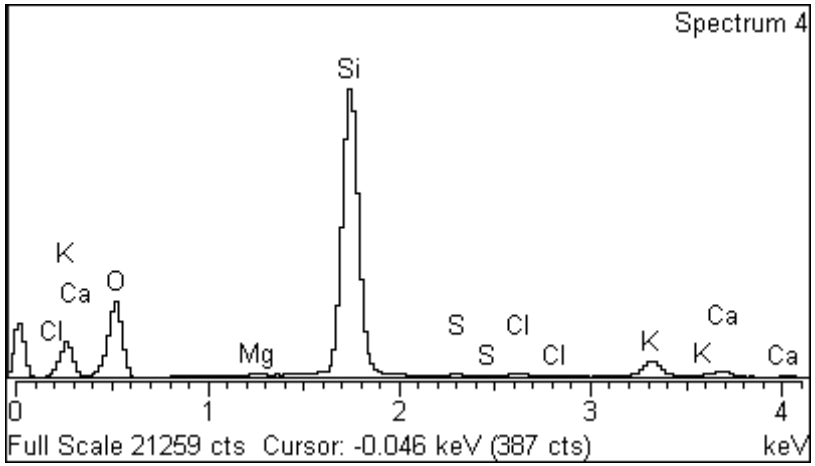

Comment:Grasses 200 6Hrs point

INCA

Ashes to ashes

03-Jun-16 11:40:11 AM

Spectrum processing :
No peaks omitted

Processing option : All elements analyzed (Normalised)
Number of iterations = 3

Standard :
O SiO2 1-Jun-1999 12:00 AM
Na Albite 1-Jun-1999 12:00 AM
Mg MgO 1-Jun-1999 12:00 AM
Si SiO2 1-Jun-1999 12:00 AM
P GaP 1-Jun-1999 12:00 AM
Cl KCl 1-Jun-1999 12:00 AM
K MAD-10 Feldspar 1-Jun-1999 12:00 AM
Ca Wollastonite 1-Jun-1999 12:00 AM
Mo Mo 1-Jun-1999 12:00 AM

Element	Weight%	Atomic%
O K	17.99	31.62
Na K	1.22	1.49
Mg K	2.45	2.83
Si K	24.10	24.13
P K	2.03	1.84
Cl K	19.46	15.43
K K	26.21	18.85
Ca K	4.65	3.26
Mo L	1.89	0.55
Totals	100.00	

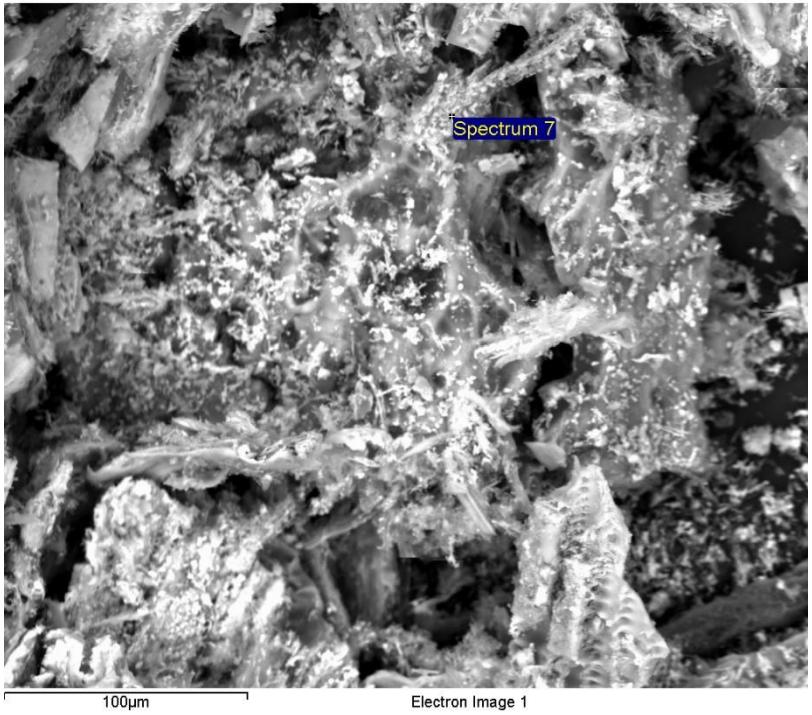

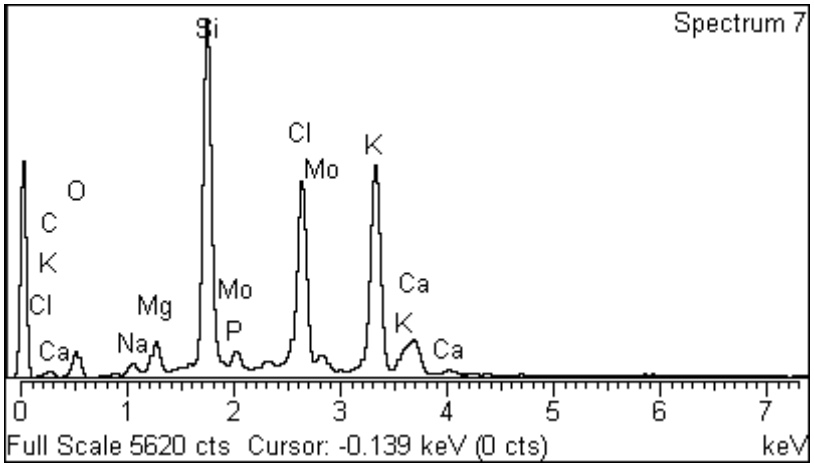

Comment:Grasses 400 6 hrs

INCA

Ashes to ashes

23-Jun-16 11:38:12 AM

Spectrum processing :
Peak possibly omitted : 5.850 keV

Processing option : All elements analyzed (Normalised)
Number of iterations = 4

Standard :
O SiO2 1-Jun-1999 12:00 AM
Na Albite 1-Jun-1999 12:00 AM
Mg MgO 1-Jun-1999 12:00 AM
Al Al2O3 1-Jun-1999 12:00 AM
Si SiO2 1-Jun-1999 12:00 AM
P GaP 1-Jun-1999 12:00 AM
Cl KCl 1-Jun-1999 12:00 AM
K MAD-10 Feldspar 1-Jun-1999 12:00 AM
Ca Wollastonite 1-Jun-1999 12:00 AM
Fe Fe 1-Jun-1999 12:00 AM

Element	Weight%	Atomic%
O K	50.65	66.39
Na K	5.22	4.77
Mg K	4.25	3.67
Al K	0.83	0.64
Si K	15.21	11.36
P K	5.05	3.42
Cl K	0.18	0.11
K K	7.13	3.82
Ca K	10.22	5.35
Fe K	1.26	0.47
Totals	100.00	

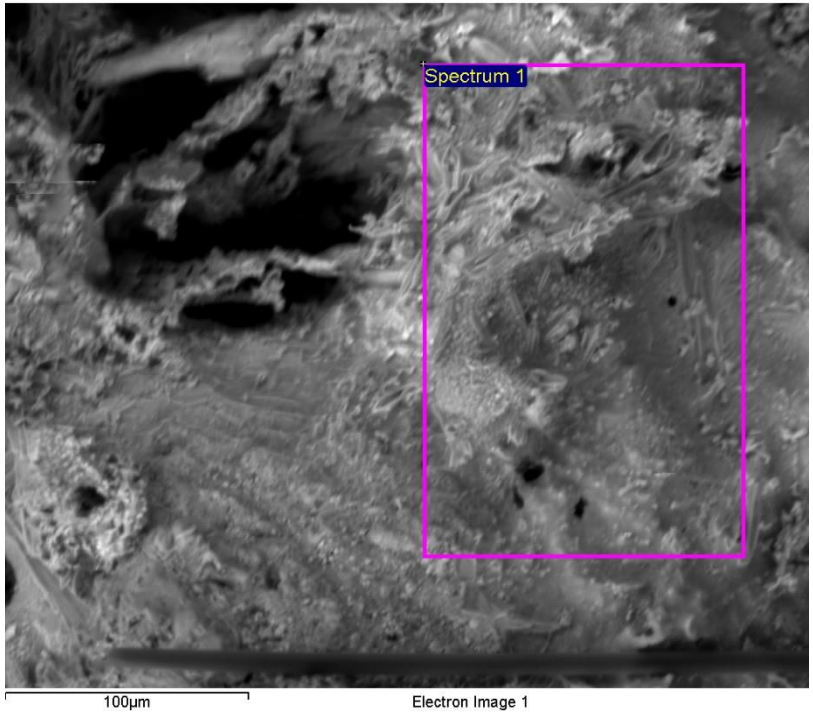

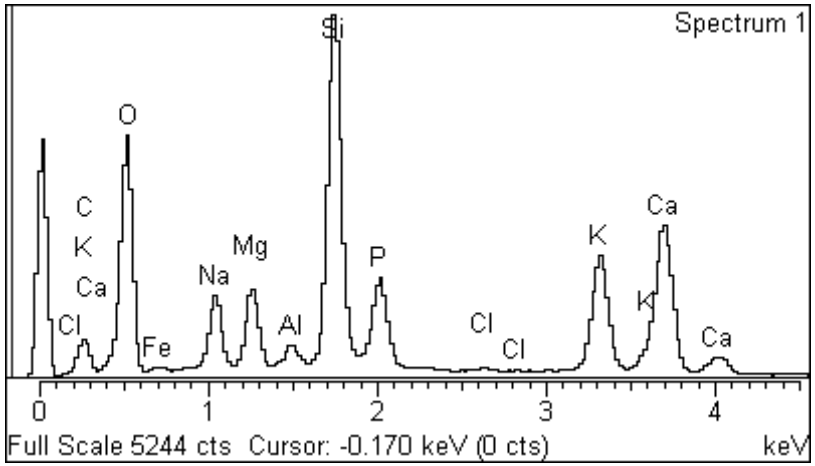

Comment: Grasses 900 6Hrs

Ashes to ashes

21-Apr-16 10:22:35 AM

Spectrum processing :
No peaks omitted

Processing option : All elements analyzed (Normalised)
Number of iterations = 3

Standard :
O SiO2 1-Jun-1999 12:00 AM
Na Albite 1-Jun-1999 12:00 AM
Mg MgO 1-Jun-1999 12:00 AM
Al Al2O3 1-Jun-1999 12:00 AM
Si SiO2 1-Jun-1999 12:00 AM
P GaP 1-Jun-1999 12:00 AM
S FeS2 1-Jun-1999 12:00 AM
K MAD-10 Feldspar 1-Jun-1999 12:00 AM
Ca Wollastonite 1-Jun-1999 12:00 AM
Mn Mn 1-Jun-1999 12:00 AM
Fe Fe 1-Jun-1999 12:00 AM

Element	Weight%	Atomic%
O K	23.55	37.92
Na K	0.80	0.89
Mg K	1.91	2.03
Al K	15.02	14.34
Si K	25.17	23.09
P K	4.24	3.53
S K	1.66	1.33
K K	14.84	9.78
Ca K	6.47	4.16
Mn K	0.97	0.46
Fe K	5.37	2.48
Totals	100.00	

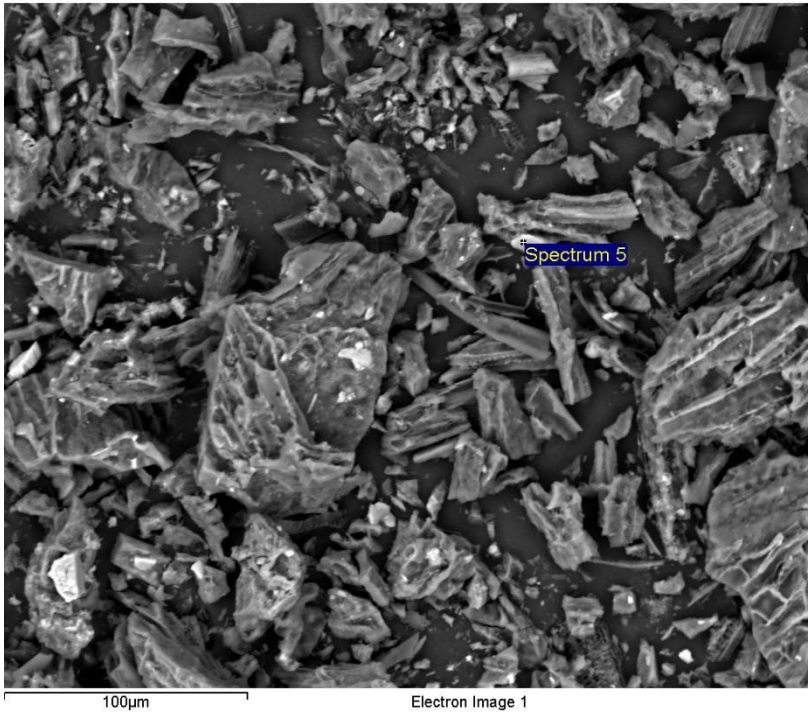

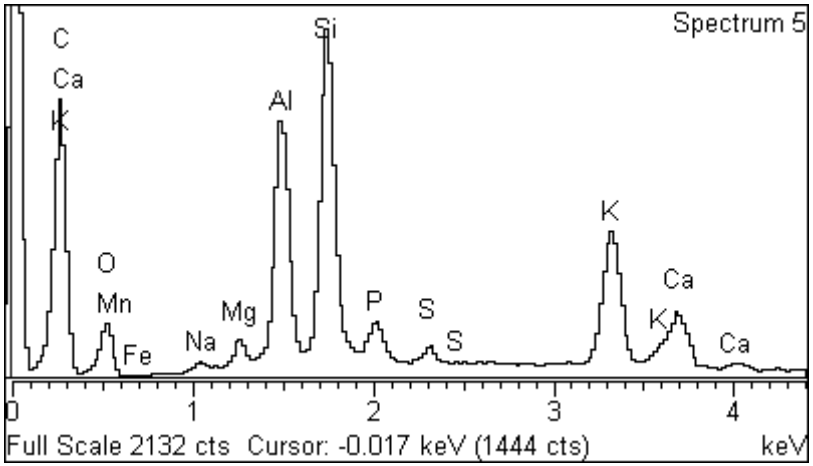

Comment: Sample 1, Sheep dung 200-6hrs

Ashes to ashes

03-Jun-16 11:35:45 AM

Spectrum processing :
No peaks omitted

Processing option : All elements analyzed (Normalised)
Number of iterations = 4

Standard :
O SiO2 1-Jun-1999 12:00 AM
Na Albite 1-Jun-1999 12:00 AM
Mg MgO 1-Jun-1999 12:00 AM
Al Al2O3 1-Jun-1999 12:00 AM
Si SiO2 1-Jun-1999 12:00 AM
P GaP 1-Jun-1999 12:00 AM
S FeS2 1-Jun-1999 12:00 AM
Cl KCl 1-Jun-1999 12:00 AM
K MAD-10 Feldspar 1-Jun-1999 12:00 AM
Ca Wollastonite 1-Jun-1999 12:00 AM
Ti Ti 1-Jun-1999 12:00 AM
Mn Mn 1-Jun-1999 12:00 AM
Fe Fe 1-Jun-1999 12:00 AM

Element	Weight%	Atomic%
O K	45.61	63.79
Na K	1.11	1.08
Mg K	6.39	5.88
Al K	1.53	1.27
Si K	8.26	6.58
P K	6.47	4.67
S K	2.09	1.46
Cl K	0.31	0.20
K K	5.71	3.27
Ca K	17.34	9.68
Ti K	0.47	0.22
Mn K	2.67	1.09
Fe K	2.04	0.82
Totals	100.00	

Comment:Sheep Dung 400 6hrs

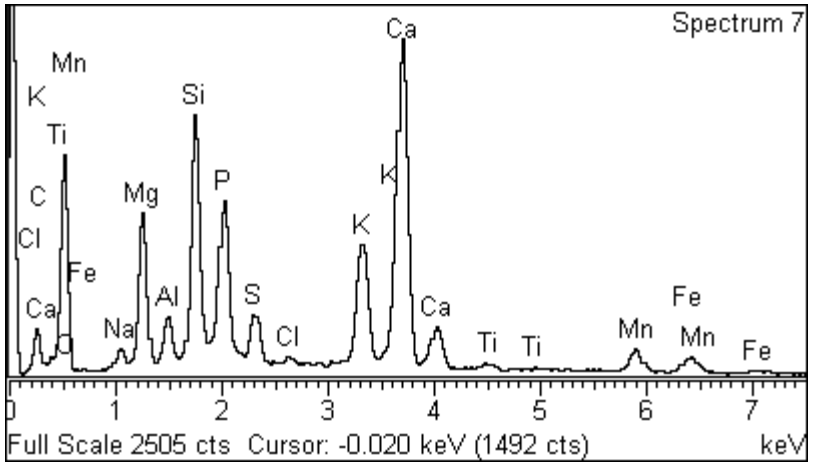

INCA

Ashes to ashes

23-Jun-16 10:35:11 AM

Spectrum processing :
No peaks omitted

Processing option : All elements analyzed (Normalised)
Number of iterations = 4

Standard :
O SiO2 1-Jun-1999 12:00 AM
Na Albite 1-Jun-1999 12:00 AM
Mg MgO 1-Jun-1999 12:00 AM
Al Al2O3 1-Jun-1999 12:00 AM
Si SiO2 1-Jun-1999 12:00 AM
P GaP 1-Jun-1999 12:00 AM
K MAD-10 Feldspar 1-Jun-1999 12:00 AM
Ca Wollastonite 1-Jun-1999 12:00 AM
Ti Ti 1-Jun-1999 12:00 AM
Mn Mn 1-Jun-1999 12:00 AM
Fe Fe 1-Jun-1999 12:00 AM

Element	Weight%	Atomic%
O K	46.67	63.33
Na K	1.88	1.78
Mg K	5.07	4.52
Al K	3.76	3.03
Si K	16.79	12.97
P K	5.27	3.69
K K	4.68	2.60
Ca K	12.19	6.60
Ti K	0.50	0.23
Mn K	1.54	0.61
Fe K	1.65	0.64
Totals	100.00	

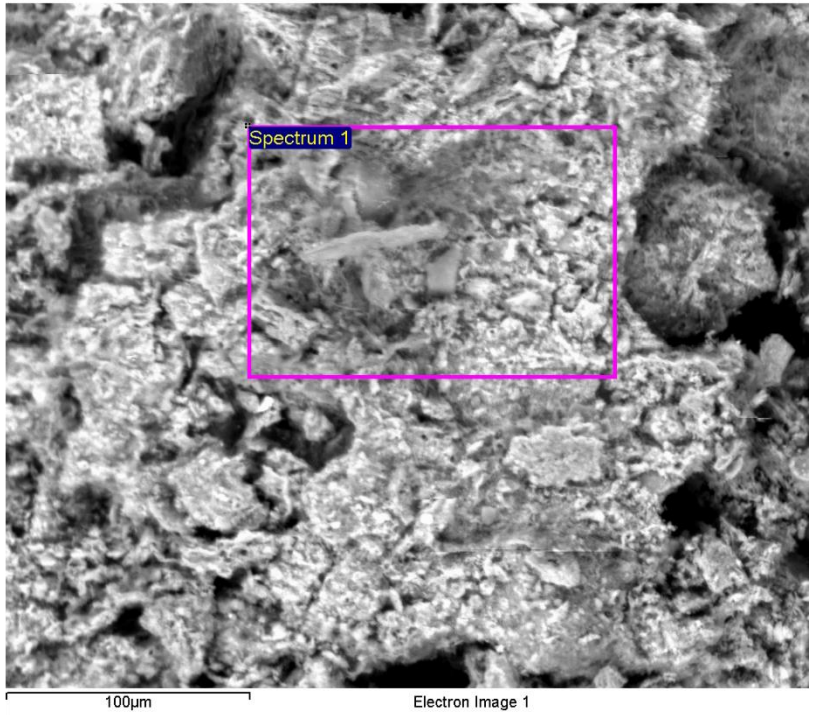

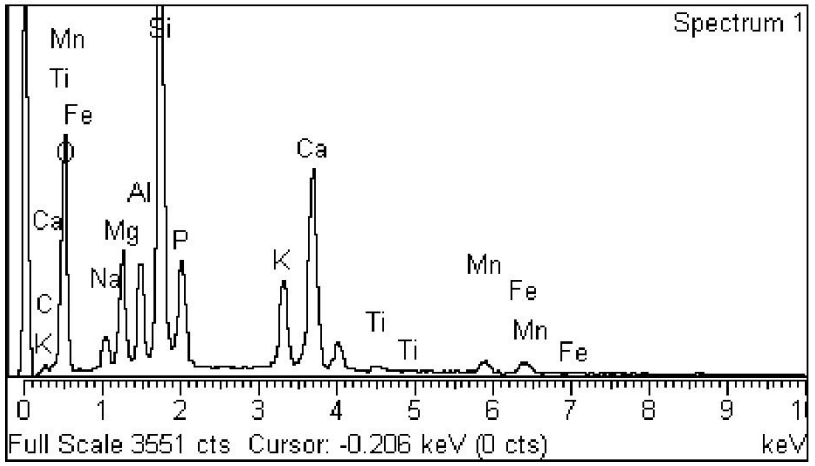

Comment:Sheep Dung 900 6Hrs

INCA

Ashes to ashes

12-Dec-16 10:34:49 AM

Spectrum processing :
No peaks omitted

Processing option : All elements analyzed (Normalised)
Number of iterations = 4

Standard :
C CaCO3 1-Jun-1999 12:00 AM
O SiO2 1-Jun-1999 12:00 AM
Na Albite 1-Jun-1999 12:00 AM
Mg MgO 1-Jun-1999 12:00 AM
Al Al2O3 1-Jun-1999 12:00 AM
Si SiO2 1-Jun-1999 12:00 AM
P GaP 1-Jun-1999 12:00 AM
S FeS2 1-Jun-1999 12:00 AM
Cl KCl 1-Jun-1999 12:00 AM
K MAD-10 Feldspar 1-Jun-1999 12:00 AM
Ca Wollastonite 1-Jun-1999 12:00 AM
Mn Mn 1-Jun-1999 12:00 AM
Fe Fe 1-Jun-1999 12:00 AM

Element	Weight%	Atomic%
C K	2.94	6.60
O K	19.90	33.48
Na K	3.55	4.16
Mg K	1.33	1.48
Al K	0.41	0.41
Si K	8.39	8.05
P K	2.74	2.38
S K	5.10	4.28
Cl K	16.80	12.76
K K	31.22	21.50
Ca K	6.49	4.36
Mn K	0.40	0.20
Fe K	0.72	0.35
Totals	100.00	

Comment:Cow Dung 200 6Hrs

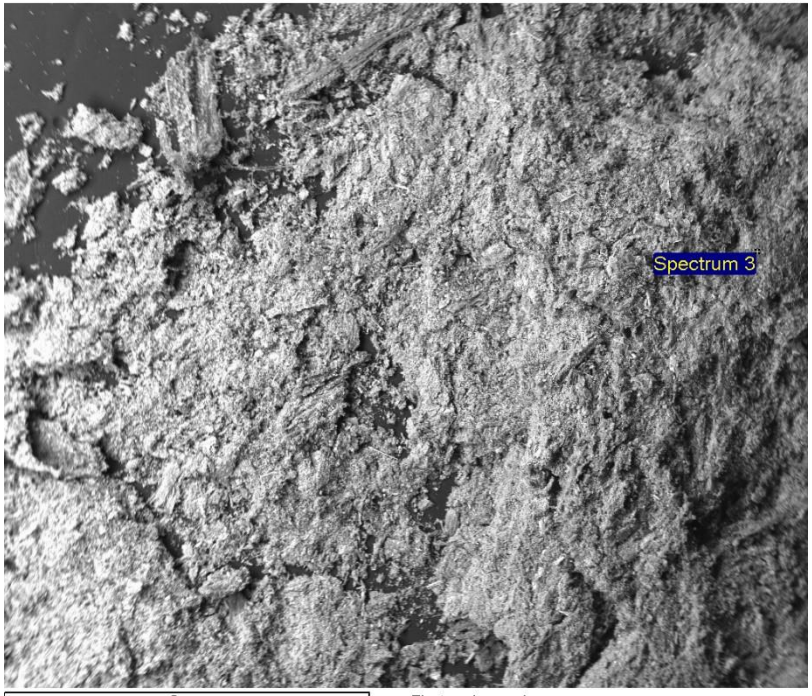

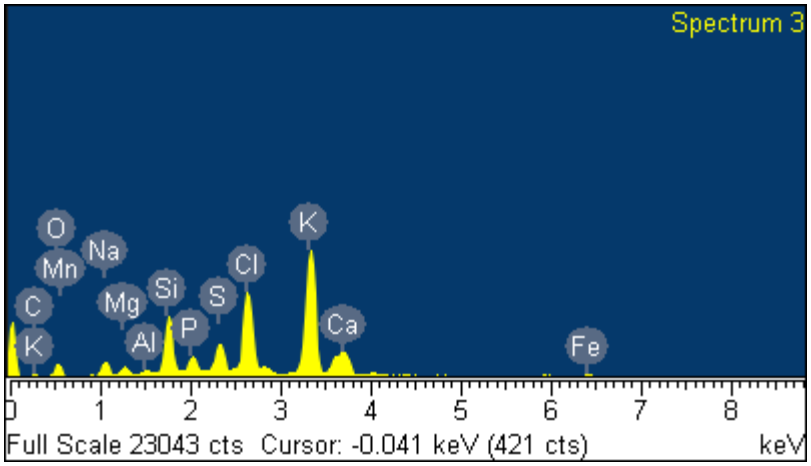

INCA

Ashes to ashes

12-Dec-16 10:24:05 AM

Spectrum processing :
No peaks omitted

Processing option : All elements analyzed (Normalised)
Number of iterations = 5

Standard :
C CaCO3 1-Jun-1999 12:00 AM
O SiO2 1-Jun-1999 12:00 AM
Na Albite 1-Jun-1999 12:00 AM
Mg MgO 1-Jun-1999 12:00 AM
Al Al2O3 1-Jun-1999 12:00 AM
Si SiO2 1-Jun-1999 12:00 AM
P GaP 1-Jun-1999 12:00 AM
S FeS2 1-Jun-1999 12:00 AM
Cl KCl 1-Jun-1999 12:00 AM
K MAD-10 Feldspar 1-Jun-1999 12:00 AM
Ca Wollastonite 1-Jun-1999 12:00 AM
Mn Mn 1-Jun-1999 12:00 AM
Fe Fe 1-Jun-1999 12:00 AM

Element	Weight%	Atomic%
C K	7.84	13.99
O K	38.10	51.04
Na K	5.17	4.82
Mg K	2.39	2.11
Al K	0.26	0.20
Si K	6.17	4.71
P K	5.18	3.58
S K	0.82	0.55
Cl K	10.50	6.35
K K	12.46	6.83
Ca K	10.28	5.50
Mn K	0.33	0.13
Fe K	0.48	0.19
Totals	100.00	

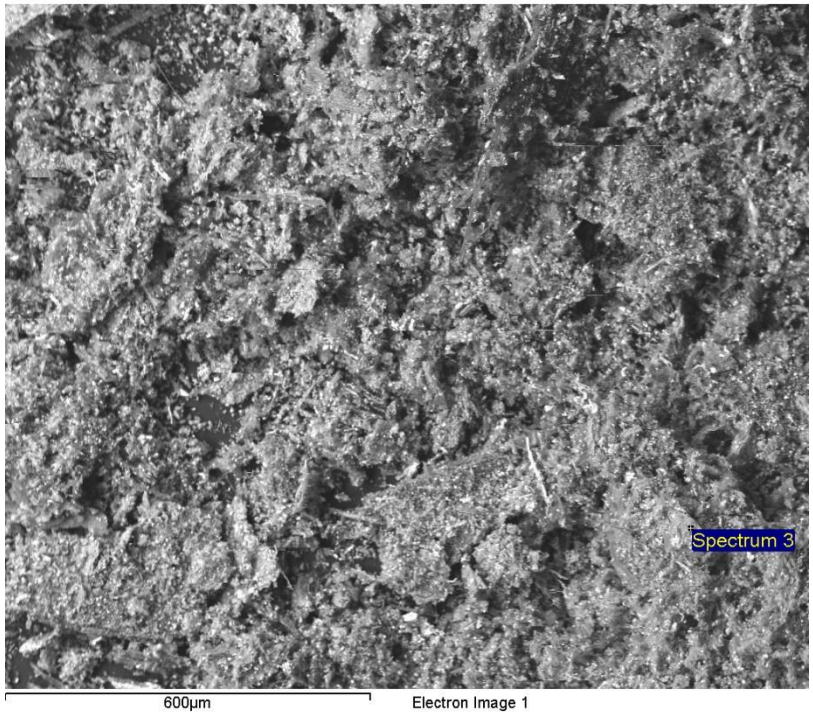

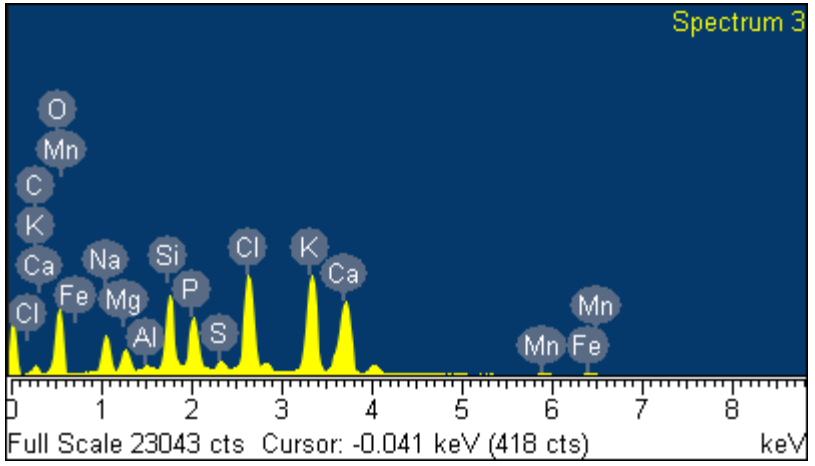

Comment:Cow Dung 400 6Hrs

INCA

Ashes to ashes

23-Jun-16 11:00:19 AM

Spectrum processing :
No peaks omitted

Processing option : All elements analyzed (Normalised)
Number of iterations = 4

Standard :
O SiO2 1-Jun-1999 12:00 AM
Na Albite 1-Jun-1999 12:00 AM
Mg MgO 1-Jun-1999 12:00 AM
Si SiO2 1-Jun-1999 12:00 AM
P GaP 1-Jun-1999 12:00 AM
S FeS2 1-Jun-1999 12:00 AM
Cl KCl 1-Jun-1999 12:00 AM
K MAD-10 Feldspar 1-Jun-1999 12:00 AM
Ca Wollastonite 1-Jun-1999 12:00 AM

Element	Weight%	Atomic%
O K	38.29	56.68
Na K	4.94	5.09
Mg K	2.38	2.32
Si K	7.65	6.45
P K	0.61	0.46
S K	0.57	0.42
Cl K	17.84	11.92
K K	18.43	11.16
Ca K	9.28	5.48
Totals	100.00	

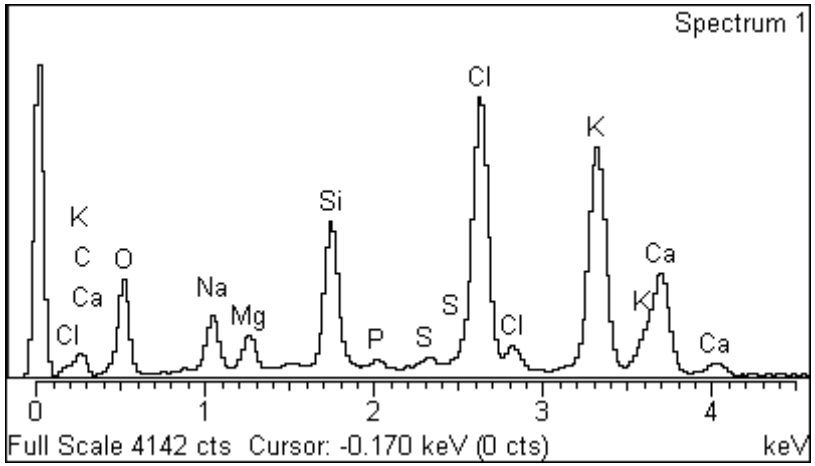

Comment: Cow Dung 900 6hrs

INCA

Ashes to ashes

13-Dec-16 10:35:15 AM

Spectrum processing :
Peak possibly omitted : 3.689 keV

Processing option : All elements analyzed (Normalised)
Number of iterations = 4

Standard :
C CaCO3 1-Jun-1999 12:00 AM
O SiO2 1-Jun-1999 12:00 AM
Mg MgO 1-Jun-1999 12:00 AM
S FeS2 1-Jun-1999 12:00 AM

Element	Weight%	Atomic%
C K	69.19	75.11
O K	30.19	24.60
Mg K	0.25	0.14
S K	0.37	0.15
Totals	100.00	

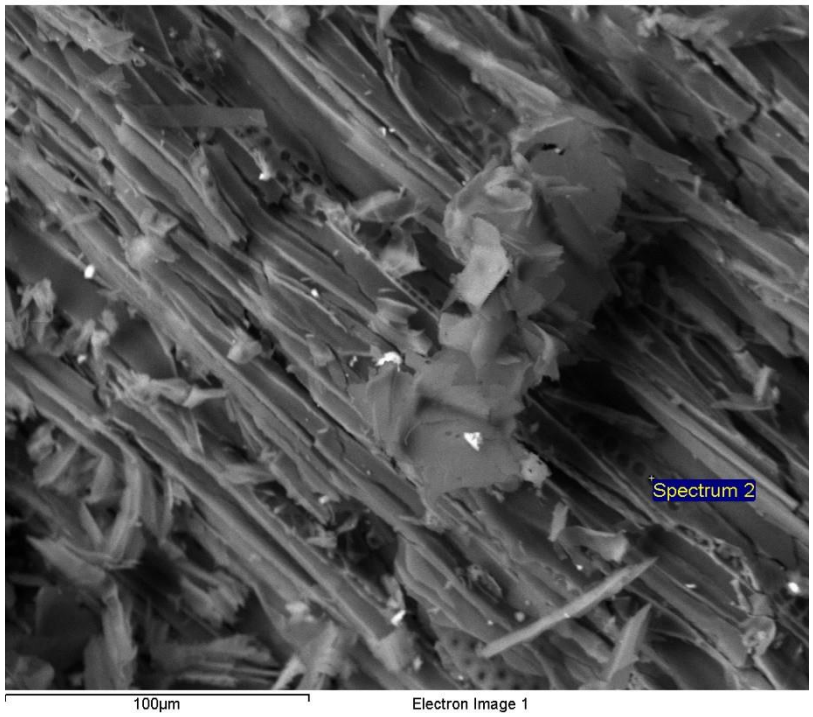

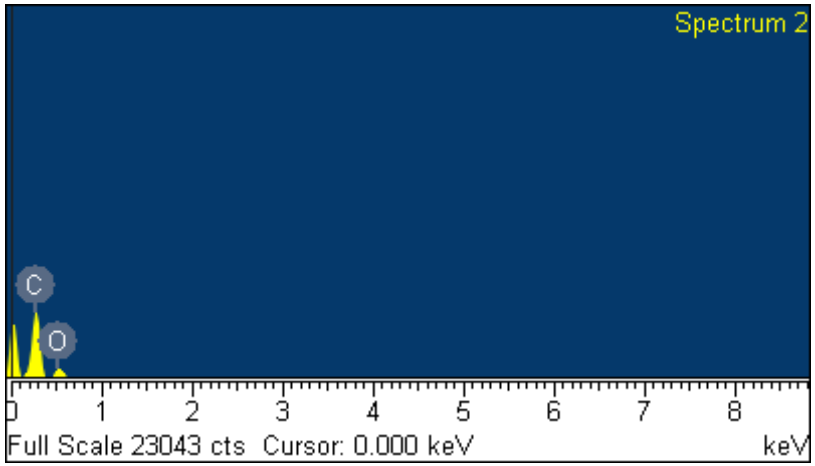

Comment:Hazel 200 6Hrs

INCA

Ashes to ashes

13-Dec-16 10:48:34 AM

Spectrum processing :
No peaks omitted

Processing option : All elements analyzed (Normalised)
Number of iterations = 4

Standard :
C CaCO3 1-Jun-1999 12:00 AM
O SiO2 1-Jun-1999 12:00 AM
Na Albite 1-Jun-1999 12:00 AM
Mg MgO 1-Jun-1999 12:00 AM
Al Al2O3 1-Jun-1999 12:00 AM
Si SiO2 1-Jun-1999 12:00 AM
P GaP 1-Jun-1999 12:00 AM
S FeS2 1-Jun-1999 12:00 AM
Cl KCl 1-Jun-1999 12:00 AM
K MAD-10 Feldspar 1-Jun-1999 12:00 AM
Ca Wollastonite 1-Jun-1999 12:00 AM
Fe Fe 1-Jun-1999 12:00 AM

Element	Weight%	Atomic%
C K	14.58	23.01
O K	42.35	50.18
Na K	6.18	5.09
Mg K	7.82	6.10
Al K	1.90	1.34
Si K	3.89	2.63
P K	3.29	2.01
S K	2.73	1.62
Cl K	0.28	0.15
K K	4.03	1.95
Ca K	11.46	5.42
Fe K	1.49	0.50
Totals	100.00	

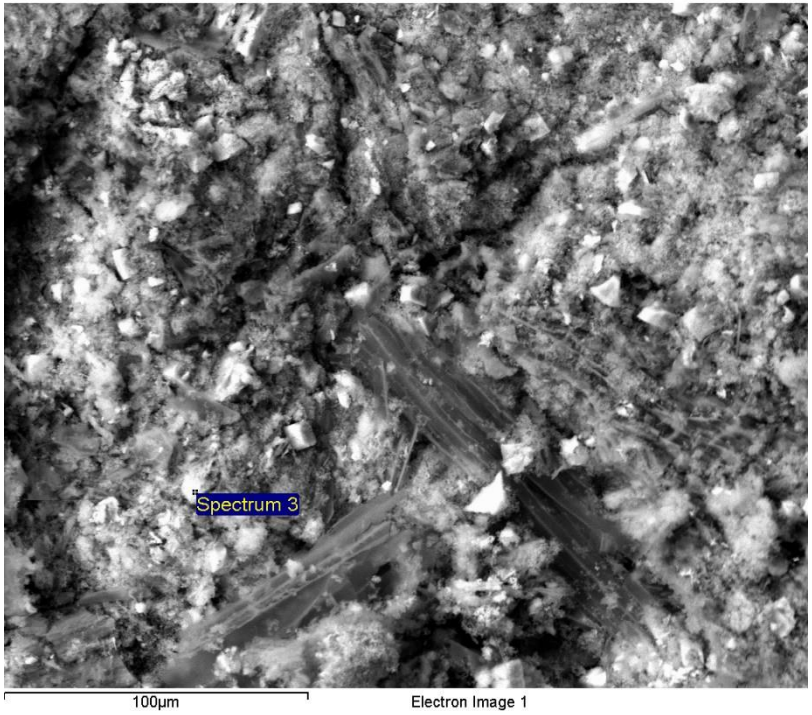

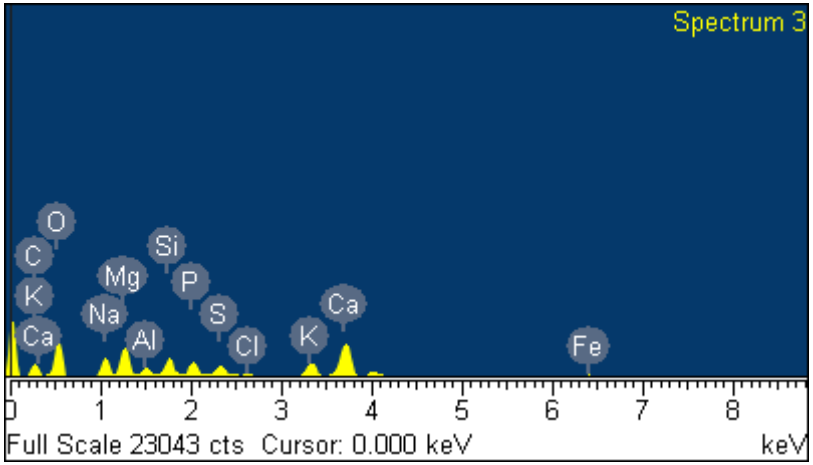

Comment:Hazel 400 6Hrs

INCA

Ashes to ashes

03-Jun-16 11:45:32 AM

Spectrum processing :
No peaks omitted

Processing option : All elements analyzed (Normalised)
Number of iterations = 5

Standard :
O SiO2 1-Jun-1999 12:00 AM
Na Albite 1-Jun-1999 12:00 AM
Mg MgO 1-Jun-1999 12:00 AM
Si SiO2 1-Jun-1999 12:00 AM
P GaP 1-Jun-1999 12:00 AM
S FeS2 1-Jun-1999 12:00 AM
K MAD-10 Feldspar 1-Jun-1999 12:00 AM
Ca Wollastonite 1-Jun-1999 12:00 AM
Fe Fe 1-Jun-1999 12:00 AM
Br KBr 1-Jun-1999 12:00 AM

Element	Weight%	Atomic%
O K	70.20	82.21
Na K	8.15	6.64
Mg K	2.45	1.89
Si K	1.82	1.21
P K	3.04	1.84
S K	1.06	0.62
K K	6.39	3.06
Ca K	3.36	1.57
Fe K	1.25	0.42
Br L	2.28	0.53
Totals	100.00	

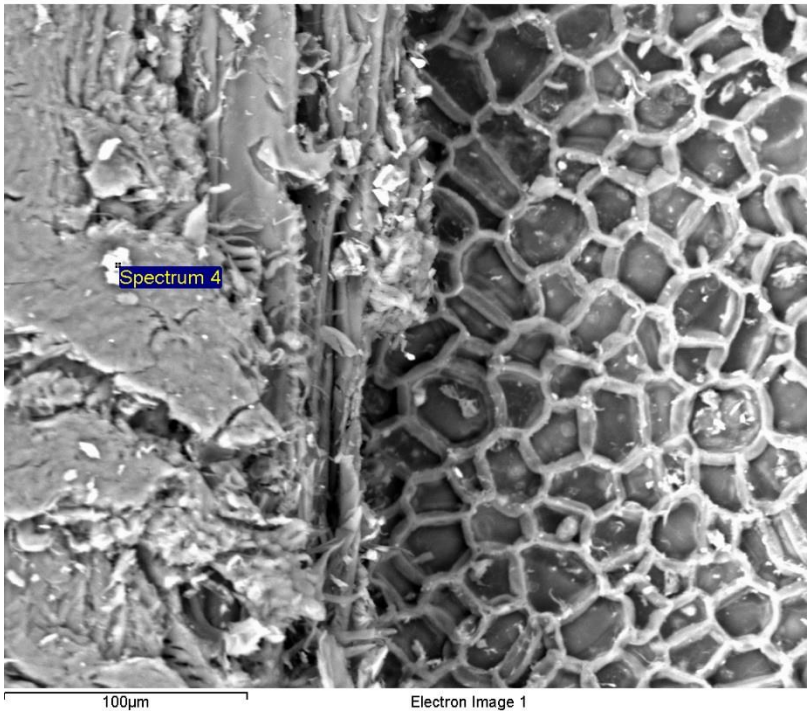

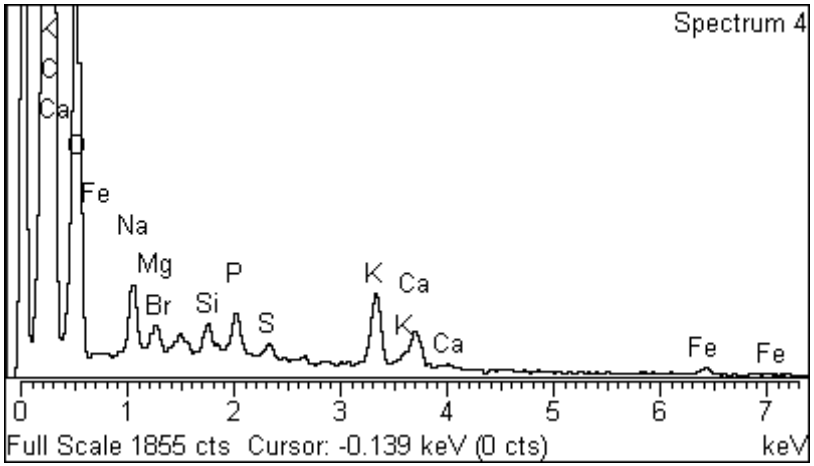

Comment:Heather 200 6Hrs

INCA

Ashes to ashes

12-Dec-16 10:49:20 AM

Spectrum processing :
No peaks omitted

Processing option : All elements analyzed (Normalised)
Number of iterations = 5

Standard :
C CaCO3 1-Jun-1999 12:00 AM
O SiO2 1-Jun-1999 12:00 AM
Na Albite 1-Jun-1999 12:00 AM
Mg MgO 1-Jun-1999 12:00 AM
Al Al2O3 1-Jun-1999 12:00 AM
Si SiO2 1-Jun-1999 12:00 AM
P GaP 1-Jun-1999 12:00 AM
S FeS2 1-Jun-1999 12:00 AM
Cl KCl 1-Jun-1999 12:00 AM
K MAD-10 Feldspar 1-Jun-1999 12:00 AM
Ca Wollastonite 1-Jun-1999 12:00 AM
Ti Ti 1-Jun-1999 12:00 AM
Fe Fe 1-Jun-1999 12:00 AM

Element	Weight%	Atomic%
C K	16.49	25.16
O K	45.16	51.75
Na K	6.08	4.85
Mg K	4.87	3.67
Al K	1.80	1.22
Si K	4.57	2.98
P K	3.59	2.13
S K	3.65	2.09
Cl K	0.32	0.16
K K	5.11	2.40
Ca K	6.42	2.94
Ti K	0.19	0.07
Fe K	1.74	0.57
Totals	100.00	

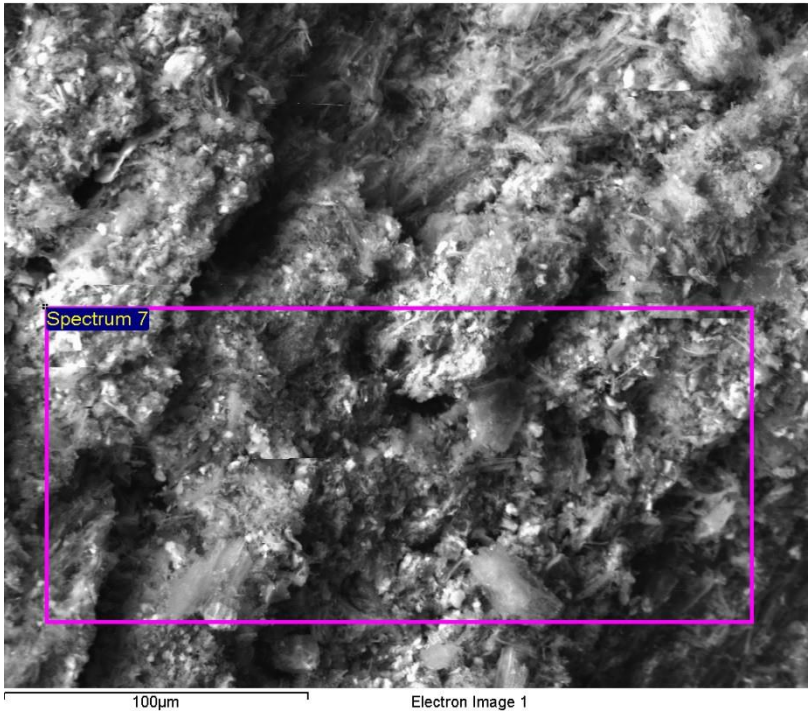

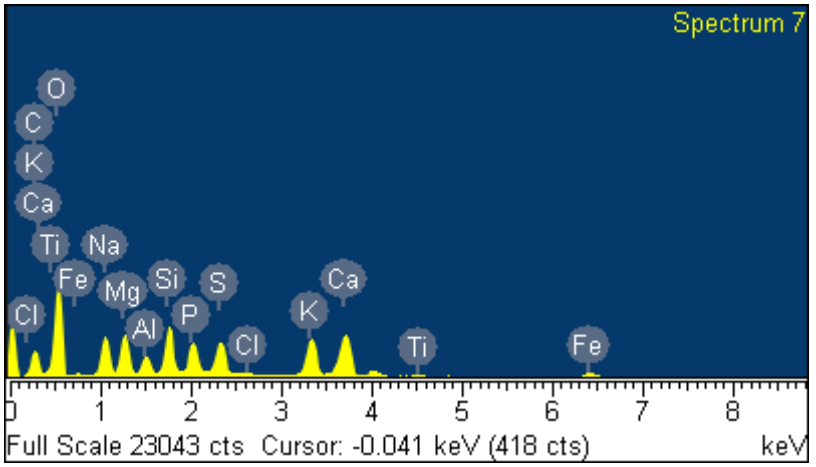

Comment:Heather 400 6Hrs

Ashes to ashes

13-Dec-16 10:17:24 AM

Spectrum processing :
No peaks omitted

Processing option : All elements analyzed (Normalised)
Number of iterations = 6

Standard :
C CaCO3 1-Jun-1999 12:00 AM
O SiO2 1-Jun-1999 12:00 AM
Al Al2O3 1-Jun-1999 12:00 AM
Ca Wollastonite 1-Jun-1999 12:00 AM
I Not defined 1-Jun-1999 12:00 AM

Element	Weight%	Atomic%
C K	37.64	50.25
O K	38.28	38.36
Al K	17.62	10.47
Ca K	0.37	0.15
I L	6.08	0.77
Totals	100.00	

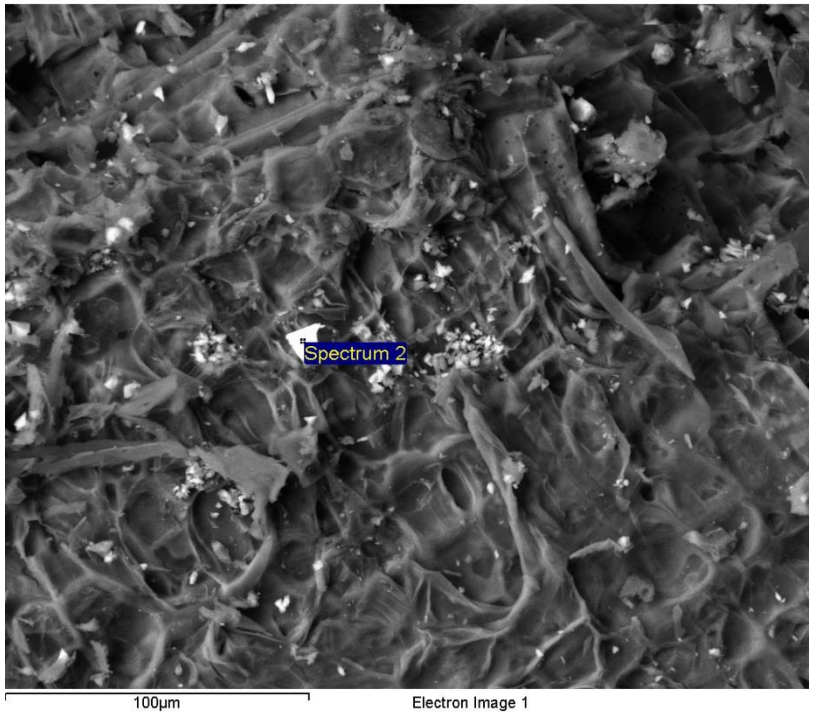

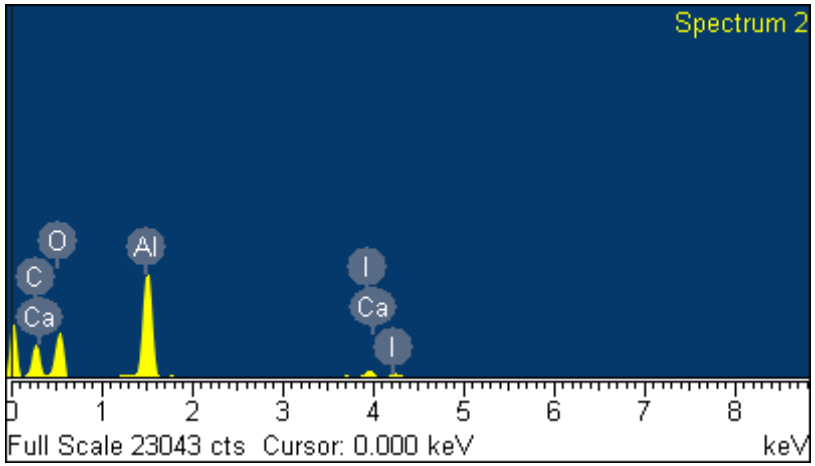

Comment:Willow 200 6Hrs

INCA

Ashes to ashes

13-Dec-16 10:26:27 AM

Spectrum processing :
No peaks omitted

Processing option : All elements analyzed (Normalised)
Number of iterations = 4

Standard :
C CaCO3 1-Jun-1999 12:00 AM
O SiO2 1-Jun-1999 12:00 AM
Na Albite 1-Jun-1999 12:00 AM
Mg MgO 1-Jun-1999 12:00 AM
P GaP 1-Jun-1999 12:00 AM
S FeS2 1-Jun-1999 12:00 AM
Cl KCl 1-Jun-1999 12:00 AM
K MAD-10 Feldspar 1-Jun-1999 12:00 AM
Ca Wollastonite 1-Jun-1999 12:00 AM

Element	Weight%	Atomic%
C K	16.39	27.39
O K	39.13	49.08
Na K	1.05	0.92
Mg K	0.43	0.36
P K	2.71	1.75
S K	1.46	0.91
Cl K	0.48	0.27
K K	9.83	5.05
Ca K	28.51	14.28
Totals	100.00	

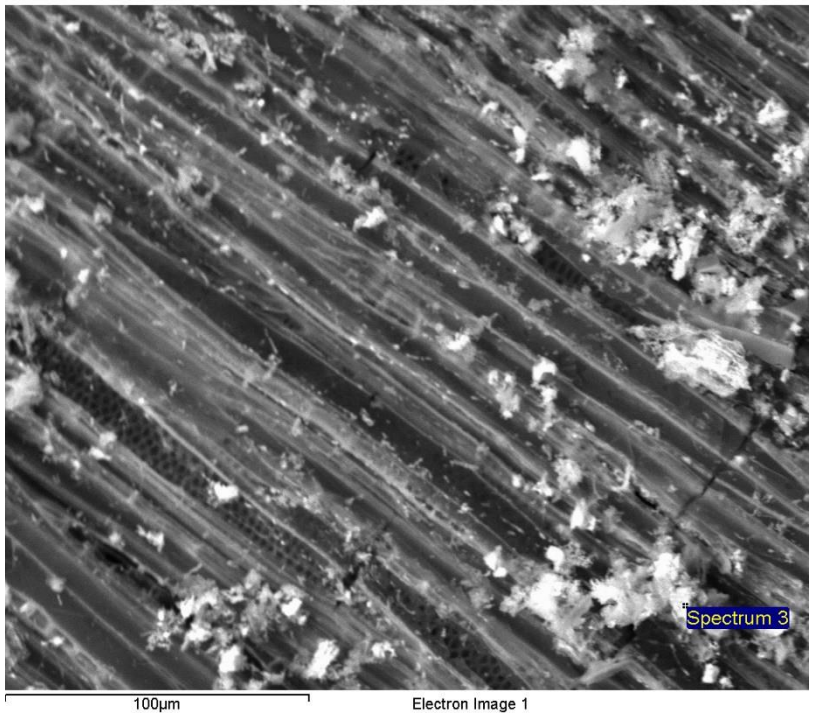

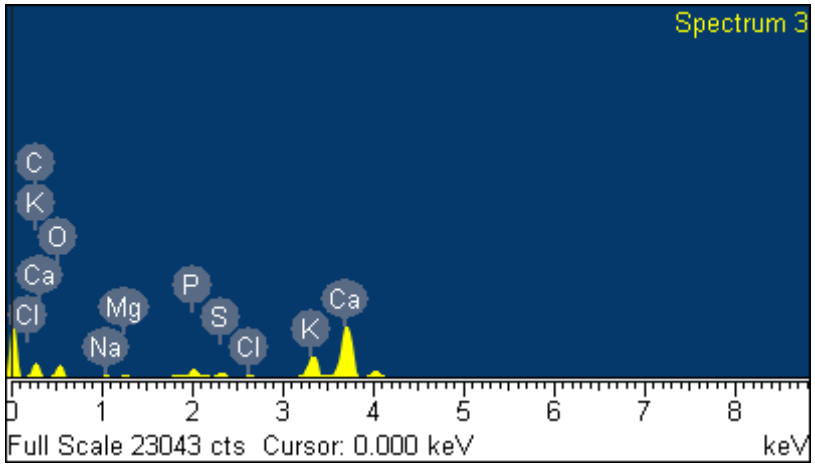

Comment:Willow 400 6Hrs

INCA

Ashes to ashes

12-Dec-16 11:17:53 AM

Spectrum processing :
No peaks omitted

Processing option : All elements analyzed (Normalised)
Number of iterations = 5

Standard :
C CaCO3 1-Jun-1999 12:00 AM
O SiO2 1-Jun-1999 12:00 AM
Na Albite 1-Jun-1999 12:00 AM
Mg MgO 1-Jun-1999 12:00 AM
P GaP 1-Jun-1999 12:00 AM
Ca Wollastonite 1-Jun-1999 12:00 AM
Sn Sn 1-Jun-1999 12:00 AM
I Not defined 1-Jun-1999 12:00 AM

Element	Weight%	Atomic%
C K	20.72	32.95
O K	38.10	45.48
Na K	0.65	0.54
Mg K	0.46	0.36
P K	13.01	8.02
Ca K	26.28	12.52
Sn L	0.42	0.07
I L	0.37	0.06
Totals	100.00	

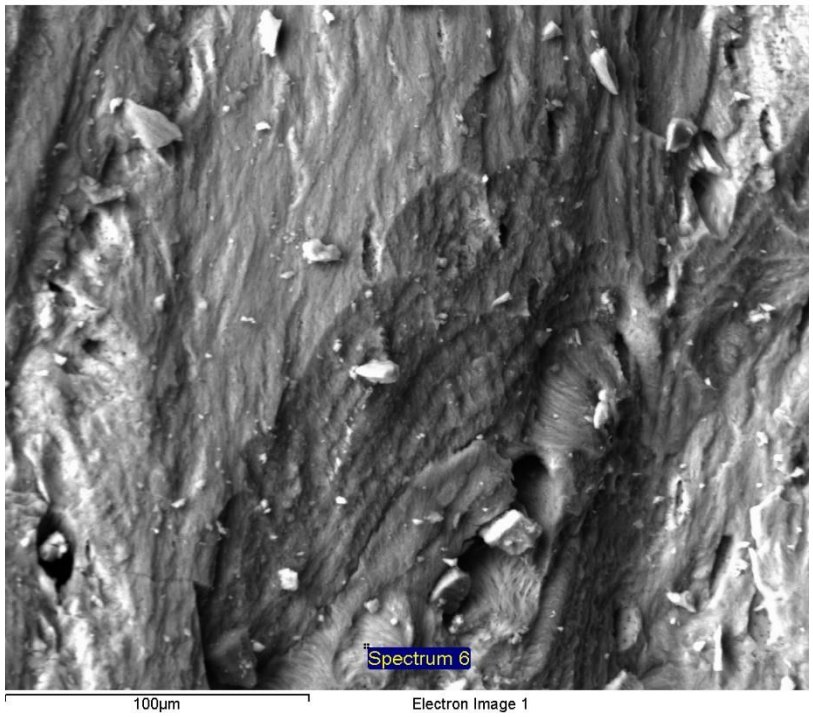

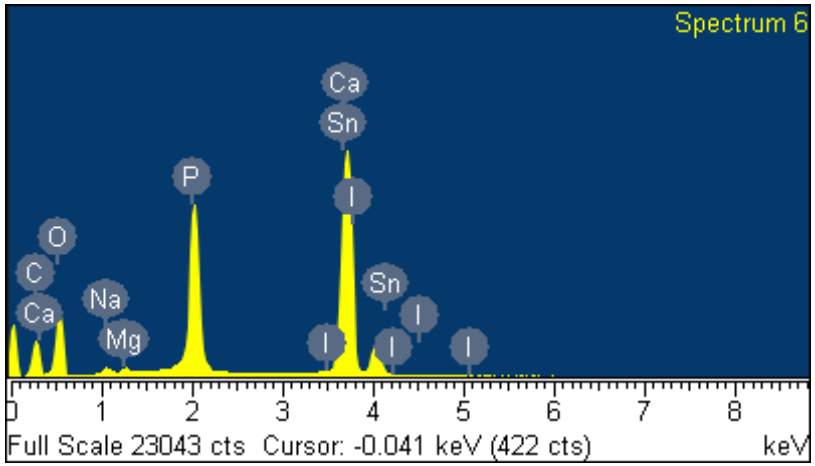

Comment:Bone 200 6Hrs

Ashes to ashes

13-Dec-16 9:59:02 AM

Spectrum processing :
No peaks omitted

Processing option : All elements analyzed (Normalised)
Number of iterations = 4

Standard :
O SiO2 1-Jun-1999 12:00 AM
Na Albite 1-Jun-1999 12:00 AM
P GaP 1-Jun-1999 12:00 AM
Ca Wollastonite 1-Jun-1999 12:00 AM

Element	Weight%	Atomic%
O K	50.90	70.04
Na K	1.19	1.14
P K	15.54	11.05
Ca K	32.36	17.77
Totals	100.00	

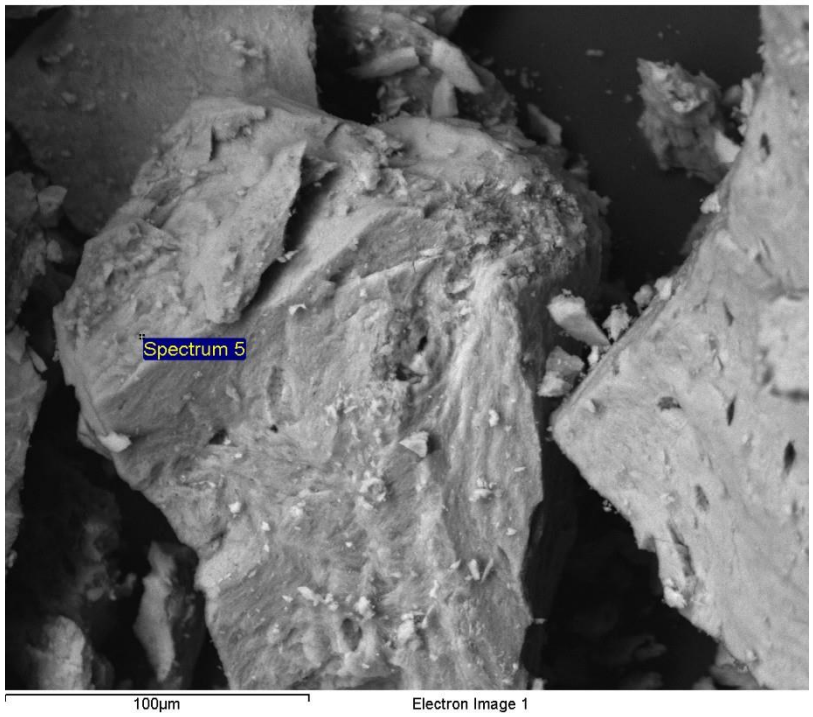

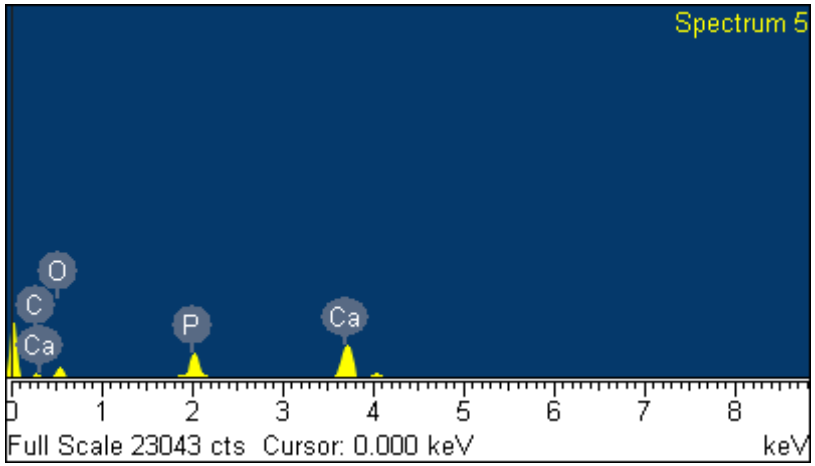

Comment:Bone 400 6Hrs

INCA

Ashes to ashes

13-Dec-16 10:07:53 AM

Spectrum processing :
Peaks possibly omitted : 2.610, 8.571 keV

Processing option : All elements analyzed (Normalised)
Number of iterations = 4

Standard :
C CaCO3 1-Jun-1999 12:00 AM
O SiO2 1-Jun-1999 12:00 AM
Na Albite 1-Jun-1999 12:00 AM
Mg MgO 1-Jun-1999 12:00 AM
P GaP 1-Jun-1999 12:00 AM
Ca Wollastonite 1-Jun-1999 12:00 AM

Element	Weight%	Atomic%
C K	10.74	17.97
O K	46.30	58.13
Na K	0.52	0.46
Mg K	0.45	0.37
P K	13.76	8.92
Ca K	28.22	14.15
Totals	100.00	

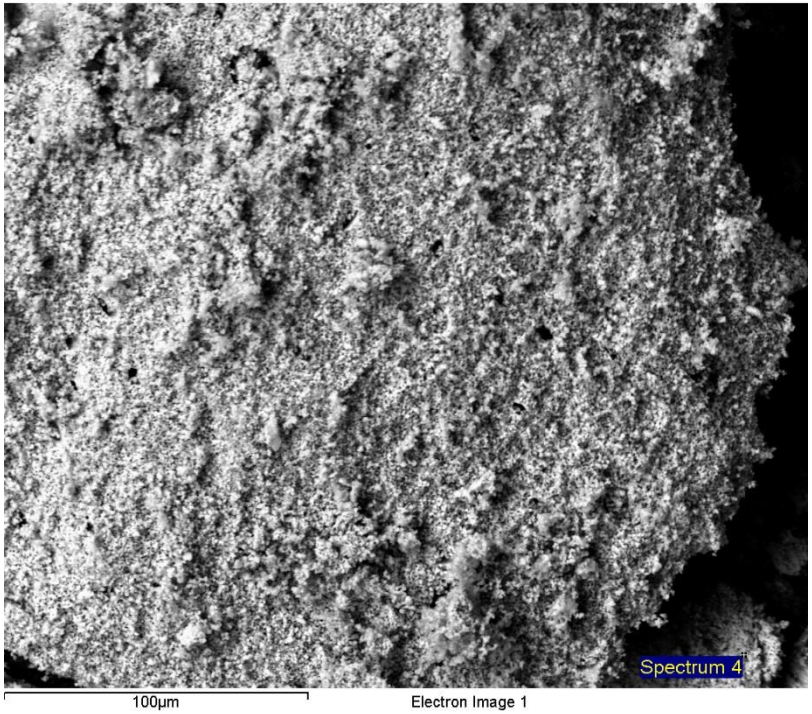

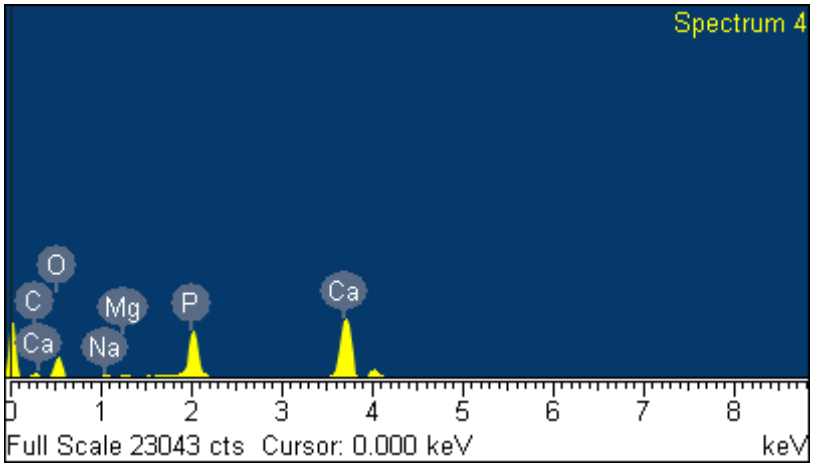

Comment:Bone 900 6Hrs

Ashes to ashes

21-Apr-16 10:41:33 AM

Spectrum processing :
No peaks omitted

Processing option : All elements analyzed (Normalised)
Number of iterations = 4

Standard :
O SiO2 1-Jun-1999 12:00 AM
Na Albite 1-Jun-1999 12:00 AM
Mg MgO 1-Jun-1999 12:00 AM
Al Al2O3 1-Jun-1999 12:00 AM
Si SiO2 1-Jun-1999 12:00 AM
S FeS2 1-Jun-1999 12:00 AM
Ca Wollastonite 1-Jun-1999 12:00 AM
Fe Fe 1-Jun-1999 12:00 AM
Ir Ir 1-Jun-1999 12:00 AM

Element	Weight%	Atomic%
O K	70.45	84.30
Na K	2.28	1.90
Mg K	4.56	3.59
Al K	3.27	2.32
Si K	2.44	1.66
S K	5.39	3.22
Ca K	3.41	1.63
Fe K	2.34	0.80
Ir M	5.87	0.58
Totals	100.00	

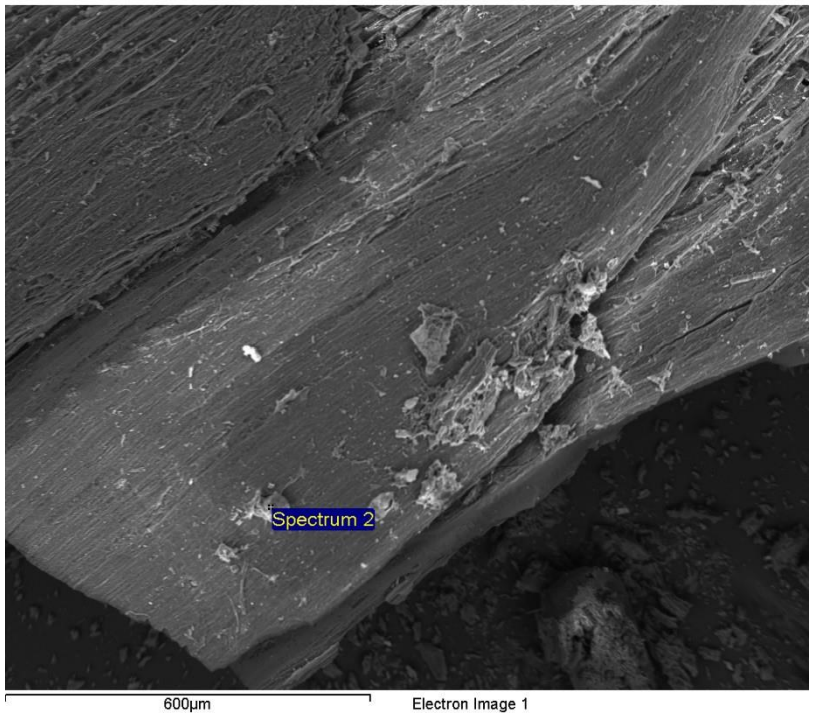

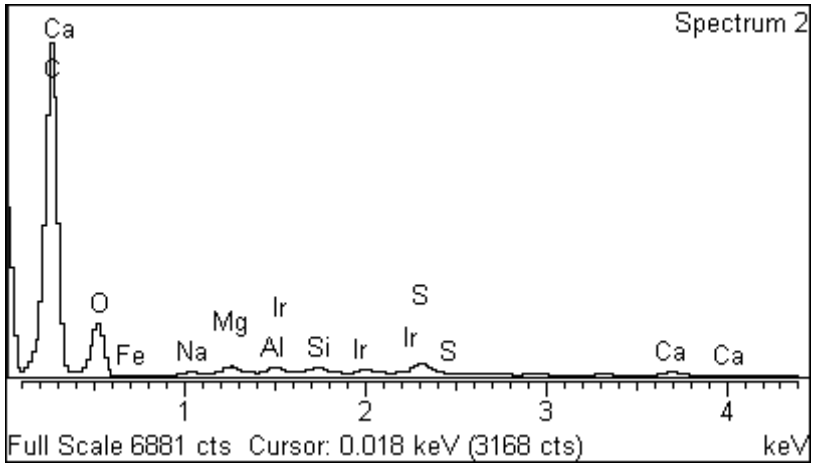

Comment: Peat at 200 degrees- 6hrs

Ashes to ashes

03-Jun-16 11:43:43 AM

Spectrum processing :
No peaks omitted

Processing option : All elements analyzed (Normalised)
Number of iterations = 3

Standard :
O SiO2 1-Jun-1999 12:00 AM
Na Albite 1-Jun-1999 12:00 AM
Mg MgO 1-Jun-1999 12:00 AM
Al Al2O3 1-Jun-1999 12:00 AM
S FeS2 1-Jun-1999 12:00 AM
Cl KCl 1-Jun-1999 12:00 AM
Ca Wollastonite 1-Jun-1999 12:00 AM
Fe Fe 1-Jun-1999 12:00 AM

Element	Weight%	Atomic%
O K	38.68	56.35
Na K	1.86	1.88
Mg K	14.01	13.43
Al K	2.02	1.74
S K	18.82	13.68
Cl K	1.82	1.19
Ca K	13.48	7.84
Fe K	9.31	3.89
Totals	100.00	

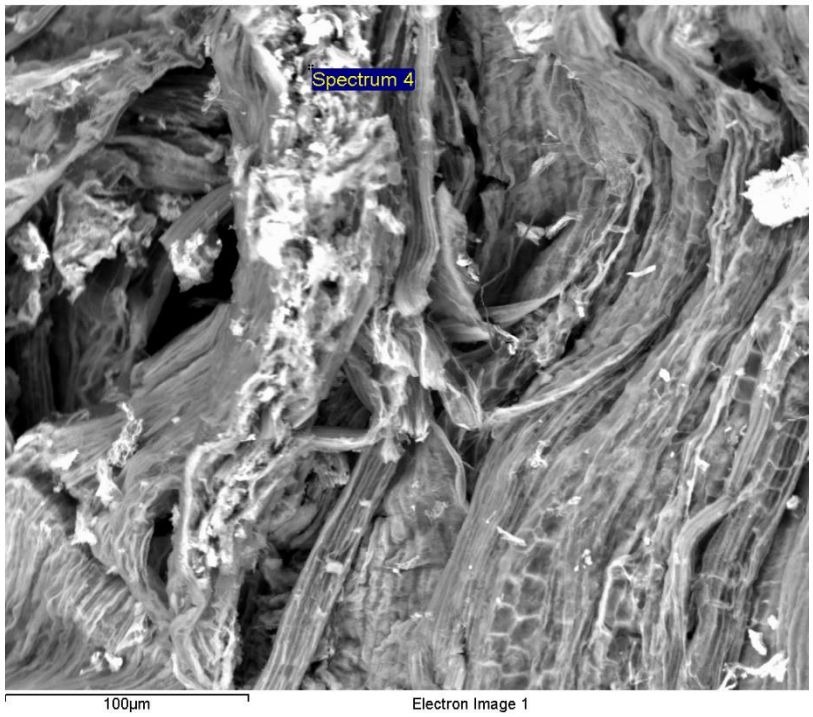

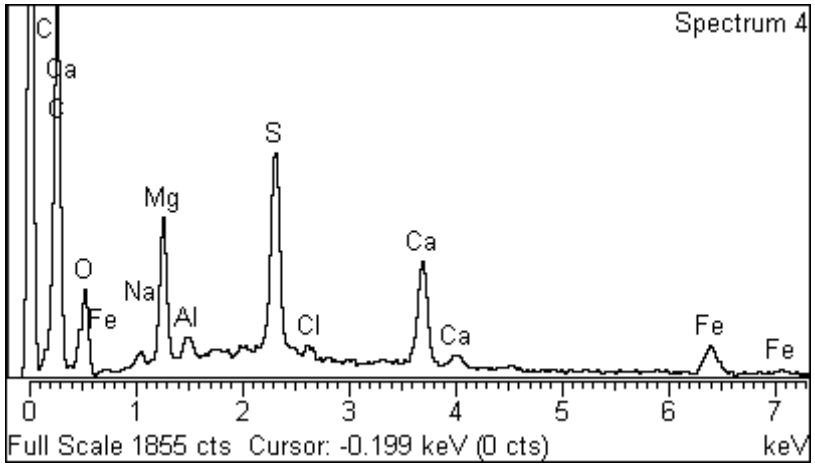

Comment:Peat 400 6 hrs

INCA

Ashes to ashes

12-Dec-16 9:58:00 AM

Spectrum processing :
Peak possibly omitted : 4.500 keV

Processing option : All elements analyzed (Normalised)
Number of iterations = 4

Standard :
O SiO2 1-Jun-1999 12:00 AM
Na Albite 1-Jun-1999 12:00 AM
Mg MgO 1-Jun-1999 12:00 AM
Al Al2O3 1-Jun-1999 12:00 AM
Si SiO2 1-Jun-1999 12:00 AM
P GaP 1-Jun-1999 12:00 AM
S FeS2 1-Jun-1999 12:00 AM
Cl KCl 1-Jun-1999 12:00 AM
K MAD-10 Feldspar 1-Jun-1999 12:00 AM
Ca Wollastonite 1-Jun-1999 12:00 AM
Fe Fe 1-Jun-1999 12:00 AM

Element	Weight%	Atomic%
O K	43.35	62.14
Na K	2.35	2.35
Mg K	12.08	11.40
Al K	1.66	1.41
Si K	2.77	2.27
P K	0.88	0.65
S K	8.41	6.01
Cl K	0.70	0.45
K K	1.27	0.75
Ca K	10.38	5.94
Fe K	16.14	6.63
Totals	100.00	

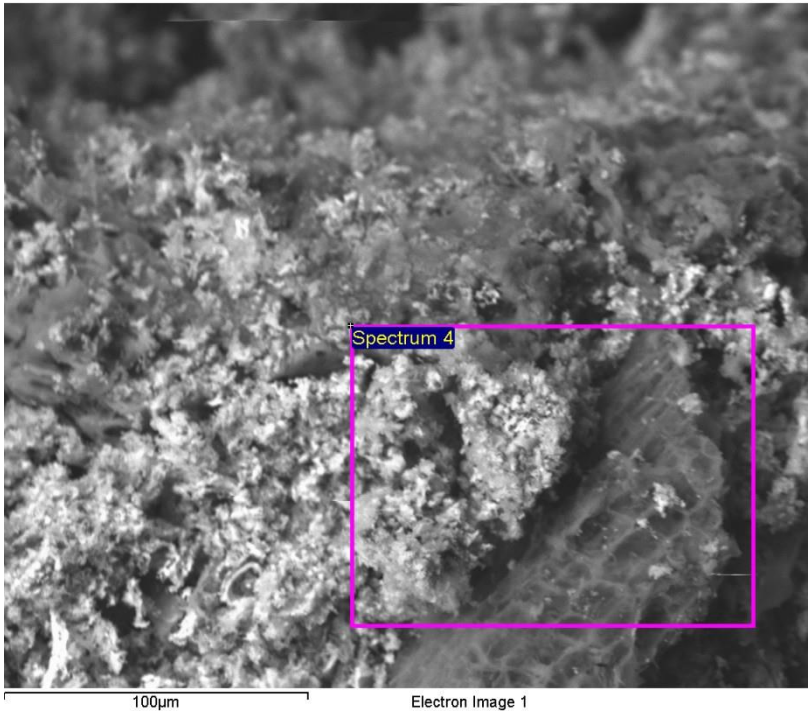

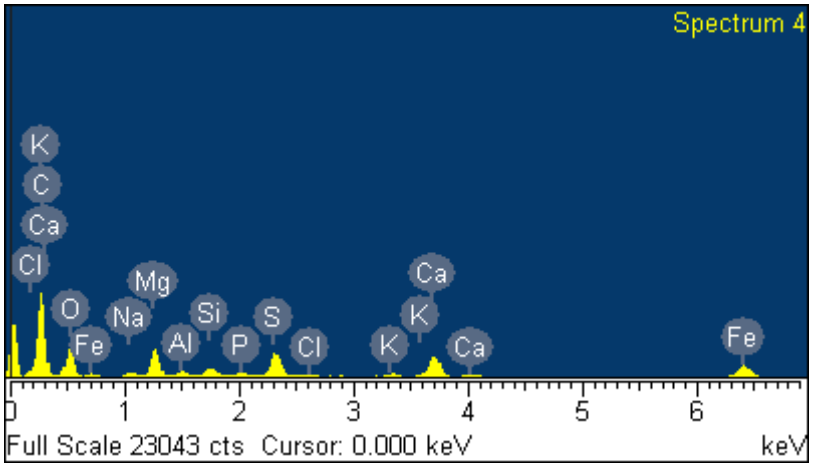

Comment:Peat 900 6 hrs

INCA

Ashes to ashes

14-Dec-16 1:55:26 PM

Spectrum processing :
No peaks omitted

Processing option : All elements analyzed (Normalised)
Number of iterations = 4

Standard :
C CaCO3 1-Jun-1999 12:00 AM
O SiO2 1-Jun-1999 12:00 AM
Mg MgO 1-Jun-1999 12:00 AM
Al Al2O3 1-Jun-1999 12:00 AM
Si SiO2 1-Jun-1999 12:00 AM
S FeS2 1-Jun-1999 12:00 AM
Cl KCl 1-Jun-1999 12:00 AM
Ca Wollastonite 1-Jun-1999 12:00 AM
Fe Fe 1-Jun-1999 12:00 AM

Element	Weight%	Atomic%
C K	56.01	65.60
O K	34.06	29.95
Mg K	2.69	1.55
Al K	1.01	0.53
Si K	0.77	0.39
S K	1.91	0.84
Cl K	0.40	0.16
Ca K	1.99	0.70
Fe K	1.17	0.30
Totals	100.00	

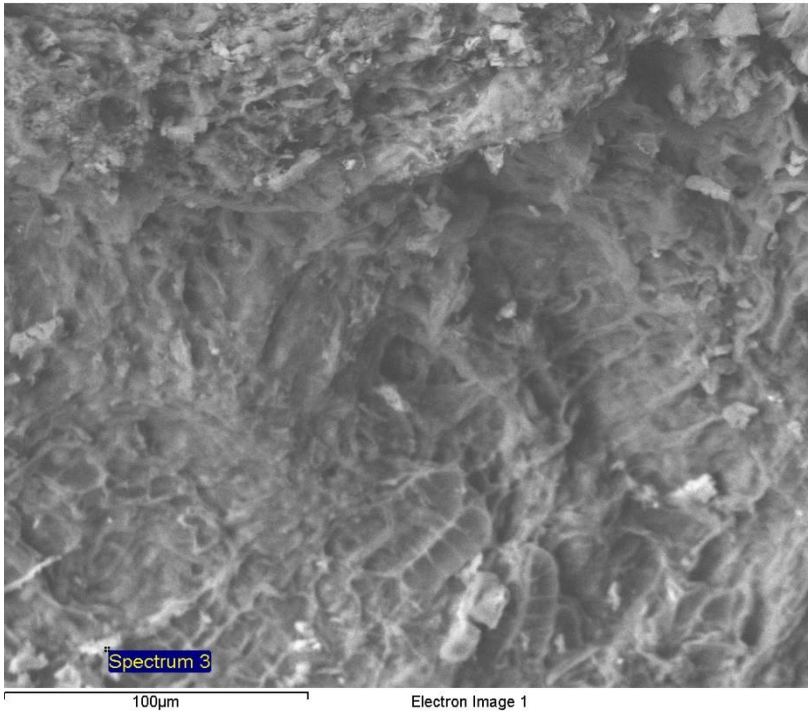

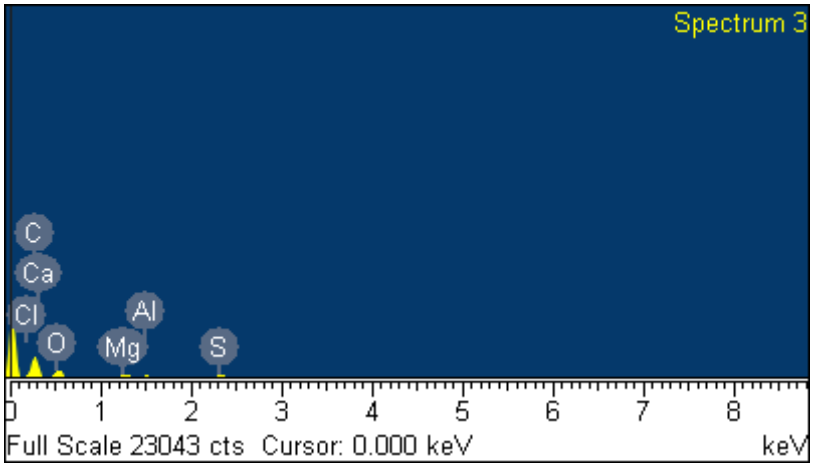

Comment: Fozzy Peat 200 6Hrs

INCA

Ashes to ashes

14-Dec-16 2:10:00 PM

Spectrum processing :
No peaks omitted

Processing option : All elements analyzed (Normalised)
Number of iterations = 4

Standard :
C CaCO3 1-Jun-1999 12:00 AM
O SiO2 1-Jun-1999 12:00 AM
Na Albite 1-Jun-1999 12:00 AM
Mg MgO 1-Jun-1999 12:00 AM
Al Al2O3 1-Jun-1999 12:00 AM
Si SiO2 1-Jun-1999 12:00 AM
S FeS2 1-Jun-1999 12:00 AM
Ca Wollastonite 1-Jun-1999 12:00 AM
Fe Fe 1-Jun-1999 12:00 AM

Element	Weight%	Atomic%
C K	59.70	69.00
O K	30.79	26.71
Na K	0.59	0.36
Mg K	1.43	0.82
Al K	0.97	0.50
Si K	2.10	1.04
S K	1.51	0.66
Ca K	2.04	0.71
Fe K	0.87	0.22
Totals	100.00	

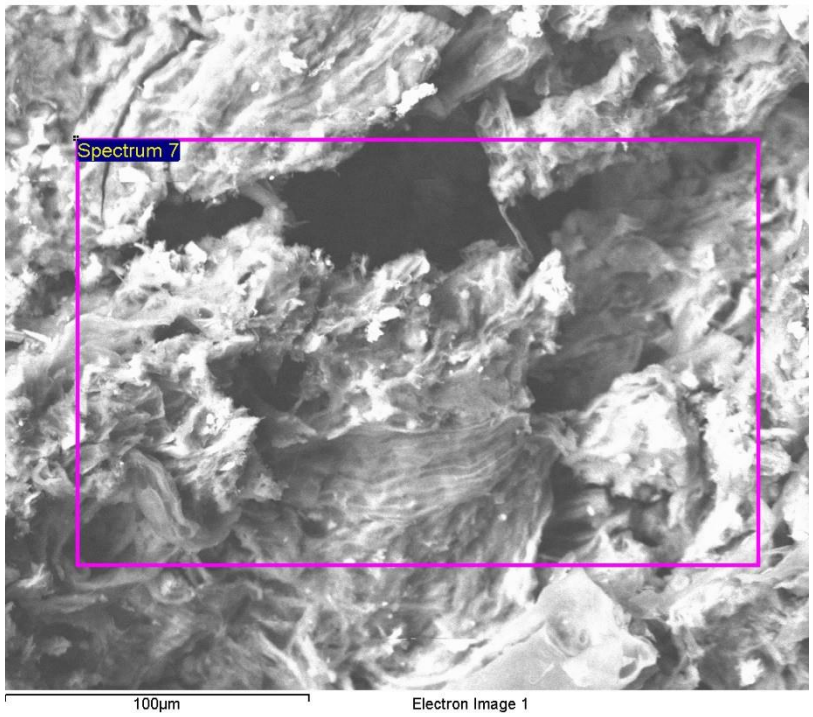

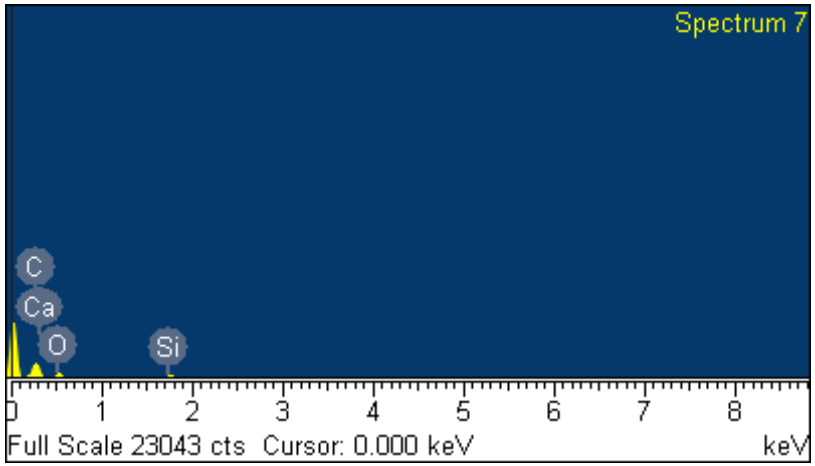

Comment: Fozzy Peat 400 6Hrs

INCA

Ashes to ashes

14-Dec-16 2:39:08 PM

Spectrum processing :
Peak possibly omitted : 8.090 keV

Processing option : All elements analyzed (Normalised)
Number of iterations = 4

Standard :
C CaCO3 1-Jun-1999 12:00 AM
O SiO2 1-Jun-1999 12:00 AM
Na Albite 1-Jun-1999 12:00 AM
Mg MgO 1-Jun-1999 12:00 AM
Al Al2O3 1-Jun-1999 12:00 AM
Si SiO2 1-Jun-1999 12:00 AM
P GaP 1-Jun-1999 12:00 AM
S FeS2 1-Jun-1999 12:00 AM
Cl KCl 1-Jun-1999 12:00 AM
K MAD-10 Feldspar 1-Jun-1999 12:00 AM
Ca Wollastonite 1-Jun-1999 12:00 AM
Ti Ti 1-Jun-1999 12:00 AM
Fe Fe 1-Jun-1999 12:00 AM

Element	Weight%	Atomic%
C K	4.07	7.01
O K	46.20	59.76
Na K	2.76	2.48
Mg K	13.71	11.67
Al K	3.73	2.86
Si K	3.41	2.51
P K	1.17	0.78
S K	6.51	4.20
Cl K	0.20	0.12
K K	0.68	0.36
Ca K	11.65	6.02
Ti K	0.63	0.27
Fe K	5.28	1.95
Totals	100.00	

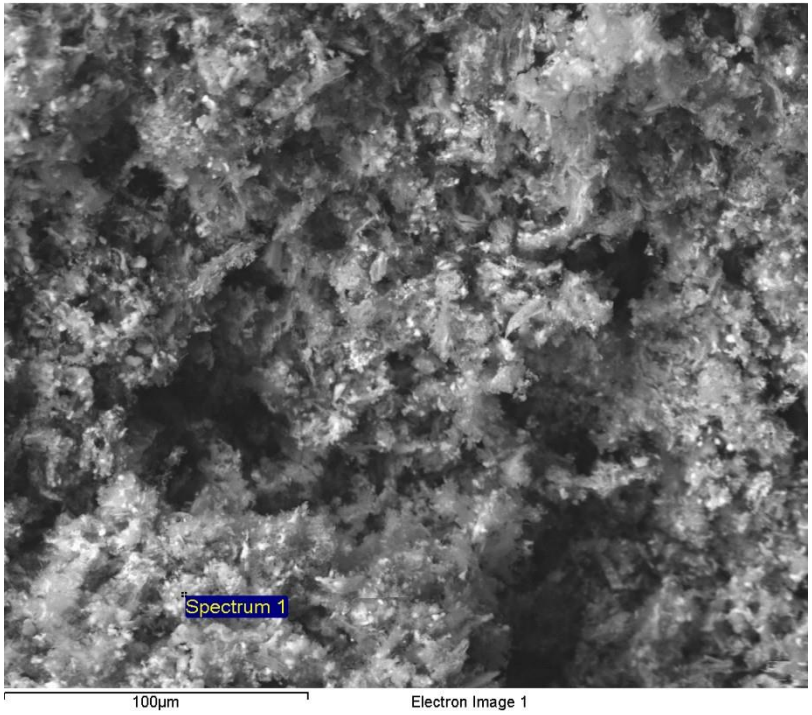

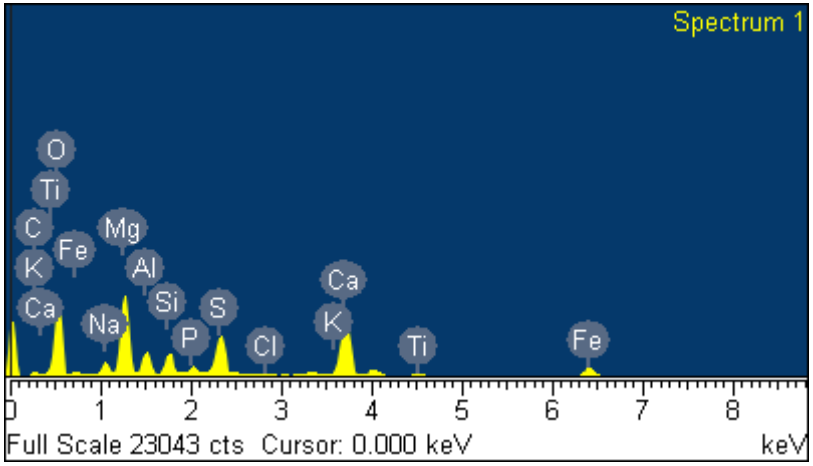

Comment:Fozzy Peat 900 6Hrs 2

INCA

Ashes to ashes

14-Dec-16 2:49:07 PM

Spectrum processing :
No peaks omitted

Processing option : All elements analyzed (Normalised)
Number of iterations = 5

Standard :
C CaCO3 1-Jun-1999 12:00 AM
O SiO2 1-Jun-1999 12:00 AM
Na Albite 1-Jun-1999 12:00 AM
Mg MgO 1-Jun-1999 12:00 AM
Al Al2O3 1-Jun-1999 12:00 AM
Si SiO2 1-Jun-1999 12:00 AM
K MAD-10 Feldspar 1-Jun-1999 12:00 AM
Ca Wollastonite 1-Jun-1999 12:00 AM
Ti Ti 1-Jun-1999 12:00 AM
Fe Fe 1-Jun-1999 12:00 AM

Element	Weight%	Atomic%
C K	8.28	12.90
O K	52.64	61.54
Na K	4.55	3.70
Mg K	0.52	0.40
Al K	5.28	3.66
Si K	23.81	15.86
K K	0.90	0.43
Ca K	1.08	0.50
Ti K	0.37	0.14
Fe K	2.57	0.86
Totals	100.00	

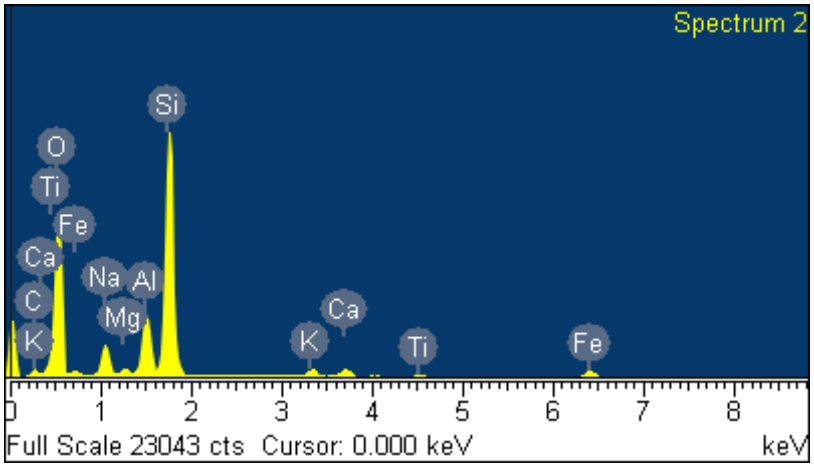

Comment:Mid Peat 200 6Hrs

INCA

Ashes to ashes

14-Dec-16 3:06:02 PM

Spectrum processing :
No peaks omitted

Processing option : All elements analyzed (Normalised)
Number of iterations = 3

Standard :
C CaCO3 1-Jun-1999 12:00 AM
O SiO2 1-Jun-1999 12:00 AM
Na Albite 1-Jun-1999 12:00 AM
Mg MgO 1-Jun-1999 12:00 AM
Al Al2O3 1-Jun-1999 12:00 AM
Si SiO2 1-Jun-1999 12:00 AM
P GaP 1-Jun-1999 12:00 AM
S FeS2 1-Jun-1999 12:00 AM
Ca Wollastonite 1-Jun-1999 12:00 AM
Ti Ti 1-Jun-1999 12:00 AM
Fe Fe 1-Jun-1999 12:00 AM
W W 1-Jun-1999 12:00 AM

Element	Weight%	Atomic%
C K	11.29	21.31
O K	26.85	38.04
Na K	1.06	1.04
Mg K	9.76	9.10
Al K	1.68	1.41
Si K	1.25	1.01
P K	0.53	0.39
S K	18.08	12.78
Ca K	20.53	11.61
Ti K	0.64	0.30
Fe K	7.01	2.85
W M	1.32	0.16
Totals	100.00	

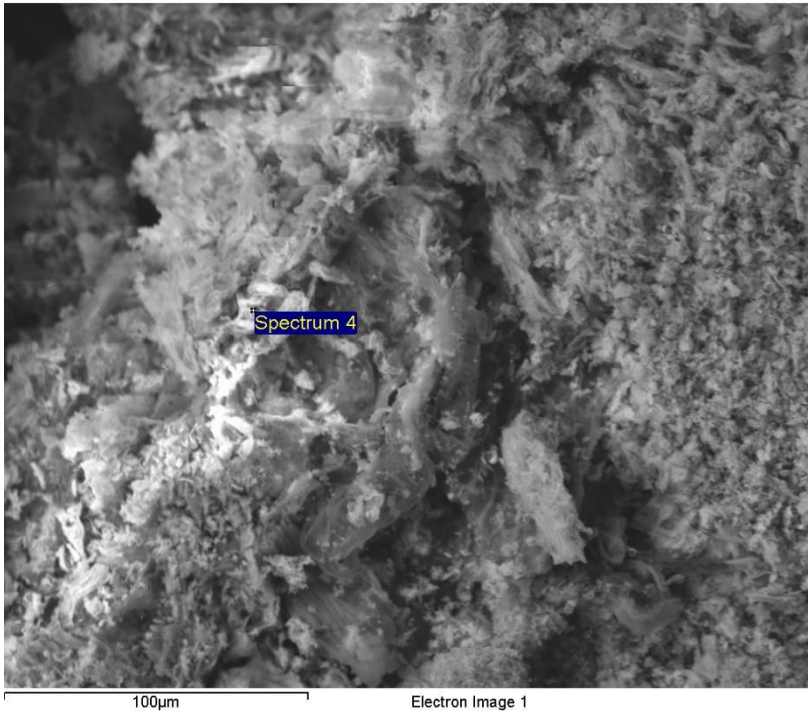

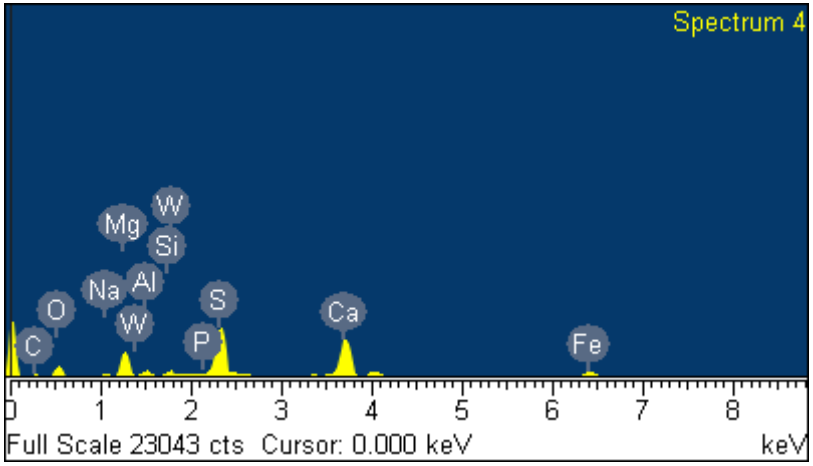

Comment:Mid Peat 400 6Hrs

INCA

Ashes to ashes

14-Dec-16 3:24:16 PM

Spectrum processing :
No peaks omitted

Processing option : All elements analyzed (Normalised)
Number of iterations = 4

Standard :
C CaCO3 1-Jun-1999 12:00 AM
O SiO2 1-Jun-1999 12:00 AM
Na Albite 1-Jun-1999 12:00 AM
Mg MgO 1-Jun-1999 12:00 AM
Al Al2O3 1-Jun-1999 12:00 AM
Si SiO2 1-Jun-1999 12:00 AM
P GaP 1-Jun-1999 12:00 AM
S FeS2 1-Jun-1999 12:00 AM
Cl KCl 1-Jun-1999 12:00 AM
K MAD-10 Feldspar 1-Jun-1999 12:00 AM
Ca Wollastonite 1-Jun-1999 12:00 AM
Ti Ti 1-Jun-1999 12:00 AM
Fe Fe 1-Jun-1999 12:00 AM

Element	Weight%	Atomic%
C K	2.22	3.95
O K	44.97	60.09
Na K	1.84	1.71
Mg K	12.43	10.93
Al K	3.80	3.01
Si K	5.87	4.47
P K	1.32	0.91
S K	6.99	4.66
Cl K	0.37	0.23
K K	1.02	0.56
Ca K	14.01	7.47
Ti K	0.57	0.26
Fe K	4.57	1.75
Totals	100.00	

Comment:Mid Peat 900 6Hrs

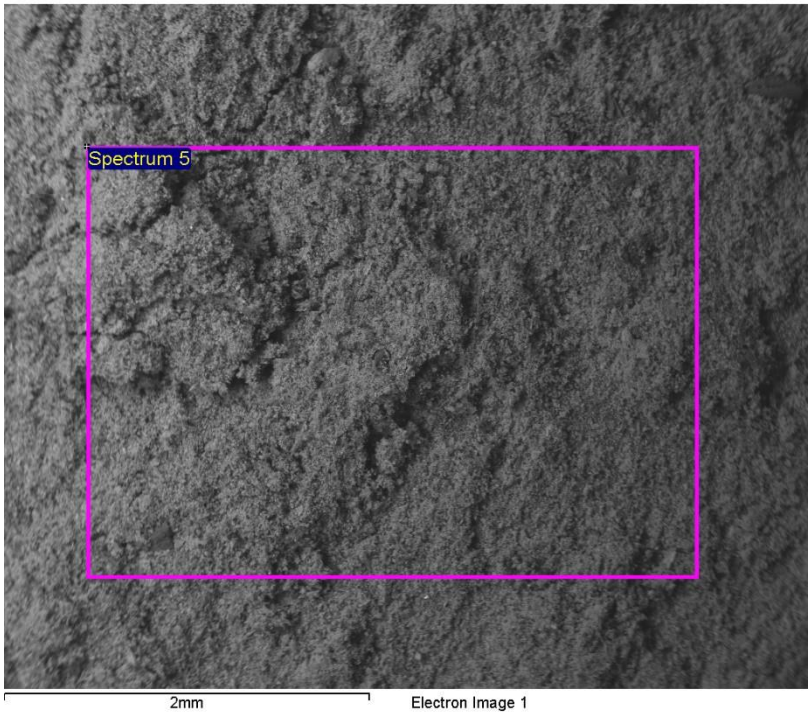

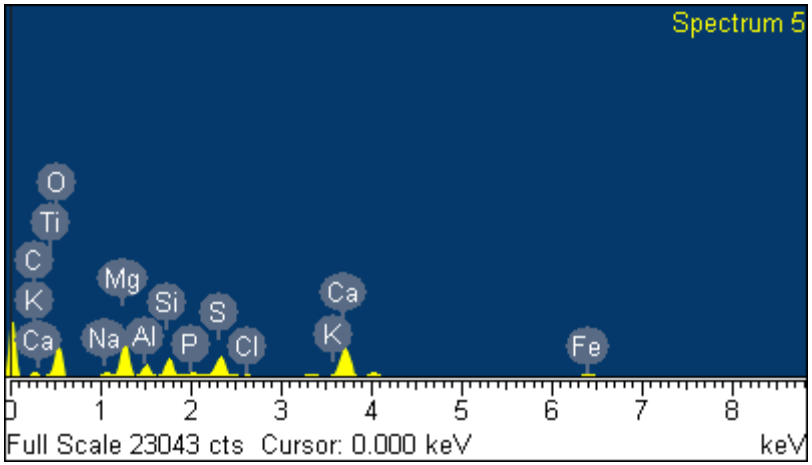

INCA

Ashes to ashes

14-Dec-16 3:36:32 PM

Spectrum processing :
No peaks omitted

Processing option : All elements analyzed (Normalised)
Number of iterations = 5

Standard :
C CaCO3 1-Jun-1999 12:00 AM
O SiO2 1-Jun-1999 12:00 AM
Na Albite 1-Jun-1999 12:00 AM
Mg MgO 1-Jun-1999 12:00 AM
Al Al2O3 1-Jun-1999 12:00 AM
Si SiO2 1-Jun-1999 12:00 AM
P GaP 1-Jun-1999 12:00 AM
S FeS2 1-Jun-1999 12:00 AM
Ca Wollastonite 1-Jun-1999 12:00 AM
Ti Ti 1-Jun-1999 12:00 AM
Fe Fe 1-Jun-1999 12:00 AM

Element	Weight%	Atomic%
C K	37.70	50.42
O K	37.03	37.18
Na K	0.69	0.48
Mg K	5.41	3.57
Al K	1.11	0.66
Si K	1.93	1.10
P K	0.30	0.16
S K	5.92	2.97
Ca K	5.20	2.08
Ti K	0.28	0.09
Fe K	4.42	1.27
Totals	100.00	

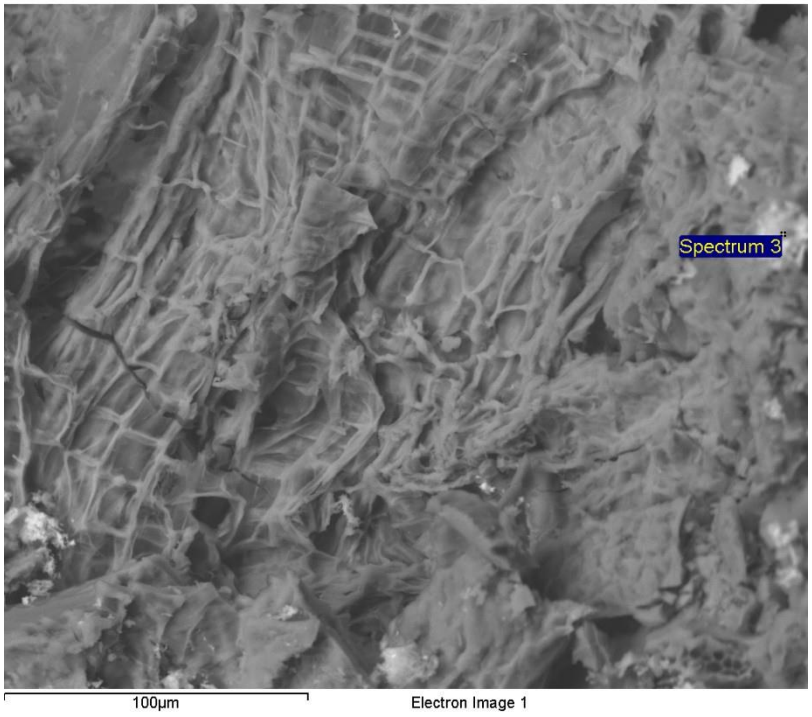

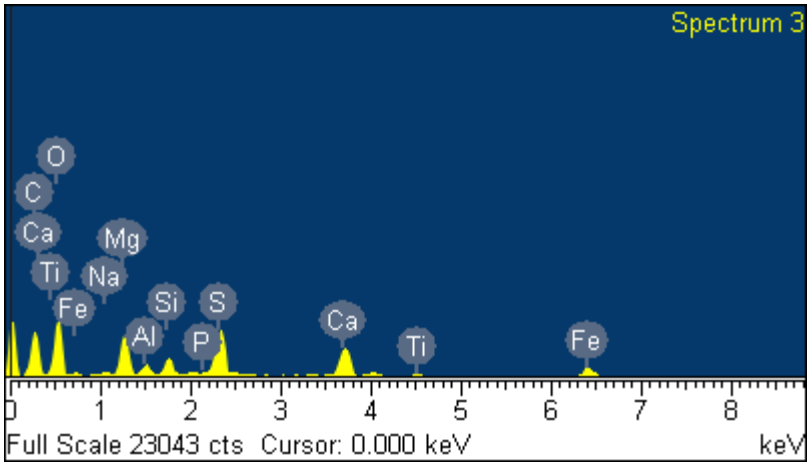

Comment:Low Peat 200 6Hrs

inca

Ashes to ashes

14-Dec-16 3:43:49 PM

Spectrum processing :
No peaks omitted

Processing option : All elements analyzed (Normalised)
Number of iterations = 4

Standard :
C CaCO3 1-Jun-1999 12:00 AM
O SiO2 1-Jun-1999 12:00 AM
Na Albite 1-Jun-1999 12:00 AM
Mg MgO 1-Jun-1999 12:00 AM
Al Al2O3 1-Jun-1999 12:00 AM
Si SiO2 1-Jun-1999 12:00 AM
P GaP 1-Jun-1999 12:00 AM
S FeS2 1-Jun-1999 12:00 AM
Ca Wollastonite 1-Jun-1999 12:00 AM
Ti Ti 1-Jun-1999 12:00 AM
Fe Fe 1-Jun-1999 12:00 AM

Element	Weight%	Atomic%
C K	57.35	68.99
O K	27.19	24.56
Na K	0.50	0.31
Mg K	2.30	1.36
Al K	0.45	0.24
Si K	0.58	0.30
P K	0.25	0.12
S K	3.94	1.78
Ca K	3.97	1.43
Ti K	0.32	0.10
Fe K	3.14	0.81
Totals	100.00	

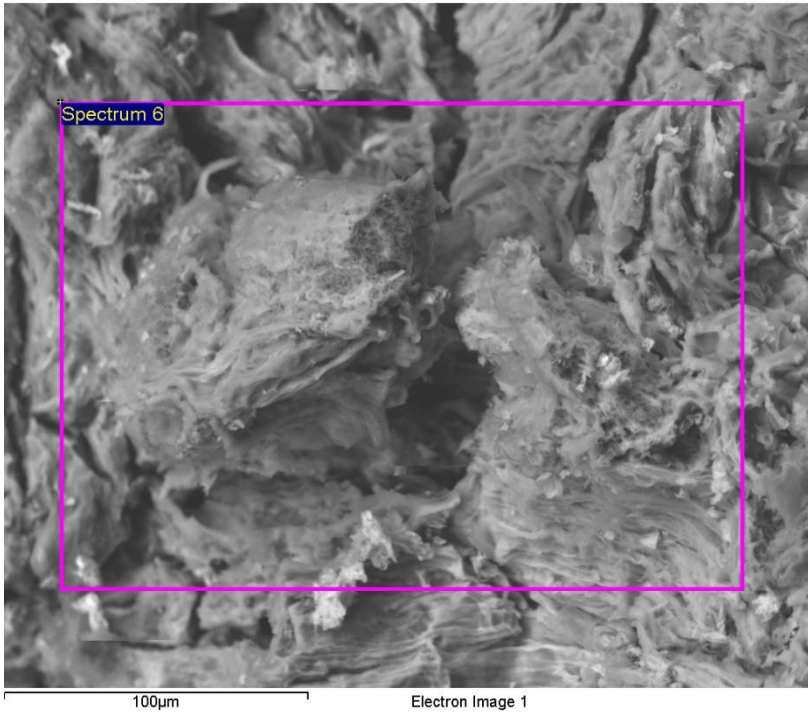

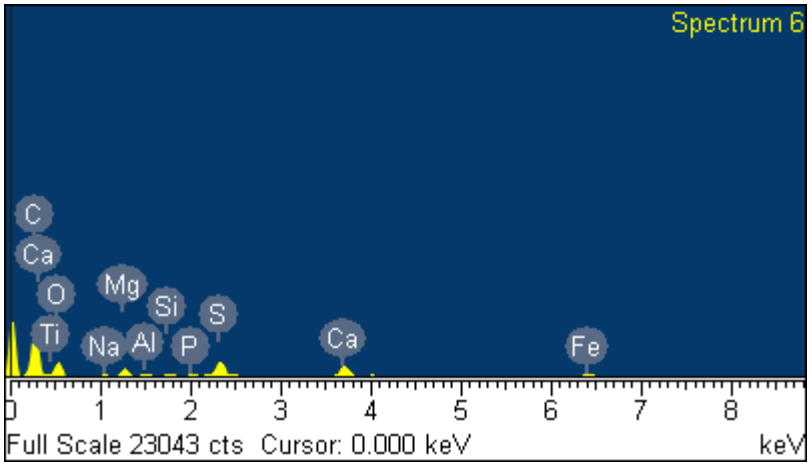

Comment:Low Peat 400 6Hrs

Ashes to ashes

14-Dec-16 3:51:16 PM

Spectrum processing :
No peaks omitted

Processing option : All elements analyzed (Normalised)
Number of iterations = 5

Standard :
C CaCO3 1-Jun-1999 12:00 AM
O SiO2 1-Jun-1999 12:00 AM
Na Albite 1-Jun-1999 12:00 AM
Mg MgO 1-Jun-1999 12:00 AM
Al Al2O3 1-Jun-1999 12:00 AM
Si SiO2 1-Jun-1999 12:00 AM
P GaP 1-Jun-1999 12:00 AM
S FeS2 1-Jun-1999 12:00 AM
K MAD-10 Feldspar 1-Jun-1999 12:00 AM
Ca Wollastonite 1-Jun-1999 12:00 AM
Ti Ti 1-Jun-1999 12:00 AM
Fe Fe 1-Jun-1999 12:00 AM

Element	Weight%	Atomic%
C K	38.66	55.09
O K	25.24	27.00
Na K	0.49	0.37
Mg K	5.16	3.63
Al K	3.38	2.14
Si K	2.04	1.24
P K	1.16	0.64
S K	4.77	2.55
K K	0.35	0.15
Ca K	11.51	4.92
Ti K	0.90	0.32
Fe K	6.33	1.94
Totals	100.00	

Comment:Low Peat 900 6Hrs

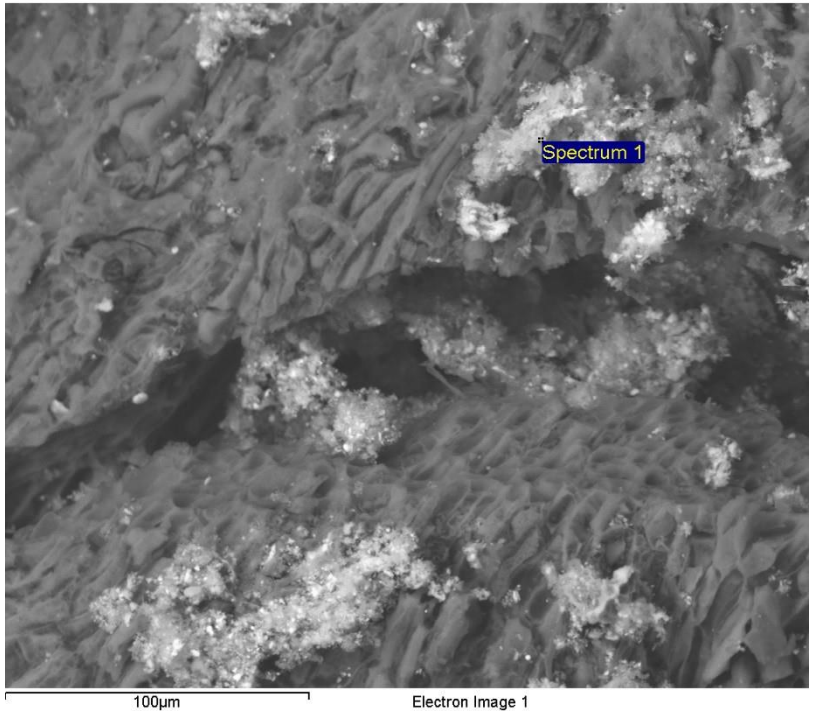

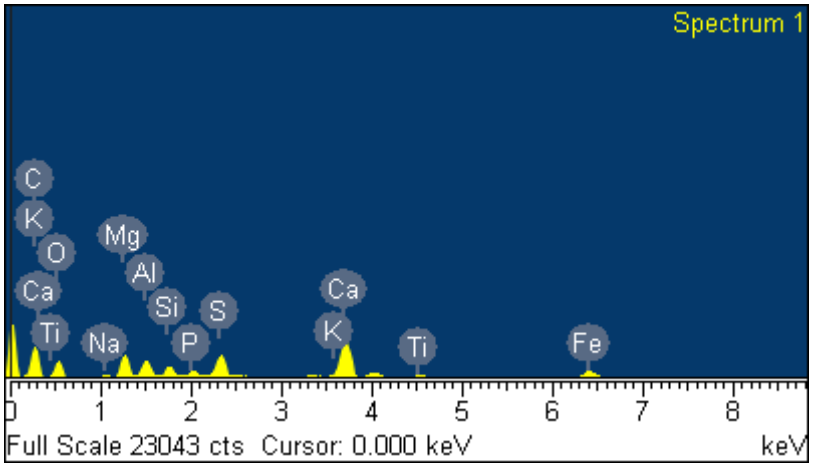

INCA

Ashes to ashes

14-Dec-16 3:59:13 PM

Spectrum processing :
No peaks omitted

Processing option : All elements analyzed (Normalised)
Number of iterations = 5

Standard :
C CaCO3 1-Jun-1999 12:00 AM
O SiO2 1-Jun-1999 12:00 AM
Na Albite 1-Jun-1999 12:00 AM
Mg MgO 1-Jun-1999 12:00 AM
Al Al2O3 1-Jun-1999 12:00 AM
Si SiO2 1-Jun-1999 12:00 AM
S FeS2 1-Jun-1999 12:00 AM
K MAD-10 Feldspar 1-Jun-1999 12:00 AM
Ca Wollastonite 1-Jun-1999 12:00 AM
Ti Ti 1-Jun-1999 12:00 AM
Fe Fe 1-Jun-1999 12:00 AM

Element	Weight%	Atomic%
C K	56.72	67.45
O K	29.93	26.72
Na K	0.26	0.16
Mg K	0.52	0.31
Al K	1.19	0.63
Si K	3.95	2.01
S K	2.76	1.23
K K	0.65	0.24
Ca K	2.17	0.77
Ti K	0.27	0.08
Fe K	1.58	0.40
Totals	100.00	

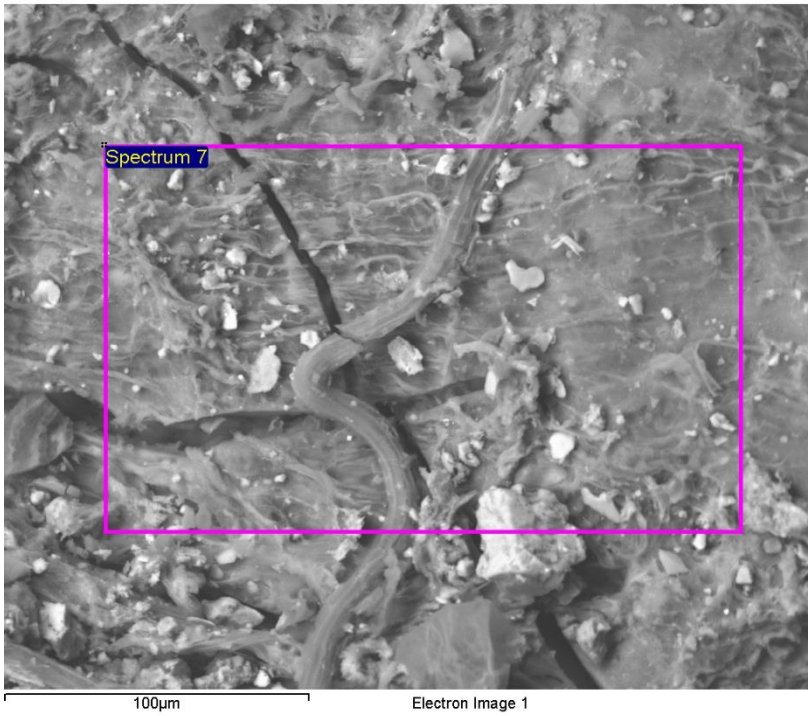

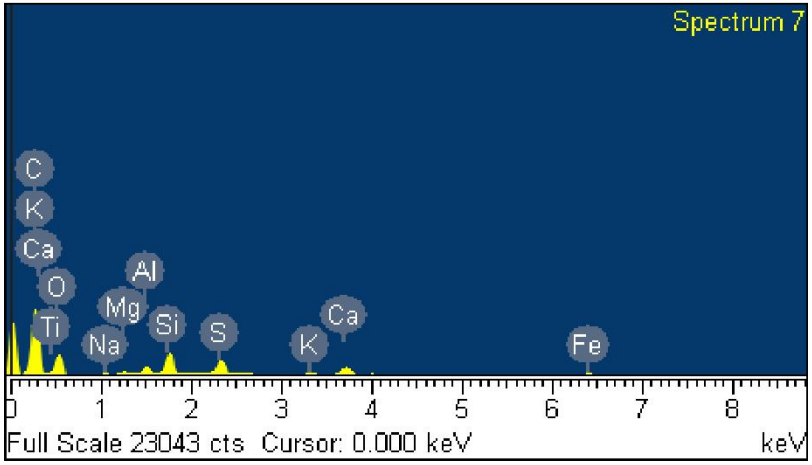

Comment:Highland Park Peat 200 6Hrs

INCA

Ashes to ashes

14-Dec-16 4:08:12 PM

Spectrum processing :
No peaks omitted

Processing option : All elements analyzed (Normalised)
Number of iterations = 5

Standard :
C CaCO3 1-Jun-1999 12:00 AM
O SiO2 1-Jun-1999 12:00 AM
Na Albite 1-Jun-1999 12:00 AM
Mg MgO 1-Jun-1999 12:00 AM
Al Al2O3 1-Jun-1999 12:00 AM
Si SiO2 1-Jun-1999 12:00 AM
P GaP 1-Jun-1999 12:00 AM
S FeS2 1-Jun-1999 12:00 AM
K MAD-10 Feldspar 1-Jun-1999 12:00 AM
Ca Wollastonite 1-Jun-1999 12:00 AM
Ti Ti 1-Jun-1999 12:00 AM
Fe Fe 1-Jun-1999 12:00 AM

Element	Weight%	Atomic%
C K	25.31	36.97
O K	42.37	46.46
Na K	1.27	0.97
Mg K	2.94	2.12
Al K	2.50	1.63
Si K	3.07	1.92
P K	0.26	0.15
S K	7.94	4.35
K K	0.50	0.22
Ca K	7.00	3.06
Ti K	0.22	0.08
Fe K	6.62	2.08
Totals	100.00	

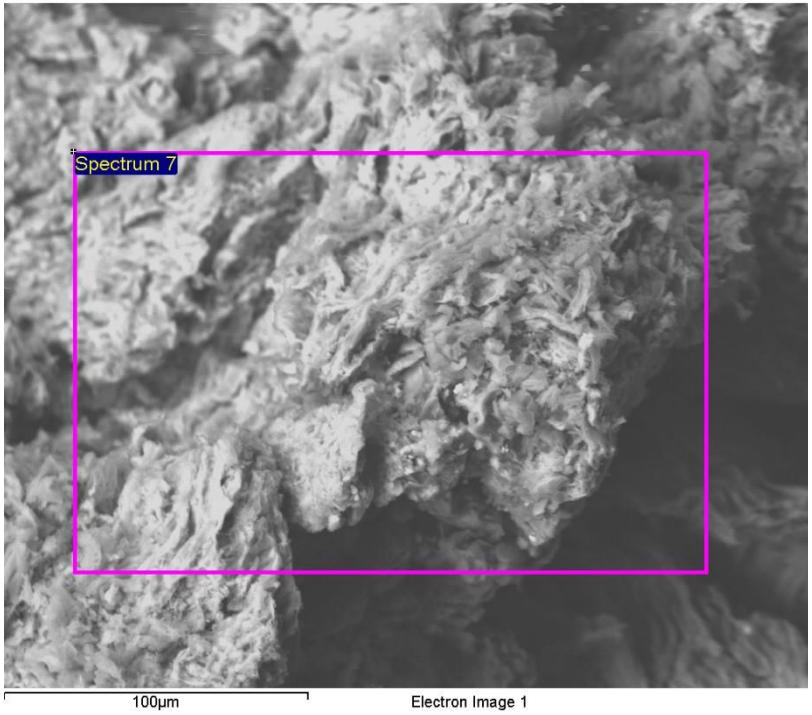

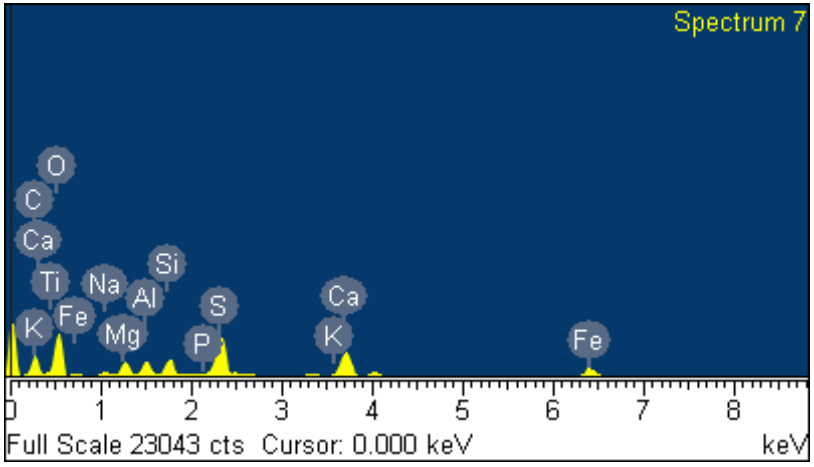

Comment:Highland Park Peat 400 6Hrs

INCA

Ashes to ashes

14-Dec-16 4:17:39 PM

Spectrum processing :
No peaks omitted

Processing option : All elements analyzed (Normalised)
Number of iterations = 5

Standard :
C CaCO3 1-Jun-1999 12:00 AM
O SiO2 1-Jun-1999 12:00 AM
Na Albite 1-Jun-1999 12:00 AM
Mg MgO 1-Jun-1999 12:00 AM
Al Al2O3 1-Jun-1999 12:00 AM
Si SiO2 1-Jun-1999 12:00 AM
P GaP 1-Jun-1999 12:00 AM
S FeS2 1-Jun-1999 12:00 AM
Cl KCl 1-Jun-1999 12:00 AM
K MAD-10 Feldspar 1-Jun-1999 12:00 AM
Ca Wollastonite 1-Jun-1999 12:00 AM
Ti Ti 1-Jun-1999 12:00 AM
Fe Fe 1-Jun-1999 12:00 AM

Element	Weight%	Atomic%
C K	6.08	10.21
O K	45.43	57.30
Na K	2.58	2.27
Mg K	14.25	11.83
Al K	4.10	3.07
Si K	5.02	3.60
P K	1.03	0.67
S K	6.94	4.37
Cl K	0.35	0.20
K K	1.10	0.57
Ca K	8.06	4.06
Ti K	0.56	0.23
Fe K	4.50	1.63
Totals	100.00	

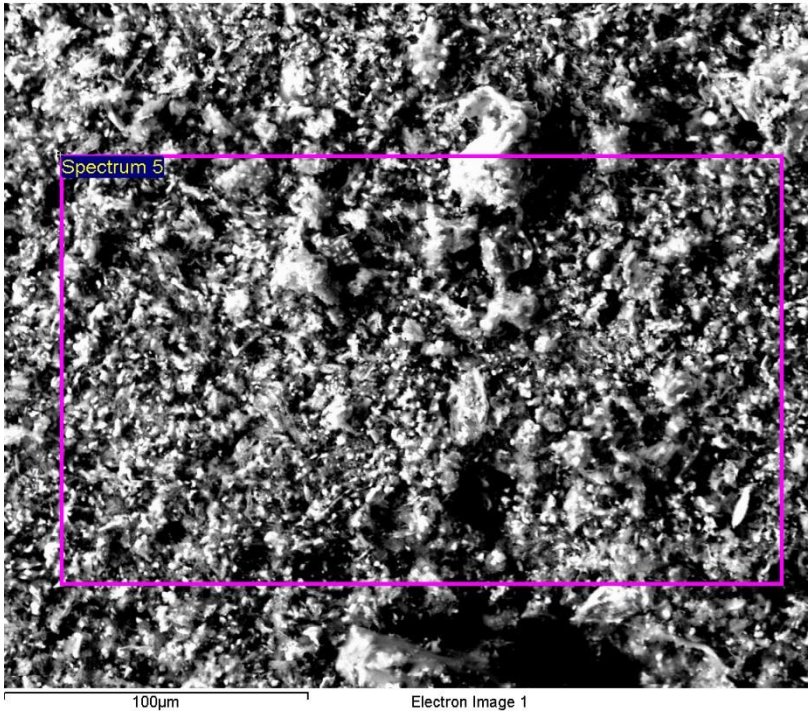

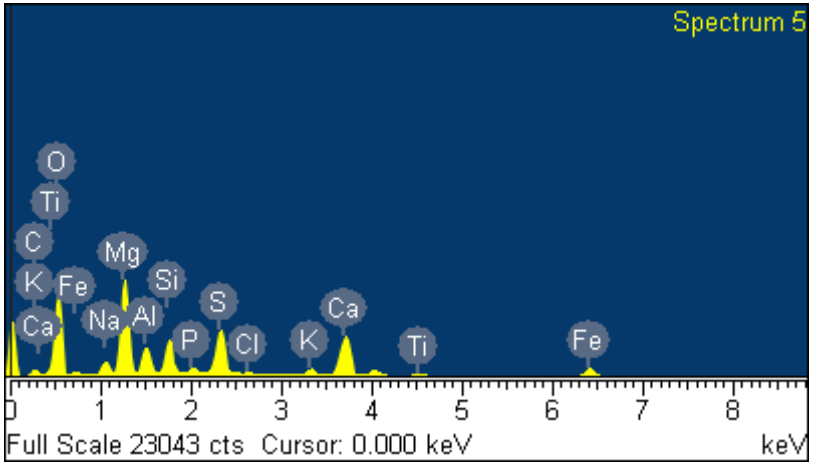

Comment:Highland Park Peat 900 6Hrs

INCA

Ashes to ashes

10-Jan-17 2:21:04 PM

Spectrum processing :
No peaks omitted

Processing option : All elements analyzed (Normalised)
Number of iterations = 3

Standard :
C CaCO3 1-Jun-1999 12:00 AM
O SiO2 1-Jun-1999 12:00 AM
Na Albite 1-Jun-1999 12:00 AM
Mg MgO 1-Jun-1999 12:00 AM
Al Al2O3 1-Jun-1999 12:00 AM
Si SiO2 1-Jun-1999 12:00 AM
P GaP 1-Jun-1999 12:00 AM
S FeS2 1-Jun-1999 12:00 AM
K MAD-10 Feldspar 1-Jun-1999 12:00 AM
Ca Wollastonite 1-Jun-1999 12:00 AM
Ti Ti 1-Jun-1999 12:00 AM
Fe Fe 1-Jun-1999 12:00 AM

Element	Weight%	Atomic%
C K	7.14	13.36
O K	40.21	56.51
Na K	0.55	0.54
Mg K	1.92	1.77
Al K	3.91	3.26
Si K	7.29	5.83
P K	0.48	0.35
S K	4.40	3.09
K K	1.02	0.59
Ca K	8.47	4.75
Ti K	0.46	0.22
Fe K	24.16	9.73
Totals	100.00	

Comment:Corrigal Caithness Peat

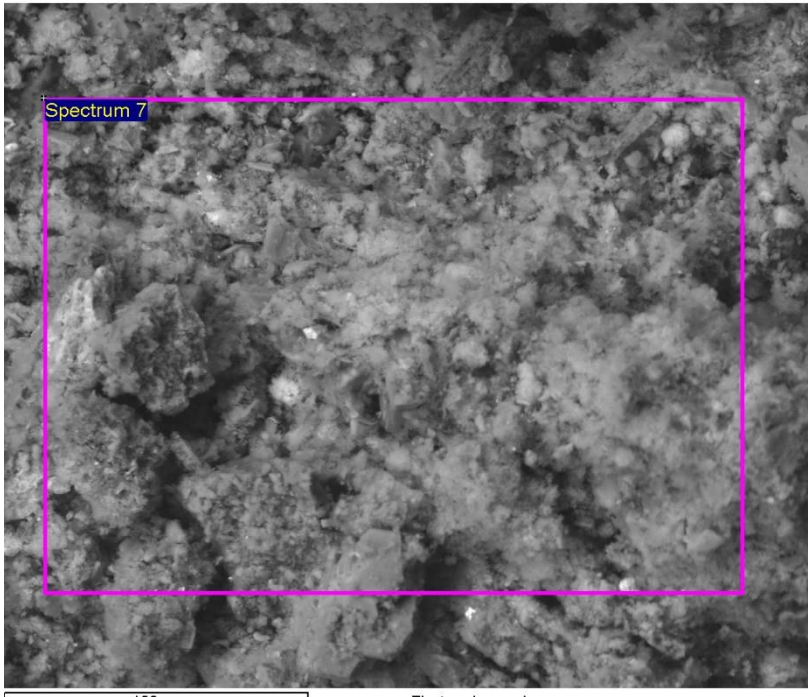

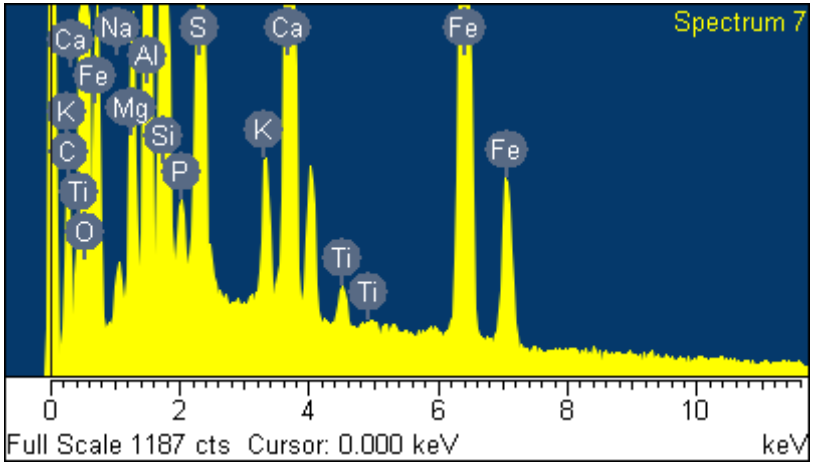

INCA

Ashes to ashes

10-Jan-17 2:01:51 PM

Spectrum processing :
No peaks omitted

Processing option : All elements analyzed (Normalised)
Number of iterations = 4

Standard :
C CaCO3 1-Jun-1999 12:00 AM
O SiO2 1-Jun-1999 12:00 AM
Na Albite 1-Jun-1999 12:00 AM
Mg MgO 1-Jun-1999 12:00 AM
Al Al2O3 1-Jun-1999 12:00 AM
Si SiO2 1-Jun-1999 12:00 AM
P GaP 1-Jun-1999 12:00 AM
S FeS2 1-Jun-1999 12:00 AM
Cl KCl 1-Jun-1999 12:00 AM
K MAD-10 Feldspar 1-Jun-1999 12:00 AM
Ca Wollastonite 1-Jun-1999 12:00 AM
Ti Ti 1-Jun-1999 12:00 AM
Fe Fe 1-Jun-1999 12:00 AM

Element	Weight%	Atomic%
C K	15.07	24.80
O K	39.53	48.83
Na K	1.44	1.24
Mg K	5.08	4.13
Al K	3.08	2.26
Si K	7.90	5.56
P K	0.68	0.43
S K	6.78	4.18
Cl K	0.37	0.21
K K	1.05	0.53
Ca K	7.79	3.84
Ti K	0.42	0.17
Fe K	10.81	3.83
Totals	100.00	

Comment:Corrigal Orkney Peat

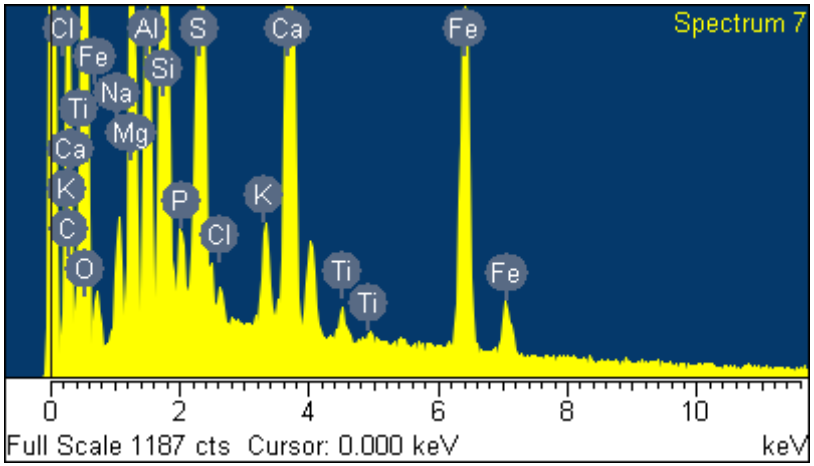

INCA

Ashes to ashes

19-Dec-16 3:04:07 PM

Spectrum processing :
No peaks omitted

Processing option : All elements analyzed (Normalised)
Number of iterations = 4

Standard :
C CaCO3 1-Jun-1999 12:00 AM
O SiO2 1-Jun-1999 12:00 AM
Na Albite 1-Jun-1999 12:00 AM
Mg MgO 1-Jun-1999 12:00 AM
Al Al2O3 1-Jun-1999 12:00 AM
Si SiO2 1-Jun-1999 12:00 AM
P GaP 1-Jun-1999 12:00 AM
S FeS2 1-Jun-1999 12:00 AM
Cl KCl 1-Jun-1999 12:00 AM
K MAD-10 Feldspar 1-Jun-1999 12:00 AM
Ca Wollastonite 1-Jun-1999 12:00 AM
Ti Ti 1-Jun-1999 12:00 AM
Fe Fe 1-Jun-1999 12:00 AM
W W 1-Jun-1999 12:00 AM

Element	Weight%	Atomic%
C K	11.78	19.57
O K	41.70	52.01
Na K	4.76	4.14
Mg K	5.38	4.42
Al K	2.12	1.57
Si K	3.49	2.48
P K	1.12	0.72
S K	7.10	4.42
Cl K	3.85	2.17
K K	5.78	2.95
Ca K	9.10	4.53
Ti K	0.32	0.13
Fe K	2.15	0.77
W M	1.34	0.15
Totals	100.00	

Comment:Mix Fuels 500 6Hrs 2

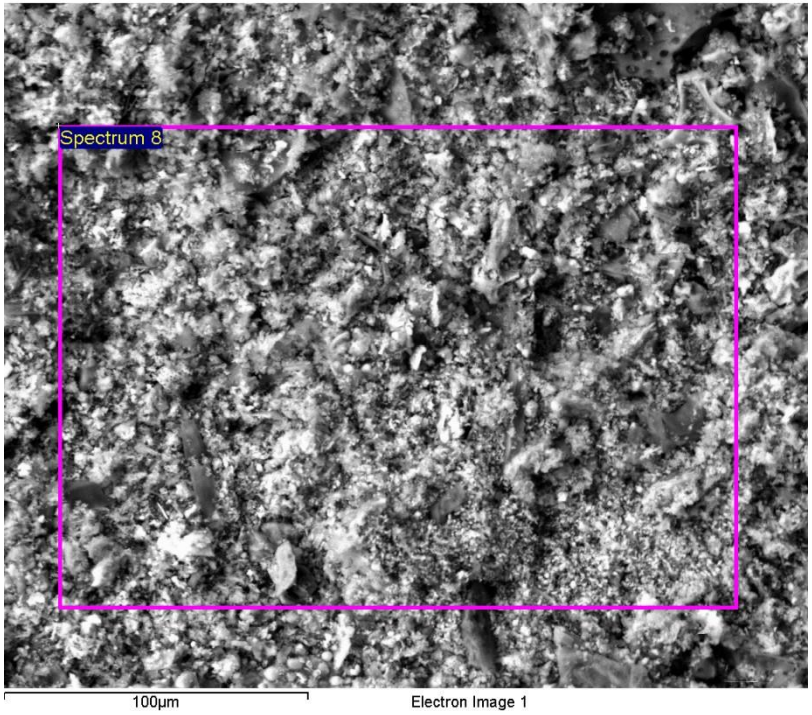

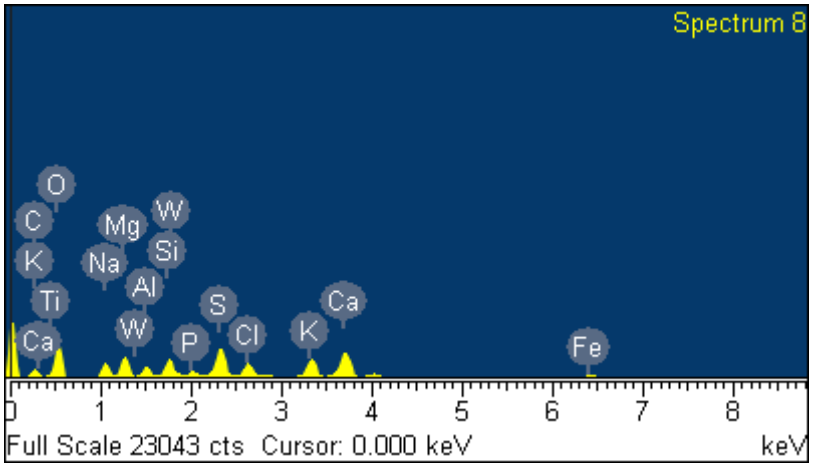

inca

Ashes to ashes

10-Jan-17 2:44:09 PM

Spectrum processing :
No peaks omitted

Processing option : All elements analyzed (Normalised)
Number of iterations = 4

Standard :
C CaCO3 1-Jun-1999 12:00 AM
O SiO2 1-Jun-1999 12:00 AM
Na Albite 1-Jun-1999 12:00 AM
Mg MgO 1-Jun-1999 12:00 AM
Al Al2O3 1-Jun-1999 12:00 AM
Si SiO2 1-Jun-1999 12:00 AM
P GaP 1-Jun-1999 12:00 AM
S FeS2 1-Jun-1999 12:00 AM
Cl KCl 1-Jun-1999 12:00 AM
K MAD-10 Feldspar 1-Jun-1999 12:00 AM
Ca Wollastonite 1-Jun-1999 12:00 AM
Ti Ti 1-Jun-1999 12:00 AM
Fe Fe 1-Jun-1999 12:00 AM

Element	Weight%	Atomic%
C K	9.44	15.64
O K	46.73	58.14
Na K	1.09	0.94
Mg K	7.12	5.83
Al K	2.30	1.69
Si K	3.10	2.20
P K	0.93	0.59
S K	5.64	3.50
Cl K	0.67	0.38
K K	3.34	1.70
Ca K	16.88	8.39
Ti K	0.13	0.05
Fe K	2.64	0.94
Totals	100.00	

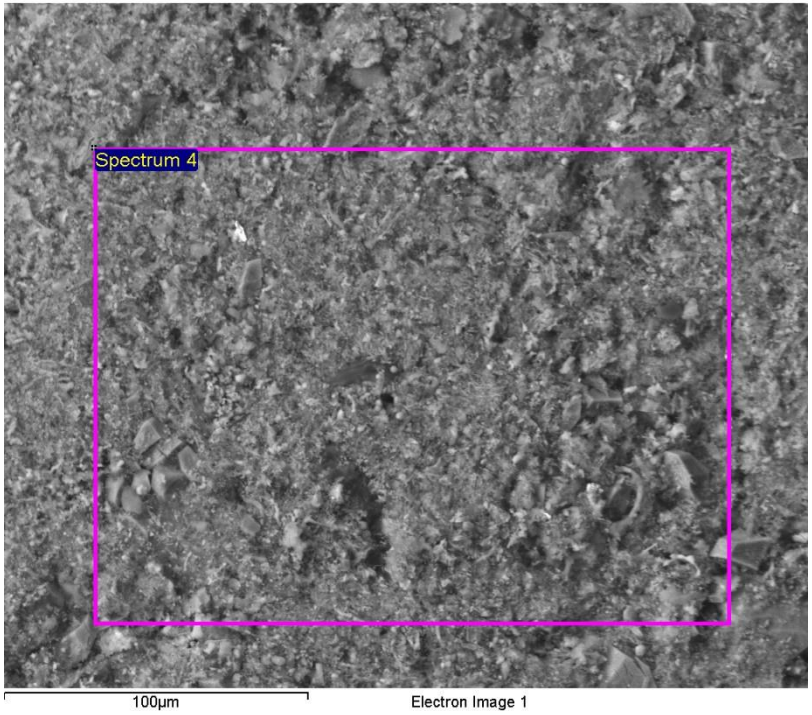

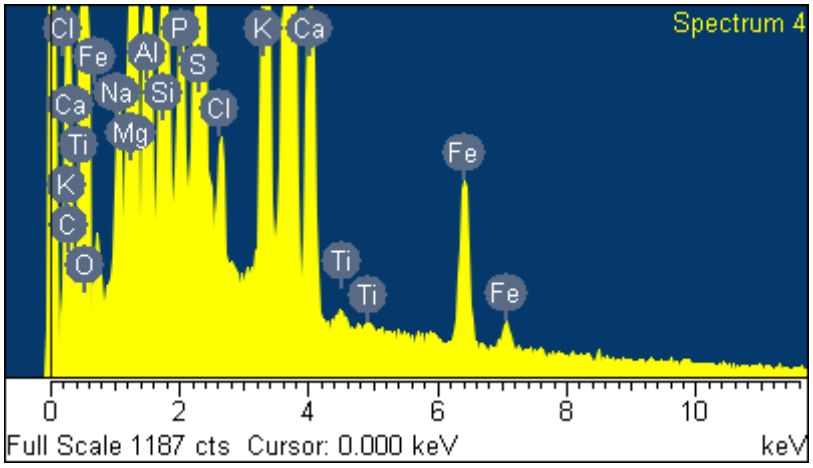

Comment:Peat + Wood

inca

Ashes to ashes

16-Jan-17 2:58:14 PM

Spectrum processing :
No peaks omitted

Processing option : All elements analyzed (Normalised)
Number of iterations = 4

Standard :
C CaCO3 1-Jun-1999 12:00 AM
O SiO2 1-Jun-1999 12:00 AM
Na Albite 1-Jun-1999 12:00 AM
Mg MgO 1-Jun-1999 12:00 AM
Al Al2O3 1-Jun-1999 12:00 AM
Si SiO2 1-Jun-1999 12:00 AM
P GaP 1-Jun-1999 12:00 AM
K MAD-10 Feldspar 1-Jun-1999 12:00 AM
Ca Wollastonite 1-Jun-1999 12:00 AM
Fe Fe 1-Jun-1999 12:00 AM

Element	Weight%	Atomic%
C K	13.91	21.48
O K	47.19	54.71
Na K	0.85	0.68
Mg K	0.61	0.47
Al K	5.76	3.96
Si K	22.16	14.63
P K	0.83	0.50
K K	2.64	1.25
Ca K	2.36	1.09
Fe K	3.70	1.23
Totals	100.00	

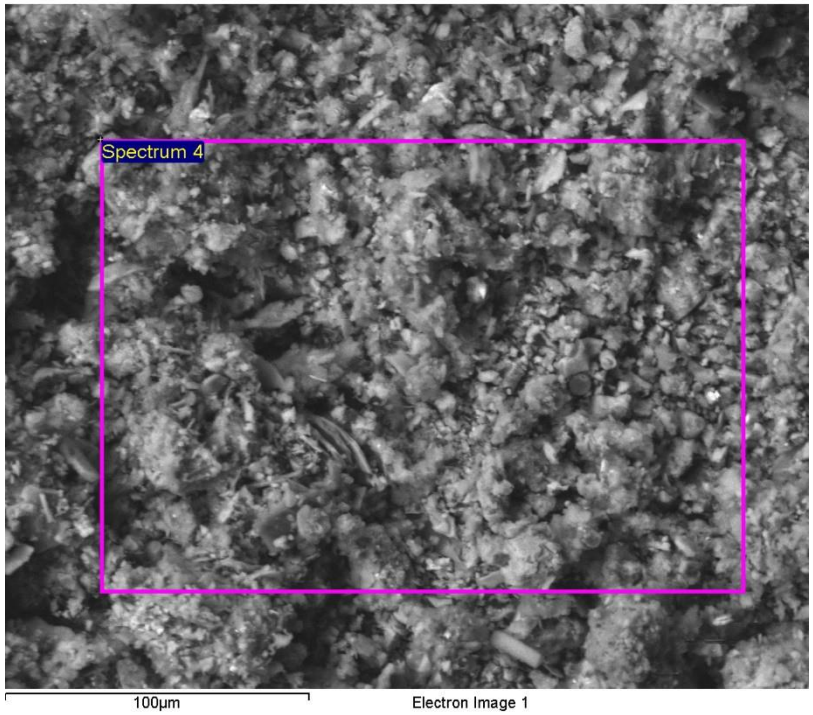

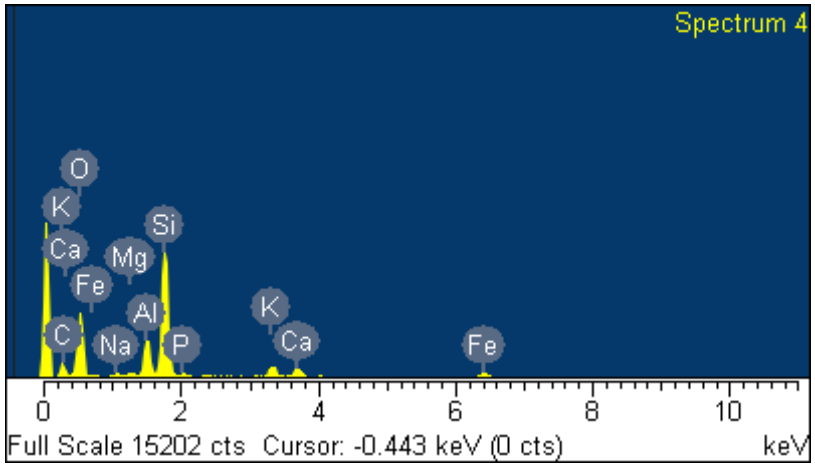

Comment:NoB 15 2617-1

INCA

Ashes to ashes

16-Jan-17 2:40:14 PM

Spectrum processing :
No peaks omitted

Processing option : All elements analyzed (Normalised)
Number of iterations = 4

Standard :
C CaCO3 1-Jun-1999 12:00 AM
O SiO2 1-Jun-1999 12:00 AM
Na Albite 1-Jun-1999 12:00 AM
Mg MgO 1-Jun-1999 12:00 AM
Al Al2O3 1-Jun-1999 12:00 AM
Si SiO2 1-Jun-1999 12:00 AM
P GaP 1-Jun-1999 12:00 AM
K MAD-10 Feldspar 1-Jun-1999 12:00 AM
Ca Wollastonite 1-Jun-1999 12:00 AM
Ti Ti 1-Jun-1999 12:00 AM
Fe Fe 1-Jun-1999 12:00 AM

Element	Weight%	Atomic%
C K	9.08	14.72
O K	46.49	56.61
Na K	1.09	0.92
Mg K	1.20	0.96
Al K	8.44	6.09
Si K	23.60	16.37
P K	0.48	0.30
K K	3.44	1.72
Ca K	0.67	0.33
Ti K	0.98	0.40
Fe K	4.53	1.58
Totals	100.00	

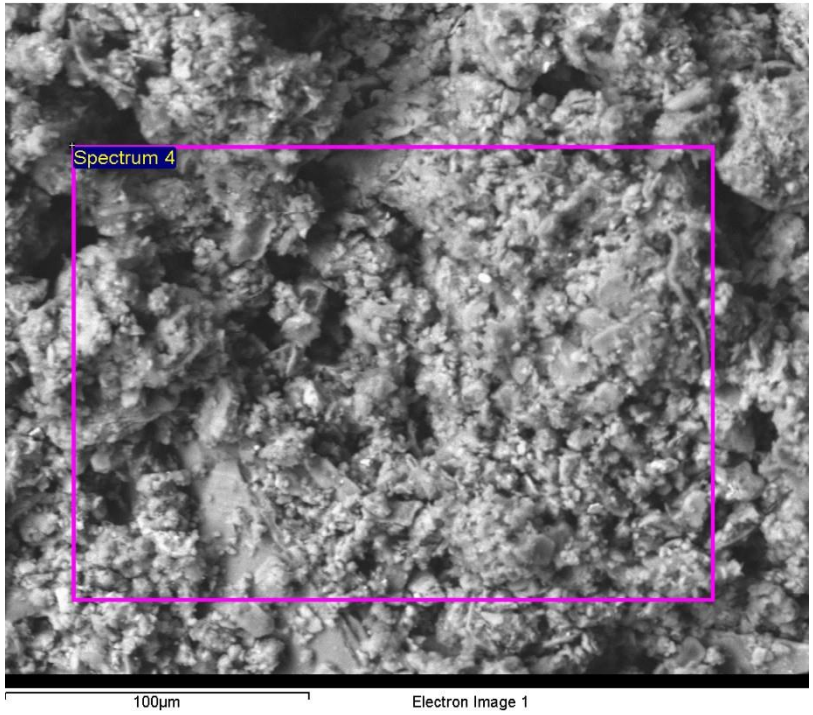

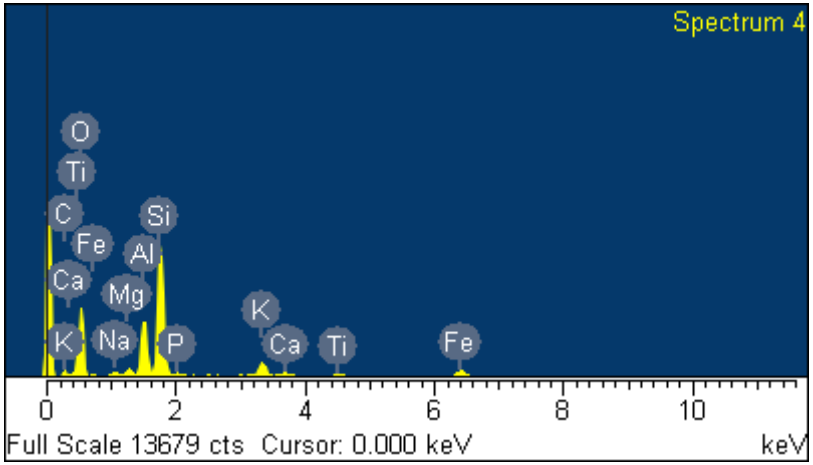

Comment:NoB 15 3851

INCA

Ashes to ashes

16-Jan-17 3:49:17 PM

Spectrum processing :
No peaks omitted

Processing option : All elements analyzed (Normalised)
Number of iterations = 4

Standard :
C CaCO3 1-Jun-1999 12:00 AM
O SiO2 1-Jun-1999 12:00 AM
Na Albite 1-Jun-1999 12:00 AM
Mg MgO 1-Jun-1999 12:00 AM
Al Al2O3 1-Jun-1999 12:00 AM
Si SiO2 1-Jun-1999 12:00 AM
P GaP 1-Jun-1999 12:00 AM
K MAD-10 Feldspar 1-Jun-1999 12:00 AM
Ti Ti 1-Jun-1999 12:00 AM
Fe Fe 1-Jun-1999 12:00 AM

Element	Weight%	Atomic%
C K	11.12	18.01
O K	43.45	52.85
Na K	1.32	1.11
Mg K	0.88	0.70
Al K	7.62	5.49
Si K	25.42	17.61
P K	0.51	0.32
K K	3.25	1.62
Ti K	0.60	0.24
Fe K	5.85	2.04
Totals	100.00	

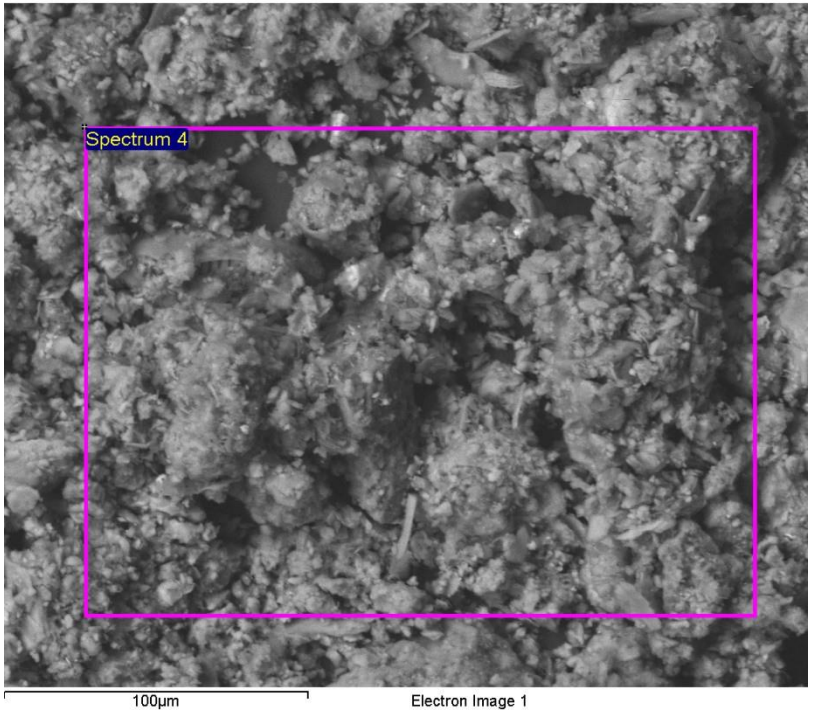

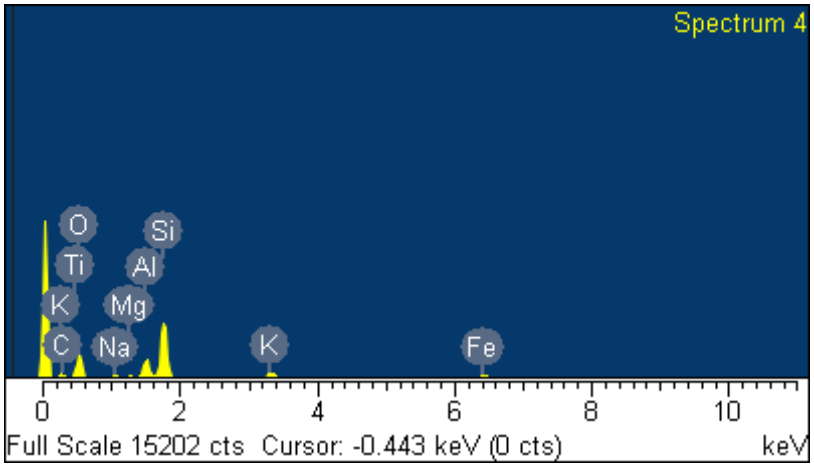

Comment:NoB 15 3857

INCA

Ashes to ashes

16-Jan-17 2:19:10 PM

Spectrum processing :
No peaks omitted

Processing option : All elements analyzed (Normalised)
Number of iterations = 3

Standard :
O SiO2 1-Jun-1999 12:00 AM
Na Albite 1-Jun-1999 12:00 AM
Mg MgO 1-Jun-1999 12:00 AM
Al Al2O3 1-Jun-1999 12:00 AM
Si SiO2 1-Jun-1999 12:00 AM
P GaP 1-Jun-1999 12:00 AM
K MAD-10 Feldspar 1-Jun-1999 12:00 AM
Ca Wollastonite 1-Jun-1999 12:00 AM
Ti Ti 1-Jun-1999 12:00 AM
Mn Mn 1-Jun-1999 12:00 AM
Fe Fe 1-Jun-1999 12:00 AM
Mo Mo 1-Jun-1999 12:00 AM

Element	Weight%	Atomic%
O K	49.80	65.42
Na K	1.03	0.94
Mg K	0.80	0.69
Al K	5.64	4.39
Si K	30.60	22.90
P K	1.14	0.78
K K	3.09	1.66
Ca K	2.02	1.06
Ti K	0.46	0.20
Mn K	0.42	0.16
Fe K	4.42	1.66
Mo L	0.58	0.13
Totals	100.00	

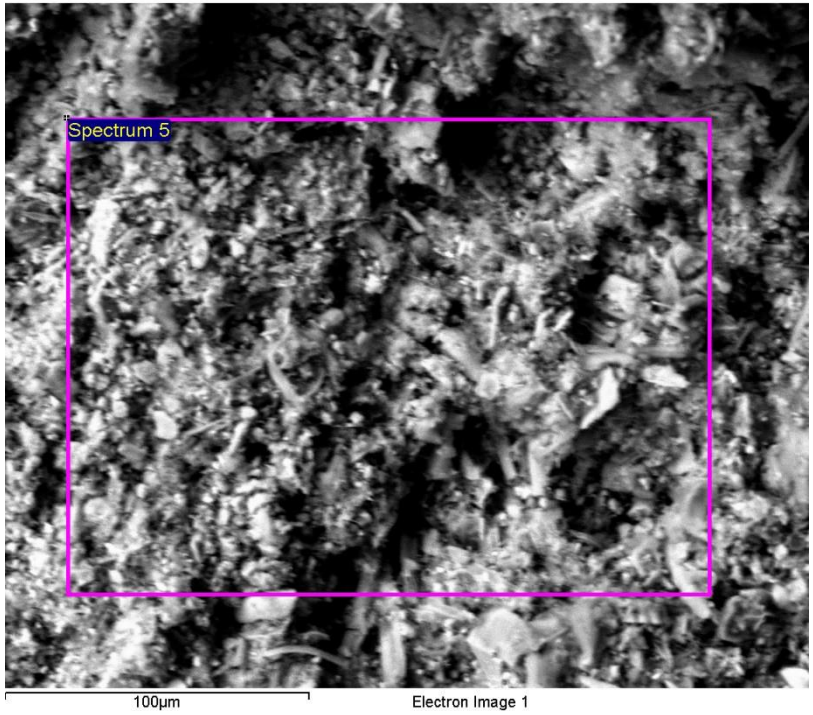

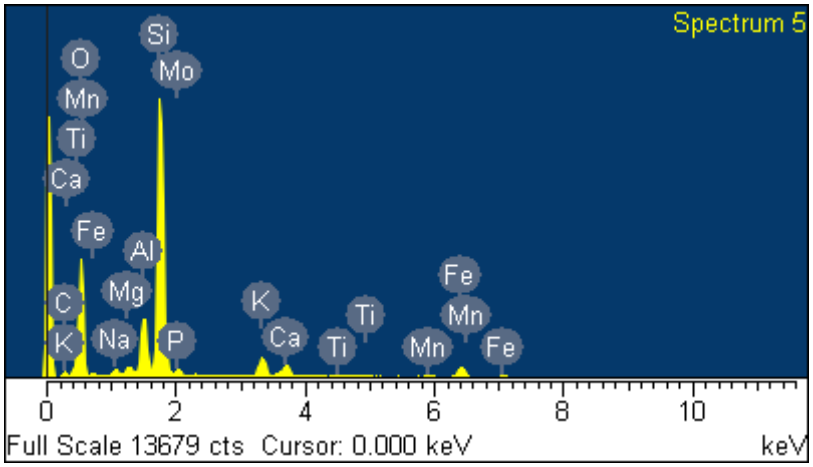

Comment:NoB 15 4264

INCA

Ashes to ashes

16-Jan-17 3:56:30 PM

Spectrum processing :
No peaks omitted

Processing option : All elements analyzed (Normalised)
Number of iterations = 3

Standard :
O SiO2 1-Jun-1999 12:00 AM
Na Albite 1-Jun-1999 12:00 AM
Mg MgO 1-Jun-1999 12:00 AM
Al Al2O3 1-Jun-1999 12:00 AM
Si SiO2 1-Jun-1999 12:00 AM
P GaP 1-Jun-1999 12:00 AM
K MAD-10 Feldspar 1-Jun-1999 12:00 AM
Ca Wollastonite 1-Jun-1999 12:00 AM
Ti Ti 1-Jun-1999 12:00 AM
Fe Fe 1-Jun-1999 12:00 AM

Element	Weight%	Atomic%
O K	46.44	62.24
Na K	1.32	1.23
Mg K	1.23	1.08
Al K	9.40	7.47
Si K	28.15	21.49
P K	1.19	0.83
K K	4.63	2.54
Ca K	1.00	0.53
Ti K	0.64	0.29
Fe K	6.00	2.30
Totals	100.00	

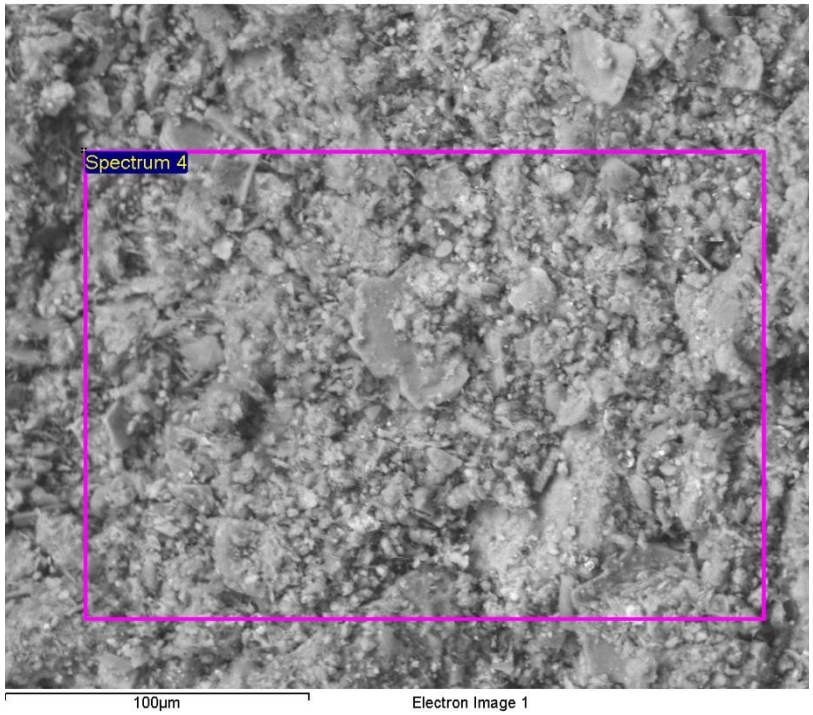

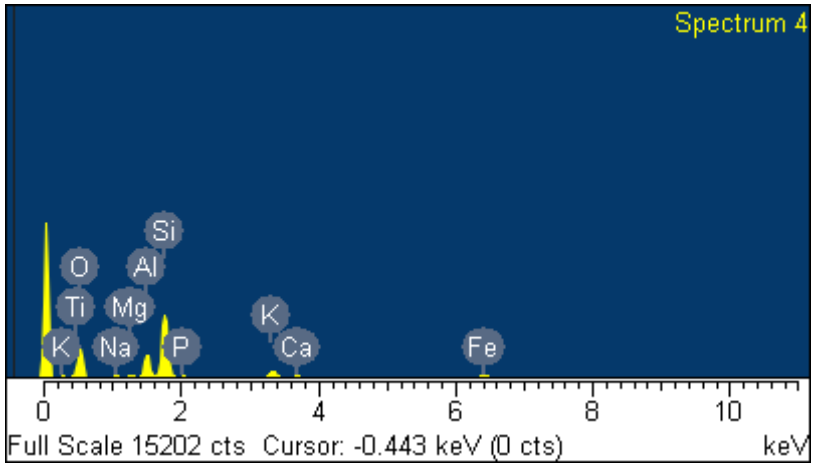

Comment:NoB 15 4656

INCA

Ashes to ashes

16-Jan-17 3:41:47 PM

Spectrum processing :
No peaks omitted

Processing option : All elements analyzed (Normalised)
Number of iterations = 5

Standard :
C CaCO3 1-Jun-1999 12:00 AM
O SiO2 1-Jun-1999 12:00 AM
Na Albite 1-Jun-1999 12:00 AM
Mg MgO 1-Jun-1999 12:00 AM
Al Al2O3 1-Jun-1999 12:00 AM
Si SiO2 1-Jun-1999 12:00 AM
P GaP 1-Jun-1999 12:00 AM
K MAD-10 Feldspar 1-Jun-1999 12:00 AM
Ca Wollastonite 1-Jun-1999 12:00 AM
Ti Ti 1-Jun-1999 12:00 AM
Mn Mn 1-Jun-1999 12:00 AM
Fe Fe 1-Jun-1999 12:00 AM

Element	Weight%	Atomic%
C K	18.98	28.97
O K	40.80	46.73
Na K	0.68	0.54
Mg K	0.98	0.74
Al K	6.86	4.66
Si K	22.40	14.62
P K	0.76	0.45
K K	2.47	1.16
Ca K	0.84	0.39
Ti K	0.61	0.23
Mn K	0.33	0.11
Fe K	4.30	1.41
Totals	100.00	

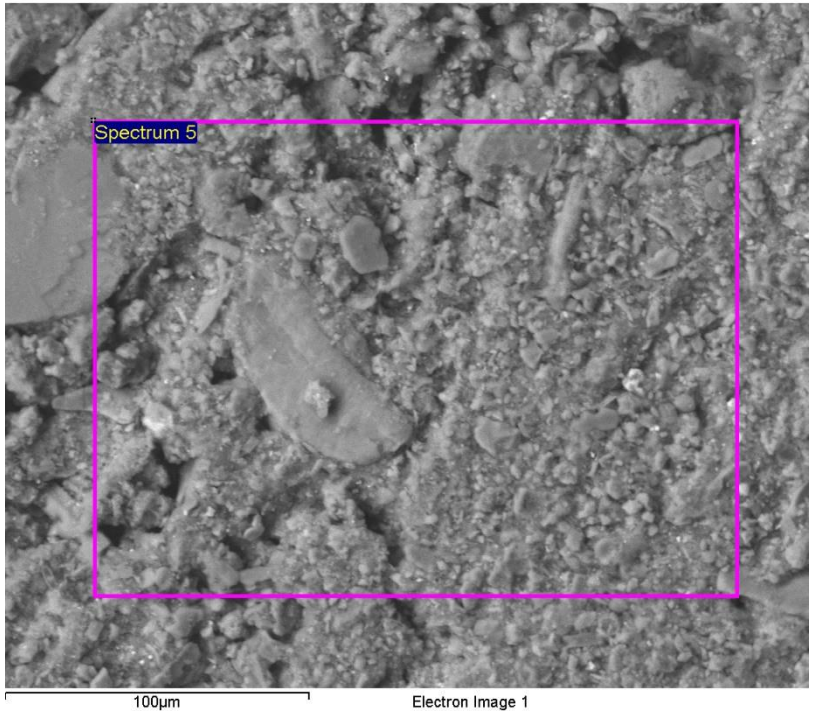

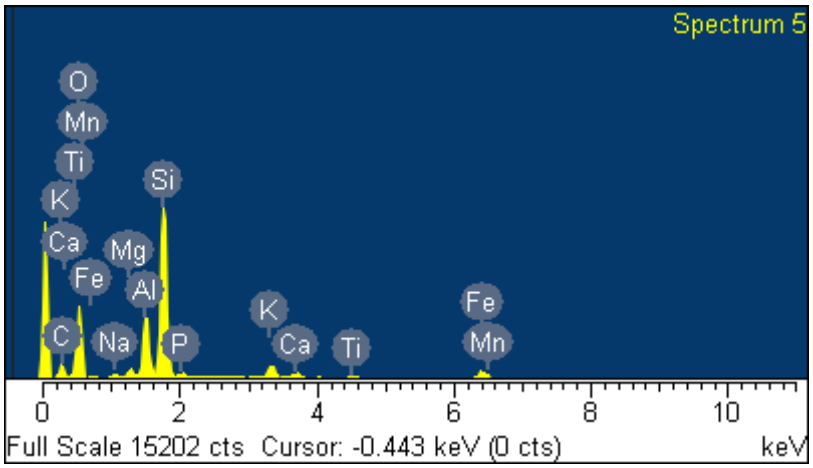

Comment:NoB 15 4674

INCA

Ashes to ashes

16-Jan-17 3:07:19 PM

Spectrum processing :
No peaks omitted

Processing option : All elements analyzed (Normalised)
Number of iterations = 4

Standard :
C CaCO3 1-Jun-1999 12:00 AM
O SiO2 1-Jun-1999 12:00 AM
Na Albite 1-Jun-1999 12:00 AM
Mg MgO 1-Jun-1999 12:00 AM
Al Al2O3 1-Jun-1999 12:00 AM
Si SiO2 1-Jun-1999 12:00 AM
P GaP 1-Jun-1999 12:00 AM
K MAD-10 Feldspar 1-Jun-1999 12:00 AM
Ca Wollastonite 1-Jun-1999 12:00 AM
Ti Ti 1-Jun-1999 12:00 AM
Mn Mn 1-Jun-1999 12:00 AM
Fe Fe 1-Jun-1999 12:00 AM

Element	Weight%	Atomic%
C K	16.13	25.54
O K	40.51	48.16
Na K	0.75	0.62
Mg K	0.74	0.58
Al K	7.12	5.02
Si K	21.40	14.49
P K	1.25	0.77
K K	3.40	1.65
Ca K	1.29	0.61
Ti K	0.59	0.23
Mn K	0.33	0.12
Fe K	6.50	2.21
Totals	100.00	

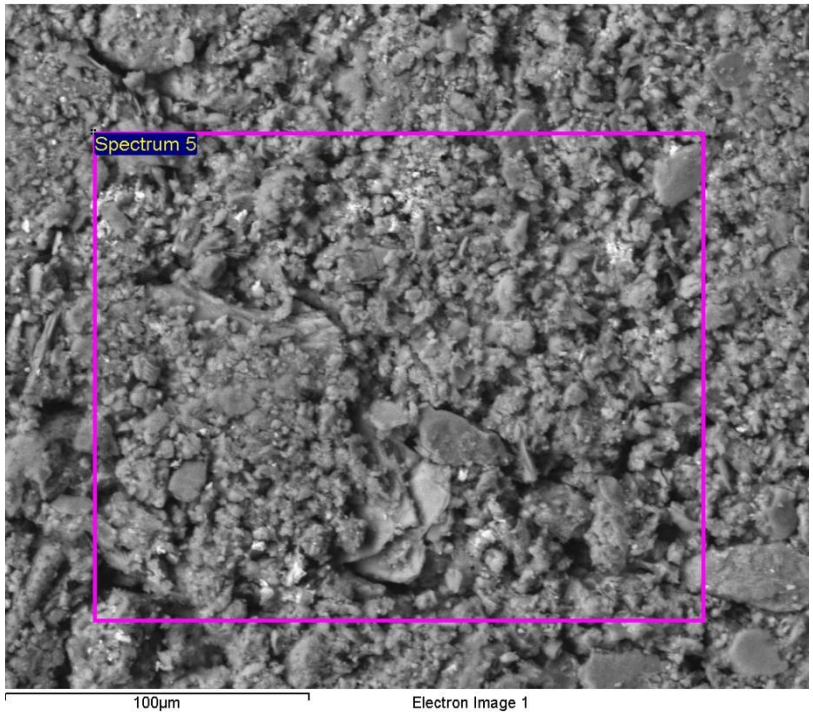

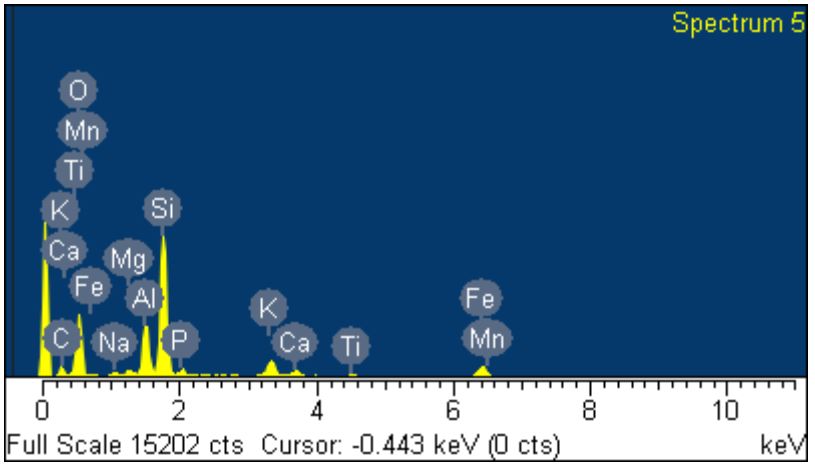

Comment:NoB 15 5332

INCA

Ashes to ashes

16-Jan-17 3:16:07 PM

Spectrum processing :
Peak possibly omitted : 5.460 keV

Processing option : All elements analyzed (Normalised)
Number of iterations = 4

Standard :
C CaCO3 1-Jun-1999 12:00 AM
O SiO2 1-Jun-1999 12:00 AM
Na Albite 1-Jun-1999 12:00 AM
Mg MgO 1-Jun-1999 12:00 AM
Al Al2O3 1-Jun-1999 12:00 AM
Si SiO2 1-Jun-1999 12:00 AM
P GaP 1-Jun-1999 12:00 AM
K MAD-10 Feldspar 1-Jun-1999 12:00 AM
Ca Wollastonite 1-Jun-1999 12:00 AM
Ti Ti 1-Jun-1999 12:00 AM
Fe Fe 1-Jun-1999 12:00 AM

Element	Weight%	Atomic%
C K	10.39	16.58
O K	46.68	55.91
Na K	1.13	0.94
Mg K	0.48	0.38
Al K	6.90	4.90
Si K	25.70	17.53
P K	0.66	0.41
K K	3.01	1.48
Ca K	0.73	0.35
Ti K	0.56	0.22
Fe K	3.76	1.29
Totals	100.00	

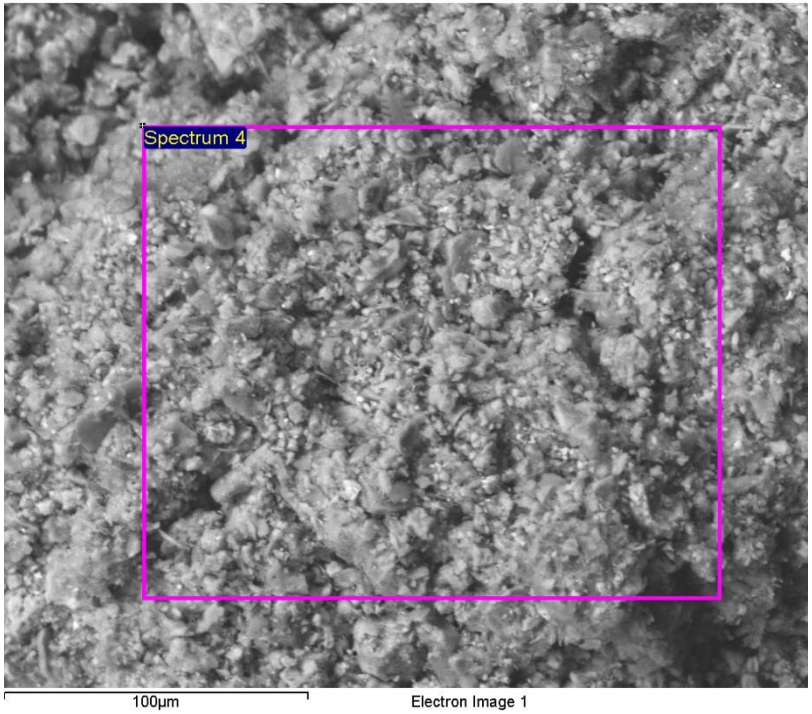

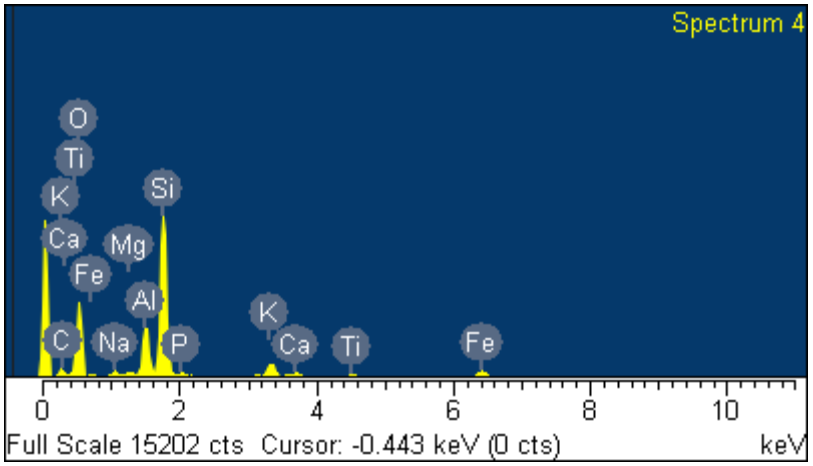

Comment:NoB 15 6156

Ashes to ashes

16-Jan-17 3:24:36 PM

Spectrum processing :
No peaks omitted

Processing option : All elements analyzed (Normalised)
Number of iterations = 3

Standard :
O SiO2 1-Jun-1999 12:00 AM
Na Albite 1-Jun-1999 12:00 AM
Mg MgO 1-Jun-1999 12:00 AM
Al Al2O3 1-Jun-1999 12:00 AM
Si SiO2 1-Jun-1999 12:00 AM
P GaP 1-Jun-1999 12:00 AM
K MAD-10 Feldspar 1-Jun-1999 12:00 AM
Ca Wollastonite 1-Jun-1999 12:00 AM
Ti Ti 1-Jun-1999 12:00 AM
Fe Fe 1-Jun-1999 12:00 AM

Element	Weight%	Atomic%
O K	50.51	65.58
Na K	1.02	0.92
Mg K	0.91	0.78
Al K	8.44	6.50
Si K	29.04	21.48
P K	1.25	0.84
K K	2.74	1.46
Ca K	0.92	0.48
Ti K	0.64	0.28
Fe K	4.52	1.68
Totals	100.00	

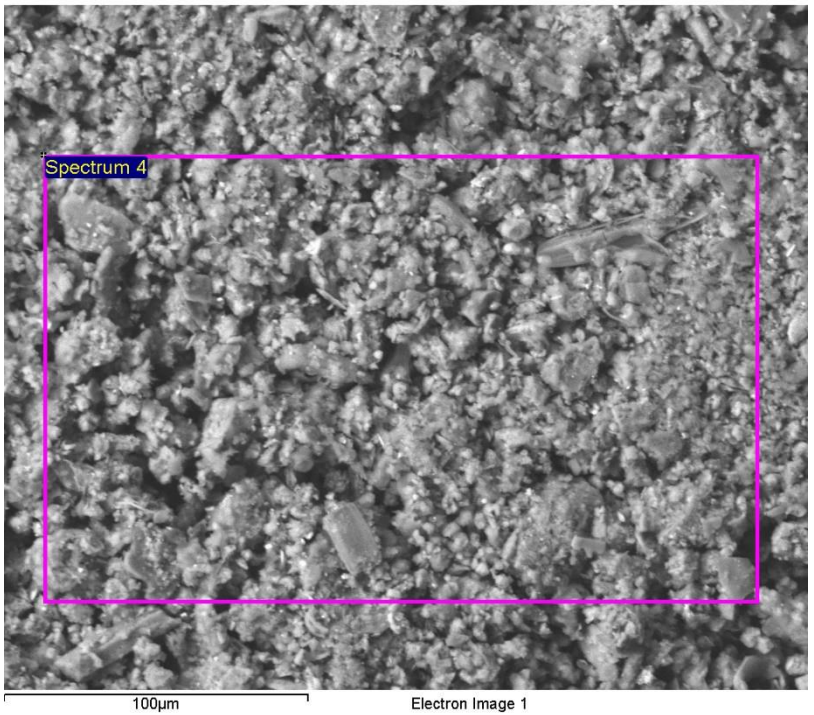

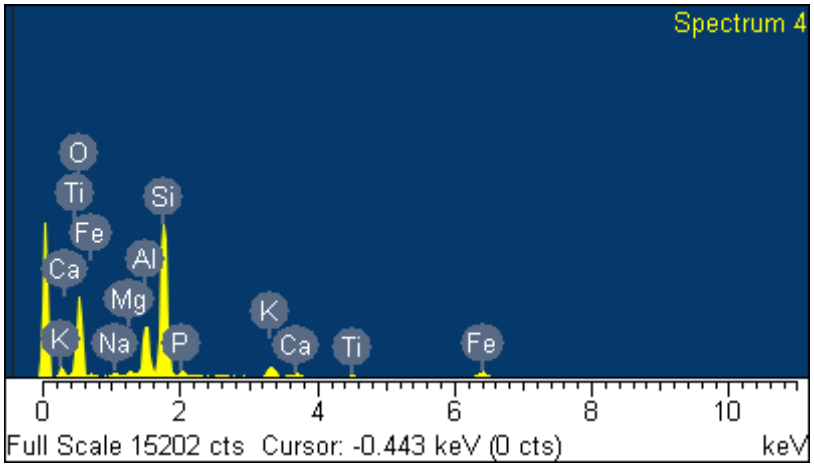

Comment:NoB 15 5013

INCA

Ashes to ashes

16-Jan-17 3:33:17 PM

Spectrum processing :
Peak possibly omitted : 5.880 keV

Processing option : All elements analyzed (Normalised)
Number of iterations = 3

Standard :
O SiO2 1-Jun-1999 12:00 AM
Na Albite 1-Jun-1999 12:00 AM
Mg MgO 1-Jun-1999 12:00 AM
Al Al2O3 1-Jun-1999 12:00 AM
Si SiO2 1-Jun-1999 12:00 AM
P GaP 1-Jun-1999 12:00 AM
K MAD-10 Feldspar 1-Jun-1999 12:00 AM
Ca Wollastonite 1-Jun-1999 12:00 AM
Ti Ti 1-Jun-1999 12:00 AM
Fe Fe 1-Jun-1999 12:00 AM

Element	Weight%	Atomic%
O K	49.45	64.75
Na K	0.92	0.84
Mg K	0.67	0.58
Al K	9.23	7.17
Si K	29.05	21.67
P K	0.79	0.53
K K	3.72	1.99
Ca K	0.63	0.33
Ti K	0.98	0.43
Fe K	4.56	1.71
Totals	100.00	

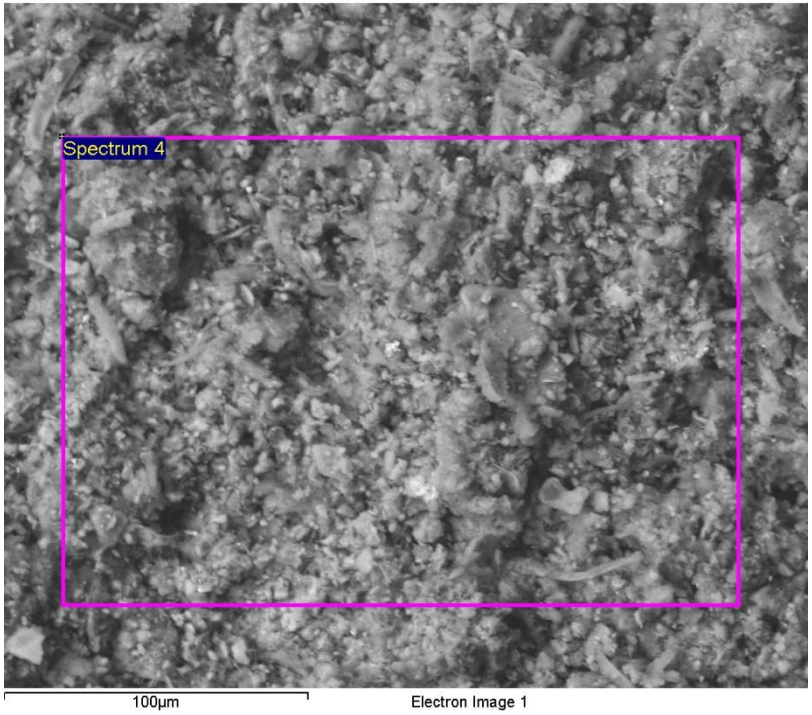

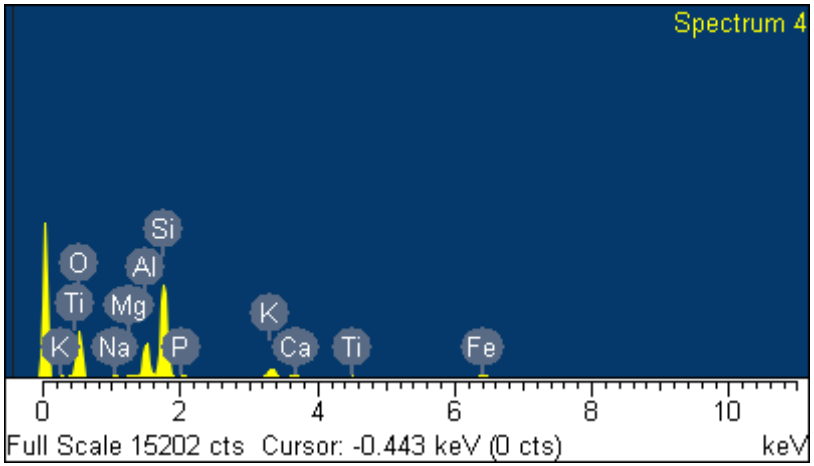

Comment:NoB 15 3783

INCA

Ashes to ashes

20-Dec-16 2:15:04 PM

Spectrum processing :
No peaks omitted

Processing option : All elements analyzed (Normalised)
Number of iterations = 4

Standard :
C CaCO3 1-Jun-1999 12:00 AM
O SiO2 1-Jun-1999 12:00 AM
Mg MgO 1-Jun-1999 12:00 AM
Al Al2O3 1-Jun-1999 12:00 AM
Si SiO2 1-Jun-1999 12:00 AM
P GaP 1-Jun-1999 12:00 AM
K MAD-10 Feldspar 1-Jun-1999 12:00 AM
Ca Wollastonite 1-Jun-1999 12:00 AM
Ti Ti 1-Jun-1999 12:00 AM
Fe Fe 1-Jun-1999 12:00 AM

Element	Weight%	Atomic%
C K	7.11	12.83
O K	40.36	54.65
Mg K	1.14	1.01
Al K	9.14	7.34
Si K	18.36	14.16
P K	0.90	0.63
K K	2.06	1.14
Ca K	0.55	0.30
Ti K	0.51	0.23
Fe K	19.87	7.71
Totals	100.00	

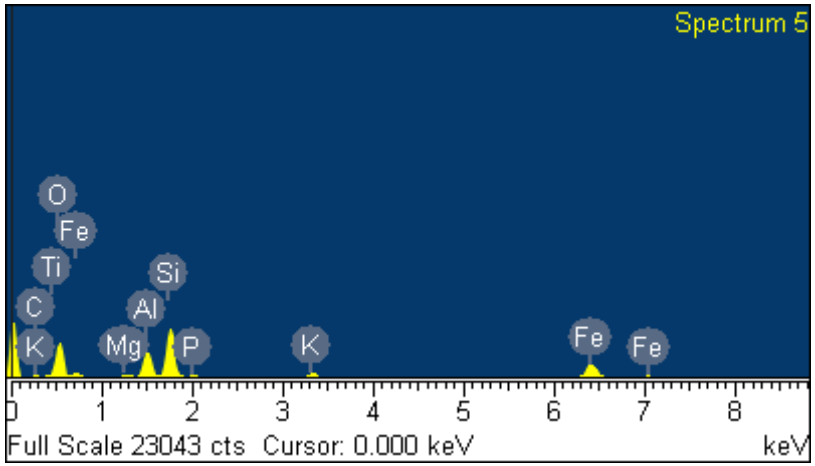

Comment:NoB16 3851

INCA

Ashes to ashes

10-Jan-17 1:45:02 PM

Spectrum processing :
No peaks omitted

Processing option : All elements analyzed (Normalised)
Number of iterations = 4

Standard :
C CaCO3 1-Jun-1999 12:00 AM
O SiO2 1-Jun-1999 12:00 AM
Na Albite 1-Jun-1999 12:00 AM
Mg MgO 1-Jun-1999 12:00 AM
Al Al2O3 1-Jun-1999 12:00 AM
Si SiO2 1-Jun-1999 12:00 AM
P GaP 1-Jun-1999 12:00 AM
K MAD-10 Feldspar 1-Jun-1999 12:00 AM
Ca Wollastonite 1-Jun-1999 12:00 AM
Ti Ti 1-Jun-1999 12:00 AM
Mn Mn 1-Jun-1999 12:00 AM
Fe Fe 1-Jun-1999 12:00 AM
Mo Mo 1-Jun-1999 12:00 AM

Element	Weight%	Atomic%
C K	4.77	8.15
O K	47.31	60.65
Na K	0.77	0.69
Mg K	1.81	1.53
Al K	5.99	4.55
Si K	23.74	17.34
P K	2.07	1.37
K K	2.26	1.18
Ca K	2.94	1.51
Ti K	0.44	0.19
Mn K	0.45	0.17
Fe K	7.08	2.60
Mo L	0.37	0.08
Totals	100.00	

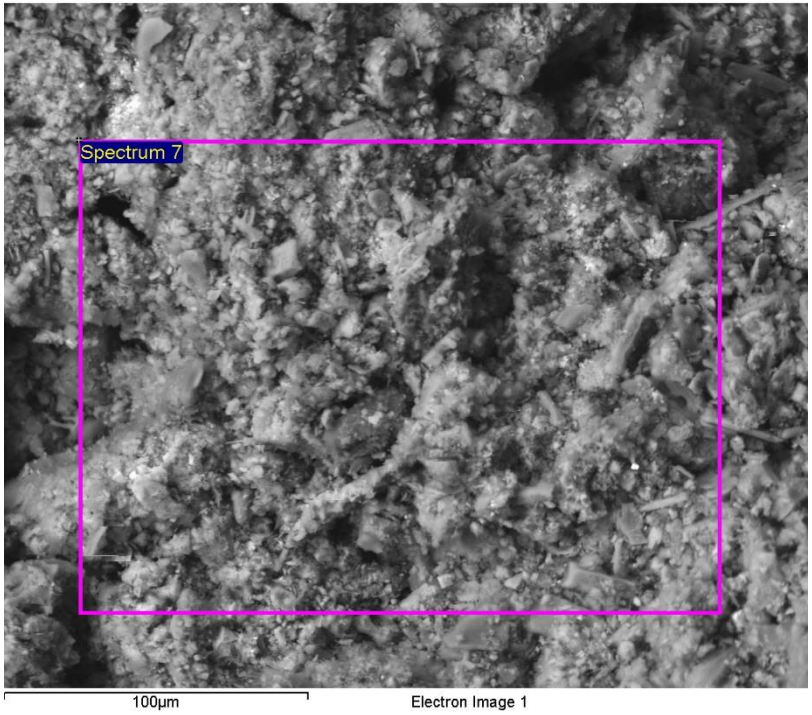

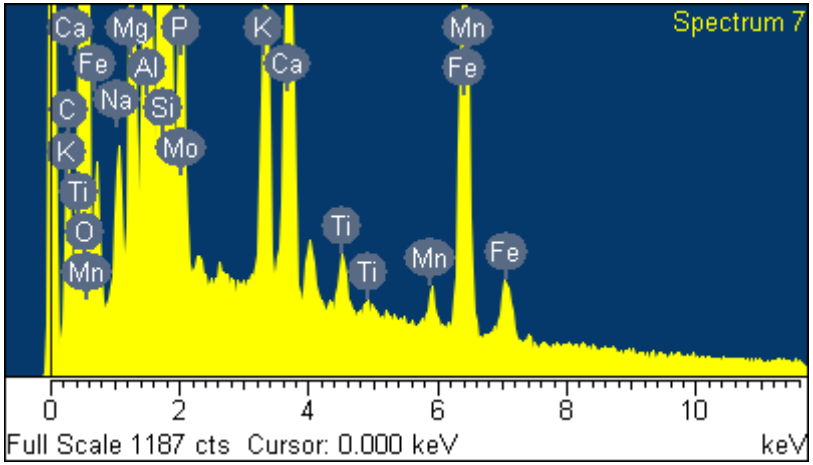

Comment:NoB 16 6339

Ashes to ashes

10-Jan-17 1:25:05 PM

Spectrum processing :
No peaks omitted

Processing option : All elements analyzed (Normalised)
Number of iterations = 4

Standard :
O SiO2 1-Jun-1999 12:00 AM
Na Albite 1-Jun-1999 12:00 AM
Mg MgO 1-Jun-1999 12:00 AM
Al Al2O3 1-Jun-1999 12:00 AM
Si SiO2 1-Jun-1999 12:00 AM
P GaP 1-Jun-1999 12:00 AM
K MAD-10 Feldspar 1-Jun-1999 12:00 AM
Ca Wollastonite 1-Jun-1999 12:00 AM
Ti Ti 1-Jun-1999 12:00 AM
Mn Mn 1-Jun-1999 12:00 AM
Fe Fe 1-Jun-1999 12:00 AM
Mo Mo 1-Jun-1999 12:00 AM

Element	Weight%	Atomic%
O K	51.39	66.71
Na K	0.92	0.83
Mg K	2.46	2.10
Al K	10.22	7.86
Si K	23.10	17.08
P K	0.91	0.61
K K	3.48	1.85
Ca K	1.13	0.59
Ti K	0.58	0.25
Mn K	0.18	0.07
Fe K	5.31	1.98
Mo L	0.32	0.07
Totals	100.00	

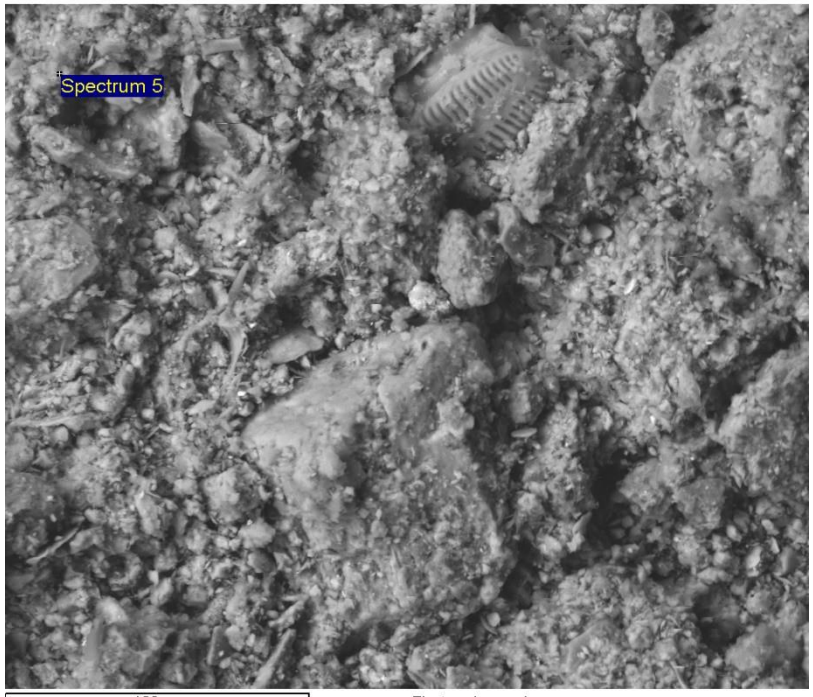

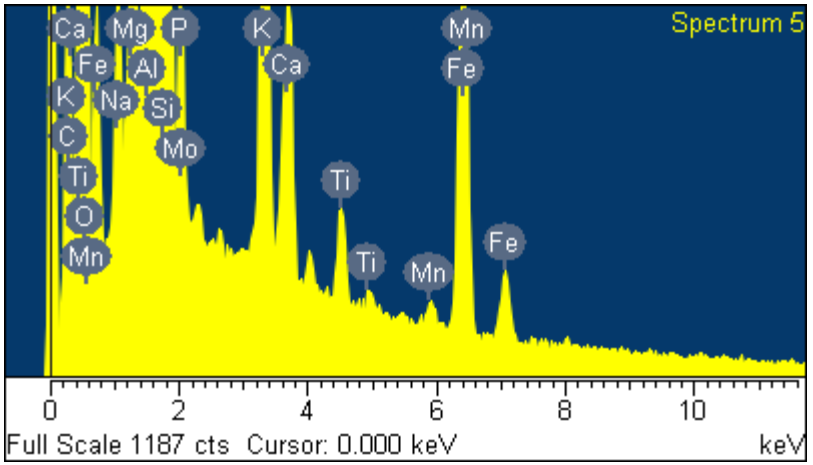

Comment:NoB 16 6346

Ashes to ashes

20-Dec-16 3:43:19 PM

Spectrum processing :
No peaks omitted

Processing option : All elements analyzed (Normalised)
Number of iterations = 5

Standard :
C CaCO3 1-Jun-1999 12:00 AM
O SiO2 1-Jun-1999 12:00 AM
Na Albite 1-Jun-1999 12:00 AM
Mg MgO 1-Jun-1999 12:00 AM
Al Al2O3 1-Jun-1999 12:00 AM
Si SiO2 1-Jun-1999 12:00 AM
P GaP 1-Jun-1999 12:00 AM
S FeS2 1-Jun-1999 12:00 AM
K MAD-10 Feldspar 1-Jun-1999 12:00 AM
Ca Wollastonite 1-Jun-1999 12:00 AM
Ti Ti 1-Jun-1999 12:00 AM
Fe Fe 1-Jun-1999 12:00 AM

Element	Weight%	Atomic%
C K	16.32	24.69
O K	46.84	53.21
Na K	0.51	0.40
Mg K	2.33	1.74
Al K	4.35	2.93
Si K	19.41	12.56
P K	2.09	1.23
S K	0.25	0.14
K K	1.51	0.70
Ca K	2.38	1.08
Ti K	0.25	0.10
Fe K	3.75	1.22
Totals	100.00	

Comment:NoB 16 6348-2

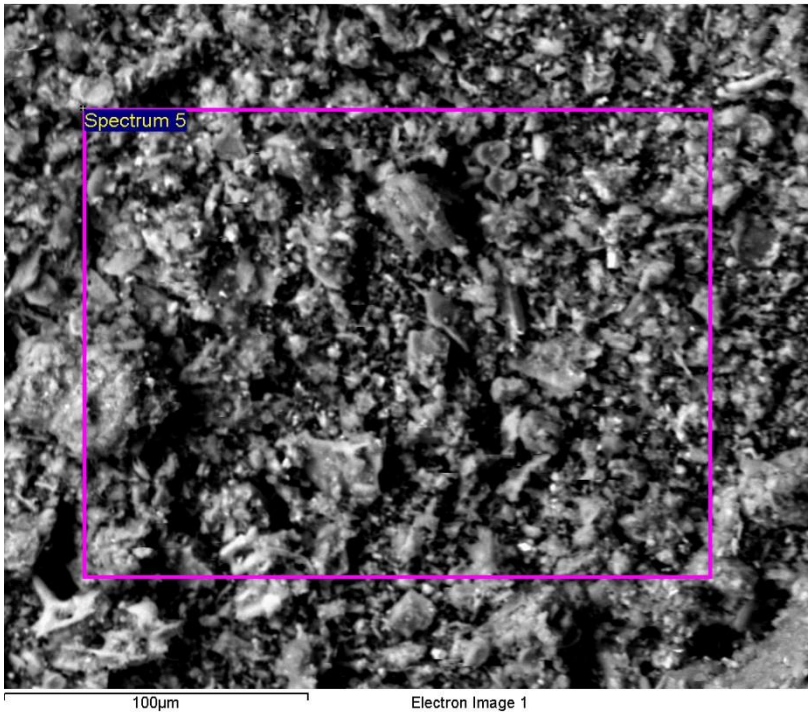

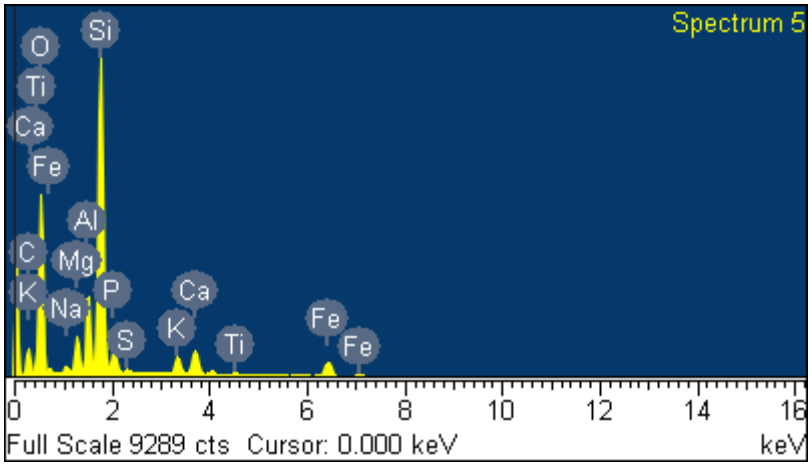

INCA

Ashes to ashes

20-Dec-16 1:51:37 PM

Spectrum processing :
No peaks omitted

Processing option : All elements analyzed (Normalised)
Number of iterations = 3

Standard :
O SiO2 1-Jun-1999 12:00 AM
Na Albite 1-Jun-1999 12:00 AM
Mg MgO 1-Jun-1999 12:00 AM
Al Al2O3 1-Jun-1999 12:00 AM
Si SiO2 1-Jun-1999 12:00 AM
P GaP 1-Jun-1999 12:00 AM
K MAD-10 Feldspar 1-Jun-1999 12:00 AM
Ca Wollastonite 1-Jun-1999 12:00 AM
Ti Ti 1-Jun-1999 12:00 AM
Fe Fe 1-Jun-1999 12:00 AM

Element	Weight%	Atomic%
O K	51.62	66.72
Na K	1.74	1.56
Mg K	0.89	0.75
Al K	7.17	5.50
Si K	27.55	20.29
P K	1.25	0.83
K K	2.73	1.44
Ca K	1.68	0.87
Ti K	0.72	0.31
Fe K	4.65	1.72
Totals	100.00	

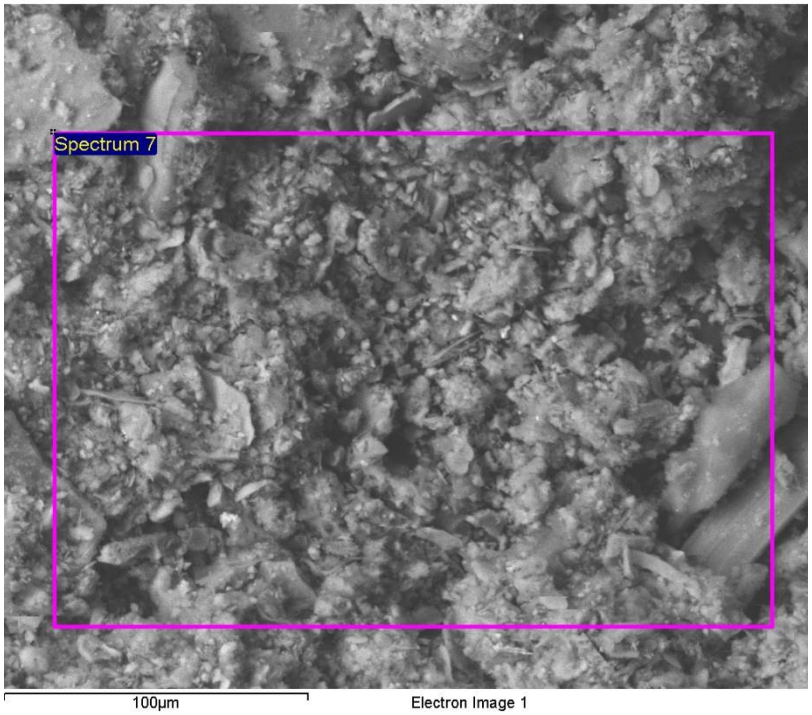

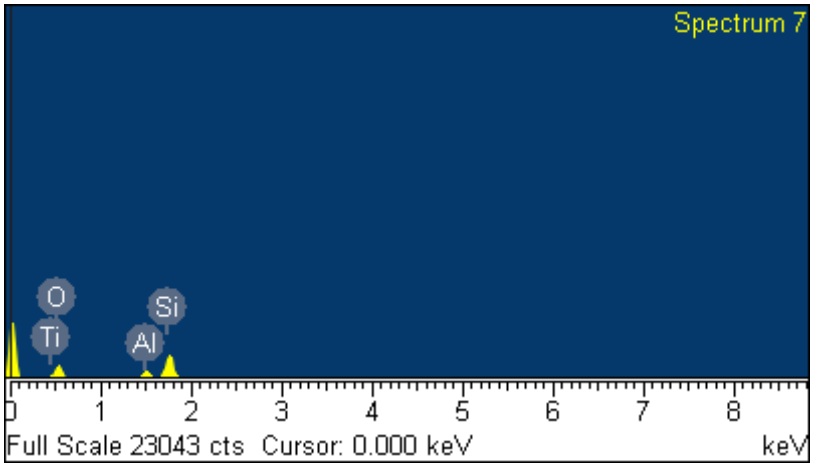

Comment:NoB16 6351

INCA

Ashes to ashes

20-Dec-16 2:49:08 PM

Spectrum processing :
No peaks omitted

Processing option : All elements analyzed (Normalised)
Number of iterations = 5

Standard :
C CaCO3 1-Jun-1999 12:00 AM
O SiO2 1-Jun-1999 12:00 AM
Na Albite 1-Jun-1999 12:00 AM
Mg MgO 1-Jun-1999 12:00 AM
Al Al2O3 1-Jun-1999 12:00 AM
Si SiO2 1-Jun-1999 12:00 AM
K MAD-10 Feldspar 1-Jun-1999 12:00 AM
Ca Wollastonite 1-Jun-1999 12:00 AM
Ti Ti 1-Jun-1999 12:00 AM
Mn Mn 1-Jun-1999 12:00 AM
Fe Fe 1-Jun-1999 12:00 AM
Mo Mo 1-Jun-1999 12:00 AM

Element	Weight%	Atomic%
C K	18.64	27.61
O K	46.58	51.80
Na K	1.52	1.17
Mg K	0.82	0.60
Al K	5.88	3.88
Si K	19.48	12.34
K K	2.64	1.20
Ca K	0.23	0.10
Ti K	0.55	0.20
Mn K	0.42	0.14
Fe K	2.63	0.84
Mo L	0.63	0.12
Totals	100.00	

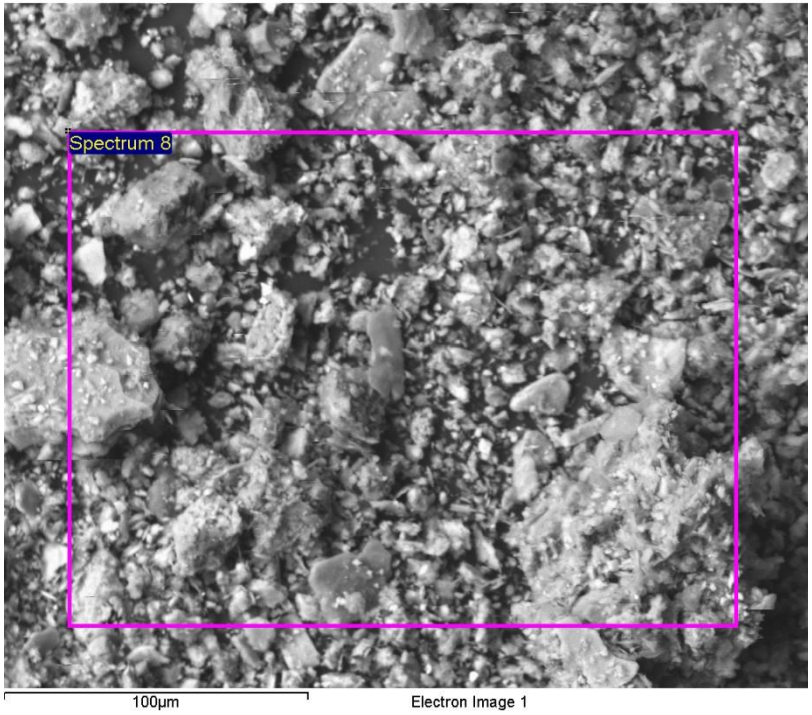

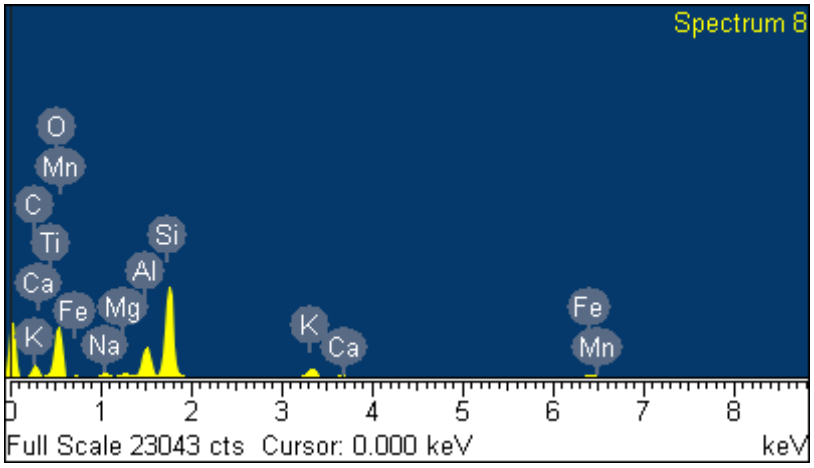

Comment:NoB16 6354

INCA

Ashes to ashes

20-Dec-16 2:38:04 PM

Spectrum processing :
No peaks omitted

Processing option : All elements analyzed (Normalised)
Number of iterations = 5

Standard :
C CaCO3 1-Jun-1999 12:00 AM
O SiO2 1-Jun-1999 12:00 AM
Na Albite 1-Jun-1999 12:00 AM
Mg MgO 1-Jun-1999 12:00 AM
Al Al2O3 1-Jun-1999 12:00 AM
Si SiO2 1-Jun-1999 12:00 AM
P GaP 1-Jun-1999 12:00 AM
K MAD-10 Feldspar 1-Jun-1999 12:00 AM
Ca Wollastonite 1-Jun-1999 12:00 AM
Ti Ti 1-Jun-1999 12:00 AM
Fe Fe 1-Jun-1999 12:00 AM

Element	Weight%	Atomic%
C K	11.94	18.36
O K	50.43	58.24
Na K	0.66	0.53
Mg K	0.99	0.75
Al K	9.07	6.21
Si K	18.98	12.49
P K	0.80	0.48
K K	3.00	1.42
Ca K	0.89	0.41
Ti K	0.77	0.30
Fe K	2.48	0.82
Totals	100.00	

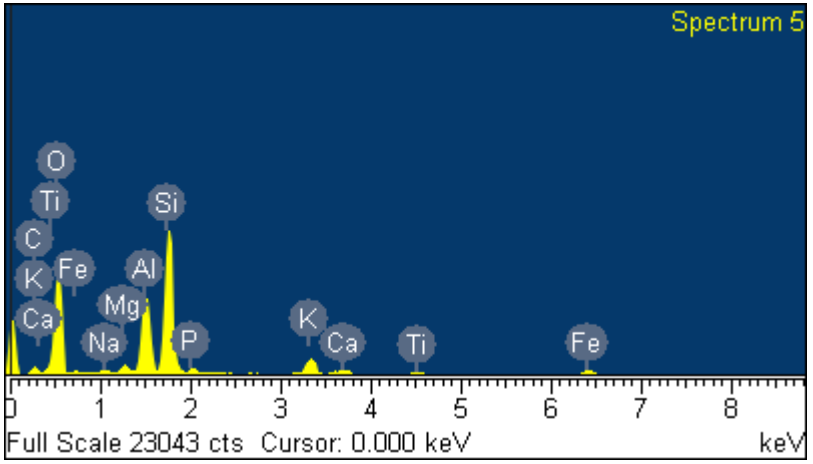

Comment:NoB16 6355

INCA

Ashes to ashes

20-Dec-16 2:59:34 PM

Spectrum processing :
No peaks omitted

Processing option : All elements analyzed (Normalised)
Number of iterations = 4

Standard :
C CaCO3 1-Jun-1999 12:00 AM
O SiO2 1-Jun-1999 12:00 AM
Na Albite 1-Jun-1999 12:00 AM
Mg MgO 1-Jun-1999 12:00 AM
Al Al2O3 1-Jun-1999 12:00 AM
Si SiO2 1-Jun-1999 12:00 AM
P GaP 1-Jun-1999 12:00 AM
Cl KCl 1-Jun-1999 12:00 AM
K MAD-10 Feldspar 1-Jun-1999 12:00 AM
Ca Wollastonite 1-Jun-1999 12:00 AM
Ti Ti 1-Jun-1999 12:00 AM
Mn Mn 1-Jun-1999 12:00 AM
Fe Fe 1-Jun-1999 12:00 AM

Element	Weight%	Atomic%
C K	6.25	10.48
O K	47.32	59.56
Na K	0.72	0.63
Mg K	2.05	1.70
Al K	5.04	3.76
Si K	24.63	17.66
P K	1.57	1.02
Cl K	0.17	0.10
K K	2.20	1.13
Ca K	2.14	1.08
Ti K	0.56	0.24
Mn K	0.43	0.16
Fe K	6.92	2.50
Totals	100.00	

Comment:NoB16 6356

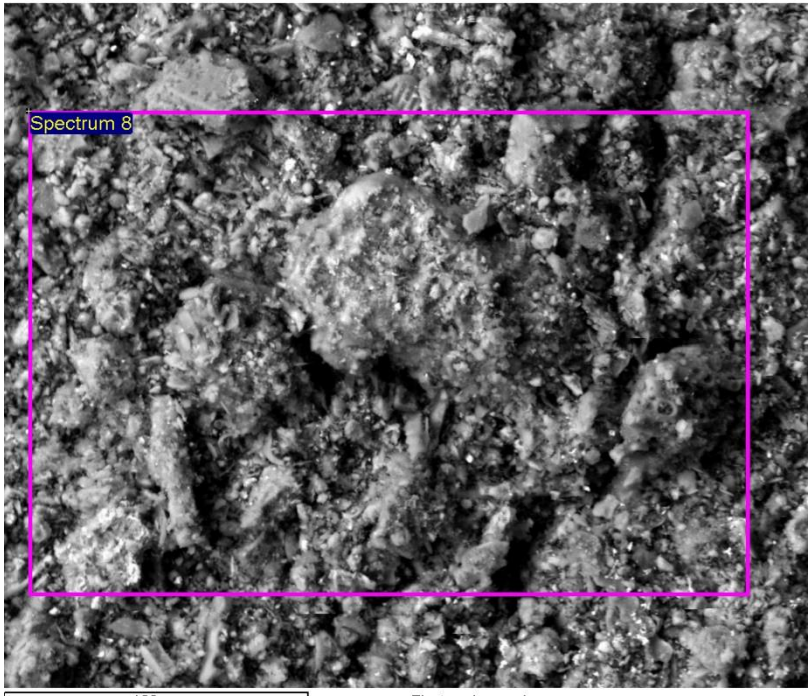

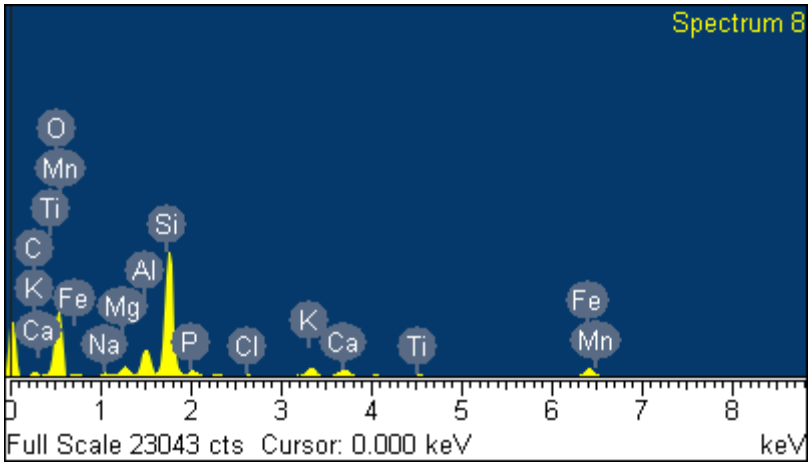

INCA

Ashes to ashes

19-Dec-16 2:07:13 PM

Spectrum processing :
No peaks omitted

Processing option : All elements analyzed (Normalised)
Number of iterations = 3

Standard :
C CaCO3 1-Jun-1999 12:00 AM
O SiO2 1-Jun-1999 12:00 AM
Na Albite 1-Jun-1999 12:00 AM
Mg MgO 1-Jun-1999 12:00 AM
Al Al2O3 1-Jun-1999 12:00 AM
Si SiO2 1-Jun-1999 12:00 AM
P GaP 1-Jun-1999 12:00 AM
K MAD-10 Feldspar 1-Jun-1999 12:00 AM
Ca Wollastonite 1-Jun-1999 12:00 AM
Ti Ti 1-Jun-1999 12:00 AM
Fe Fe 1-Jun-1999 12:00 AM

Element	Weight%	Atomic%
C K	5.05	8.32
O K	50.68	62.67
Na K	1.10	0.95
Mg K	0.54	0.44
Al K	7.54	5.53
Si K	24.37	17.16
P K	1.25	0.80
K K	3.24	1.64
Ca K	1.68	0.83
Ti K	0.87	0.36
Fe K	3.69	1.31
Totals	100.00	

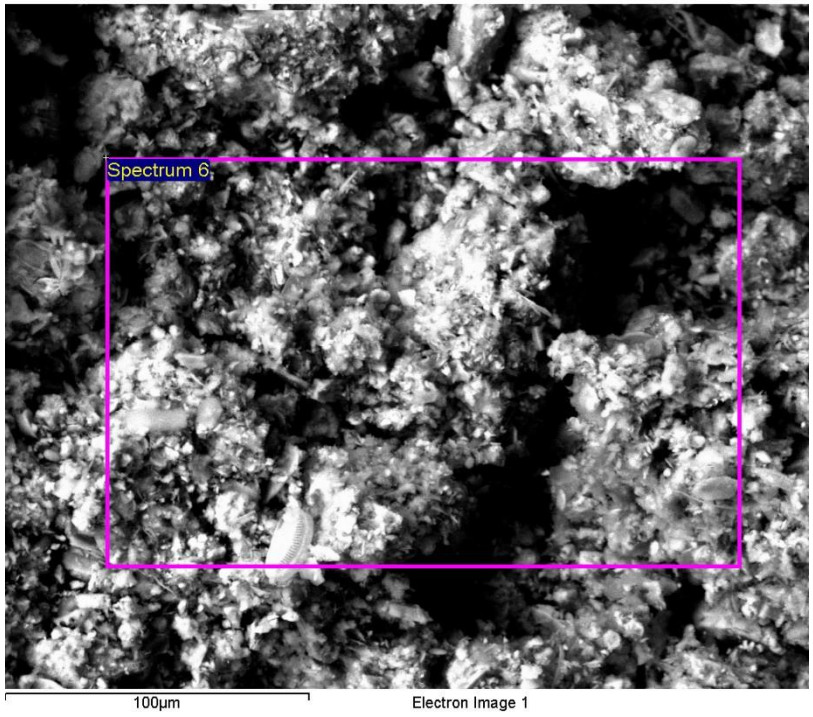

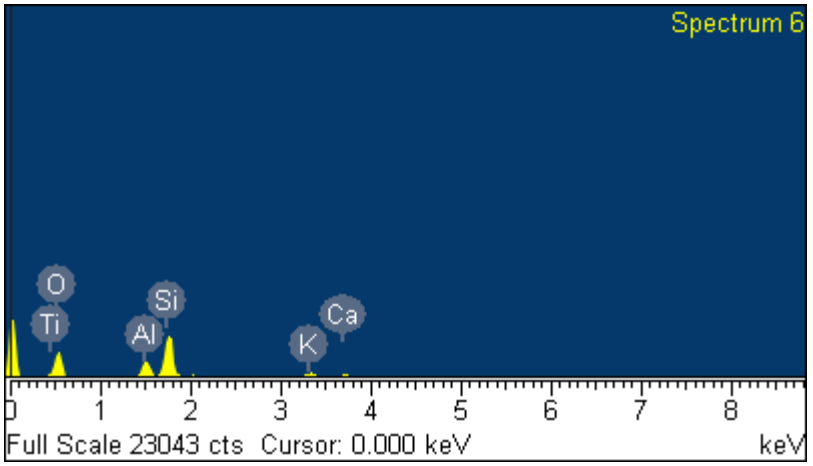

Comment:NoB T 4825

INCA

Ashes to ashes

19-Dec-16 1:50:15 PM

Spectrum processing :
No peaks omitted

Processing option : All elements analyzed (Normalised)
Number of iterations = 3

Standard :
C CaCO3 1-Jun-1999 12:00 AM
O SiO2 1-Jun-1999 12:00 AM
Na Albite 1-Jun-1999 12:00 AM
Mg MgO 1-Jun-1999 12:00 AM
Al Al2O3 1-Jun-1999 12:00 AM
Si SiO2 1-Jun-1999 12:00 AM
P GaP 1-Jun-1999 12:00 AM
K MAD-10 Feldspar 1-Jun-1999 12:00 AM
Ca Wollastonite 1-Jun-1999 12:00 AM
Ti Ti 1-Jun-1999 12:00 AM
Fe Fe 1-Jun-1999 12:00 AM

Element	Weight%	Atomic%
C K	-0.97	-1.67
O K	52.85	68.40
Na K	1.21	1.09
Mg K	0.81	0.69
Al K	8.61	6.61
Si K	26.27	19.37
P K	2.02	1.35
K K	3.13	1.66
Ca K	1.46	0.75
Ti K	0.58	0.25
Fe K	4.03	1.49
Totals	100.00	

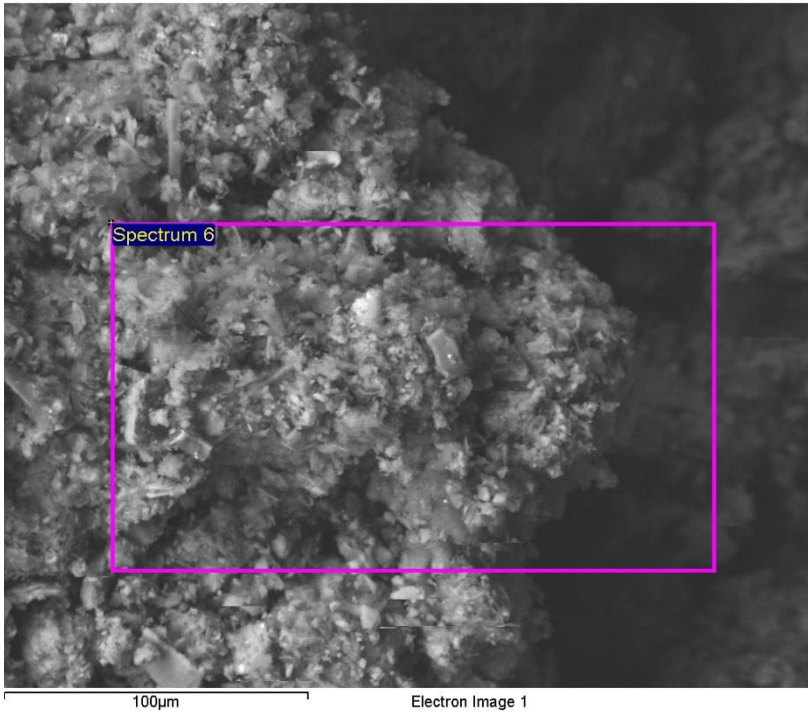

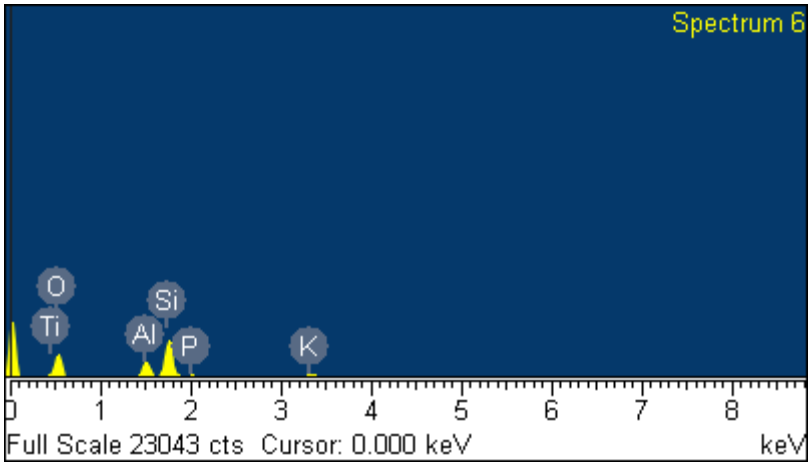

Comment:NoB T 4831

INCA

Ashes to ashes

19-Dec-16 2:28:19 PM

Spectrum processing :
No peaks omitted

Processing option : All elements analyzed (Normalised)
Number of iterations = 2

Standard :
O SiO2 1-Jun-1999 12:00 AM
Si SiO2 1-Jun-1999 12:00 AM
K MAD-10 Feldspar 1-Jun-1999 12:00 AM
Fe Fe 1-Jun-1999 12:00 AM
Br KBr 1-Jun-1999 12:00 AM

Element	Weight%	Atomic%
O K	38.21	63.94
Si K	15.36	14.64
K K	6.30	4.31
Fe K	25.34	12.15
Br L	14.78	4.95
Totals	100.00	

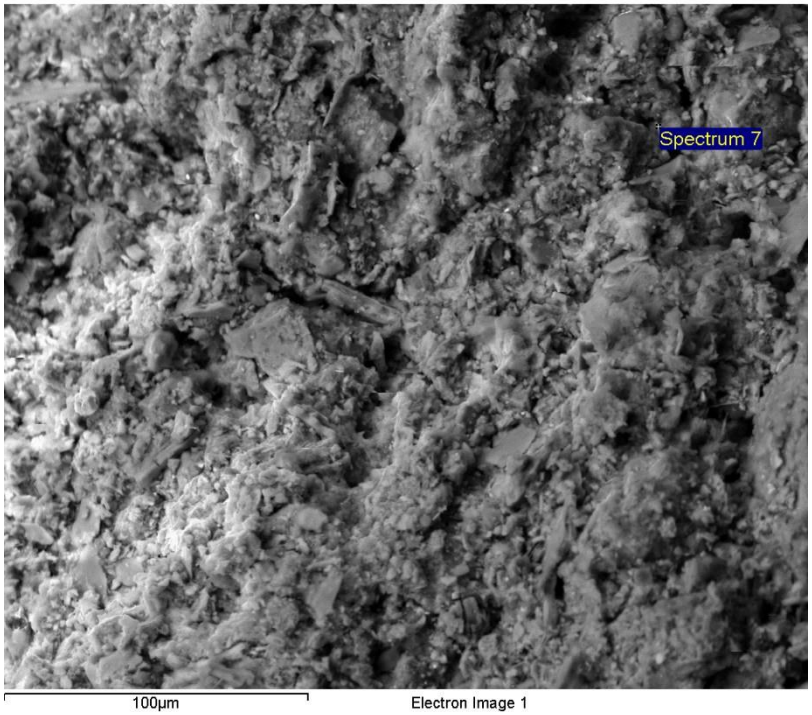

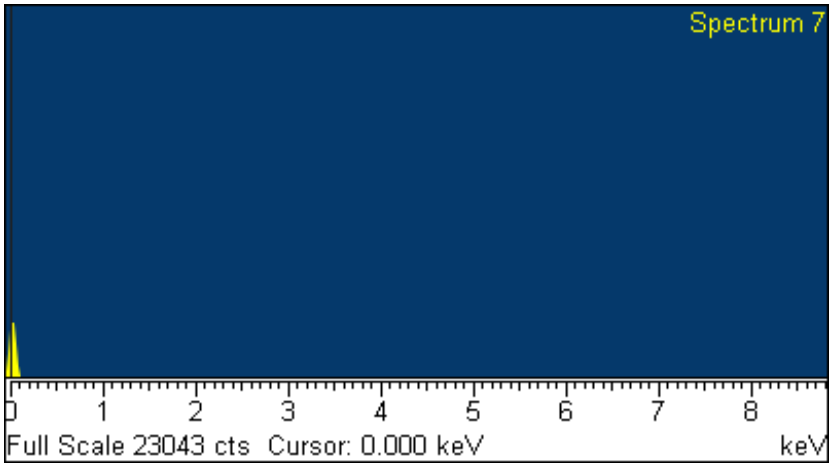

Comment:NoB T 4860-2

Ashes to ashes

19-Dec-16 2:36:47 PM

Spectrum processing :
No peaks omitted

Processing option : All elements analyzed (Normalised)
Number of iterations = 5

Standard :
C CaCO3 1-Jun-1999 12:00 AM
O SiO2 1-Jun-1999 12:00 AM
Na Albite 1-Jun-1999 12:00 AM
Mg MgO 1-Jun-1999 12:00 AM
Al Al2O3 1-Jun-1999 12:00 AM
Si SiO2 1-Jun-1999 12:00 AM
P GaP 1-Jun-1999 12:00 AM
K MAD-10 Feldspar 1-Jun-1999 12:00 AM
Ca Wollastonite 1-Jun-1999 12:00 AM
Ti Ti 1-Jun-1999 12:00 AM
Fe Fe 1-Jun-1999 12:00 AM
Mo Mo 1-Jun-1999 12:00 AM

Element	Weight%	Atomic%
C K	22.82	32.62
O K	46.60	50.00
Na K	1.05	0.78
Mg K	0.64	0.45
Al K	5.08	3.23
Si K	16.99	10.38
P K	0.53	0.29
K K	2.14	0.94
Ca K	0.84	0.36
Ti K	0.34	0.12
Fe K	2.18	0.67
Mo L	0.80	0.14
Totals	100.00	

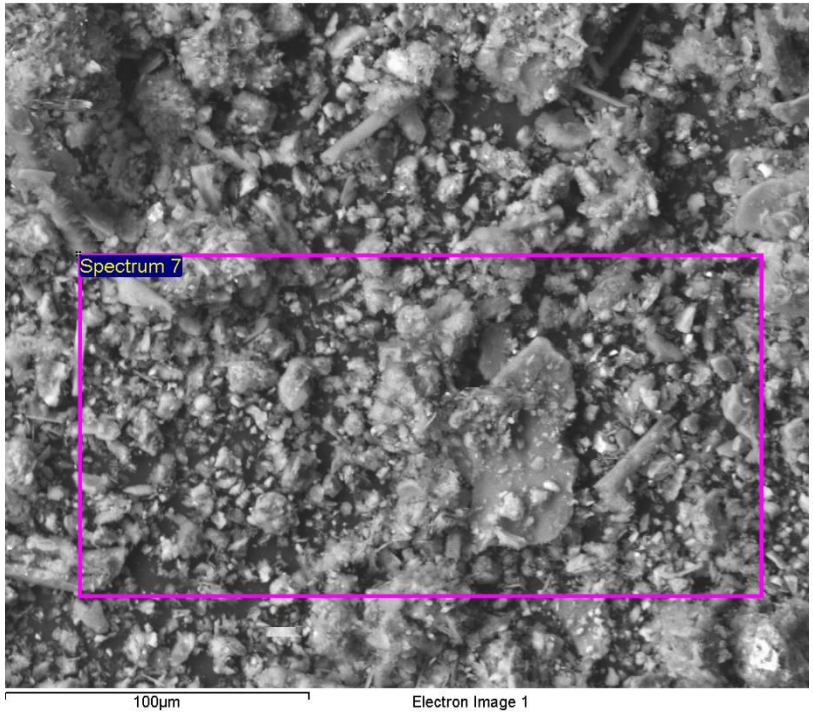

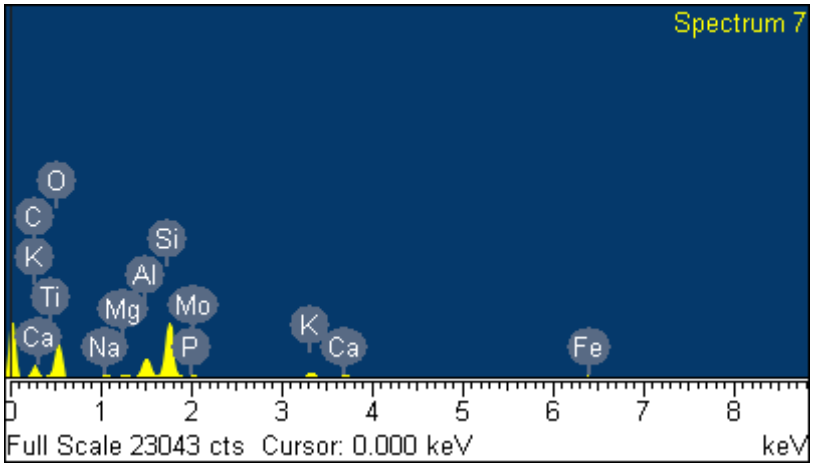

Comment:NoB T 5810

INCA

Ashes to ashes

19-Dec-16 2:45:28 PM

Spectrum processing :
No peaks omitted

Processing option : All elements analyzed (Normalised)
Number of iterations = 4

Standard :
C CaCO3 1-Jun-1999 12:00 AM
O SiO2 1-Jun-1999 12:00 AM
Na Albite 1-Jun-1999 12:00 AM
Mg MgO 1-Jun-1999 12:00 AM
Al Al2O3 1-Jun-1999 12:00 AM
Si SiO2 1-Jun-1999 12:00 AM
P GaP 1-Jun-1999 12:00 AM
K MAD-10 Feldspar 1-Jun-1999 12:00 AM
Ca Wollastonite 1-Jun-1999 12:00 AM
Ti Ti 1-Jun-1999 12:00 AM
Fe Fe 1-Jun-1999 12:00 AM

Element	Weight%	Atomic%
C K	10.57	17.31
O K	46.03	56.62
Na K	0.70	0.60
Mg K	0.67	0.54
Al K	5.49	4.01
Si K	20.25	14.19
P K	1.72	1.09
K K	1.85	0.93
Ca K	1.46	0.72
Ti K	0.56	0.23
Fe K	10.70	3.77
Totals	100.00	

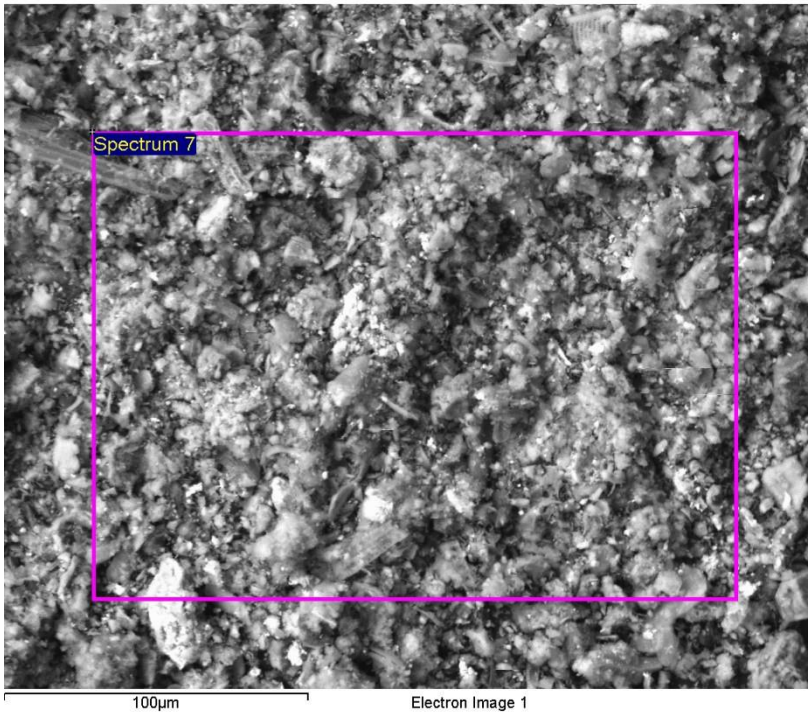

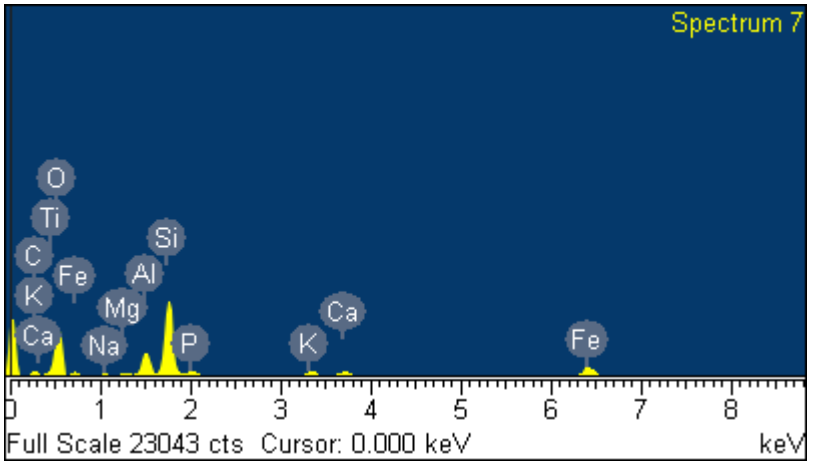

Comment:NoB T 5849

INCA

Ashes to ashes

19-Dec-16 2:16:22 PM

Spectrum processing :
No peaks omitted

Processing option : All elements analyzed (Normalised)
Number of iterations = 5

Standard :
C CaCO3 1-Jun-1999 12:00 AM
O SiO2 1-Jun-1999 12:00 AM
Na Albite 1-Jun-1999 12:00 AM
Mg MgO 1-Jun-1999 12:00 AM
Al Al2O3 1-Jun-1999 12:00 AM
Si SiO2 1-Jun-1999 12:00 AM
P GaP 1-Jun-1999 12:00 AM
K MAD-10 Feldspar 1-Jun-1999 12:00 AM
Ca Wollastonite 1-Jun-1999 12:00 AM
Ti Ti 1-Jun-1999 12:00 AM
Mn Mn 1-Jun-1999 12:00 AM
Fe Fe 1-Jun-1999 12:00 AM

Element	Weight%	Atomic%
C K	31.76	44.77
O K	37.93	40.14
Na K	0.42	0.31
Mg K	0.41	0.29
Al K	6.21	3.90
Si K	9.36	5.64
P K	1.58	0.87
K K	1.61	0.70
Ca K	0.96	0.41
Ti K	0.42	0.15
Mn K	2.74	0.84
Fe K	6.60	2.00
Totals	100.00	

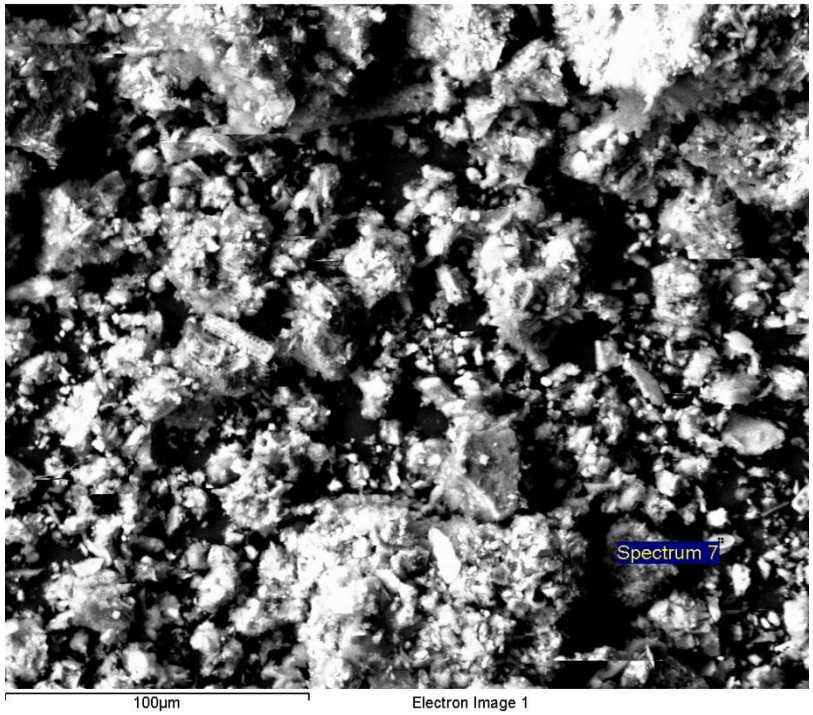

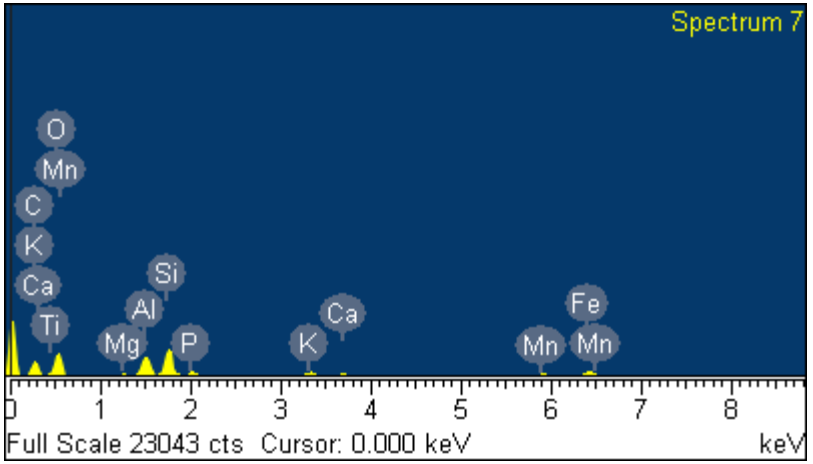

Comment:NoB T 5855

INCA

Ashes to ashes

23-Jan-17 2:55:09 PM

Spectrum processing :
No peaks omitted

Processing option : All elements analyzed (Normalised)
Number of iterations = 4

Standard :
C CaCO3 1-Jun-1999 12:00 AM
O SiO2 1-Jun-1999 12:00 AM
Mg MgO 1-Jun-1999 12:00 AM
Al Al2O3 1-Jun-1999 12:00 AM
Si SiO2 1-Jun-1999 12:00 AM
K MAD-10 Feldspar 1-Jun-1999 12:00 AM
Ca Wollastonite 1-Jun-1999 12:00 AM
Fe Fe 1-Jun-1999 12:00 AM
Zr Zr 1-Jun-1999 12:00 AM

Element	Weight%	Atomic%
C K	28.06	42.52
O K	39.49	44.92
Mg K	0.88	0.66
Al K	1.73	1.17
Si K	8.93	5.79
K K	0.58	0.27
Ca K	1.15	0.52
Fe K	2.56	0.83
Zr L	16.62	3.32
Totals	100.00	

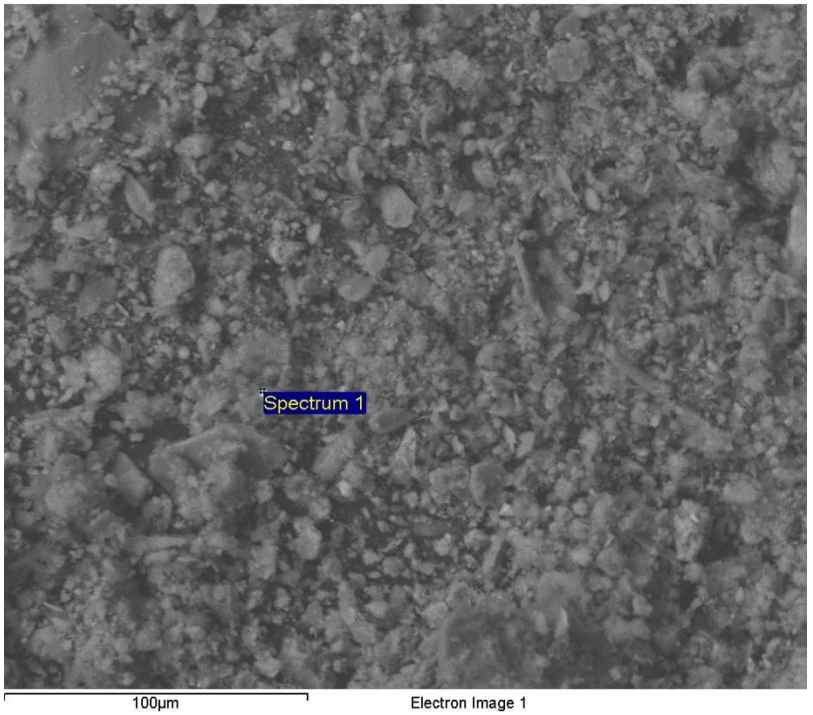

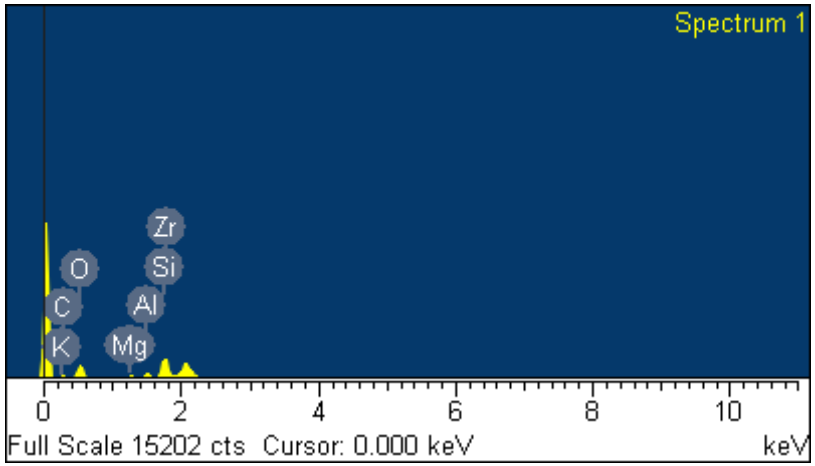

Comment:KoS 2039

INCA

Ashes to ashes

23-Jan-17 2:46:11 PM

Spectrum processing :
No peaks omitted

Processing option : All elements analyzed (Normalised)
Number of iterations = 4

Standard :
C CaCO3 1-Jun-1999 12:00 AM
O SiO2 1-Jun-1999 12:00 AM
Na Albite 1-Jun-1999 12:00 AM
Mg MgO 1-Jun-1999 12:00 AM
Al Al2O3 1-Jun-1999 12:00 AM
Si SiO2 1-Jun-1999 12:00 AM
P GaP 1-Jun-1999 12:00 AM
K MAD-10 Feldspar 1-Jun-1999 12:00 AM
Ca Wollastonite 1-Jun-1999 12:00 AM
Fe Fe 1-Jun-1999 12:00 AM

Element	Weight%	Atomic%
C K	12.43	18.92
O K	51.91	59.32
Na K	0.71	0.56
Mg K	1.23	0.92
Al K	1.98	1.34
Si K	23.95	15.59
P K	1.42	0.84
K K	1.46	0.68
Ca K	1.72	0.79
Fe K	3.20	1.05
Totals	100.00	

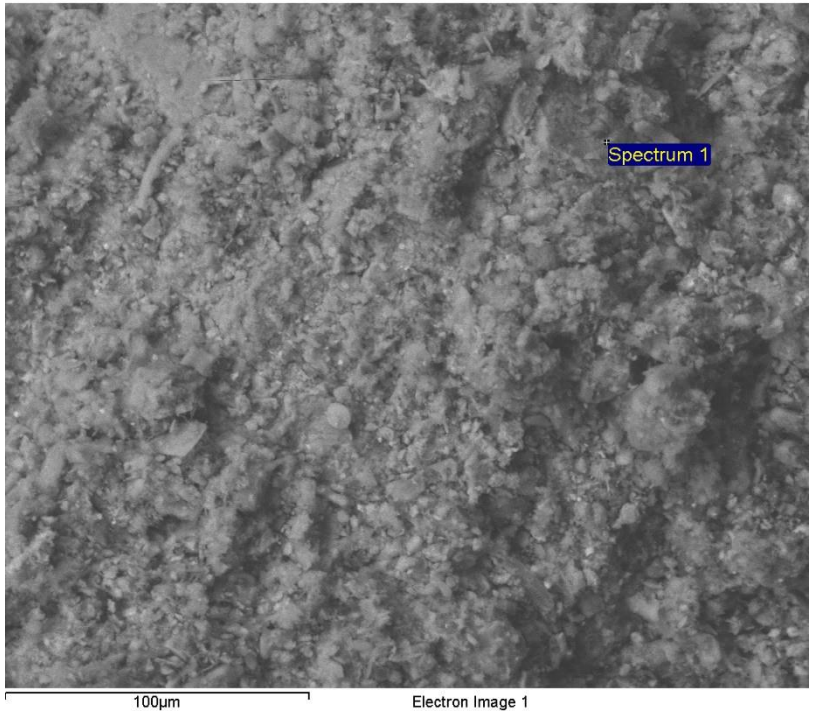

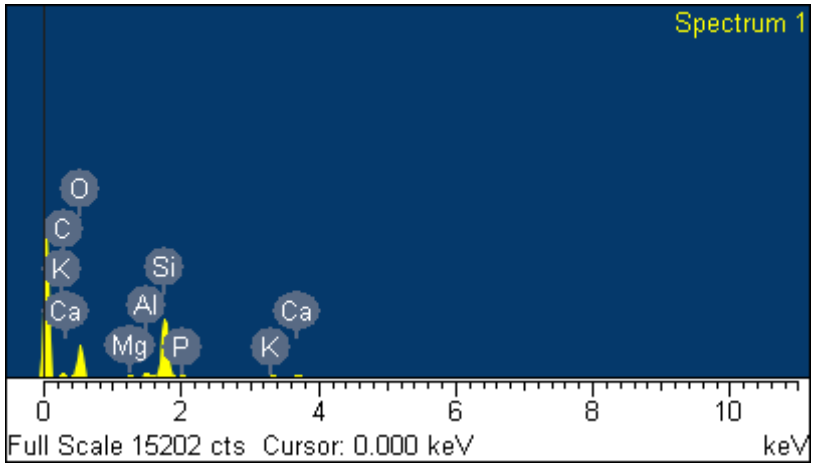

Comment:KoS 3081

INCA

Ashes to ashes

23-Jan-17 2:19:37 PM

Spectrum processing :
No peaks omitted

Processing option : All elements analyzed (Normalised)
Number of iterations = 2

Standard :
O SiO2 1-Jun-1999 12:00 AM
Si SiO2 1-Jun-1999 12:00 AM
K MAD-10 Feldspar 1-Jun-1999 12:00 AM
Br KBr 1-Jun-1999 12:00 AM

Element	Weight%	Atomic%
O K	35.35	51.92
Si K	49.13	41.11
K K	7.85	4.72
Br L	7.66	2.25
Totals	100.00	

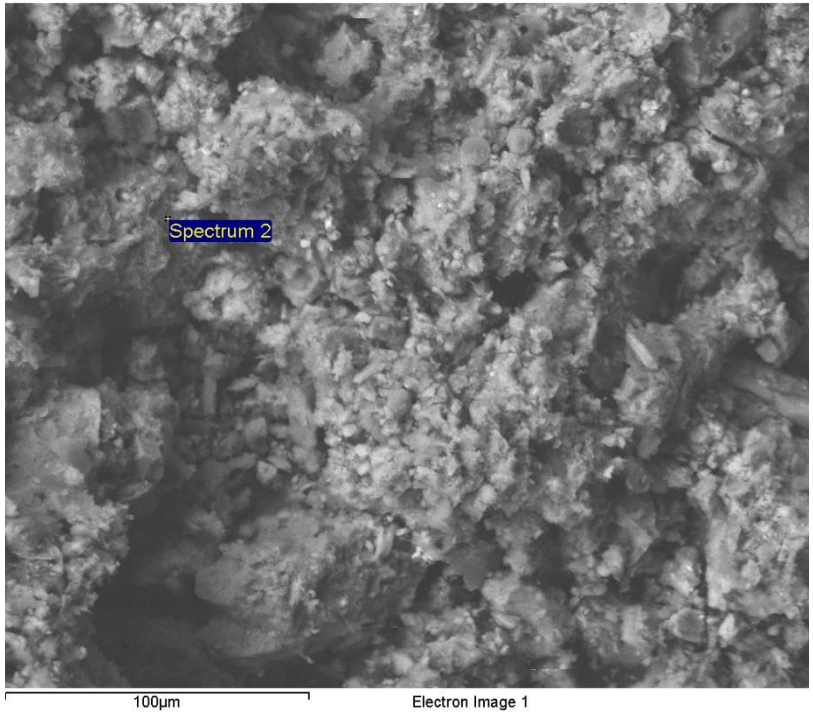

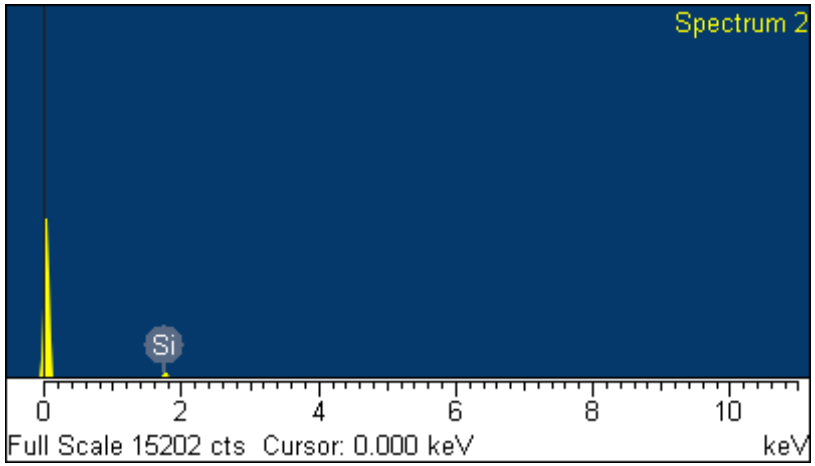

Comment:KoS 3196

INCA

Ashes to ashes

23-Jan-17 1:46:46 PM

Spectrum processing :
No peaks omitted

Processing option : All elements analyzed (Normalised)
Number of iterations = 4

Standard :
O SiO2 1-Jun-1999 12:00 AM
Mg MgO 1-Jun-1999 12:00 AM
Al Al2O3 1-Jun-1999 12:00 AM
Si SiO2 1-Jun-1999 12:00 AM
P GaP 1-Jun-1999 12:00 AM
Ca Wollastonite 1-Jun-1999 12:00 AM

Element	Weight%	Atomic%
O K	62.47	78.36
Mg K	2.55	2.11
Al K	1.61	1.20
Si K	6.44	4.60
P K	1.72	1.11
Ca K	25.21	12.62
Totals	100.00	

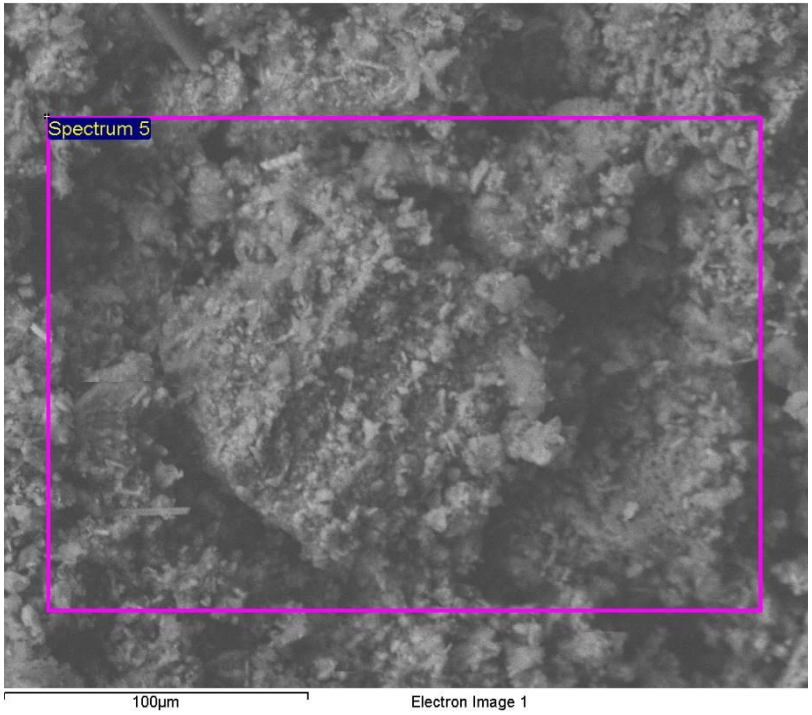

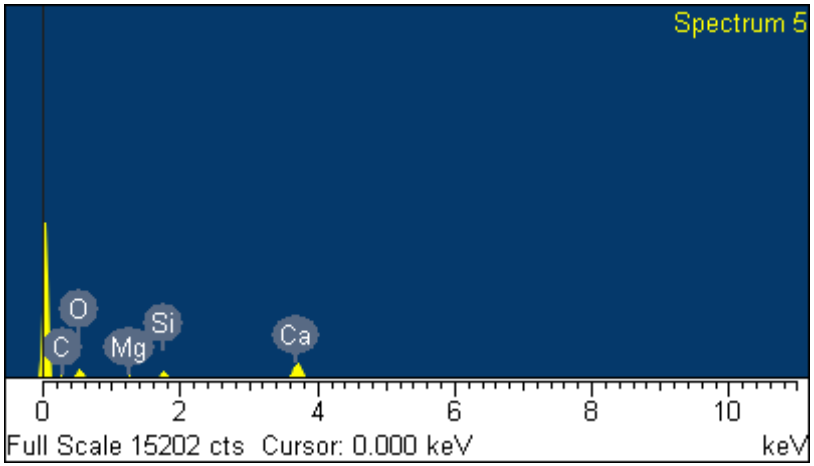

Comment:KoS 3201

INCA

Ashes to ashes

23-Jan-17 2:09:54 PM

Spectrum processing :
No peaks omitted

Processing option : All elements analyzed (Normalised)
Number of iterations = 3

Standard :
C CaCO3 1-Jun-1999 12:00 AM
O SiO2 1-Jun-1999 12:00 AM
Na Albite 1-Jun-1999 12:00 AM
Mg MgO 1-Jun-1999 12:00 AM
Al Al2O3 1-Jun-1999 12:00 AM
Si SiO2 1-Jun-1999 12:00 AM
P GaP 1-Jun-1999 12:00 AM
K MAD-10 Feldspar 1-Jun-1999 12:00 AM
Ca Wollastonite 1-Jun-1999 12:00 AM
Fe Fe 1-Jun-1999 12:00 AM

Element	Weight%	Atomic%
C K	5.68	9.57
O K	46.79	59.14
Na K	1.10	0.97
Mg K	0.90	0.74
Al K	5.16	3.87
Si K	26.66	19.20
P K	1.52	0.99
K K	2.81	1.45
Ca K	4.70	2.37
Fe K	4.68	1.70
Totals	100.00	

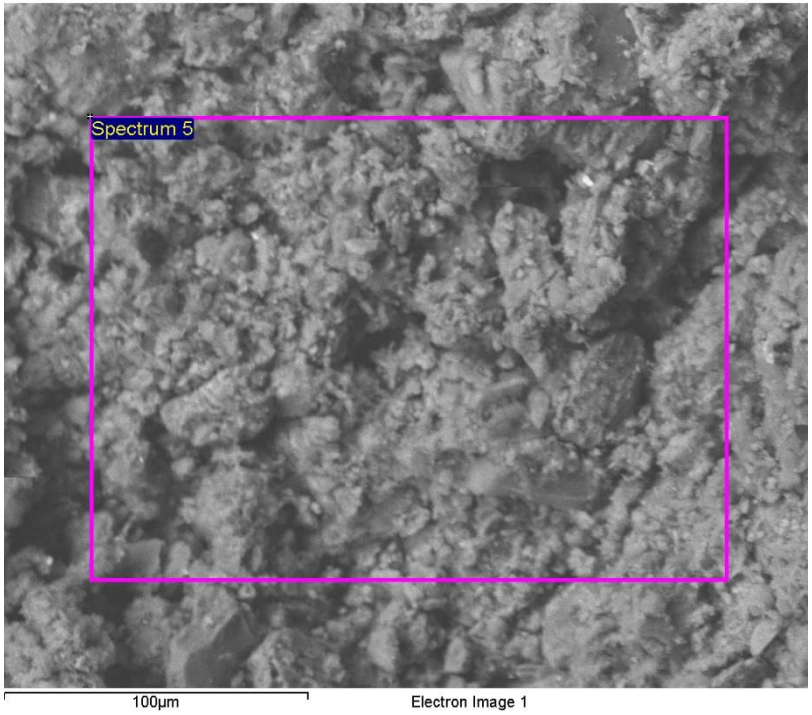

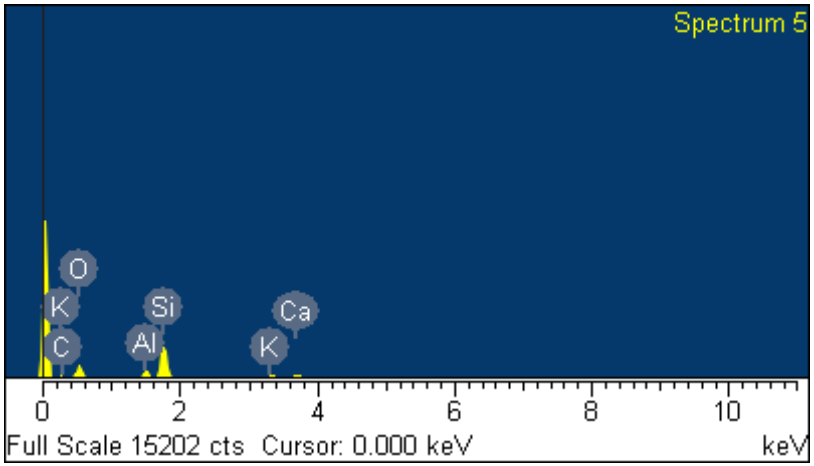

Comment:KoS 3217

INCA

Ashes to ashes

23-Jan-17 1:59:32 PM

Spectrum processing :
No peaks omitted

Processing option : All elements analyzed (Normalised)
Number of iterations = 3

Standard :
C CaCO3 1-Jun-1999 12:00 AM
O SiO2 1-Jun-1999 12:00 AM
Mg MgO 1-Jun-1999 12:00 AM
Al Al2O3 1-Jun-1999 12:00 AM
Si SiO2 1-Jun-1999 12:00 AM
P GaP 1-Jun-1999 12:00 AM
K MAD-10 Feldspar 1-Jun-1999 12:00 AM
Ca Wollastonite 1-Jun-1999 12:00 AM
Fe Fe 1-Jun-1999 12:00 AM

Element	Weight%	Atomic%
C K	12.62	19.51
O K	50.84	59.03
Mg K	1.56	1.19
Al K	5.88	4.05
Si K	15.18	10.04
P K	2.58	1.55
K K	2.10	1.00
Ca K	4.30	1.99
Fe K	4.94	1.64
Totals	100.00	

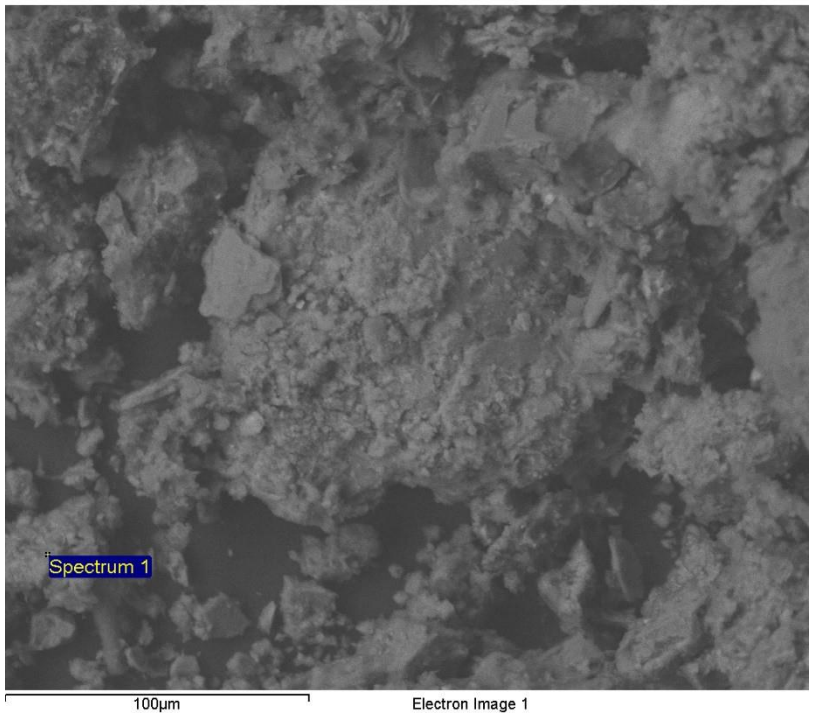

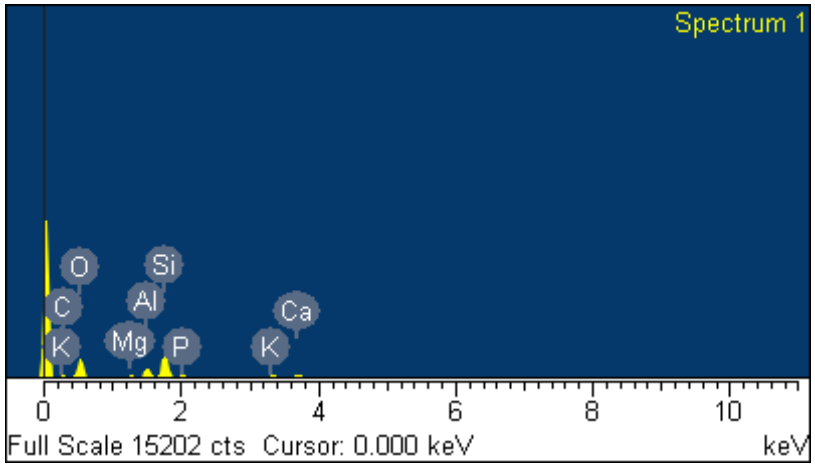

Comment:KoS 3225

INCA

Ashes to ashes

23-Jan-17 2:28:36 PM

Spectrum processing :
No peaks omitted

Processing option : All elements analyzed (Normalised)
Number of iterations = 3

Standard :
O SiO2 1-Jun-1999 12:00 AM
Na Albite 1-Jun-1999 12:00 AM
Mg MgO 1-Jun-1999 12:00 AM
Al Al2O3 1-Jun-1999 12:00 AM
Si SiO2 1-Jun-1999 12:00 AM
P GaP 1-Jun-1999 12:00 AM
K MAD-10 Feldspar 1-Jun-1999 12:00 AM
Ca Wollastonite 1-Jun-1999 12:00 AM
Fe Fe 1-Jun-1999 12:00 AM

Element	Weight%	Atomic%
O K	49.02	64.27
Na K	2.37	2.17
Mg K	0.80	0.69
Al K	7.20	5.60
Si K	29.12	21.75
P K	0.86	0.58
K K	3.60	1.93
Ca K	2.53	1.33
Fe K	4.49	1.69
Totals	100.00	

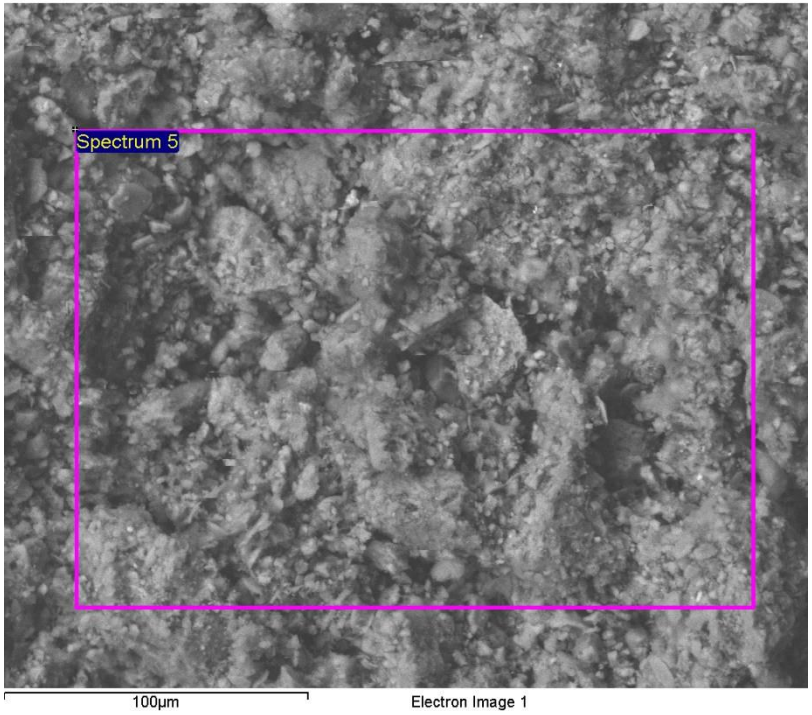

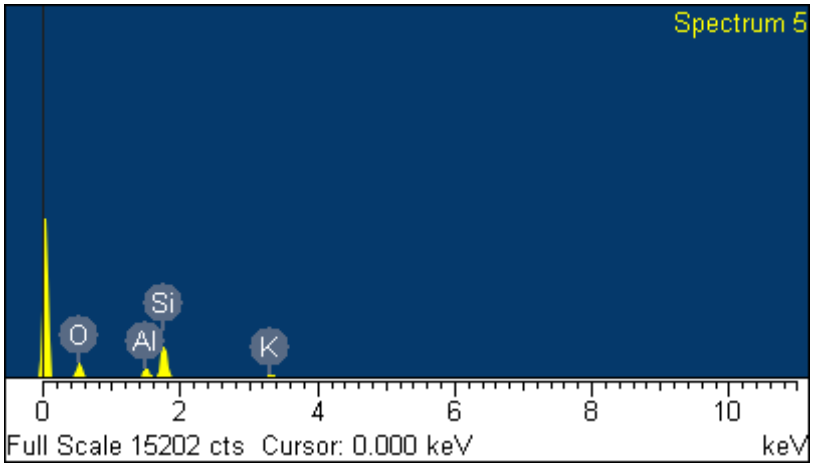

Comment:KoS 3238

INCA

Ashes to ashes

23-Jan-17 2:39:04 PM

Spectrum processing :
No peaks omitted

Processing option : All elements analyzed (Normalised)
Number of iterations = 3

Standard :
C CaCO3 1-Jun-1999 12:00 AM
O SiO2 1-Jun-1999 12:00 AM
Na Albite 1-Jun-1999 12:00 AM
Mg MgO 1-Jun-1999 12:00 AM
Al Al2O3 1-Jun-1999 12:00 AM
Si SiO2 1-Jun-1999 12:00 AM
P GaP 1-Jun-1999 12:00 AM
K MAD-10 Feldspar 1-Jun-1999 12:00 AM
Ca Wollastonite 1-Jun-1999 12:00 AM
Fe Fe 1-Jun-1999 12:00 AM

Element	Weight%	Atomic%
C K	7.18	11.50
O K	49.87	59.97
Na K	1.78	1.49
Mg K	0.75	0.60
Al K	5.12	3.65
Si K	29.11	19.94
P K	0.65	0.40
K K	2.16	1.06
Ca K	1.61	0.77
Fe K	1.78	0.61
Totals	100.00	

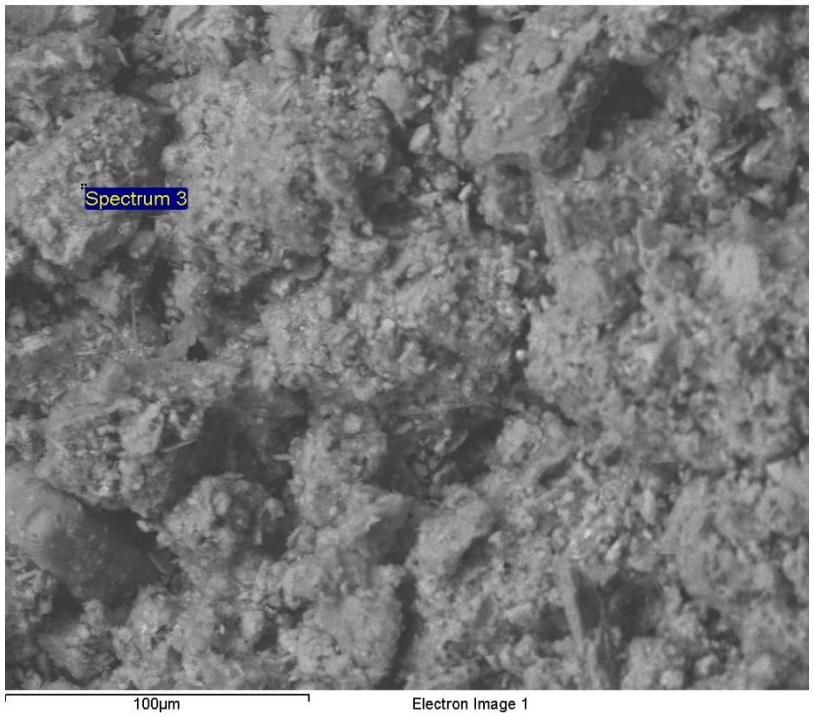

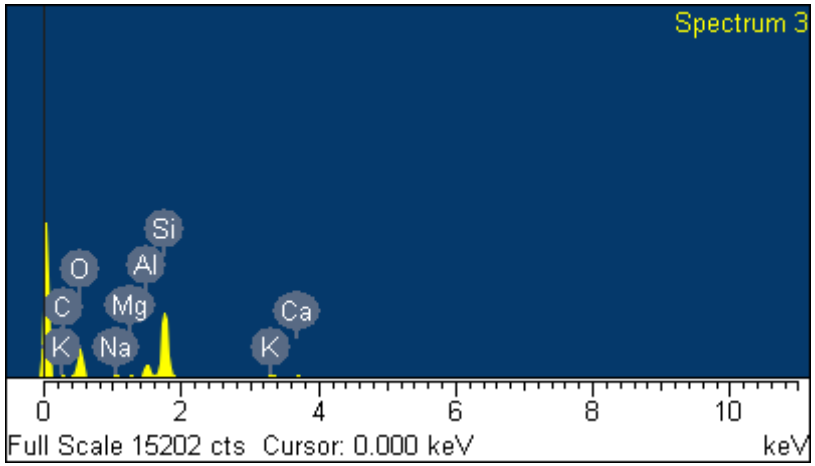

Comment:KoS 3255

INCA

Ashes to ashes

11-Jan-17 11:34:55 AM

Spectrum processing :
No peaks omitted

Processing option : All elements analyzed (Normalised)
Number of iterations = 4

Standard :
O SiO2 1-Jun-1999 12:00 AM
Na Albite 1-Jun-1999 12:00 AM
Mg MgO 1-Jun-1999 12:00 AM
Al Al2O3 1-Jun-1999 12:00 AM
Si SiO2 1-Jun-1999 12:00 AM
P GaP 1-Jun-1999 12:00 AM
K MAD-10 Feldspar 1-Jun-1999 12:00 AM
Ti Ti 1-Jun-1999 12:00 AM
Fe Fe 1-Jun-1999 12:00 AM

Element	Weight%	Atomic%
O K	49.97	64.67
Na K	1.23	1.11
Mg K	0.42	0.36
Al K	7.55	5.79
Si K	33.11	24.41
P K	0.42	0.28
K K	3.86	2.05
Ti K	1.09	0.47
Fe K	2.33	0.86
Totals	100.00	

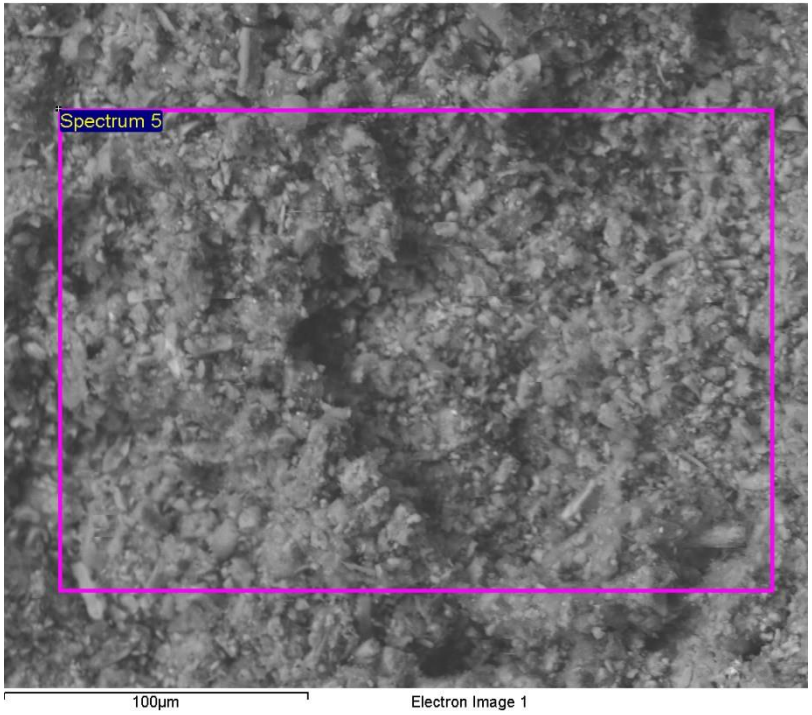

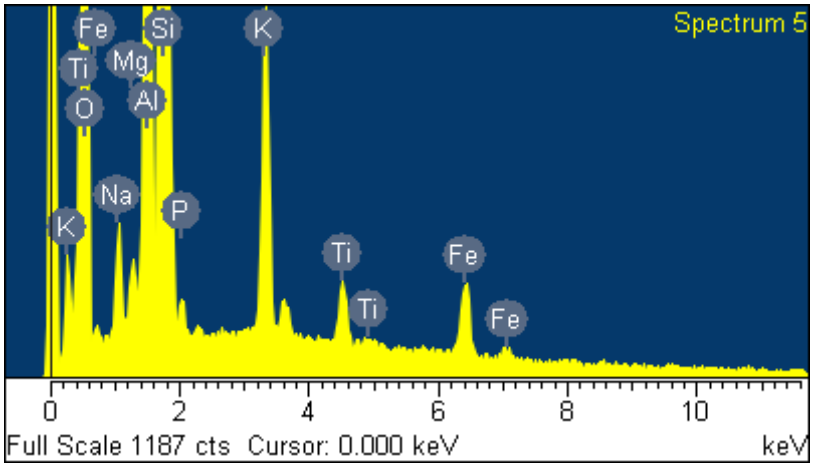

Comment:RDL 031

INCA

Ashes to ashes

11-Jan-17 12:23:24 PM

Spectrum processing :
No peaks omitted

Processing option : All elements analyzed (Normalised)
Number of iterations = 2

Standard :
C CaCO3 1-Jun-1999 12:00 AM
O SiO2 1-Jun-1999 12:00 AM
Al Al2O3 1-Jun-1999 12:00 AM
Si SiO2 1-Jun-1999 12:00 AM
Fe Fe 1-Jun-1999 12:00 AM

Element	Weight%	Atomic%
C K	28.15	41.87
O K	37.39	41.75
Al K	3.28	2.17
Si K	13.38	8.51
Fe K	17.81	5.70
Totals	100.00	

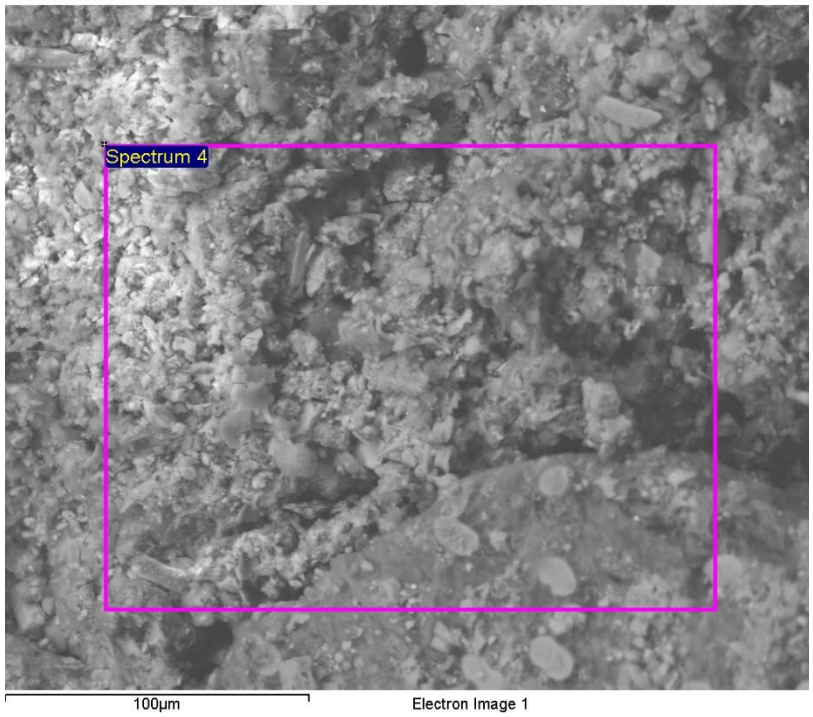

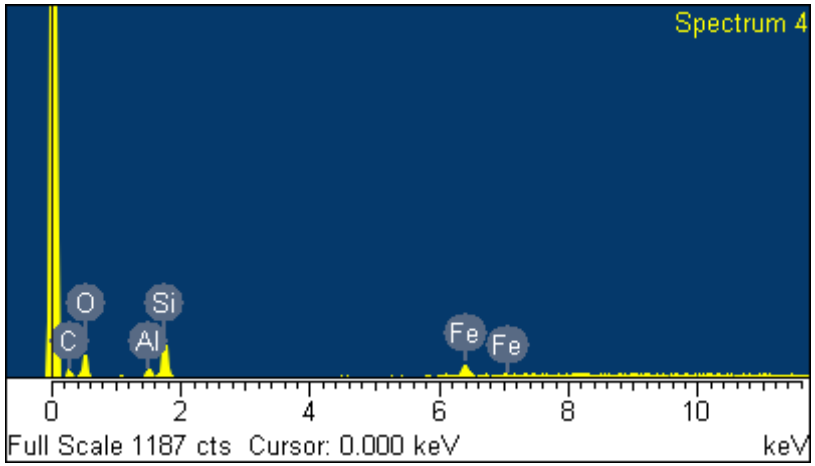

Comment:RDL 001

INCA

Ashes to ashes

11-Jan-17 12:32:43 PM

Spectrum processing :
No peaks omitted

Processing option : All elements analyzed (Normalised)
Number of iterations = 4

Standard :
C CaCO3 1-Jun-1999 12:00 AM
O SiO2 1-Jun-1999 12:00 AM
Na Albite 1-Jun-1999 12:00 AM
Al Al2O3 1-Jun-1999 12:00 AM
Si SiO2 1-Jun-1999 12:00 AM
P GaP 1-Jun-1999 12:00 AM
K MAD-10 Feldspar 1-Jun-1999 12:00 AM
Ti Ti 1-Jun-1999 12:00 AM
Fe Fe 1-Jun-1999 12:00 AM

Element	Weight%	Atomic%
C K	19.49	29.64
O K	42.35	48.34
Na K	0.79	0.63
Al K	4.84	3.28
Si K	22.03	14.32
P K	0.29	0.17
K K	1.67	0.78
Ti K	0.92	0.35
Fe K	7.62	2.49
Totals	100.00	

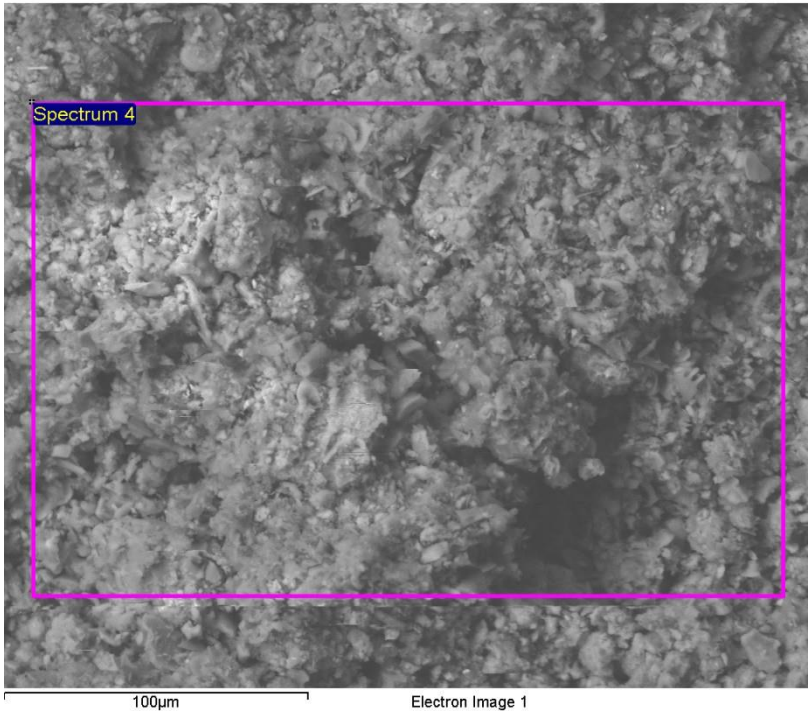

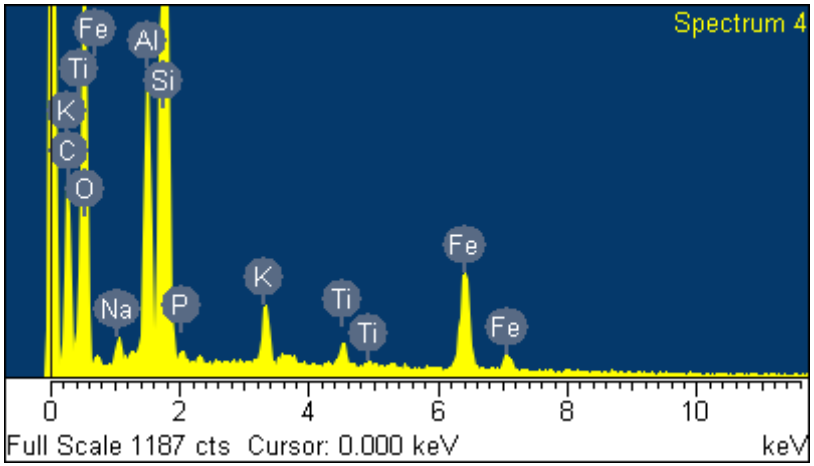

Comment:RDL 004

INCA

Ashes to ashes

11-Jan-17 11:21:25 AM

Spectrum processing :
Peak possibly omitted : 9.770 keV

Processing option : All elements analyzed (Normalised)
Number of iterations = 4

Standard :
C CaCO3 1-Jun-1999 12:00 AM
O SiO2 1-Jun-1999 12:00 AM
Na Albite 1-Jun-1999 12:00 AM
Mg MgO 1-Jun-1999 12:00 AM
Al Al2O3 1-Jun-1999 12:00 AM
Si SiO2 1-Jun-1999 12:00 AM
P GaP 1-Jun-1999 12:00 AM
K MAD-10 Feldspar 1-Jun-1999 12:00 AM
Ti Ti 1-Jun-1999 12:00 AM
Mn Mn 1-Jun-1999 12:00 AM
Fe Fe 1-Jun-1999 12:00 AM

Element	Weight%	Atomic%
C K	6.33	10.23
O K	51.03	61.87
Na K	1.01	0.86
Mg K	0.50	0.40
Al K	6.76	4.86
Si K	26.80	18.51
P K	0.67	0.42
K K	2.98	1.48
Ti K	0.48	0.20
Mn K	0.17	0.06
Fe K	3.24	1.13
Totals	100.00	

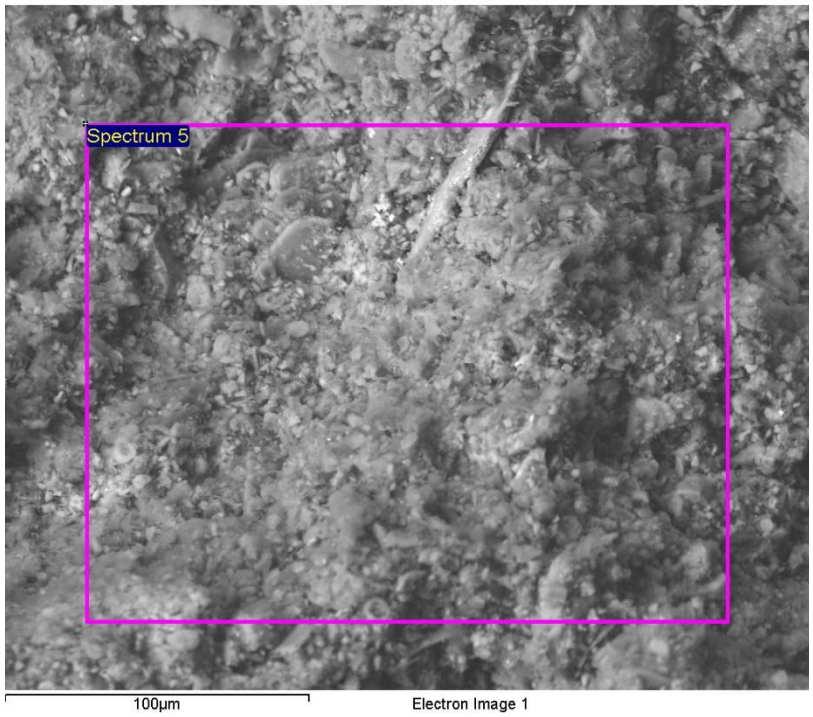

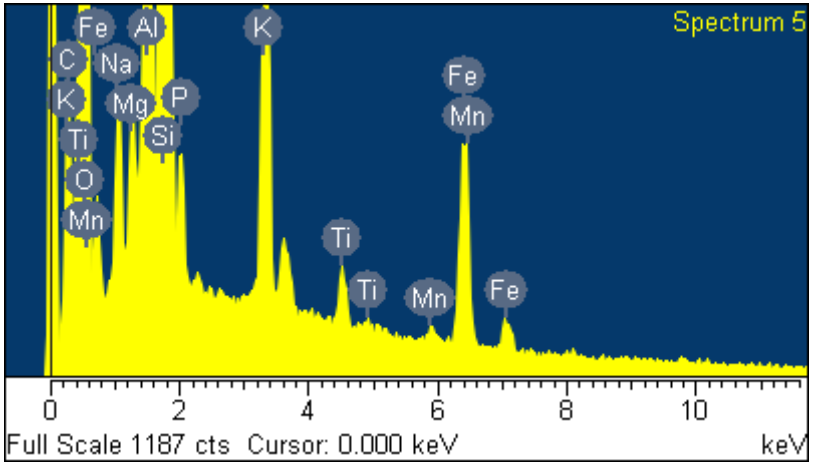

Comment:RDL 006

INCA

Ashes to ashes

11-Jan-17 12:41:51 PM

Spectrum processing :
No peaks omitted

Processing option : All elements analyzed (Normalised)
Number of iterations = 4

Standard :
C CaCO3 1-Jun-1999 12:00 AM
O SiO2 1-Jun-1999 12:00 AM
Na Albite 1-Jun-1999 12:00 AM
Mg MgO 1-Jun-1999 12:00 AM
Al Al2O3 1-Jun-1999 12:00 AM
Si SiO2 1-Jun-1999 12:00 AM
P GaP 1-Jun-1999 12:00 AM
K MAD-10 Feldspar 1-Jun-1999 12:00 AM
Ti Ti 1-Jun-1999 12:00 AM
Fe Fe 1-Jun-1999 12:00 AM

Element	Weight%	Atomic%
C K	15.12	22.81
O K	47.41	53.70
Na K	1.20	0.94
Mg K	0.31	0.23
Al K	5.70	3.83
Si K	25.70	16.58
P K	0.28	0.16
K K	2.40	1.11
Ti K	0.49	0.18
Fe K	1.39	0.45
Totals	100.00	

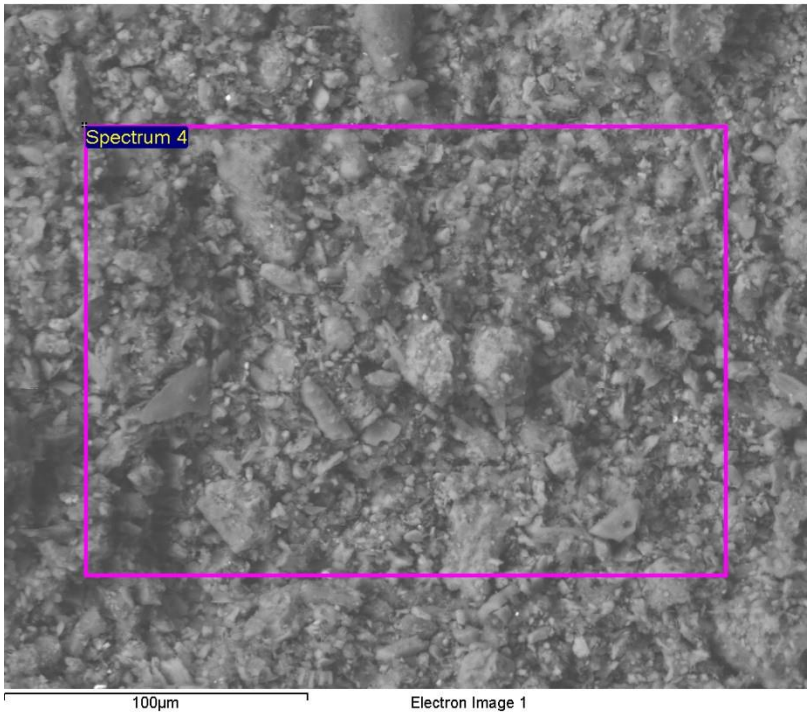

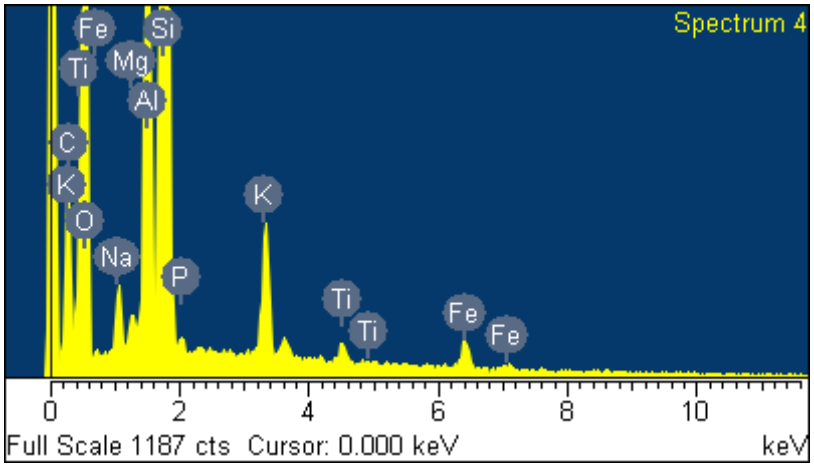

Comment:RDL 009

INCA

Ashes to ashes

11-Jan-17 11:47:25 AM

Spectrum processing :
No peaks omitted

Processing option : All elements analyzed (Normalised)
Number of iterations = 5

Standard :
C CaCO3 1-Jun-1999 12:00 AM
O SiO2 1-Jun-1999 12:00 AM
Na Albite 1-Jun-1999 12:00 AM
Mg MgO 1-Jun-1999 12:00 AM
Al Al2O3 1-Jun-1999 12:00 AM
Si SiO2 1-Jun-1999 12:00 AM
P GaP 1-Jun-1999 12:00 AM
K MAD-10 Feldspar 1-Jun-1999 12:00 AM
Ca Wollastonite 1-Jun-1999 12:00 AM
Ti Ti 1-Jun-1999 12:00 AM
Mn Mn 1-Jun-1999 12:00 AM
Fe Fe 1-Jun-1999 12:00 AM

Element	Weight%	Atomic%
C K	16.12	24.42
O K	47.42	53.95
Na K	0.69	0.55
Mg K	0.80	0.60
Al K	6.64	4.48
Si K	18.75	12.16
P K	1.37	0.81
K K	2.12	0.99
Ca K	0.29	0.13
Ti K	0.48	0.18
Mn K	0.55	0.18
Fe K	4.77	1.56
Totals	100.00	

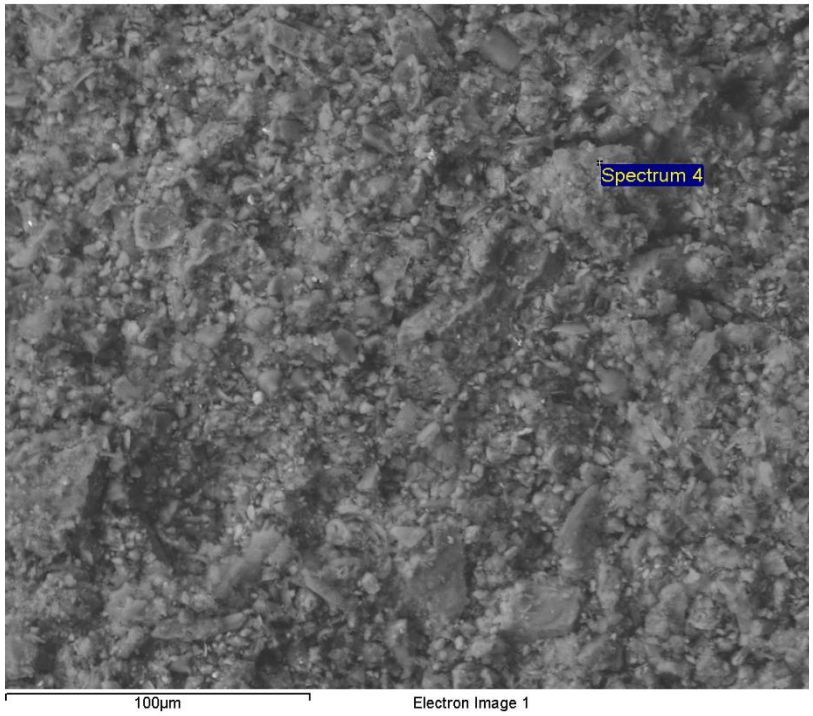

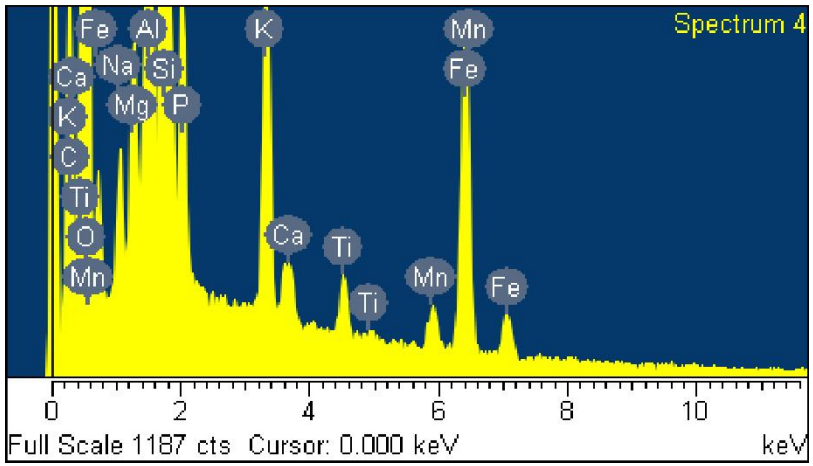

Comment:RDL 007

INCA

Ashes to ashes

11-Jan-17 12:52:15 PM

Spectrum processing :
No peaks omitted

Processing option : All elements analyzed (Normalised)
Number of iterations = 4

Standard :
C CaCO3 1-Jun-1999 12:00 AM
O SiO2 1-Jun-1999 12:00 AM
Na Albite 1-Jun-1999 12:00 AM
Mg MgO 1-Jun-1999 12:00 AM
Al Al2O3 1-Jun-1999 12:00 AM
Si SiO2 1-Jun-1999 12:00 AM
P GaP 1-Jun-1999 12:00 AM
K MAD-10 Feldspar 1-Jun-1999 12:00 AM
Ti Ti 1-Jun-1999 12:00 AM
Mn Mn 1-Jun-1999 12:00 AM
Fe Fe 1-Jun-1999 12:00 AM

Element	Weight%	Atomic%
C K	5.28	8.82
O K	47.07	59.04
Na K	1.84	1.61
Mg K	0.42	0.34
Al K	7.15	5.32
Si K	29.33	20.96
P K	0.76	0.49
K K	2.75	1.41
Ti K	1.09	0.46
Mn K	0.33	0.12
Fe K	3.99	1.43
Totals	100.00	

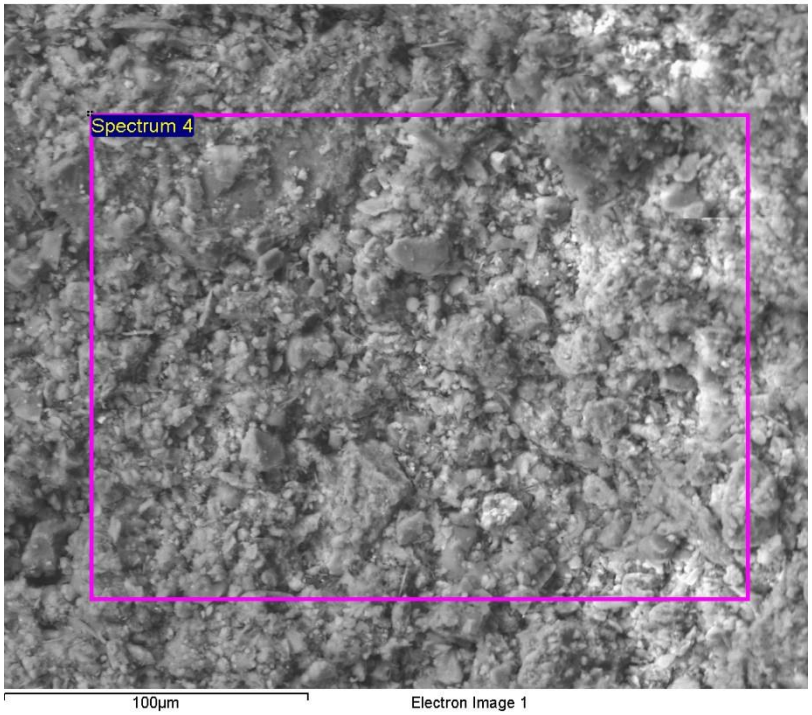

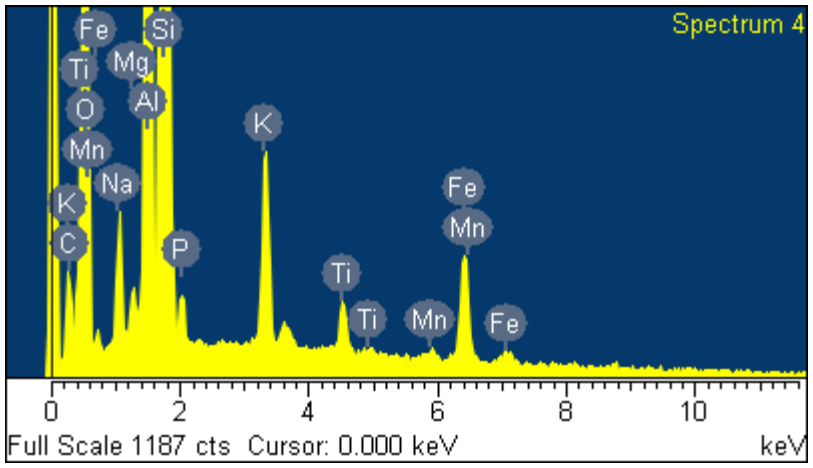

Comment:RDL 013

INCA

Ashes to ashes

11-Jan-17 12:01:22 PM

Spectrum processing :
No peaks omitted

Processing option : All elements analyzed (Normalised)
Number of iterations = 4

Standard :
C CaCO3 1-Jun-1999 12:00 AM
O SiO2 1-Jun-1999 12:00 AM
Na Albite 1-Jun-1999 12:00 AM
Mg MgO 1-Jun-1999 12:00 AM
Al Al2O3 1-Jun-1999 12:00 AM
Si SiO2 1-Jun-1999 12:00 AM
P GaP 1-Jun-1999 12:00 AM
K MAD-10 Feldspar 1-Jun-1999 12:00 AM
Ti Ti 1-Jun-1999 12:00 AM
Mn Mn 1-Jun-1999 12:00 AM
Fe Fe 1-Jun-1999 12:00 AM

Element	Weight%	Atomic%
C K	4.98	8.22
O K	49.45	61.24
Na K	0.91	0.79
Mg K	0.40	0.33
Al K	5.88	4.32
Si K	30.75	21.69
P K	0.31	0.20
K K	3.89	1.97
Ti K	0.52	0.22
Mn K	0.25	0.09
Fe K	2.65	0.94
Totals	100.00	

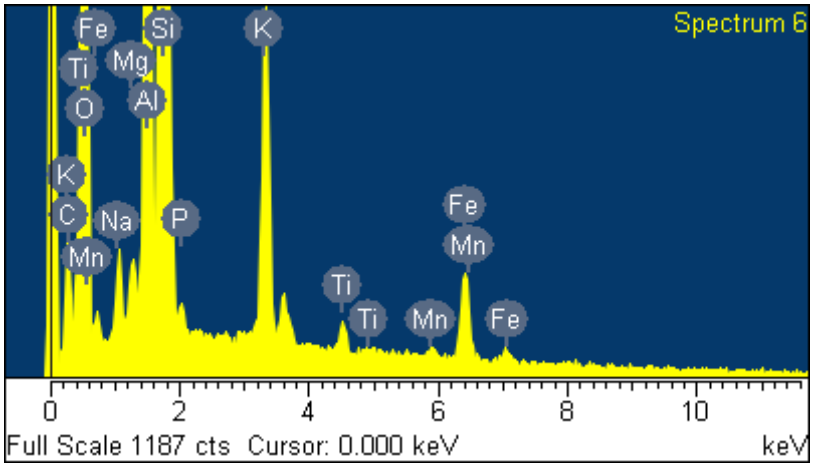

Comment:RDL 016

INCA

Ashes to ashes

11-Jan-17 12:12:31 PM

Spectrum processing :
No peaks omitted

Processing option : All elements analyzed (Normalised)
Number of iterations = 4

Standard :
O SiO2 1-Jun-1999 12:00 AM
Na Albite 1-Jun-1999 12:00 AM
Mg MgO 1-Jun-1999 12:00 AM
Al Al2O3 1-Jun-1999 12:00 AM
Si SiO2 1-Jun-1999 12:00 AM
P GaP 1-Jun-1999 12:00 AM
K MAD-10 Feldspar 1-Jun-1999 12:00 AM
Ti Ti 1-Jun-1999 12:00 AM
Mn Mn 1-Jun-1999 12:00 AM
Fe Fe 1-Jun-1999 12:00 AM

Element	Weight%	Atomic%
O K	49.96	64.81
Na K	1.89	1.70
Mg K	0.55	0.47
Al K	7.47	5.75
Si K	31.79	23.49
P K	0.41	0.28
K K	3.25	1.72
Ti K	0.61	0.26
Mn K	0.31	0.12
Fe K	3.75	1.39
Totals	100.00	

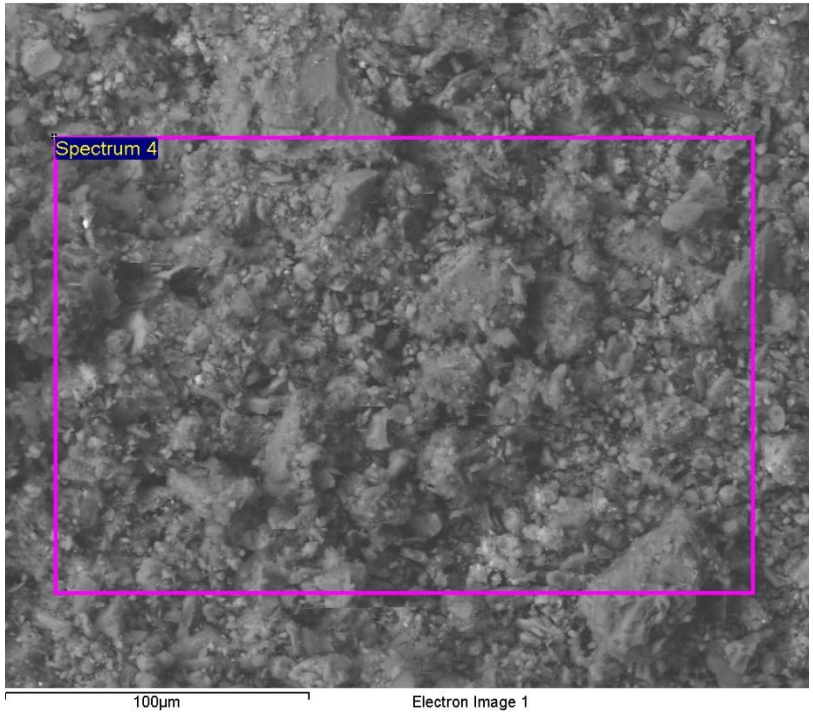

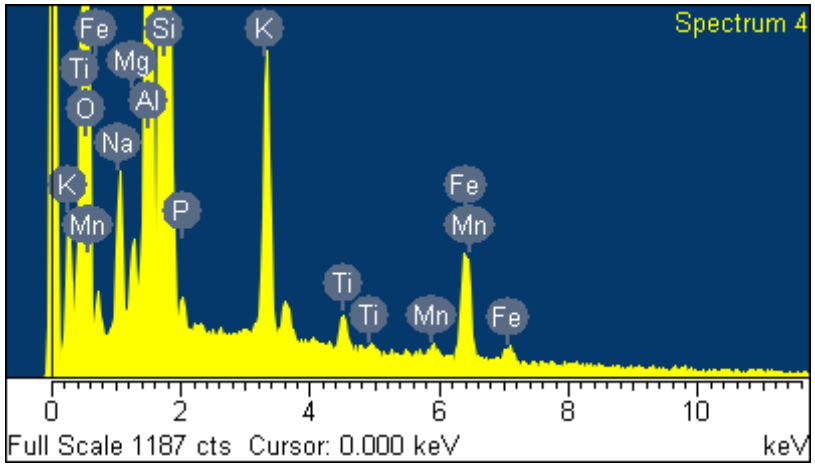

Comment:RDL 023

INCA

Ashes to ashes

11-Jan-17 11:05:43 AM

Spectrum processing :
Peak possibly omitted : 8.060 keV

Processing option : All elements analyzed (Normalised)
Number of iterations = 5

Standard :
C CaCO3 1-Jun-1999 12:00 AM
O SiO2 1-Jun-1999 12:00 AM
Na Albite 1-Jun-1999 12:00 AM
Mg MgO 1-Jun-1999 12:00 AM
Al Al2O3 1-Jun-1999 12:00 AM
Si SiO2 1-Jun-1999 12:00 AM
P GaP 1-Jun-1999 12:00 AM
S FeS2 1-Jun-1999 12:00 AM
K MAD-10 Feldspar 1-Jun-1999 12:00 AM
Ti Ti 1-Jun-1999 12:00 AM
Mn Mn 1-Jun-1999 12:00 AM
Fe Fe 1-Jun-1999 12:00 AM

Element	Weight%	Atomic%
C K	17.14	25.79
O K	45.51	51.40
Na K	1.15	0.91
Mg K	0.44	0.33
Al K	5.47	3.66
Si K	23.57	15.16
P K	0.50	0.29
S K	0.20	0.11
K K	2.64	1.22
Ti K	0.48	0.18
Mn K	0.28	0.09
Fe K	2.61	0.84
Totals	100.00	

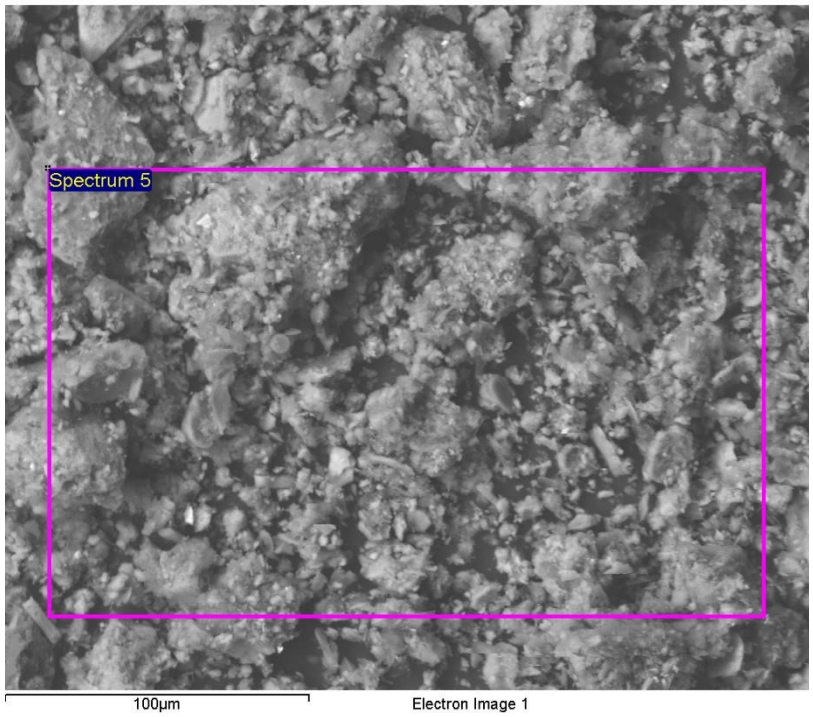

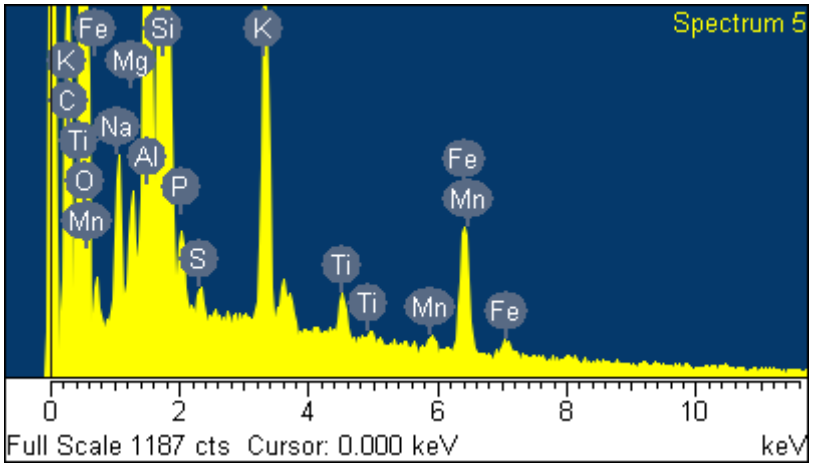

Comment:RDL 032

INCA

Ashes to ashes

23-Jan-17 3:29:01 PM

Spectrum processing :
No peaks omitted

Processing option : All elements analyzed (Normalised)
Number of iterations = 2

Standard :
C CaCO3 1-Jun-1999 12:00 AM
O SiO2 1-Jun-1999 12:00 AM
Al Al2O3 1-Jun-1999 12:00 AM
Si SiO2 1-Jun-1999 12:00 AM
K MAD-10 Feldspar 1-Jun-1999 12:00 AM
Fe Fe 1-Jun-1999 12:00 AM

Element	Weight%	Atomic%
C K	13.23	20.45
O K	49.04	56.91
Al K	6.04	4.16
Si K	23.23	15.35
K K	2.25	1.07
Fe K	6.20	2.06
Totals	100.00	

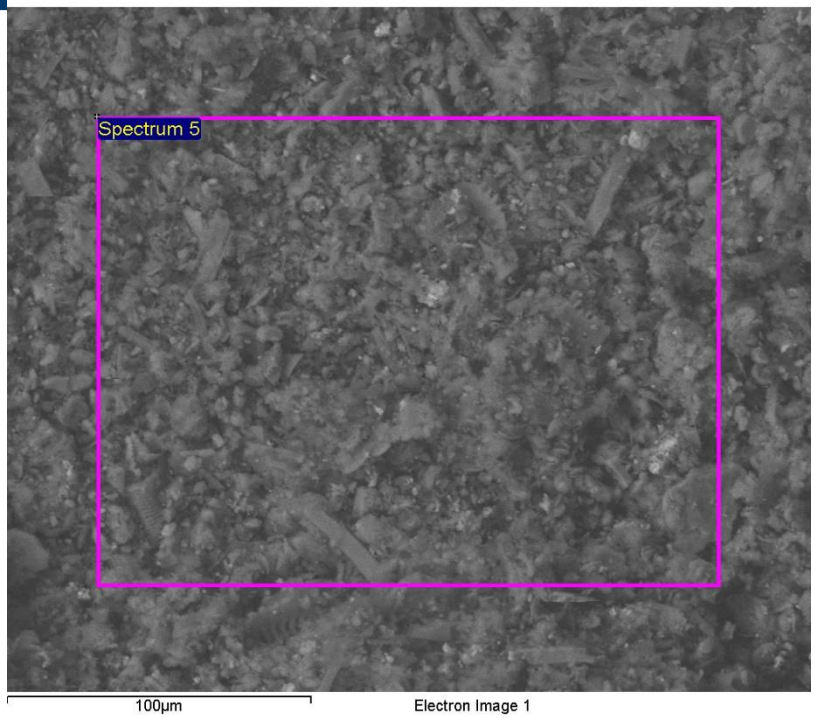

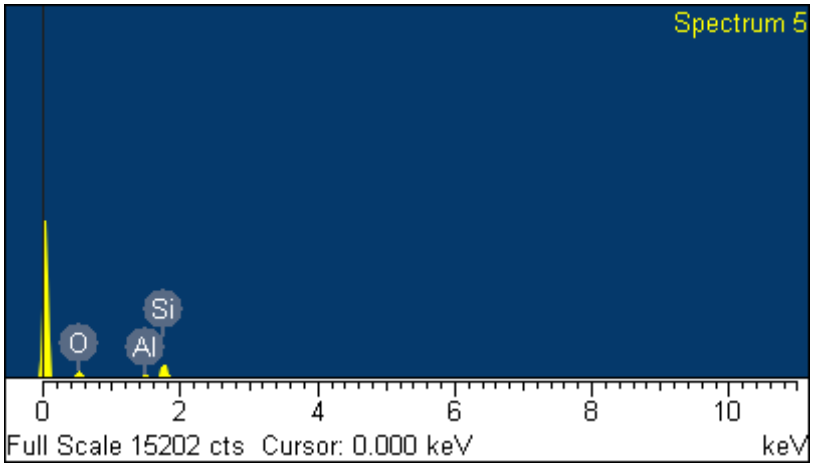

Comment:SMQ 1-2

INCA

Ashes to ashes

23-Jan-17 3:35:06 PM

Spectrum processing :
Peak possibly omitted : 1.040 keV

Processing option : All elements analyzed (Normalised)
Number of iterations = 3

Standard :
O SiO2 1-Jun-1999 12:00 AM
Al Al2O3 1-Jun-1999 12:00 AM
Si SiO2 1-Jun-1999 12:00 AM
P GaP 1-Jun-1999 12:00 AM
K MAD-10 Feldspar 1-Jun-1999 12:00 AM
Ti Ti 1-Jun-1999 12:00 AM
Fe Fe 1-Jun-1999 12:00 AM

Element	Weight%	Atomic%
O K	47.49	63.42
Al K	7.33	5.80
Si K	32.93	25.05
P K	0.97	0.67
K K	4.19	2.29
Ti K	1.02	0.46
Fe K	6.07	2.32
Totals	100.00	

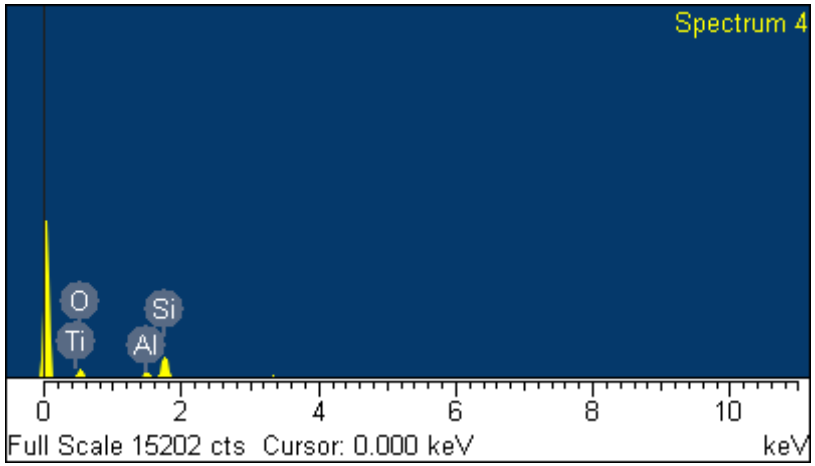

Comment:SMQ 2

INCA

Ashes to ashes

23-Jan-17 3:13:16 PM

Spectrum processing :
No peaks omitted

Processing option : All elements analyzed (Normalised)
Number of iterations = 4

Standard :
C CaCO3 1-Jun-1999 12:00 AM
O SiO2 1-Jun-1999 12:00 AM
Na Albite 1-Jun-1999 12:00 AM
Mg MgO 1-Jun-1999 12:00 AM
Al Al2O3 1-Jun-1999 12:00 AM
Si SiO2 1-Jun-1999 12:00 AM
P GaP 1-Jun-1999 12:00 AM
K MAD-10 Feldspar 1-Jun-1999 12:00 AM
Ca Wollastonite 1-Jun-1999 12:00 AM
Ti Ti 1-Jun-1999 12:00 AM
Fe Fe 1-Jun-1999 12:00 AM

Element	Weight%	Atomic%
C K	14.62	22.08
O K	51.30	58.15
Na K	0.73	0.58
Mg K	1.74	1.30
Al K	4.77	3.21
Si K	15.26	9.85
P K	1.85	1.08
K K	1.82	0.84
Ca K	2.50	1.13
Ti K	0.41	0.15
Fe K	4.99	1.62
Totals	100.00	

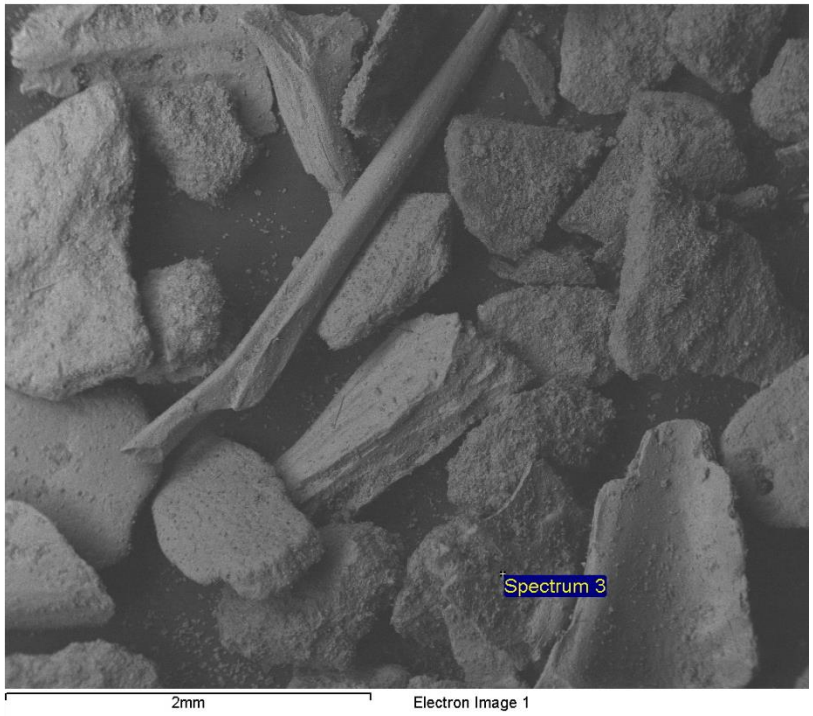

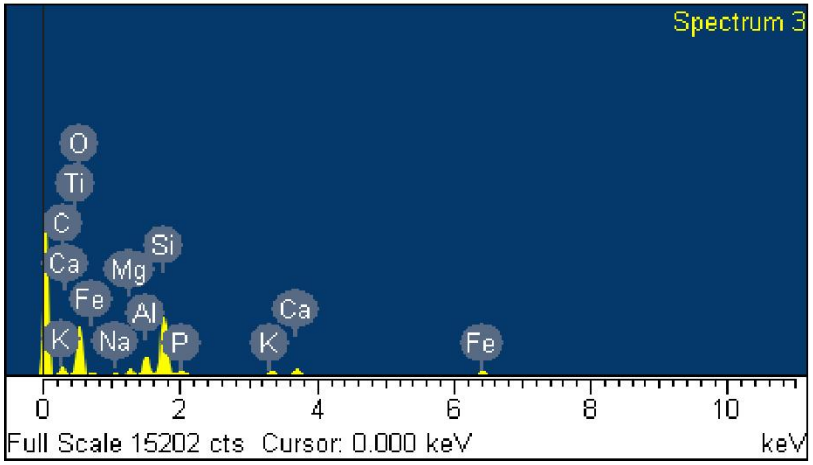

Comment:Arch U/B

Ashes to ashes

23-Jan-17 3:19:53 PM

Spectrum processing :
No peaks omitted

Processing option : All elements analyzed (Normalised)
Number of iterations = 3

Standard :
C CaCO3 1-Jun-1999 12:00 AM
O SiO2 1-Jun-1999 12:00 AM
Mg MgO 1-Jun-1999 12:00 AM
Al Al2O3 1-Jun-1999 12:00 AM
P GaP 1-Jun-1999 12:00 AM
S FeS2 1-Jun-1999 12:00 AM
Cl KCl 1-Jun-1999 12:00 AM
Ca Wollastonite 1-Jun-1999 12:00 AM
Fe Fe 1-Jun-1999 12:00 AM

Element	Weight%	Atomic%
C K	17.90	30.15
O K	34.25	43.30
Mg K	0.48	0.40
Al K	0.84	0.63
P K	13.62	8.89
S K	0.67	0.42
Cl K	0.45	0.26
Ca K	31.14	15.71
Fe K	0.64	0.23
Totals	100.00	

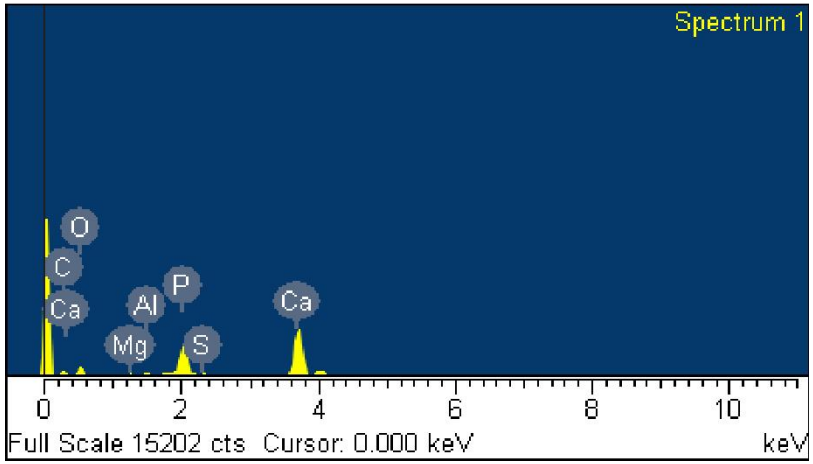

Comment:UB 900

INCA

Appendix 4 Additional PCA

The following PCA plots show the analysis of the data that are not present within the main body of the thesis. These were excluded due to their lack of relevance to the arguments; however, their presence here is to demonstrate why they did not help the investigation, and to demonstrate why the plots presented within the thesis are necessary and germane to the evidence that is being presented. The following plots include the other archaeological matrix mixing simulations including 2:1, 3:1, and 4:1, the analysis with the addition of Munsell data as a variable, and the analysis repeated with outliers removed.

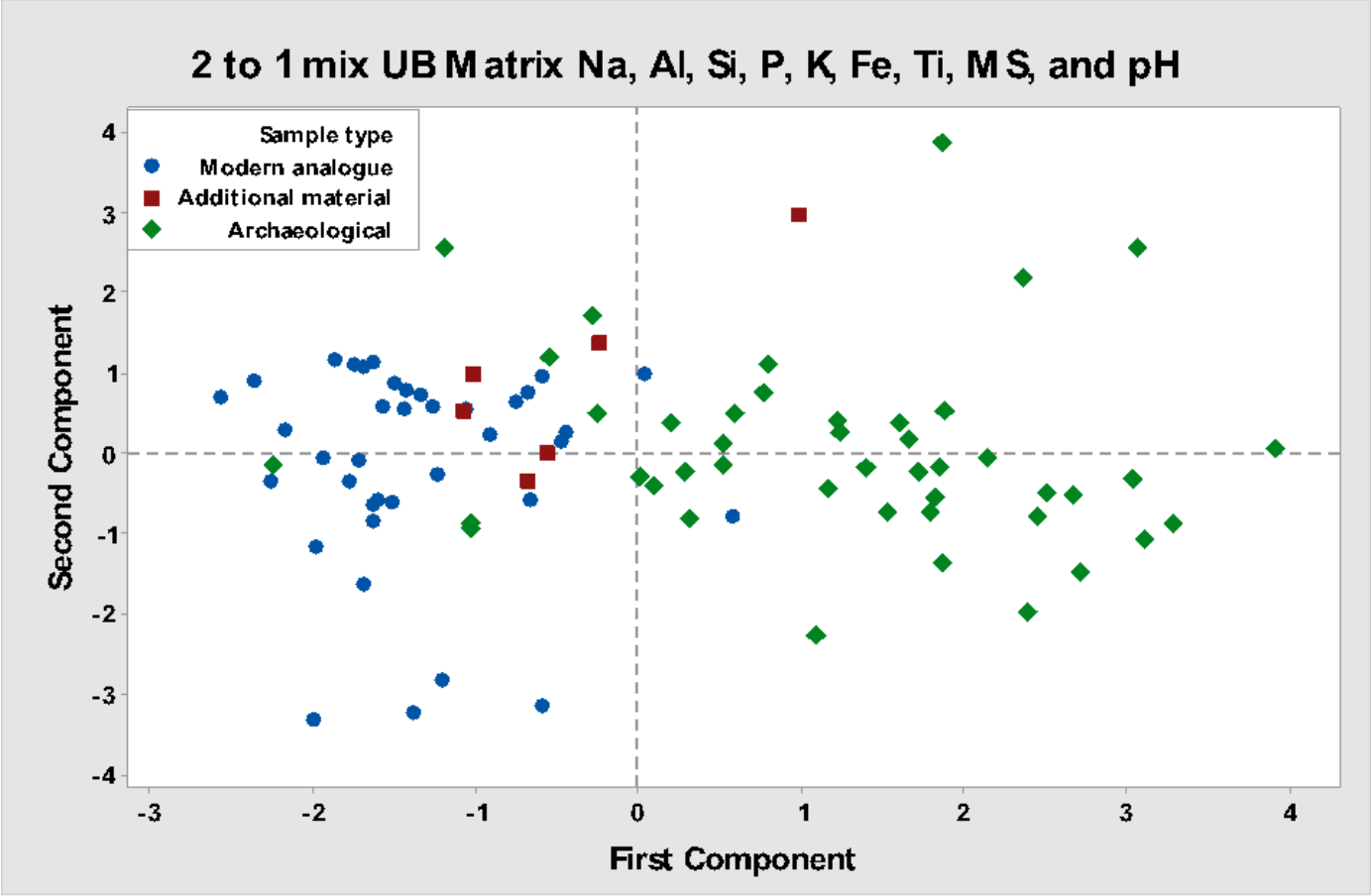

- The PCA of the data considering adjustment for a 2:1 ratio of archaeological matrix to modern analogue ash material. This shows a wide distribution of the data, with the modern analogue data focused on the left hemisphere of the plot, and the archaeological material on the right. There is very little overlap between the sample types which shows a lack of relationships between the adjusted modern analogue data and the archaeological data. The 1:1 mix ratio PCA (figure 7.40 pg 295) shows a much tighter grouping of the data and is indicative of significantly more matching between modern analogue ash and archaeological sample material which is why this plot was excluded from the discussion.

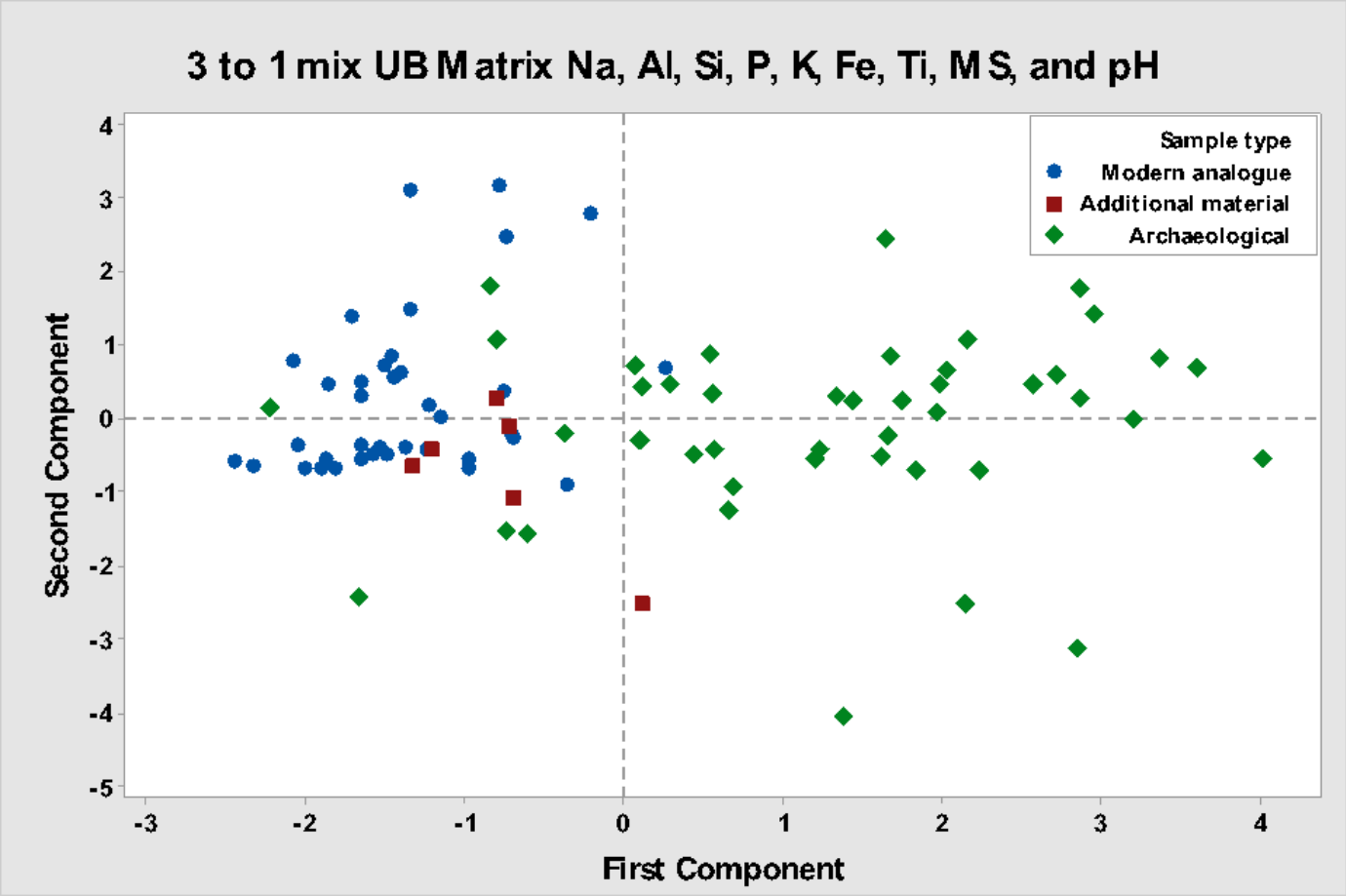

- The PCA of the data considering adjustment for a 3:1 ratio of archaeological matrix to modern analogue ash material. This analysis shows a similar distribution to that of the 2:1 mix ratio when considering the archaeological material data and shows a more compact grouping of the modern analogue data. This analysis does not show a significant relationship between the archaeological material and modern ash, therefore this plot was excluded from the discussion.

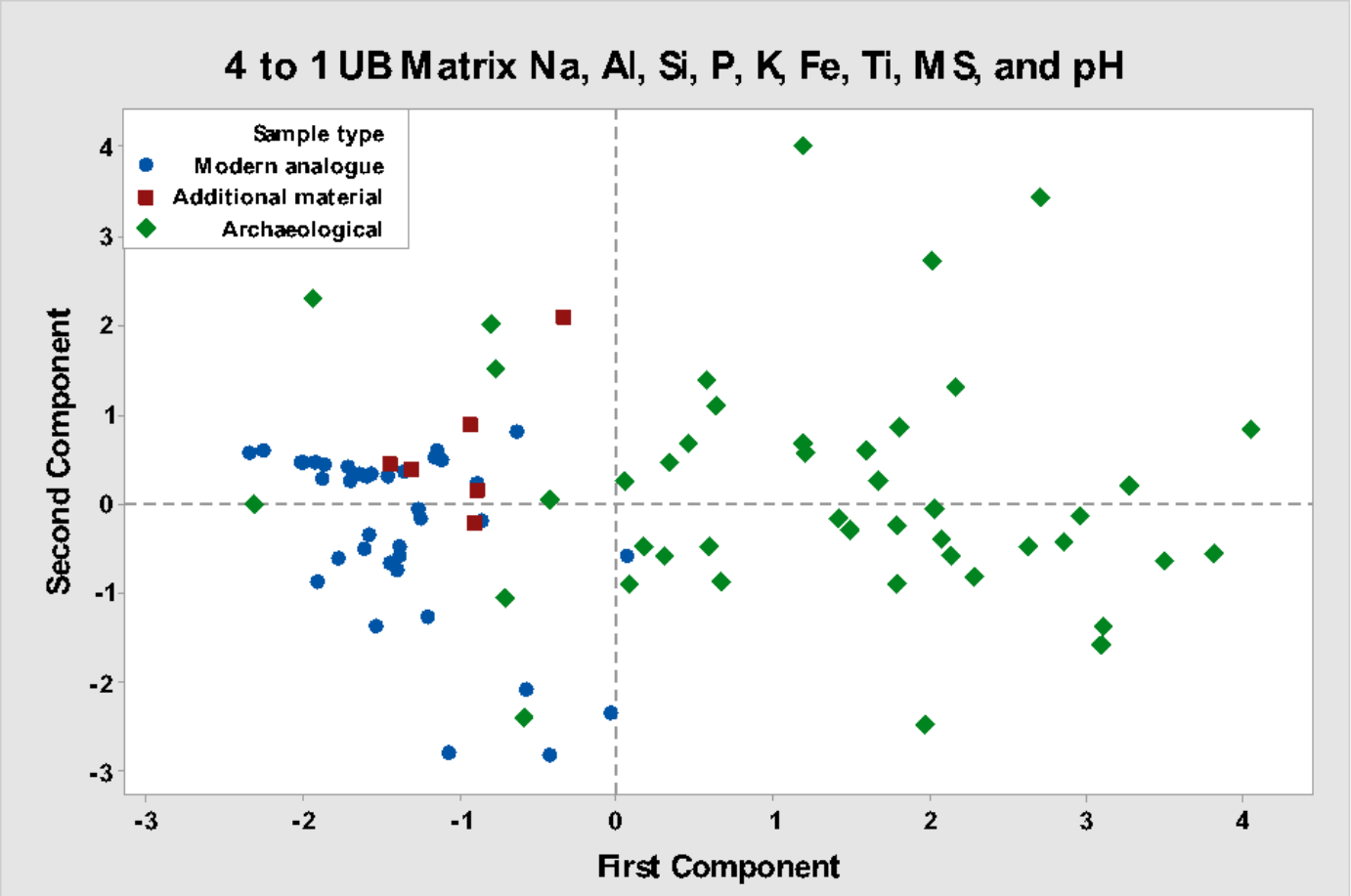

- The PCA of the data considering adjustment for a 4:1 ratio of archaeological matrix to modern analogue ash material. Where the 2:1 and 3:1 ratio analyses have a similar distribution of data, the 4:1 mix simulation is a complete departure. This analysis only indicates a relationship with several archaeological samples and the modern analogue material. The modern analogue data is clustered together, and the archaeological data is distributed more greatly than the two-previous permutations of the mixing simulation. This plot was excluded from the discussion due to the lack of relationships between the archaeological material and the modern analogue ash.

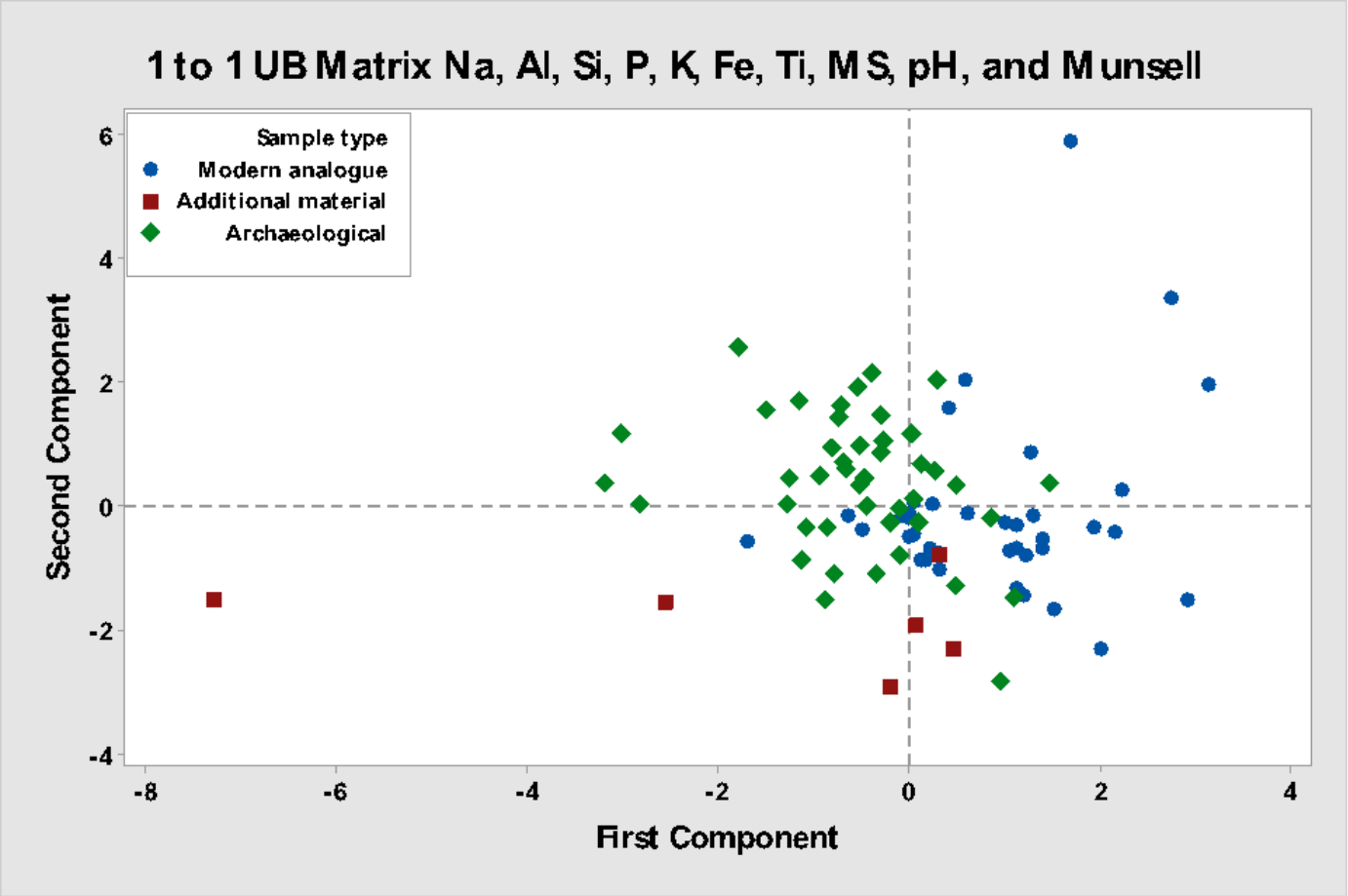

- The PCA of the data with the additional variable of Munsell colour assignment is indicative of a relationship between the archaeological material and the modern analogue ash. This correlation of the two datasets is not to the same degree that is achieved by the PCA that does not consider the Munsell colour assignment. This analysis does show more relationships within the data than the PCA considering the 2:1, 3:1, or 4:1 ratio of unburnt matrix adjusted data, but it does not achieve the same level of correlation shown in figure 7.40. That is why this plot was excluded from the discussion.

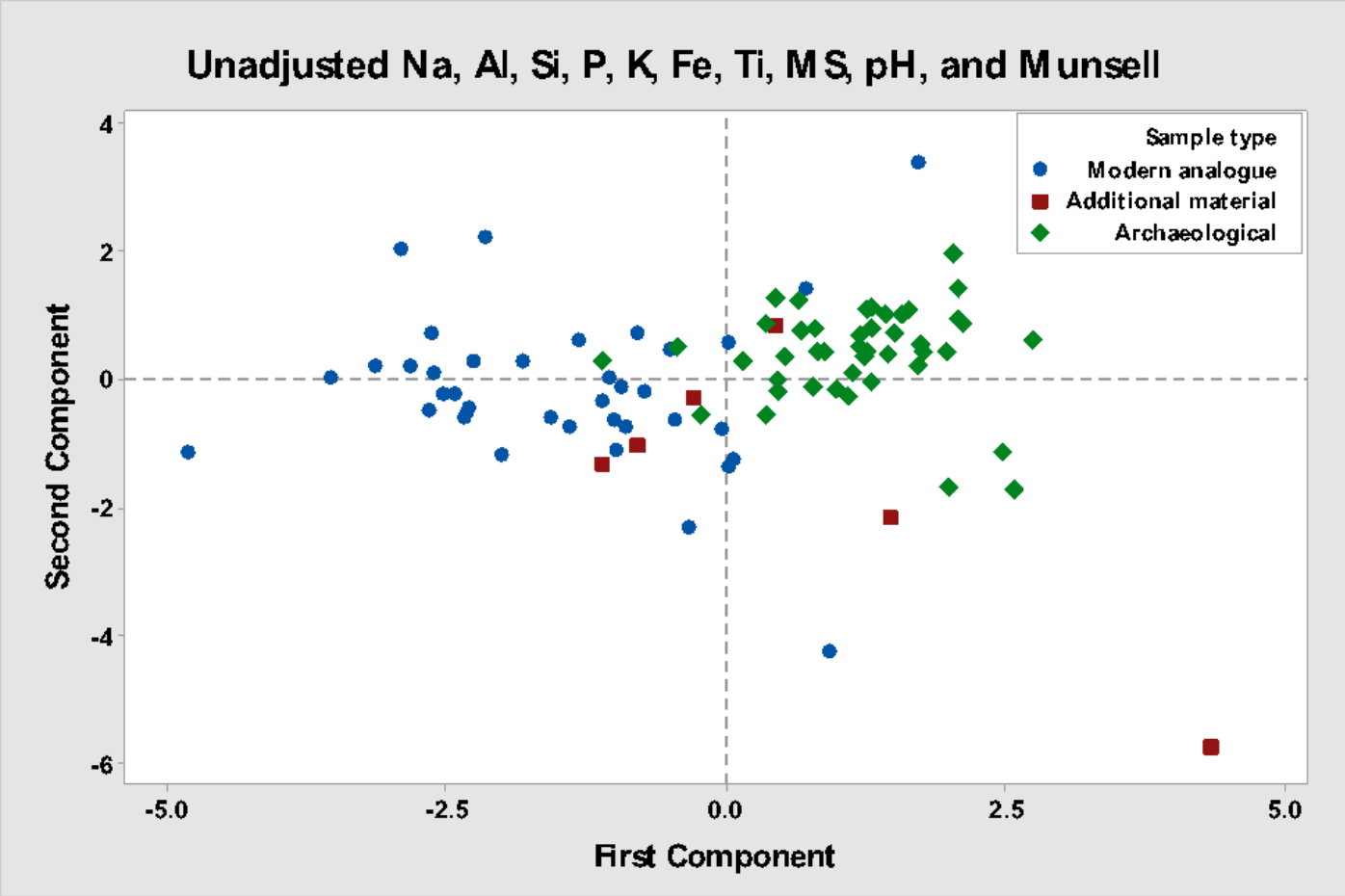

- This plot shows the PCA of the unadjusted data with the additional variable of Munsell colour assignment. The archaeological material and the modern analogue ash are divided almost entirely along the Y axis, with the modern material on the left hemisphere and the archaeological material on the right with only minimal crossover. This analysis does indicate some relationship between the archaeological material and the modern analogue ash, but not to the same extent as the 1:1 mix ratio PCA (figure 7.40 pg 295). That is why this plot was excluded from the discussion.

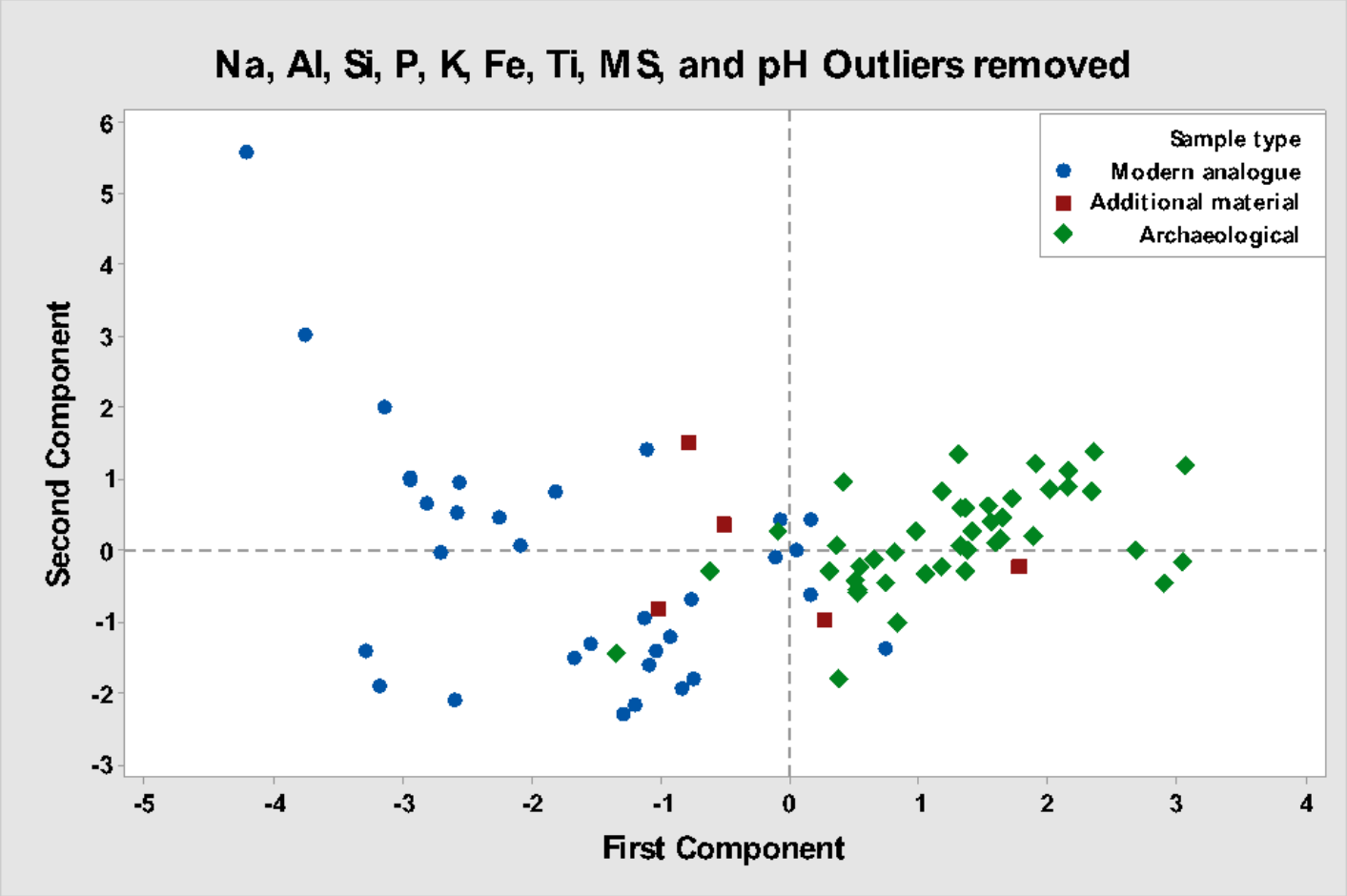

- The PCA plot considering the unadjusted data with 10 outliers removed does show some correlation between the modern analogue ash and the archaeological material. The PCA shows a wide distribution of the modern analogue material within the left hemisphere of the plot and a tight cluster of the archaeological material on the right. This plot was not used in the discussion due to the lack of similarity shown between the modern analogue and the archaeological material.

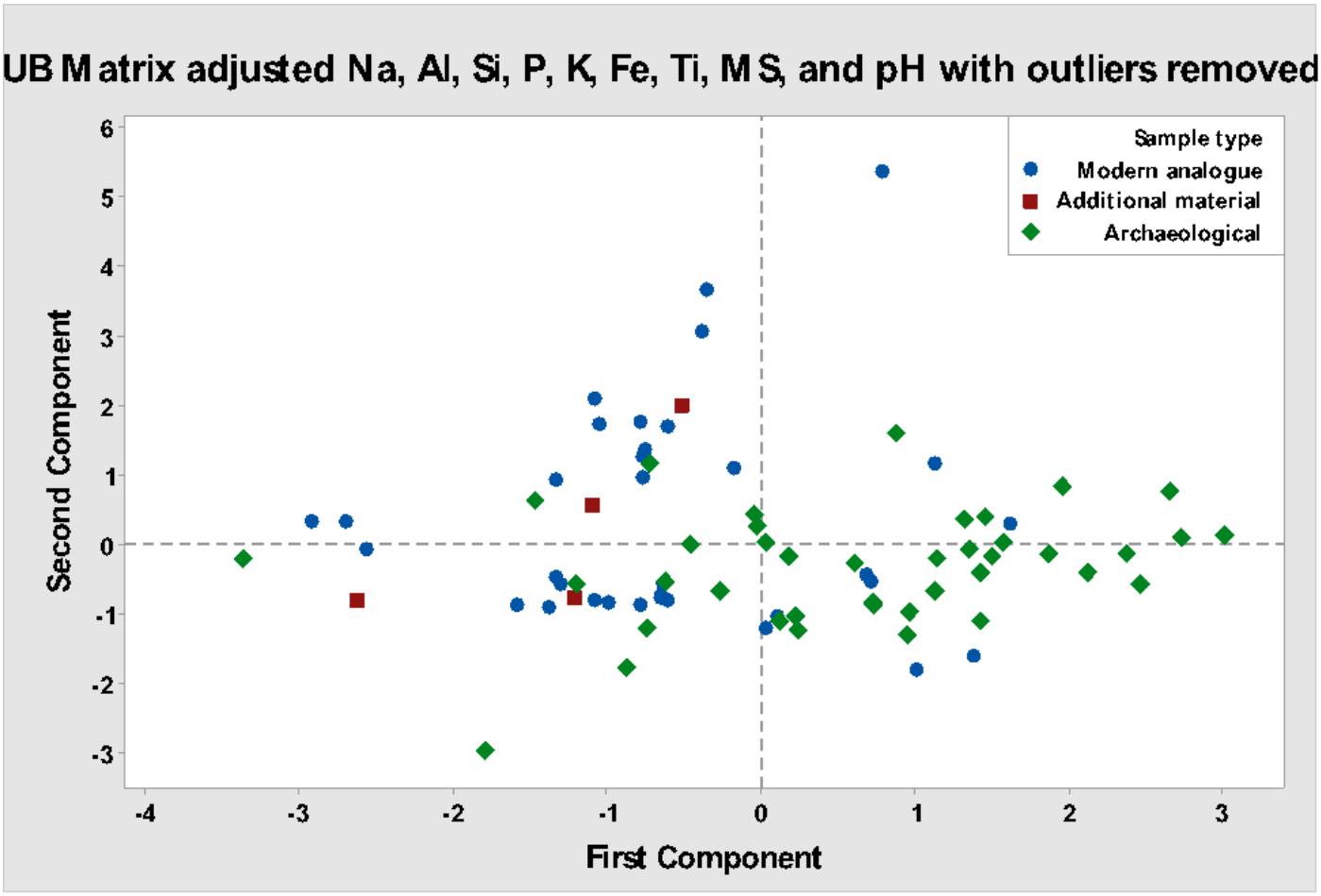

- The PCA of the unburnt archaeological matrix adjusted data with 10 outliers removed does show some similarity between the modern analogue ash and archaeological material. This relationship is more evident than among the unadjusted sample material, but still not as strong as the correlation shown by the 1:1 ratio unburnt archaeological matrix adjusted data with all of the observations included, that is why this plot was not included in the discussion.

Appendix 5 Compete Mass Lost Datasheet

The following presents the complete mass lost dataset for the modern analogue ashing experiments. The data is organised by sample type and temperature. The plots that were used in the main body of the thesis summarize this data.

Mass Lost Data						
Sample	Crucible mass	Crucible + Sample mass	Sample mass	Mass after heating	(Burnt - Unburnt)/Unburnt x 100	% Mass Lost
Driftwood 200^{0}C 3Hrs	142.5	197.1	54.6	44.9	-17.8	18%
Driftwood 200^{0}C 6Hrs	142.5	206	63.5	51.5	-18.9	19%
Driftwood 400^{0}C 2Hrs	142.7	200.9	58.2	16.5	-71.6	72%
Driftwood 400^{0}C 6Hrs	142.6	200.8	58.2	0.9	-98.5	98%
Driftwood 900^{0}C 6Hrs	134.4	191.1	56.7	0.8	-98.6	99%
Seaweed 200^{0}C 3Hrs	168.5	278.6	110.1	80.6	-26.8	27%
Seaweed 200^{0}C 6Hrs	168.5	273.5	105	74.6	-29.0	29%
Seaweed 400^{0}C 2Hrs	168.6	279.9	111.3	58.4	-47.5	48%
Seaweed 400^{0}C 6Hrs	168.7	280	111.3	38.2	-65.7	66%
Seaweed 900^{0}C 6Hrs	168.7	231.9	63.2	23.9	-62.2	62%
Grasses 200^{0}C 3Hrs	151.7	180.3	28.6	16.1	-43.7	44%
Grasses 200^{0}C 6Hrs	151.7	172.9	21.2	15.1	-28.8	29%
Grasses 400^{0}C 2Hrs	151.7	173.6	21.9	8.9	-59.4	59%
Grasses 400^{0}C 6Hrs	151.8	173.7	21.9	4.1	-81.3	81%
Grasses 900^{0}C 6Hrs	151.8	165	13.2	0.1	-99.2	99%
Sheep dung 200^{0}C 3Hrs	162.7	246.7	84	56.1	-33.2	33%
Sheep dung 200^{0}C 6Hrs	162.7	235.2	72.5	48.6	-33.0	33%
Sheep dung 400^{0}C 2Hrs	162.8	230	67.2	27.6	-58.9	59%
Sheep dung 400^{0}C 6Hrs	162.7	229.9	67.2	15	-77.7	78%
Sheep dung 900^{0}C 6Hrs	162.7	225.5	62.8	9.8	-84.4	84%
Cow dung 200^{0}C 3Hrs	136.2	173.8	37.6	21.1	-43.9	44%
Cow dung 200^{0}C 6Hrs	136.2	171.7	35.5	19	-46.5	46%
Cow dung 400^{0}C 2Hrs	136.2	168.2	32	13.7	-57.2	57%

Cow dung 400^{0}C 6Hrs	136.3	168.3	32	5.4	-83.1	83%
Cow dung 900^{0}C 6Hrs	136.3	171.3	35	4.3	-87.7	88%
Heather 200^{0}C 3Hrs	134.6	236.4	101.8	39.3	-61.4	61%
Heather 200^{0}C 6Hrs	134.6	224.1	89.5	70.2	-21.6	22%
Heather 400^{0}C 2Hrs	134.8	197.2	62.4	18.2	-70.8	71%
Heather 400^{0}C 6Hrs	134.7	197.1	62.4	19.9	-68.1	68%
Heather 900^{0}C 6Hrs	142.4	205.6	63.2	0.2	-99.7	100%
Willow 200^{0}C 6Hrs	162.7	225.1	62.4	40.5	-35.1	35%
Willow 400^{0}C 6Hrs	152	196.5	44.5	3.9	-91.2	91%
Willow 900^{0}C 6Hrs	152.1	224.1	72	1	-98.6	99%
Hazel 200^{0}C 6Hrs	162.7	208.9	46.2	29.8	-35.5	35%
Hazel 400^{0}C 6Hrs	162.7	210.5	47.8	2.8	-94.1	94%
Hazel 900^{0}C 6Hrs	162.7	224.7	62	0.8	-98.7	99%
Animal Bone 200^{0}C 6Hrs	151.9	282.5	130.6	121.6	-6.9	7%
Animal Bone 400^{0}C 6Hrs	162.7	297.5	134.8	96	-28.8	29%
Animal Bone 900^{0}C 6Hrs	142.5	275.5	133	88.8	-33.2	33%
Rousay Peat 200^{0}C 3Hrs	150.9	199.1	48.2	26.5	-45.0	45%
Rousay Peat 200^{0}C 6Hrs	150.9	255.3	104.4	32.9	-68.5	68%
Rousay Peat 400^{0}C 2Hrs	151	247	96	13	-86.5	87%
Rousay Peat 400^{0}C 6Hrs	150.8	246.8	96	3.8	-96.0	96%
Rousay Peat 900^{0}C 6Hrs	150.8	252.6	101.8	6	-94.1	94%
Fozzy Peat 200^{0}C 6Hrs	162.7	236.7	74	11.5	-84.5	84%
Fozzy Peat 400^{0}C 6Hrs	162.7	253.5	90.8	11.6	-87.2	87%
Fozzy Peat 900^{0}C 6Hrs	151	242.2	91.2	3.9	-95.7	96%
Middle Peat 200^{0}C 6Hrs	162.7	254.4	91.7	27.1	-70.4	70%

Middle Peat 400^{0}C 6Hrs	152	260.6	108.6	7.6	-93.0	93%
Middle Peat 900^{0}C 6Hrs	151.8	256	104.2	3.3	-96.8	97%
Low Peat 200^{0}C 6Hrs	162.7	291	128.3	20.4	-84.1	84%
Low Peat 400^{0}C 6Hrs	152	275.5	123.5	14.7	-88.1	88%
Low Peat 900^{0}C 6Hrs	150.8	302.6	151.8	18.1	-88.1	88%
Highland Park Peat 200^{0}C 6Hrs	162.7	253.6	90.9	30.2	-66.8	67%
Highland Park Peat 400^{0}C 6Hrs	162.7	236.9	74.2	5.8	-92.2	92%
Highland Park Peat 900^{0}C 6Hrs	151.2	255	103.8	2	-98.1	98%
Mixed Fuel 500^{0}C 6Hrs	162.7	251.6	88.9	10.6	-88.1	88%